THE DEVELOPMENT OF A BEARING OF HIGH STIFFNESS AND A WIDE SPEED RANGE.

By

T. M. SALEM, B.Sc., (Eng.), 1968
El - Menia University, Egypt.

THESIS PRESENTED FOR THE DEGREE OF
DOCTOR OF PHILOSOPHY.

Department of Mechanical Engineering,
Brunel University,
England.

May 1980.

TO MY WIFE AND CHILDREN WHO

MADE ALL THIS WORK WORTHWHILE

إلى زوجتي وأطفالي الذين

جعلوا هذا العمل يرى النور

SUMMARY

"Summary"

The thesis describes work carried out in the development of a bearing for a wide speed range, and of high stiffness. The intended speed range is from zero to 9000 rpm, and the intended load capacity is approximately 6.6×10^4N (6.7 tonne) in the low speed range and 4×10^3N (0.41 tonne) in the high speed range. The intended stiffness is approximately 8.75×10^8 Nm^{-1} (2300 tonne in^{-1}) in the low speed range and 3.5×10^8 Nm^{-1} (905 tonne in^{-1}) in the high speed range.

It appeared that the bearing would have to work hydrostatically at low speed, and would, of course, become self generating at high speed. The bearing which has been designed is of three-lobe form with the intention of enhancing stiffness and stability in the self-generating regime. High pressure inlets with no pockets are provided in the mid lobe positions, and low pressure inlets are provided at the apices of the lobes.

Two development bearings of 135 mm bore and 127 mm width have been made. A bearing-spindle system has been investigated in two full scale test rigs. In the first test rig in which there was no rotation of the journal, the hydrostatic performance of the bearing and the hydrostatic performance of the oil control devices were tested. These tests showed the bearing to be satisfactory with respect to load capacity, stiffness and with respect to the operation of the constant volume flow valves which were chosen as the control devices. The second test rig was built to represent an actual

arrangement for a machine tool spindle. The three lobe bearing in both externally pressurized and self-generating regimes has been tested over a speed range from zero to 7000rpm, which was the limit for the available drive, and with two oils of different viscosities. The results from these tests showed that the behaviour of the bearing was satisfactory up to the highest speed (7000rpm) and revealed that spindle deflection had a significant effect upon overall stiffness. Typically at 7000rpm, the power loss was 8.6KW, and the oil temperature rise through the bearing was 39°C.

In addition to the design study and the test work, theoretical studies have been carried out. In the initial design stage an approximate analytical prediction was made of bearing stiffness in the hydrostatic regime in order to establish that feasible and convenient values for supply pressure, oil flow quantity and pumping power were possible. An approximate prediction was also made (and this drew upon published results for circular bore bearings) of the stiffness of the bearing in the hydrodynamic regime. The evaluations from these approximate analyses were made by means of two programmes written for the purpose. Later, to provide more realistic solutions, Reynolds equation was expressed in finite difference form, and a computer programme was written for the numerical solution of Reynolds equation. Various versions of this programme have been developed for several particular applications. The applications which have been investigated are:

1) A programme for the self-generating regime. In one version of the programme the boundary conditions at the low pressure grooves are assigned to zero dimensionless pressure (i.e. the conventional boundary conditions at the inlet grooves), and in another version the boundary conditions are assigned to non-zero dimensionless pressure. The listings (i.e. the

programmes themselves) and a sample of the outputs are given in Appendices. Outputs from these programmes have been compared with test results of the three-lobe bearings, and with the published results for circular bore bearings.

II) A programme for the self-generating regime of full circular bore journal bearings. The results from this programme have been compared with published results for full circular bore bearings (360 degree bearings).

III) A programme in which the oil flow quantity is fixed to a pre-calculated oil flow for a stationary journal centred within its bearing. This programme has been applied to hydrostatic operation without journal rotation, and to the operation with journal rotation in which self-generating might be present to limited or to dominant extents. In one version of the programme the fixed oil flow is supplied at mid-lobe positions and in another version the fixed oil flow is supplied at the apices of the lobes. Outputs from these versions are compared with test results and with calculated results from (I).

The dimensionless outputs of these programmes have been used in a further programme "The Design Programme" which gives values of power loss, oil flow, oil temperature rise, load and stiffness for a bearing specified dimensionally.

The question always arises in a development of a programme whether all errors have been eliminated. As a confirmation of the correctness of the programmes they have been used to give predictions

which should correspond with published results. A close agreement has been found.

The principal use of the programmes has been to give calculated values to set besides the test results, and also to predict the behaviour of a wider range of three lobe bearings than could be tested experimentally. The comparison between test and numerical prediction has been found to be satisfactory. Suggestions are made for future work. In the present work there is only a brief discussion of the stability characteristics of the three-lobe journal bearings, and a fuller discussion is outstanding. It is also suggested that a head with a stiffer shaft should be designed, and possibly running in a bearing with modified geometry to give an even higher stiffness together with a reduction in oil temperature rise.

CONTENTS

CONTENTS

NOMENCLATURE

NOMENCLATURE

C	Bearing diametral clearance or the lobe clearance.	m
$\overline{C}$	Maximum diametral clearance	m
$\underline{\underline{C}}$	Minimum diametral clearance	m
C_M	Mean diametral clearance	m
C_t	Power constant	$Nm\ s^{-1}$
D	Bearing Diameter or lobe diameter	m
F_H	Horizontal Component of force	N
F_R	Radial force	N
F_t	Total force	N
F_v	Vertical component of force	N
H^*	Dimensionless oil film thickness, h/C	
Hp	Pumping power	KW
Hs	Shear Power Loss	KW
K	Specific heat	$cal\ gm^{-1}\,^oC^{-1}$
L	Bearing Length	m
N	Shaft speed	r.p.m.
P_i	Pressure at bearing inlets	Nm^{-2}
P_o	Pressure at zero journal eccentricity	Nm^{-2}
$P^*_{i,j}$	Dimensionless pressure, $\frac{P_{i,j}}{P_o}$	
P_s	Supply pressure (i.e. pump pressure)	Nm^{-2}
P_θ	Pressure along the direction of rotation	Nm^{-2}
$Q_{A,a}$	Axial flow	litres s^{-1}
Q_c	Induced pressure circumferential flow	litres s^{-1}
Q_h	Hydrodynamic flow	litres s^{-1}

Q_n	Velocity Induced flow	litres s^{-1}
Q_p	Zero speed flow	litres s^{-1}
Q_t	Total flow	litres s^{-1}
Q_v	Flow through constant flow device	litres s^{-1}
S	Duty Parameter,* $\frac{\mu NLD}{W} (D/C)^2$	litres s^{-1}
Sp	Speed Paramter, $\frac{N}{P_O} \left(\frac{D}{C}\right)^2$	
T	Oil Temperature	^oC
U	Surface speed	ms^{-1}
W	Bearing load	N
W_x	Load component in the direction of the attitude line	N
W_y	Load component in the direction perpendicular on the attitude direction	N
$\overline{W}_t$	Dimensionless load, $\frac{W}{LD\ P_O}$	
X*	Dimensionless distance. x/D	
Z*	Dimensionless distance, z/L	
d	Journal diameter	m
fo	Heat loss factor	
h	Oil film thickness	m
h_{min}	Minimum oil film thickness	m
κ	Number of iterations	
ℓ	Axial length of oil inlets	m
n	Number of mesh points in the direction of rotation	
m	Number of mesh points across the bearing	
q_a	Axial flow coefficient, $6\mu\ Q_A/C^3P_O$	

* Also used as pressure parameter in figure 3.2

q_c Induced pressure circumferential flow coefficient

$$\frac{12 \mu Q_c}{C^3 P_o}$$

q_h Hydrodynamic flow coefficient, $\frac{4 Q_h}{\pi DLCN}$

q_n Velocity induced flow coefficient $\frac{2Q_n}{C\pi DNL}$

q_p Pressure flow coefficient

χ Bearing distance measured in the direction of rotation

z Bearing distance measured perpendicular to the direction of rotation — m

α The axial groove angle — degree

β Load angle for each lobe

γ Load angle for the complete bearing — degree

δ Bearing eccentricity — m

δ_1, δ_2 and δ_3 Lobes eccentricity — m

Δ_r Bearing offset — m

Δx and Δy Dimensionless and height of the mesh square set

ΔT Temperature rise — ^oC

ε_o Offset ratio,

$$\frac{2 \Delta r}{C}$$

ε_B Bearing eccentricity ratio $\frac{2\delta}{C_{min}}$

ε Eccentricity ratio, $\varepsilon_B (1 - \varepsilon_o)$

ε_I Eccentricity ratio of the bottom lobe

ε_J	Eccentricity ratio of the left lobe	
ε_K	Eccentricity ratio of the right lobe	
θ	Lobe angle	degree
θ_I, θ_J and θ_K	Angle between the position of minimum film thickness and the starting of the lobe in the direction of rotation.	degree
λ	Bearing stiffness	Nm^{-1}
$\bar{\lambda}$	Dimensionless stiffness	
μ	Dynamic viscosity of the lubricant	poise
$\bar{\mu}$	Dimensionless viscosity	
ρ	Oil density	$gm\ cm^{-3}$
Γ	Shear stress	
ϕ	Bearing attitude angle	degree
ϕ_I	The bottom lobe attitude angle	degree
ϕ_J	The left lobe attitude angle	degree
ϕ_K	The right lobe attitude angle	degree
Ω	Optimum over-relaxation factor	

SUBSCRIPTS

HL	Horizontal
VL	Vertical
i	Reference to the count in the axial direction
I,J,K	Refer to the considered lobe

j	Reference to the count in the direction of rotation
Max	Maximum
Min	Minimum
o	Point of zero eccentricity
1,2	Inlet and outlet

TERMINOLOGY

The following conditions are met in this thesis:

i) No rotation of journal, controlled high pressure oil only.

ii) With rotating journal, controlled high pressure only.

iii) With rotating journal, uncontrolled low pressure oil only.

Conditions i) and ii) will be referred to as being hydrostatic or externally pressurized, where in condition ii) the journal speed with other factors is sufficient to produce very considerable self-generating pressure the term externally pressurized will only be used. Condition iii) will be as hydrodynamic or self-generating.

CHAPTER 1.

INTRODUCTION

INTRODUCTION

1.1 General

The problems associated with friction, wear and the introduction of a lubricant between moving surfaces, have been appreciated for a long time. The subject of lubrication received much attention since the later part of the 19th Century when Reynolds published the first theorectical analysis for the fluid film problem. Reynolds' analysis was based on the experimental work carried out by Tower (refs. 1,2,3).

In this investigation, lubrication of journal bearings may be classified, as self-generating bearings* (hydrodynamic bearings) or externally pressurized bearings (hydrostatic bearings). In the hydrodynamic bearings the creation of a fluid film between the bearing and journal surfaces depends on the relative velocity and the presence of a wedge shape between the two surfaces. Hydrodynamic journal bearings have received much attention and a list of references covering the theory and test results are given in References 1 to 11.

The main advantages of self-generating bearings are high load capacity at high speed and eccentricities, high overload tolerance and the absence of a high pressure supply line. However, there are some applications where hydrodynamic bearings fail to provide the required load and stiffness characteristics especially at low speeds and at low values of eccentricity.

* See 'Terminology'

1.2. Externally Pressurized Bearings

In contrast with the self-generating bearings, in the externally pressurized bearings the load carrying capacity is produced by externally pressurized fluid in the gap between the sliding surfaces. Hence the main advantage of externally pressurized bearings (i.e. high stiffness, high load carrying capacity at low values of eccentricity and zero speed, accurate journal position, low friction coefficients and consequently a minimum starting torque and wear) is dependent as much upon the characteristics of the high pressure system (i.e. pressure, flow and method of compensation) as upon the bearing configuration. Specific bearing requirements within a wide range can be met by appropriate design.

The main disadvantage of externally pressurized bearings is the need of a high pressure supply line with means for providing volume flows to the inlets which are substantially constant and independent of the condition of operation of the bearing. A failure in the high pressure supply may lead to a complete failure of the bearing system.

Hydrostatic bearings, (i.e. externally pressurized bearings), have been known since 1862, when the Frenchman, Girard invented the first hydrostatic bearing (ref. 11). The next publication on the subject of hydrostatic bearings was by Lord Rayleigh who described a hydrostatic thrust bearing and solved the equation for load, flow and frictional torque (ref. 11). The name "hydrostatic bearing" became adopted after Fuller (12) had presented an analysis of a pressurized pad bearing, which he described as an oil lift.

Oil lifts are normally used with large rotors to reduce the starting torque. The analysis had been made for a single pad of 180 degree arc, and was simplified by considering the case of an infinitely long bearing, so that there was no axial flow of the oil to be considered.

1.3. The Conventional Externally Pressurized Journal Bearings.

The idea of the conventional externally pressurized journal bearing, in which high pressure pockets have been introduced around the circumference, was described by Shaw and Macks (13). The pockets may contain up to 90% of the bearing surface area, so the load capacity may be increased, while the power loss due to the shaft rotation may be decreased; but at high speeds, the turbulence within the pockets increases the power loss.

The first analysis and performance characteristics for the conventional externally pressurized journal bearing was presented by Raimondi and Boyd (14), for a bearing which was compensated by an orifice or by capillary tube.

In the last 25 years different approaches for the analysis of conventional hydrostatic journal bearings have been described in the literature (15-24); the analyses are generally restricted to bearings which are compensated by capillary tubes or by orifices. With these devices the flow has to be defined in terms of the supply pressure and the downstream pressure. In general the results of the analysis have been expressed as mathematical relations without any numerical evaluation for specific applications. There has been little experimental verification of the expressions and the majority of the experimental work which has been reported relates to a small diameter bearing with the shaft stationary or rotating slowly.

In addition to the analytical approaches various numerical solutions for the hydrostatic bearings have been published, references (25-28). These methods would be quite impracticable but for the electronic computer.

1.4. External Compensation

In the simple hydrodynamic bearing which in general has a circular bore the only oil supply requirement is to fill the convergent space between journal and bearing with oil. In practice, supply pressure from 1.5×10^5 Nm^{-2} (20 psi) to 7.5×10^5 Nm^{-2} (100 psi) is used, Reference (29). In some instances arrangements are made within the bearing to permit additional flows of oil, which do not pass through the confine of journal and bearing, and whose function is cooling rather than lubrication. However, it may be said that the behaviour of hydrodynamic bearings is more dependent upon bearing configurations than upon the oil supply system. In contrast, the behaviour of hydrostatic and externally pressurized bearings is dependent as much upon the oil supply system as upon the configuration of the bearing itself.

In a hydrostatic bearing, to create the bearing load carrying capacity, there must be a pressure drop between the supply pressure, and the pressure of the pad. Furthermore, to develop a restoring force when the journal is displaced it is necessary that the pressure at a pad should rise when the journal approaches the pad. For this to happen the rate of flow through the inlets should be held substantially constant irrespective of the pressure downstream of the control means . This requirement can be satisfied, in principle, by

using orifices, capillary tubes, constant flow devices, or diaphragm valves. These devices are described in Table 1.1.

The control devices have received much attention because it has been realised that the control devices (compensation devices) have a considerable effect on the performance of externally pressurized bearings. In particular, the stiffness is directly dependent on the type of compensation device.

Loeb and Rippel (30),Malonski and Loeb (31), have investigated the effect of the capillary, orifice, and flow control valves as compensation devices, on the stiffness of the lubricant film; as might be expected they found a constant flow device, which might be a constant flow valve or constant displacement pump , to produce the greater the stiffness. Also they found that the performance of a constant flow control valve is independent of the pressure ratio (i.e. the ratio between the pad pressure and the pump pressure at zero eccentricity).

Mohsin (32), De Gast (33), and Morsi (34), have described control devices which cause the flow rate to increase as the load increases. By this means, in principle, the bearing stiffness may be made infinite over a limited range of conditions.

The different methods of compensation applicable for the externally pressurized bearings have been described in several references summarized by O'Donoghue and Hooke (35), where the advantages, disadvantages and the limitation in using each method are described. In references (36-38) several applications where no external compensation is used are described.

Table 1.1 Comparison between different types of compensating devices

Compensation device		Description	Formula defining the flow	Advantage	Disadvantage
Capillary tubes	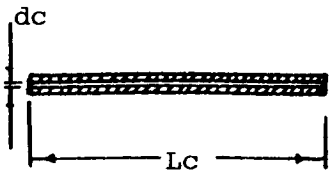	A simple tube having a large length diameter ratio. Capillaries are available as glass or hypodermic.	$Qc = \frac{Ps - Pi}{Kc\ \eta}$ (for Laminar flow) K_c is the capillary constant.	Simplicity and bearing load and stiffness are independent of oil viscosity.	Low stiffness and high power loss due to the required pressure drop.

Table 1.1 Comparison between different types of compensating devices

Compensation device		Description	Formula defining the flow	Advantage	Disadvantage
Orifices	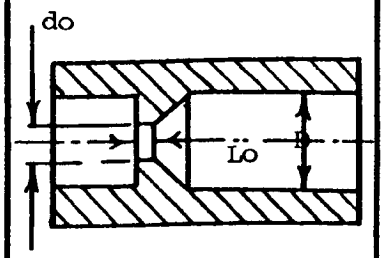		$Q_o = \frac{\pi d_o^2}{4} C_d \sqrt{\frac{2}{\rho}(ps-pi)}$ Cd: is the discharge coefficient.	Can be accommodated in small space and leads to slightly higher stiffness than the capillary.	Greater flow variation the flow characteristics change as the viscosity changes, increased tendency to blockage, and difficult to predict the exact performance.

Table 1.1 Comparison between different types of compensating devices

Compensation device.		Description	Formula defining the flow.	Advantages	Disadvantages
Constant flow control	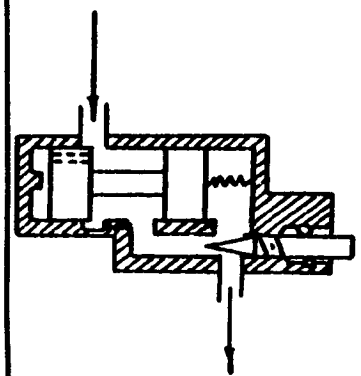	The constant flow may be achieved by using a fixed displacement pump or by spool valve. The spool is controlled by a low modulus spring ensuring a constant force within the limits of its movement.	-	High stiffness, low power loss, stiffness independent of the supply pressure and pressure ratio and the valve may be adjusted to cope with different conditions.	The bearing stiffness is dependent on the oil viscosity and temperature variation.

Table 1.1. Comparison between different types of compensating devices.

Compensation device		Description	Formula defining the flow	Advantages	Disadvantages
Diaphragm Valves	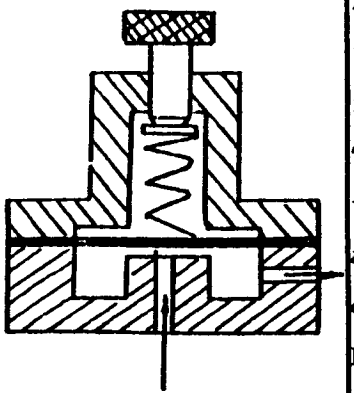	A diaphragm is used to control the flow rate to the bearing. The fluid is supplied through a control pad and its flow rate depends on the gap between the diaphragm and pad.	-	High stiffness, and no sticking.	Needs a separate design for each case and may lead to a negative stiffness.

1.5. Applications of Externally Pressurized Bearings

The advantages of the externally pressurized bearings, as described above, have led to their choice for some applications in which they have been used successfully, references (39-41). Uses of externally pressurized bearings in the machine tool industry are discussed in references (42-49). The uses include applications to slide ways and to spindles. The use of externally pressurized bearings in particular gives enhanced finish, permits smaller tolerances, and allows items of precision to be obtained at moderate cutting speeds when they are demanded by the material.

Compressible fluids (gas), such as air, have been used as a lubricant, and externally pressurized gas bearings have been developed for machine tools of very high speed, where finishing to ultra-tolerances is required. Gas lubricated bearings have been fully described by Grassam and Powell (50), and the various applications of the externally pressurized gas lubricated bearings have been presented and discussed by Decker (51) and Wunch and Nimo (52).

1.6. Externally Pressurized Bearing System.

It has been stated previously in paragraph 1.3, that most of the literature which has been published in the field of externally pressurized bearings has concentrated on the analysis of a single bearing, without reference to the behaviour of the complete machine tool spindle and without reference to specified design requirements. Little experimental test results have been published for externally pressurized bearings.

Kher and Cowely (53), have given an approximate theoretical analysis and have described some test results for a capillary compensated externally pressurized journal bearing. The analysis is simplified by considering the short bearing circumstance which has been solved for a stationary journal. Two pocket bearings of 50 m m diameter circular bore were tested over a limited range of speed (1900 rpm).

Decker and Shapiro (54-55) have presented a theoretical study of the development of a hydrostatic bearing for a milling spindle. The maximum speed of the spindle was 2000 rpm, and the maximum radial load was 8910 N. Results for pumping power, shearing power loss, temperature rise and stiffness are presented. In the absence of experimental verification it is difficult to judge how far these results would hold in practice.

Davies and Andvig (56) have presented results obtained from tests on an orifice compensated hydrostatic journal bearing with four pockets under the action of steady radial loads which produce severe bending of the shaft. The bending was produced with a shaft of 76 m m diameter and the overhang of load was 65 m m. The results are presented in terms of journal eccentricity, and it has been deduced by the writer that loads typically of 3400N were employed. An important conclusion of Davies and Andvig is that the severe shaft bending had no serious effect upon the performance of the hydrostatic bearing.

Recently, Parsiegla (57), in his paper presented at the 6th

Conference on "The Optimization Problems in Design and Production of Machines", has presented an experimental investigation of hydrostatic bearings for heavy duty machine tools with high rotational speeds. A system of two conventional hydrostatic journal bearings and one thrust bearing were used for a machine tool spindle of 130 m m diameter. Measurements of power loss and temperature rise are presented for speeds up to 10^4 rpm. To minimize power loss, a very thin oil (μ = 2.5 Cp at 40°C) was used. At 10^4 rpm the power loss due to the rotation of the shaft was approximately 70KW, however, it was noted that the load capacity was reduced because of the low viscosity actually within the bearing. At speeds greater than 4000 rpm it was noted that the power loss exceeded the calculated power loss and this was attributed to the development of turbulence in the pockets. There was no provision for supplying the bearing with low pressure oil, and the hydrodynamic operation at high speed depended upon the externally pressurized supply. It seems reasonable to suppose that hydrodynamic operation was severely affected detrimentally by the presence of the pockets.

1.7. The object of the present investigation.

The purpose of the present investigation is to develop a single journal bearing for a wide speed range and high stiffness. The development work was originated by an enquiry for a machine tool bearing of 152 m m diameter, and with the specification given in table 1.2.

The preliminary analysis showed that the rolling element bearings cannot match the required load, diameter, stiffness and running speed.

Rolling bearings have well known limited working capabilities, they cannot withstand static loads for a long time, or shock and impulse loads; they are not suitable for working at high temperatures. The higher stiffness exists only with pre-loading which reduces the working life (58-60).

It seemed possible, from a feasibility study, that the specification of table 1.2 could be met by a journal bearing which operates hydrostatically at low speed, and which becomes self-generating as the speed of rotation is increased. In a self-generating bearing of circular bore (Figure 1.1a) the stiffness of the bearing arises in the locality of the position of minimum film thickness, and the remainder of the surface contributes little to the stiffness but a great deal to the shearing loss within the bearing. However, if the journal bearing is a multi-lobe bearing (Figure 1.b), then there is a position of film convergence at each lobe, and each lobe contributes to the overall stiffness in the self-generating regime. By adopting a multi-lobe journal bearing it was considered that the required stiffness in the self-generating regime could be obtained at a lower power loss and oil temperature rise than would be possible with a bearing of circular bore. This concept reacted upon the design of the bearing in its hydrostatic aspect.

In a journal bearing which is entirely hydrostatic the advantages of the high pressure pockets (Figure 1.1c) are well known, but as reported in references (61, 62, 63), the consequent removal of surface greatly diminishes the load carrying capacity of the bearing as a

Table 1.2. Specification.

Regime	Speed rpm	Max. Bearing Pressure Nm^{-2}	Torque Nm	Power kw	Deflection m	Mean Stiffness Nm^{-1}
Low speed	8 - 40	3.86×10^{6}	6.1×10^{4}	-	unimportant	-
	40 - 840	3.86×10^{6}	-	22	"	-
Finishing	840 - 1800	1.18×10^{6}	-	-	2.5×10^{-5}	8×10^{8}
High Speed	1800-9000	2.34×10^{5}	-	-	1.25×10^{-5}	3.2×10^{8}

For the above bearing pressuresmaximum loads for a bearing of 135 m m diameter and 127 m m long become 6.6×10^{4}N, 6.6×10^{4}N, 2.0×10^{4}N and 4.0×10^{3}N respectively.

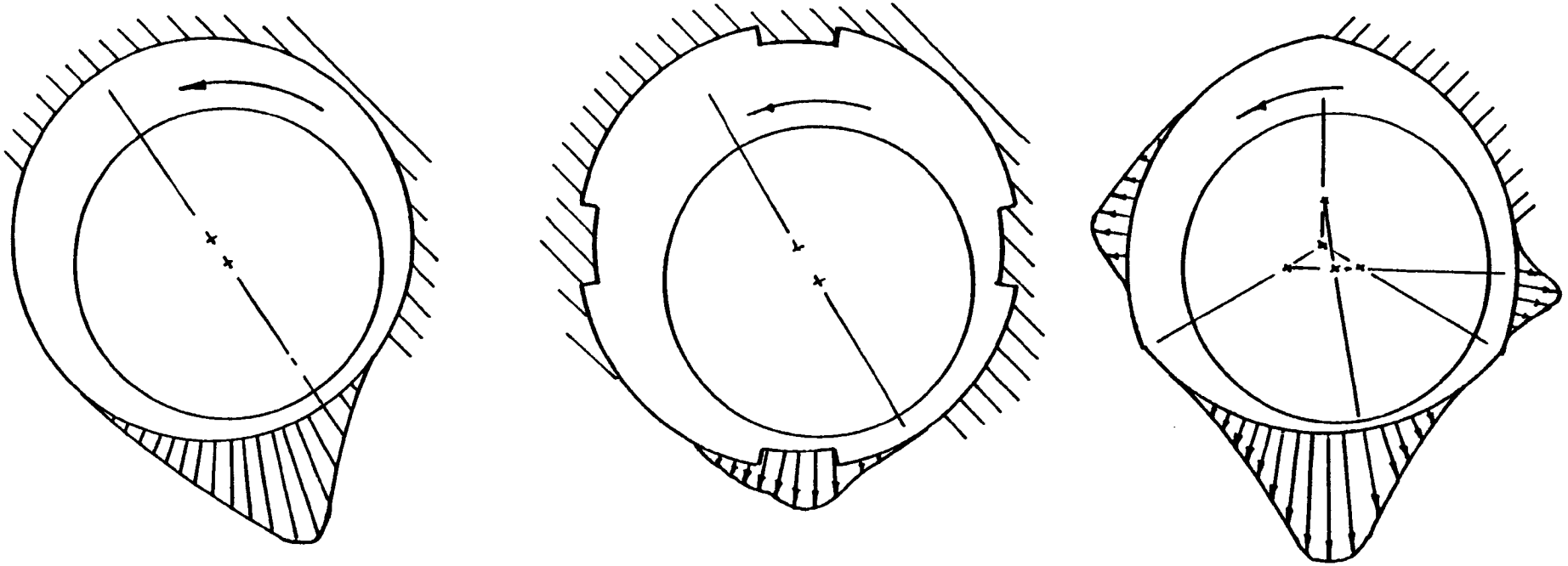

a. Circular Cylindrical 360° bearing. b. Four recesses bearing. c. Three-lobe bearing

Figure 1.1. Hydrodynamic pressure distribution around three different bearings.

self-generating bearing. Furthermore, in reference (64) it has been shown that the turbulence within the pockets increases the power loss, and the resisting torque due to the pocket friction is not always negligible and becomes dominant at high rotational speeds. The dynamic behaviour of the pocket bearings has been investigated by Optiz et al (65), Davies and Leonard (66) and Leonard and Rowe (67). It has been reported that the hydrostatic bearings with high pressure pockets are liable to dynamic instability as self-generating bearings, and the bearing damping is reduced by incorporating the pockets. Consequently, it was decided that the journal bearing would be designed with three-lobes, and without pockets. A high pressure oil inlet for the hydrostatic regime is provided at the centre of each lobe, and a low pressure inlet is provided for the self-generating regime at each conjunction of the lobes. The required characteristics in the hydrostatic regime would be obtained by employing a sufficiently high inlet pressure. Multi-lobe bearings have been analysed by Pinkus (68-70). They have been proposed as having good anti-whirl and anti-vibration properties and as having high stiffness and damping characteristics, references (71-72).

The proposed bearing will be protected from severe damage should the high pressure supply fail due to blockage or pipe failure because of the continuous supply to it of low pressure oil.

In the present investigation a system of bearings is proposed to support a machine tool spindle. A three-lobe journal bearing for hydrostatic and hydrodynamic operation which is compensated by constant volume flow valves is used as the main front bearing to

provide the required load capacity and stiffness. Rolling elements are chosen for tail and thrust bearing, both for economy of construction and to reduce the total power loss of the spindle.

The bearing spindle system has been investigated in two full scale test rigs. In the first test rig the hydrostatic performance of the three-lobe bearing was tested but without rotation of the journal. Also the characteristics of the compensation devices were tested. The second test rig was built to represent an actual arrangement for a machine tool spindle. The three-lobe bearing in both externally pressurized and self-generating regimes has been tested over a speed range from 0 to 7000 rpm,and with two oils of different viscosities. Measurements have been made of power loss, oil flow rate, oil temperature rise and journal displacement in both vertical and horizontal directions under the influence of a steady vertical load.

Two bearings of the three-lobe type have been machined with different lobe clearances, offset ratios and axial groove dimensions. These bearings have been tested in the second test rig, and the second bearing was also tested with high pressure oil admitted at the conjunctions rather than at the centre of the lobes. The method used to produce the three-lobe bearings is described. A different method for producing the three-lobe bearing has been examined experimentally and the results are outlined.

The behaviour of the spindle assembly has been investigated with special reference to the bending of the spindle and the stiffness of

the tail bearing assembly. With the aid of a computer programme for calculating spindle deflection, several arrangements for the complete assembly have been examined, and alternative arrangements of tail and thrust bearing have been outlined.

In addition to the test work and the design study mentioned above, a theoretical investigation has been carried out, and the theoretical predictions have been compared with test results and published data. The initial theoretical work was based upon the analytical solution of Reynolds' equation and was limited to the infinitely wide bearing instance. A three-lobe externally pressurized bearing with a stationary journal was considered. In addition an approximate analytical study of the three-lobe bearing in the hydrodynamic regime was carried out. Originally the concept was quantified on the basis of these approximate analytical studies. Later Reynolds' equation was expressed in finite difference form and a computer programme for its solution was written. Programmes of this kind have been applied to the following circumstances.

I. Self-generating regime with a vertical load directed towards the centre of a lobe.

II. As above, but with a vertical load directed towards the conjunction between the lobes.

III) Self-generating regime with dimensionless pressure at the inlet grooves assigned to non-zero values.

IV. Externally pressurized regime with a vertical load as (I) and (II).

V. Externally pressurized regime with the high pressure oil admitted at the conjunction of the lobes.

VI. Self-generating regime for the full circular bore bearing (360° journal bearing).

The principal output of these programmes is :-

a)	Dimensionless pressure	Hydrodynamic regime
b)	Duty parameter	
c)	Attitude angle	
d)	Load angle	
e)	Hydrodynamic flow coefficient	
f)	Pressure flow coefficient	
g)	Total flow coefficient	
h)	Dimensionless pressure at each inlet	externally pressurized regime
i)	Flow coefficient	
j)	load factor	
k)	load angle	

A further computer programme which is called "The Design Programme" has been written, where in this programme the dimensionless output of the finite difference programmes may be used as an input for the calculation of actual oil flow, temperature rise, power loss, actual load and actual stiffness. As appropriate this programme has been run in connection with test bearings, but has also been run in connection with bearings which are cited in the literature. This has been done in particular to seek assurance that the programmes are correct. The programme has also been used for calculation of a small bearing which is of interest in another connection .

All the computer programmes which have been used in this investigation have been written by the author except the computer programme which has been used to calculate the spindle deflection. The computer programmes' list as well as a sample of the output are presented in the Appendices.

Comparison between theory and experiment is presented. Modification for the test rig* and computer programmes for future investigation have been outlined. Figure 1.2 shows a flow chart for the sequence of the investigation.

* The writer designed, drew, assembled and commissioned the rig himself. He also carried out some machining and fitting.

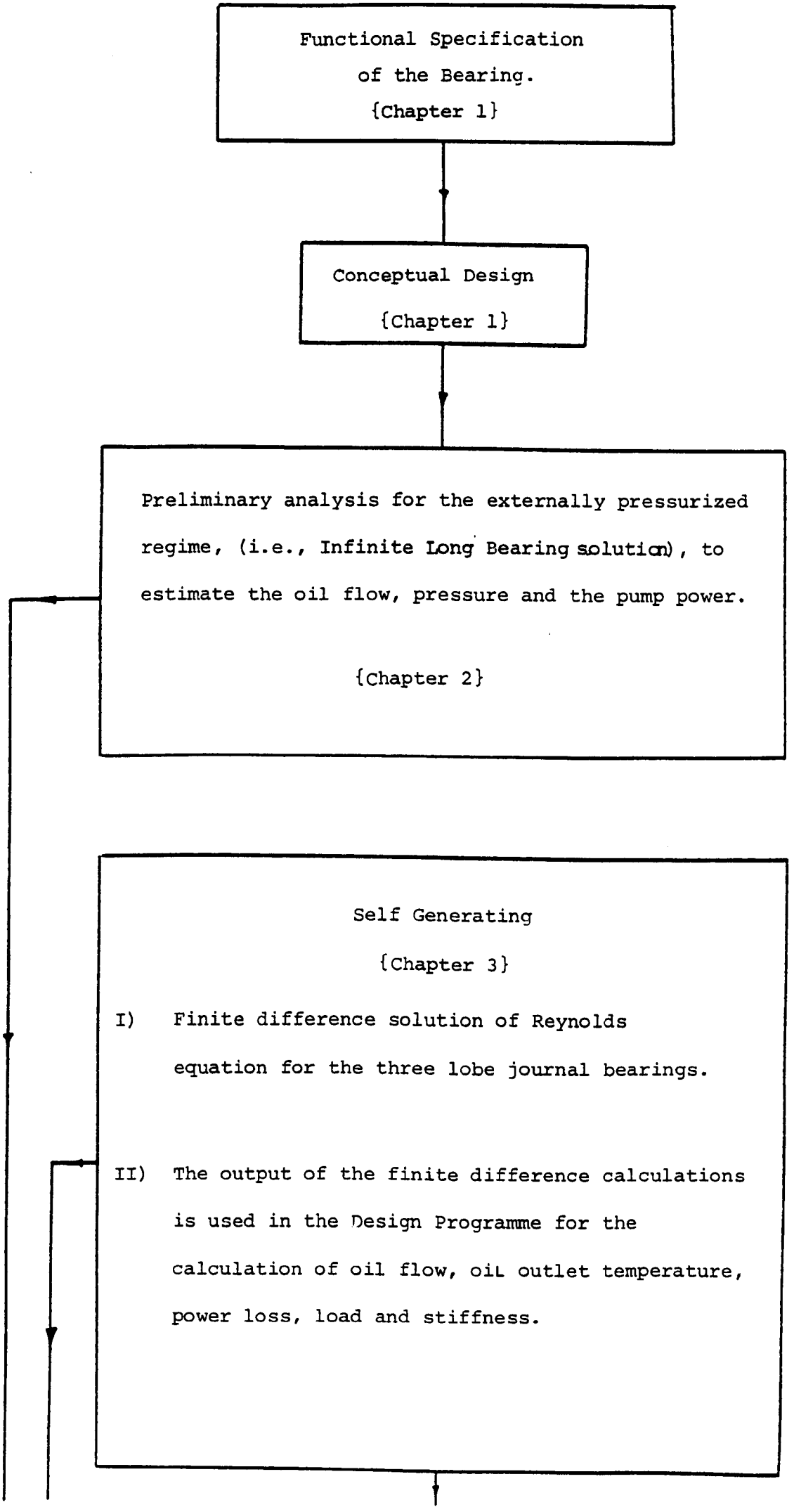
Functional Specification
of the Bearing.
{Chapter 1}
Conceptual Design
{Chapter 1}
Preliminary analysis for the externally pressurized regime, (i.e., Infinite Long Bearing solution), to estimate the oil flow, pressure and the pump power.
{Chapter 2}
Self Generating
{Chapter 3}
I) Finite difference solution of Reynolds equation for the three lobe journal bearings.
II) The output of the finite difference calculations is used in the Design Programme for the calculation of oil flow, oil outlet temperature, power loss, load and stiffness.

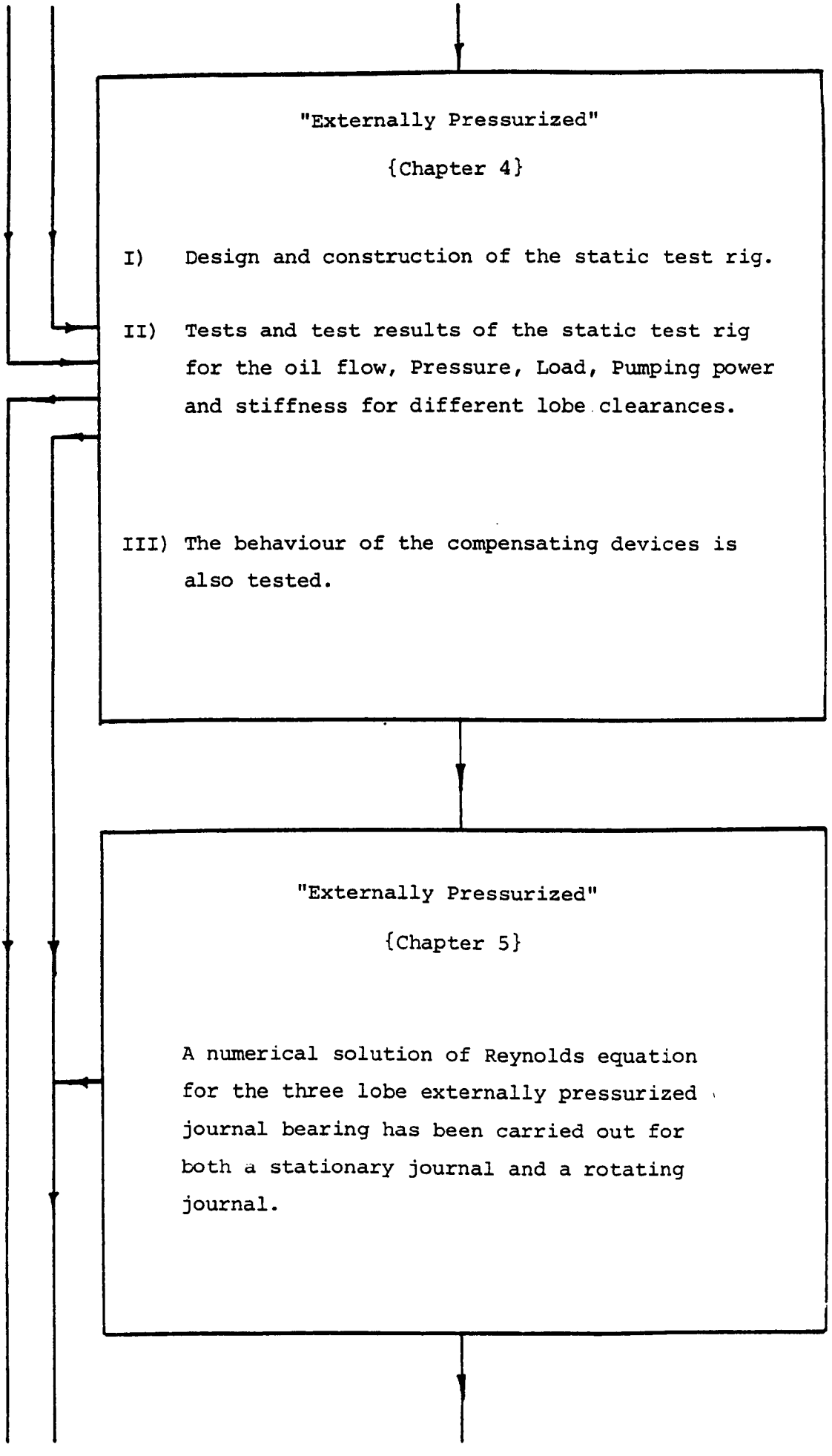
"Externally Pressurized"
{Chapter 4}
I) Design and construction of the static test rig.
II) Tests and test results of the static test rig for the oil flow, Pressure, Load, Pumping power and stiffness for different lobe clearances.
III) The behaviour of the compensating devices is also tested.
"Externally Pressurized"
{Chapter 5}
A numerical solution of Reynolds equation for the three lobe externally pressurized journal bearing has been carried out for both a stationary journal and a rotating journal.

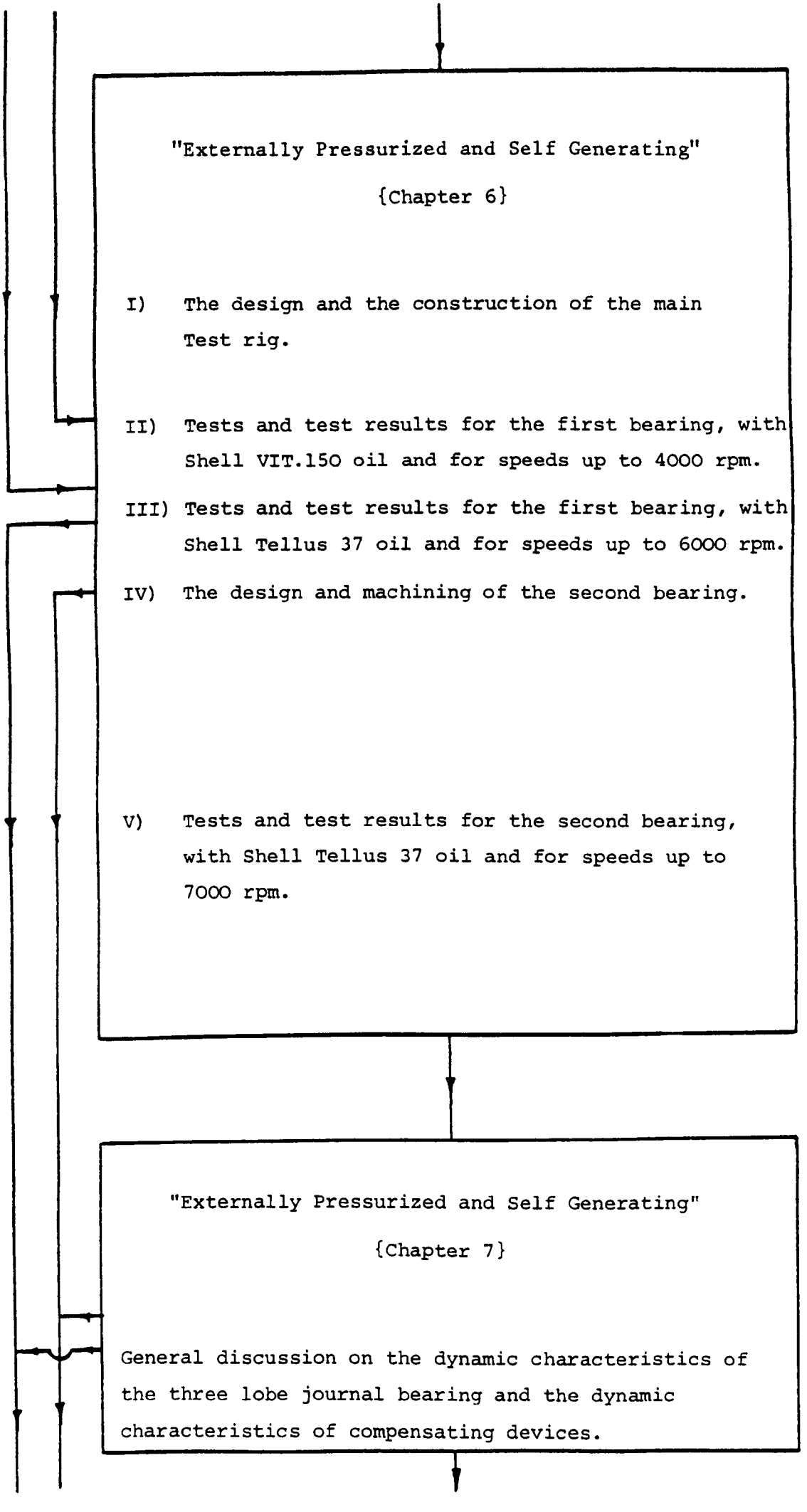
"Externally Pressurized and Self Generating"
{Chapter 6}
I) The design and the construction of the main Test rig.
II) Tests and test results for the first bearing, with Shell VIT.150 oil and for speeds up to 4000 rpm.
III) Tests and test results for the first bearing, with Shell Tellus 37 oil and for speeds up to 6000 rpm.
IV) The design and machining of the second bearing.
V) Tests and test results for the second bearing, with Shell Tellus 37 oil and for speeds up to 7000 rpm.
"Externally Pressurized and Self Generating"
{Chapter 7}
General discussion on the dynamic characteristics of the three lobe journal bearing and the dynamic characteristics of compensating devices.

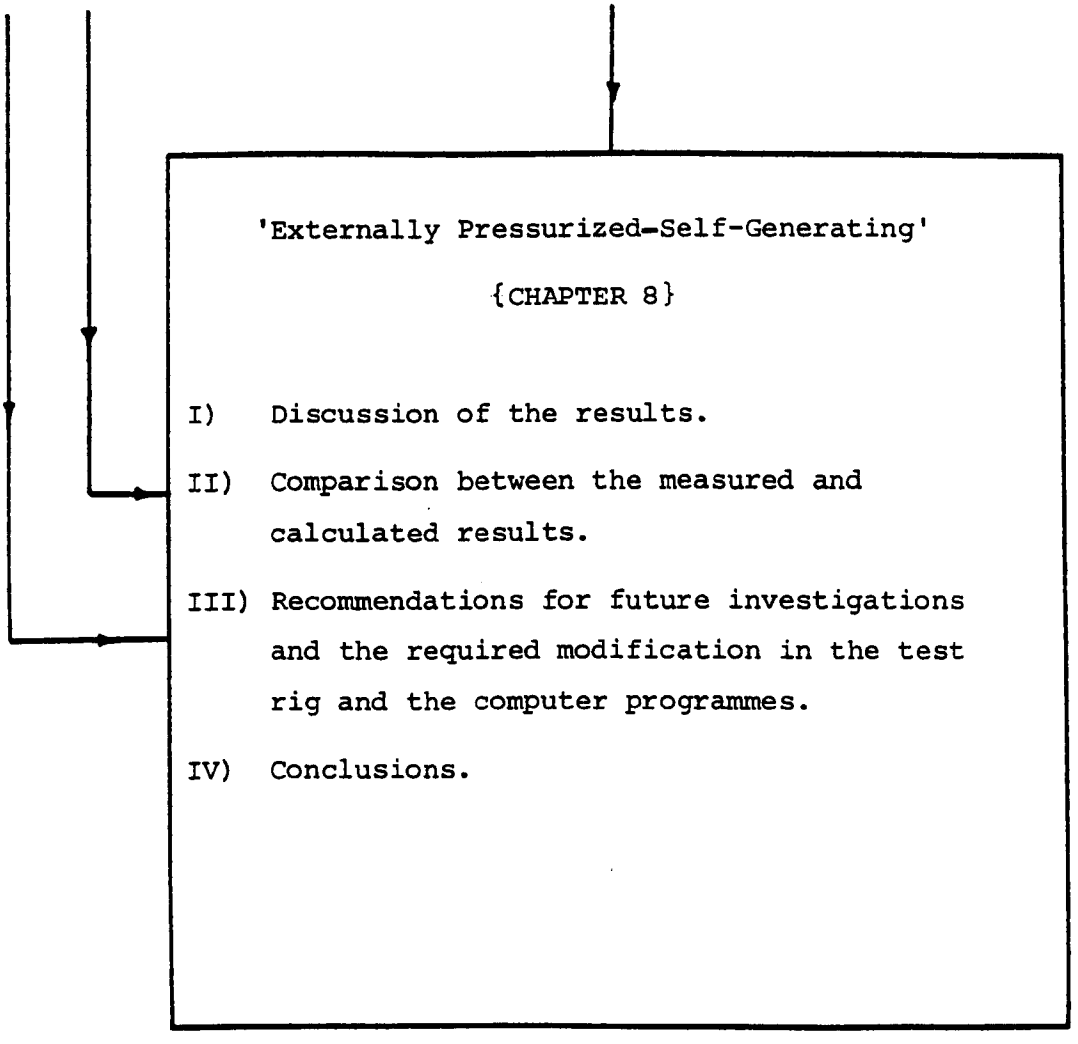

Figure 1.2 Flow Chart for the Sequence of the Investigation.

C H A P T E R 2

2. ANALYSIS OF A THREE-LOBE EXTERNALLY PRESSURIZED JOURNAL BEARING

2.1 Introduction

In paragraph 1.7 the conceptual design of a three-lobe bearing intended to meet the functional specification was described. To design an actual test bearing the concept has to be quantified, and in this chapter the quantification with relation to the hydrostatic mode of operation of the bearing, with no journal rotation, will be described. In the first instance the bearing is treated as if it were infinitely long. This treatment takes no cognizance of the axial oil flow which exists with an actual bearing, and narrow bearing theory is used to estimate the axial oil flow.

The discussion of the problem in this chapter is based upon elementary theory and is approximate. In later chapters less approximate treatments based upon finite difference solutions are presented for the hydrostatic (Chapter 5) and hydrodynamic (Chapter 3) regimes. The predictions which are required are:
Pressure distribution, the supply pressure, resultant force, stiffness, oil flow and pump power.

With reference to the present approximate treatment the appropriate expressions are described as functions of the gap between journal and a single lobe with the journal symmetrically disposed. The treatment of stiffness is based upon a journal displaced from its central position within the complete bearing so that different gaps obtain at each lobe. The journal can then no longer be symmetrically disposed with respect to each lobe, however the departures from symmetry are small, and in the analysis symmetry is assumed.

The circumferential oil flow is based upon the solution for an infinitely wide bearing. To obtain a very approximate estimate for the side leakage it has been assumed that one half of the maximum pressure calculated for the infinitely wide lobe exists along the centre line of the lobe, and that the pressure falls off linearly to the sides to give constant axial pressure gradient. This is an arbitrary procedure but the sum of the flows so calculated is reasonably close to the oil flow found experimentally, and to the more precise calculation of oil flow by the finite difference method.

The initial calculation will now be presented and discussed with reference to the choice of dimensions for an actual test bearing.

2.2 Infinitely Wide Bearing Solution

The general arrangement of the bearing is illustrated in Figure 2.1. The high pressure oil is admitted to each lobe through a series of holes, which in the analysis are treated as if they provided a uniform supply of oil over the full width of the lobe. The oil is assumed to flow circumferentially into axial grooves of zero pressure, and in consequence each lobe is taken as being isolated without any interaction with another.

2.3 Single Lobe

The coordinates of the analysis are indicated in Figure 2.2. In the steady state condition and, when the bearing is considered to be infinitely wide, the NaVier, Stoke's equation may be taken in the approximate form

$$\frac{\partial P}{\partial x} = \mu \frac{\partial_2 U}{\partial y^2} \qquad (2.3.1)$$

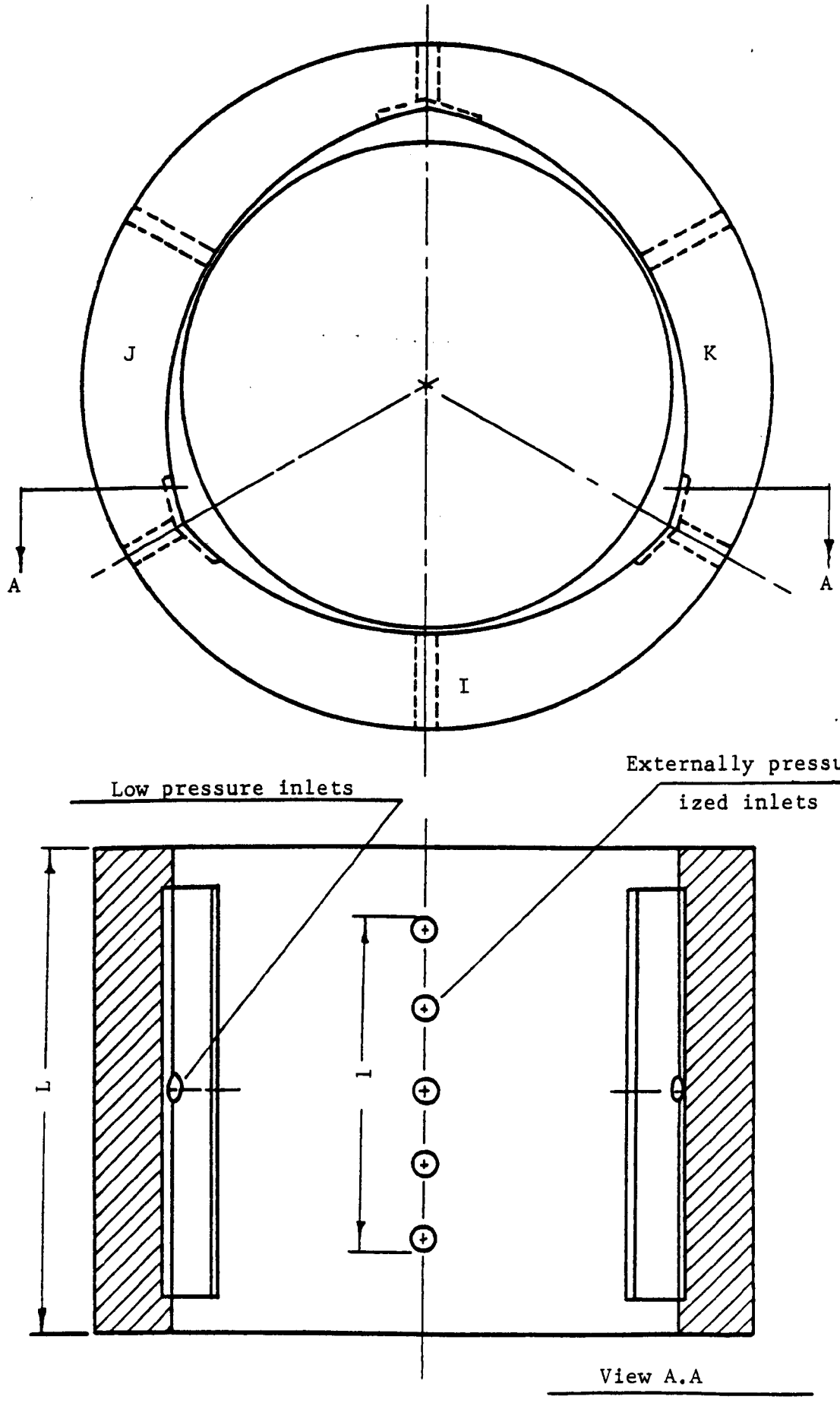

FIG.2.1 Arrangement of externally pressurized inlets.

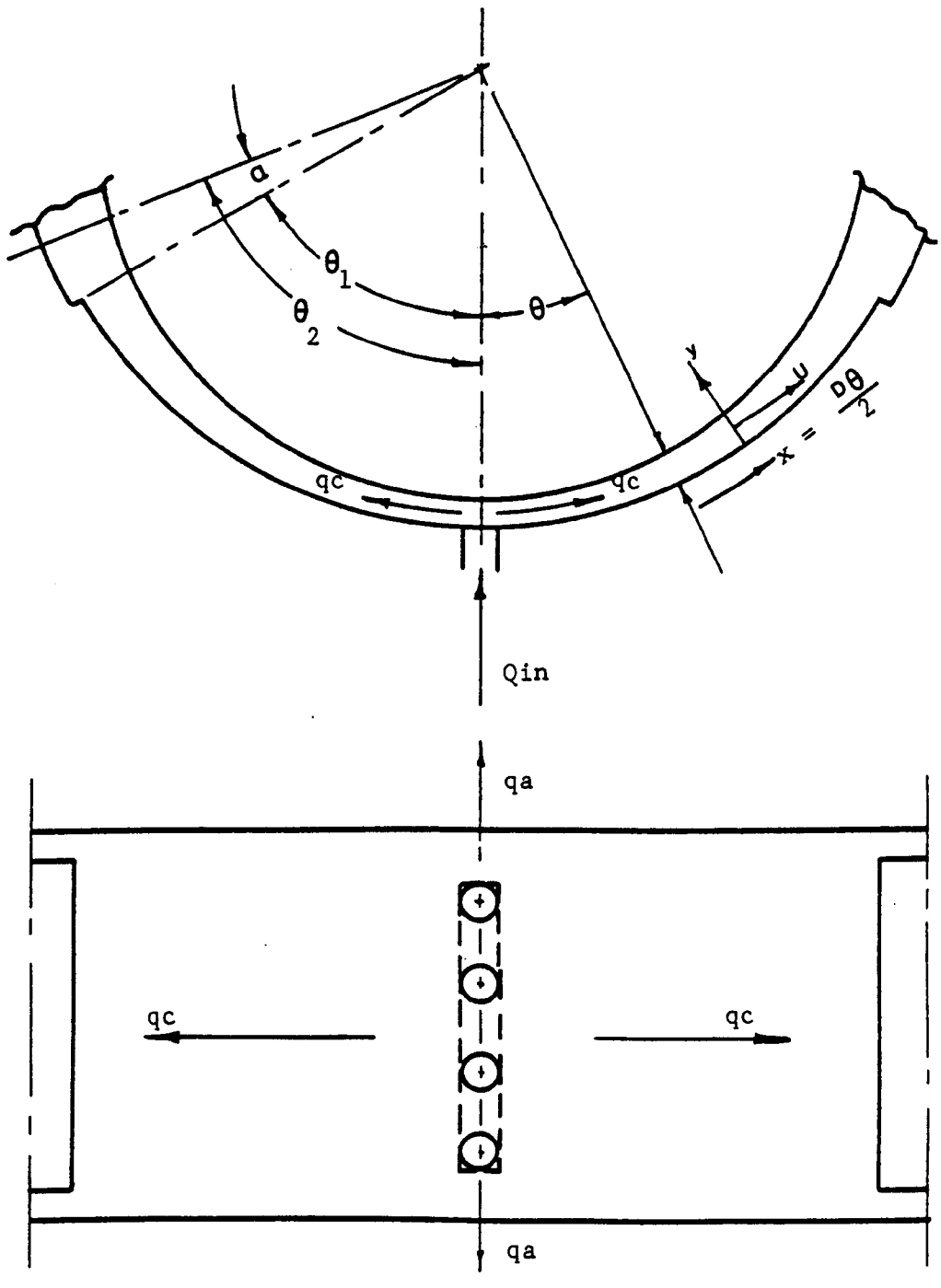

FIG.2.2 Co-ordinates and flow from a hydrostatic bearing lobe.

Repeated integration with respect to y, with the following boundary conditions, U = o when y = h and U = o when y = o, leads to

$$U = \frac{1}{2\mu} y(y-h) \frac{\partial P}{\partial x} \qquad (2.3.2)$$

The circumferential oil flow to right and left of the oil inlet may be expressed as

$$q_c = 2L \int_o^h U \, dy \qquad (2.3.3)$$

Substitution from(2.3.2) into equation(2.3.3) and integration leads to

$$\frac{\partial P}{\partial \theta} = - \frac{D}{L} \cdot 3\mu \cdot q_c \cdot \frac{1}{h^3} \qquad (2.3.4)$$

The oil film thickness may be expressed as

$$h = C/2 \ (1 - \varepsilon \cos\theta) \qquad (2.3.5)$$

where,

$$\varepsilon = \frac{\text{the distance between the journal centre and the centre of the pad}}{\text{the lobe radial clearance}} = \frac{\delta}{c} .$$

From(2.3.5) and(2.3.4) it follows that

$$\frac{\partial P}{\partial \theta} = - \frac{24 D q_c \mu}{L \, C^3} \left(\frac{1}{1-\varepsilon \cos\theta} \right)^3$$

and it follows that

$$P_\theta = - \frac{24 D q_c \mu}{L \, C^3} \int \left(\frac{1}{1-\varepsilon \cos\theta} \right)^3 d\theta$$

It is convenient to write the above equation in the form

$$P_\theta \Big/ \frac{24\mu D q_c}{L\, C^3} = \int \left(\frac{}{1-\varepsilon\cos\theta}\right)^3 d\theta \qquad (2.3.6)$$

The integration of equation (2.3.6) is carried out by using the Sommerfeld variable defined by

$$\cos\gamma = \frac{-\varepsilon + \cos\theta}{1-\varepsilon\cos\theta}$$

The result of integration is given by

$$P_\theta \Big/ \frac{24\mu D q_c}{L\, C^3} = \frac{-1}{(1-\varepsilon^2)^{5/2}} \left[\gamma\left(1+\frac{\varepsilon^2}{2}\right) + 2\varepsilon\sin\gamma + \frac{\varepsilon^2}{2}\sin\gamma\cos\gamma \right] + S \qquad (2.3.7)$$

The constant of integration is to be evaluated from:

$P = o$ at $\theta = \theta_1$ where θ_1 defines an extremity of the lobe. The associated value of γ will be denoted by γ_1 .

It then follows that

$$S = \frac{1}{(1-\varepsilon^2)^{5/2}} \left[\gamma_1\left(1+\frac{\varepsilon^2}{2}\right) + 2\varepsilon\sin\gamma_1 + \frac{\varepsilon^2}{2}\sin\gamma_1\cos\gamma_1 \right] \qquad (2.3.8)$$

In Figure 2.3, S is plotted as a function of ε, for various values of θ_1 . At the inlet $P = P_o$, $\theta = o$, $\cos\gamma = 1$, $\sin\gamma = o$ and from (2.3.7)

$$P_o \Big/ \left(\frac{24\mu D q_c}{L\, C^3}\right) = S \qquad 2.3.9)$$

and the pressure distribution along the lobe is given by

$$P_\theta \Big/ \left[24\mu D q_c / LC^3\right] \qquad 2.3.10)$$

$$= \frac{1}{(1-\varepsilon^2)^{\frac{5}{2}}} \left[(1+\varepsilon^2/2)(\gamma_1-\gamma) + 2\varepsilon(\sin\gamma_1 - \sin\gamma) + \frac{\varepsilon^2}{2} (\sin\gamma_1\cos\gamma_1 - \sin\gamma\cos\gamma) \right]$$

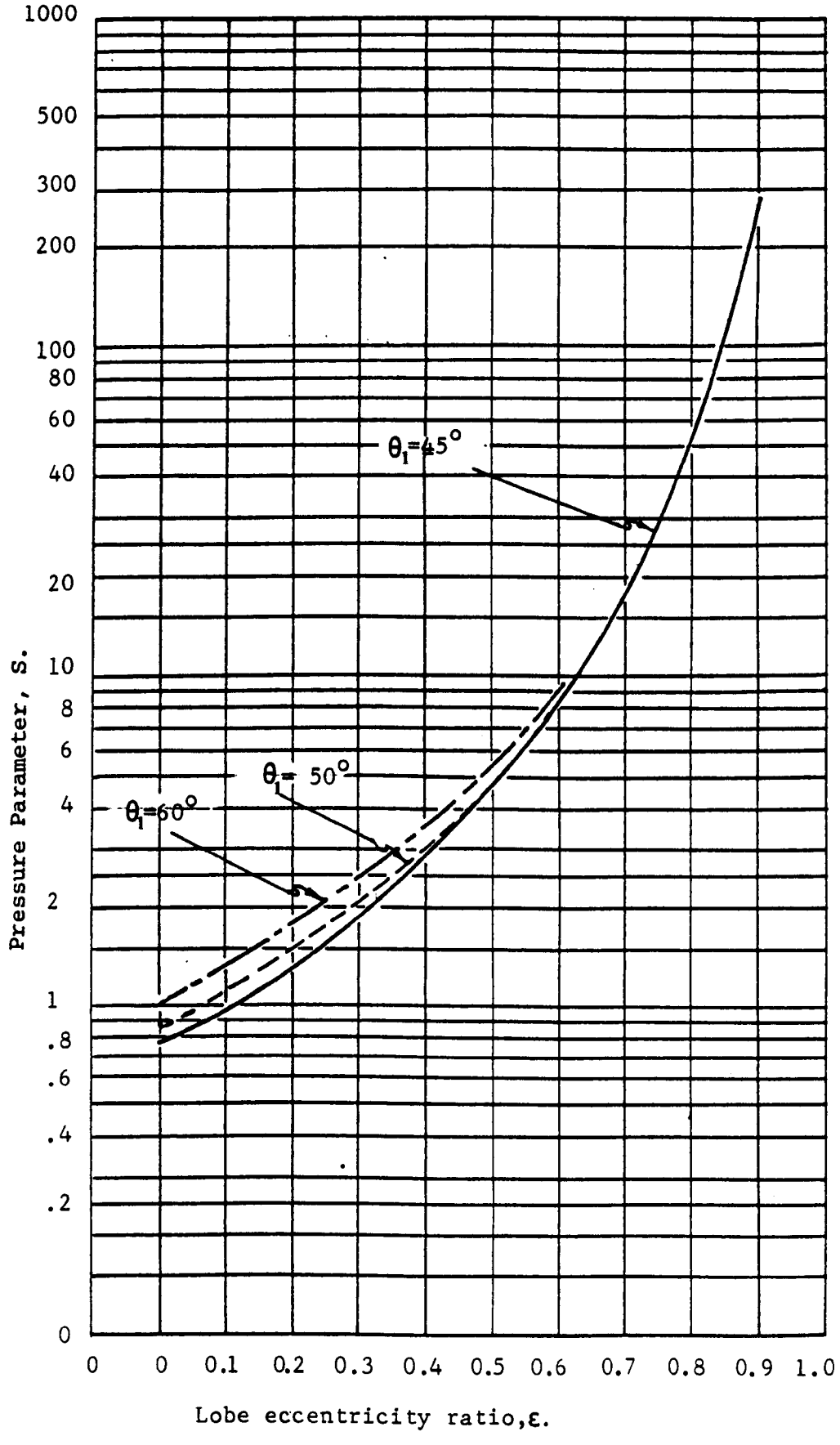

FIG.2.3 Variation of pressure parameter with lobe eccentricity ratio.

2.4 The Hydrostatic Force of a Single Lobe

The hydrostatic force generated by a lobe may be evaluated from

$$F = 2 \int_o^{\theta_1} LRP_\theta \cos\theta \, d\theta$$

$$= LD \left[P_\theta \sin\theta \right]_o^{\theta_1} - \int_o^{\theta_1} \frac{\partial P}{\partial \theta} \sin\theta \, d\theta \cdot \qquad (2.4.1)$$

The pressure P_θ is equal to zero at $\theta = \theta_1$ and $\sin\theta$ is zero at $\theta = o$, thus the hydrostatic force per lobe is expressed by

$$F = \frac{24\mu D^2 q_c}{C^3} \int_o^{\theta_1} \frac{1}{(1-\varepsilon \cos\theta)^3} \sin\theta \, d\theta \qquad (2.4.2)$$

Equation(2.4.2) is integrated by using the Sommerfeld substitution and the result is

$$F = \frac{24\mu D^2 q_c}{C^3} \frac{1}{(1-\varepsilon^2)^2} \left[-\cos\gamma - \frac{\varepsilon}{4} \cos 2\gamma \right]_o^{\gamma_1} \qquad (2.4.3)$$

By substituting from equation (2.3.9) into (2.4.3) and rearranging, the force is given by

$$F = LDP_o E \qquad (2.4.4)$$

where

$$E = (1-\varepsilon^2)^{\frac{1}{2}} \left[\frac{-(1+\cos\gamma_1) - \varepsilon/4 (1+\cos 2\gamma_1)}{\gamma_1 (1+\varepsilon^2/2) + 2\varepsilon \cos\gamma_1 + \varepsilon^2/2 \sin\gamma_1 \cdot \cos\gamma_1} \right]$$

In Figure 2.4, E is plotted as function of ε for various values of θ_1 .

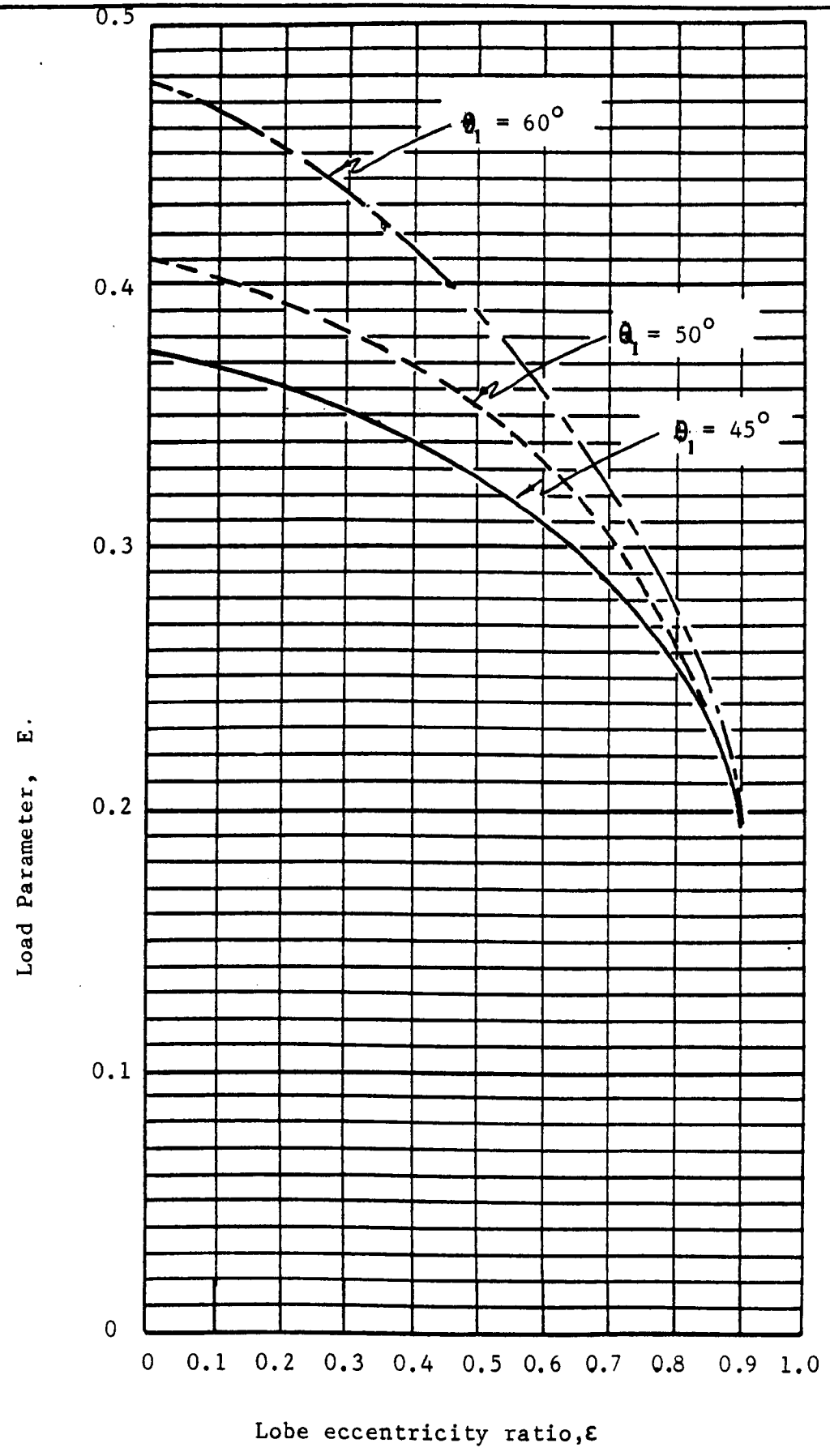

FIG.2.4 Variation of lobe load parameter with the lobe eccentricity ratio.

2.5 The Complete Bearing

The calculation of the total force, total oil flow and overall stiffness require that the eccentricity ratio at each lobe should be related to the eccentricity of the journal within the complete bearing. With reference to Figure 2.5a the journal centre is at the centre of the bearing at O, and is displaced by Δr from the centres of the lobes at $O_{I,J,K}$. In Figure 2.5b the journal centre is at O_1, and is displaced from the bearing centre at O by the distance δ. The eccentricity ratio with reference to each lobe is given by

$$\varepsilon_I = \frac{2\delta_I}{C} = \frac{2\{\delta^2 + \Delta r^2 + 2.\delta.\Delta r.\cos\phi\}^{\frac{1}{2}}}{C}$$

$$\varepsilon_J = \frac{2\delta_J}{C} = \frac{2\delta_J}{C} = \frac{2\{\delta^2 + \Delta_r^2 - 2.\delta.\Delta_r \cos(\Pi/3-\phi)\}^{\frac{1}{2}}}{C}$$

$$\varepsilon_K = \frac{2\delta_K}{C} = \frac{2\{\delta^2 + \Delta_r^2 - 2.\delta.\Delta_r \cos(\Pi/3+\phi)\}^{\frac{1}{2}}}{C}$$

When ϕ is zero (i.e. the centre of the journal moves vertically downward) the eccentricity ratios for the lobes are given by

$$\varepsilon_I = \frac{2\delta_I}{C} = \frac{2(\delta + \Delta_r)}{C}$$

$$\varepsilon_J = \varepsilon_K = \frac{2\delta_{J,K}}{C} = \frac{2\{\delta^2 + \Delta_r^2 - 8.\Delta_r\}^{\frac{1}{2}}}{C}$$

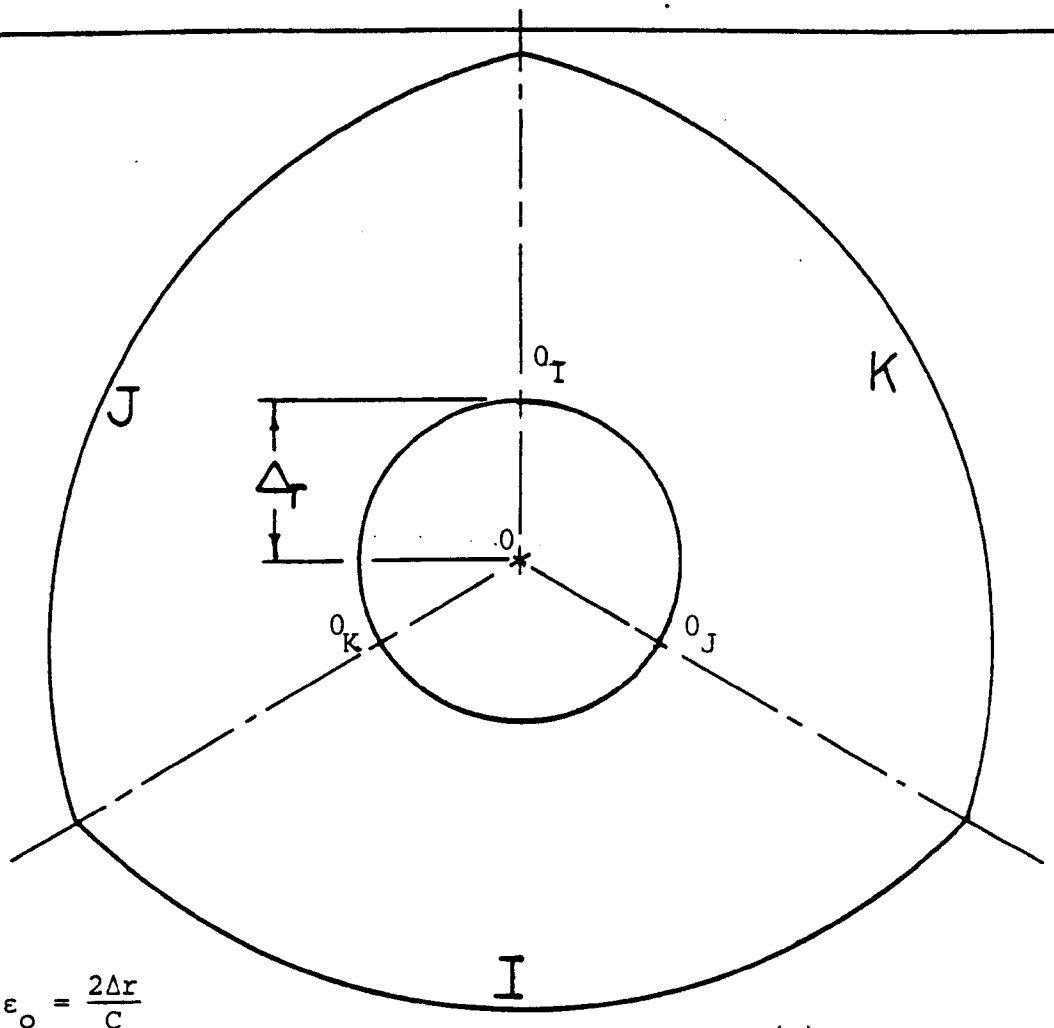

$$\varepsilon_o = \frac{2\Delta r}{C}$$

$$\varepsilon = \frac{2\delta}{C}$$

(a)

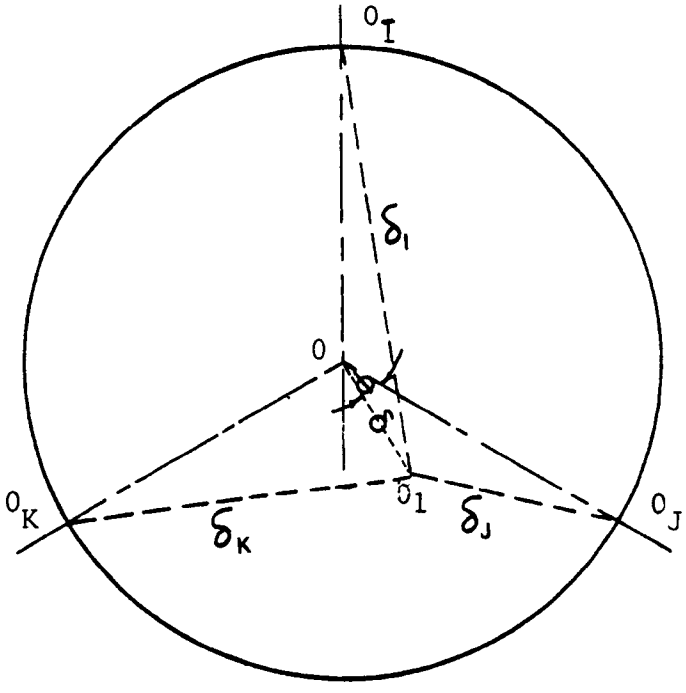

(b)

FIG.2.5 Displacements relationships.

and when ϕ is 180 degrees (i.e. the centre of the journal moves vertically upward), the eccentricity ratios are given by

$$\varepsilon_I = \frac{2\delta_I}{C} = \frac{2(\Delta_r - \delta)}{C}$$

$$\varepsilon_J = \varepsilon_K = \frac{2\delta_{j,k}}{C} = \frac{2\{\Delta_r + \delta^2 + \delta.\Delta_r\}^{\frac{1}{2}}}{C} \quad .$$

2.6 The Total Force

If the load acts in an arbitrary direction, then the force from each lobe will be such that the vector sum of the forces will balance the applied load.

The total hydrostatic force is given by

$$\vec{F}_t = \sum_{I-K} \vec{F} \qquad (2.6.1)$$

When the external load is applied vertically downward the total force is given by

$$F_t = \left\{ F_I - (F_J + F_K) \sin 30 \right\} \qquad (2.6.2)$$

By substitution from (2.4.4) it follows that

$$F_t = LD\left[(P_oE)_I - \left\{(P_oE)_J + (P_oE)_K\right\}\sin 30\right] \qquad (2.6.3)$$

$$= LD\, P_{oI}\left[E_I - \left\{\frac{(P_oE)_J}{P_{oI}} + \frac{(P_oE)_K}{P_{oI}}\right\}\sin 30\right].$$

from(2.3.9) and(2.3.6) it follows that

$$F_t = LD\ P_{oI}\left[E_I - \left\{ E_I \frac{S_J}{S_I} + E_K \frac{S_K}{S_I} \right\} \sin 30 \right] \qquad (2.6.4)$$

When the external load is considered to be applied from the opposite direction the total hydrostatic force is given by

$$F_t = LD\ P_{o\,J,K}\left[(E_J + E_K) \sin 30 - E_I \frac{S_I}{S_J} \right] \qquad (2.6.5)$$

2.7 The Oil Flow

2.7.1 The Circumferential Oil Flow

When the shaft is stationary by symmetry the flow divides equally to left and right, and therefore the rate of flow in the circumferential direction for one lobe is given by expression(2.3.9) which will be written as

$$q_c = \left[P_o\ L\ C^3/24\mu D \right] \cdot \frac{1}{S} \qquad (2.7.1)$$

2.7.2 The Axial Flow

It is clear from Figure 2.2 that the oil flows out of a hydrostatic lobe from the sides as well as in the circumferential direction.

The approporiate form of the approximate Navier, Stoke's equation in the axial direction is

$$\frac{\partial^2 w}{\partial y^2} = \frac{1}{\mu} \frac{\partial P}{\partial z} \qquad (2.7.2)$$

Repeated integration of equation(2.7.2) with respect to y, with the following boundary conditions:

$w = y$ at $y = h$ and $w = o$ at $y = o$

leads to

$$w = \frac{1}{2\mu} \frac{\partial P}{\partial z} (y-h)y \ . \qquad (2.7.3)$$

The total axial flow from one lobe is given by

$$q_a = 4 \int_o^{\theta_1} \int_o^{h_1} Rw \, d\theta \, dy \qquad (2.7.4)$$

which, from (2.7.3) may be written as

$$q_a = \frac{-4R}{2\mu} \frac{\partial P}{\partial z} \int_o^{\theta_1} d\theta \int_o^{h} (y-h)y \, dy \ . \qquad (2.7.5)$$

After integration and substituting for the oil film thickness by $C/2 \ (1 - \varepsilon \cos\theta)$, equation (2.7.5) may be expressed as

$$q_a = - \frac{4R}{2\mu} \frac{C^3}{8x6} \frac{\partial P}{\partial z} \int_o^{\theta_1} (1-\varepsilon \cos\theta)^3 \, d\theta \ . \qquad (2.7.6)$$

The pressure at the lobe centre line is deemed to fall linearly to zero at the extremities of the bearing, however the pressure gradient $\frac{\partial P}{\partial z}$ is to be represented by

$$\frac{\partial P}{\partial z} = \pm \frac{P_o}{2} \qquad (2.7.7)$$

After substituting from 2.7.7) in 2.7.6), and integrating the axial oil flow for one lobe is given by

$$q_a = - \frac{DC^3 P_o}{48\mu L} \Big| K \Big|_o^{\theta_1} \qquad (2.7.8)$$

where

$$K = \left[\theta(1+\tfrac{3}{2}\varepsilon^2 + \varepsilon^3 \sin\theta + \tfrac{3}{4}\varepsilon^2 \sin 2\theta - 3\varepsilon \sin\theta - \frac{1}{3}\varepsilon^3 \sin 3\theta\right]_o^{\theta_1}$$

In Figure 2.6, K is plotted as a function of ε for one value of θ_1.

2.7.3 The Total Oil Flow

The total oil flow out of one lobe will be taken as

$$q_t = q_c + q_a \qquad (2.7.9)$$

and the total flow out of the bearing as

$$Q_t = q_{tI} + q_{tJ} + q_{tK} \qquad (2.7.10)$$

In an externally pressurized bearing the oil is admitted to the bearing via a constant flow device, however the oil flow is the same for each pad and the total oil flow is taken as

$$Q_t = 3q_t \qquad (2.7.11)$$

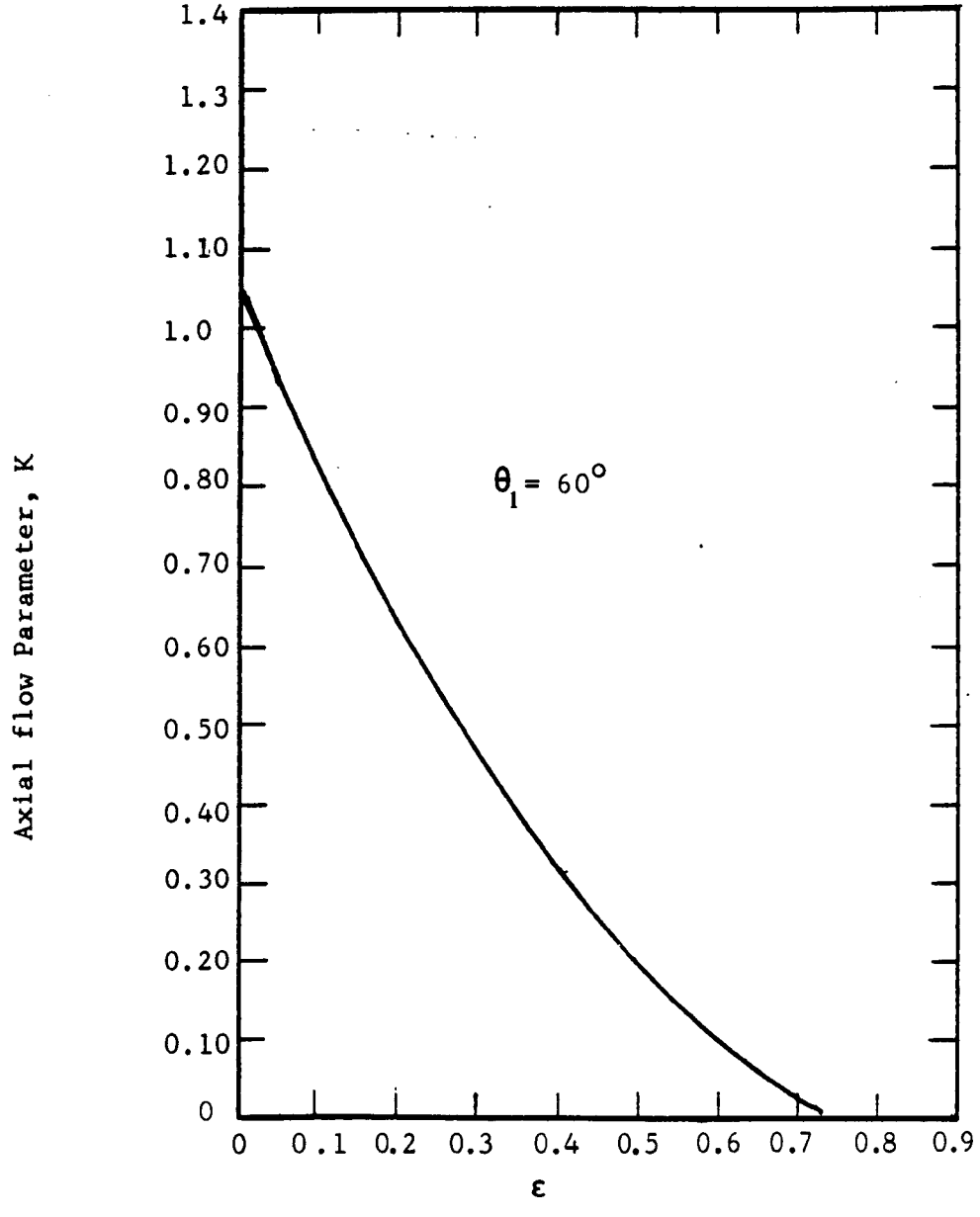

FIG.2.6 Axial flow parameter versus eccentricity ratio.

2.8 Stiffness

2.8.1 Single Lobe Stiffness

The stiffness of the externally pressurized bearing will be taken as the negative derivative of the force with respect to the oil film thickness. Because the load-displacement relationship is approximately linear the stiffness given by the derivation and the secent stiffness, are essentially coincident.

The stiffness is given by

$$\lambda \simeq \frac{dF}{d\delta} \simeq \frac{dF}{c/2 d\varepsilon} \tag{2.8.1}$$

and it follows from equation(2.4.3) that

$$\lambda / \left| 48\mu q_c D^2/C^4 \right| = - \frac{1}{(1-\varepsilon^2)^3} \left| \left\{ -\varepsilon(4+\varepsilon)+\varepsilon(4\cos\gamma_1 - \varepsilon\cos 2\gamma_1) \right\} \right. \tag{2.8.2}$$
$$\left. +(1-\varepsilon^2)\left\{ -0.25-\sin\gamma_1 - \tfrac{1}{2}\varepsilon\sin 2\gamma_1 + \tfrac{1}{4}\cos 2\gamma_1 \right\} \right| = \bar{\lambda}$$

In Figure 2.7 $\bar{\lambda}$ is shown as a function of ε for various values of θ_1 (γ_1) .

2.8.2 Total Stiffness

To calculate the total bearing stiffness resulting from the stiffness of each lobe, (Figure 2.8)the stiffness of each lobe is represented by springs of stiffness λ_I, λ_J and λ_K respectively. When the journal centre is displaced from O to O', each spring will be displaced a distance δ_I, δ_J and δ_K respectively.

The stiffness for the complete bearing is given by

$$\lambda_e = \lambda_I + \lambda_J \sin^2 30 + \lambda_K \sin^2 30 \qquad (2.8.3)$$

The direction for the load with relation to the pad repeats itself every 60° as the load is rotated. Consequently, the above expression of stiffness λ_e is valid for 6 specific directions of the load within the bearing. It is highly improbable that the stiffness will vary significantly as the load is swung through 60°, and it is considered that the above expression sufficiently represents the stiffness of the bearing for all directions of the load.

2.9 Compensation Method

In paragraph 1.4 various methods of external compensation for the externally pressurized bearings were discussed. In the present investigation the high pressure oil was supplied to the high pressure inlets via individual control valves. Volume control valves were chosen in contrast with orifices or capillaries to minimise the loss and therefore the pump power, to minimise the pressure of the pump, and also to provide a greater stiffness. Furthermore, by using the control valves, any change in bearing dimension, oil flow and the supply pressure can be accommodated by changing the setting of the valves whereas otherwise new orifices or capillaries would be required.

2.10 Pump Power

The pumping power required to pump the oil to the high pressure inlet is given by

$$H_p = \frac{P_s Q_t}{C_t} \qquad (2.10.1)$$

$$P_s = P_o + \Delta P \qquad (2.10.2)$$

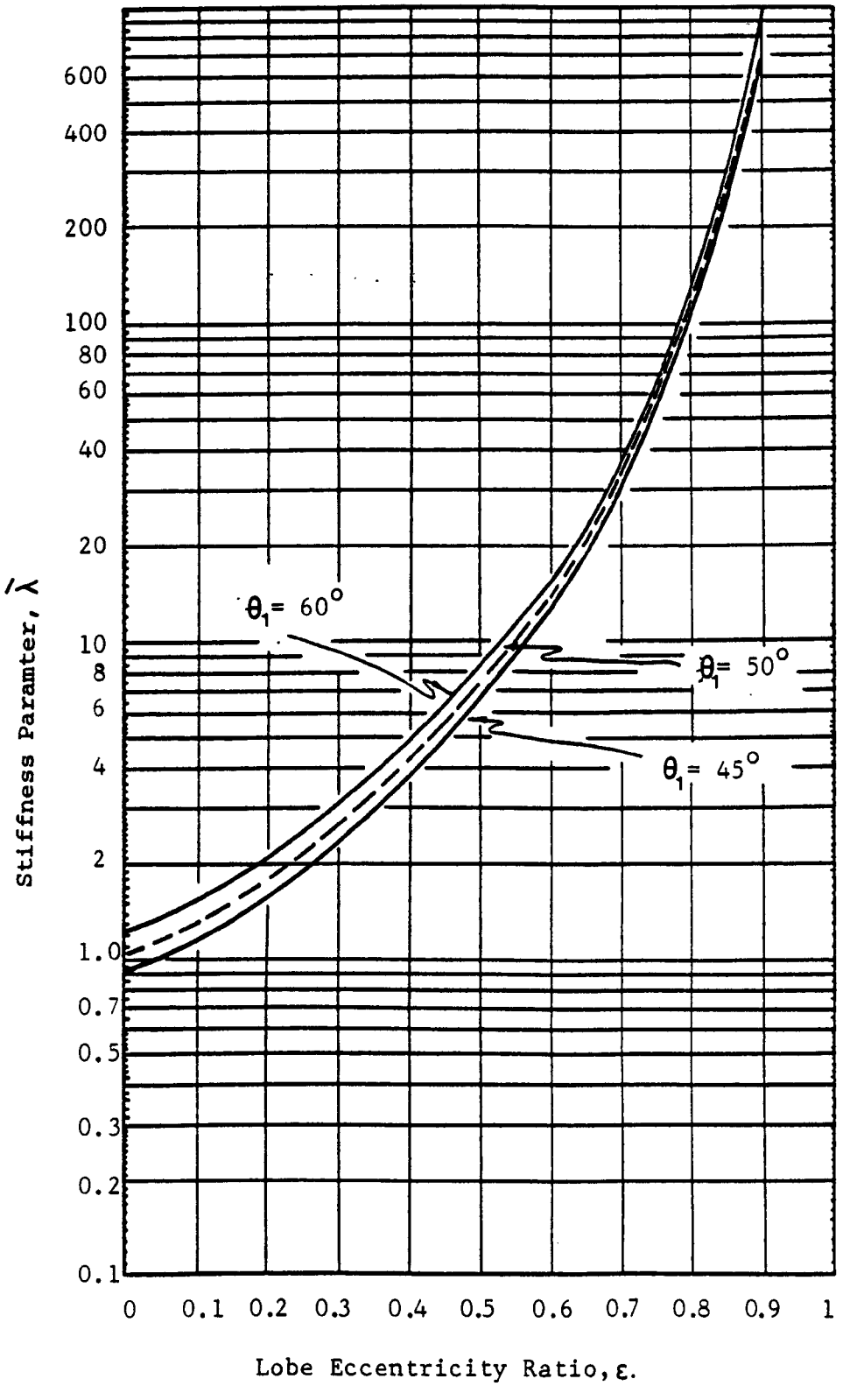

FIG.2.7 Variation of the stiffness parameter with the lobe eccentricity ratio.

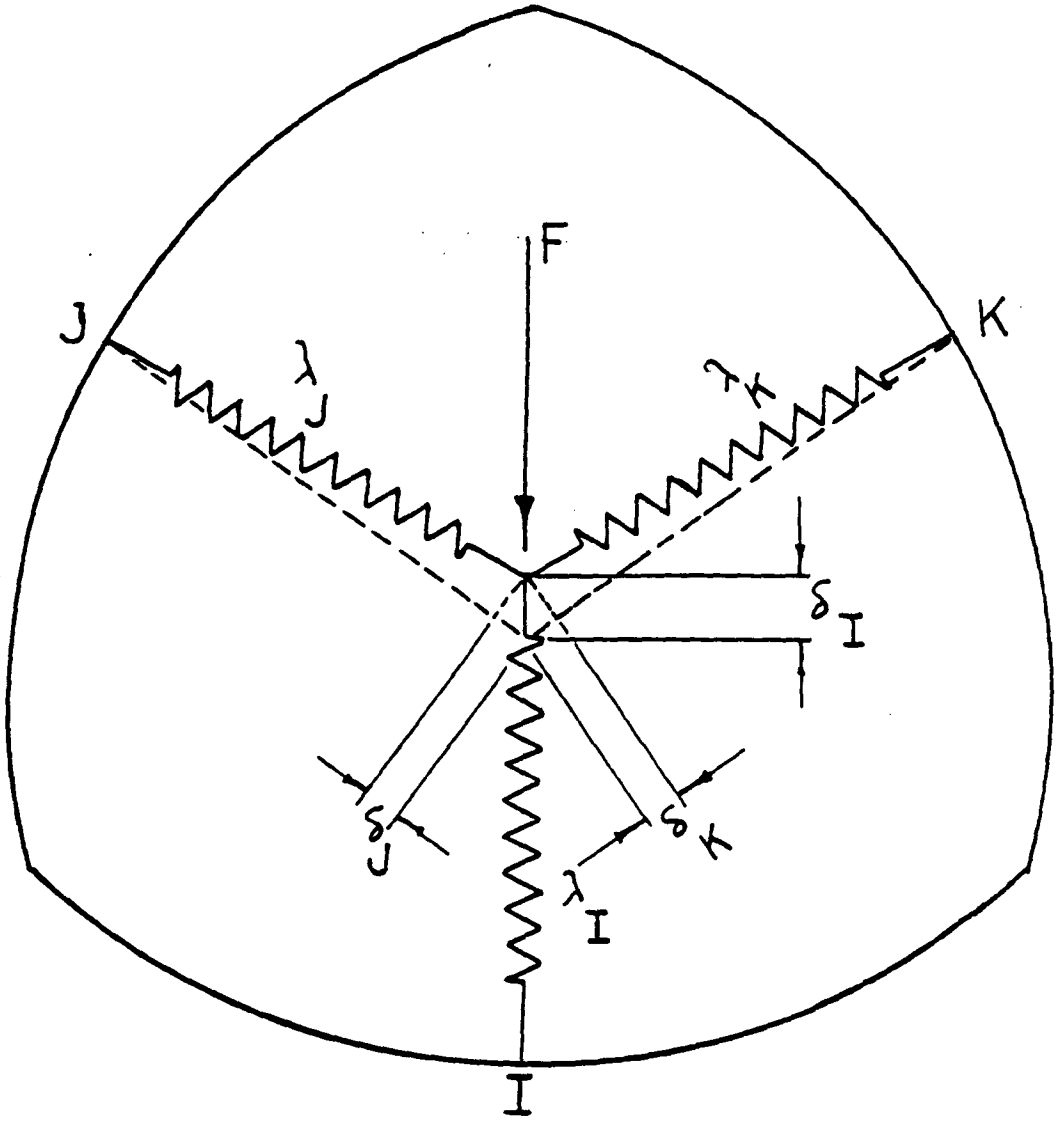

$$(\lambda_e)_I = \lambda_I + \lambda_J \sin^2 30 + \lambda_K \sin^2 30$$

FIG. 2.8 Stiffness Analogy

where

ΔP: is the pressure drop in the control valve

2.11 Results of the Computations

The purpose of these initial calculations was to choose dimensions for the first test bearing*. The hydrostatic calculations alone are insufficient because the bearing has also to be suitable for high speed of rotation (i.e. choice of dimensions has to be made with reference to both hydrostatic and hydrodynamic predictions). The hydrodynamic predictions are described in the next chapter, and the choice of dimensions is described. Here the appropriate calculations and curves, required for the choice, but pertaining only to the hydrostatic regime, are presented. In nondimensional form the complete cross section of journal and bearing is defined uniquely by (ε) and the lobe diametral clearance when the journal is centred within the bearing. The addition of an actual diameter, and an actual length define the dimensions of the bearing in all respects. The results of calculations which will be presented relate to a journal of nominal diameter 135 mm (5.30in), and to a bearing length of 127mm(5in).

The choice of journal diameter follows from the specifications of Chapter 1, and the length of the bearing was an initial guess which in fact happened to remain a suitable length with respect to load carrying capacity after the assessment had been completed.

The inputs to the computer programme were chosen to include appropriate quantities which appear in the specification of the bearing. The inputs of that kind are:

bearing load, journal displacement and journal diameter.

* The calculations were carried out by means of a computer programme which embodies the expressions already developed.

The inputs are completed by bearing length, oil viscosity and the distance between the centre of each lobe and the centre of the bearing (Δr), and the lobe diametral clearance (c).

The outputs from the programme are:

The overall stiffness (eqn. 2.8.3)

The total oil flow (i.e. the sum of the axial and circumferential flows (eqns 2.7.1, 2.7.8 and 2.7.10)

The inlet pressure at each pad (eqn. 2.3.9)

The supply pressure which is taken to be the greatest of the three inlet pressures (eqn. 2.3.9)

The pumping power (eqn. 2.10.1)

It is sufficient to take the supply pressure as being equal to the greatest inlet pressure because the minimum pressure drop across a control valve necessary for it to perform its constant flow function is small in comparison with the inlet pressure ($\sim$ 10%).

The computer programme itself is given in Appendix (A1.2). Calculations were carried out for the following values of the variables:
Load: 2.232×10^4, 2.932×10^4, 2.632×10^4 and 4.332×10^4N.
Journal displacement: 2.545×10^{-5}, 5.089×10^{-5}, 7.634×10^{-5} and 10.178×10^{-5}m.
Lobe Diametral Clearance: 2.05×10^{-4}, 2.3×10^{-4}, 2.8×10^{-4}, 3.05×10^{-4} and 2.33×10^{-4}m.
Bearing offset (Δr) = 5.86×10^{-5}m, Oil viscosity = 0.2 poise.

Typical plots of stiffness, pump power, supply pressure and oil flow as functions of lobe diametral clearance are given in Figure 2.9. In Figure 2.10 in which supply pressure and the geometry of the bearing

are constant, bearing load and stiffness are shown as functions of the displacement of the journal from its central position in the bearing.

Figure 2.9 shows that as the lobe diametral clearance is increased, the oil flow increases and also the pumping power, and that the stiffness falls substantially. Also it may be seen from figure 2.9 that the functional specification stiffness (8×10^{8} Nm^{-1}) can be obtained with a diametrical clearance of 2.8×10^{-4}m, with a supply pressure of 6.1×10^{6} Nm^{-2}, with a total volume flow of 1.2×10^{-2} $l\ s^{-1}$ with a pumping power of 0.8 kw. However, the final choice of the bearing dimensions should be made to give a compromise solution for the requirements of both the hydrostatic and the hydrodynamic regimes and this will be discussed in Chapter 3.

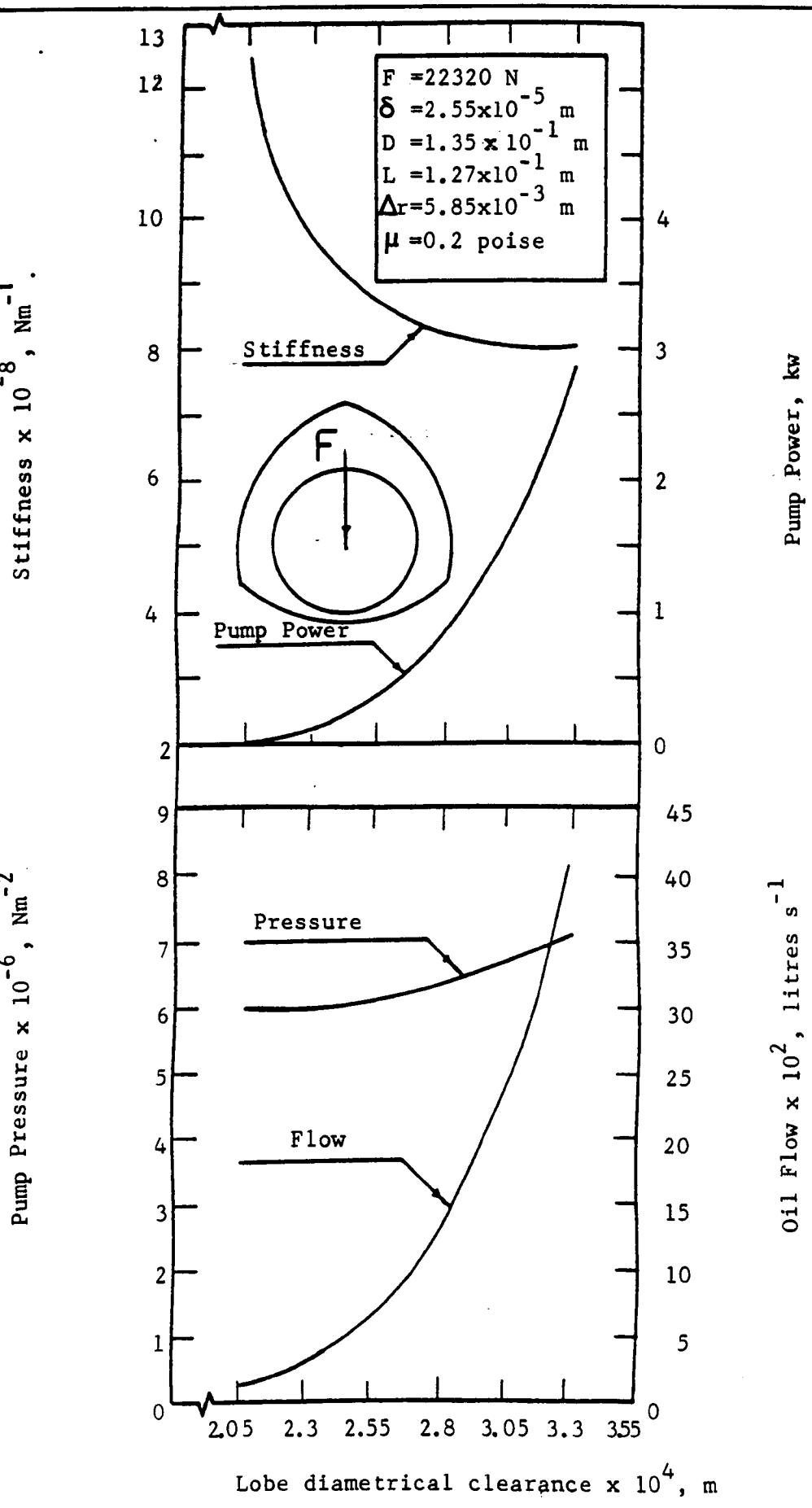

FIG. 2.9 The calculated bearing parameters.

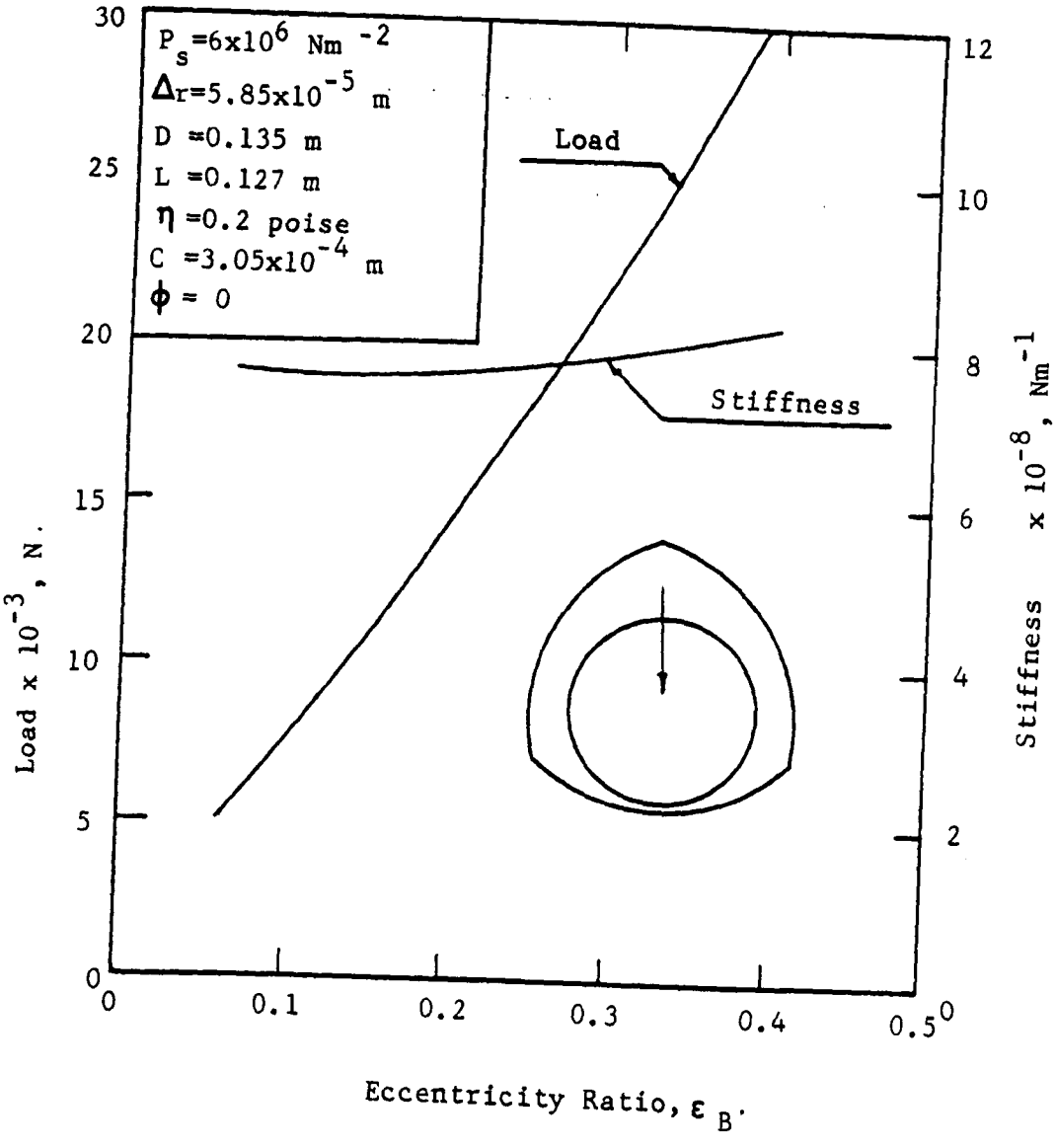

FIG.2.10 Variation of load and stiffness with the bearing eccentricity ratio.

CHAPTER 3

NUMERICAL SOLUTION FOR THE THREE-LOBE JOURNAL BEARING

3. NUMERCIAL SOLUTION FOR THE THREE-LOBE SELF-GENERATING JOURNAL BEARING

3.1 Introduction

In paragraph 2.11 the point was made that the dimensions of the bearing have to be chosen with reference to both hydrostatic and hydrodynamic regimes and the hydrostatic characteristics of the bearing were derived in an approximate manner. In the historical sequence of the work an approximate analysis was made of the hydrodynamic characteristics of the bearing, and the dimensions of the first test bearing were chosen with reference to this approximate treatment. However, the degree of approximation in the hydrodynamic instance is large with respect to power loss, oil flow, and with respect to viscosity. It has seemed to be preferable therefore to commence this chapter with the better discussion of the hydrodynamic regime based upon a finite difference treatment, rather than with a discussion of the very approximate treatment. However, at the end of the chapter the approximate treatment is briefly described, and its predictions are compared with those of the finite difference calculations.

3.2 Finite Difference Solution

In principle the numerical solution of Reynolds' equation may be performed either by using the finite difference formulation or by the finite element technique (Ref.81). The advantage of the finite element method is that irregular mesh elements can be used, however in the context of bearings there is no need for irregular elements, and the finite difference formulation is to be preferred because it leads to quicker solutions.

The assumptions of the finite difference solution are the usual assumptions implicit in Reynolds' equation including constant viscosity. A calculation commences by inserting some reasonable value for the viscosity, however the intention is that the constant viscosity should be the viscosity at the outlet of the bearing. The calculation approaches the desired viscosity by an iteration in which viscosity, power loss, oil flow and outlet temperature all become self-consistent within a limit set within the programme. Each calculation within an iteration comprises the solution of typically 648 simultaneous equations which are solved by an over relaxation technique.

As is usual in bearing calculations, there is a mathematical solution containing negative pressures and a more realistic solution which has none. When a negative pressure arises at a mesh point that pressure is set to zero before the point is again invoked within the calculation. In that way the solution is constrained towards the realistic solution. It leads not only to zero pressure at the trailing edge of the film but also to zero pressure gradient. A criterion has to be provided for completion of the iterations, and the criterion which has been used is that the dimensionless pressures of the final iteration should differ by no more than 0.0001 from those of the penultimate iteration. To put this into perspective the maximum dimensionless pressure is typically 60. In precise terms a dimensionless pressure less than -0.0001 would be set to zero whereas a dimensionless pressure of -0.0001 would stand.

The required form of Reynolds' equation is,

$$\partial/\partial x\left(\frac{1}{\mu}\, h^3\frac{\partial P}{\partial x}\right)+\frac{\partial}{\partial z}\left(\frac{1}{\mu}\, h^3\, \frac{\partial P}{\partial z}\right) = 6U\, \frac{dh}{dx} \qquad (3.1)$$

The following dimensionless forms are introduced.

$$X^* = {}^{x}/_{D} \quad , \quad Z^* = z/\ell$$

$$H^* = h/C \quad , \quad \mu^* = \frac{\mu}{\mu_{avg}} = 1$$

$$U^* = \Pi DN \quad , \quad P^* = \frac{P}{\mu_{avg} N} (C/D)^2$$

and in dimensionless form equation (3.1) becomes

$$\partial/\partial X^* \left(H^{*3} \frac{\partial P^*}{\partial X^*} \right) + (D/L)^2 \frac{\partial}{\partial Z^*} \left(H^{*3} \frac{\partial P^*}{\partial Z} \right) = 6\Pi \frac{dH^*}{dX^*} \tag{3.2}$$

With reference to Figure 3.1 the individual terms, in finite difference form become respectively

$$\partial/\partial X^* \left(H^{*3} \frac{\partial P^*}{\partial X^*} \right)_j \approx \frac{(P^*_{i,j+2} - P^*_{i,j}) \times H^{3*}_{i,j+1} - (P^*_{i,j} - P^*_{i,j-2}) \times H^{*3}_{i,j-1}}{\Delta X^{*2}} \tag{3.3}$$

$$\partial/\partial Z^* \left(H^* \frac{\partial P^*}{\partial Z^*} \right)_i \approx \frac{(P^*_{i+1,j} - P^*_{i,j}) \times H^*_{i+1,j} - (P^*_{i,j} - P^*_{i-1,j}) \times H^*_{i-1,j}}{\Delta Z^{*2}} \tag{3.4}$$

$$\left(\frac{dH}{dX} \right)^*_j = -\frac{1}{2} \varepsilon \sin\theta \tag{3.5}$$

$$\left(\frac{dH}{dX} \right)^*_j = \frac{H^*_{i,j+1} - H^*_{i,j-1}}{\Delta X^*} \tag{3.6}$$

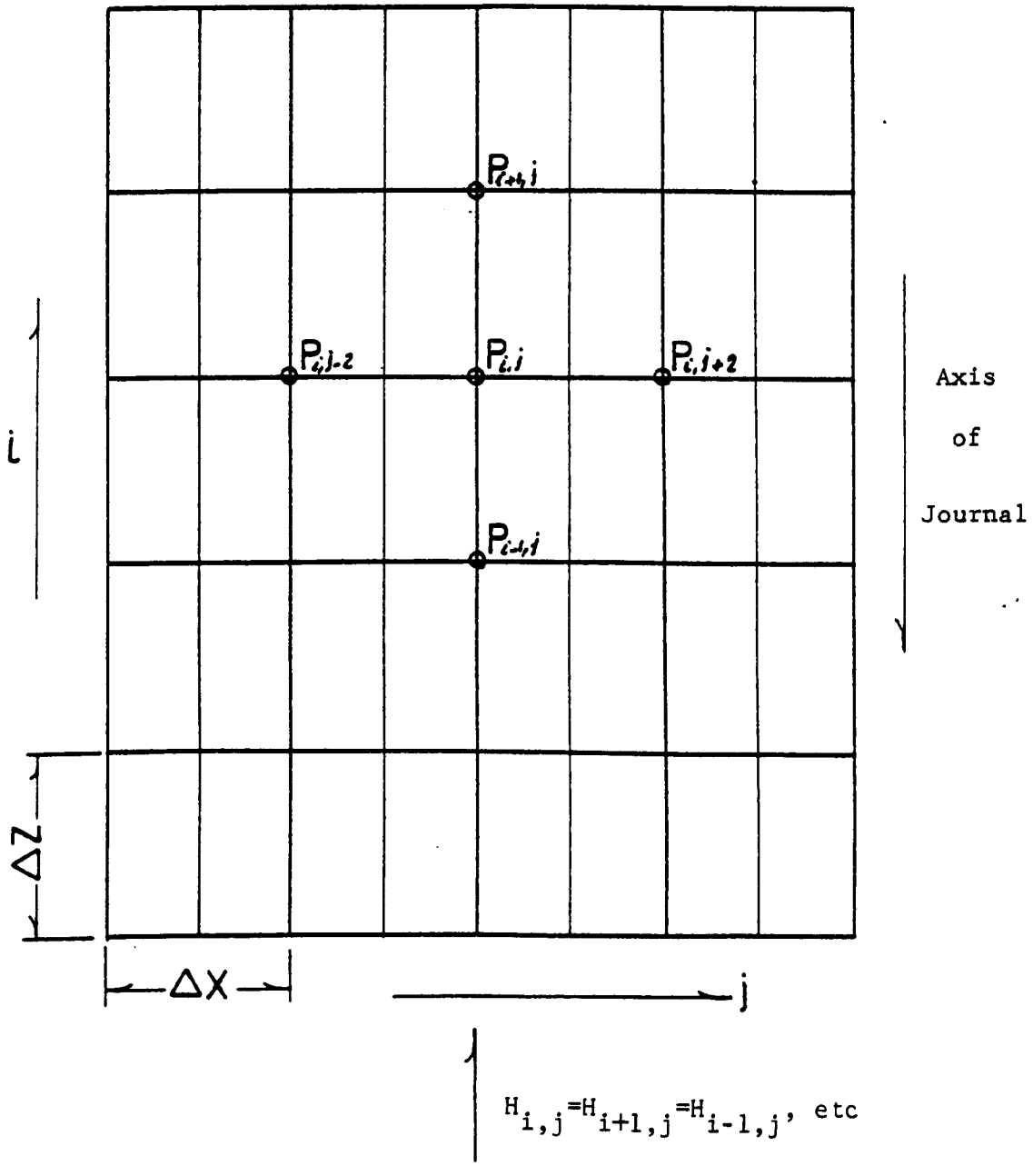

Values for H are calculated for each value of j

Values for P are calculated for each value of i but only for odd values of j.

FIG.3.1 Finite difference representation.

By substituting (3.3), (3.4) and (3.6) into (3.2) and solving for $P_{i,j}$, the finite difference equation becomes

$$\left\{P_{i,j}\right\}^{*}_{K+1} = \left[\begin{array}{l} \left\{6\Pi\left(\frac{H_{i,j-1} - H_{i,j+1}}{\Delta X}\right)\right\} + \left\{P_{i,j+2})(H^3_{i,j+1})/\Delta X^2\right\} \\ \quad + \left\{(P_{i,j-2})(H^3_{i,j-1})/\Delta X^2\right\} \\ \dfrac{\left\{(D/L)^2 \times (P_{i+1,j})(H^3_{i+1,j}/\Delta Z^2)\right\} + \left\{(D/L)^2 (P_{i-1,j})/\Delta Z^2)\right\}}{(H^3_{i,j+1})/\Delta X^2 + (H^3_{i,j-1}/\Delta X^2)} \\ \quad + (D/L)^2 \times (H^3_{i+1,j}/\Delta Z^2) + (D/L)^2 H^3_{i-1,j}/\Delta Z^2) \end{array}\right]^{*}_{K} \qquad (3.7)$$

For a mesh of i = 1 to m + 1 and j = 1 to n + 1 where n is even, and with the assumption that pressures at the boundary are known, then there are (n - 1) x (m - 1) linear simultaneous equations to be solved. These equations are of the form

$$\{P_{i,j}\}^{*}_{K+1} = \{C_1 + C_2 P_{i,j+2} + C_3 P_{i,j-2} + C_4 P_{i+1,j} + C_5 P_{i-1,j}\}^{*}_{K} \qquad (3.8)$$

where K relates to the sequence of iterations and denotes that the values of $P_{i,j}$ are those already calculated, and K + 1 denotes the current value of $P_{i,j}$,

$$C_1 = \frac{6\Pi\left(\frac{H_{i,j-1} - H_{i,j+1}}{\Delta X}\right)^{*}}{A}, \quad C_2 = \frac{(H^3_{i,j+1})^{*}/\Delta X^{2*}}{A}, \quad C_3 = \frac{(H^{*}_{i,j-1})/\Delta X^{*2}}{A}$$

$$C_4 = \frac{(D/L)^2 H^{*3}_{i+1,j})/\Delta Z^{*2}}{A}, \quad C_5 = \frac{(D/L)^2 (H^{*}_{i+1,j})/\Delta Z^{*2}}{A} \quad \text{and}$$

$$A = (H^{*3}_{i,j+1}/\Delta X^{*2}) + (H^{*3}_{i,j-1}/\Delta X^{*2}) + (D/L)^2 (H^{*3}_{i+1,j}/\Delta Z^{*2}) + (D/L)^2 (H^3_{i-1,j}/\Delta Z^{*2})$$

The set of simultaneous equations, in each of which there are only five nonzero coefficients, are solved by a modified Gauss-Seidel technique. The condition for the procedure to converge is that in each equation the coefficients on the leading diagonal of the array should exceed the sum of all other coefficients on the line. The modification of the Gauss-Seidel method is the speeding up of convergence by use of an overrelaxation factor (Ω) so that equation (3.8) becomes,

$$\left\{P_{i,j}\right\}^{*}_{k+1} = \Omega\left\{C_1 + C_2\, P_{i,j+2} + C_3\, P_{i,j-2} + C_4\, P_{i+1,j} + C_5\, P_{i-1}\right\}^{*}_{k} + (1-\Omega)\left\{P_{i,j}\right\}^{*}_{k} \qquad (3.9)$$

The over relaxation factor (Ω) is given by (Ref. 85)

$$\Omega = 2\,\frac{1 - (1-\zeta^2)^{\frac{1}{2}}}{\zeta^2} \qquad (3.10)$$

where, $\zeta = 1 - \dfrac{\Pi^2[4+(\Pi D/L)^2}{2[m^2+(\,Dn/L)^2}$

The iteration procedures starts with the P's around the boundary set to boundary values (which might be zero) and with all internal P's set to zero. The solution was performed for boundary values at the axial grooves between 0 and 5.

The particular grid employed in the calculations for each lobe is shown in Figure 3.2, i = 1 to 29(m = 28), j = 1 to 51(n = 50) so that there are 27x24 = 648 equations to be solved. The pressures around the boundary are zero except in the axial grooves which may be taken as any appropriate value. The pressures must be symmetrical about the line i = 15, and

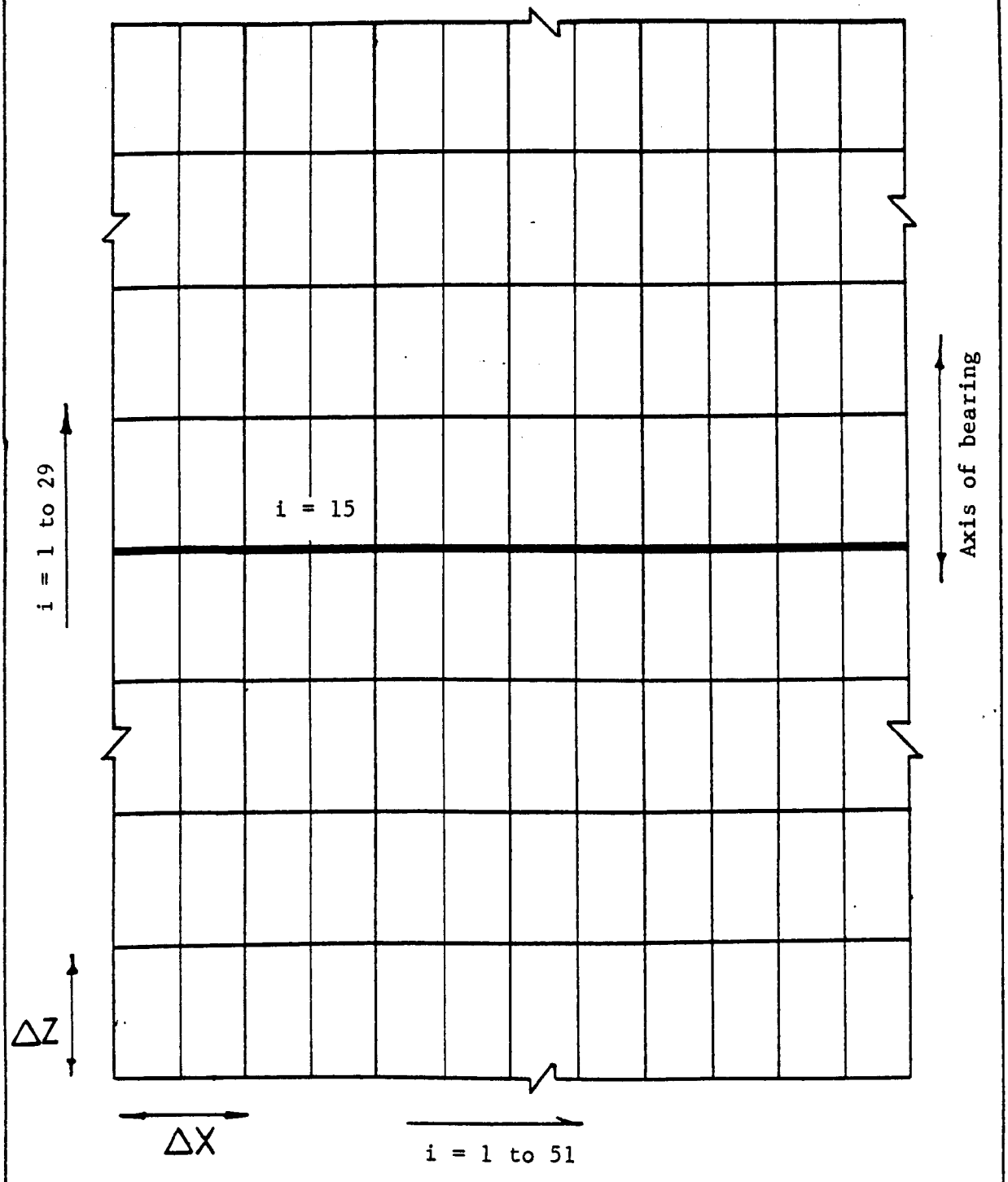

FIG.3.2 One lobe grid.

the symmetry could be used to reduce the number of equations to be solved. However a test in which that was done gave no reduction in time of computation, and consequently the full set of equations has been retained with the advantage that, as a check upon the programme, the output can be inspected for the symmetry which must exist.

The symmetry of the output may be seen in Figure 3.10 which is typical. To provide for the axial grooves which separate the lobes, the grooves in each lobe were allocated 20°, and the dimensionless pressure in these grooves may be taken as zero or any dimensionless value which is expressed by $P^* = \frac{P}{\mu N}\left(\frac{C}{D}\right)^2$.

3.3 Method of Solution for Complete Bearing

With reference to Figure 3.3 the centre of the journal is displaced from the centre of the bearing by a distance δ, and δ is included in the input to the calculation as the dimensionless displacement given by $2\delta/C_{min} = \varepsilon_B$.

The journal is fixed at given eccentricity by assuming an attitude angle ϕ which is also included in the input. The forces due to the hydrodynamic pressures at each lobe are then evaluated, and the resultant force in the vertical, and in the horizontal direction are calculated. The total hydrodynamic force and the angle between the vertical direction and the direction of the total force are also calculated, and then the journal displacements in the direction of the total force and in the direction perpendicular to the total force direction are calculated. ϕ is then increased by a small increment (i.e. $\pm 10^{\circ}$), the calculation is repeated until ϕ is equal to $\pm 60^{\circ}$ and then ε_B is then increased by a small increment (i.e. +0.1), the calculation is repeated and stiffness

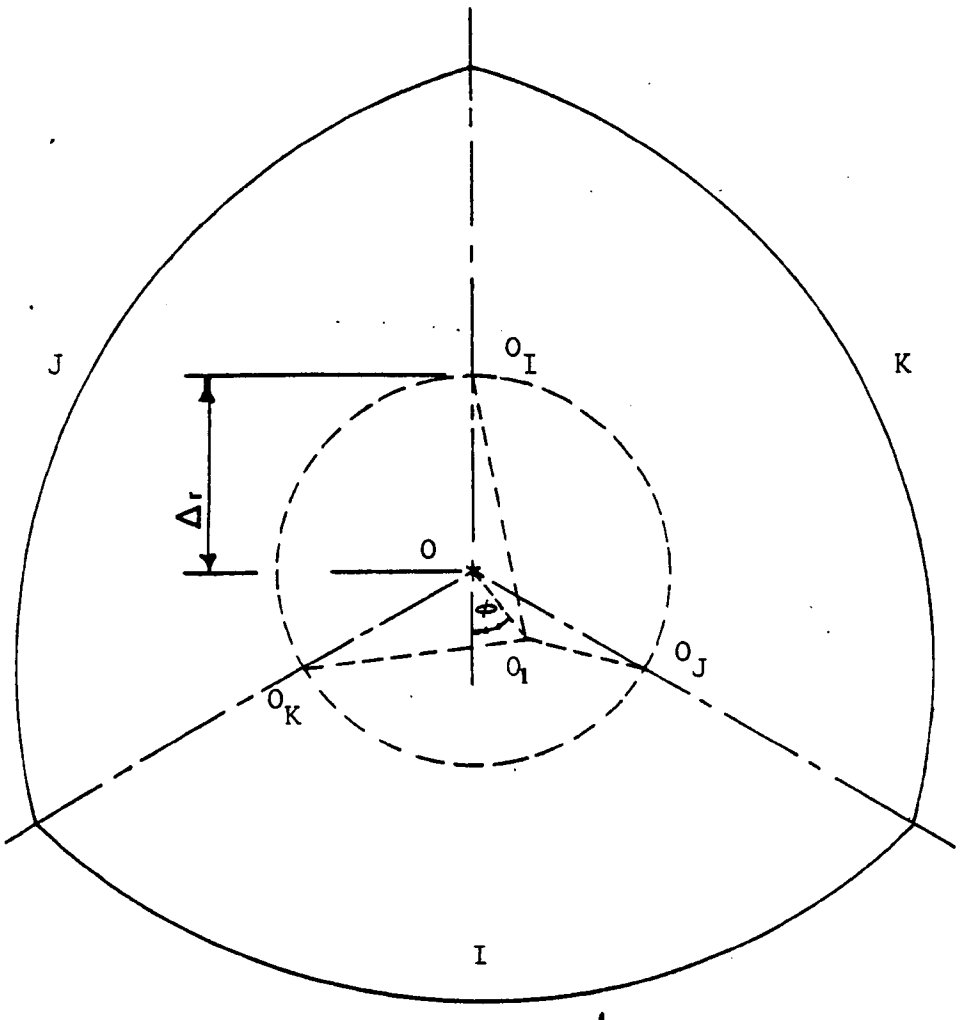

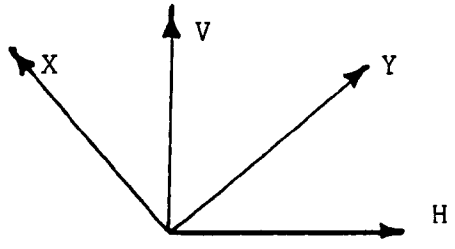

$$OO_1 = \delta$$

$$\varepsilon_o = \frac{2\,\Delta r}{C}$$

$$\varepsilon_b = \frac{2\,\delta}{C_{MIN}}$$

FIG.3.3 Bearing geometry.

coefficient is evaluated as $\frac{\text{change in dimensionless vertical load}}{\text{change in displacement}}$.

A conceptual flow chart of the routine used for the solution of the self-generating three lobe journal bearing is shown in Figure 3.4.

To revert now to individual lobes, the expression for the film thickness at each lobe, and the position of minimum film thickness at each lobe, in terms of ε_B, ϕ and ε_o are given in Figure 3.5.

Film thickness together with an initial value of viscosity, which is to be taken as constant, permits the calculation of the pressures at each lobe. With reference to Figure 3.6 the hydrodynamic forces in the direction of the lobe attitude line, and in the direction perpendicular to the lobe attitude line may be calculated from:

$$(W_x^*) = \int_0^{\theta} \int_0^{L} P_\theta^* \cos\theta \; d\theta \tag{3.11}$$

$$(W_y^*) = \int_0^{\theta} \int_0^{L} P_\theta^* \sin\theta \, d\theta \tag{3.12}$$

In numerical form equations (3.11) and (3.12) become

$$(W_x^*)_{I,J,K} = \sum_{i=1}^{m+1} \sum_{j=1}^{n+1} P_{i,j}^*, \; \Delta X^* . \Delta Z^* . \cos\theta_j \tag{3.13}$$

$$(W_y^*)_{I,J,K} = \sum_{i=1}^{m+1} \sum_{j=1}^{n+1} P_{i,j}^*, \; \Delta X^* . \Delta Z^* . \sin\theta_j \tag{3.14}$$

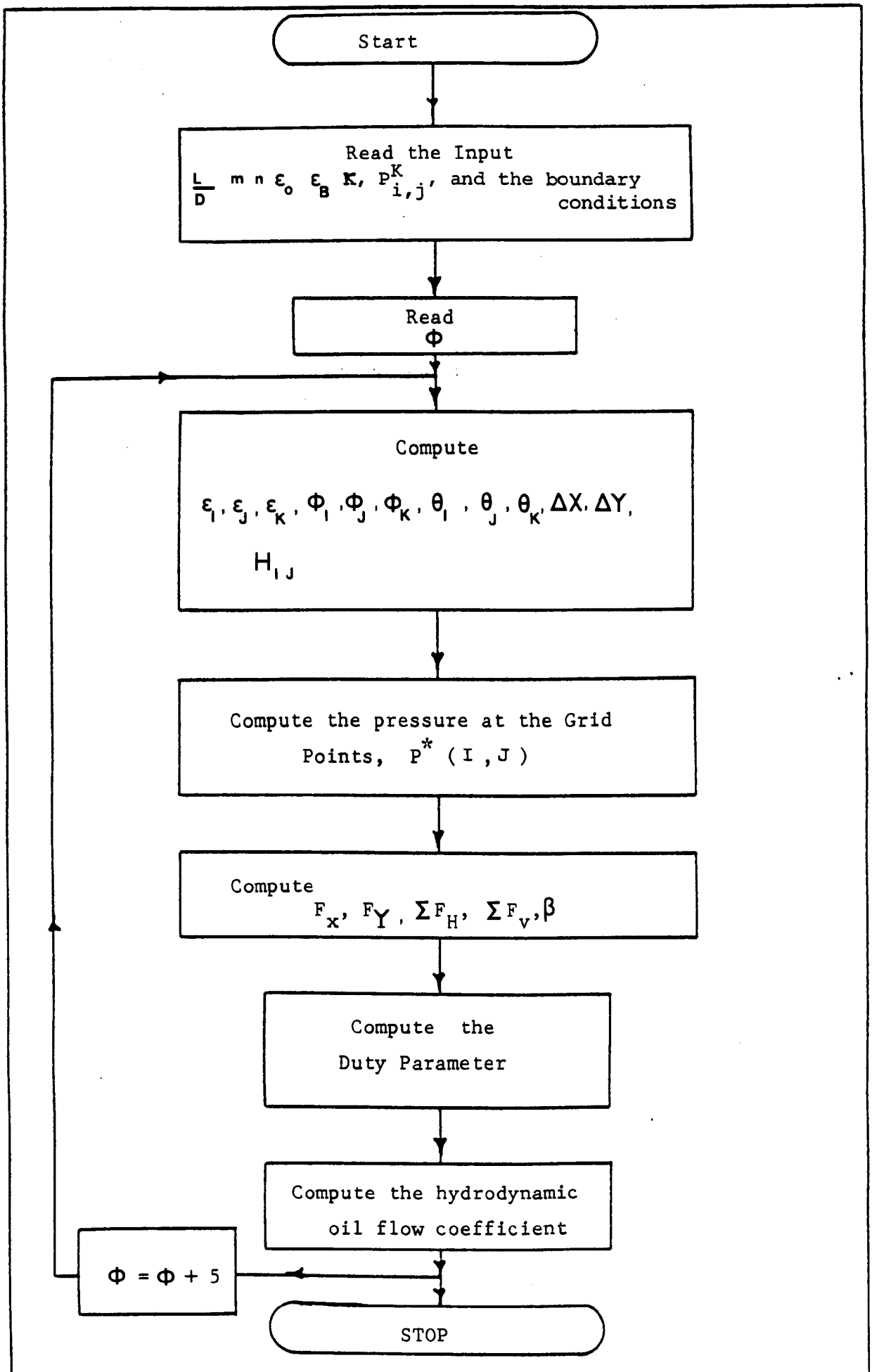

FIG.3.4 Flow chart for the hydrodynamic computer programme.

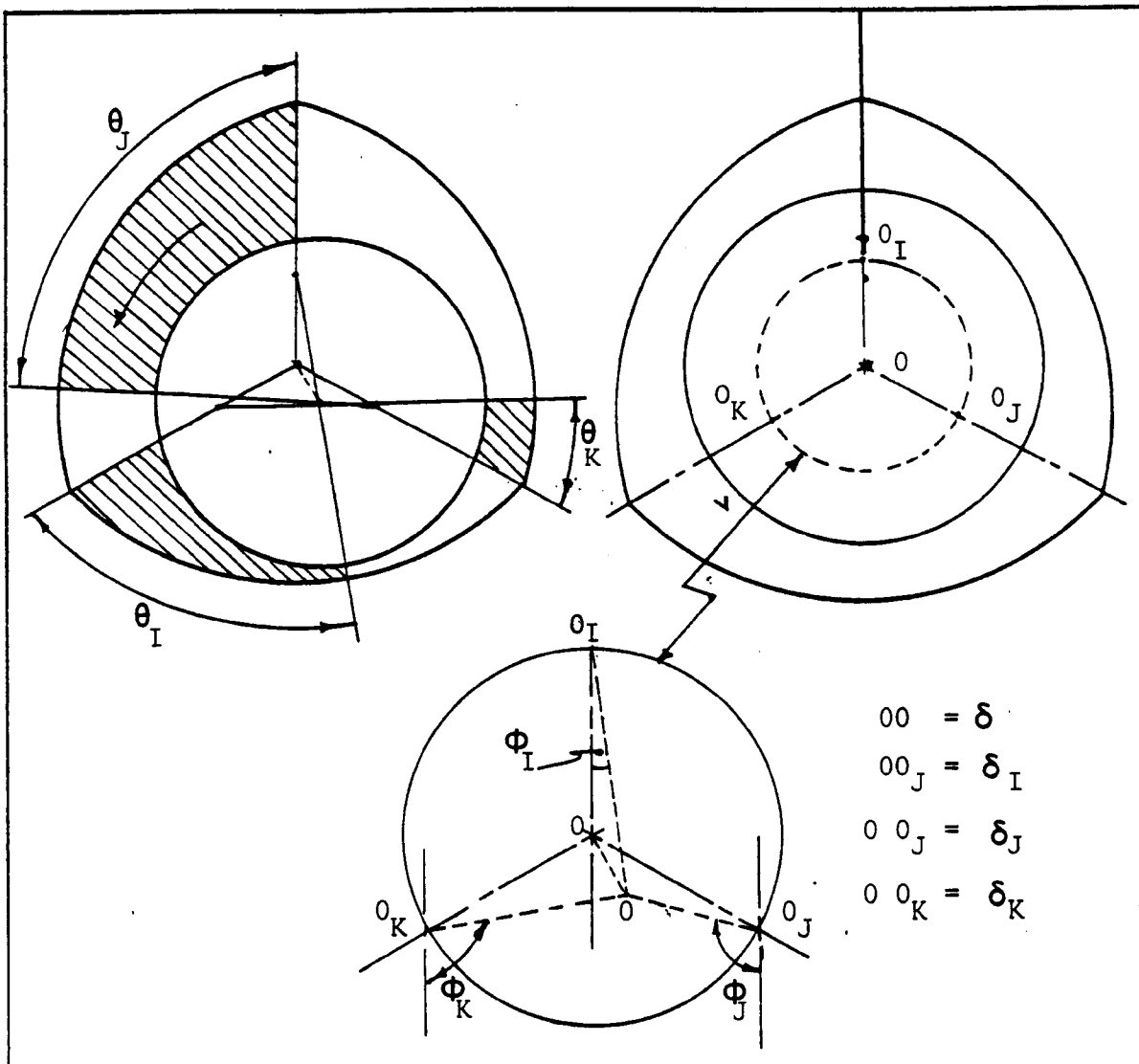

$$\varepsilon_B = \frac{2\delta}{C_{MIN}} \qquad \varepsilon_o = \frac{2\Delta r}{C} \qquad \varepsilon = \varepsilon_B\,(1 - \varepsilon_o)$$

$$\varepsilon_I = (\varepsilon_o^2 + \varepsilon^2 + 2 \times \varepsilon_o \times \varepsilon \times \cos\phi)^{\frac{1}{2}}$$

$$\phi_I = \sin^{-1}\{\varepsilon \times \sin\phi / \varepsilon_I\} \quad , \quad \theta_I = 50 + \phi_I$$

$$\varepsilon_J = \{\varepsilon_o^2 + \varepsilon^2 - 2 \times \varepsilon\varepsilon_o \times \cos(\pi/3 - \phi)\}^{\frac{1}{2}}$$

$$\phi_J = \sin^{-1}\{\varepsilon \times \sin(\pi/3 - \phi)/\varepsilon_J\} - 2\pi/3 \quad , \quad \theta_J = 170 - \phi_J$$

$$\varepsilon_K = \{\varepsilon^2 + \varepsilon_o^2 + 2 \times \varepsilon \times \varepsilon_o \times \cos(2\pi/3 - \phi)\}^{\frac{1}{2}}$$

$$\Phi_K = 2\pi/3 - \sin^{-1}\{\varepsilon \times \sin(2\pi/3 - \phi)/\varepsilon_K\}, \quad \theta_K = \phi_K - 70$$

FIG.3.5 Bearing geometry.

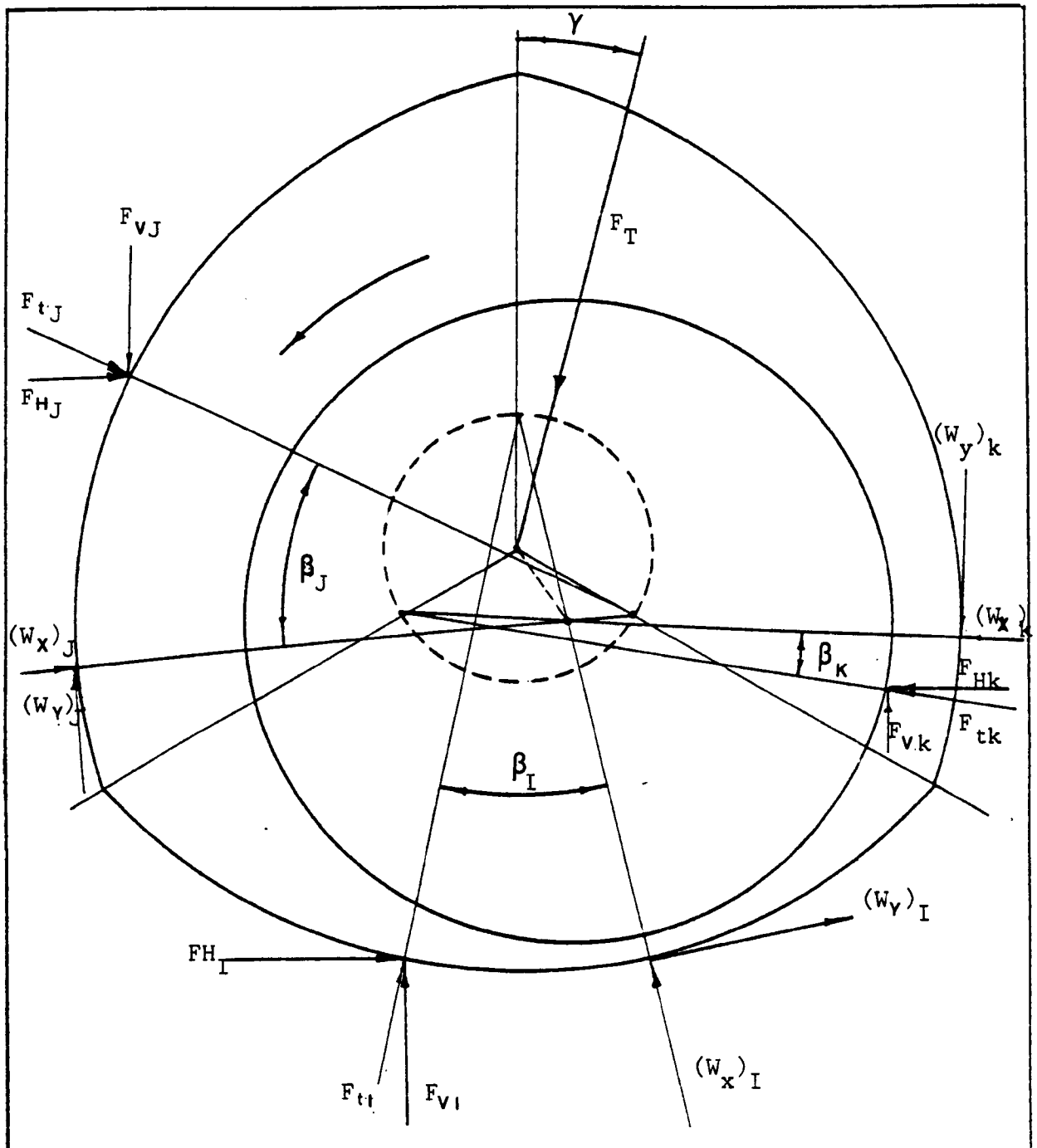

$$(F_H)_t = F_{HI} + F_{HJ} + F_{HK}$$

$$(F_V)_t = F_{VI} + F_{VJ} + F_{VK}$$

FIG.3.6 Hydrodynamic forces relationship.

and the resultant force is given by

$$(F_t^*)_{I.J.K} = \left\{(W_x)^2 + (W_y)^2\right\}^{\frac{1}{2}} \qquad (3.15)$$

and the angle between the direction of the force and the displacement is given by

$$\beta_{I,J,K} = \sin^{-1} (W_y/F_t)_{I,J,K} \qquad (3.16)$$

The force (F_t) is then decomposed into a horizontal and into a vertical force at each lobe. The total force is then given from:

$$F_T^* = (F_{Vt}^* + F_{Ht}^*)^{\frac{1}{2}} \qquad (3.17)$$

and the angle between the vertical direction and the direction of the total force is given by

$$\gamma = \tan^{-1} (- F_{Ht}^*/F_{Vt}^*) \qquad (3.18)$$

where $\vec{F}_{Vt} = F_{VI} + F_{Vj} + F_{Vk}$ and $\vec{F}_{Ht} = F_{HI} + \vec{F}_{HJ} + F_{HK}$

The bearing duty parameter is given by:

$$S = \frac{1}{F_T^*} \qquad (3.19)$$

Where $S = \frac{\mu N}{P} (D/C)^2$ and $P = F_T/LD$

3.4 Stiffness

For a steady state running condition the lubricant film stiffness in the radial direction will be defined by

$$\lambda = \frac{dF_R}{dh_{min}} = \frac{dF_T \cos\Phi}{dh_{min}} \tag{3.20}$$

since

$$F_T = \frac{\mu DLN}{S} (D/C)^2 \tag{3.21}$$

and

$$h_{min} = C/2(1-\varepsilon) \tag{3.22}$$

$$\lambda = \frac{2\mu DLN}{C} (D/C)^2 \frac{d(\frac{\cos\phi}{S})}{d\varepsilon} \tag{3.23}$$

and the stiffness coefficient is given by

$$\lambda^{\wedge} = \frac{\lambda}{2\mu DLN/(D/C)^2} = \frac{d(\frac{\cos\phi}{S})}{d\varepsilon} \tag{3.24}$$

where $\varepsilon = \varepsilon_B(1 - \varepsilon_o)$

The stiffness coefficient has been calculated from the numerical solution of Reynolds equation. A typical calculation of the stiffness coefficient for the three lobe bearing is given in Figure 3.15. The calculations have been carried up to eccentricity ratios larger than those appropriate in practical use of the bearing, and with reference to the functional specifications of the three lobe bearing, the maximum eccentricity ratio (ε_B) would be 0.17 (the eccentricity ratio is calculated for a lobe clearance of 2.6×10^{-4}m).

3.5 Oil Flow

The oil flow fed to a bearing serves a dual purpose. Whilst its primary functions is to act as a lubricant in the creation of a load carrying film, it is also called upon to carry away the heat generated in the bearing. As a consequence, the rate of flow of oil through a bearing is an important consideration in bearing design and operation, and has to be known so that the oil system can be designed.

Oil is normally supplied to the inlet grooves under pressure, and with the journal stationary there would be a flow of oil through the clearances of the bearing. This kind of flow will be called the pressure flow. There would be also a flow of oil if oil were supplied at zero pressure, and the journal is rotating. This flow is due to the pumping action of the moving surface, and must also escape axially from the bearing. This flow will be called the hydrodynamic flow. The total oil flow will be regarded as the sum of the pressure flow (Poiseuille flow) and the hydrodynamic flow (Couette flow).

In the description of the finite difference technique in paragraph 3.2. it was mentioned that the pressures around the boundary of the film do not have to be zero but may be finite. The finite difference method may be used to calculate the hydrodynamic oil flow by inserting zero dimensionless pressure along the boundary which is the boundary of the axial oil inlet grooves. Also the finite difference method may be used to calculate the total oil flow (i.e. hydrodynamic oil flow and pressure oil flow) by inserting the pressure of the inlet oil along the boundary of the axial grooves. The oil inlet pressure in dimensionless

form is given by

$$P^* = P/_{\mu N} \, (C/_D)^2 \tag{3.25}$$

where P: is the oil pressure at the inlet (Figure 3.7).

From this point of view the total side-leakage oil flow or the hydrodynamic oil flow from one lobe and from both the bearing ends is given by

$$Q_{t,h} = 2 \int \frac{1}{12\mu} h^3 \frac{\partial P}{\partial z} dx \tag{3.26}$$

where $\frac{dp}{dz}$ is axial pressure gradient at the ends of the bearing. The above expression may be used for the calculation of the total oil flow or for the hydrodynamic oil only. Subscript t denotes the total oil flow (i.e. $P^* \neq 0$) whereas subscript h denotes the hydrodynamic oil flow (i.e. $P^* = 0$).

It is convenient to express the oil flow in terms of a dimensionless flow coefficient which relates the oil flow to the Petroff oil flow i.e.

$$Q_{t,h} = q. \frac{\Pi}{4}. N.D.L.C. \tag{3.27}$$

By equating equation (3.26) and (3.27), the oil flow coefficient is given by

$$\left(q_{t,h}\right)_{I.J.K} = \frac{2}{3\Pi} \cdot \frac{1}{NDLC} \int \frac{1}{\mu} h^3 \frac{\partial P}{\partial z} dx \tag{3.28}$$

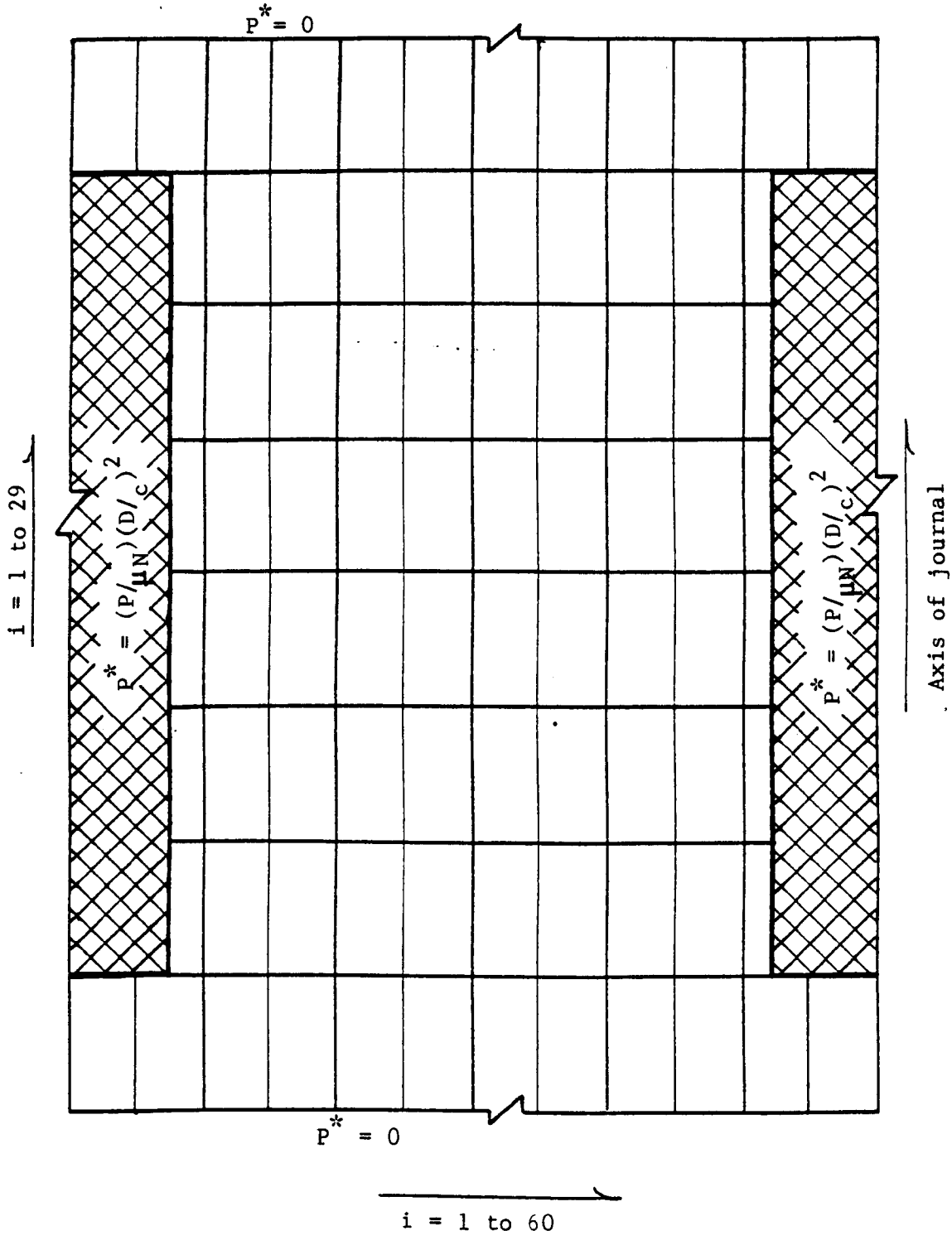

FIG.3.7 Boundary conditions for the calculation of the total oil flow.

After substituting dimensionless forms for $\frac{\partial P}{\partial z}$, h^3, μ and dx and after rearranging the oil flow coefficient is given by

$$(q_{t,h})_{I,J,K} = \frac{2}{3\Pi} \cdot (D/L)^2 \int H^{*3} \frac{\partial P^*}{\partial z^*} \cdot dx^*. \qquad (3.29)$$

In numerical form equation (3.29) becomes

$$(q_{t,h})_{I.J.K} = (2/3\Pi)\ (D/L)^2 \sum_{i=1}^{n+1} H^*_{m,i} \left(\frac{P_{m-1,j} - P_{m+1,j}}{2.\Delta Z}\right)^* \Delta X^*. \qquad (3.30)$$

The calculation of $q_{t,h}$ from expression (3.30) depends upon a prior solution of Reynolds equation (3.7) to give the pressure distribution over the complete bearing. The calculations of $q_{t,h}$ is incorporated in the same computer programme. The term 'solution of Reynolds equation' will denote the calculation of the pressure distribution, and the oil flow coefficient by the finite difference procedure.

The dimensionless flow coefficient $(q_{t,h})$ has been calculated separately for each lobe and have been summed to give the oil flow coefficient of the complete bearing which may be expressed as

$$q_{o(t,h)} = \sum_{I,J,K} (q_{t,h}) \qquad (3.31)$$

Reynolds equation has been solved for inlet pressures (P*) of 0,0.5, 1,2,3 and 5. Typical results of calculation are shown in Figure 3.8. At P* = o, the calculated flowcoefficient is the hydrodynamic flow coefficient $(q_o)_h$ and where P* $\neq$ 0, the calculated flow coefficient

is the total flow coefficient $(q_o)_t$, which comprises the hydrodynamic flow coefficient and the pressure flow coefficient $(q_o)_p$. It may be seen from Figure 3.8 that the pressure flow coefficient varies linearly with the dimensionless inlet pressure, and consequently, in general for any value of ε_B (or duty parameter) it is necesssary only to solve Reynolds equation for two values of P*. Also it may be seen that at higher values of offset ratio the pressure flow coefficient is increasing marginally as the dimensionless inlet pressure increases. The notion was proposed at the start of this paragraph that the pressure flow depends only upon the inlet pressure and the bearing clearance, and clearly Figure 3.8 is consistent with that notion. An alternative way for the calculation of the pressure flow is considered below.

It would appear from Figure 3.8 that at low offset ratios the pressure flow is in general substantially greater than the hydrodynamic flow, however with normal values of inlet pressure, viscosity, clearance and speed the value of the dimensionless inlet pressure does not rise above a value of two in practice. The results of the oil flow coefficient calculations have been used to calculate the actual oil flow, the power loss and the temperature rise. Typical results of calculations are listed in Table 3.1 where it may be seen that the dimensionless inlet pressure decreases as the speed and the eccentricity ratio increase.

A second way in which total oil flows can be assessed is to calculate the pressure flow from the solution of Reynolds equation when the shaft is stationary. For a stationary shaft Reynolds equation reduces

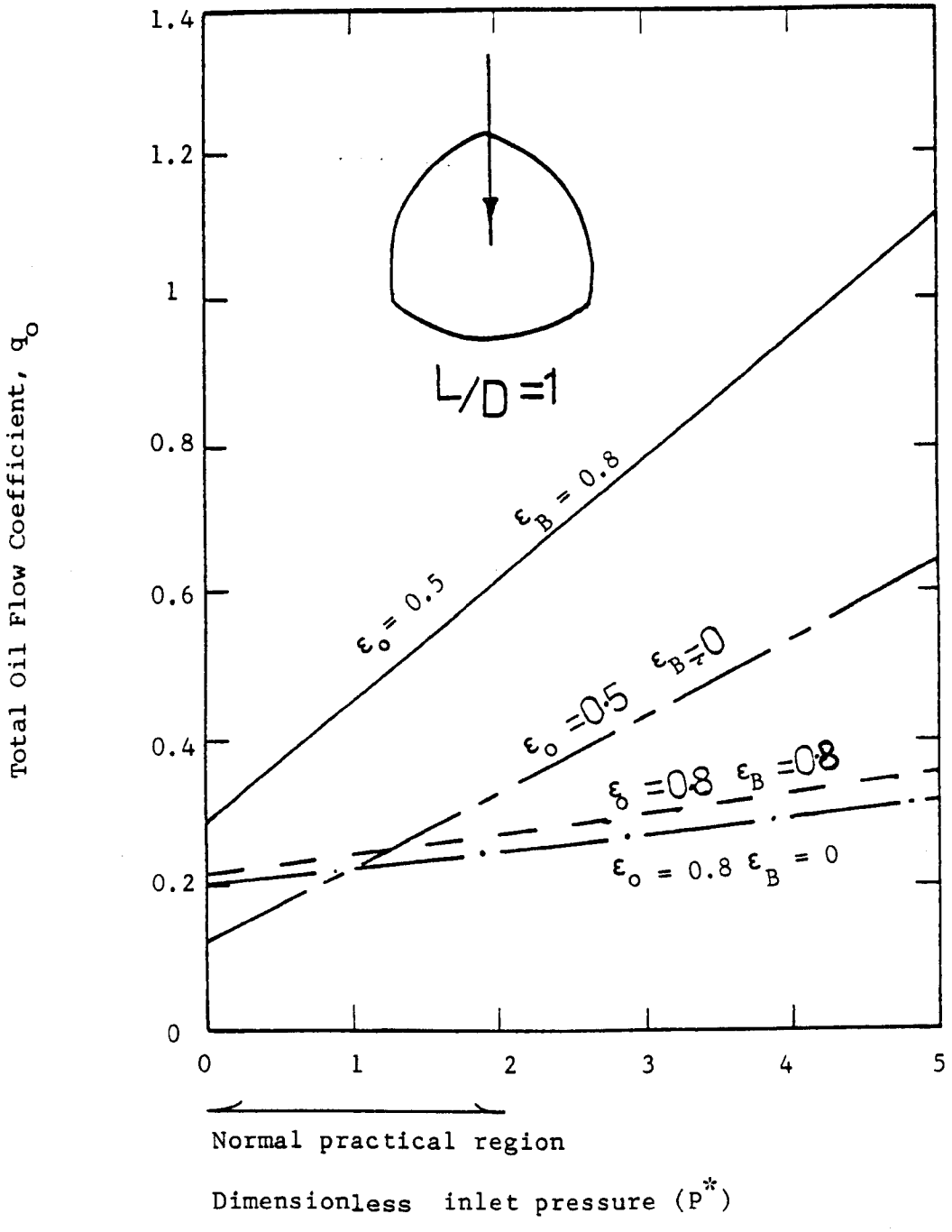

FIG.3.8 Variation of the total oil flow coefficient with the inlet dimensionless pressure.

TABLE 3.1 Power loss, oil flow, temperature rise and dimensionless inlet pressure for the three-lobe Journal bearing.

$L = 1.27 \times 10^{-1}$ m $D = 1.35 \times 10^{-1}$ m $C = 3 \times 10^{-4}$ m

$\varepsilon_o = 0.4$ $T_1 = 40^{\circ}$ C $P = 1.47 \times 10^{5}$ Nm^{-2}

$\mu = 33$ C.P. at 40° C

$\varepsilon_B = 0$

N rpm	Q_h $l\ s^{-1}$	Q_p $l\ s^{-1}$	Q_t $l\ s^{-1}$	H_s kw	T_2 ^{o}C	$P^* = \frac{P}{\mu N}(C/D)^2$
1000	0.0066	0.0214	0.028	0.49	51	2.06
3000	0.0198	0.0382	0.058	2.48	65	1.14
5000	0.033	0.0525	0.855	5	74	0.9
7000	0.0462	0.0658	0.112	7.86	79.5	0.737
9000	0.0594	0.0796	0.139	10.77	84	0.64

$\varepsilon_B = 0.6$

N rpm	Q_h $l\ s^{-1}$	Q_p $l\ s^{-1}$	Q_t $l\ s^{-1}$	H_s kw	T_2 ^{o}C	$P^* = \frac{P}{\mu N}(C/D)^2$
1000	0.016	0.0265	0.0425	0.56	48.5	1.87
3000	0.048	0.0438	0.0918	3.06	60	0.97
5000	0.080	0.0587	0.1387	6.34	67	0.71
7000	0.112	0.069	0.181	10.5	73	0.615
9000	0.144	0.0820	0.226	14.72	77	0.524

to the form

$$\frac{\partial}{\partial x}\left(h^3 \frac{\partial P}{\partial X}\right) + \frac{\partial}{\partial z}\left(h^3 \frac{\partial P}{\partial z}\right) = 0 \qquad (3.32)$$

The solution of equation(3.32) is also required in connection with the hydrostatic aspect of the bearing, and this solution is discussed in Chapter 5. Here it is sufficient to note that the pressure flow coefficient is given by

$$(q_p)_{I,J \text{ and } K} = \int h^3 \frac{\partial P}{\partial z}\, dx \qquad (3.33)$$

The dimensionless pressure flow coefficient has been calculated separately for each lobe and have been summed to give the oil flow coefficient of the complete bearing which may be expressed as

$$q_{op} = \sum_{I,J \text{ and } K} q_p \qquad (3.34)$$

and the pressure flow is calculated from

$$Q_p = \frac{P\, C^3 q_{op}}{6\mu} \qquad (3.35)$$

In expression(3.33) the axial pressure gradient at the end of the bearing denoted by $\frac{dP}{dz}$, is actually calculated from the solution of equation(3.32).

The pressure flow was measured experimentally, simply by collecting the oil flow out of the bearing when the shaft is stationary. In such tests the only thing which can vary is oil viscosity and from

expression (3.35) one would expect $Q_p x \mu$ to be constant. The experiment gave a value of $Q_p x \mu$ of 8.36 dyne cm whereas the calculated value is 9.24. The two results are in close agreement. However, the pressure flow as measured or calculated in the context of a stationary shaft is not necessarily the pressure flow which will arise when the shaft is rotating, because the temperature is then influenced additionally by the rotation of the shaft. It was found that if the pressure flow with a rotating shaft is based upon oil outlet temperature then the calculation leads to a pressure flow somewhat in excess of the pressure flow as derived by subtracting the calculated hydrodynamic flow from the calculated total oil flow or from the measured total flow. For instance at a speed of 6000 rpm, the calculated total oil flow is $0.1151 s^{-1}$, the calculated hydrodynamic oil flow is $0.0381 s^{-1}$, which gives a pressure flow of $0.0771 s^{-1}$. The measured total oil flow was $0.1061 s^{-1}$ which gives a pressure flow of $0.0681 s^{-1}$, while the calculated pressure flow from expressure (3.35) is $0.1281 s^{-1}$. The trend shown by the results is to be expected because clearly the mean oil temperature to be associated with the pressure flow is somewhere between inlet and outlet temperatures. It has been found from the experimental tests which are reported in Chapter 6, that agreement between the calculated pressure flows and the experimentally derived pressure flows is obtained by taking a mean temperature given by

$$T_m = T_1 + (T_2 - T_1) \times 0.65 \qquad (3.36)$$

Semi empirical expressions are frequently used for the calculation of the pressure flow, e.g. Ref 11 and Ref 70 give the following

expressions for the calculations of the pressure oil flow.

$$Q_p = \frac{C^3 PDM}{96\mu L}\left(q^*_{o,g} + \frac{46}{D(1-\ell/_L)}\right) \qquad \text{(ref: 11)}$$

$$Q_p = \frac{PC^3V}{24\mu} \qquad \text{(ref: 70)}$$

The first expression was modified to take into account the presence of the three axial grooves and also to take into account the change in the oil film thickness within each lobe. In Ref. 11 it has been pointed out that it is often difficult to give precise values to the viscosity when the bearing is hot, but a thermocouple placed at the inlet manifold and not in the bearing spill should give tolerable accuracy. However, a viscosity associated with the mean temperature given by equation (3.36) has been used in the semi-empirical formula for the calculation of the pressure flow.

Quite clearly there are several ways of dealing with the pressure flow and the results given by the various methods in one particular instance are listed in Table 3.2. In that table line A gives the calculated hydrodynamic oil flow, line B gives the calculated total oil flow and line C is pressure flow. Line D gives the pressure flow as calculated with a stationary shaft and using the mean oil temperature given by expression(3.36) while line F gives the pressure flow by using the oil outlet temperature. Line E gives the total oil flow as implied by lines A and D. Line G gives the pressure flow as calculated from semi-empirical expression (Ref. 11) and by using the mean oil temperature given by expression(3.36) while line H gives the

TABLE 3.2 Calculated oil flow for the three lobe Journal bearing*

Line	Type of Flow	Origin	Oil Flow $l\ s^{-1}$
A	Hydrodynamic flow	Eqn.3.27	0.038
B	Total oil flow	Eqn.3.27	0.115
C	Pressure flow	B-A	0.077
D	Pressure flow	Eqns.3.35-3.36	0.0735
E	Total oil flow	A+D	0.1115
F	Pressure flow	Eqn.3.35	0.128
G	Pressure flow**	Refll +eqn.3.36	0.060
H	Total oil flow	A+G	0.098
I	Measured flow	Chapter 6	0.106

*N = 6000 rpm $T_1 = 40^{\circ}$ C

$D = 1.35 \times 10^{-1}$ m $L = 1.27 \times 10^{-1}$ m $l = 1.07 \times 10^{-1}$ m

$b = 0.0353$ m $P = 1.47 \times 10^{5}$ Nm^{-2} $C = 3.25 \times 10^{-4}$ m

$\varepsilon_B = 0$ $\Delta r = 5.85 \times 10^{-5}$ m $\varepsilon_o = 0.35$ $\alpha = 30^{\circ}$

μ = 33 C.P. at 40°C

**The expression given in ref. 11 has been adapted to be used for the three lobe bearing.

total oil flow as implied by lines A and G. Line I gives the measured total oil flow. It may be seen from the table that the same result is obtained whether the total oil flow is calculated directly as in line B or is obtained by summing the hydrodynamic and pressure flows as in line E provided that the mean temperature is used in calculating the latter. It may also be seen that the pressure flow given by the modified semi-empirical expression is in substantial agreement with the other calculated pressure flows.* The calculated total oil flow given by line B and line E are greater than the total measured oil flow by approximately 8.5% which gives a reasonable tolerance for the design of the oil system. However, by using the previous methods for the calculations of the oil flow to calculate the power loss and the oil temperature rise, a very close agreement between the calculated and the measured (Chapter 6) power loss and oil temperature is achieved.

The question arises, which is the preferred method for calculating total oil flow. Because of its simplicity of conception the one step method of equation(3.27) is preferred. It is of interest to compare the pressure distribution given by this one step method with the pressure distribution given when the hydrodynamic flow alone is considered (eqn. 3.7). The comparison is shown in Figure 3.9 which shows that both calculations place the peak pressure in the same position but at a typical eccentricity ratio of 0.4, the peak pressure for the total calculation is slightly higher than that for the hydrodynamic flow alone.

3.6 Results of the Numerical Computations

The validity of the computer programme and its accuracy has been

*Line F gives a pressure flow $>$ the total oil flow

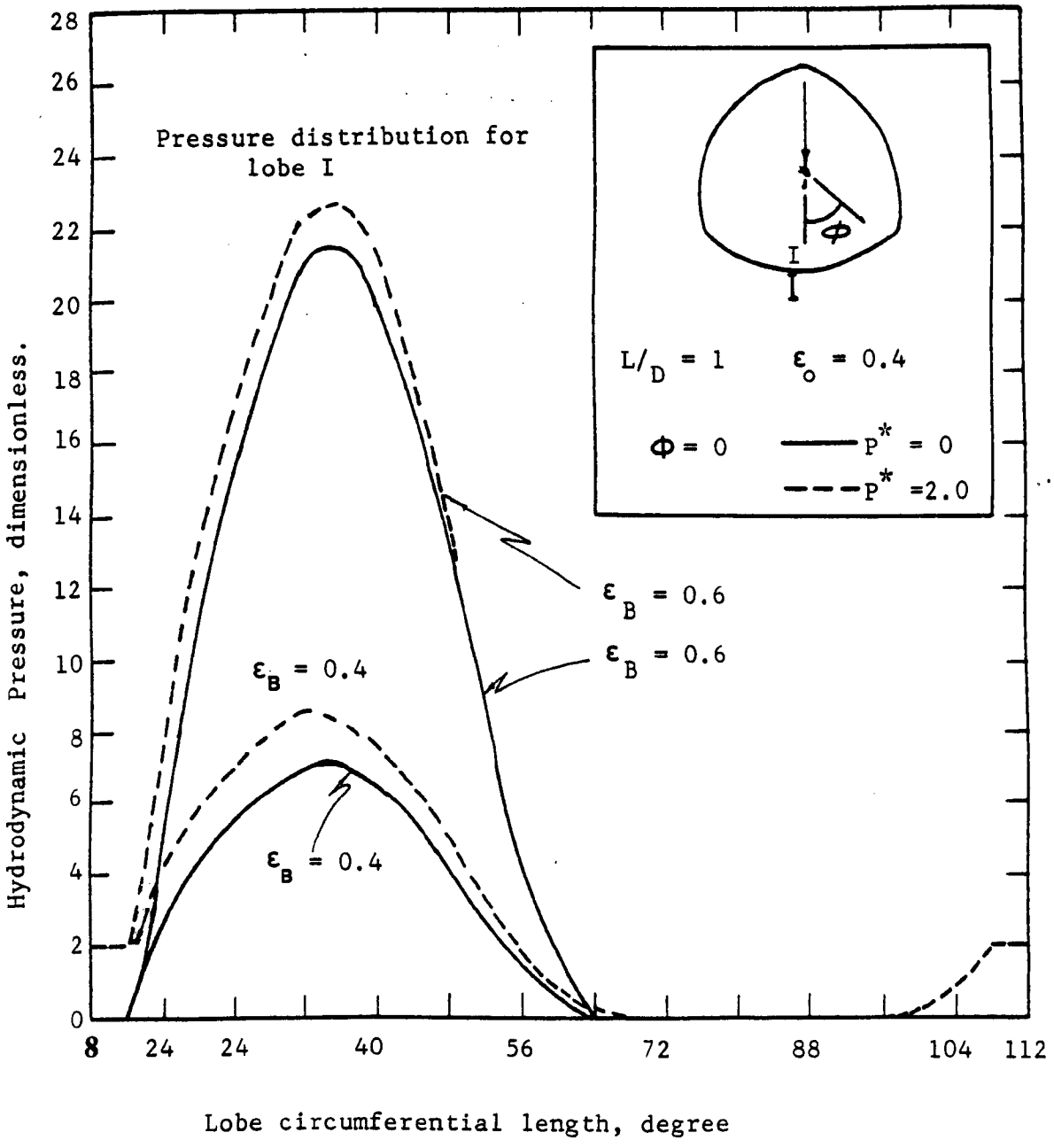

FIG.3.9 Pressure distribution at the axial mid-plane.

examined by using the computer programme to solve Reynolds equation for a journal bearing of full circular bore. Table 3.3 compares the result of the present programme with results previously published in Refs.1,2, and very close agreement is obtained. Also it has been pointed out that the solution of Reynolds equation for the pressure distribution was carried over the full mesh and the symmetry of the pressure distribution around the bearing centre can be used as a check upon calculation. In Figure 3.10 a complete output for the pressure distribution is given and it may be seen that the pressure is symmetrical around the bearing axial mid-plane. As a further check upon the accuracy of the computer programme, Figure 3.11 shows the pressure distribution at the axial mid-plane. It may be seen that the pressure film is terminated beyond the position of the minimum film thickness. Also it may be seen from Figure 3.11 that the condition of zero pressure and zero pressure gradient at the trailing edge has been satisfied in the solution. The computer routine has written in Fortran VI language and it has been performed on the I.C.I. 1900 Computer, and on the C.D.C.7600 computer.

All of the input and the output of the finite difference programme is in dimensionless form. The output comprises the load angle γ , the attitude angle ϕ, duty parameter, the hydrodynamic oil flow coefficient, the pressure oil flow coefficient, the total oil flow coefficient and the dimensionless pressure at the mesh points.

The computer programme was performed for the following values of the variables

ε_o: 0.3, 0.4, 0.5,....., and 0.8.

ε_B: 0, 0.1, 0.2,....., and 0.9.

TABLE 3.3 Comparison of the present computer programme with those of references 1—2 for the 360° degree Journal bearing.

$L_{/D}$	ε	Present Computer Programme						Refs. 1 – 2					
		$P_{max/P}$	γ	α	Φ	S	q_h	$P_{/Pmax}$	γ	α	Φ	S	q_h
$1_{/2}$	0.2	2.04	12	18	75.16	2.18	0.352	1.97	11.9	17.5	74.9	2.03	0.376
	0.4	2.31	17.5	18	61.76	0.84	0.71	2.27	16.9	17.5	61.5	0.779	0.75
	0.6	2.8	18	16	48	0.34	1.06	2,74	17.1	17	48.1	0.319	1.12
	0.8	3.76	15	12	32.86	0.097	1.415	3.67	15.3	11	33.3	0.0923	1.455
1	0.2	1.943	10	32	73.95	0.671	0.3	1.89	9.2	32	74.0	0.631	0.316
	0.4	2.13	18	28	62.6	0.276	0.595	2.07	16.5	28	63.1	0.264	0.595
	0.6	2.48	18	24	50.5	0.128	0.883	2.40	18.2	22	50.6	0.121	0.938
	0.8	3.23	20	16	36	0.047	1.17	3.17	18.2	16	36.2	0.0446	1.24
$1\frac{1}{2}$	0.2	1.88	10	40	72.4	0.388	0.245	--	-	-	-	-	-

TABLE 3.3 Contd.

L/D	ϵ	Present Computer Programme					
		$P_{max/P}$	γ	α	Φ	S	q_h
$1\frac{1}{2}$	0.4	2.02	16	36	62.7	0.168	0.475
	0.6	2.31	20	28	52.0	0.085	0.70
	0.8	2.94	22	21	38	0.0355	0.9

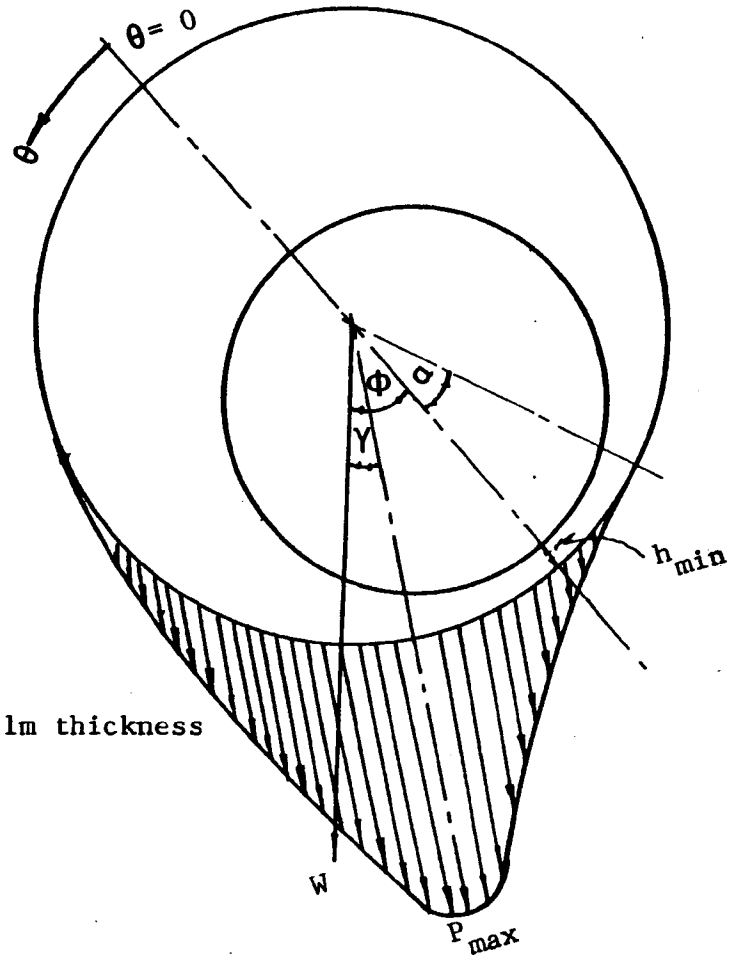

P_{max} : is the peak pressure on the bearing mid-plane = P^* N $(D/C)^2$

P ; total load/unit projected area, W/LD= $N(D/C)^2 \cdot \frac{1}{S}$

$Pmax_{/P}$ = P^* . S

γ : Angular distance of peak pressure beyond the load time

α : Angular distance of zero pressure beyond the position of minimum oil film thickness

Φ: Attitude angle

S : Duty parameter

q_h : Hydrodynamic flow coefficient

EPS	MAXIT	EB	L	D	M	ELIPIT
.00010	100	.6000	2	2.000	50	.500

THE OVER RELAXATION FACTOR OMEGA = 1.7736

THE BEARING ATTITUDE ANGLE ALPHA = .959444

E	EL1	EL2	EL3	ALPHA1	ALPHA2	ALPHA3	THETA1	THETA2
.3000	.7157	.2028	.6833	20.088	112.593	96.548	70.086	

DY = .0348888 DX = .03488889

CYCLE NUMBER ITN = 53

	11	12	13	14	15	16	17	18	19	
	0	0	0	0	0	0	0	0	0	
	7.31084	7.46896	7.55707	7.61547	7.63467	7.61548	7.55709	7.45699	7.31088	1
	15.68528	16.02479	16.25788	16.39406	16.43885	16.39408	16.25792	16.02484	15.68535	7
	23.81202	24.34820	24.71728	24.93327	25.00438	24.93330	24.71733	24.34827	23.81211	13
	27.93970	28.59386	29.04568	29.31068	29.39805	29.31071	29.04571	28.59393	27.93978	19
	23.08740	23.98545	24.10080	24.34531	24.42605	24.34534	24.10083	23.68550	23.08745	25
	10.42438	10.76631	11.03981	11.18984	11.23951	11.18985	11.03982	10.78633	10.42440	31
	.83676	.91663	.97303	1.00658	1.01769	1.00658	.97303	.91683	.83676	37
	0	0	0	0	0	0	0	0	0	43
										49

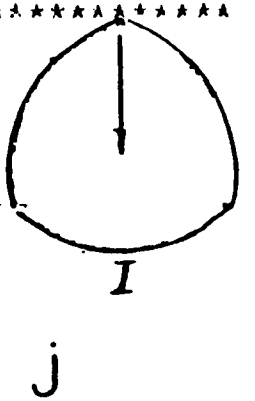

Figure 3.10 Pressure distribution Map for the Bottom to be (I).

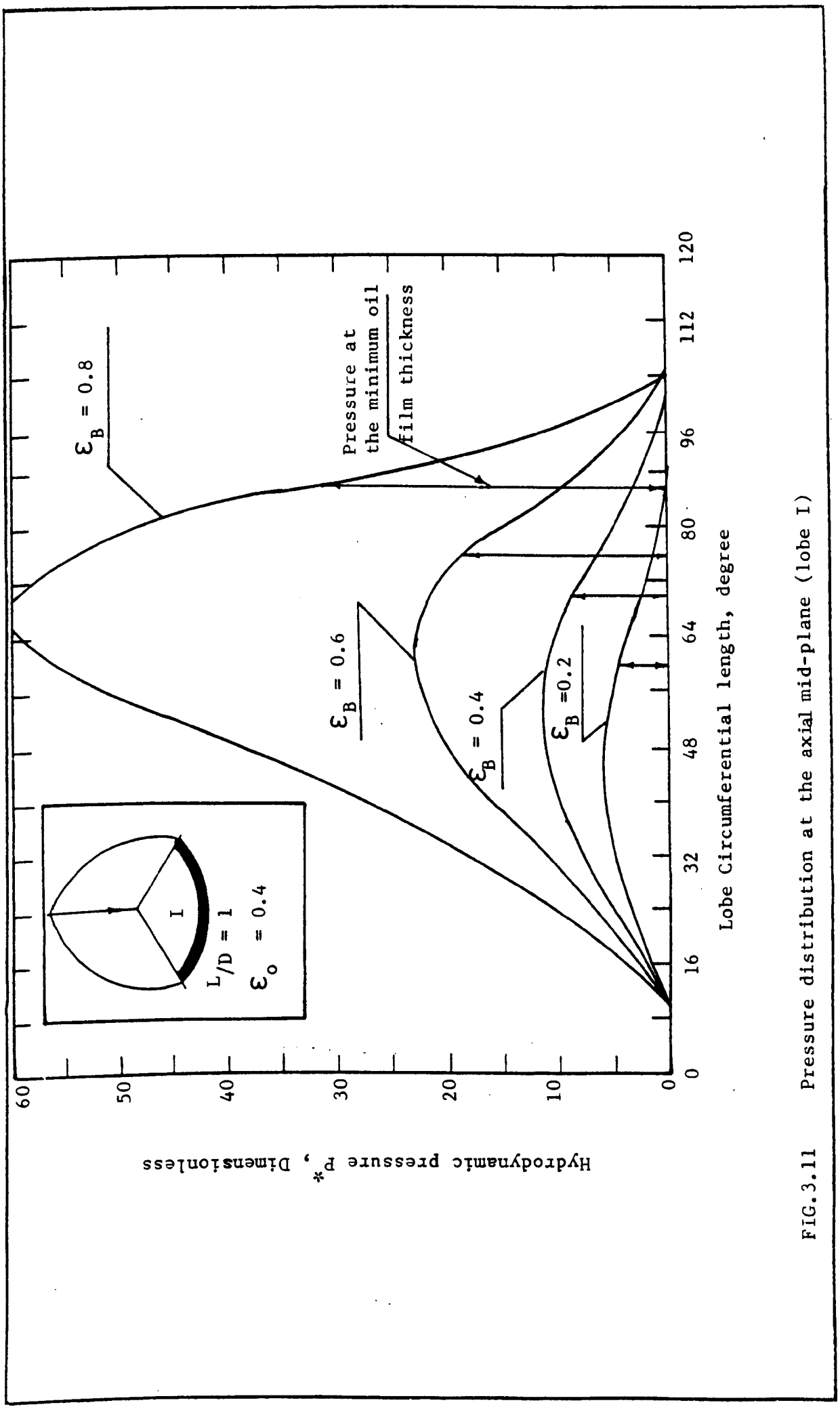

FIG.3.11 Pressure distribution at the axial mid-plane (lobe I)

P*: 0, 1, 2 and 5.

The results of calculation are presented in Tables 3.4 - 3.8. Table 3.4 relates to a load acting towards the centre of a lobe, and Table 3.5 relates to a load acting towards a conjunction of adjacent lobes. Tables 3.6 and 3.7 relate to calculation in which a finite pressure has been entered at the oil inlets. Journal position is given by Table 3.6 and the total oil flow coefficient for axial grooves of 30 degree width are given in Table 3.7. In Table 3.8 pressure flow coefficients as calculated from expression(3.32) are given.

Typical results from Tables 3.4 - 3.5 will be discussed and compared with available results for other bearing designs. Figure 3.12 shows the variation of the hydrodynamic flow coefficient with the eccentricity ratio. It may be seen from Figure 3.12, at high values of eccentricity the hydrodynamic flow coefficient decreases as the offset ratio increases, however in real terms the increase of the offset ratio leads to an increase in the lobe diametral clearance and it will be shown in paragraph 3.9 that the actual hydrodynamic flow increases as the offset ratio increases. It may also be seen from Figure 3.12 that at low values of eccentricity the flow coefficient increases as the offset ratio increases. This trend in the characteristics of the hydrodynamic flow coefficient is attributable to the finite lobe eccentricity which exist at zero bearing eccentricity. As the offset ratio reaches zero (i.e. full circular bore with three groove bearing) the hydrodynamic action is diminished and the hydrodynamic flow coefficient becomes zero.* Another important factor in the hydrodynamic

*the flow coefficient relates to the axial flow and in this instance no pressures are developed, and in principal there is no axial flow.

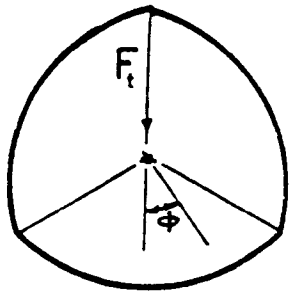

Table 3.4. Results of Computation for* the three-lobe bearings

ε_o	L/D	ε_B	Φ	S	q_h
0.8	½	0.1	30	0.4	0.328
		0.2	32	0.2	0.328
		0.3	35	0.129	0.3285
		0.4	38	0.091	0.33
		0.5	38	0.0625	0.33
		0.6	38	0.0454	0.332
		0.7	40	0.0345	0.333
		0.8	42	0.0263	0.334
		0.9	42	0.0172	0.335
	1	0.1	30	0.286	0.16
		0.2	33	0.139	0.161
		0.3	35	0.088	0.161
		0.4	37	0.0625	0.161
		0.5	40	0.0454	0.162
		0.6	40	0.033	0.162
		0.7	41	0.025	0.163
		0.8	42	0.0189	0.164
		0.9	42	0.015	0.1645

* Vertical Load

Table 3.4. continued Results of Computation for the Three-lobe Journal Bearings

ε_o	L/D	ε_B	Φ	S	q_h
0.7	½	0.1	40	0.884	0.305
		0.2	42	0.426	0.306
		0.3	42	0.27	0.308
		0.4	45	0.188	0.312
		0.5	45	0.134	0.316
		0.6	46	0.096	0.32
		0.7	47	0.071	0.336
		0.8	47	0.0476	0.33
		0.9	46	0.03	0.337
	1	0.1	42	0.556	0.152
		0.2	44	0.263	0.154
		0.3	45	0.168	0.155
		0.4	47	0.118	0.157
		0.5	47	0.087	0.159
		0.6	47	0.0625	0.162
		0.7	47	0.0454	0.164
		0.8	47	0.033	0.166
		0.9	45	0.02	0.172
0.6	½	0.1	43	1.37	0.272
		0.2	50	0.65	0.276
		0.3	51	0.4	0.282
		0.4	51	0.26	0.29
		0.5	52	0.203	0.3
		0.6	52	0.167	0.31
		0.7	51	0.1124	0.32
		0.8	50	0.066	0.334
		0.9	47	0.037	0.353

Table 3.4 continued Results of Computation for the Three-lobe Journal Bearings.

ε_o	L/D	ε_B	Φ	S	q_h
0.6	1	0.1	50	0.76	0.139
		0.2	52	0.36	0.142
		0.3	53	0.22	0.145
		0.4	53	0.16	0.15
		0.5	53	0.112	0.154
		0.6	52	0.0855	0.16
		0.7	51	0.069	0.166
		0.8	50	0.0417	0.173
		0.9	45	0.022	0.191
0.5	½	0.1	57	2.04	0.235
		0.2	58	0.995	0.240
		0.3	59	0.62	0.253
		0.4	58	0.425	0.268
		0.5	58	0.298	0.283
		0.6	57	0.204	0.310
		0.7	55	0.137	0.323
		0.8	53	0.095	0.357
		0.9	45	0.048	0.415
	1	0.1	55	1.11	0.122
		0.2	55	0.502	0.127
		0.3	60	0.323	0.134
		0.4	60	0.22	0.143
		0.5	55	0.156	0.152
		0.6	55	0.112	0.162
		0.7	55	0.076	0.173
		0.8	53	0.056	0.193
		0.9	45	0.0255	0.22

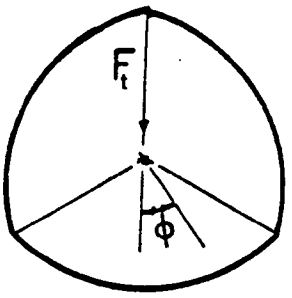

Table 3.4 continued Results of Computation for the Three-lobe Journal Bearings.

ε_o	L/D	ε_B	Φ	S	q_h
0.4	½	0.1	65	2.89	0.195
		0.2	66	1.34	0.208
		0.3	65	0.85	0.226
		0.4	64	0.544	0.243
		0.5	61	0.38	0.276
		0.6	58	0.258	0.306
		0.7	55	0.168	0.354
		0.8	50	0.109	0.414
		0.9	35	0.037	0.505
	1	0.1	63	1.445	0.103
		0.2	63	0.683	0.11
		0.3	60	0.425	0.115
		0.4	60	0.268	0.138
		0.5	60	0.187	0.153
		0.6	59	0.131	0.17
		0.7	55	0.085	0.197
		0.8	50	0.051	0.23
		0.9	37	0.028	0.273

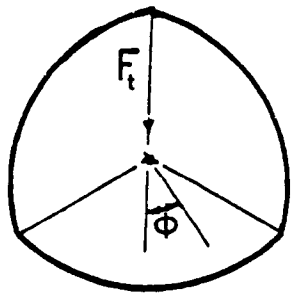

Table 3.4 continued Results of Computation for the Three-lobe Journal Bearings.

ξ_o	L/D	ξ_B	Φ	S	q_h
0.3	½	0.1	73	3.76	0.154
		0.2	70	1.7	0.177
		0.3	70	1.063	0.214
		0.4	65	0.655	0.244
		0.5	62	0.48	0.30
		0.6	58	0.356	0.361
		0.7	50	0.20	0.43
		0.8	47	0.111	0.50
		0.9	34	0.039	0.574
	1	0.1	73	1.81	0.083
		0.2	70	0.855	0.099
		0.3	70	0.48	0.12
		0.4	64	0.31	0.14
		0.5	60	0.25	0.174
		0.6	54	0.161	0.215
		0.7	50	0.104	0.244
		0.8	42	0.059	0.290
		0.9	35	0.025	0.321

Table 3.5 Results of Computation for the Three Lobe Journal Bearing*

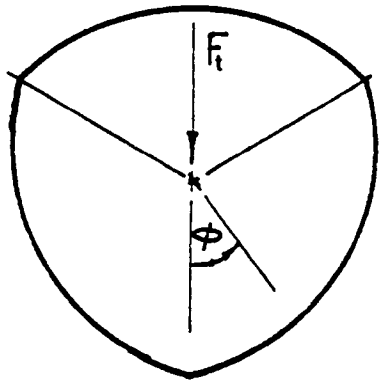

ε_o	L/D	ε_B	ϕ	s	q_h
0.8	$\frac{1}{2}$	0.1	25	0.455	0.327
		0.2	22	0.23	0.328
		0.3	20	0.149	0.329
	1	0.1	27	0.303	0.161
		0.2	25	0.15	0.161
		0.3	22	0.10	0.161
		0.4	20	0.073	0.161
0.7	$\frac{1}{2}$	0.1	35	0.91	0.304
		0.2	30	0.455	0.305
		0.3	27	0.294	0.308
		0.4	24	0.208	0.312
		0.5	22	0.16	0.317
		0.6	18	0.125	0.322
	1	0.1	37	0.568	0.153
		0.2	34	0.28	0.154
		0.3	31	0.184	0.155
		0.4	27	0.132	0.158
		0.5	25	0.1	0.16
0.6	$\frac{1}{2}$	0.1	43	1.36	0.272
		0.2	40	0.654	0.276
		0.3	35	0.425	0.283
		0.4	32	0.293	0.293
		0.5	28	0.218	0.305

* The results which are listed in this table are obtained from the solution of Reynolds equation (3.7) for zero dimensionless pressure at the axial grooves.

Table 3.5 cont. Results of Computation for the Three Lobe Journal Bearing

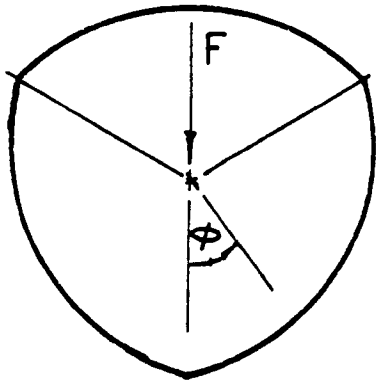

ε_o	L/D	ε_B	ϕ	s	q_h
0.6	$\frac{1}{2}$	0.6	25	0.157	0.319
		0.7	22	0.113	0.33
	1	0.1	47	0.78	0.139
		0.2	44	0.38	0.142
		0.3	40	0.29	0.147
		0.4	37	0.20	0.153
		0.5	33	0.15	0.16
		0.6	29	0.09	0.17
		0.7	25	0.069	0.18
		0.8	22	0.05	0.186
		0.9	18	0.035	0.191
0.5	$\frac{1}{2}$	0.1	57	2.07	0.235
		0.2	49	1.03	0.245
		0.3	44	0.644	0.262
		0.4	40	0.44	0.284
		0.5	35	0.315	0.311
		0.6	31	0.217	0.34
		0.7	27	0.155	0.37
		0.8	22	0.103	0.411
	1	0.1	57	1.15	0.122
		0.2	52	0.56	0.129
		0.3	50	0.35	0.14
		0.4	45	0.244	0.157
		0.5	40	0.175	0.176

Table 3.5 cont. Results of Computation for the Three Lobe Journal Bearing

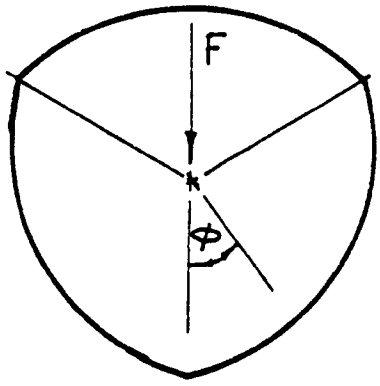

ε_o	L/D	ε_B	ϕ	s	q_h
0.5	1	0.6	36	0.125	0.191
		0.7	31	0.09	0.215
		0.8	26	0.06	0.22
		0.9	22	0.04	0.244
0.4	$\frac{1}{2}$	0.1	62	2.98	0.196
		0.2	57	1.44	0.215
		0.3	52	0.9	0.25
		0.4	46	0.61	0.30
		0.5	42	0.425	0.354
		0.6	36	0.283	0.41
		0.7	32	0.20	0.446
		0.8	26	0.121	0.488
		0.9	21	0.074	0.524
	1	0.1	65	1.58	0.104
		0.2	62	0.766	0.118
		0.3	57	0.476	0.142
		0.4	52	0.327	0.173
		0.5	47	0.23	0.203
		0.6	42	0.165	0.239
		0.7	36	0.114	0.269
		0.8	28	0.081	0.295
		0.9	24	0.0472	0.302

Table 3.6 Results of Computation for the Three Lobe Journal Bearing

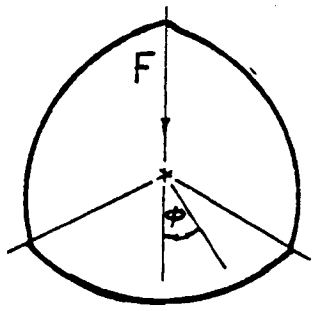

$P^* = 1.0$

ε_o	L/D	ε_B	ϕ	s	q_t
0.5	$\frac{1}{2}$	0	-	-	0.58
		0.2	60	1.02	0.604
		0.4	61	0.434	0.667
		0.6	61	0.22	0.77
		0.8	55	0.10	0.9
	1	0	-	-	0.204
		0.2	60	0.54	0.212
		0.4	60	0.225	0.24
		0.6	55	0.105	0.33
		0.8	53	0.066	0.36

P^* is the dimensionless pressure at the axial grooves

Table 3.7 Results of Computation of Three Lobe Journal Bearing

$\alpha = 30^{o}$

ε_o	L/D	ε_B	p^*	q_t
0.5	$\frac{1}{2}$	0	0	0.219
		0.2	0	0.240
		0.4	0	0.268
		0.6	0	0.310
		0.8	0	0.357
	1	0	0	0.1191
		0.2	0	0.127
		0.4	0	0.143
		0.6	0	0.162
		0.8	0	0.193
0.5	$\frac{1}{2}$	0	2	0.964
		0.2	2	1.005
		0.4	2	1.144
		0.6	2	1.361
		0.8	2	1.646
	1	0	2	0.303
		0.2	2	0.321
		0.4	2	0.383
		0.6	2	0.47
		0.8	2	0.577
0.5	$\frac{1}{2}$	0	5	2.153
		0.2	5	2.249
		0.4	5	2.51
		0.6	5	2.95
		0.8	5	3.55
	1	0	5	0.621
		0.2	5	0.663
		0.4	5	0.761
		0.6	5	0.91
		0.8	5	1.108

Table 3.7 cont. Results of Computation of the Three Lobe Journal Bearing

$\alpha = 30^{o}$

ε_o	L/D	ε_B	p^*	q_t
0.4	$\frac{1}{2}$	0	0	0.179
		0.2	0	0.208
		0.4	0	0.243
		0.6	0	0.306
		0.8	0	0.414
	1	0	0	0.098
		0.2	0	0.115
		0.4	0	0.138
		0.6	0	0.170
		0.8	0	0.230
0.4	$\frac{1}{2}$	0	5	2.79
		0.2	5	2.93
		0.4	5	3.35
		0.6	5	4.0
		0.8	5	4.94
	1	0	5	0.83
		0.2	5	0.875
		0.4	5	1.123
		0.6	5	1.251
		0.8	5	1.558
0.3	$\frac{1}{2}$	0	0	0.1362
		0.2	0	0.177
		0.4	0	0.243
		0.6	0	0.365
		0.8	0	0.50
	1	0	0	0.075
		0.2	0	0.111
		0.4	0	0.142
		0.6	0	0.218
		0.8	0	0.290
0.3	$\frac{1}{2}$	0	5	3.6
		0.2	5	3.78

Table 3.7 cont. Results of Computation of the Three Lobe Journal Bearing

$\alpha = 30^{o}$

ε_o	L/D	ε_B	p^*	q_t
0.3	$\frac{1}{2}$	0.4	5	4.35
		0.6	5	5.34
		0.8	5	6.73
	1	0	5	1.1
		0.2	5	1.156
		0.4	5	1.364
		0.6	5	1.7
		0.8	5	2.14
0.6	$\frac{1}{2}$	0	0	0.270
		0.2	0	0.276
		0.4	0	0.29
		0.6	0	0.31
		0.8	0	0.334
	1	0	0	0.134
		0.2	0	0.142
		0.4	0	0.150
		0.6	0	0.160
		0.8	0	0.173
0.7	$\frac{1}{2}$	0	0	0.300
		0.2	0	0.306
		0.4	0	0.312
		0.6	0	0.32
		0.8	0	0.33
	1	0	0	0.150
		0.2	0	0.154
		0.4	0	0.157
		0.6	0	0.162
		0.8	0	0.166
0.8	$\frac{1}{2}$	0	0	0.326
		0.2	0	0.328
		0.4	0	0.33

Table 3.7 cont. Results of Computation of the Three Lobe Journal Bearing

$\alpha = 30^{o}$

ε_o	L/D	ε_B	p^*	q_t
0.8	$\frac{1}{2}$	0.6	0	0.332
		0.8	0	0.334
	1	0	0	0.164
		0.2	0	0.164
		0.4	0	0.165
		0.6	0	0.196
		0.8	0	0.199
0.6	$\frac{1}{2}$	0	3.0	0.961
		0.2	3.0	0.985
		0.4	3.0	1.041
		0.6	3.0	1.2
		0.8	3.0	1.394
	1	0	3.0	0.328
		0.2	3.0	0.337
		0.4	3.0	0.368
		0.6	3.0	0.427
		0.8	3.0	0.504
0.7	$\frac{1}{2}$	0	3.0	0.811
		0.2	3.0	0.823
		0.4	3.0	0.858
		0.6	3.0	0.918
		0.8	3.0	1.003
	1	0	3.0	0.291
		0.2	3.0	0.295
		0.4	3.0	0.308
		0.6	3.0	0.329
		0.8	3.0	0.363
0.8	$\frac{1}{2}$	0	3.0	0.695
		0.2	3.0	0.699
		0.4	3.0	0.710
		0.6	3.0	0.731
		0.8	3.0	0.76

Table 3.7 cont. Results of Computation of the Three Lobe Journal Bearing

$\alpha = 30^{o}$

ε_o	L/D	ε_B	p^*	η_t
	1	0	3.0	0.263
		0.2	3.0	0.264
		0.4	3.0	0.278
		0.6	3.0	0.279
		0.8	3.0	0.285
0.45	$\frac{1}{2}$	0	5	2.45
		0.2	5	2.68
		0.4	5	2.92
		0.6	5	3.46
		0.8	5	4.19
	1	0	5	0.713
		0.2	5	0.75
		0.4	5	0.883
		0.6	5	1.07
		0.8	5	1.3
0.45	$\frac{1}{2}$	0	0	0.198
		0.2	0	0.218
		0.4	0	0.279
		0.6	0	0.374
		0.8	0	0.47
	1	0	0	0.109
		0.2	0	0.12
		0.4	0	0.141
		0.6	0	0.165
		0.8	0	0.222
0.35	$\frac{1}{2}$	0	5	3.18
		0.2	5	3.34
		0.4	5	3.85
		0.6	5	4.63
		0.8	5	5.99

Table 3.7 cont. Results of Computation of the Three Lobe Journal Bearing

$\alpha = 30^{o}$

ε_o	L/D	ε_B	p^*	q_t
0.35	1	0	5	0.96
		0.2	5	1.006
		0.4	5	1.18
		0.6	5	1.46
		0.8	5	1.84
	$\frac{1}{2}$	0	0	0.158
		0.2	0	0.192
		0.4	0	0.303
		0.6	0	0.43
		0.8	0	0.549
	1	0	0	0.087
		0.2	0	0.11
		0.4	0	0.140
		0.6	0	0.20
		0.8	0	0.260

Table 3.8 Results of Computation for the Three Lobe Journal Bearing

$\alpha = 20^{o}$

ε_o	L/D	ε_B	q_p
0.5	$\frac{1}{2}$	0	1.149
		0.2	1.187
		0.4	1.298
		0.6	1.388
		0.8	1.76
	1	0	0.704
		0.2	0.73
		0.4	0.8
		0.6	0.921
		0.8	1.1
0.4	$\frac{1}{2}$	0	1.48
		0.2	1.53
		0.4	1.71
		0.6	2.0
		0.8	2.43
	1	0	0.926
		0.2	0.962
		0.4	1.08
		0.6	1.27
		0.8	1.54
0.3	$\frac{1}{2}$	0	1.86
		0.2	1.94
		0.4	2.2
		0.6	2.64
		0.8	3.58
	1	0	1.194
		0.2	1.25
		0.4	1.42
		0.6	1.71
		0.8	2.1

Table 3.8 Results of Computation for the Three Lobe Journal Bearing.

$\alpha = 30°$

ε_o	L/D	ε_B	q_p
0.5	$\frac{1}{2}$	0	1.34
		0.2	1.4
		0.4	1.52
		0.6	1.79
		0.8	2.07
	1	0	0.783
		0.2	0.81
		0.4	0.89
		0.6	1.131
		0.8	1.23
0.4	$\frac{1}{2}$	0	1.74
		0.2	1.806
		0.4	2.016
		0.6	2.37
		0.8	2.89
	1	0	1.038
		0.2	1.082
		0.4	1.212
		0.6	1.432
		0.8	1.752
0.3	$\frac{1}{2}$	0	2.21
		0.2	2.31
		0.4	2.52
		0.6	3.15
		0.8	3.93
	1	0	1.35
		0.2	1.41
		0.4	1.6
		0.6	1.938
		0.8	2.41

flow coefficient is that at higher offset ratios (i.e. $\varepsilon_o > 0.6$) the hydrodynamic flow coefficient is nearly constant for eccentricity ratio up to 0.9. The implication of the hydrodynamic flow coefficient for the bearing performance will be examined in paragraph 3.9.

The locus of journal centre is shown in Figure 3.13. At low values of eccentricity all three lobes contribute to the hydrodynamic performance of the bearing so that they all have a marked effect on the attitude angle which is lower than the angle of the other circular bearings (E and F of the Figure). At high values of eccentricity the hydrodynamic contribution of the two upper lobes decreases. For instance at $\varepsilon_B = 0.3$ the generated dimensionless hydrodynamic force at the bottom and the upper lobes is 1.133, 0.093 and 0.228 respectively while at $\varepsilon_B = 0.9$, the dimensionless hydrodynamic forces become 11.28, 0.046 and 0.467 respectively. Consequently it can be seen that as the eccentricity increase the hydrodynamic effect of the upper lobes decreases, so that the attitude angle tends to increase. Also it may be seen that the increase of the offset ratio has a marked effect on decreasing the attitude angle.

The other important dimensionless parameters which are used to describe the bearing performance are the duty parameter and the stiffness coefficient. In Figure 3.14 the duty parameter is plotted against the bearing eccentricity ratio and in Figure 3.15 the stiffness coefficient as defined in paragraph 3.4 is shown. Quite clearly, from Figure 3.14 and 3.15, increasing the offset ratio leads to a decrease in the duty parameter (i.e. increasing the load capacity) and leads to an increase in the stiffness coefficient. However, because the offset ratio and lobe clearance are not variable independently, the changes in duty parameter and stiffness coefficient do not necessarily imply similar

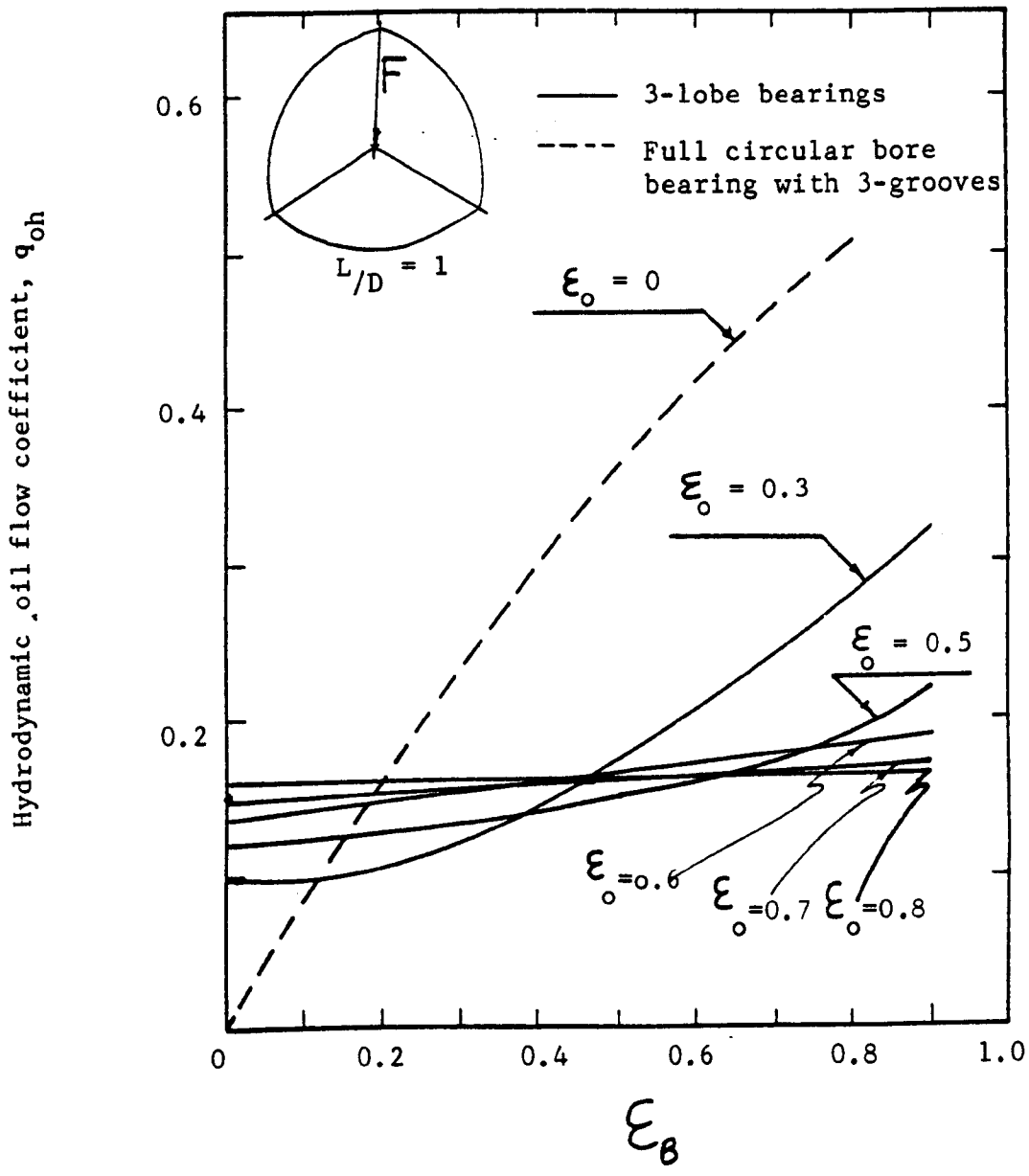

FIG.3.12 Variation of the hydrodynamic flow coefficient with the eccentricity ratio.

A = ε_o = 0.8)
B = ε_o = 0.6)
C = ε_o = 0.5) Three-lobe bearing
D = ε_o = 0.4)

E : Full circular bore bearing with three-groove)
F : Full circular bore bearing)

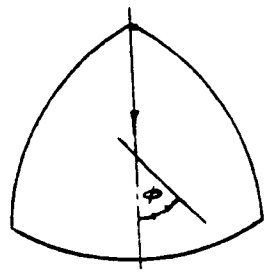

ε_o = 0

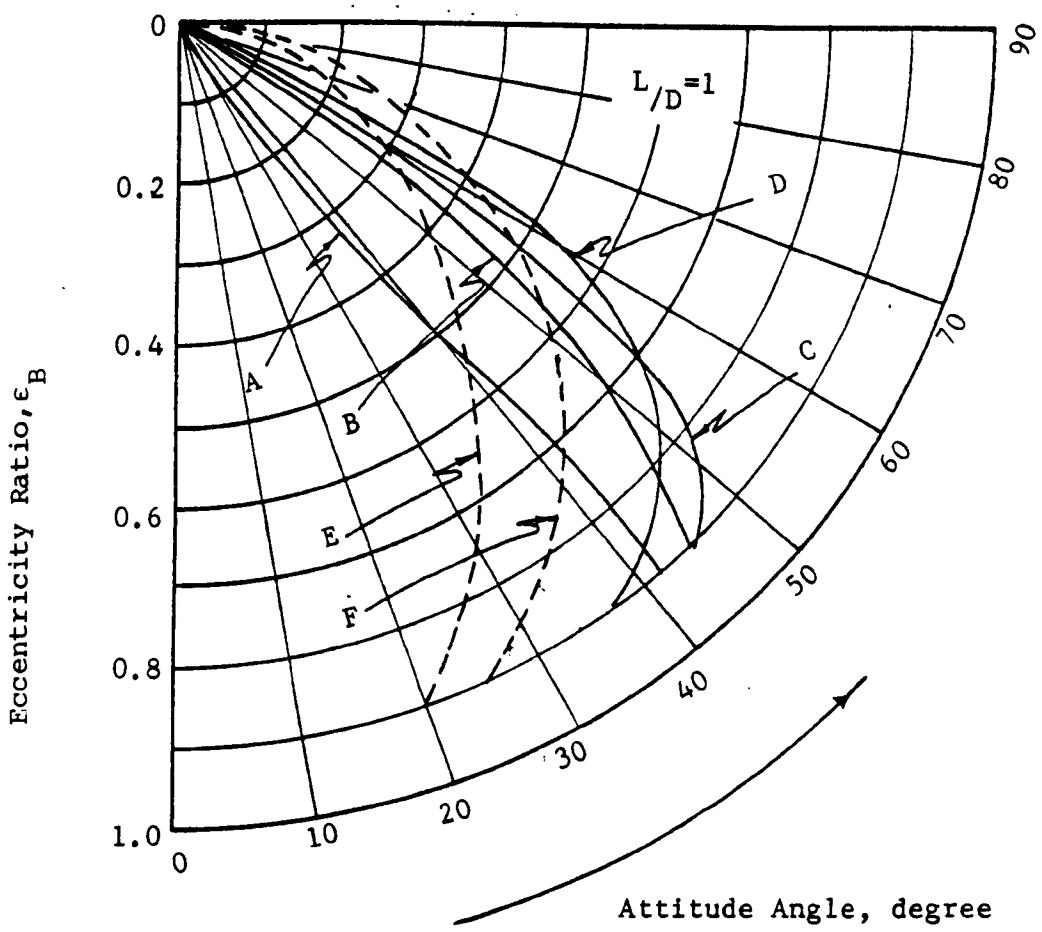

FIG.3.13 Variation of attitude angle with the eccentricity ratio.

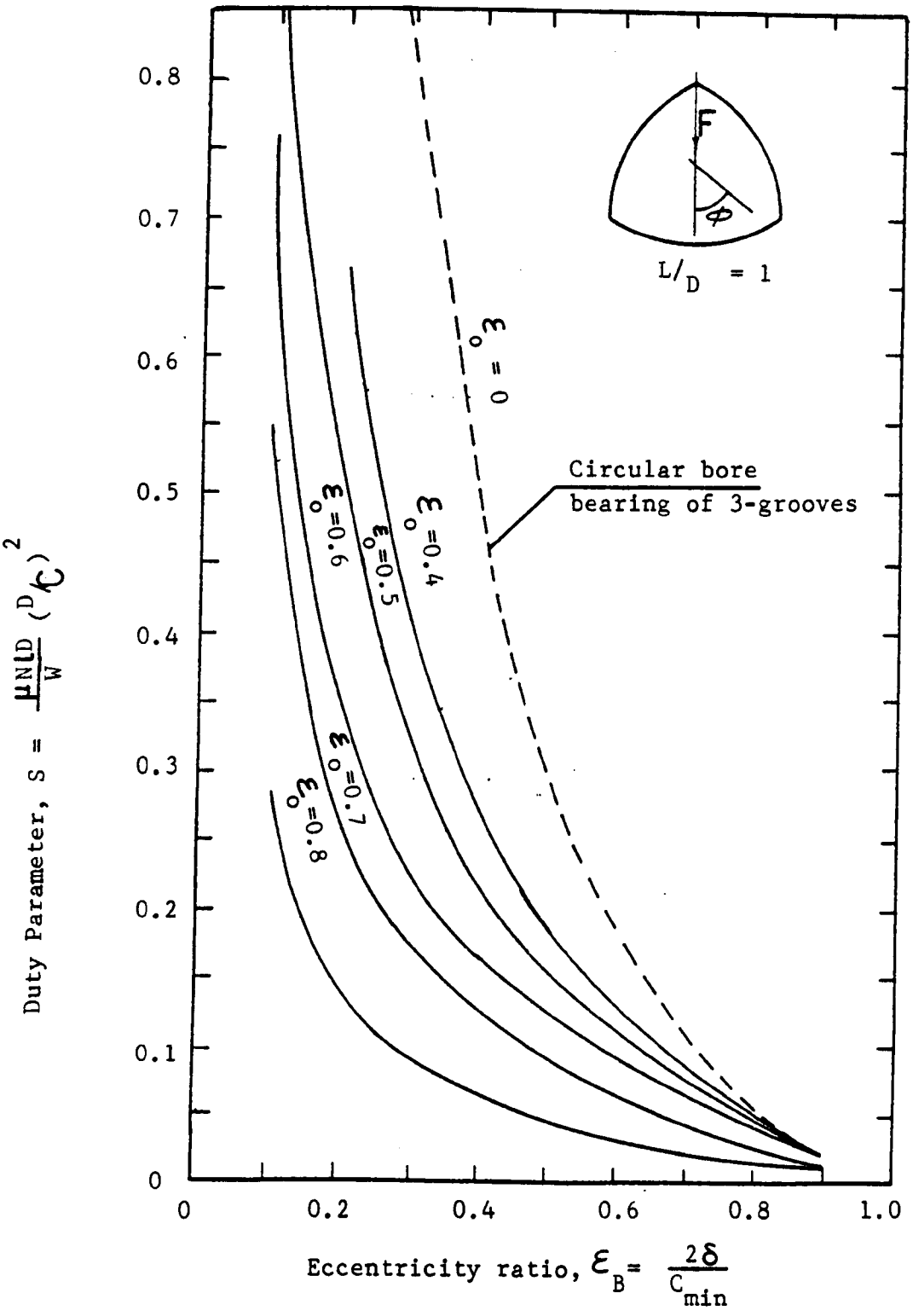

FIG.3.14 Variation of the duty parameter with the eccentricity ratio.

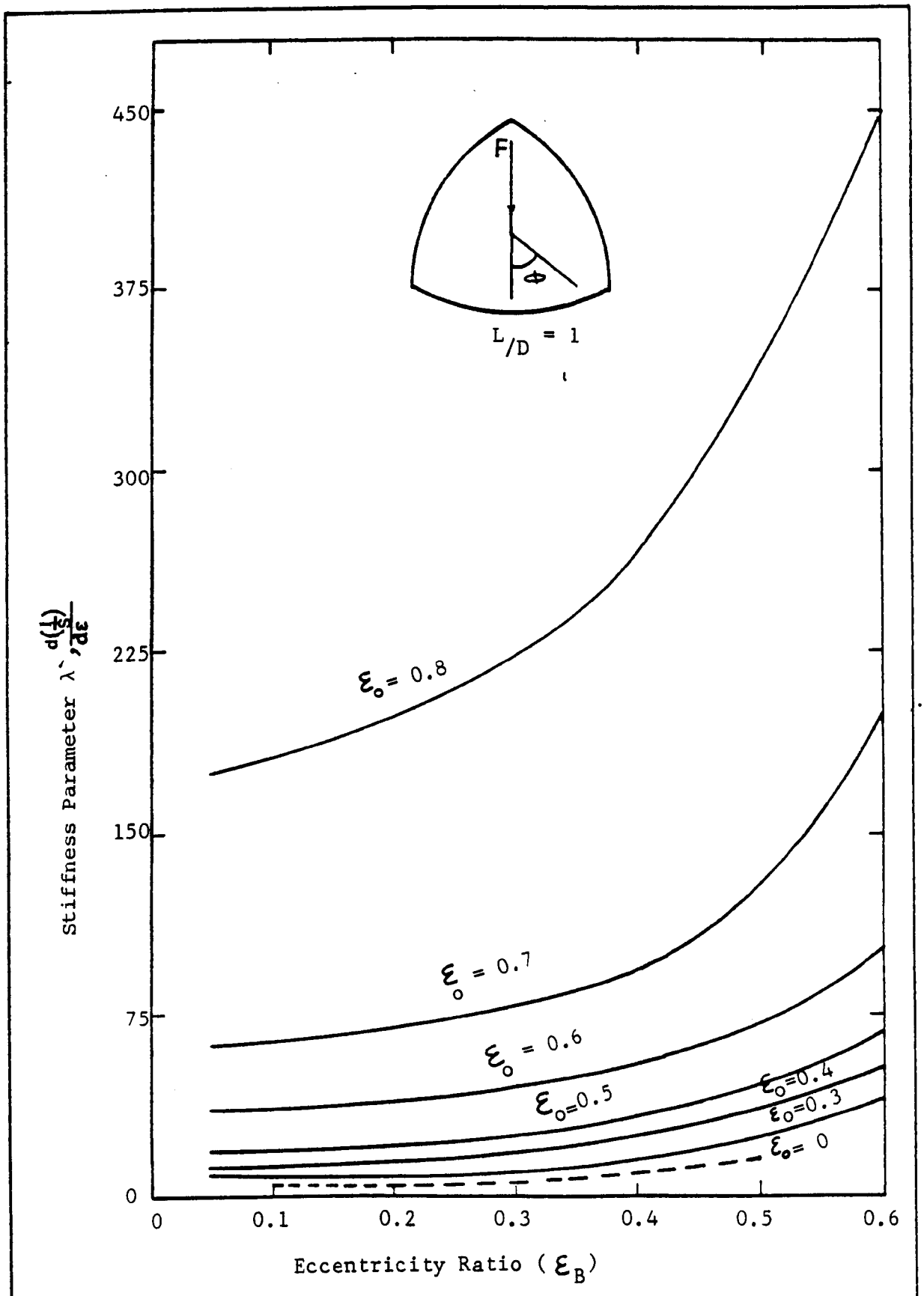

FIG.3.15 Variation of the stiffness coefficient with the eccentricity ratio.

changes in actual load capacity and in actual stiffness. The trend in these and other physical quantities must be found by applying the non-dimensional relationship to bearings which are defined in terms of actual dimensions and to oils of specified viscosity. The calculations pertaining to such specific circumstances are presented and discussed in paragraph 3.9.

Figures 3.16 and 3.17 show the variation of the duty parameter and the attitude angle with the eccentricity ratio for a vertical load directed towards the centre of a lobe and for a vertical load directed towards the conjunction of adjacent lobes. It may be seen from Figure 3.16 that the duty parameter is nearly independent of the load direction while it can be seen from Figure 3.17 that there is a big difference in the attitude angle.

3.7 Power Loss

The total friction force acting upon the journal is given essentially by

$$F = \int_0^L \int_0^{2\Pi} \frac{\mu U R d\theta}{h} dy. \qquad (3.37)$$

For a three lobe journal bearing and with the journal centred in the bearing (Figure 3.18) the force due to all three lobes is given by

$$F = 6 \int_0^L \int_{\Pi}^{2\Pi/3} \frac{\mu U R d\theta}{h} dy. \qquad (3.38)$$

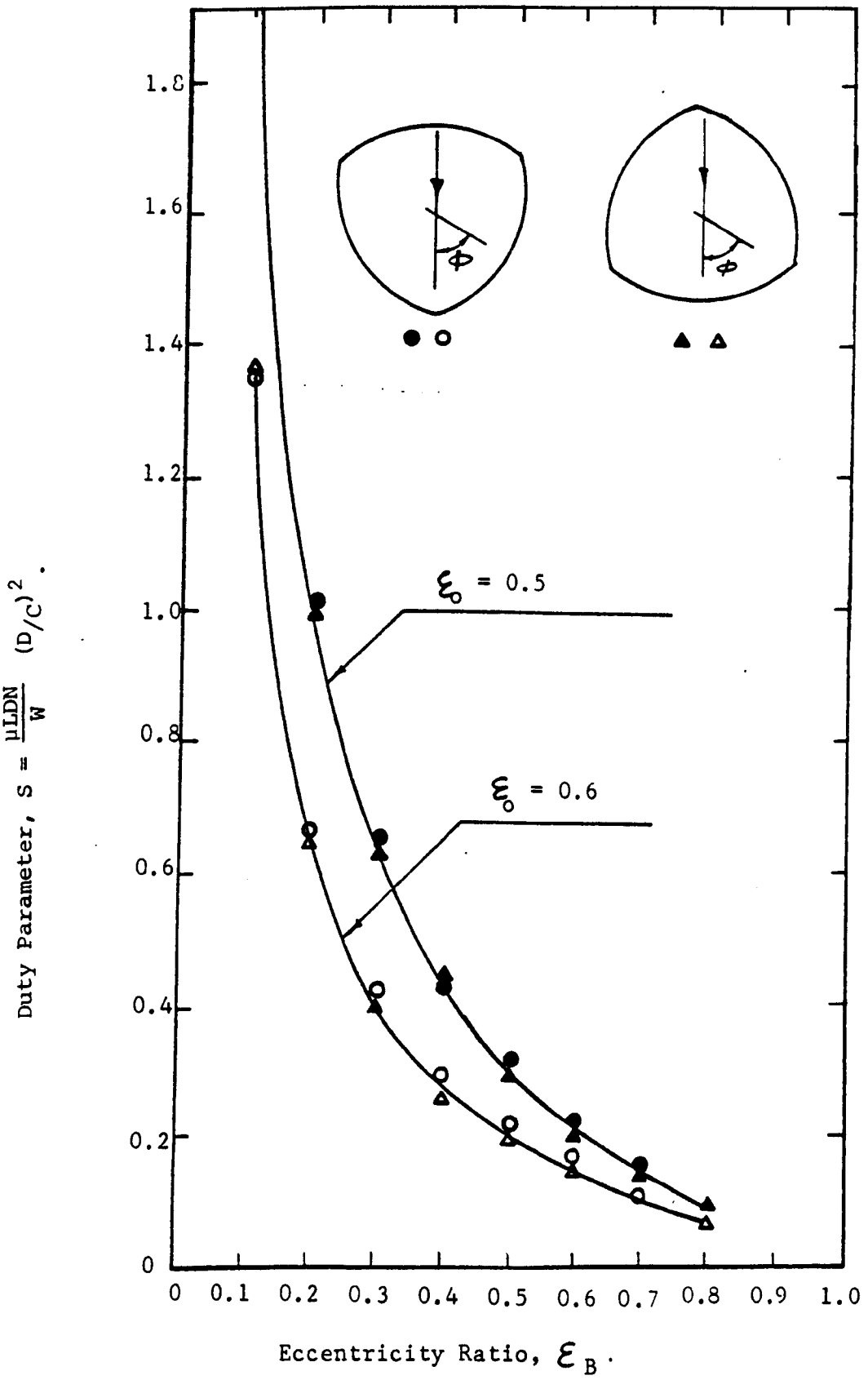

FIG.3.16 Variation of the duty parameter with the eccentricity ratio.

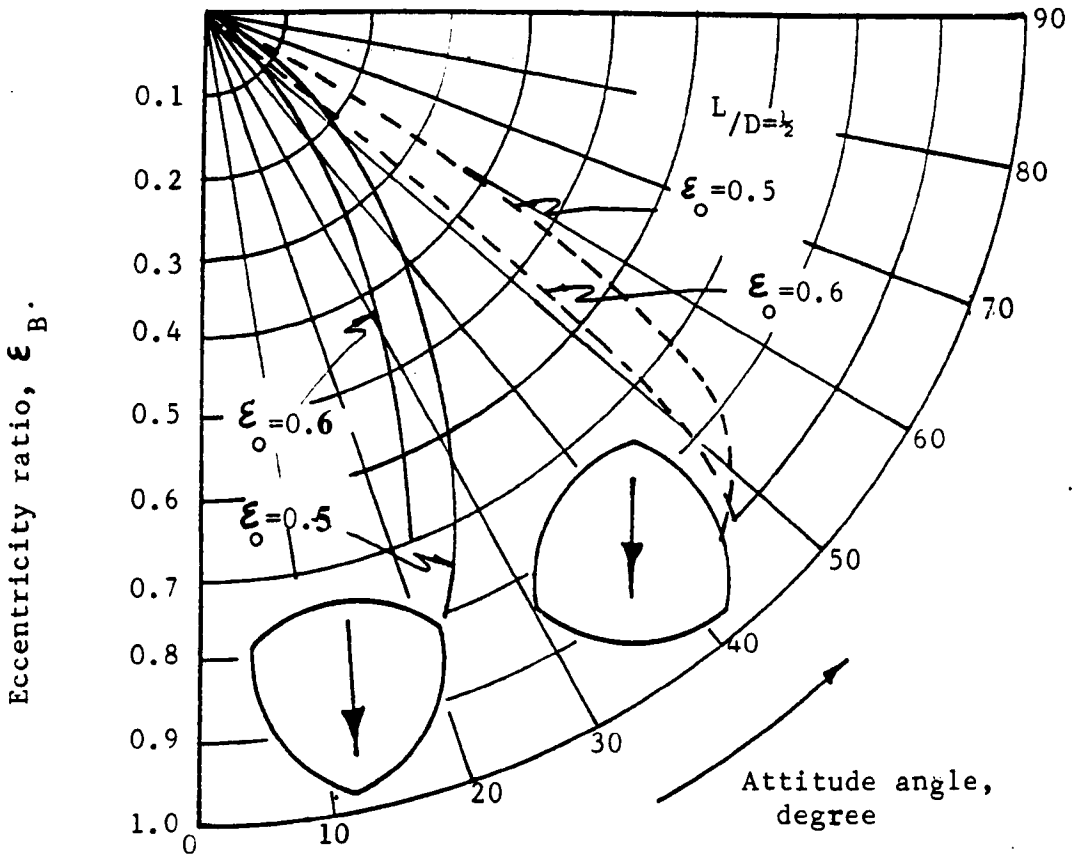

FIG.3.17 Locus of shaft centre.

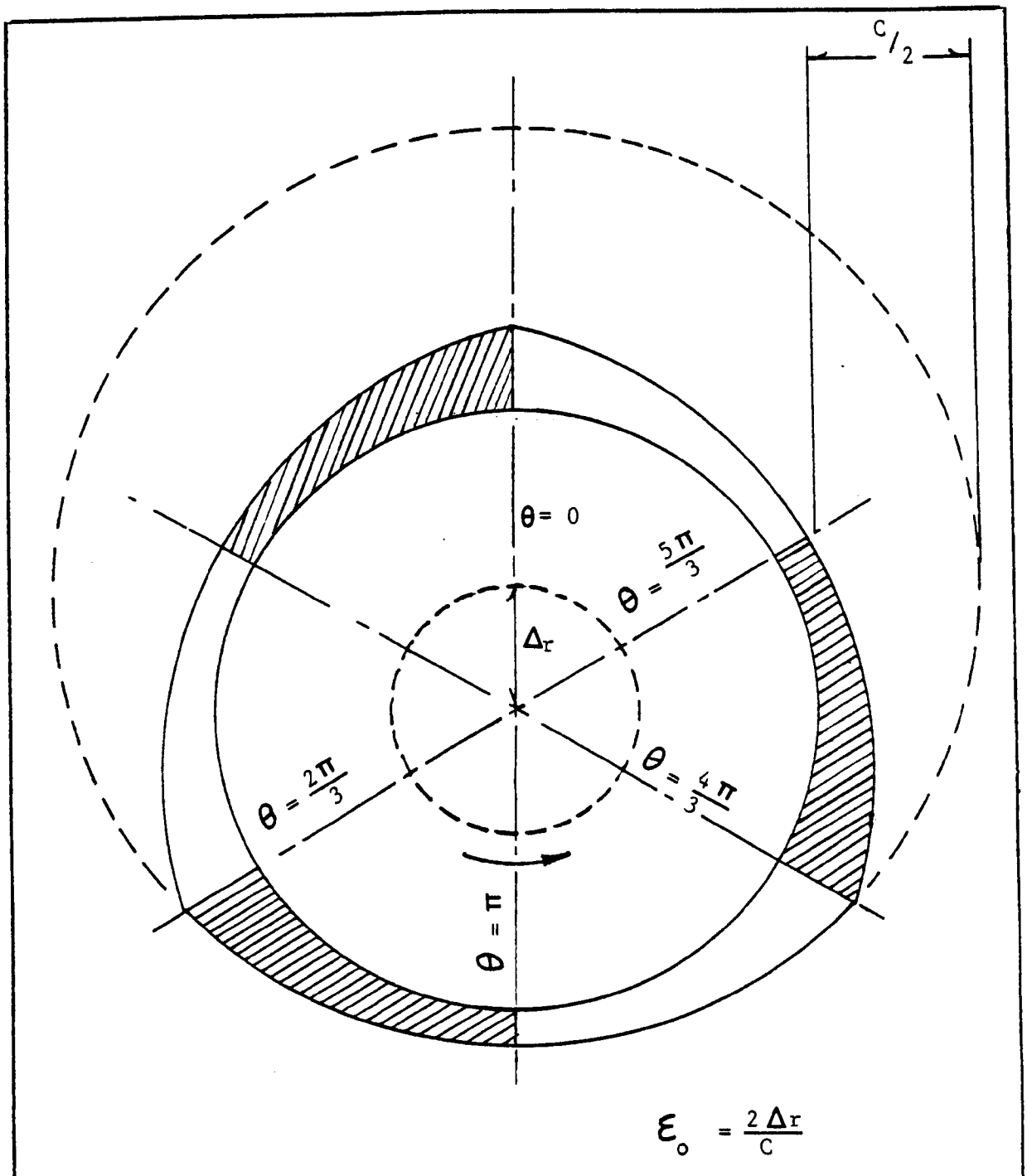

FIG. 3.18 Power loss analogy for a three-lobe bearing.

The oil film thickness is expressed by:

$$h = {}^{C}/_{2} \ (1 + \varepsilon_o \cos \theta) \qquad (3.39)$$

With viscosity treated as being constant it follows from (3.38) and (3.39) that

$$F = 6L \frac{U\mu D}{C} \int_{\Pi}^{2\Pi/3} \frac{d\theta}{(1+\varepsilon_o \cos \theta)} \qquad (3.40)$$

Expression (3.40) may be integrated by using the Sommerfeld substitution which is given in Chapter 2. The result is

$$F = \frac{6 \ UDL}{C(1-\varepsilon_o^2)^{\frac{1}{2}}} \left\{ \cos^{-1} \frac{-1+\varepsilon_o}{1-\varepsilon_o} - \cos^{-1} \frac{-0.5+\varepsilon_o}{1-0.5 \ \varepsilon_o} \right\} \qquad (3.41)$$

and the power loss is given by

$$H_s = \frac{6\Pi^2 \mu L N^2 D^3}{C(1-\varepsilon_o^2)^{\frac{1}{2}}} \left\{ \cos^{-1} \frac{-1+\varepsilon_o}{1-\varepsilon_o} - \cos^{-1} \frac{-0.5+\varepsilon_o}{1-0.5\varepsilon_o} \right\} . \qquad (3.42)$$

Equation (3.42) may be used with any system of units. However, when μ is given in poise, L in cm, D in cm, N in r.p.m., C cm, the power loss in KW is given by

$$H_s = 1.646 \times 10^{-12} \frac{\mu L N^2 D^3}{C} \frac{1}{(1-\varepsilon_o^2)^{\frac{1}{2}}} \left\{ \cos^{-1} \frac{-1+\varepsilon_o}{1-\varepsilon_o} - \cos^{-1} \frac{-0.5+\varepsilon_o}{1-0.5 \ \varepsilon_o} \right\}$$

(3.43)

For a circular bore bearing $\varepsilon_o = 0$, and equation(3.42) reduces to

$$H_p = \frac{6\Pi^2\mu LN^2D^3}{C} \cdot \frac{\Pi}{3} = \frac{2\Pi^3\mu LN^2D^3}{C} \qquad (3.44)$$

which is the Petroff's loss for a circular bearing. The ratio between the power loss of the three lobe bearing and the Petroff power loss of a circular bore bearing which has a diametral clearance equal to the lobe diametral clearances of the three lobe bearing is defined as the power loss factor, and is given by

$$j_s = \frac{H_s}{H_p} = \frac{3}{\Pi}\left\{\cos^{-1}\frac{-1+\varepsilon_o}{1-\varepsilon_o} - \cos^{-1}\frac{-0.5+\varepsilon_o}{1-0.5\varepsilon_o} \times \frac{1}{(1-\varepsilon_o^2)^{\frac{1}{2}}}\right\} \qquad (3.45)$$

In Figure 3.19 the power loss factor is plotted against the offset ratio. The relation shows that for the same lobe clearance (i.e. the clearance of the circular bore bearing is equal to the lobe clearance of the three lobe bearing), and the same viscosity, the power loss of the three lobe bearing is greater than the power loss of the circular bore bearing by the factor Js. However, because the offset ratio and lobe clearance are not variable independently, the changes in the offset ratio do not necessarily imply that the actual power loss will follow the power loss factor.

The power losses in a particular bearing of circular bore and in a particular three lobe bearing will now be discussed. In the first instance the power loss of a circular bore bearing will be considered. The computer programme has been used to calculate the power loss simply

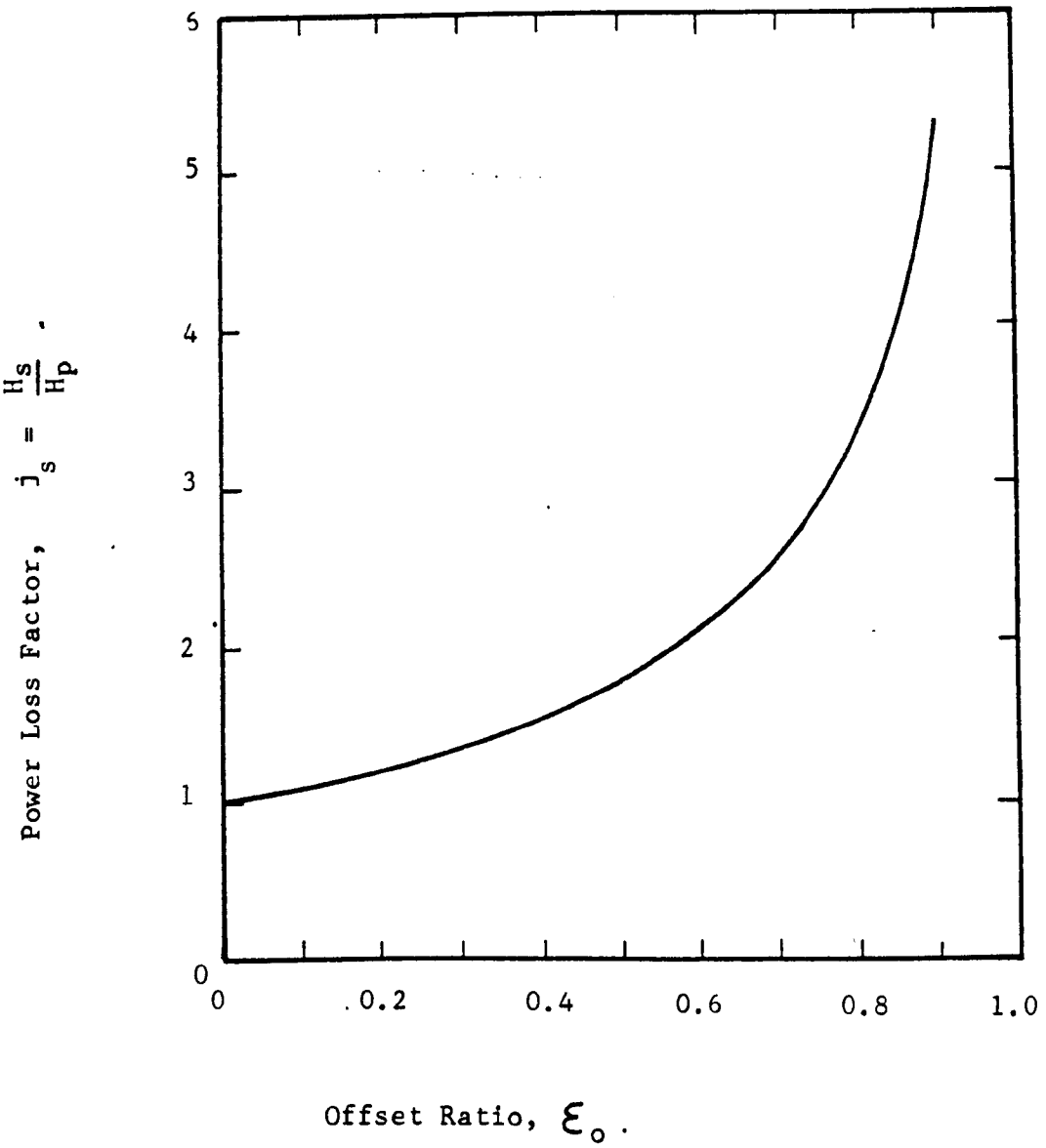

FIG.3.19 Variation of the power loss factor with the offset ratio.

by setting the offset ratio $\varepsilon_o = 0$. In Figure 3.20a the calculated power loss is shown as functions of speed. It has previously been shown in paragraph 3.6 that the flow coefficients given by the computer programme are substantially the same as those given in the literature. It follows from this that at any particular speed the oil outlettemperature given by the 'design programme', which will be discussed in paragraph 3.8, is the same as the temperature arising from the published values of flow coefficient. Because of this, it is valid in comparing the calculated power loss as given by the programme with power loss found from published power loss coefficient to take as the oil viscosity that found by means of the design programme.

The power loss of the three-lobe bearing will now be considered. The calculation of the power loss as given by the programme for an offset ratio of $\varepsilon_o = 0.35$ is shown in Figure 3.20b together with the measured power loss as reported in Chapter 6. The calculated power loss is somewhat greater than that measured at low speed but measured and calculated losses become substantially equal at a speed of 5000 rpm.

There is no unique basis for comparing the power loss of a circular bore and a three-lobe bearing, but a reasonable basis seems to be between bearings of equal minimum clearance. The diametral clearance of the circular bore bearing of Figure 3.20a is the same as the minimum clearance of the three-lobe bearing of Figure 3.20b. In Figure 3.20c the power loss of that particular circular bore bearing and of that particular three-lobe bearing are compared, and it may be seen that the circular bore bearing gives somewhat less power loss over the full

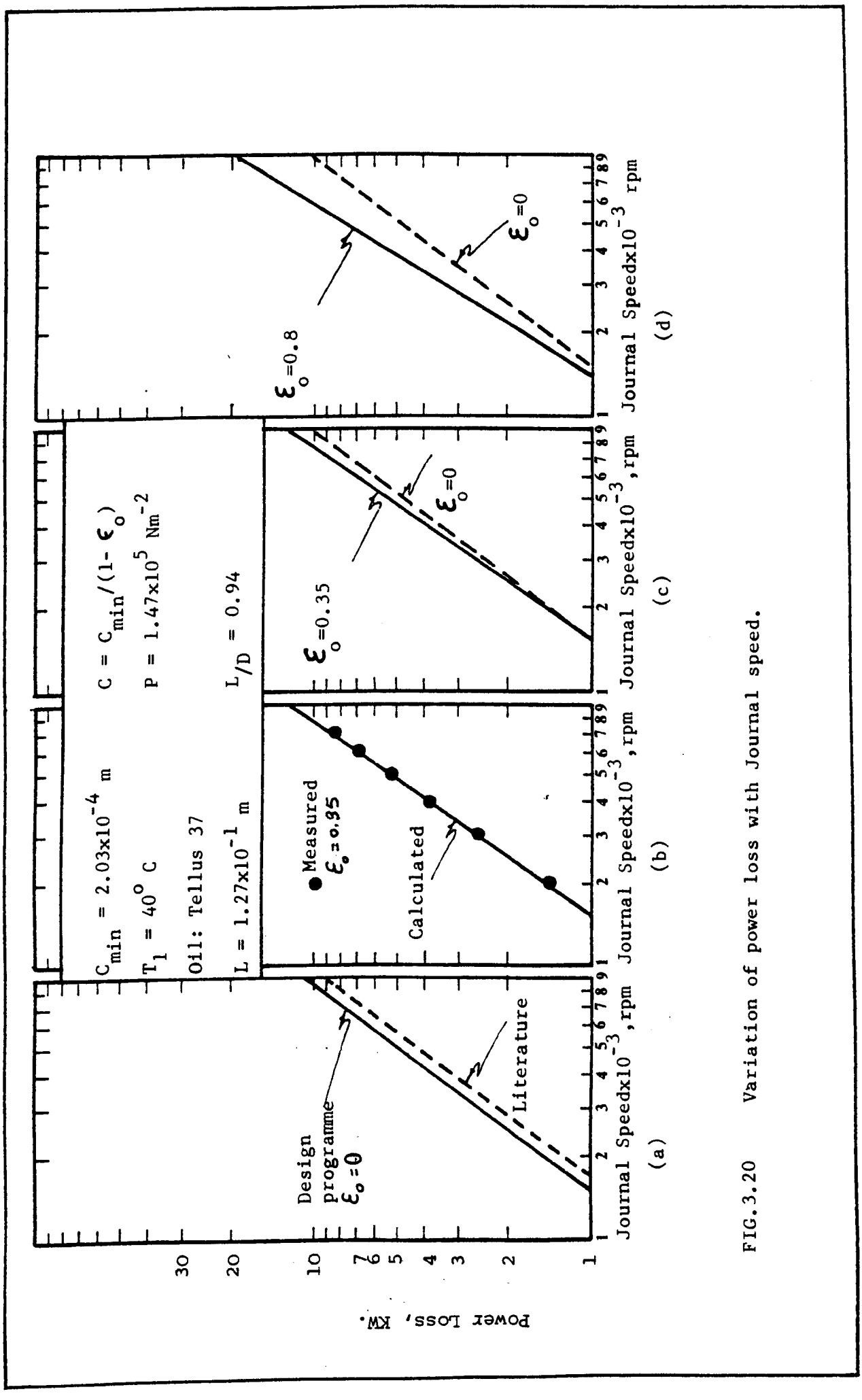

FIG.3.20 Variation of power loss with Journal speed.

speed range. This is usually so as may be seen from Figure 3.20d in which calculated results are compared in the instance that the three lobe bearing has an offset ratio of 0.8. In this instance a smaller power loss is indicated for the circular bore bearing over the full speed range. The general conclusion from this comparison is there is no major difference in power loss between circular and three lobe bearings of equal minimum clearance. However there are substantial differences in other respects and these will be discussed as they arise.

3.8 The Design Programme, "Computation of actual oil flow, temperature rise, power loss, load capacity and stiffness".

A second computer programme has been written which is in the nature of a design programme and which will be termed "The Design Programme". The input to this programme includes the dimensionless output of the finite difference programme together with dimensions and actual viscosity which completely described a real bearing situation. The output of the design programme is the actual total oil flow, the actual hydrodynamic oil flow, the actual pressure oil flow, power loss, oil temperature rise, outlet viscosity, load capacity and stiffness. The design programme includes an iteration routine by which temperature rise and outlet viscosity are brought to self consistent values. Flow and power loss are calculated on the basis that the outlet viscosity pertains throughout the bearing.

The inputs to the programme are given below, and numerical values which are given relate to the bearings which have been tested. Numerical values are not given for oil viscosity, flow coefficient, duty parameter and stiffness coefficient because different values are required for

each combination of minimum clearance and offset ratio however the numerical values which appear in brackets against these quantities are typical values just to indicate the magnitude of the quantities.

The inputs to the programme are:

Shaft diameter: 1.35×10^{-1}m.

Bearing axial length: 1.27×10^{-1}m.

Oil grooves axial length: 1.07×10^{-1}m.

Oil grooves circumferential length: 3.5×10^{-2} and 1.75×10^{-2}m.

Minimum clearance: 1.016×10^{-4}, 1.27×10^{-4}, 1.52×10^{-4}, 1.78×10^{-4}, and 2.03×10^{-4}m.

Oil inlet temperature: 30, 40 and 50°C.

Oil viscosity at the inlet temperature: Tellus 37 oil (0.53 to 0.22 poise). VIT. 150 oil (2.19 to 0.736 poise).

Pump pressure: $1.47 \times 10^{5} Nm^{-2}$

Journal Speed: 10^{3}, 2.10^{3}, 3×10^{3},.....,and 10^{4} r.p.m.

Journal displacement: 1.27×10^{-5}m.

Offset ratio: 0,0.35, 0.45, 0.6, 0.7 and 0.8.

Hydrodynamic oil flow coefficient: (from 0 to 0.26).

Total oil flow coefficient: $\{q_h + (0.023 \text{ to } 0.5 \times P^*)\}$ (paragraph 3.5)

Duty parameter: (from 2.5 to 0.13)

Stiffness coefficient: (from 210 to 5)

The iterative routine itself may be described as follows:

(1) For the considered oil, calculate the factor α by substituting the oil viscosity at 30 and 50°C into the following expression:

$$\mu_{50} = \mu_{30} \exp^{-\alpha(50-30)}$$

(2) For the considered speed, enter an arbitrary outlet temperature, T_2.

(3) Calculate the oil viscosity at the outlet from the following expression:

$$\mu_2 = \mu_1 \exp^{-\alpha(T_2-T_1)}$$

(4) The oil flow is calculated within the programme by two methods, either of which may be chosen for a particular run as follows:

.calculate the dimensionless inlet pressure (P*) from expression (3.25).

.calculate the total oil flow from expression (3.27) by using the total oil flow coefficient which is calculated from expression (3.31).

OR

.calculate the pressure oil flow by using the semi-empirical expression

.calculate the hydrodynamic oil flow from expression (3.27)

.calculate the total oil flow as the sum of the pressure flow and the hydrodynamic flow.

(5) Calculate the shear power loss from expression (3.43).

(6) Calculate the oil outlet temperature from the following expression:

$$H_s = \rho K Q_t (T_2-T_1).$$

where,

H_s is the shear power loss which is calculated in step (5), KW.

Q_t is the total oil flow which is calculated step (4), $Cm^3 S^{-1}$.

K specific heat of the oil, $\simeq$ 0.47 Cal $qm^{-1}\ ^oC^{-1}$.

ρ oil density, $\simeq$ 0.88.

$T_{1,2}$ oil inlet and outlet temperatures respectively, ^oC.

(7) If the calculated outlet temperature (T_2) in step (6) is equal to the outlet temperature which is entered in step (2), or there is a difference within $\pm$ 2°C, the procedure is completed and the calculations may be carried out for another speed. However, if the difference is greater than $\pm$ 2°C, within the programme itself a new trial value is found for T_2 and the iteration is repeated.

(8) The outputs of the computer programme are:

The oil outlet temperature (T_2), °C.

The oil outlet viscosity (μ_2), poise.

The hydrodynamic oil flow, ls^{-1}.

The pressure oil flow, ls^{-1}.

The total oil flow, ls^{-1}.

The power loss, KW.

Load carrying capacity, N.

Bearing stiffness, Nm^{-1}.

The computer programme may be used for any bearing of any dimensions providing that the oil flow coefficient, the stiffness coefficient and the duty parameter of that bearing are entered in the input. The computer programme itself as well as a sample of the output are given in Appendix A2.2.

3.9 Results of the Design Programme Computation

The validity of the design programme has been examined by comparing the quantities predicted with experimental measurements. Such comparisons have been made in the context of large turbine bearings, and in the context of test bearingsof the present work. In Table 3.9 a comparison is made between calculated and experimental results for a 19"x10"x0.023" bearing of circular bore. For convenience three equally spaced axial grooves

were assumed in the calculation where in the actual bearing the axial grooves were not equally spaced. However the table shows a good agreement and provides substantial evidence of correctness of the design programme and the calculation of the flow coefficient. In Figure 3.21a comparison is made between the prediction of the design programme and the experimental results from the test rig which will be discussed in Chapter 6. There is close agreement.

The trends predicted by the design programme will be described now. The variation of power loss with journal speed is shown in Figure 3.22. The results are plotted for minimum clearances of 1.016, 1.52 and 2.03×10^{-4}m. It may be seen that the power loss increases as the offset ratio increases and also the power loss increases marginally as the minimum clearance increases. Also it may be seen that the dependence of power loss upon the offset ratio (ε_o) decreases as the minimum clearance increases.

The variation of the oil temperature rise with the journal speed is shown in Figure 3.23. It is quite clear that as the offset ratio increases the oil temperature rise decreases over the full range of minimum clearances which have been used in the calculations. Figure 3.24 shows the variation of the oil flow with the journal speed. It may be seen that the oil flow is increased as the offset ratio and the minimum clearance increases.

Figures 3.25 and 3.26 show the variation of the bearing load and the bearing stiffness with the journal speed. In Figures 3.25 a, b and 3.26 a,b, it is quite clearly shown that the increase in the offset ratio has a marked effect on the bearing load and on the bearing stiffness and it

Table 2.9 The Design Programme Results and the Test Results for a 19 x 10 x 0.023" Turbine Journal Bearing.

The Design Programme								Refs. Smith, [10] DUFFIN [82] and Private Communication [83]							
N rpm	ε	T_1 °C	$Px10^{-5}$ Nm^{-2}	Q ℓs^{-1}	T_2 °C	μ_2 C.P.	H_s K.W.	N	W/LD** Nm^{-2}	T_1 °C	$Px10^{-5}$ Nm^{-2}	Q ℓs^{-1}	T_2 °C	μ_2 C.P.	H_s K.W.
1000	0.4	50	0.74	1.012	59	19	15.54	1000	4×10^5	50	0.74	0.872	58.33	19.4	15
2000	"	"	"	1.631	67	14	47.37	2000	"	"	"	1.63	67.78	14	54
3000*	"	"	"	2.2	74	12	91.5	3000*	"	"	"	2.88	78.9	9.7	150.5

* At Journal speed of 3000 rpm, the calculated results from the design programme is for a laminar oil flow in the bearing clearance, while the test results obtained at 3000 rpm were observed with the presence of turblent flow in the bearing clearance.

** The load on projected area was used with the test results because the value of the eccentricity ratio has not been mentioned in the quoted references.

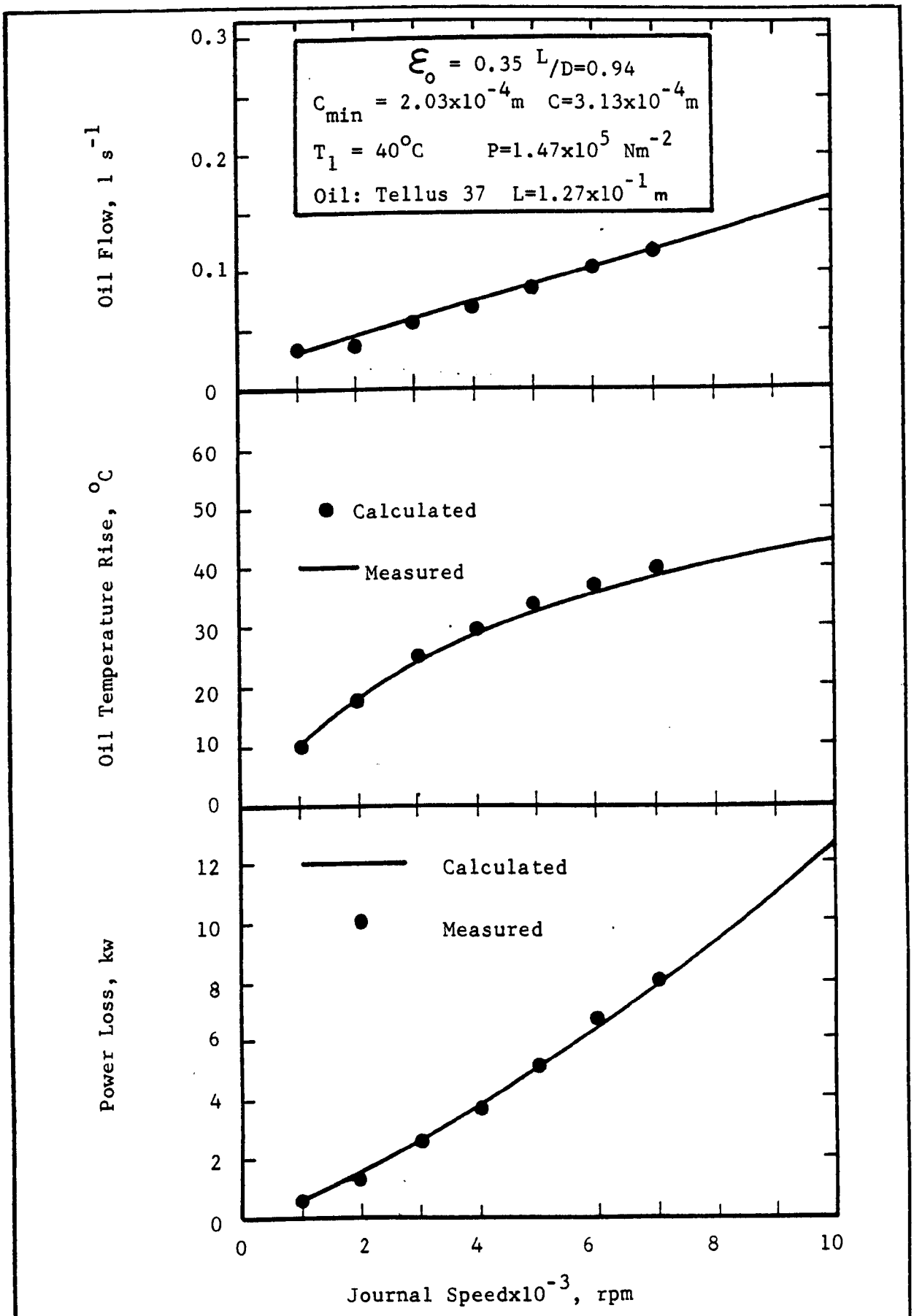

FIG.3.21 Variation of power loss, oil temperature rise, and oil flow with the Journal speed.

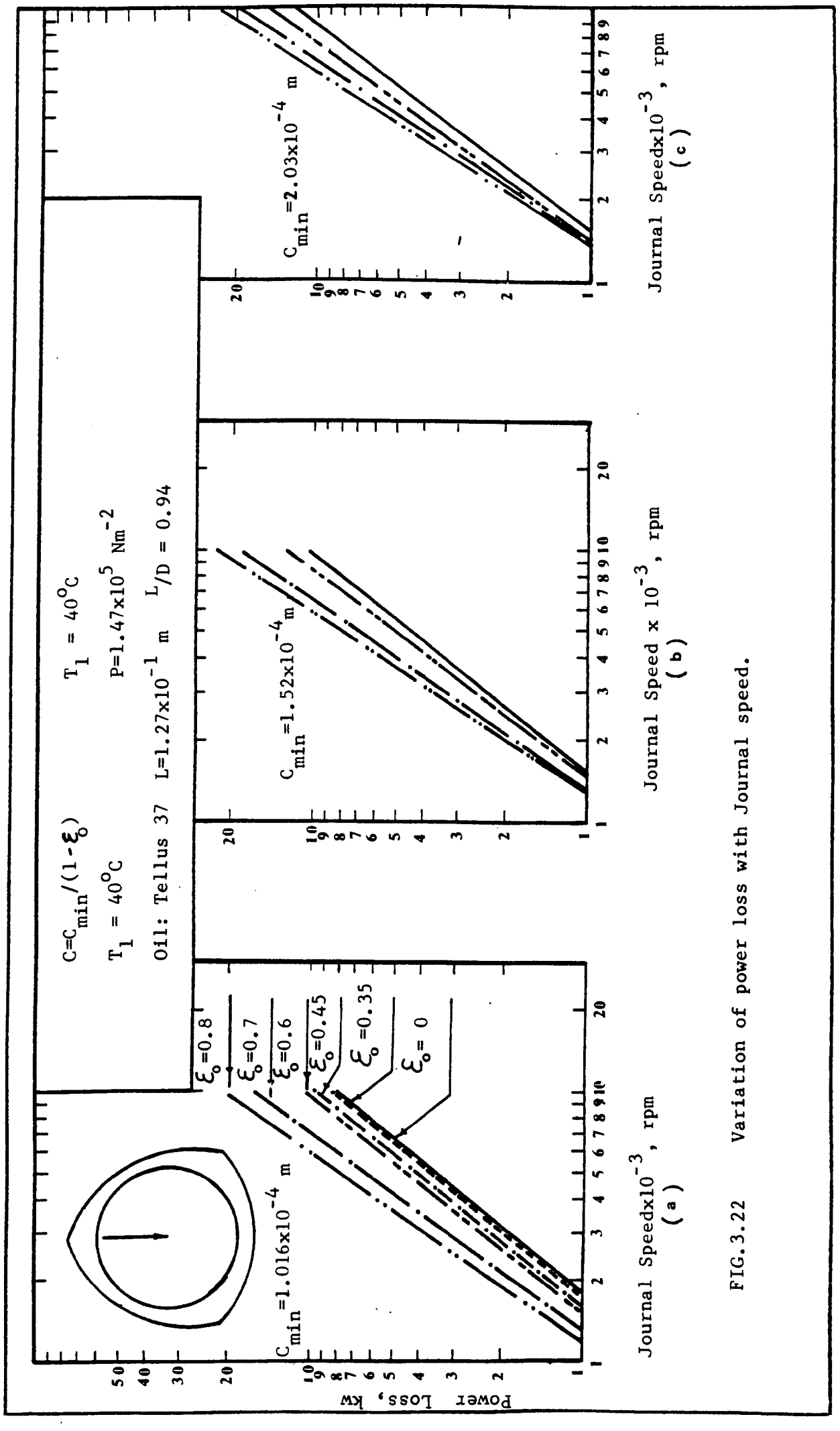

FIG.3.22 Variation of power loss with Journal speed.

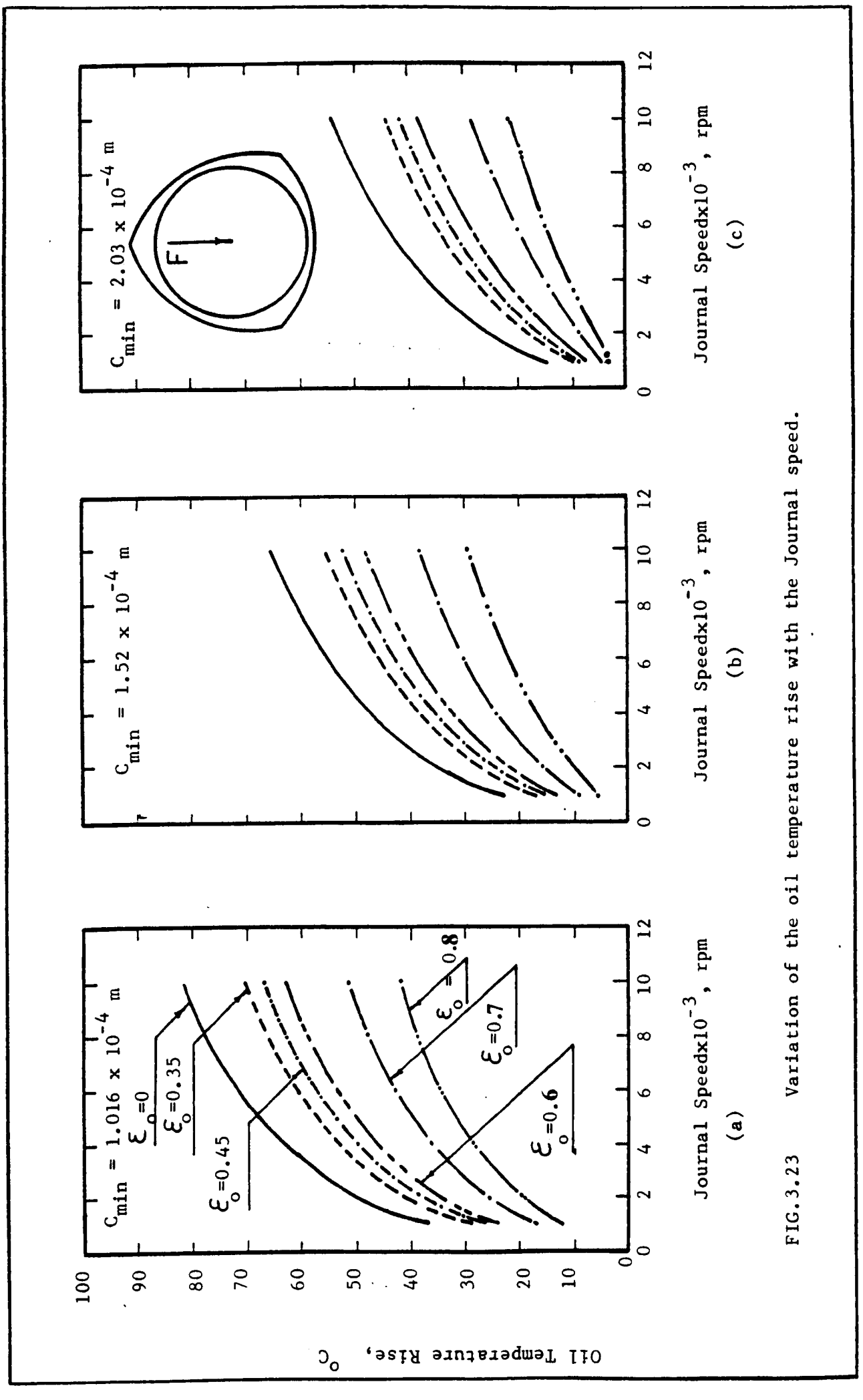

FIG.3.23 Variation of the oil temperature rise with the Journal speed.

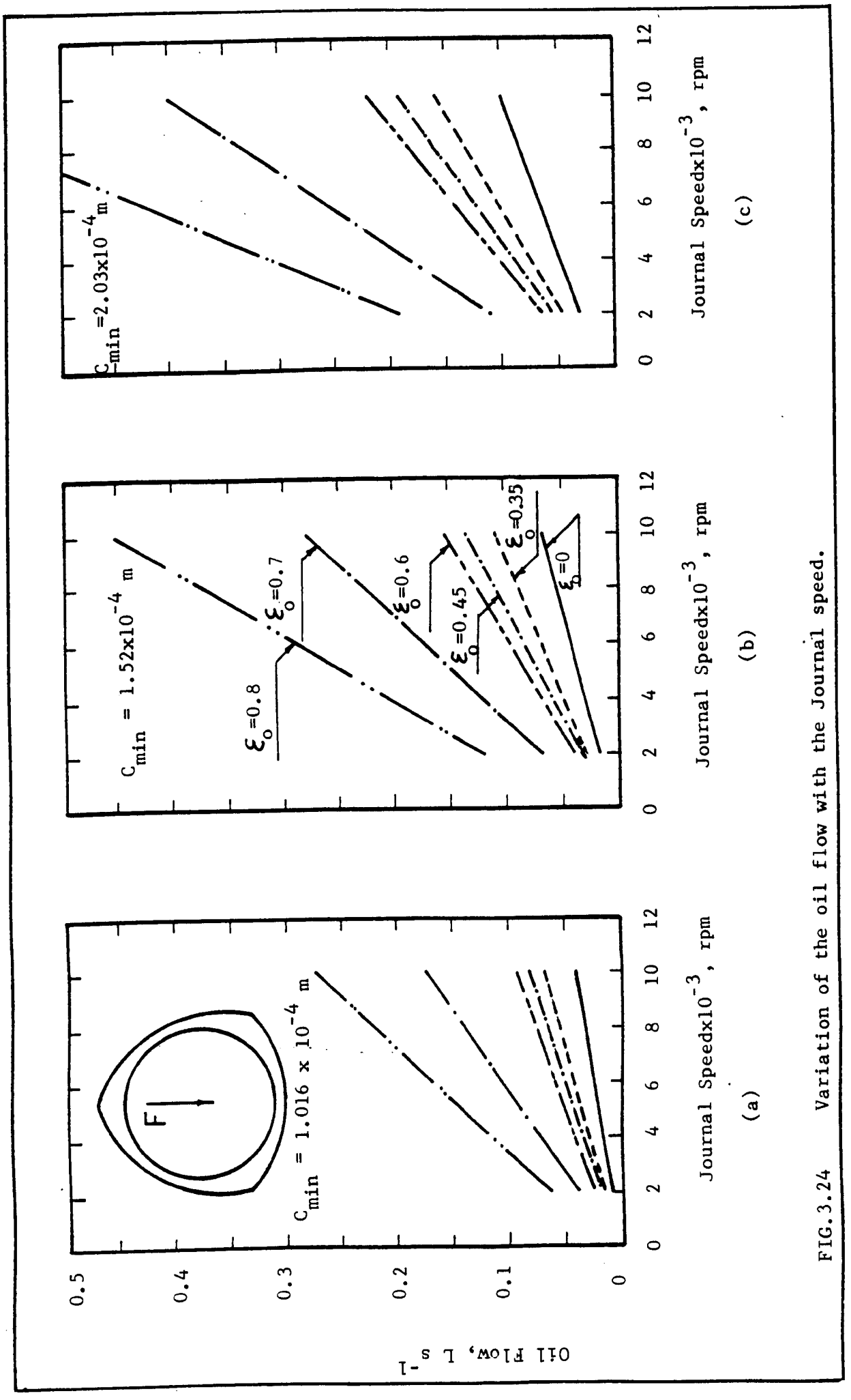

FIG.3.24 Variation of the oil flow with the Journal speed.

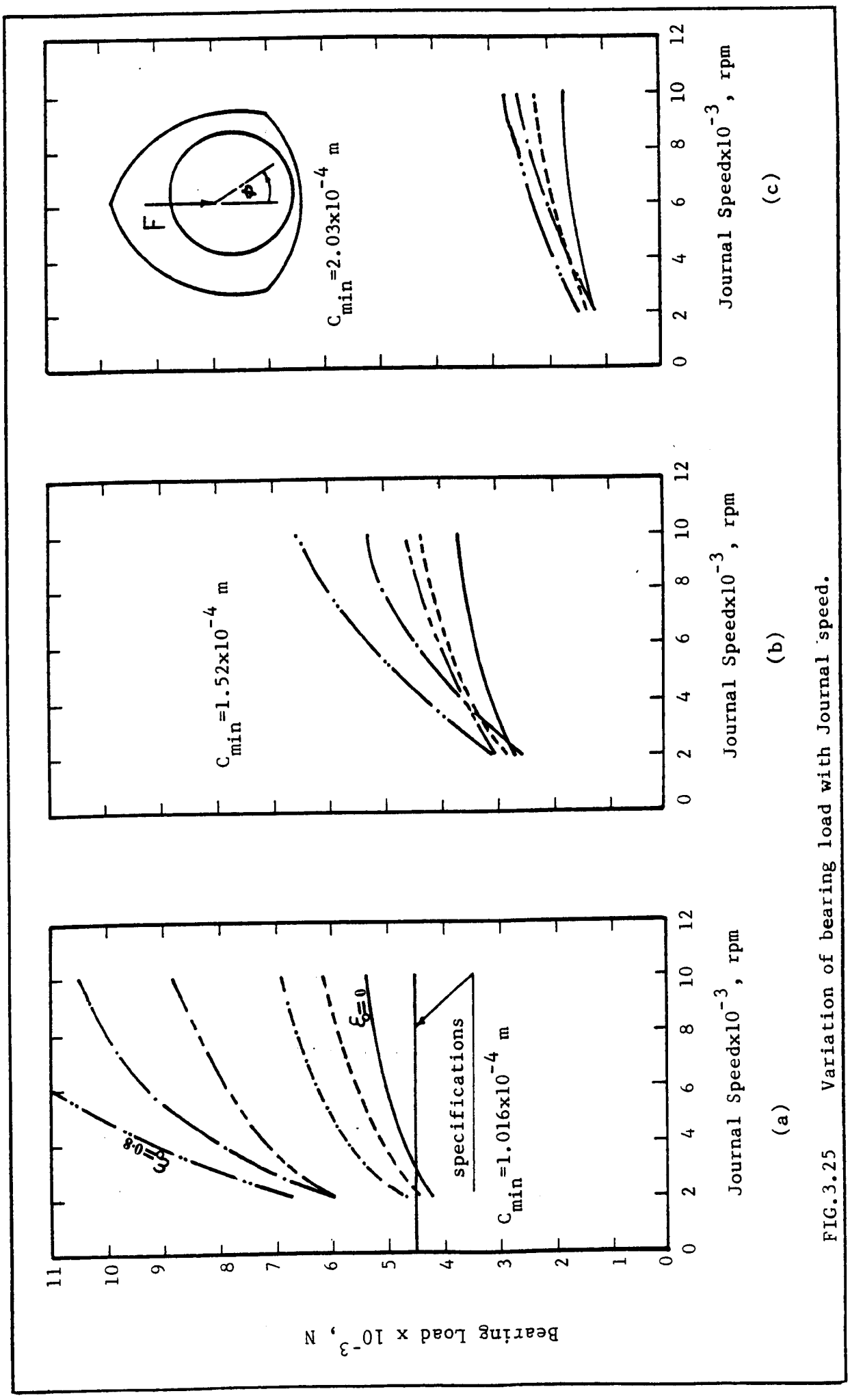

FIG.3.25 Variation of bearing load with Journal speed.

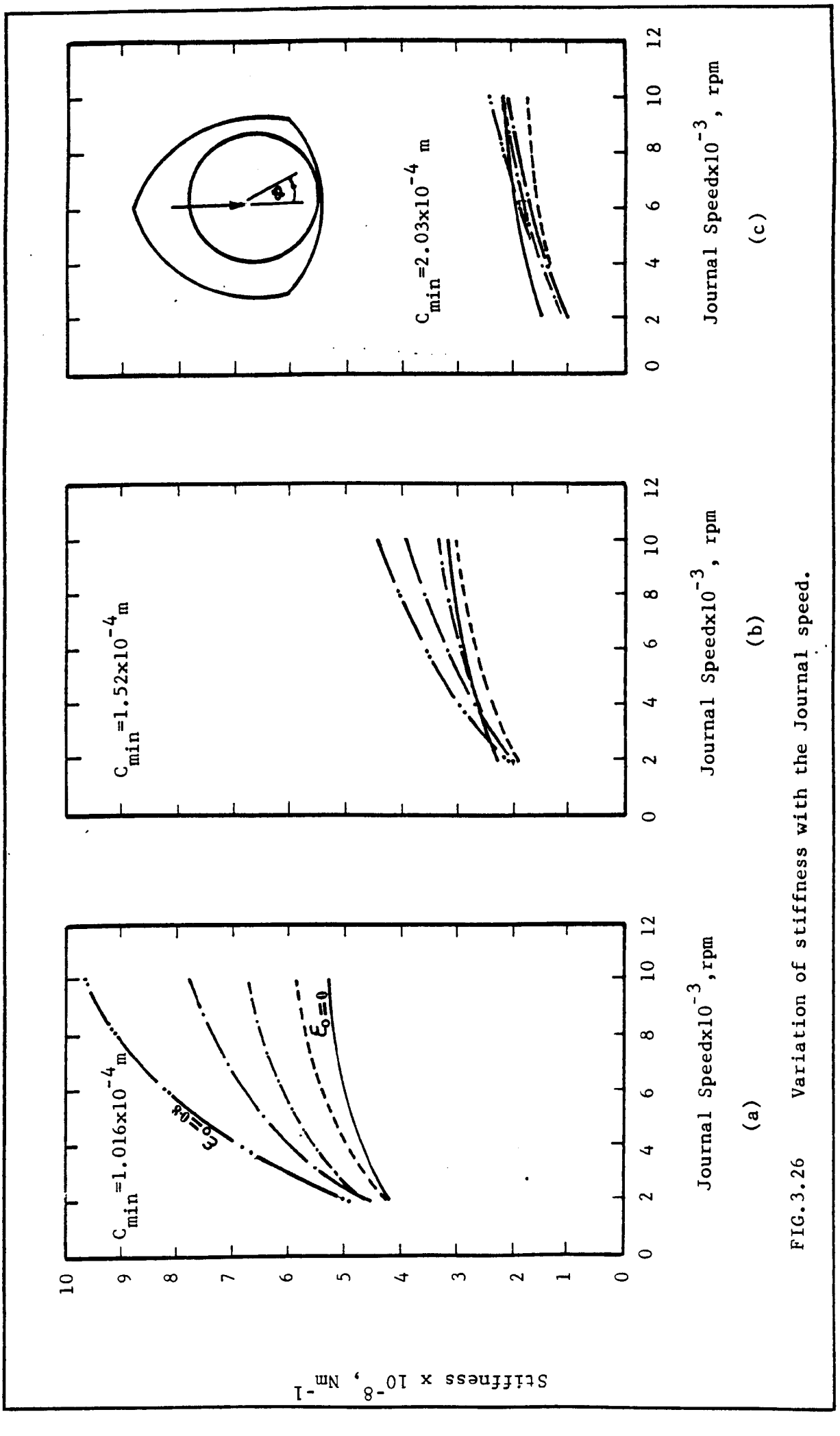

FIG.3.26 Variation of stiffness with the Journal speed.

may be seen that the load capacity and the bearing stiffness increases as the offset ratio increases over the full range of speeds. At higher values of clearances (Figure 3.25c-3.26c) there are small increases in the load capacity and bearing stiffness due to the increase in the offset ratio. It also may be seen from Figures 3.25a,b,c and 3.26a,b,c that the load capacity and the bearing stiffness decrease as the minimum clearance increases.

The use of these predictions in the design of a bearing will now be discussed. The results which are plotted in Figures 3.22-3.26 show that for a bearing of high load carrying capacity and high stiffness, the bearing should be designed with high offset ratio and with small minimum clearance. The increase in the offset ratio leads to a big decrease in the oil temperature rise, but consequently the power loss is increased. The small minimum clearance leads to an increase in the oil temperature rise but the power loss is decreased. However, the choice of the offset ratio and the minimum clearance should be made to give a compromise solution for the required load capacity, bearing stiffness and for reasonable power loss and oil temperature rise. The predictions of the design programme show that the functional spacification of Table 1.1 can be met by a bearing of offset ratio of 0.45, such a bearing would have a minimum clearance of 1.43×10^{-4}m and a lobe clearance of 2.6×10^{-4}m. At 9000rpm and for oil inlet temperature of 40°C, the power loss is 11KW, and the oil temperature rise is 51°C. A three lobe journal bearing was machined to have an offset ratio of 0.45, lobe diametral clearance of 2.6×10^{-4} and a minimum clearance of 1.43×10^{-4}m, with the intention that different clearences may be tested by reducing the journal diameter. It should be pointed out that in Chapter 2 the approximate hydrostatic analysis has shown that such

dimensions are satisfactory for the hydrostatic performance.

3.10 An Approximate Assessment of the Bearing Stiffness

The choice of dimensions for the original test bearing was based upon assessment of power loss, temperature rise and bearing stiffness made by approximate and elementary methods. All of these are now superseded by the computer programmes which have been described, but there is some value in describing the approximate treatment of stiffness and its results as a check upon the results from the numerical solution. In a bearing of full circular bore stiffness is substantially determined within a relatively small area dispose mainly ahead of the position of minimum film thickness. In elementary treatment of stiffness it was supposed that each lobe would encompass the area of significance about each position of minimum film thickness, and that in consequence the three lobe bearing could be treated in stiffness as three bearings of full circular bore placed one against another and with their centres suitably displaced.

In Figure 3.27 a journal is shown at eccentricity Δr in a bearing of full circular bore. It is running at this eccentricity, and attitude angle ϕ due to the external load F. (in the multi-lobe bearing the force F is created by the hydrodynamic pressures associated with the other lobes). By considering that under the influence of an external load with components P_{x1} and P_{y1}, the centre of the journal is further displaced by a distance δr but that the attitude angle ϕ remains unchanged, the components of the displacement are obviously

$$\left.\begin{aligned} \Delta x_1 &= \delta r \cos \phi \\ \Delta y_1 &= \delta r \, (-\sin \phi) \end{aligned}\right\} \quad (3.46)$$

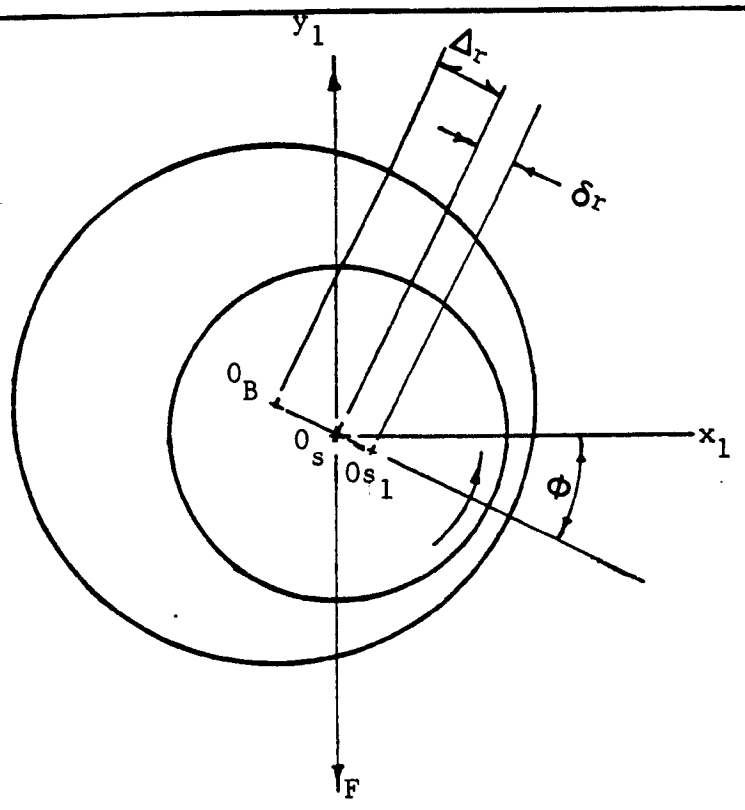

(a) Circular bore Journal bearing.

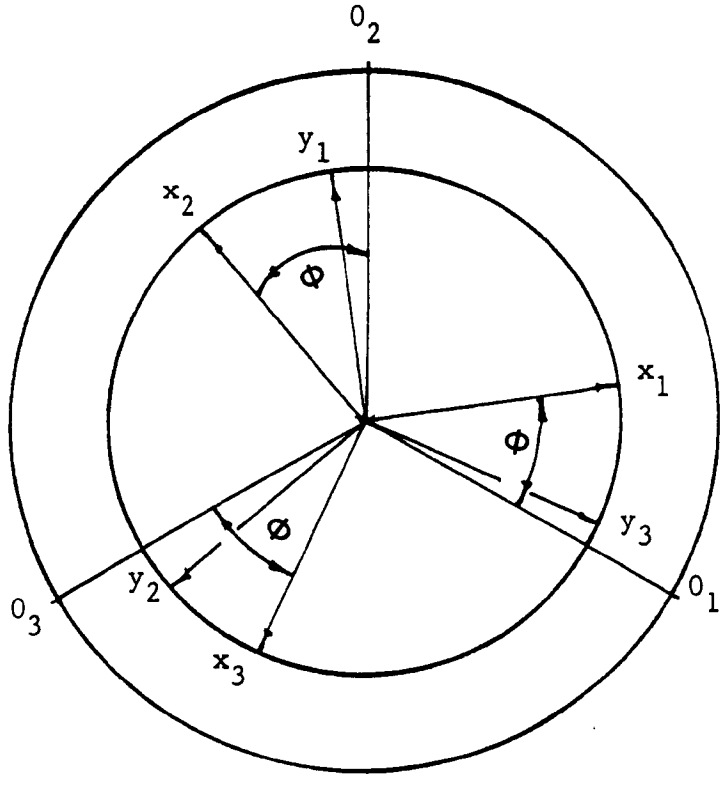

(b) Multi-lobe bearing.

FIG.3.27 Force-displacement relationship for Journal bearing.

It is clear from figure 3.27b, that this displacement δr with respect to the next lobe will produce components of displacement.

$$\left.\begin{aligned} \Delta x_2 &= \delta r[\cos(\phi+120)] \\ \Delta y_2 &= \delta r[-\sin(\phi+120)] \end{aligned}\right\} \quad (3.47)$$

and with respect to the third lobe

$$\left.\begin{aligned} \Delta x_3 &= \delta r[\cos(\phi+240)] \\ \Delta y_3 &= \delta r[-\sin(\phi+240)] \end{aligned}\right\} \quad (3.48)$$

Therefore

$$\left.\begin{aligned} \Delta x_1 &= \delta r[\cos\phi] \\ \Delta y_1 &= \delta r[-\sin\phi] \\ \Delta x_2 &= \delta r[-\tfrac{1}{2}\cos\phi - \tfrac{\sqrt{3}}{2}\sin\phi] \\ \Delta y_2 &= \delta r[\tfrac{1}{2}\sin\phi - \tfrac{\sqrt{3}}{2}\cos\phi] \\ \Delta x_3 &= \delta_r[-\tfrac{1}{2}\cos\phi + \tfrac{\sqrt{3}}{2}\sin\phi] \\ \Delta y_3 &= \delta_r[\tfrac{1}{2}\sin\phi + \tfrac{\sqrt{3}}{2}\cos\phi] \end{aligned}\right\} \quad (3.49)$$

From the theory of the dynamic characteristics of bearings, the incremental forces P_{x1} and P_{y1} are related to the displacement they produce by expressions of the form.

$$\left.\begin{aligned} P_{x1}/F &= a_{11}\frac{\Delta x_1}{C/2} + a_{12}\frac{\Delta y_1}{C/2} \\ P_{y1}/F &= a_{21}\frac{\Delta x_1}{C/2} + a_{22}\frac{\Delta y_1}{C/2} \end{aligned}\right\} \quad (3.50)$$

where a_{11}, a_{12}, a_{21}, a_{22} are the displacement coefficients (Ref. 10)

Consequently,

$$
\left.
\begin{aligned}
P_{x1}/F &= \frac{\delta r}{C/2}\,[a_{11}\cos\phi - a_{12}\sin\phi] \\
P_{y1}/F &= \frac{\delta r}{C/2}\,[a_{21}\cos\phi - a_{22}\sin\phi] \\
P_{x2}/F &= \frac{\delta r}{C/2}\,[a_{11}(-\tfrac{1}{2}\cos\phi - \frac{\sqrt{3}}{2}\sin\phi) + a_{12}(\tfrac{1}{2}\sin\phi - \frac{\sqrt{3}}{2}\cos\phi)] \\
P_{y2}/F &= \frac{\delta r}{C/2}\,[a_{21}(-\tfrac{1}{2}\cos\phi - \frac{\sqrt{3}}{2}\sin\phi) + a_{22}(\tfrac{1}{2}\sin\phi - \frac{\sqrt{3}}{2}\cos\phi)] \\
P_{x3}/F &= \frac{\delta r}{C/2}\,[a_{11}(-\tfrac{1}{2}\cos\phi + \frac{\sqrt{3}}{2}\sin\phi) + a_{12}(\tfrac{1}{2}\sin\phi - \frac{\sqrt{3}}{2}\cos\phi)] \\
P_{y3}/F &= \frac{\delta r}{C/2}\,[a_{21}(-\tfrac{1}{2}\cos\phi + \frac{\sqrt{3}}{2}\cos\phi) + a_{22}(\tfrac{1}{2}\sin\phi + \frac{\sqrt{3}}{2}\cos\phi)]
\end{aligned}
\right\} \quad (3.51)
$$

the total force in the x_1 direction is given by:

$$
(P_{x1})_{total} = P_{x1} - \tfrac{1}{2}P_{x2} - \tfrac{1}{2}P_{x3} - \frac{\sqrt{3}}{2}P_{y3} + \frac{\sqrt{3}}{2}P_{y3} \qquad (3.52)
$$

Similarly,

$$
(P_{y1})_{total} = P_{y1} - \tfrac{1}{2}P_{y2} - \tfrac{1}{2}P_{y3} + \frac{\sqrt{3}}{2}P_{x2} - \frac{\sqrt{3}}{2}P_{x3} \qquad (3.53)
$$

After substitution for P_{x1}, P_{y1},..... etc, and rearranging, the result is given by

$$
(P_{x1})_{total}/F = \frac{3}{2}\frac{\delta r}{C/2}\,[a_{11}\cos\phi + a_{12}\sin\phi + a_{21}\sin\phi + a_{22}\cos\phi]
$$

$$
(P_{y1})_{total}/F = \frac{3}{2}\frac{\delta r}{C/2}\,[a_{11}(-\sin\phi) + a_{12}(-\cos\phi) + a_{21}\cos\phi + a_{22}(-\sin\phi]
$$

(3.54)

The force F is calculated from the following expression

$$F = \frac{\mu DLN}{S} \left(D/C\right)^2 \qquad (3.55)$$

The calculated stiffness by using expression (3.54) and the calculated stiffness from the numerical solution are plotted in figure 3.28. It may be seen that there is satisfactory agreement between both methods of calculation. Furthermore, as expected the stiffness given by the approximate method is greater than the stiffness given by the numerical solution because in the approximate solution each lobe was considered to be as a full circular bore bearing whilst the actual lobe in the numerical solution was of 100^{o} arc.

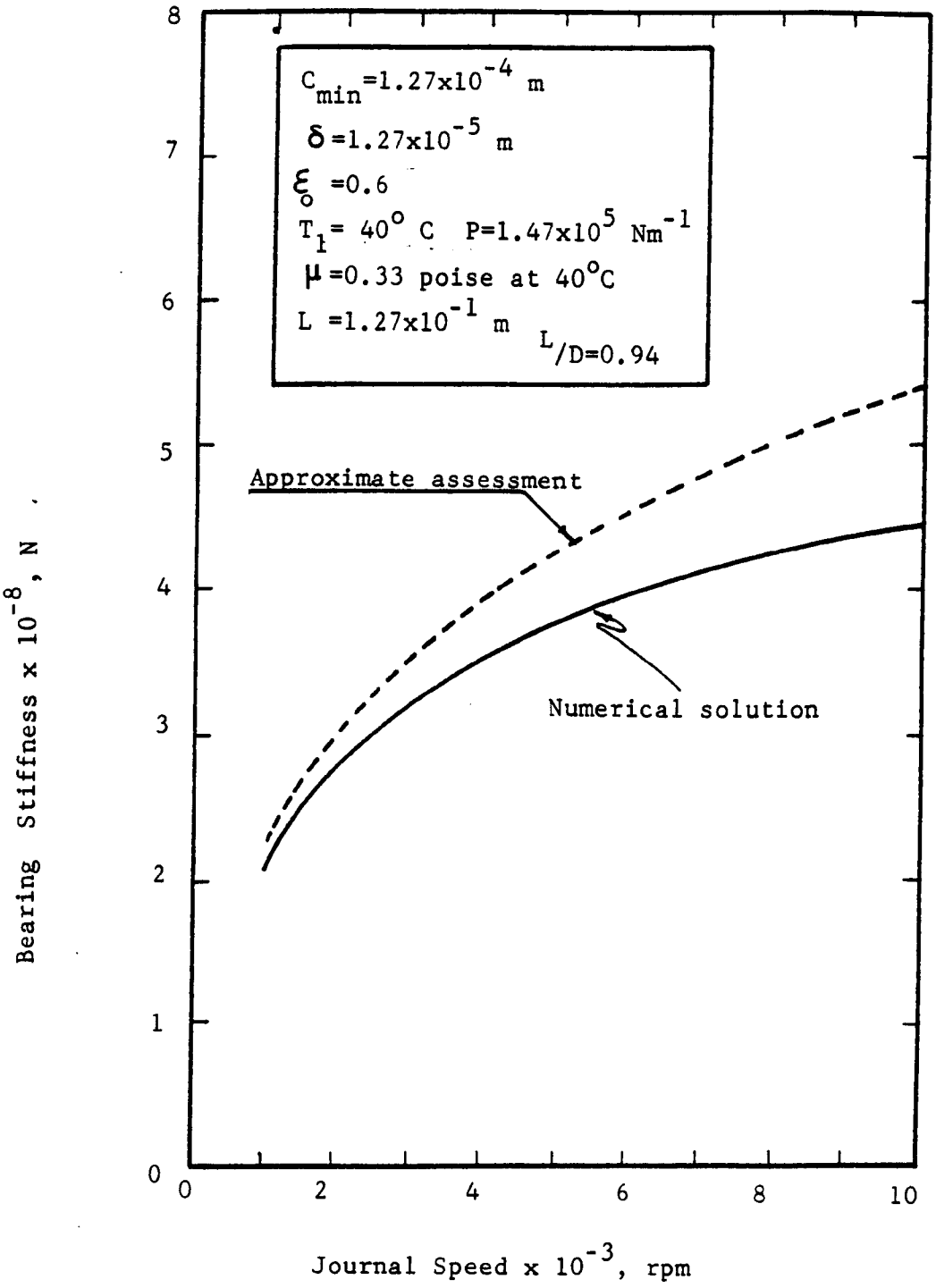

FIG.3.28 Variation of bearing stiffness with the Journal speed.

C H A P T E R 4

4. PRELIMINARY EXPERIMENTAL WORK

4.1 Introduction

The literature on hydrostatic bearings covers bearings with pockets, and with compensation by capillary or by orifices means, however nothing has been found in the literature upon a three lobe hydrostatic bearing, nor upon hydrostatic bearings of any kind which have no pockets, and which are compensated by constant volume valves. Because of this there seemed to be good reason in the first instance to investigate in a relatively simple rig, and without rotation of the journal, the hydrostatic behaviour of the bearing. Such a rig would provide a screening test before proceeding to the far greater elaboration required for high speed testing. It also seemed reasonable to suppose that a non-rotating journal would behave similarly to a journal running so slowly that little self-generation is present.

4.2 Test Rig

The bearing as arranged for hydrostatic test is shown in Figure 4.1. The rig does not permit continuous rotation, but the effect of applying the force in different directions with respect to the lobes may be tested by rotating the bearing in its frame. The force is applied by a hydraulic ram, and the force is calculated from the cross-sectional area, and the ram pressure. The movement of the journal with respect to the bearing is measured with dial gauges capable of reading down to 0.00254 mm. (0.0001 inch), and four dial test indicators, two at each end, are mounted to detect the vertical displacement as well as the horizontal displacement. The absence of metal to metal contact between journal and bearing was monitored by measuring the electrical resistance between journal and bearing. High pressure oil was supplied from the high pressure pump to the high pressure inlets via individual volume

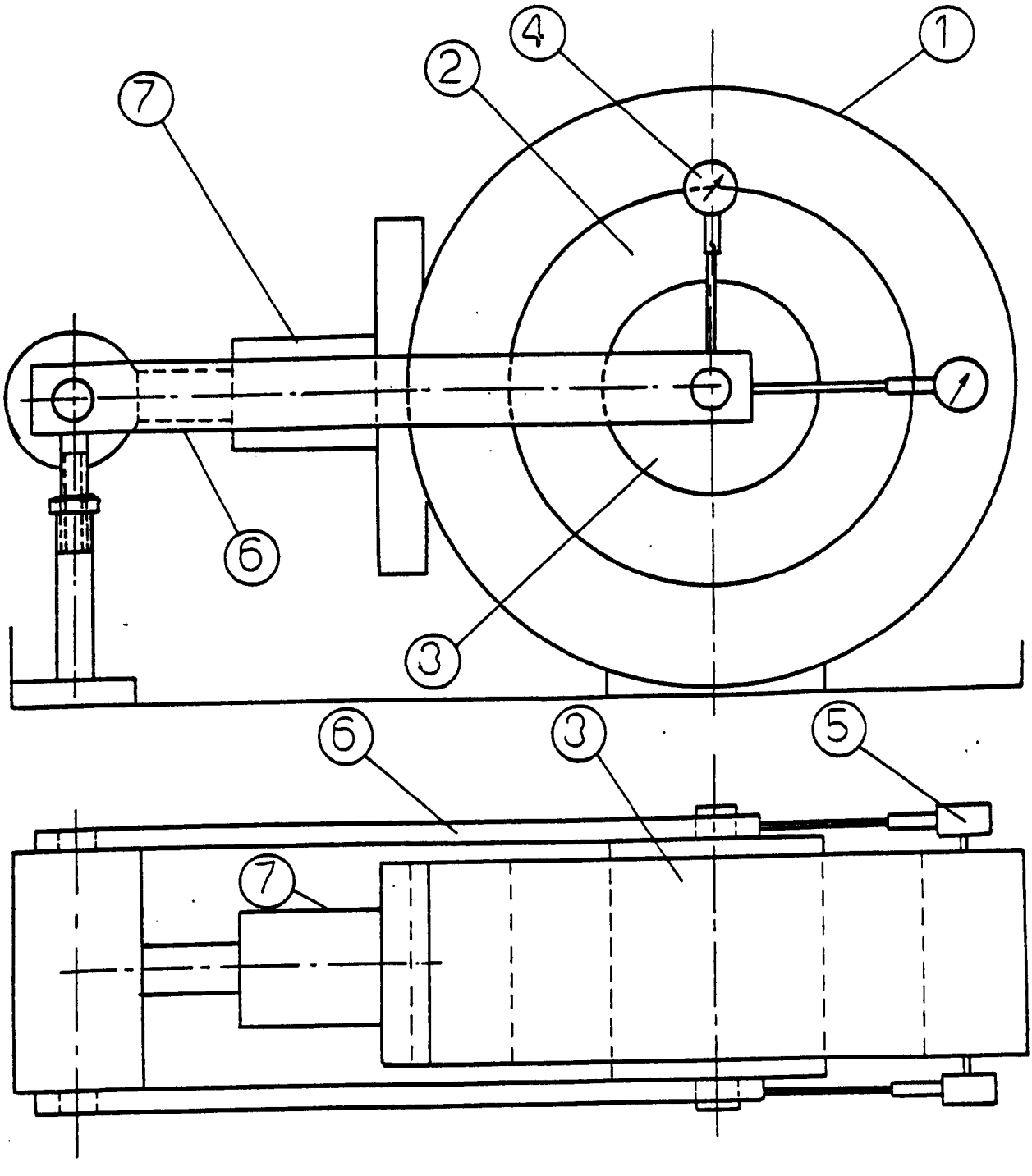

1	Steel housing	5	Dial gauge
2	Brass shell	6	Loading arms
3	Journal	7	Hydraulic ram
4	Dial gauge		

FIG.4.1 Test rig for external pressurization.

control valves. Volume control valves were chosen for the reasons which are reported in Chapter 1 and Chapter 2. The supply pressure from the pump was measured, oil temperature and pressure were measured downstream of each of the the volume control valves. A photograph of the test rig with its instrumentation is shown in Figure 4.2. The rod to be seen in the left was provided against the possibility that the journal would be angularly unstable within the bearing. However, no need arose to use the rod.

4.3 The Bearing

The concept of the bearing which was used in the experimental work is illustrated by Figure 4.3. The bearing was made by splitting a brass cylinder into three segments, by reassembling the segments but separated by shims, by boring the assembly circular, by removing the shims and finally by turning the outer surface circular (Figure 4.4). The thickness of shims (t) was calculated from $t = 2\ \Delta r \sin 60$ to provide the required offset of the centres of the lobes. Particular care had to be taken with the abutments of the three segments so that no bending was introduced on tightening (Appendix A4). A high pressure oil inlet for the hydrostatic regime is provided at the centre of each lobe, and a low pressure inlet is provided for the self-generating regime at each conjunction of the lobes. The form achieved by the process is shown by the roundness chart of Figure 4.5. The departures from the intended form are 0.00254mm ($\sim$ 5%).

4.4 Test Procedures

Before experimental testing was commenced the flow characteristics of each valve were tested by measuring volume flows at different valve settings, at different supply pressures and at different oil temperatures. Details are given in Appendix A7. It was confirmed that the valves do deliver a constant volume flow.

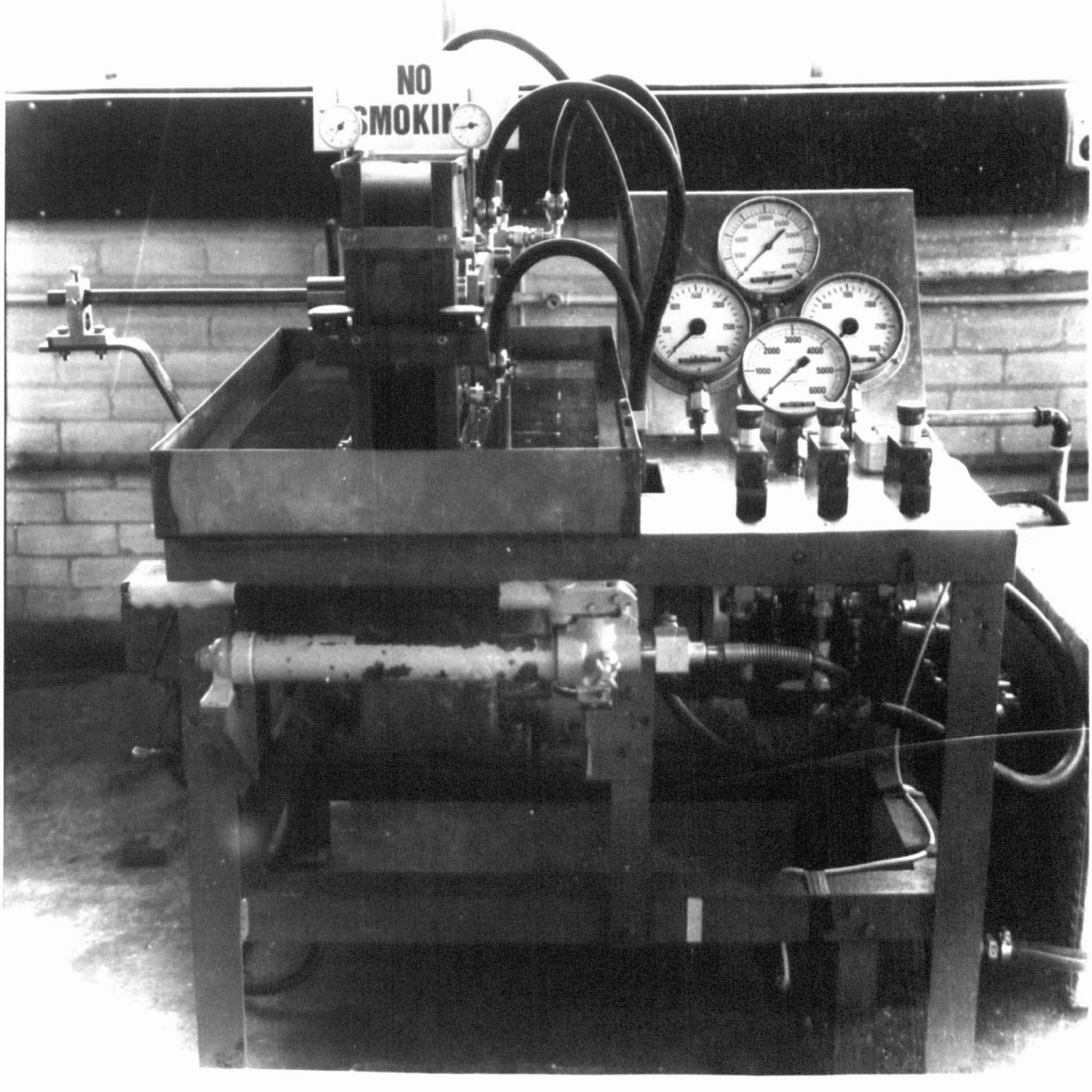

FIG. 4.2 HYDROSTATIC TEST RIG.

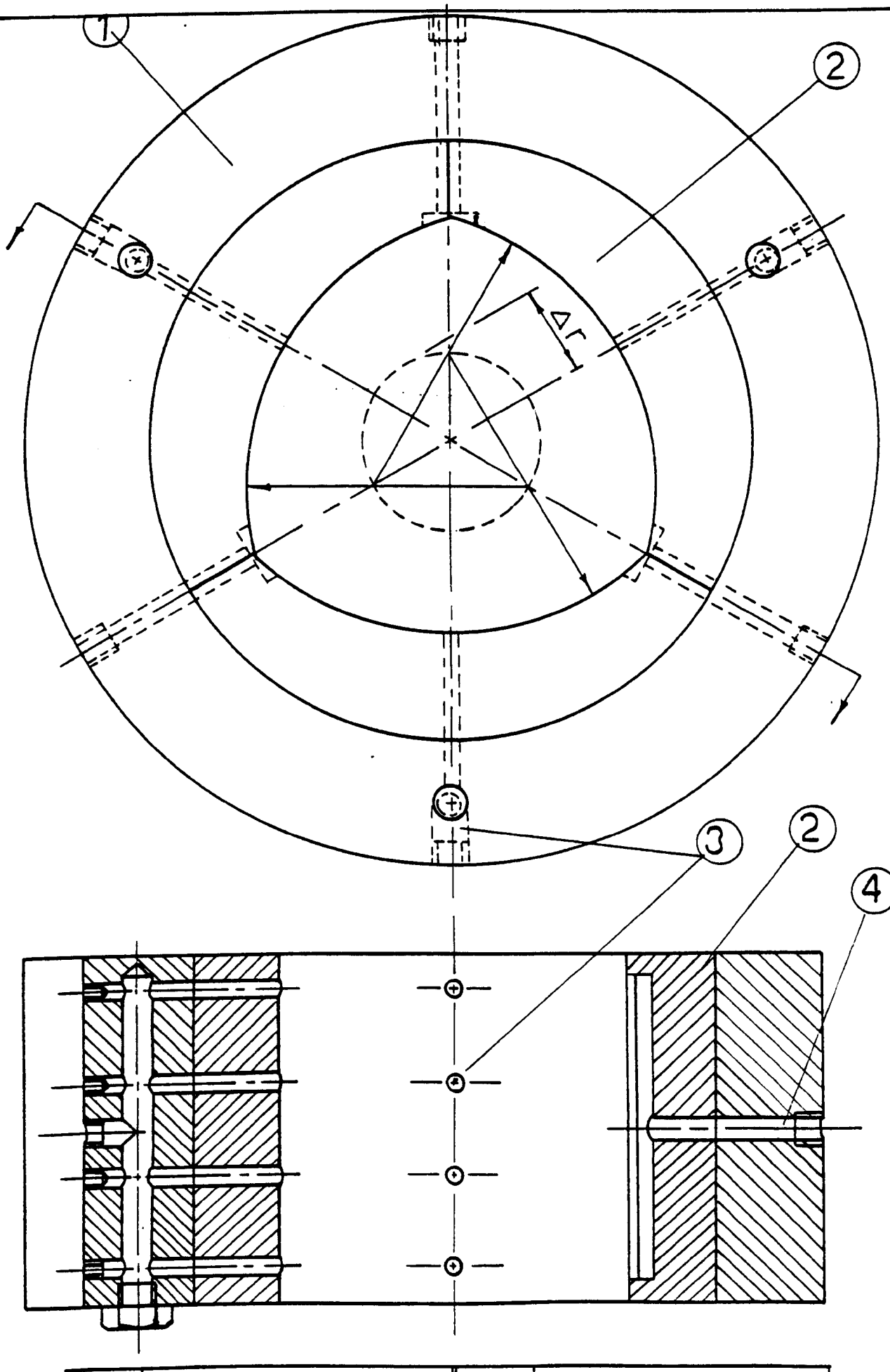

1	Steel housing	3	High pressure inlet
2	Brass shell	4	Low pressure inlet

FIG.4.3 Three lobe-bearing for hydrodynamic and hydrostatic operation.

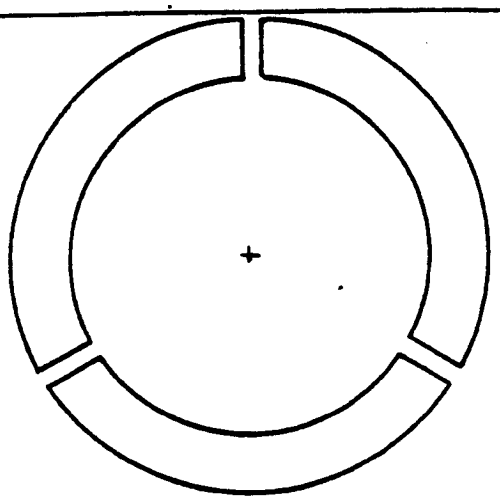

(a) A brass cylinder splitted into 3 segments.

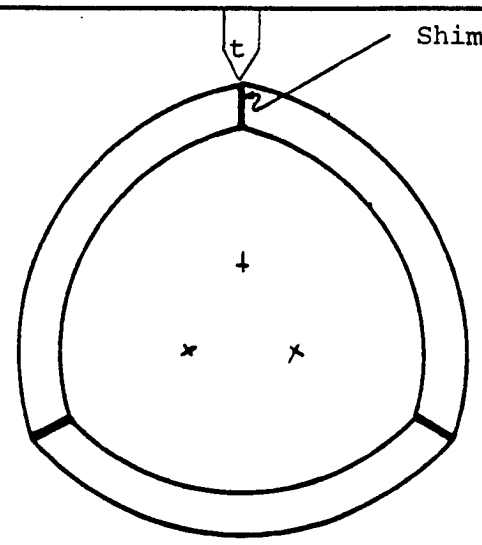

(b) The segments reassembled and separated by shims.

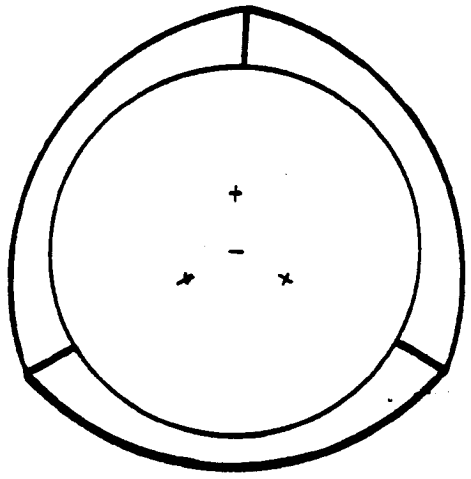

(c) The assembly bored circular.

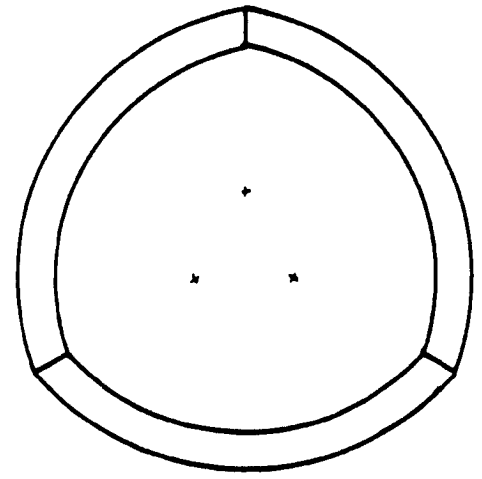

(d) The shims are removed.

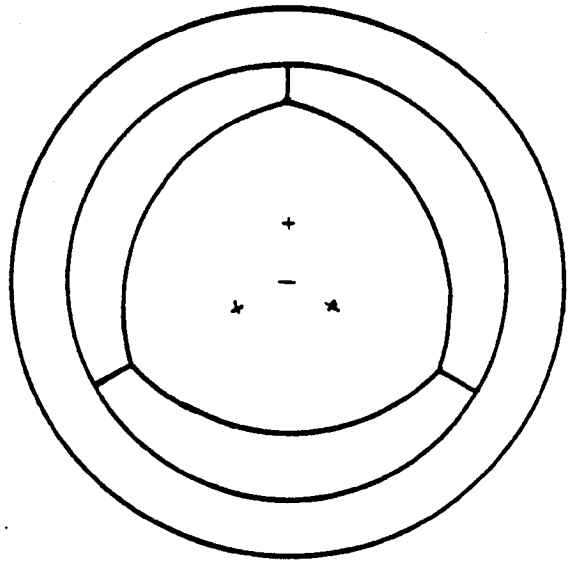

(c) The outer surface turned circular and the assembly fitted into steel housing.

FIG.4.4 The Machining steps for a bearing shell.

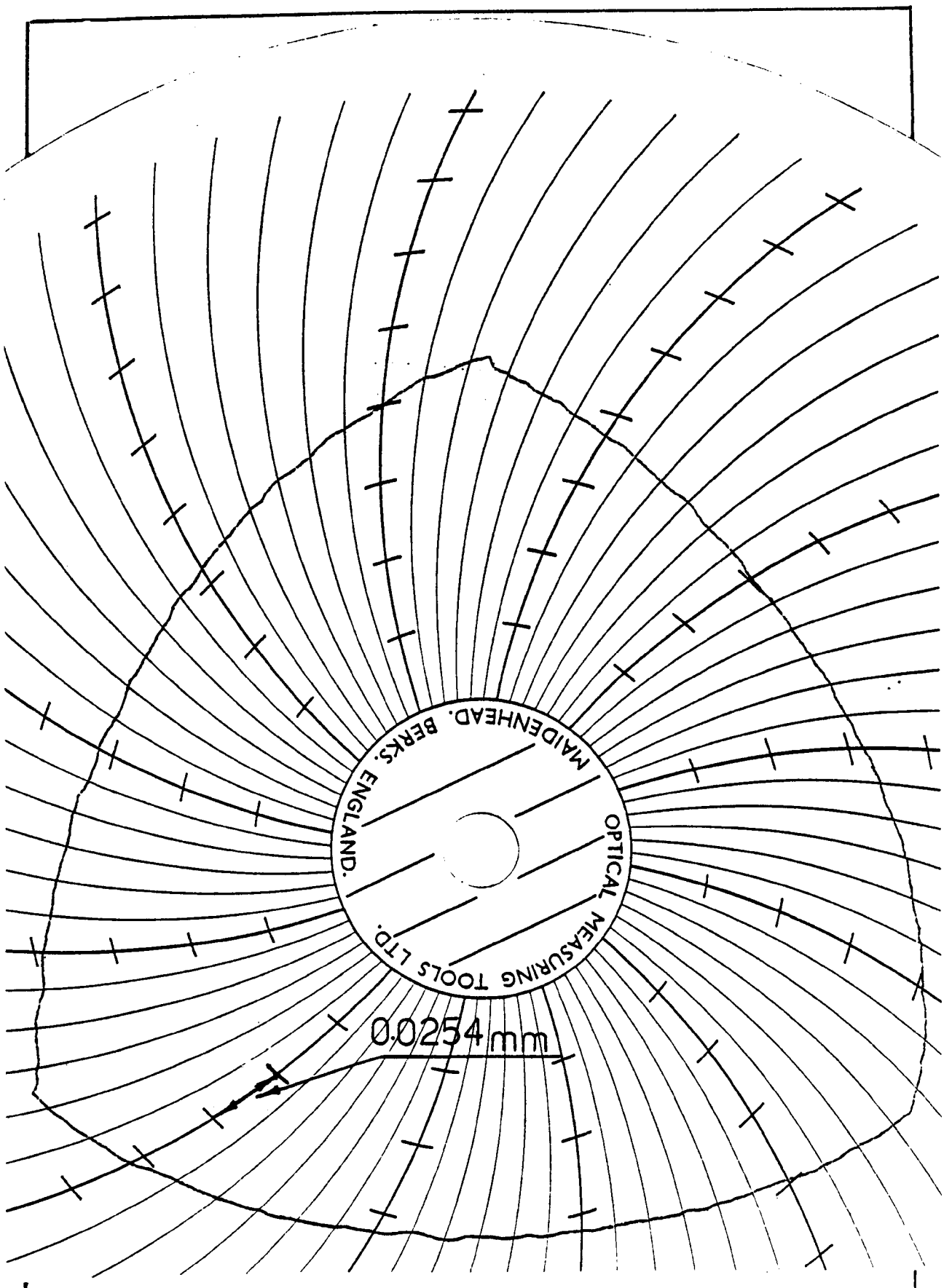

FIG.4.5 PROFILE OF FINISHED BEARING.

The bypass of the high pressure pump, and the values were adjusted to give the desired supply pressure and the desired volume flow. In the static rig no oil cooler was provided, and in consequence the oil temperature rose over the full sequence of the testing. However, within a test at particular values of supply pressure and volume flow, the oil temperature rise was small so that a particular oil temperature could be attributed to each individual test.

Horizontal load was applied to the journal by means of the hydraulic jack, the position of the journal in the bore of the bearing was measured both horizontally and vertically by means of dial gauges, and the pressure downstream of a constant flow valve, which is the inlet pressure to a lobe, was measured. It was found by careful attention to the symmetry of loading that the rig could be adjusted so that the journal remained parallel to the axis of the bearing as the journal moved. The criterion is obviously equality of dial gauge measurements at each end of the bearing. A small vertical displacement of the journal was noticed at the start of loading, but it did not increase as the load was increased.

Results were obtained with lobe diametral clearances from 2.6×10^{-4} to 3.7×10^{-4}m (0.0104 to 0.0144 inch). The dimensions of the test bearing are given in Table 4.1. The different diametral clearances were obtained by machining the journal.

4.5 Test Results

The tests were carried out with an oil which has a viscosity of 20 cp. at 75°C (Shell Vitria 150). Conditions of test were supply pressures from $1.03 \times 10^{7} Nm^{-2}$ to $2.06 \times 10^{7} Nm^{-2}$ (from 1500 to 3000 psi), total volume flow from 0.1 to 0.2 litres per second. Pumping powers were from 2.8

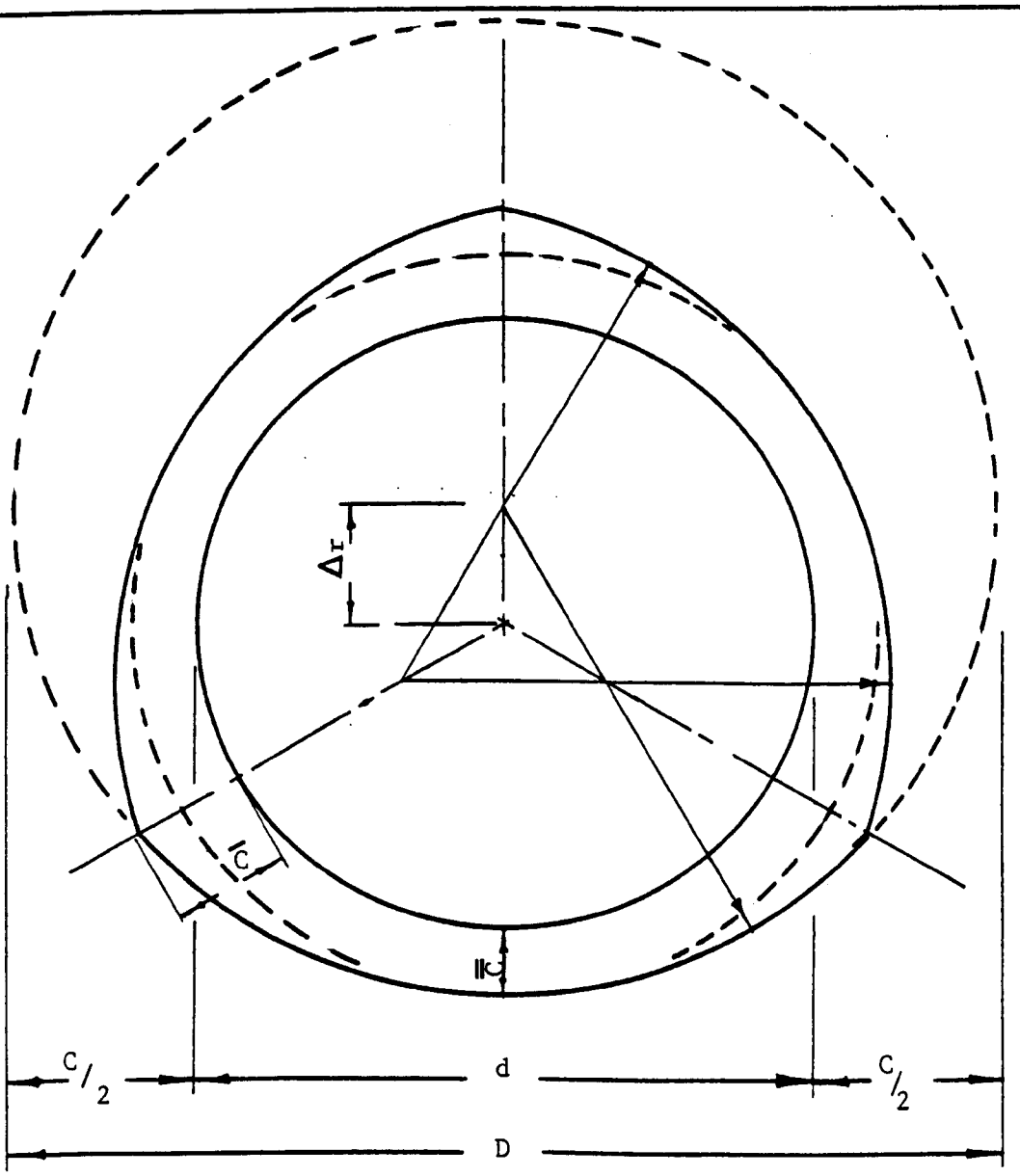

Designation of Bearing	D* m	d m	Δ_r m	C m	$\bar{C}$ m	$\bar{\bar{C}}$ m
1	1.352×10^{-1}	1.349×10^{-1}	5.75×10^{-5}	2.6×10^{-4}	1.45×10^{-4}	2.025×10^{-4}
2	1.352×10^{-1}	1.348×10^{-1}	5.75×10^{-5}	3.0×10^{-4}	1.85×10^{-4}	2.425×10^{-4}
3	1.352×10^{-1}	1.348×10^{-1}	5.75×10^{-5}	3.7×10^{-4}	2.55×10^{-4}	3.175×10^{-4}

* $L/D = 0.94$

TABLE 4.1 Dimensions of test bearings.

to 6.6 KW, oil temperatures at inlet were from 40 to 70°C. Stiffnesses were found typically of $1x10^{9}Nm^{-1}$ ($\sim 5.7x10^{6}$lb in^{-1}), and there was no metal to metal contact up to the maximum load which was $5.6x10^{4}N$ ($\sim$5.7 tons).

Specific test results are shown in Figures 4.6 to 4.10. In Figure 4.6 journal displacement is shown as a function of load for three rates of oil flow. In all tests the supply pressure was $1.7x10^{7}Nm^{-2}$ (2500 psi), and at no load the ratio between the supply pressure and the downstream pressure was approximately 0.6. The results show that the displacement load relationship is not exactly linear and that an increase in volume flow produces an increase in stiffness.

Figure 4.7 shows a plot of journal displacement and of the downstream pressure versus the external load. The circular points are for a load directed towards the conjunction of the lobes and the triangular points are for a load directed towards the centre of a lobe. The difference in the measured displacement in both directions is insignificant and the only difference was in the downstream pressure which as is to be expected has a greater value when the load is applied through the centre of the lobe.

In Figure 4.8 the lobe downstream pressure and the rate of flow are shown as functions of the external load. The oil flow was not measured directly but measured from the calibration table which is given in Appendix A7. However, in the proper bearing rig flow meters were fitted in the high pressure lines and the measurements then made confirmed the correctness of the procedure adopted in Figure 4.8.

In Figure 4.9 the bearing stiffness is plotted versus the bearing pressure ratio (i.e. the ratio between the downstream pressure at zero

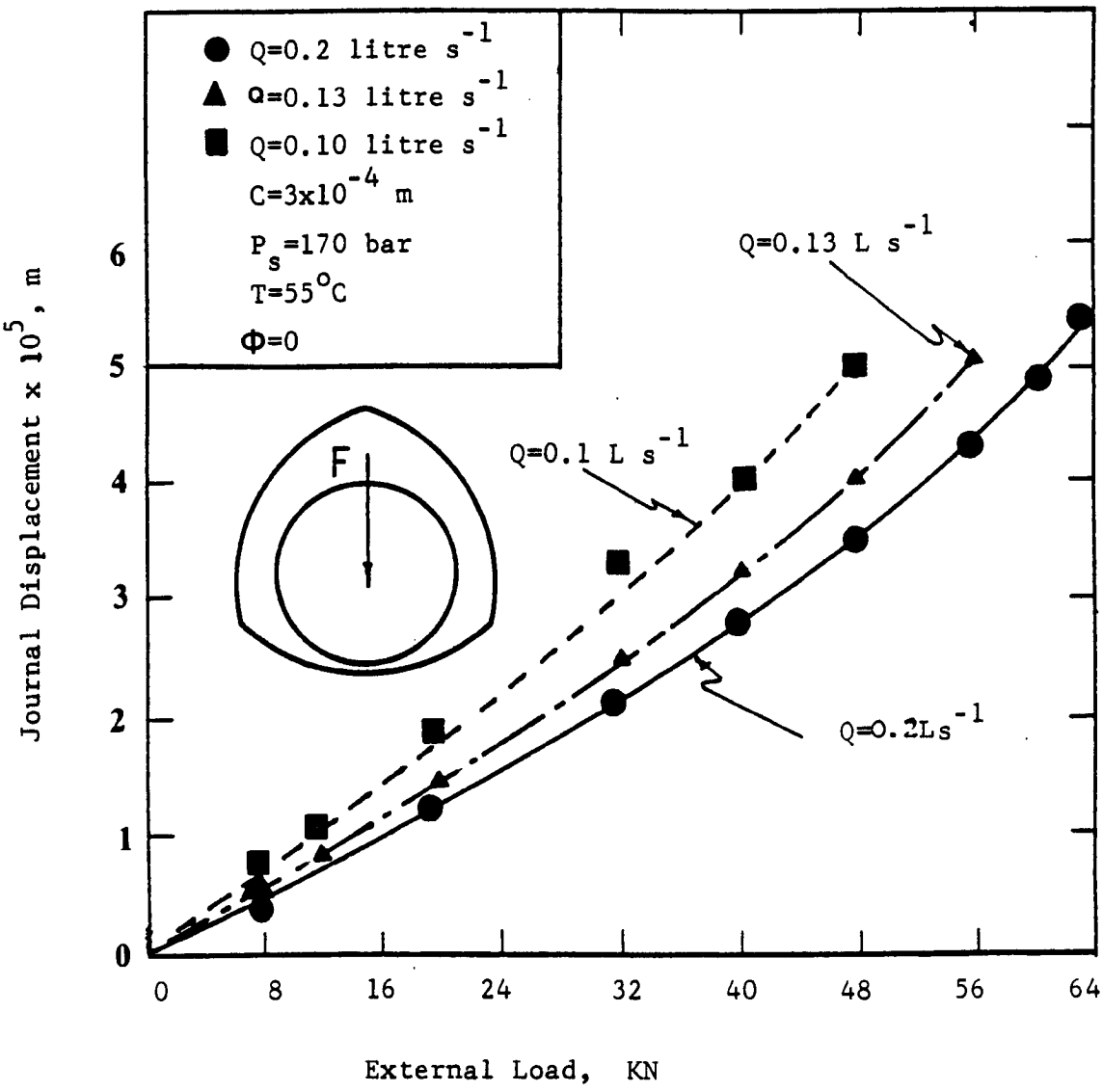

FIG.4.6 Load displacement relationship for different rates of flow.

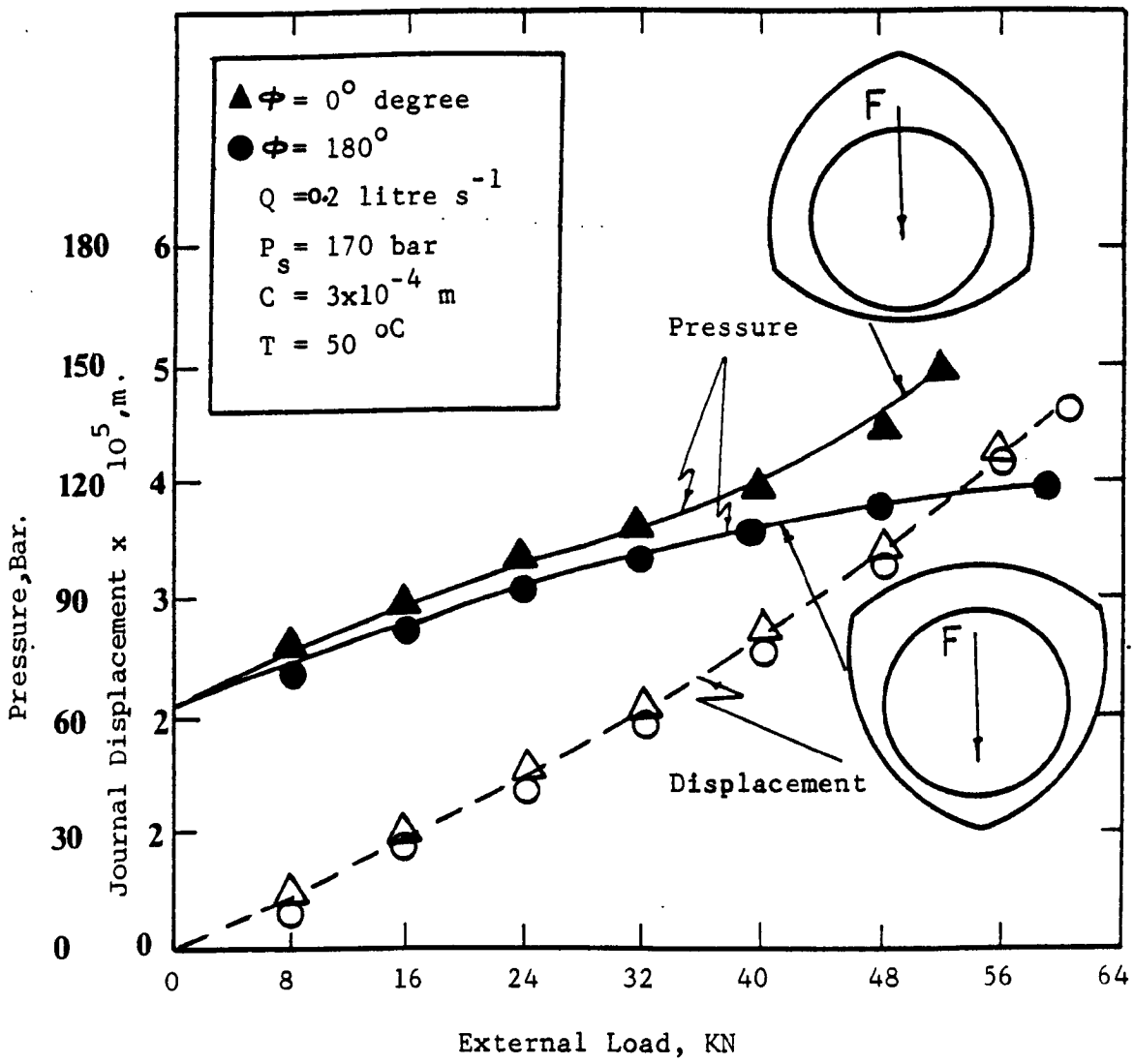

FIG.4.7 Load displacement, and load pressure relationship for two different direction of loading.

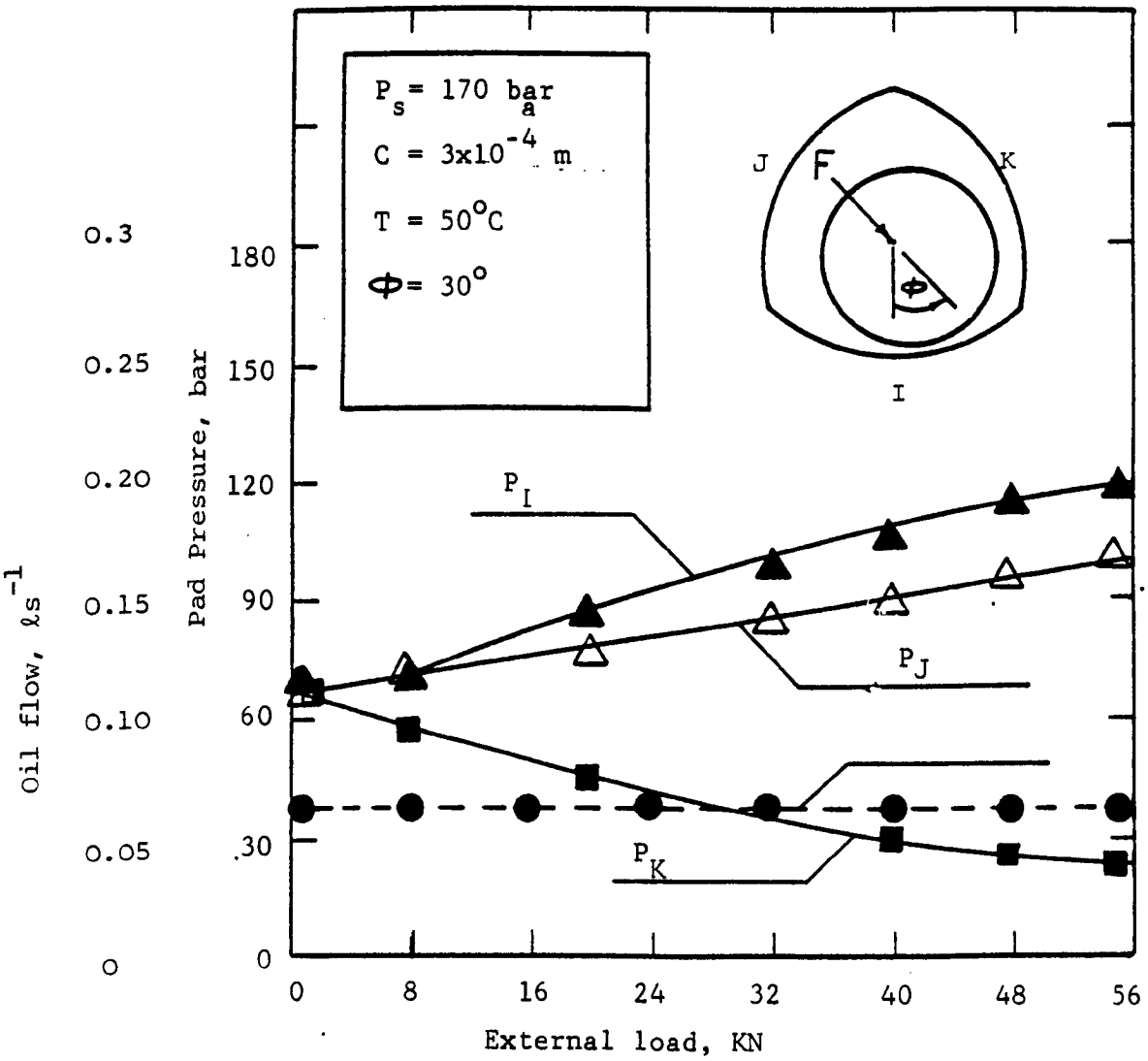

FIG.4.8 Variation of lobes pressure and oil flow with the external load.

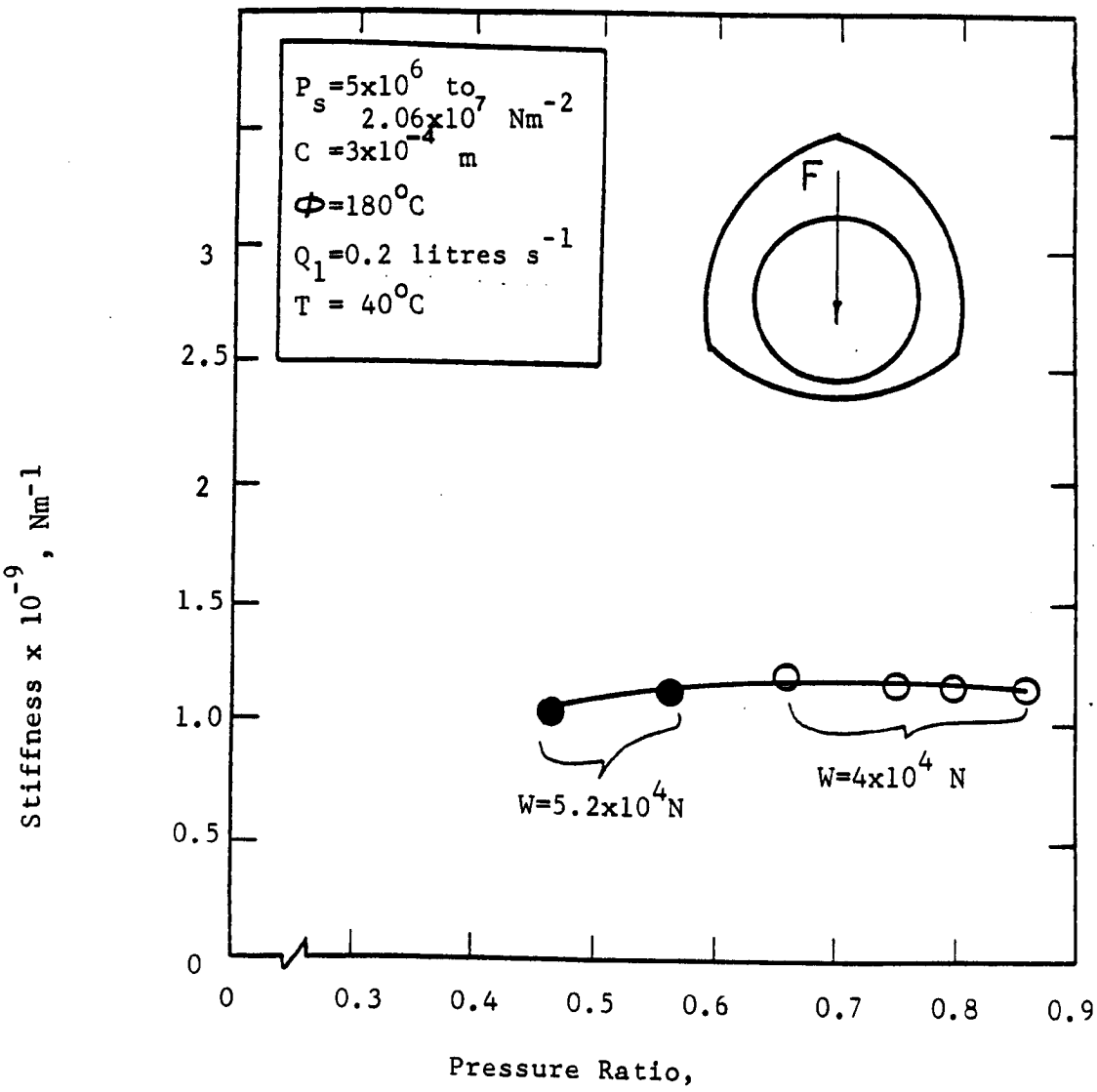

FIG.4.9 Variation of stiffness with the pressure ratio.

load and the pump pressure). For constant valve settings and constant viscosity the pressure ratio was adjusted to the desired value by adjusting the supply pressure. It may be seen from Figure 4.9 that the bearing stiffness is independent of the pressure ratio and in consequence the stiffness is independent of the supply pressure. The minimum pressure drop across a valve during this test was $7 \times 10^{5} Nm^{-2}$ ($\sim$ 100psi).

4.6 Discussion

From the tests which have been carried out with the three lobe bearing, the experimentally determined performance substantially matches or exceeds the functional specification of Table 1.1. For instance, the functional specification calls for a stiffness in finishing of $8 \times 10^{8} Nm^{-1}$ at low speed. It may be seen from Figure 4.10 that this stiffness can be obtained with a diametral clearance of $3.3 \times 10^{-4} m$, with a supply pressure of $1.7 \times 10^{7} Nm^{-2}$, with a total volume flow of 0.31 litres per second and with a pumping power of 3.8KW. Also it may be seen that at a diametral clearance of $3 \times 10^{-4} m$, a stiffness of $1 \times 10^{9} Nm^{-1}$ was achieved. In addition the functional specification calls for a pressure on projected area of $3.86 \times 10^{6} Nm^{-2}$. From Figure 4.6 a pressure of $3.73 \times 10^{6} Nm^{-2}$ on projected area* was achieved experimentally without metal to metal contact. It is concluded that the bearing configuration which has been tested is capable of satisfying the slow speed specification of the functional specification.

The hydrodynamic predictions for the bearing and journal dimensions of the hydrostatic tests were reviewed to see if an acceptable hydrodynamic performance would be likely. The hydrostatic tests have covered diametral clearances of 2.6, 3 and $3.7 \times 10^{-4} m$. It has been predicted

* The actual load is 6.4×10^{4} N.

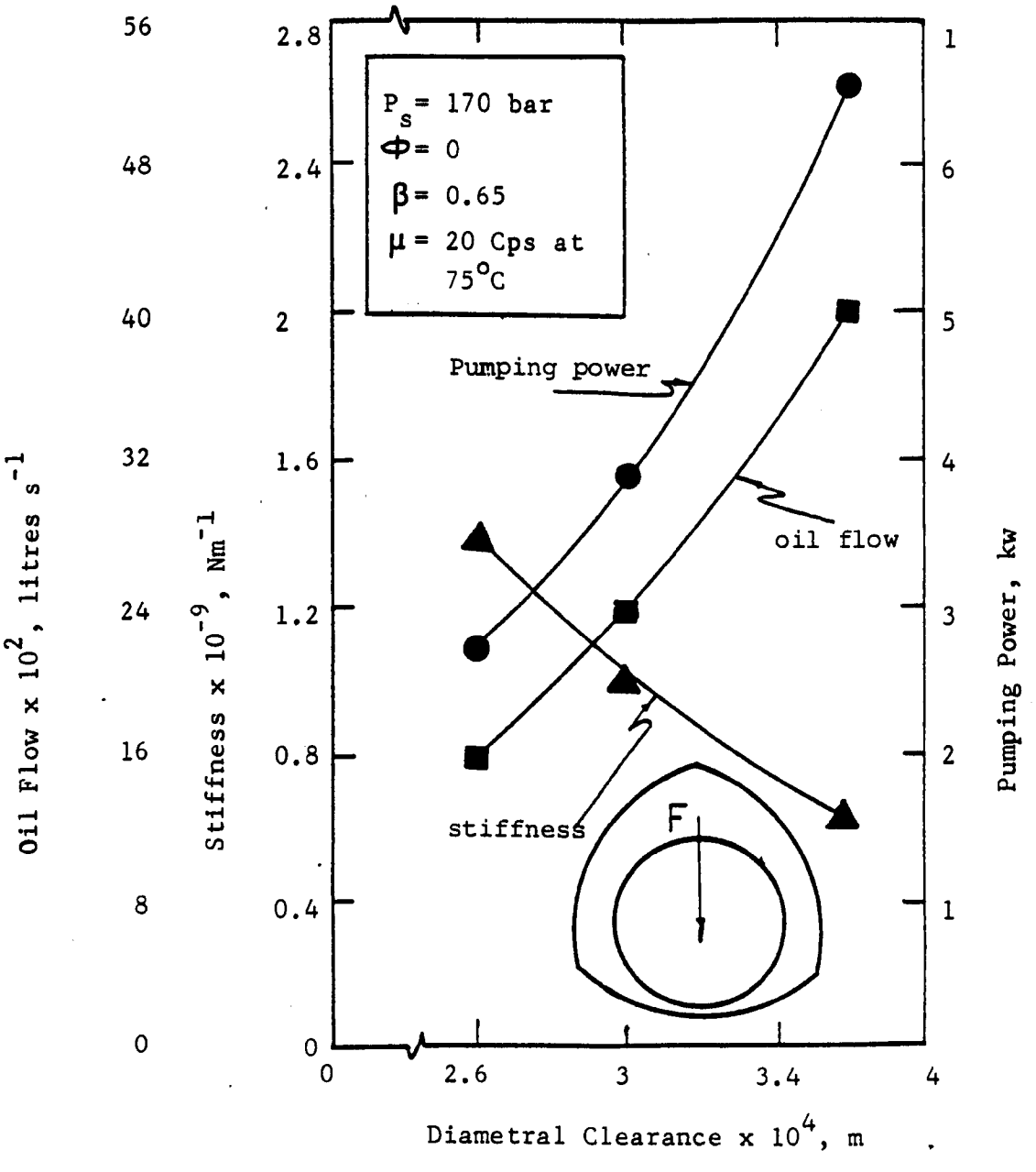

FIG.4.10 Variation of stiffness, oil flow, and pumping power with the diametral clearance.

in Chapter 3 that under hydrodynamic conditions the power loss increases marginally as the diametral clearance is increased, that the oil temperature rise falls, and that the stiffness falls marginally. However, because the predicted hydrodynamic stiffness exceeds the stiffness required by the specification the fall in stiffness as the diametral clearance is increased is of no consequence in the hydrodynamic regime, and the lesser rise in oil temperature favours a larger rather than a smaller diametral clearance, but in the hydrostatic regime the stiffness with a diametral clearance of 3.7×10^{-4}m is too low, and consequently a maximum diametral clearance between 3 and 3.7×10^{-4}m had to be set for the hydrodynamic tests. Another consideration is that it is easy to increase diametral clearance by reducing journal diameter while to decrease the clearance requires the building up of the journal. The final dimensions for hydrodynamic testing was a diametral clearance of 2.6×10^{-4}m, with the intention of employing a greater diametral clearance when a knowledge existed of the actual hydrodynamic performance of the initial clearance.

CHAPTER 5

NUMERICAL ANALYSIS OF THE THREE-LOBE EXTERNALLY PRESSURIZED JOURNAL BEARING .

5. NUMERICAL ANALYSIS OF THE THREE-LOBE EXTERNALLY PRESSURIZED JOURNAL BEARING .

5.1. Introduction

In Chapter 2 an approximate analysis has been described for the externally pressurized circumstances with zero shaft speed. The analysis has provided a reasonable prediction for the steady-state parameters, (i.e. oil flow rate, load capacity, stiffness, supply pressure and pumping power). In Chapter 2, the analysis was simplified by reducing the Navier Stoke's equation to the case of the infinitely wide journal bearing with zero speed of rotation. The pressure between the adjacent lobes was assumed to be zero, and the oil was considered to flow in the circumferential direction and then out of the bearing through the low pressure grooves. Consequently the steady state parameters (i.e. load and stiffness) were considered to be dependent only on the circumferential flow. Furthermore, the problem was simplified by taking the journal as symmetrically disposed with respect to each lobe. To obtain a closer approximation to the oil flow out of the bearing, the axial flow from both ends of the bearing was calculated on the basis of a linear pressure drop along the bearing width and a constant pressure around the lobe arc equal to half the inlet pressure. The results from these approximate calculations have been described in Chapter 2.

It is to be expected that an actual bearing would depart substantially from these simplifying assumptions. In an actual bearing the pressure at the low pressure grooves is not zero, and it was found from the experimental measurements that the pressure at the axial grooves is

about 20% of the pressure at the high pressure inlets.

In this chapter a numerical solution based upon the finite difference formulation of the Reynolds eqn. will be described. This numerical solution is distinguished from the numerical solution described in Chapter 3, in that in the present instance the following circumstances obtain:-

i) A condition which has to be satisfied is that the oil flow rate at each high pressure inlet has to be the same. This is in contrast with the condition in Chapter 3 in which the only boundary condition specified was the dimensionless pressure at the boundary of the lobe.

ii) The pressure at the high pressure inlets must be finite and becomes a specified boundary condition. Pressures are expressed non-dimensionally as $P^* = P/P_o$, where P_o is in essence the ($\xi_B = 0$) pressure downstream of the control valves.* When the journal is centred within the bearing the pressure downstream of each control valve must be the same at all the lobes. In the computer programme the dimensionless pressure downstream of the control valve of each lobe may be set as input from some small finite value to unity. The oil flow rate, in dimensionless form, is then calculated as a function of the dimensionless pressure at the high pressure inlets.

When the journal is displaced within the bearing the dimensionless pressures downstream of each control valve are no longer equal, but the nondimensional oil flow remains the same as it was when

*P_o is the pressure downstream of the control valves when the journal is centred within the bearing.

the journal was in its central position. There is an iteration procedure within the computer programme by which the dimensionless pressure downstream of each control valve is found such that the dimensionless flow through each control valve is the same, and is also equal to the dimensionless flow through each control valve when the journal was in its central position. The iteration procedure starts with the input of the same dimensionless pressure downstream of each valve as has been described in the context of the centralized journal, i.e. each calculation starts with a centralized journal and then proceeds to the displacement of the journal.

The displacement of the journal is specified within the programme, and the journal is displaced successively to ε_B = 0, 0.1, 0.2,...., 0.9. With stationary journal the load and displacement are co-linear. With journal rotation this is no longer so. The computer programme is arranged to maintain the vertical direction of journal displacement, and outputs the departure from co-linearity of the load.

iii) Reynolds' equation is to be solved both for the zero speed and finite journal speed circumstances. In the former instance the right hand side of Reynolds' equation is zero (eqn. 5.1 below).

iv) The calculation of the oil flow includes the pressure induced flow in the axial direction, the pressure induced flow in the circumferential direction and the shear flow in the circumferential direction whereas in Chapter 3 the axial flow only has been calculated.

v) Because of the possibility of circumferential oil flow from one lobe to another, Reynolds' equation has to be solved for the bearing as a whole in contrast with the lobe by lobe treatment of Chapter 3. The finite difference mesh has to cover all the lobes.

5.2. Finite Difference Solution.

The solution of Reynolds equation will be performed by using the finite difference formulation as has been described in paragraph 3.2 (Chapter 3). Also the assumptions of the finite difference solution are the usual assumptions implicit in Reynolds equation including constant viscosity which will be treated as the outlet viscosity. When the journal speed is not zero, the pressure distribution solution may yield negative pressures. Negative pressures are set to zero as was described in paragraph 3.2.

The required form of Reynolds equation is,

$$\frac{\partial}{\partial X}\left(\frac{1}{\mu}\, h^3 \frac{\partial P}{\partial X}\right) + \frac{\partial}{\partial z}\left(\frac{1}{\mu}\, h^3 \frac{\partial P}{\partial z}\right) = 6U \frac{dh}{dx} \qquad (5.1)$$

The dimensionless forms which have been used in the numerical solution of Chapter 3 will be used here except that the dimensionless pressure will be defined as

$$P^* = \frac{P}{P_O} \qquad (5.2)$$

where, P_O is the($\varepsilon_B = 0$) pressure downsteam of the control valves. When the journal is in its central position (i.e. $\varepsilon_B = 0$), the highest value for P at a high pressure inlet with the pressure drop across the control device may be used as the supply pressure.

In dimensionless form equation (5.1) becomes

$$\frac{\partial}{\partial X^*}\left(H^{*3}\ \frac{\partial P^*}{\partial X^*}\right) + \left(\frac{D}{L}\right)^2 \frac{\partial}{\partial Z^*}\left(H^*\ \frac{\partial P^*}{\partial Z^*}\right) = 6\Pi S_p\ \frac{dH^*}{dX^*} \qquad (5.3)$$

where,

$$Sp = \frac{\mu N}{P_o}\ (D/_C)^2 \qquad (5.4)$$

The speed parameter (Sp) is related to the running speed of the externally pressurized bearing, to the lobe pressure, to the outlet viscosity and to the lobe diameter - clearance ratio.

When N = O, then Sp = O and the right hand term of equation (5.3) is zero. Equation (5.3) has been transformed to a finite difference form by the same procedure used with equation (3.2) and the finite difference equation becomes:

$$\left\{P^*_{i,j}\right\}_{k+1} = \left[\frac{\begin{array}{l}\left\{6\Pi Sp\left(\frac{H_{i,j-1} - H_{i,j+1}}{\Delta X}\right)^*\right\} + \left\{(P_{i,j+2})(H_{i,j+1})^3/\Delta X^2\right\}^* \\ + \left\{(P_{i,j-2})(H_{i,j-1})^3/\Delta X^2\right\} \\ + \left\{(D/L)^2(P_{i+1,j})(H_{i+1,j})^3/\Delta Z^2\right\}^* + \left\{(D/L)^2(P_{i-1,j})(H_{i,j+1})^3/\Delta Z^2\right\}^* \end{array}}{\left\{(H_{i,j+1})^3/\Delta X^2\right\}^* + \left\{(H_{i,j+1})^3/\Delta X^2\right\}^*} \right.$$
$$\left. + (D/L)^2\left\{(H^3_{i+1,j}/\Delta Z^2)^* + (H^3_{i-1,j}/\Delta Z^2)^*\right\}\right]_K \qquad (5.5)$$

For a mesh of i = 1 to m+1 and j = 1 to n + 1 where n is even and with the assumption that pressures at the boundary are known, then there are (n-1) x (m-1) linear simultaneous equations which have to be solved by the over relaxation technique which has been previously used in Chapter 3.

The iteration procedure starts with the P's around the boundary set to zero except at the high pressure inlets where the dimensionless boundary pressure is set to a finite value $0<P^* \leq 1.0$.

The particular grid employed in the calculations for the complete bearing is shown in figure 5.1. Because the axial grooves do not break through over the full axial length of the bearing, the flow from one lobe to the adjacent lobes depends upon the pressure distribution in these adjacent lobes so that the three lobes are being treated here simultaneously, whereas in Chapter 3 each lobe has been treated separately and the pressure distribution was calculated for each lobe independently. In figure 5.1, i = 1 to 29 (m = 28), j = 1 to 181 (n = 180) so that there are 28 x 89 = 2403 equations to be solved.

5.3. Method of Solution for Complete Bearing.

To solve equation (5.5), the boundary conditions around each lobe must be stated. To find the pressure at each inlet as well as the pressure at each point of the grid when the shaft is displaced within the bearing, equation (5.5) is solved typically by setting the dimensionless pressure P* for zero journal eccentricity to unity at all the bearing inlets. The pressure at each grid point is then calculated. The oil flow out from each lobe is calculated and is considered as the reference flow. Because the journal is central within the bearing, then the pressure in all the lobes is the same and there is no pressure induced flow nor velocity induced flow in the circumferential direction to give a net delivery of oil from one lobe to another. All oil must leave each lobe axially (Fig.5.2a

Figure 5.1. Bearing Grid.

Now, when the solution is performed for an eccentricity ratio greater than zero, the solution yields a flow rate out of the lobe which is initially different from the flow calculated at $\varepsilon_B = 0$ (i.e., the reference flow). With reference to figures 5.2b and 5.5, this flow is given by

$$\left(Q_v\right)_{I,J,K} = \left\{2\, Q_a + Q_{c1} + Q_{c2} + Q_{n\ out} - Q_{n\ in}\right\}_{I,J,K} \qquad (5.6)$$

Where:

Q_a: is the flow out from the lobe through the bearing side (pressure induced flow in the **axial** direction).

$Q_{c1,2}$: is the flow from the lobe to the adjacent lobes (pressure induced flow in the circumferential direction).

$Q_{n\ out}$: is the velocity induced flow from the considered lobe to the downstream lobe.

$Q_{n\ in}$: is the velocity induced flow from the upstream lobe to the considered lobe.

Q_v: is the oil flow through the constant flow valve.

The dimensionless pressure at each inlet is then corrected and the solution is repeated until the calculated flow for each lobe is equal with the flow calculated at zero eccentricity ratio. The forces due to the hydrostatic and hydrodynamic pressures are then calculated, and the resultant force in the vertical, and in the horizontal direction are calculated at each lobe. The total force and the angle between the vertical direction and the direction of the total force are also calculated.

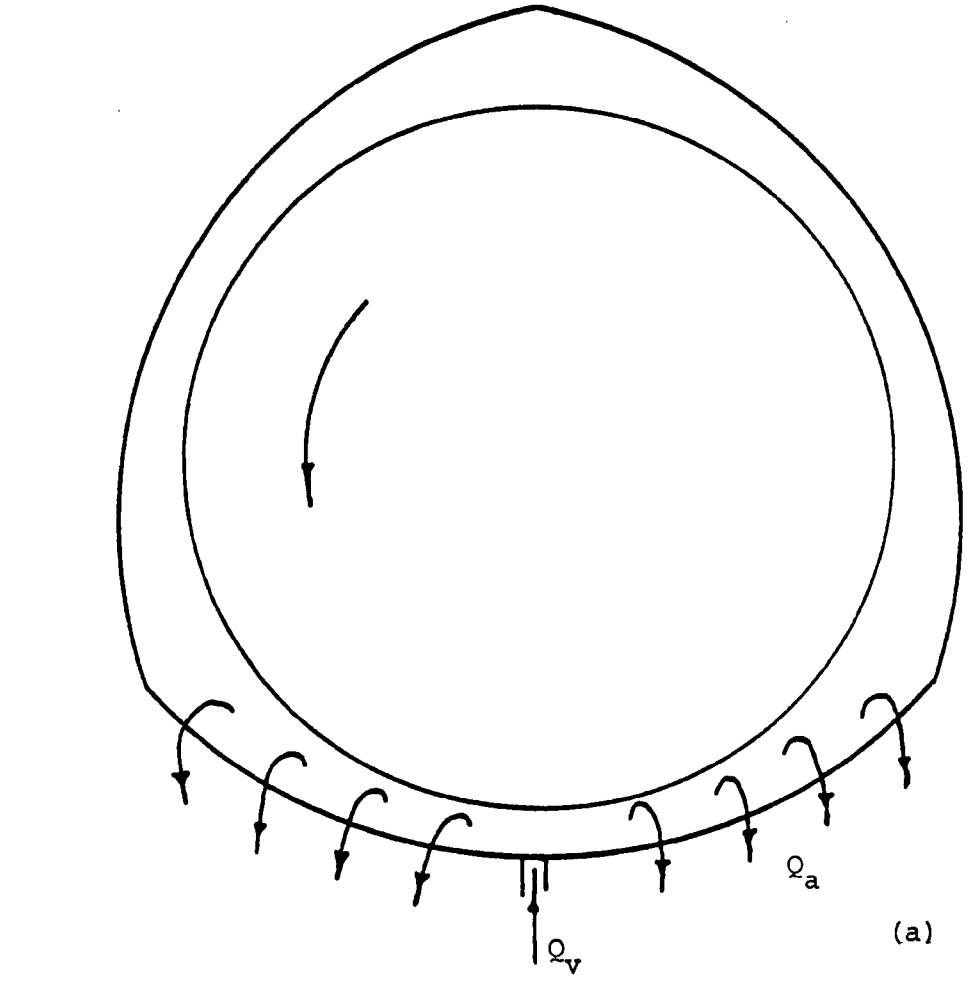

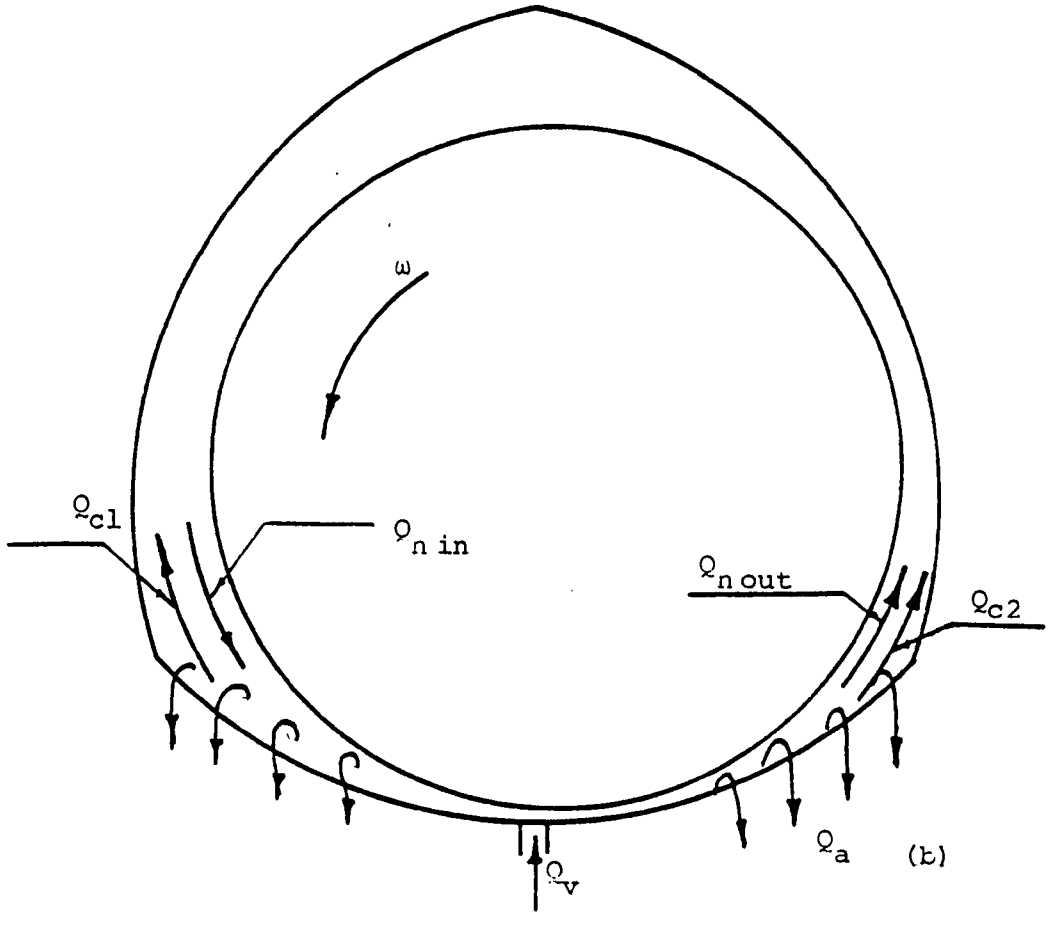

Figure 5.2. Oil Flow Pattern.

A conceptual flow chart of the routine used for the solution is shown in figure 5.3 and may be described as follows:

(1) The dimensionless pressure at the high pressure inlets is given a value of 1.0 (i.e. $P/p_o = 1.0$).

(2) For zero eccentricity ratio (i.e. $\varepsilon_B = 0$), solve equation (5.5) for the pressure distribution.

(3) Calculate the oil fow out of each lobe and retain this flow as the reference flow.

(4) For the given eccentricity ratio and displacement direction, resolve equation (5.5).

(5) Calculate the pressure induced flow and the velocity induced flow out of each lobe (i.e. $Q_v = 2Q_a + Q_{c1} + Q_{c2} + Q_{n\ out} - Q_{n\ in}$).

(6) If the flow equality is not satisfied, return to step 4 and resolve equation (5.5) with new values for the dimensionless pressure at the high pressure inlets. A routine for calculating the revised dimensionless pressures is incorperated into the computer programme and simply adjusts P* at each high pressure inlet in proportion to the departure from the desired flow.

(7) Calculate the generated forces in the direction of the attitude line and in the direction perpendicular on the altitude line, then calculate the load factor.

Two computer programmes have been written for the solution of Reynolds equation for the externally pressurized regime. In both instances the load in the journal is assumed to be towards the centre of a lobe, or to be reversed and to be towards the conjunction of each lobe. In

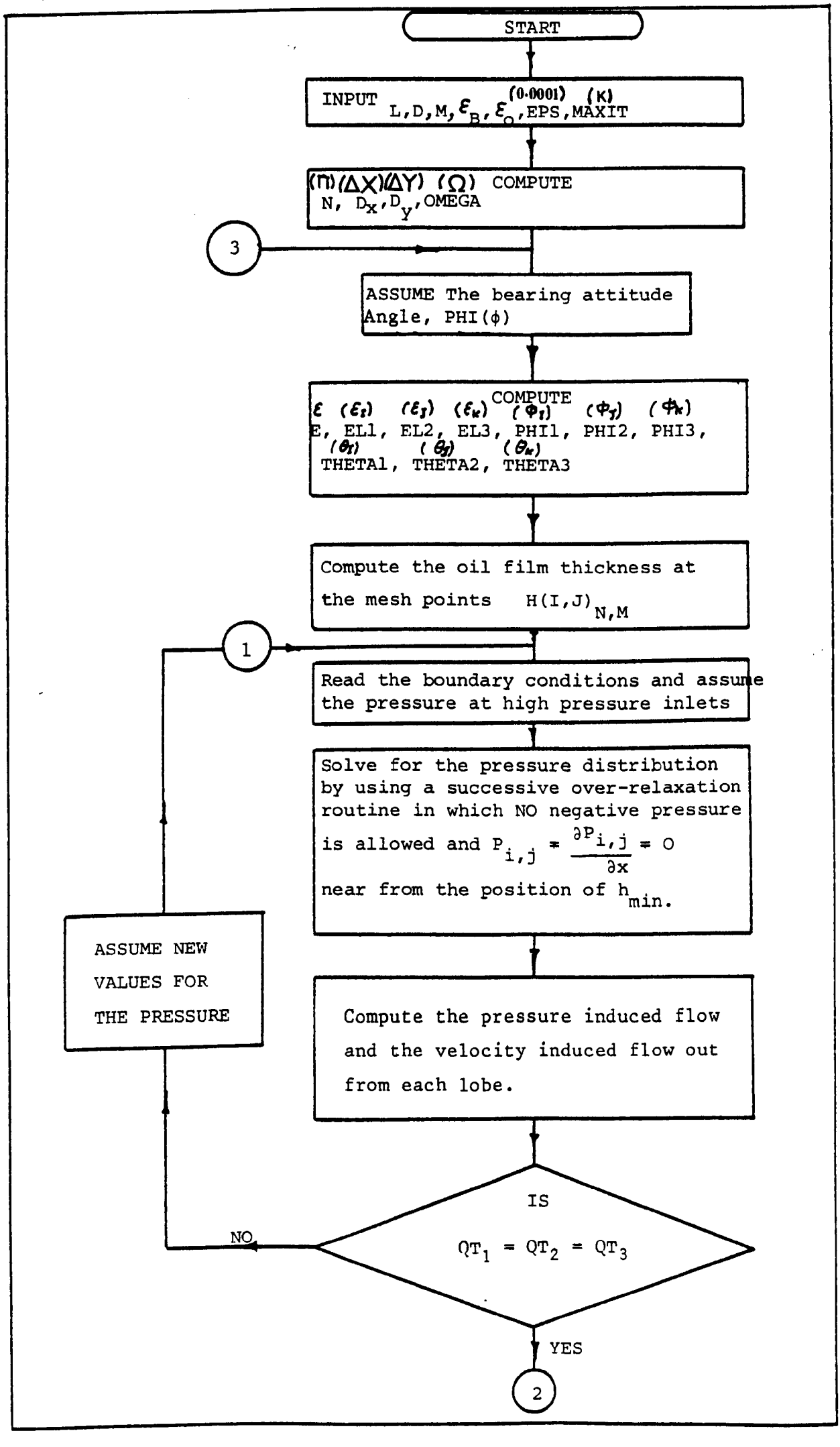
START
INPUT L,D,M, ε_B, ε_o (0.0001), EPS, MAXIT (K)
(Π) (ΔX) (ΔY) (Ω) COMPUTE
N, D_x, D_y, OMEGA
3
ASSUME The bearing attitude Angle, PHI(ϕ)
COMPUTE
ε (ε1) (ε2) (ε3) (εk) (Φ1) (Φ2) (Φ3) (Φk)
E, EL1, EL2, EL3, PHI1, PHI2, PHI3,
(θ1) (θ2) (θ3)
THETA1, THETA2, THETA3
Compute the oil film thickness at the mesh points H(I,J) N,M
1
Read the boundary conditions and assume the pressure at high pressure inlets
Solve for the pressure distribution by using a successive over-relaxation routine in which NO negative pressure is allowed and $P_{i,j} = \frac{\partial P_{i,j}}{\partial x} = 0$ near from the position of h_{min}.
ASSUME NEW VALUES FOR THE PRESSURE
Compute the pressure induced flow and the velocity induced flow out from each lobe.
IS
$QT_1 = QT_2 = QT_3$
NO
YES
2

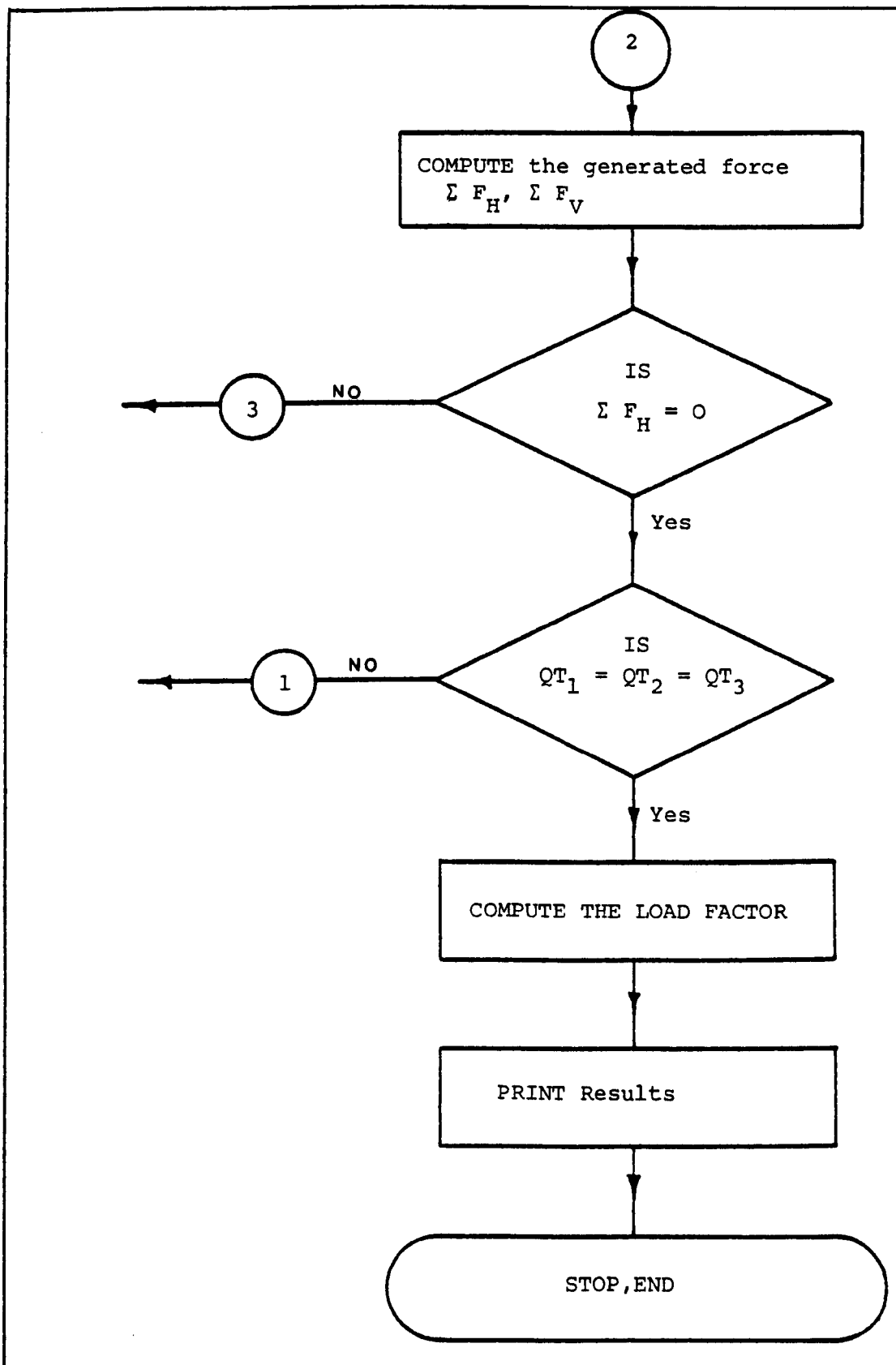

Figure 5.3. Flow Chart for the hybrid bearing computer programme.

the first computer programme, high pressure oil is admitted to the high pressure inlets at the centre of each lobe (figure 5.4., A, B and C), and in the second programme, metered high pressure oil is admitted to the "Low pressure inlets" at the conjunction of the lobes. Through a pressure of time the second programme has not been used comprehensively, and its only use has been the calculation of the pressure flow coefficient for various dimensionless speeds of rotation in the self generating regime as has been described in paragraph 3.5 in Chapeter 3. In this chapter the output of the first programme will be discussed.

5.4. Oil Flow

5.4.1. Axial Pressure induced flow

The oil flow out of a bearing lobe from both ends and which is induced by the pressure difference is given by

$$Q_a = 2 \int \frac{1}{12\mu} h^3 \frac{\partial P}{\partial z} dx \qquad (5.7)$$

where $\frac{\partial P}{\partial z}$ is the axial pressure gradient at the ends of the bearing.

After substituting dimensionless forms for $\frac{\partial P}{\partial z}$, h^3, μ and dx and after rearranging the axial pressure induced flow coefficient is given by

$$\left(q_a\right)_{I,J,K} = (D/L) \int H^{*3} . \frac{\partial P^*}{\partial z^*} . dx^* \qquad (5.8)$$

In numerical form equation (5.8) becomes

$$\left(q_a\right)_{I,J,K} = (D/L) \sum_{j=1,61,121}^{n/3+1,\ 2n/3+1 \text{ and } n+1} H^{*3}_{m,j} \frac{P_{m-1,j} - P_{m+1,j}}{2.\Delta Z}^{*} . \Delta X^* \qquad (5.9)$$

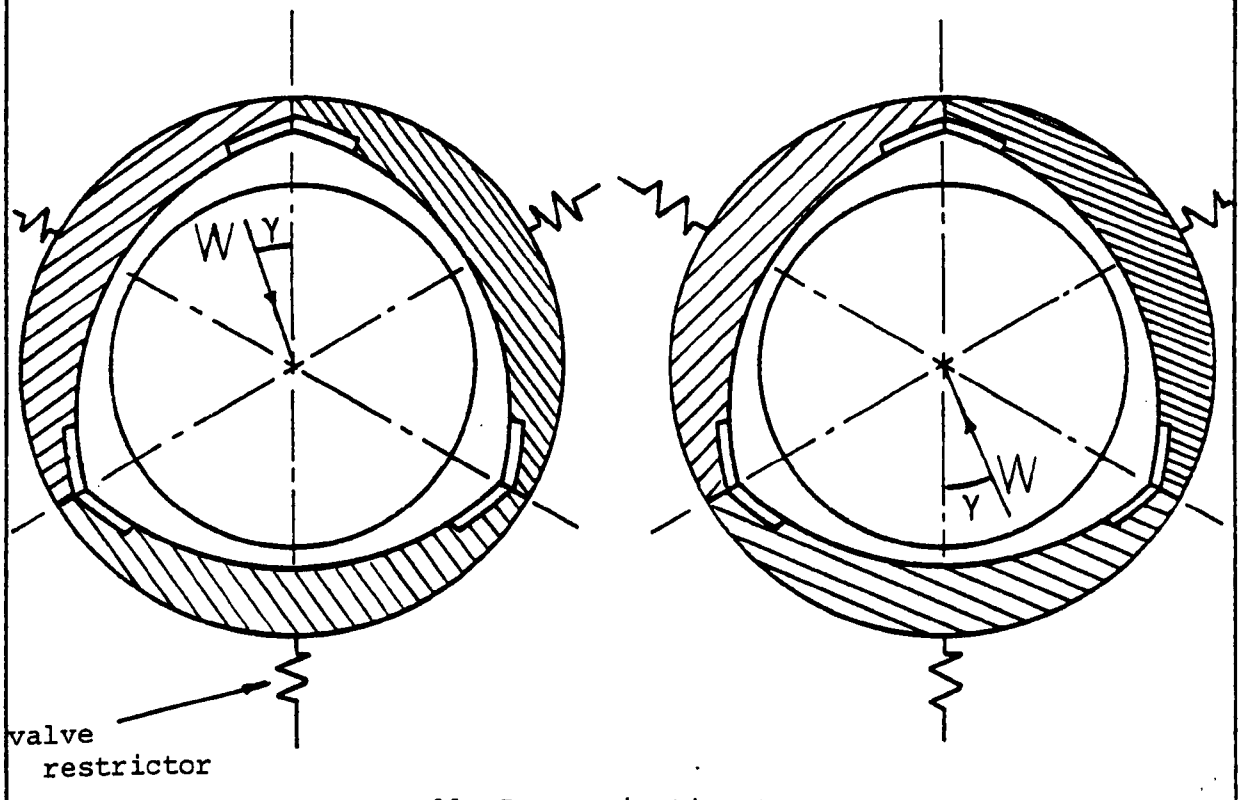

Externally Pressurization type - A

Loading type - B

Loading type - C

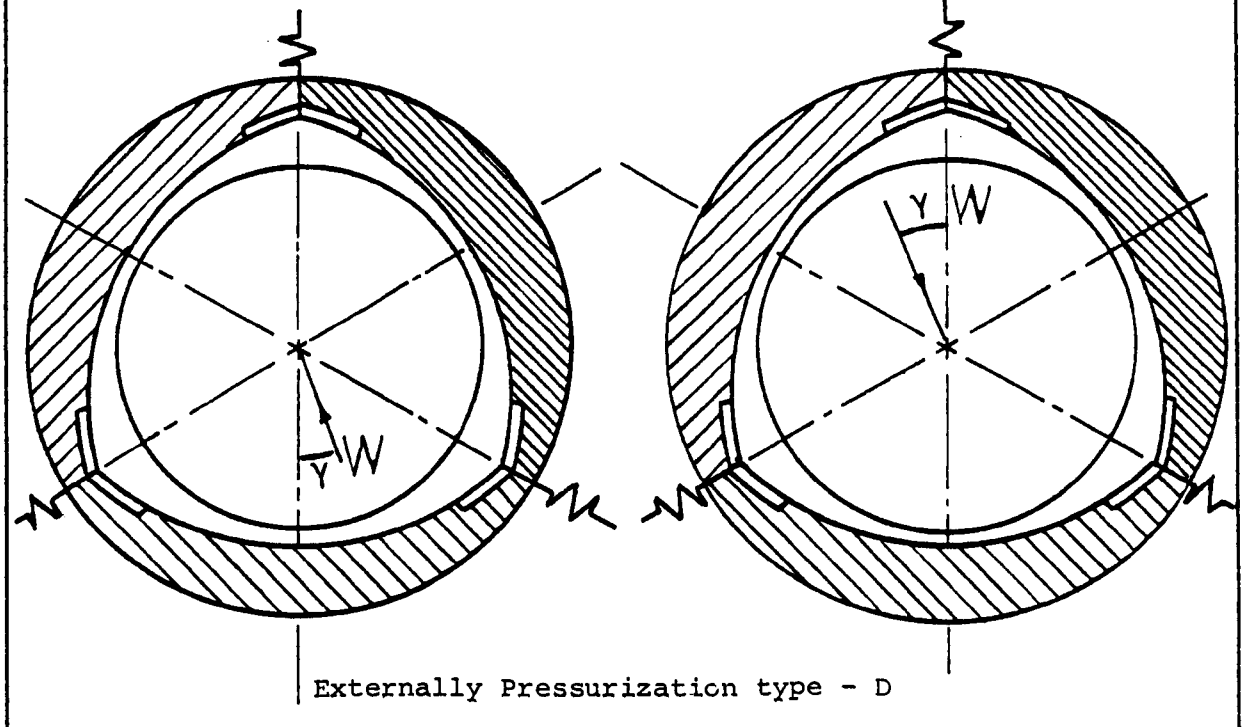

Externally Pressurization type - D

Loading type - E

Loading type - F

Figure 5.4. Arrangement of Externally Pressurization and Loading.

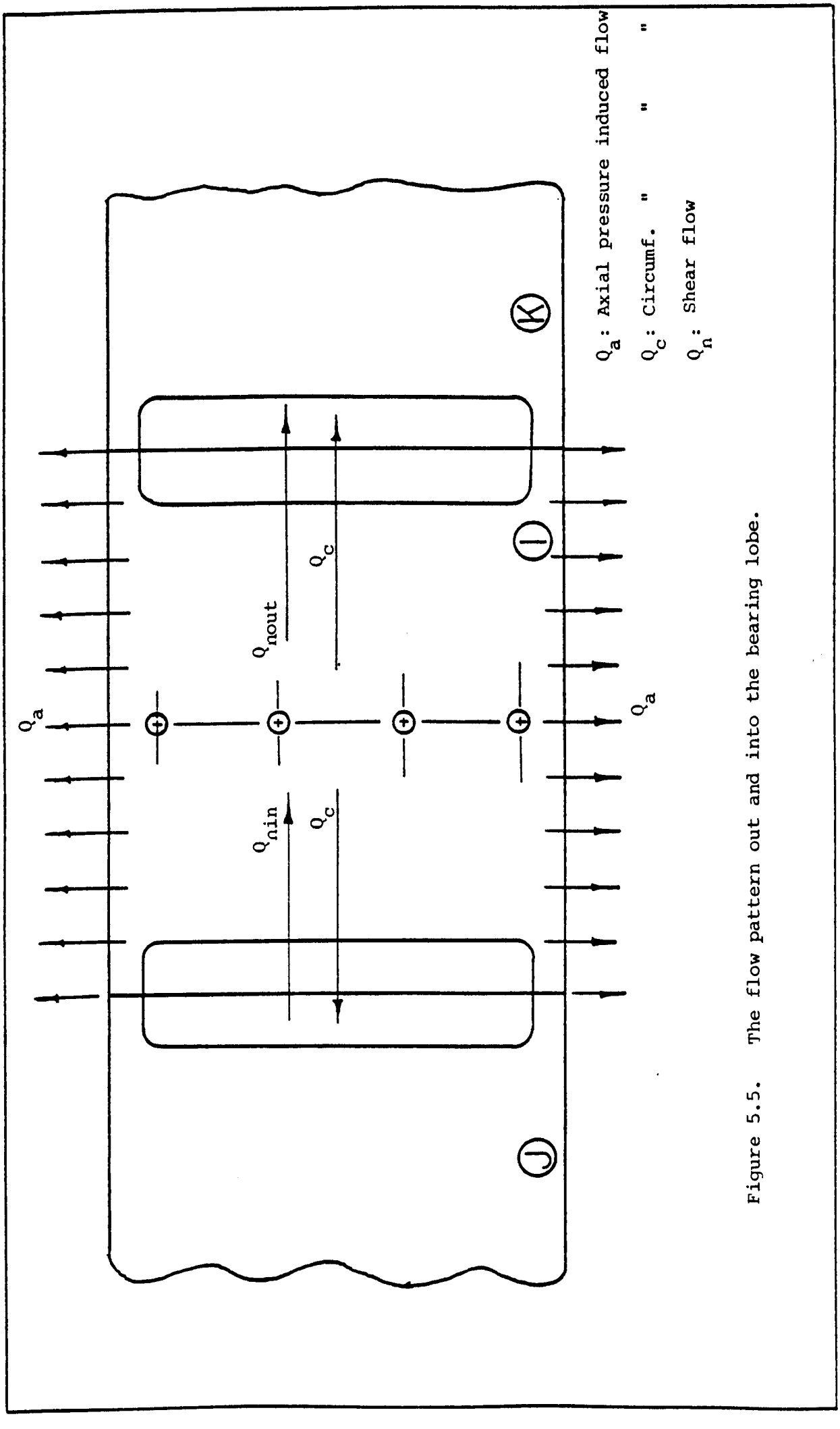

Figure 5.5. The flow pattern out and into the bearing lobe.

The calculation of q_a from expression (5.9) depends upon prior solution of Reynolds equation (5.5) to give the pressure distribution over the complete bearing. The calculation of q_a is incorporated in the same computer programme.

The oil flow out of each lobe may be expressed as

$$\left(Q_a\right)_{I,J,K} = \frac{P_o\, c^3}{6\mu} \cdot q_a \qquad (5.10)$$

5.4.2. Circumferential Pressure Induced Flow

When the bearing eccentricity is zero the pressure in all the bearing lobes is similar, and there will be no flow from one lobe to the adjacent lobes. When the journal is displaced within the bearing a differential pressure between the bearing lobes will exist and leads to a flow from one lobe to the adjacent lobes. This flow is called the circumferential pressure induced flow and is given by

$$Q_c = 2 \int \frac{1}{12\mu} h^3 \frac{\partial P}{\partial X}\, dZ \qquad (5.11)$$

where $\frac{\partial P}{\partial x}$ is the circumferential pressure gradient at the conjunction with the adjacent lobes.

After substituting dimensionless forms for $\frac{\partial P}{\partial x}$, h^3, μ and dz and after rearranging the circumferential pressure induced flow coefficient is given by

$$\left(q_c\right)_{I,J,K} = (L/D) \int H^{*3} \cdot \frac{\partial P^*}{\partial x^*} \cdot dz^* \,. \qquad (5.12)$$

In numerical form equation (5.12) becomes

$$\left(q_c\right)_{I,J,K} = (L/D) \sum_{i=1}^{m+1} H^{*3}_{n,i} \left(\frac{P_{n-1,i} - P_{n+1,i}}{2.\Delta X} \right)^{*} . \Delta Z^{*} \qquad (5.13)$$

The calculation of q_c from expression (5.13) also depends upon prior solution of Reynolds equation (5.5) to give the pressure distribution over the complete bearing. Because the pressure difference and the oil film thickness do not have to be the same at both the right and left sides of the lobe (Lines A-A and B-B in figure 5.1), the circumferential pressure induced flow coefficient (q_c) is calculated separately at each side of the lobe and that is incorporated in the same computer programme. The value of q_c is positive when the flow of lubricant is flow out of the lobe and is negative when the lubricant flows into the considered lobe.

5.4.3. Velocity Induced Flow

The flow in the direction of rotation due to the rotation of the journal is equal to the shear flow and is given by

$$Q_n = \frac{h}{2} UL \qquad (5.14)$$

After substituting dimensionless form for h and after rearranging, the velocity induced flow coefficient is given by

$$q_n = \frac{2\, Q_n}{\pi DNLC} = H^{*} \qquad (5.15)$$

Where

H^{*} is the dimensionless oil film thickness at the lobe sides (lines A-A and B-B in figure 5.1),

q_n is the velocity induced flow coefficient.

5.4.4. The Total Oil Flow

The quantity of oil which is delivered to an externally pressurized bearing is held constant whether the journal is stationary or rotating at any speed. The oil flow rate which is calculated for a concentric stationary journal is the oil flow rate which will be maintained constant at any bearing eccentricity and at any speed by the compensation device (in this investigation the compensation device is a constant volume flow valve). However, for a concentric journal within the bearing there will be no net flow in the circumferential direction, and the only flow out of the bearing is the axial pressure induced flow which is calculated at zero bearing eccentricity from expression (5.10) for each lobe.

The total flow rate through the compensating devices and out of the bearing is given by

$$Q_t = 3\, Q_v = \sum_{I,J,K} Q_a \tag{5.16}$$

where at $\varepsilon_B = 0$, $(Q_a)_I = (Q_a)_J = (Q_a)_K$

5.5. Load and Load Factors*

From the obtained pressure distribution, the load components in the direction of attitude line and the direction perpendicular on the attitude line at each lobe are found from

$$\left.\begin{aligned} (W_x)_{I,J,K} &= \int P.dx.dz.\ \cos\theta. \\ (W_y)_{I,J,K} &= \int P.dx.dz.\ \sin\theta. \end{aligned}\right\} \tag{5.17}$$

*for notation, see figure 3.6.

After substituting dimensionless forms for P, dx and dy and after rearranging, expression (5.17) may be written as:

$$\left.\begin{aligned}(W_x)_{I,J,K} / (P_o \quad LD) &= \int P^* dx^* dz^* \cos\theta \\ (W_y)_{I,J,K} / (P_o \quad LD) &= \int P^* dx^* dz^* \sin\theta\end{aligned}\right\} \qquad (5.18)$$

where

$$(W^\wedge)_{I,J,K} = (W)_{I,J,K} \; / \; (P_{max} \; LD)$$

In numerical form expression (5.18) becomes

$$\left.\begin{aligned}(W_x^\wedge)_{I,J,K} &= \sum_{i=1}^{m+1} \sum_{j=1,61,121}^{n/3+1,\,2n/3+1,\,n+1} P_{i,j} . \Delta X^* . \Delta Z^* . \cos\theta_j \\ (W_y^\wedge)_{I,J,K} &= \sum_{i=1}^{m+1} \sum_{j=1,61,121}^{n/3+1,\,2n/3+1,\,n+1} P^*_{i,j} . \Delta X^* . \Delta Z^* . \sin\theta_j\end{aligned}\right\} \qquad (5.19)$$

and the resultant dimensionless load is given by

$$(W^\wedge)_{I,J,K} = \left\{ (W_x^\wedge)^2_{I,J,K} + (W_y^\wedge)^2_{I,J,K} \right\}^{\frac{1}{2}} \qquad (5.20)$$

and the angle between the direction of the load and the displacement for each lobe is given by

$$\beta_{I,J,K} = \sin^{-1} (W_y^\wedge / W^\wedge)_{I,J,K} \qquad (5.21)$$

The $(W^\wedge)_{I,J,K}$ is then decomposed into a horizontal and into a vertical force at each lobe. The load factor is then given by

$$(W_t^\wedge) = (W_{vt}^{\wedge 2} + W_{Ht}^{\wedge 2})^{\frac{1}{2}} \qquad (5.22)$$

where, $W_{vt}^\wedge$ is the vector sum of the vertical dimensionless load at each lobe and $W_{Ht}^\wedge$ is the vector sum of the horizontal dimensionless loads at each lobe.

The angle between the vertical direction and the direction of the total load is given by

$$\gamma = \tan^{-1} (- \hat{W}_{Ht}/\hat{W}_{Vt}) \qquad (5.23)$$

$\hat{W}_t$ is called the load factor and includes both the hydrodynamic and the hydrostatic components of load.

When the journal is stationary the load factor comprises only the hydrostatic effect.

In both instances the bearing load is given by

$$W_t = \hat{W}_t . LD\ P_o \qquad (5.24)$$

The load factor ($\hat{W}_t$) is calculated in the same computer programme.

5.6. Bearing Stiffness

The bearing stiffness has been defined as:

$$\lambda = \frac{\text{change in the magnitude of the load}}{\text{change in the magnitude of the displacement}}$$

or

$$\lambda = \frac{d\ W_t}{C/2\ d\varepsilon} \qquad (5.25)$$

Since,

$$W_t = \hat{W}_t . LD\ P_o \qquad (5.26)$$

then,

$$\lambda = \frac{2LD\ P_o}{C} \frac{d\hat{W}_t}{d\varepsilon} \qquad (5.27)$$

and the stiffness coefficient is given by

$$\hat{\lambda} = \lambda \frac{C}{2LD\ P_o} = \frac{d\hat{W}_t}{d\varepsilon} \qquad (5.28)$$

The values of the load factor $\hat{W}_t$ which is evaluated at a series

of values of eccentricity ratios is used to calculate the stiffness parameter $\lambda^{`}$.

5.7. Results of the Numerical Solution

The computer routines for the solutions of Reynold's equations for the externally pressurized circumstances have been written in Fortran VI and it has been performed on the I.C.L. 1900 Computer and on the C.D.C. 7600 Computer. The computer routines and samples of the output are presented in Appendix A.3.

All the inputs and the outputs of the finite difference programmes are in dimensionless form. The output comprises the load angle γ, the attitude angle ϕ, the load factor $W_t^{`}$ (Figure 3.6), the oil flow coefficient, the pressure distribution at the mesh points, the oil film thickness at the mesh points and the pressure at the bearing inlets. The computer programme was run for the following values of the input variables:

ε_o: 0.3, 0.4, 0.5, 0.6, 0.7

ε_B: 0, 0.1, 0.2, ...,0.9.

ϕ: 0 and 180 degrees.

P*: 1

Sp: 0, 0.01, 0.03, 0.05, and 0.1.

$L/_D$: 1.0.

Results of calculation are presented in tables 5.1 to 5.9 . For tables 5.1 to 5.5 the journal displacement is directed towards the centre of a lobe whereas in table 5.6 to table 5.9 the journal displacement is directed towards a conjunction of adjacent lobes. Table 5.1 presents results for a stationary journal (Sp = 0) whereas in tables 5.2 to 5.5 the speed parameter is increased, table by table from 0.01 to 0.1. Table 5.6 is related to a stationary journal.

Tables 5.1 to 5.9 are all calculated for a mean value of the three dimensionless inlet pressure of 1.0. In tables 5.7 to 5.9 the speed parameter is also increased table by table from 0.01 to 0.1. In general the mean value of the three dimensionless pressure at the inlets was specified, and the programme calculated the individual dimensionless inlet pressure together with the common flow coefficient pertaining to each inlet. However, the calculation for tables 5.6 to 5.9 has been carried out for only a few values of eccentricity because a more refined routine is required to adjust the dimensionless pressure at each inlet.

Typical results from the computer outputs and from tables 5.1 to 5.9 will now be discussed. Figure 5.6 shows the pressure distribution at the axial mid-plane when the journal is stationary. It may be seen, at zero bearing eccentricity, that the pressure distribution is symmetrical about the inlet. Although not shown in the figure, the calculated pressures were the same at each lobe. For instance at mesh point of i = 15 and j = 5, the dimensionless pressure was 0.84576, and for the upper lobes at similar points the pressures were 0.84484 and 0.84492. When the journal is displaced within the bearing the pressure distribution for the bottom lobe is shown by the line B, and the distribution for the upper lobes by line C. Line B is symmetrical, but as is to be expected, line C is not. At ε_B= 0 (line A) it may be seen that the pressure at the axial grooves (j = 31, 91 and 151) is approximately 25% of the pressure at the high pressure inlets (j = 1, 181, 61 and 121). The test results show that this ratio is approximately 20%, however, it

Table 5.1 Results of Computation for the Three-lobe Externally Pressurezed Journal Bearing .

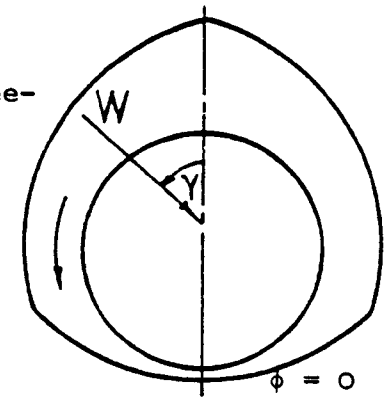

$L/D = 1$ $P^*_{\varepsilon=o} = 1$ Sp = o ϕ = o

ε_o	ε_B	γ	W_t^*	P/P_o	q_a
0.3	0	0	0	1.0	0.176
	0.1	1.5	0.121	1.23	"
	0.2	- 0.35	0.305	1.67	"
	0.3	- 0.3	0.526	2.31	"
	0.4	- 0.19	0.84	3.36	"
	0.5	- 0.16	1.35	5.3	"
	0.6	0.11	2.18	8.95	"
	0.7	0	4.0	17.93	"
	0.8	0	9.6	50.7	"
	0.9	0	41.3	295	"
0.4	0	0	0	1.0	0.116
	0.1	- 0.8	0.134	1.28	"
	0.2	- 0.45	0.292	1.69	"
	0.3	- 0.34	0.499	2.32	"
	0.4	- 0.27	0.795	3.37	"
	0.5	0.21	1.21	5.1	"
	06.	0	2.08	9.0	"
	0.7	0.1	3.75	17.93	"
	0.8	0.07	8.93	50.2	"
	0.9	0.065	36.12	276.5	"

Table 5.1 continued - Results of Computation for the Three-lobe Externally Pressurized Journal Bearing .

L/D $P^*_{\varepsilon=o} = 1$ sp = 0 ϕ = 0

ε_o	ε_B	γ	$\hat{W}_t$	P/P_o	q_a
0.5	0	0	0	1.0	0.069
	0.1	1.1	0.11	1.22	"
	0.2	- 0.3	0.264	1.64	"
	0.3	- 0.2	0.456	2.27	"
	0.4	0.3	0.68	3.16	"
	0.5	0	1.12	5.0	"
	0.6	0	1.81	8	"
	0.7	0	3.3	17	"
	0.8	0	7.67	47	"
	0.9	0	31.33	260	"
0.6	0	0	0	1.0	0.038
	0.1	1	0.096	1.22	"
	0.2	- 0.2	0.236	1.63	"
	0.3	0.46	0.38	2.18	"
	0.4	- 0.1	0.64	3.24	"
	0.5	0.2	0.96	4.9	"
	0.6	0	1.66	8.6	"
	0.7	0	3.0	17.16	"
	0.8	0	6.77	45.7	"
	0.9	0	27.8	255	"
0.7	0	0	0	1.0	0.0174
	0.1	2.3	0.056	1.15	"
	0.2	2.2	0.14	1.45	"
	0.3	1.1	0.26	2.0	"
	0.4	0.5	0.46	2.9	"
	0.5	- 0.5	0.8	5.3	"
	0.6	0.2	1.4	8.0	"
	0.7	0	2.6	17	"
	0.8	0	6.4	49	"
	0.9		22	236	"

Table 5.2. Results of Computation for the Three-lobe Externally Pressurized Journal Bearing .

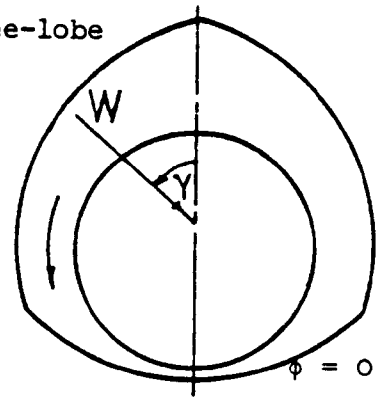

$L/D = 1$ $P^*_{\varepsilon=o} = 1$ Sp = 0.01 $\phi = o$

ε_o	ε_B	γ	W_t^*	P/P_o	q_a
0.3	0	0	0	1.0	0.176
	0.1	8	0.129	1.23	"
	0.2	5.5	0.313	1.67	"
	0.3	5.5	0.533	2.3	"
	0.4	5.3	0.85	3.34	"
	0.5	5.0	1.34	5.26	"
	0.6	5.0	2.2	8.95	"
	0.7	4	4.0	17.9	"
	0.8	2	9.61	50.6	"
	0.9	1	41.4	295	"
0.4	0	0	0	1.0	0.116
	0.1	7.0	0.14	1.27	"
	0.2	7.0	0.3	1.67	"
	0.3	7.0	0.51	2.3	"
	0.4	7.0	0.81	3.35	"
	0.5	7.0	1.23	5.0	"
	0.6	6.0	2.0	8.8	"
	0.7	5	3.75	18	"
	0.8	3	8.9	50	"
	0.9	1.2	36.4	278	"

Table 5.2 continued - Results of Computation for the Three-lobe Externally Pressurized Journal Bearing .

$L/D = 1$ $P^*_{\varepsilon=o} = 1$ Sp = 0.01 $\phi = 0$

ε_o	ε_B	γ	$\hat{W}_t$	P/P_o	q_a
0.5	0	0	0	1.0	0.069
	0.1	12.6	0.115	1.21	"
	0.2	12	0.26	1.59	"
	0.3	10	0.47	2.24	"
	0.4	10	0.71	3.15	"
	0.5	10	1.1	4.86	"
	0.6	8	1.8	8.0	"
	0.7	6	3.41	17.45	"
	0.8	4	7.6	46.0	"
	0.9	2	31.2	259	"
0.6	0	0	0	1.0	0.038
	0.1	16.6	0.113	1.21	"
	0.2	16.2	0.245	1.58	"
	0.3	15.4	0.42	2.17	"
	0.4	14.77	0.65	3.11	"
	0.5	12.8	1.037	4.92	"
	0.6	11	1.65	8.26	"
	0.7	8.42	2.94	16.5	"
	0.8	5.2	6.64	44.38	"
	0.9	2.3	24.1	221	"

Table 5.2 continued - Results of Computation for the Three-lobe Externally Pressurized Journal Bearing .

$L/D = 1$ $P^*_{\varepsilon=o} = 1$ Sp = 0.01 $\phi = 0$

ε_o	ε_B	γ	$\hat{W}_t$	P/P_{Θ}	q_a
0.8	0	0	0	1.0	0.0059
	0.1	36	0.171	1.28	"
	0.2	35	0.252	1.62	"
	0.3	35	0.32	L.98	"
	0.4	33	0.43	2.4	"
	0.5	34	0.525	2.80	"
	0.6	39	0.62	3.35	"
	0.7	48	0.71	3.45	"

Table 5.3. Results of Computation for the Three-lobe Externally Pressurized Journal Bearing .

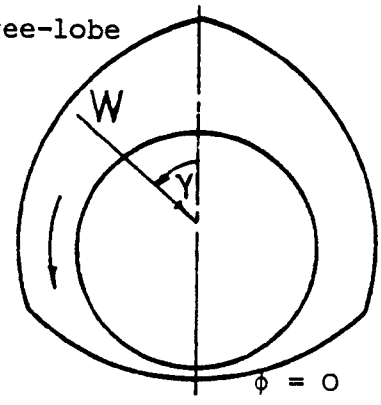

$L/D = 1$ $P^*_{\varepsilon=o} = 1$ Sp = 0.03 $\phi = 0$

ε_o	ε_B	γ	$\hat{W}_t$	P/P_o	q_a
0.3	0	0	0	1.0	0.176
	0.1	19	0.144	1.21	"
	0.2	16.4	0.336	1.65	"
	0.3	16.4	0.562	2.26	"
	0.4	15.7	0.885	3.32	"
	0.5	14.4	1.39	5.2	"
	0.6	12.7	2.22	8.86	"
	0.7	9.7	4.0	17.6	"
	0.8	7.4	9.16	46.8	"
	0.9	3	38.6	273	"
0.4	0	0	0	1.0	0.116
	0.1	23.34	0.14	1.23	"
	0.2	20.77	0.334	1.66	"
	0.3	21.0	0.554	2.27	"
	0.4	20.3	0.86	3.3	"
	0.5	19	1.29	5.0	"
	0.6	15.65	2.06	8.36	"
	0.7	12.65	3.44	15.6	"
	0.8	8.7	7.27	39.66	"
	0.9	4.0	28.3	214.76	"

Table 5.3. continued - Results of Computation for the Three-lobe Externally Pressurized Journal Bearing .

$L/D = 1$ $P^* = 1$ Sp = 0.03 $\phi = 0$

ε_o	ε_B	γ	W_t	P/P_o	q_a
0.5	0	0	0	1.0	0.069
	0.1	25	0.159	1.23	"
	0.2	27	0.333	1.61	"
	0.3	28	0.54	2.19	"
	0.4	26.5	0.8	3.0	"
	0.5	24	1.16	4.43	"
	0.6	22	1.64	6.6	"
	0.7	19	2.57	11.72	"
	0.8.	15	4.89	27.4	"
	0.9	7.7	16.17	130.0	"
0.6	0	0	0	1.0	0.038
	0.1	37	0.153	1.2	"
	0.2	35	0.342	1.6	"
	0.3	35	0.52	2.04	"
	0.4	34	0.714	2.6	"
	0.5	34	0.95	3.4	"
	0.6	36	1.23	4.41	"
	0.7	36.5	1.67	6.48	"
	0.8	39	2.29	9.96	"
	0.9	57	2.97	11.5	"
0.7	0	0	0	1.0	0.0174
	0.1	51	0.218	1.27	"
	0.2	51	0.312	1.48	"
	0.3	51	0.426	1.61	"
	0.4	54	0.573	1.84	"

Table 5.4. Results of Computation for the Three-lobe Externally Pressurized Journal Bearing .

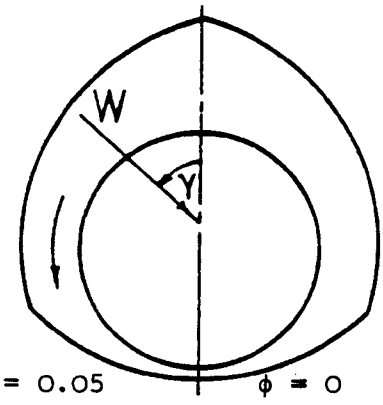

$L/D = 1$ $P^*_{\varepsilon=0} = 1$ Sp = 0.05 $\phi = 0$

ε_δ	ε_B	γ	$\tilde{W}_t$	P^*	q_a
	0	0	0	1.0	0.176
	0.1	27.7	0.163	1.22	"
	0.2	27.3	0.354	1.6	"
	0.3	27	0.59	2.2	"
0.3	0.4	25	0.926	3.22	"
	0.5	22	1.4	4.86	"
	0.6	19	2.15	7.9	"
	0.7	17	3.87	15.4	"
	0.8	11	8.15	40.3	"
	0.9	5	31.8	22.3	"
	0	0	0	1.0	0.116
	0.1	33	0.172	1.22	"
	0.2	31.5	0.382	1.64	"
	0.3	31.5	0.61	2.19	"
	0.4	30	0.913	3.0	"
0.4	0.5	28	1.28	4.26	"
	0.6	26	1.85	6.52	"
	0.7	22	3.0	12.2	"
	0.8	17	5.8	29.3	"
	0.9	9	19.2	14.2	"

Table 5.4. continued - Results of Computation for the Three-lobe Externally Pressurized Journal Bearing .

$L/D = 1$ $P^*_{\varepsilon=o} = 1$ Sp = 0.05 $\phi = 0$

ε_o	ε_B	γ	W_t^*	P^*	q_a
0.5	0	0	0	1.0	0.069
	0.1	40	0.183	1.19	"
	0.2	41	0.39	1.54	"
	0.3	38	0.605	2.0	"
	0.4	37	0.85	2.57	"
	0.5	38	1.1	3.2	"
	0.6	40	1.45	4.19	"
	0.7	42	1.95	5.9	"
	0.8	44	2.78	9.42	"
	0.9	56	4.1	13.8	"
0.7	0	0	0	1.0	0.0174
	0.1	65	0.328	1.33	"
	0.2	67	0.44	1.32	"
	0.3	72	0.566	1.05	"
0.6	0	0	0	1.0	0.038
	0.1	55	0.189	1.2	"
	0.2	50	0.362	1.46	"
	0.3	50	0.546	1.65	"
	0.4	53	0.75	1.87	"
	0.5	59	0.96	1.64	"
	0.6	68	1.232	1.35	"

Table 5.5. Results of Computation for the Three-lobe Externally Pressurized Journal Bearing .

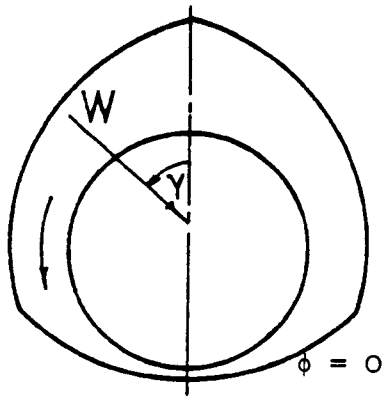

$L/D = 1$ $P^*_{\varepsilon=o}$ Sp = 0.1 ϕ = 0

ε_o	ε_B	γ	$\hat{W}_t$	p*	q_a
0.3	0	0	0	1.0	0.176
	0.1	42	0.222	1.21	"
	0.2	42	0.472	1.58	"
	0.3	40	0.735	2.0	"
	0.4	40	1.0	2.64	"
	0.5	36	1.47	3.8	"
	0.6	34	2.15	6.0	"
	0.7	32	3.4	10.6	"
	0.8	28	5.75	23.2	"
	0.9	18	16.5	104.7	"
0.4	0	0	0	1.0	0.116
	0.1	48	0.25	1.21	"
	0.2	46	0.50	1.51	"
	0.3	46	0.74	1.82	"
	0.4	47	1.02	2.2	"
	0.5	50	1.34	2.55	"
	0.6	51	1.81	3.3	"
	0.7	54	2.48	4.31	"
	0.8	65	3.38	3.4	"

Table 5.5. continued - Results of Computation for the Three-lobe Externally Pressurized Journal Bearing.

$L/D = 1$ $P^*_{\varepsilon=o}$ Sp = 0.1 $\phi = 0$

ε_o	ε_B	γ	W_t	P^*	q_a
	0	0	0	1.0	0.069
	0.1	62.5	0.25	1.18	"
0.5	0.2	56.0	0.48	1.35	"
	0.3	57.7	0.715	1.38	"
	0.4	62.8	1.0	1.44	"

Table 5.6. Results of Computation for the Three-hole Externally Pressurized Journal Bearing .

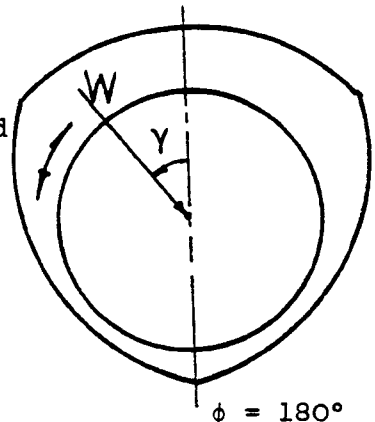

$L/D = 1$ $P^*_{\varepsilon=o} = 1$ Sp = O $\phi = 180°$

ε_o	ε_B	γ	W^*_t	P/P_o	q_a
0.3	0	0	0	1.0	0.176
	0.1	- 0.75	0.144	1.16	"
	0.2	- 0.1	0.26	1.3	"
	0.3	0.4	0.382	1.46	"
	0.4	0.28	0.519	1.67	"
	0.5	0	0.663	1.97	"
0.4	0	0	0	1.0	0.116
	0.1	0.8	0.115	1.13	"
	0.2	0	0.244	1.3	"
	0.3	0	0.366	1.48	"
	0.4	0	0.5	1.7	"
	0.5	0	0.66	1.97	"
	0.6	0	0.831	2.27	"
0.5	0	0	0	1.0	0.069
	0.1	- 2.0	0.11	1.2	"
	0.2	1.0	0.24	1.4	"
	0.3	1.0	0.285	1.5	"
	0.4	0	0.47	1.8	"
	0.5	0	0.60	2.0	"

Table 5.7. Results of Computation for the Three Lobe Externally Pressurized Journal Bearing.

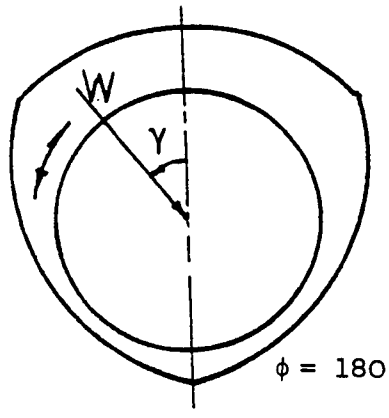

$L/D = 1$ $P^*_{\varepsilon=o} = 1$ Sp = 0.01 $\phi = 180°$

ε_o	ε_B	γ	$\hat{W}_t$	P^*	q_a
	0	0	0	1.0	0.176
	0.1	4	0.15	1.18	"
0.3	0.2	5	0.28	1.35	"
	0.3	5	0.43	1.58	"
	0.4	5	0.6	1.85	"
	0.5	5	0.738	2.17	"
	0	0	0	1.0	0.116
	0.1	7.5	0.13	1.16	"
0.4	0.2	7	0.26	1.36	"
	0.3	6	0.4	1.6	"
	0.4	6	0.71	1.8	"
	0	0	0	1.0	0.069
	0.1	10.86	0.12	1.15	"
0.5	0.2	9.4	0.24	1.35	"
	0.3	7.76	0.388	1.62	"

Table 5.8. Results of Computation for the Three Lobe Externally Pressurized Journal Bearing.

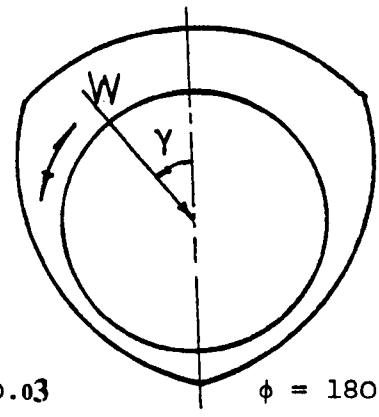

$L/D = 1$ $\quad P^*_{\varepsilon=o} = 1$ $\quad Sp = 0.03$ $\quad \phi = 180°$

ε_o	ε_B	γ	W_t	P^*	q_a
0.3	0	0	0	1.0	0.176
	0.1	15	0.155	1.19	"
	0.3	13	0.494	1.73	"
0.4	0	0	0	1.0	0.116
	0.1	19	0.154	1.22	"
	0.2	17	0.32	1.5	"
	0.3	15	0.48	1.7	"
0.5	0	0	0	1.0	0.069
	0.1	21.4	0.161	1.25	"
	0.2	20.64	0.322	1.55	"
	0.3	21	0.47	1.6	"
0.6	0	0	0	1.0	0.038
	0.1	29	0.147	1.24	"
	0.2	27	0.293	1.54	"
	0.3	24	0.44	1.9	"

Table 5.9. Results of Computation for the Three-Lobe Externally Pressurized Journal Bearings.

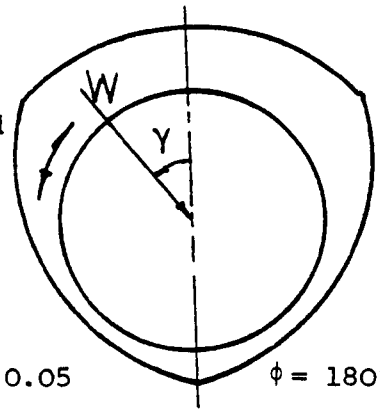

$L/D = 1$ $P^*_{\varepsilon=o} = 1$ Sp = 0.05 $\phi = 180°$

ε_o	ε_B	γ	$\hat{W}_t$	P^*	q_a
0.3	0	0	0	1.0	0.176
	0.1	19	0.19	1.26	"
	0.2	20	0.362	1.53	"
0.4	0	0	0	1.0	0.069
	0.1	24	0.194	1.3	"
	0.3	21	0.6	2.0	"
0.5	0	0	0	1.0	0.069
	0.1	32	0.183	1.3	"
	0.2	28.8	0.372	1.65	"
	0.3	24.7	0.6	2.13	"
0.6	0	0	0	1.0	0.038
	0.1	47	0.076	1.0	"
	0.2	44	0.193	1.12	"
	0.3	39	0.32	1.38	"

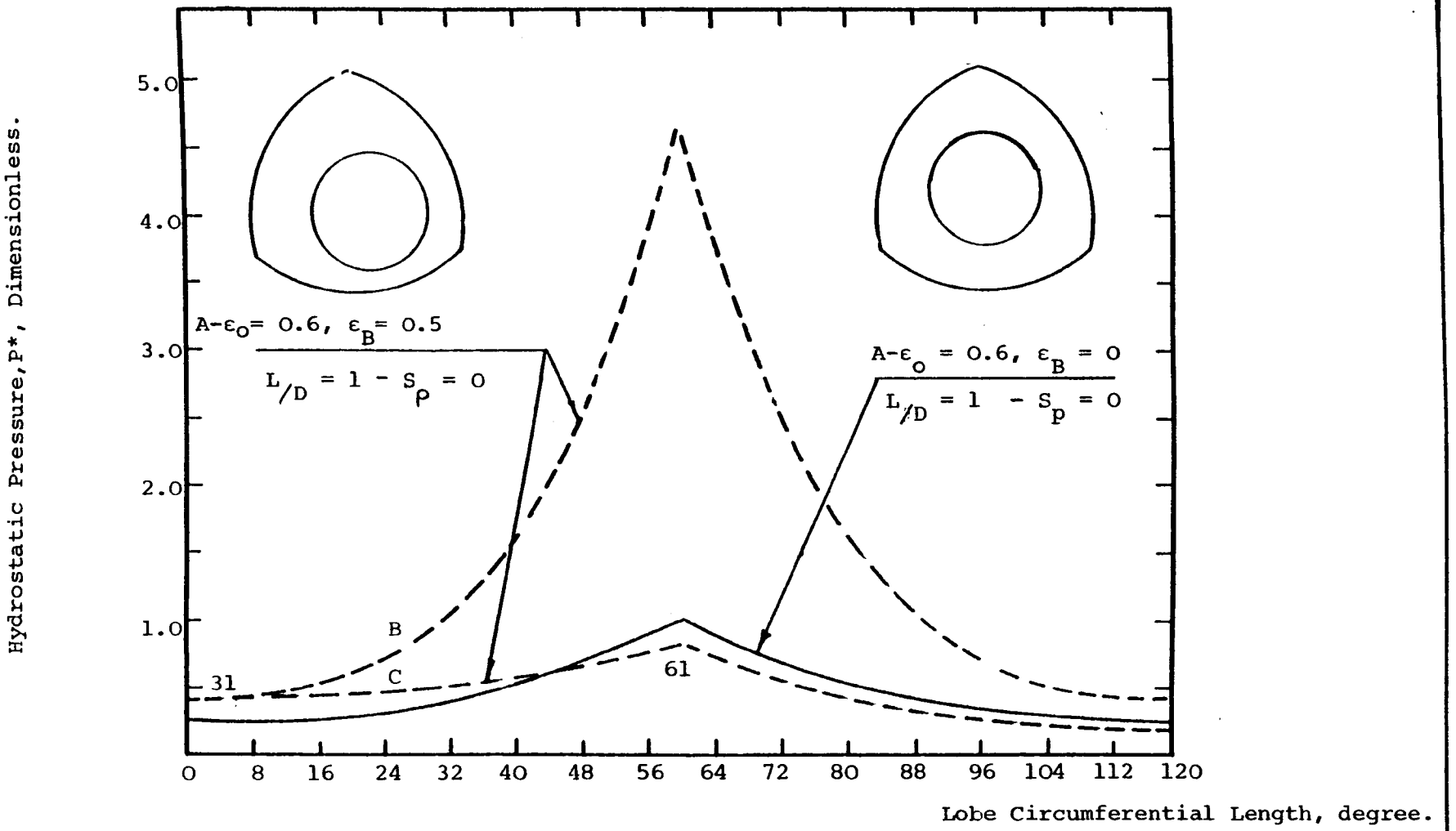

Figure 5.6. Dimensionless Pressure Distribution Along The Axial Mid-PLANE

may be mentioned that in the computer programme, the oil grooves are not represented and the bearing surface is assumed to be continued.

Figures 5.7 and 5.8 relate to a rotating journal and are respectively for speed parameter of 0.03 and 0.1. With reference to figure 5.7 it may be seen that the pressure distribution is no longer symmetric about the lobe (i.e. $\theta = 60°$), but the maximum dimensionless pressure for all ε_B is still at the position of the high pressure inlets (i.e. $\theta = 60°$). Also it may be seen that as the bearing eccentricity ratio (ε_B) increases the hydrodynamic effect increases, and negative pressures start to develop at the trailing end of the lobes, and as the eccentricity increases, the pressure distribution curve is terminated before the end of the lobe circumferential length. With reference to Fig. 5.8, at a speed parameter of 0.1, the bearing is behaving as a self generating bearing. The pressure distribution curves are similar to those plotted in Chapter 3. Also it may be seen that the maximum pressure position is no longer located at the high pressure inlets but the high pressure positions are now located before the minimum film thickness as has been found in the self generating analysis.

Figure 5.9, which relates to a stationary journal, shows the variation of the dimensionless pressure at high pressure inlets with the bearing eccentricity ratio. Line A is drawn for a vertical load directed towards the centre of the bottom lobe (i.e., towards the high pressure inlet). Line B is drawn for a vertical load directed towards the conjunction of the lobes and the journal movement is not directly against the high pressure inlets. It may be seen that for the case represented by line A the dimensionless pressure P* increases

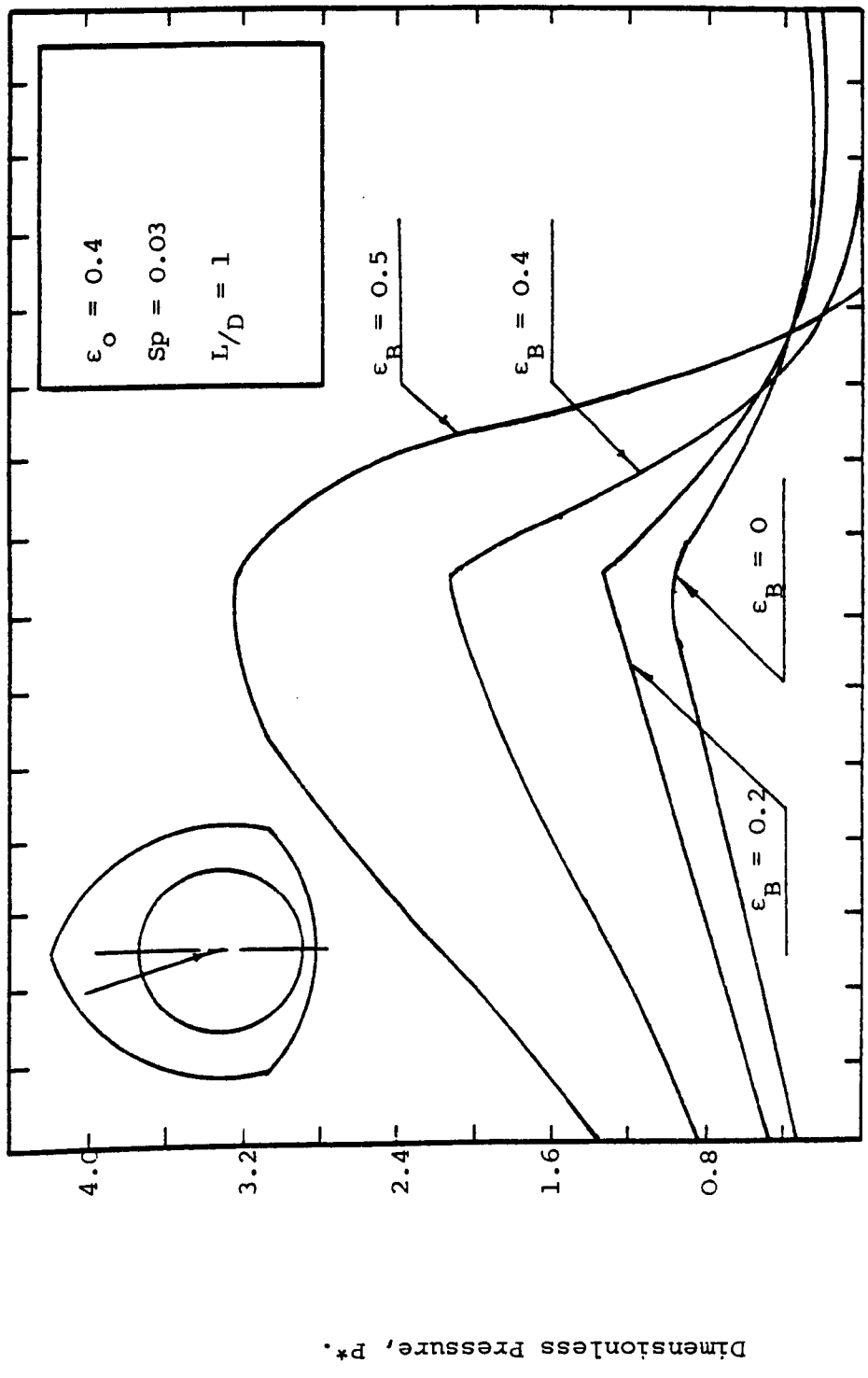

Figure 5.7. Dimensionless Pressure Distribution Along THE AXIAL MID-PLANE.

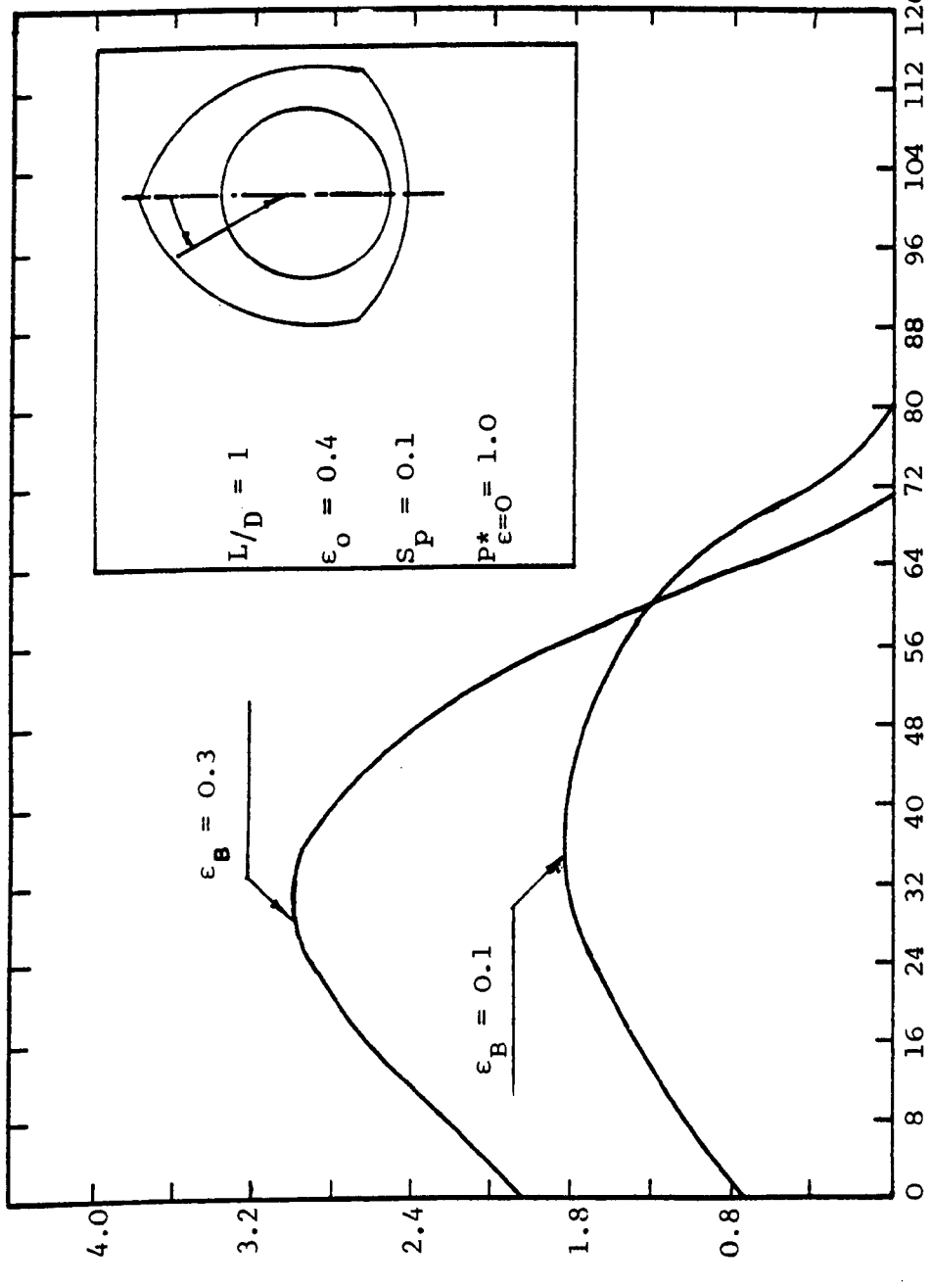

Figure 5.8 Dimensionless Pressure Distribution Along the Axial Mid Plane.

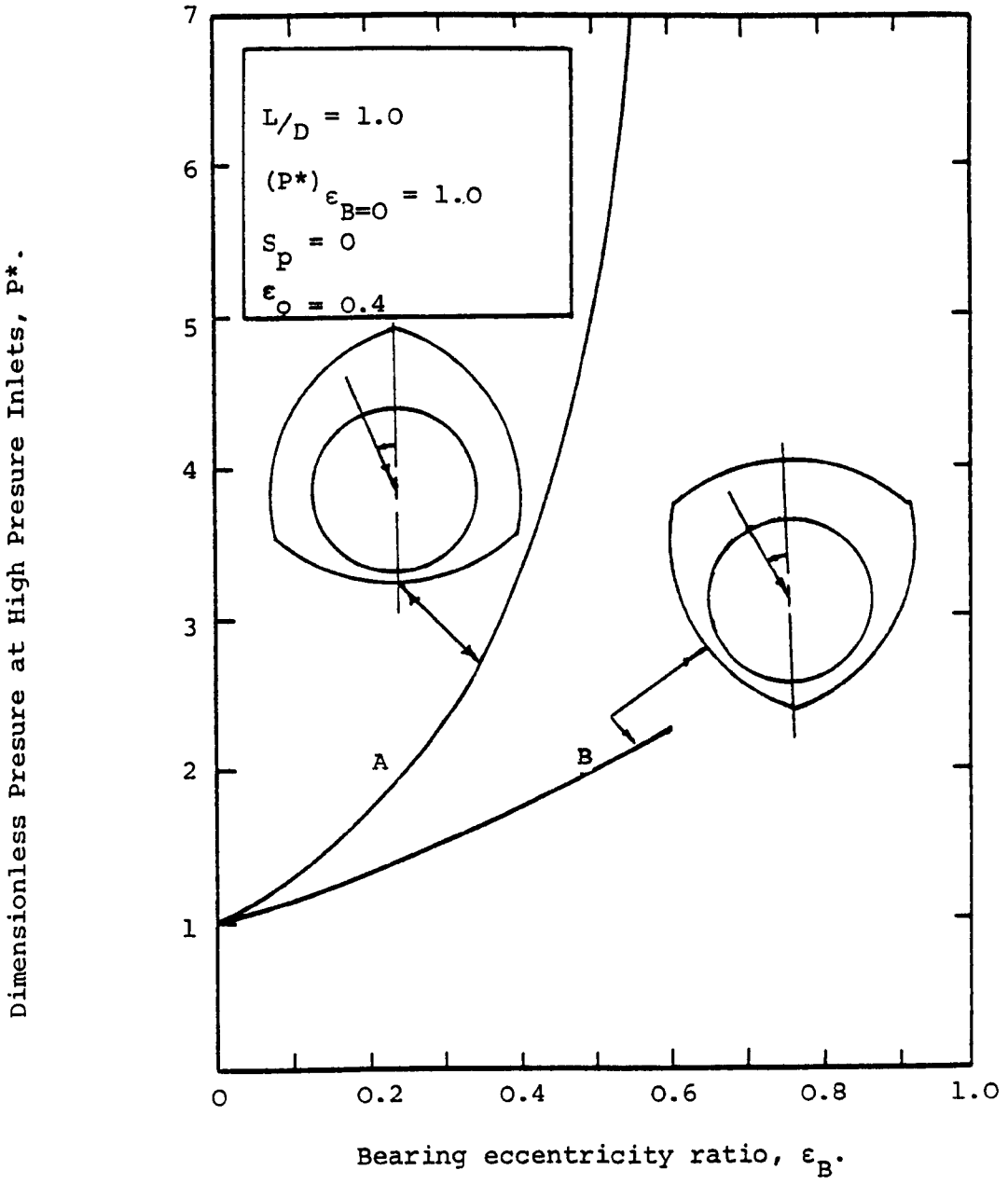

Figure 5.9. Dimensionless Inlet Pressure - Bearing Eccentricity Characteristics.

rapidly as the journal moves towards the high pressure inlet.

The oil flow through the bearing is determined by the setting of the constant volume valves, and is independent of whether the journal is rotating or not, loaded or not. However, with the journal central and for a particular value of P^* the oil flow required to establish that pressure will be a function of the way in which the space between journal and the lobes varies (i.e. function of the offset ratio ε_o). In figure 5.10 the variation of the oil flow coefficient against offset ratio is plotted for a central journal. It may be seen that the oil flow coefficient decreases as the offset ratio increases, however, in real terms the increase of the offset ratio leads to an increase in the lobe diametral clearance so that the actual oil flow may be increased as the offset ratio increases.

The effect of the variation of bearing eccentricity ratio on load factor is shown in figure 5.11. The results obtained are for zero speed and for various offset ratios. It may be seen that the load factor increases as the eccentricity ratio increases but the load factor decreases as the offset ratio increases. The decrease in the load factor as the offset ratio increases may be attributed to the departure from a uniform oil film thickness around the journal which will affect the pressure distribution.

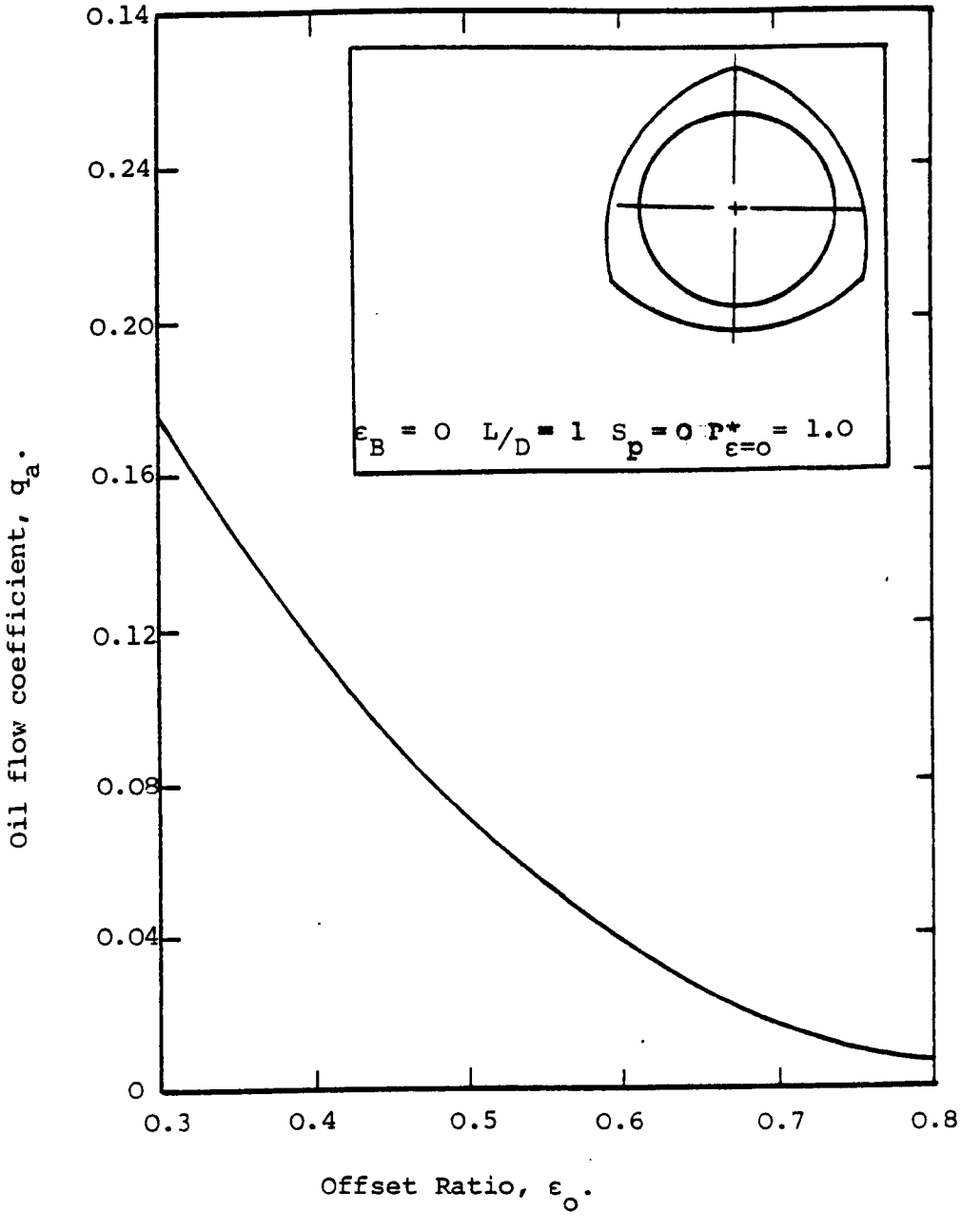

Figure 5.10. Oil Flow Coefficient - Bearing Offset Ratio Characteristics.

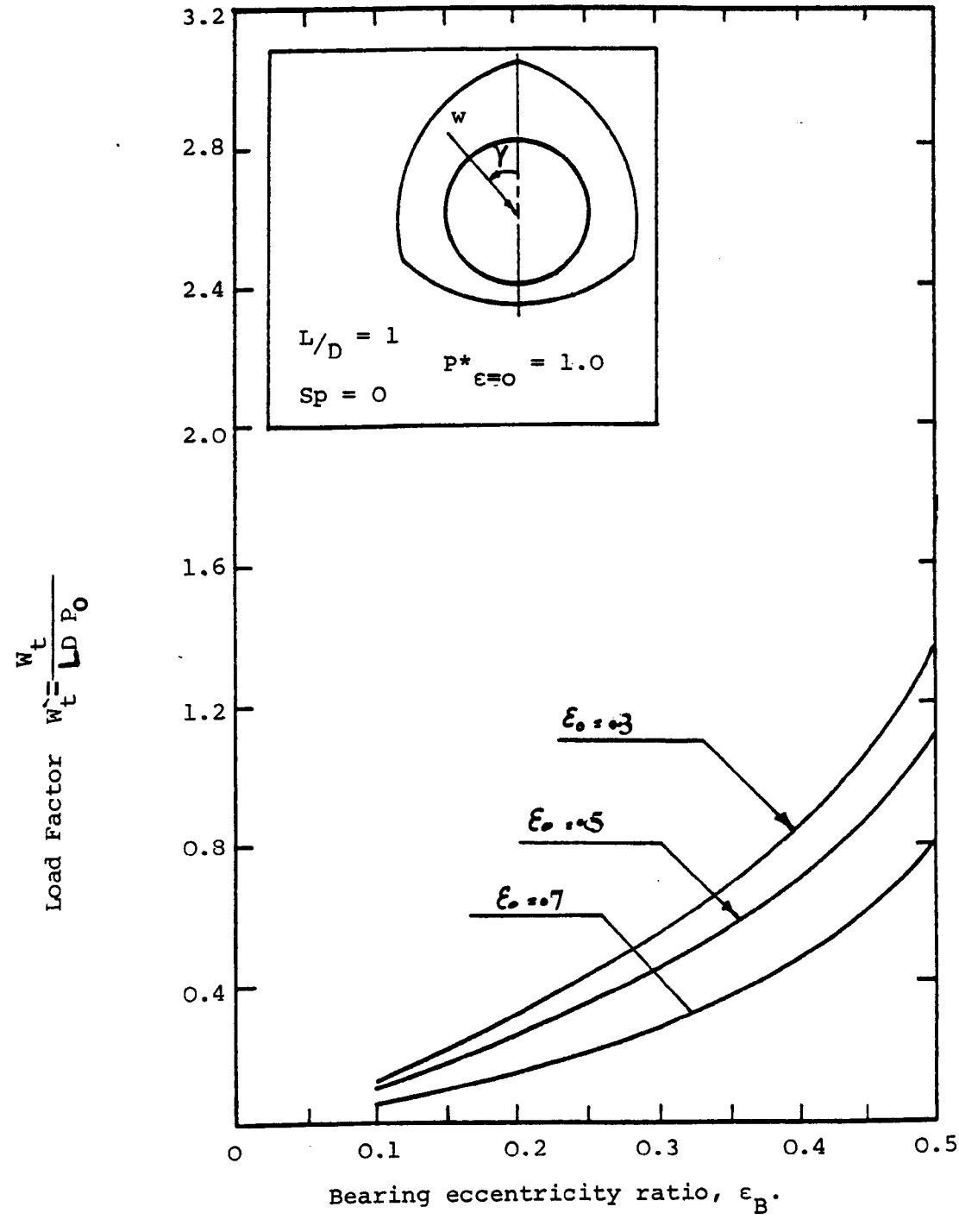

Figure 5.11. Load Factor - Bearing Eccentricity Characteristics.

In figure 5.12 the effect of the variation of speed on load factor is shown. It is quite clear that as the speed parameter increases the hydrodynamic effects on the load parameter increases, so that the load factor $\hat{w}_t$ and the bearing load increase as the speed increases. Also it may be seen from figure 5.12 that an increase in eccentricity ratio leads to an increase in hydrodynamic effects which is typically what has been found by the hydrodynamic solution in chapter 3. In figure 5.13 the load factor is plotted against the speed parameter for two different offset ratios. As the speed parameter increases it may be seen that the effect of offset ratios upon the load factor decreases. However, at speed parameters beyond 0.09 a cross-over occurs. This trend in the characteristics of load factor is attributed to the increase in the hydrodynamic effects as the speed parameter and the offset ratio increases; also this trend in the characteristics of the load factor is consistent with results which have been discussed in Chapter 3, where it has been shown that the bearing duty parameter (i.e. bearing load) increases as the offset ratio increases.

Figure 5.14 shows the variation of the stiffness coefficient $\hat{\lambda}$ as defined by expression (5.28) with the bearing eccentricity ratio. Quite clearly, from figure 5.14 increasing the eccentricity ratio increases the stiffness coefficient, also

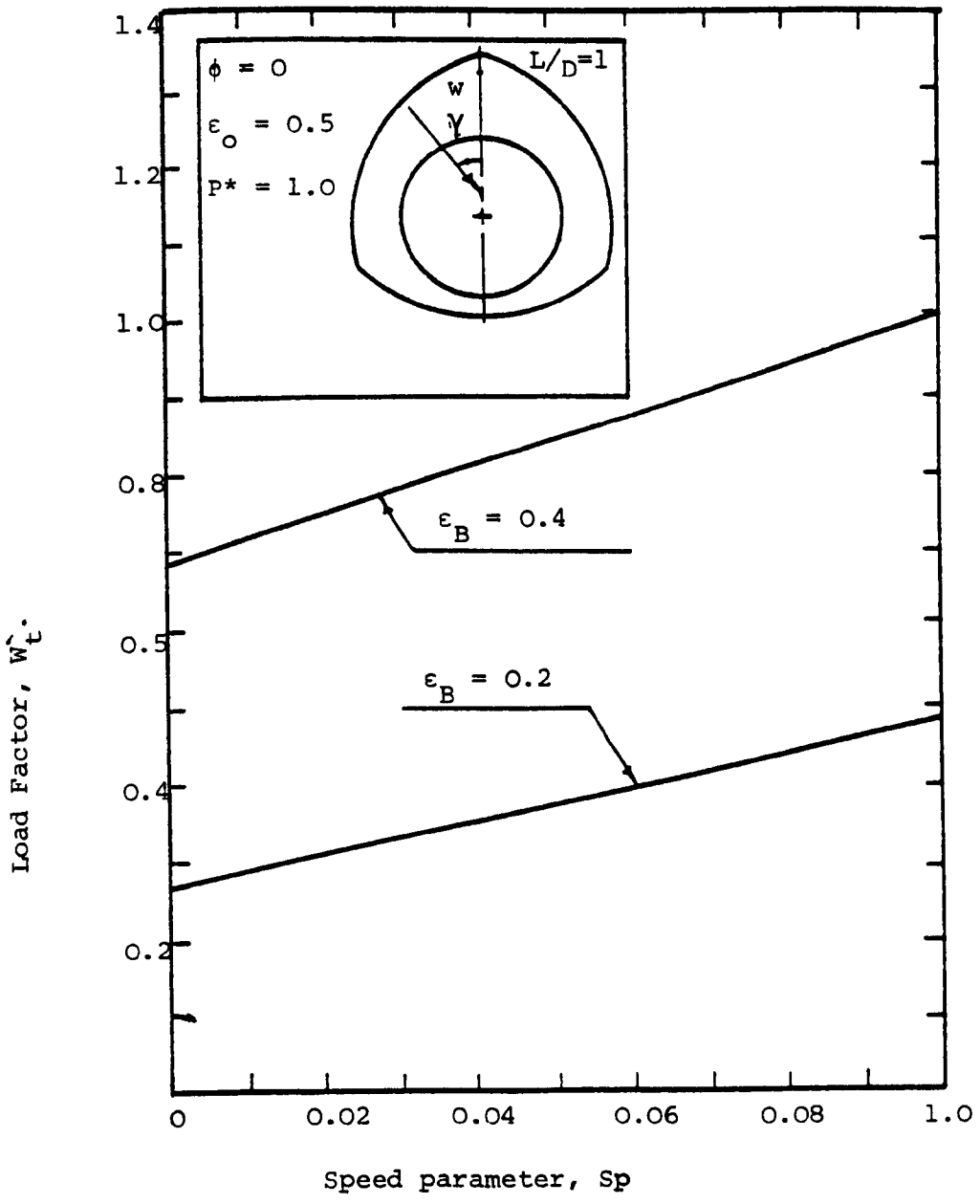

Figure 5.12. Load Factor - Speed Parameter Characteristics.

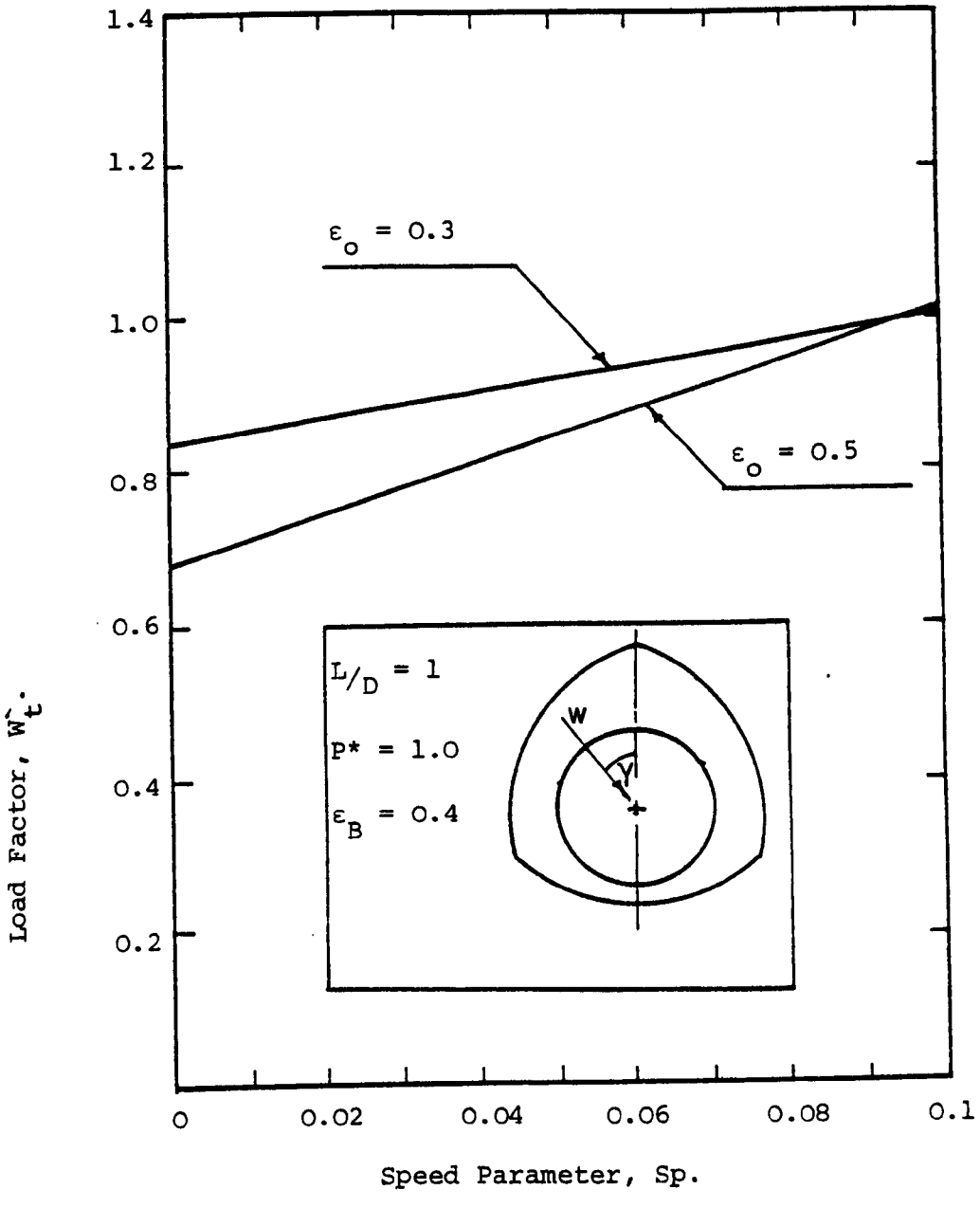

Figure 5.13. Load factor - Speed Parameter Characteristics.

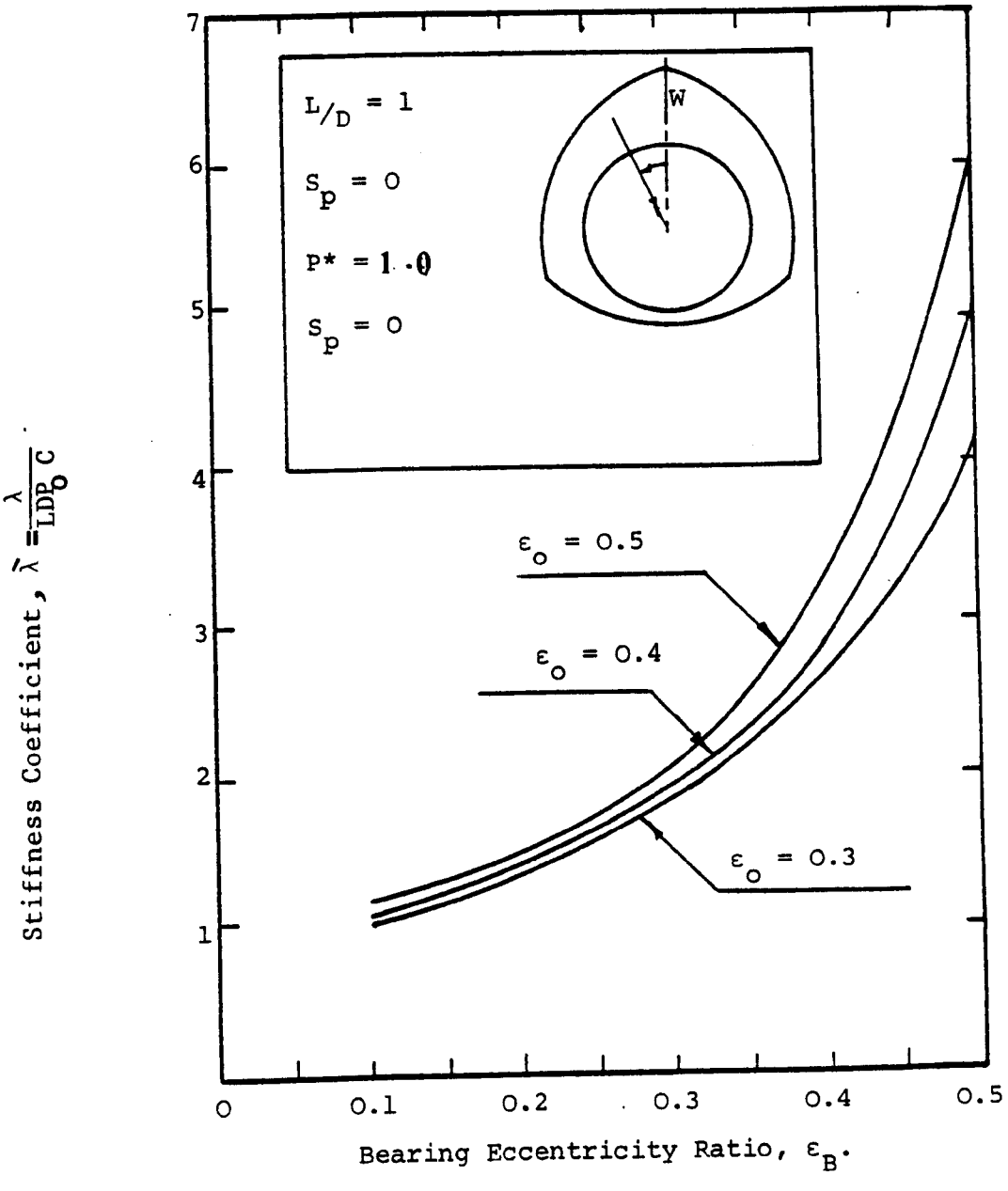

Figure 5.14. Stiffness Coefficient - Eccentricity Ratio Characteristics.

the stiffness coefficient increases with the offset ratio. However, because the stiffness coefficient is dependent on the lobe clearance, and because the offset ratio and lobe clearance are not variable independently the change in the stiffness coefficient does not necessarily imply similar changes in actual stiffness.

The effect of speed parameter on the load angle γ , is shown in figure 5.15. When the speed parameter is zero (i.e. stationary journal) the load angle γ is zero for all the eccentricity ratio values,, and the load is in the same sense as the journal displacement. When the speed parameter increases, the angle between the vertical direction of the journal displacement and the load direction increases. Also it may be seen that at speed parameters beyond 0.85 a cross-over occurs which may be attributed to the increase in the hydro-dynamic effects.

In figure 5.16 it may be seen that an increase in the offset ratio increases the load angle. In both figures 5.15 and 5.16 the load angles are comparable to the load angles for the self generating circumstances which have been reported in chapter 3.

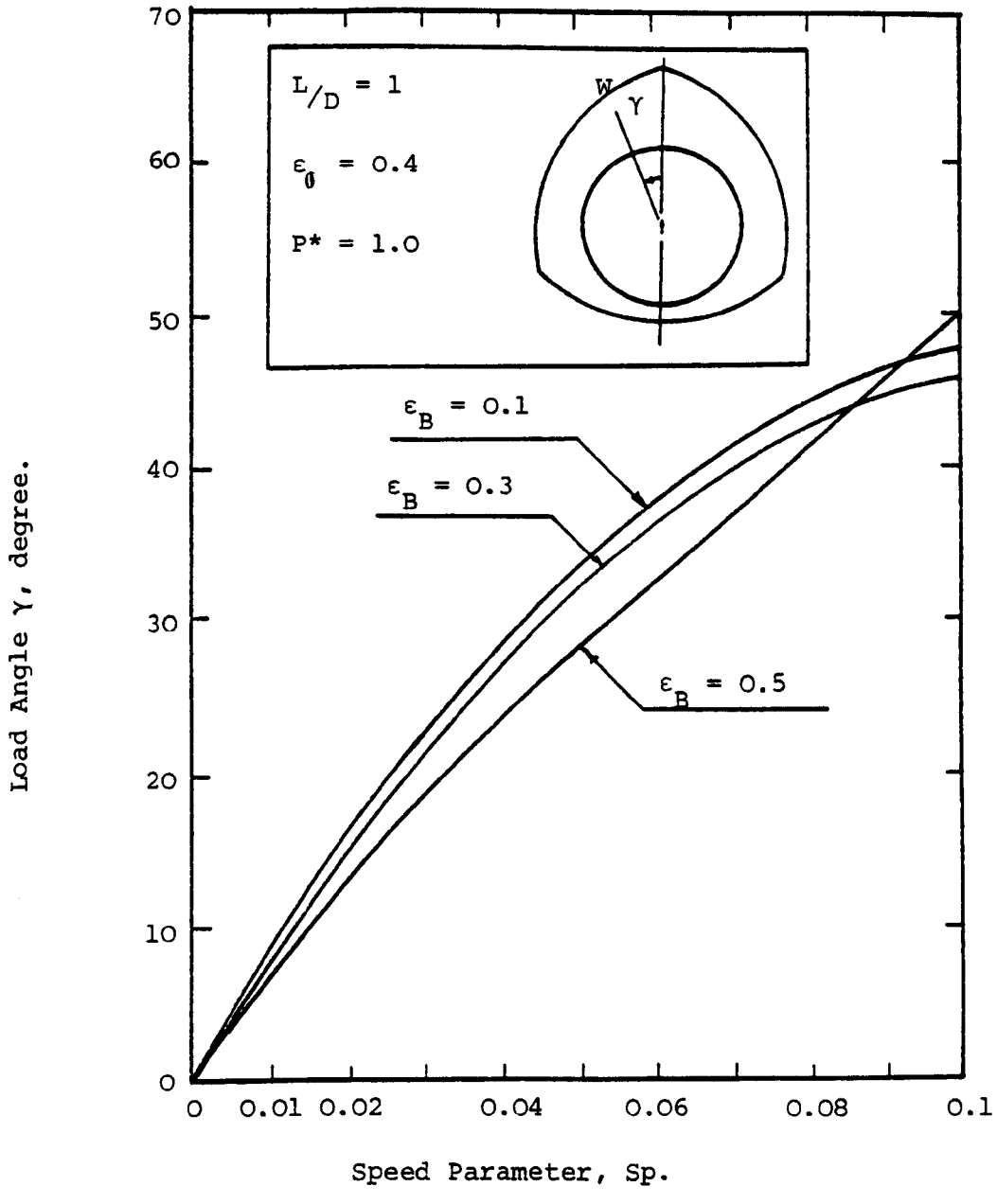

Figure 5.15. Load Angle - Speed Parameter Characteristics.

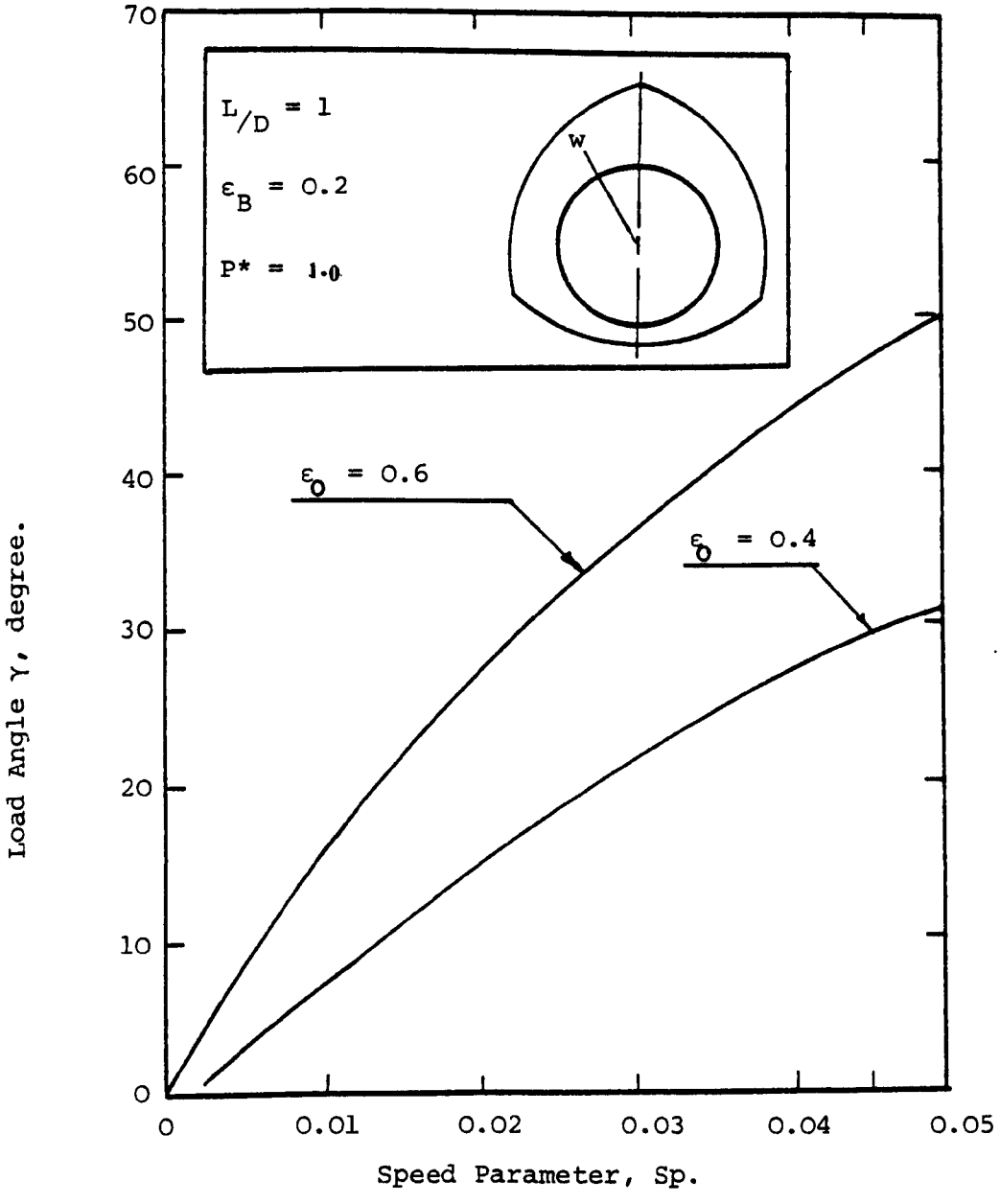

Figure 5.16. Load Angle - Speed Parameter Characteristics.

5.8. Design procedure

In this paragraph a numerical example will be worked in order to show how to predict the performance of a three lobe bearing from the results which have been presented. The numerical values which are used in this example relate to the bearing which has been tested. Also, the load and the displacement values which are used in this example relate to the functional specification given in table 1.1. The numerical values are:

$D = 135$ m m $L = 127$ m m $C = 0.26$ m m $\delta = 0.0254$ m m

$\varepsilon_o = 0.45$ $W_t = 22270$ N $N = 0 \rightarrow 5000$ rpm

Oil: Tellus 37

The eccentricity ratio $\varepsilon = \frac{2\delta}{C} = \frac{2 \times 0.0254}{0.26} = 0.1954$

The bearing eccentricity ratio $\varepsilon_B = \frac{\varepsilon}{(1-\varepsilon_o)} = \frac{0.1954}{(1 - 0.45)} = 0.355$

The load factor $W_t^{\wedge} = 0.62$ (Figure 5.11)

$$P_o = W_t / LD\, W_t^{\wedge} = \frac{22270}{0.127 \times 0.135 \times 0.25} = 2.1 \times 10^6 \text{ Nm}^{-2}$$

The oil flow coefficient, $q_a = 0.09$ (Figure 5.10)

$\mu = 0.22$ at 50°C (The operating temperature is considered to be 50°C).

$$Q_a = \frac{q_a P_o C^3}{6\mu} = \frac{0.09 \times 2.1 \times 10^6 \times (0.026)^3 \; 981000}{6 \times 0.22 \times 1000 \times 9.81 \times 10^4} = 0.025 \text{ ℓs}^{-1}$$

The total oil flow $= 3 \times Q_a = 0.075$ ℓs^{-1} (1.0 G.P.M.)

From table 5.1 and for $\varepsilon_B = 0.355$ then $P^* = 2.77$

The pressure at the highest pressure inlet for bearing eccentricity ratio of 0.355 = $2.1 \times 10^6 \times 2.77 = 5.82 \times 10^6$ NM^{-2}

The supply pressure, Ps = 5.82×10^6 + the pressure drop across constant volume flow valve.

$$Ps = 5.82 \times 10^6 + 6.67 \times 10^5 = 6.487 \times 10^6 \ NM^{-2}$$

By considering the shaft is rotated at 1000 rpm:-

The speed parameter, $Sp = \frac{\mu N}{P_o} (D/C)^2$

$$= \frac{0.22 \times \frac{1000}{60} \times 9.81}{2.1 \times 10^2 \times 981000} \left(\frac{13.5}{0.026}\right) = 0.044$$

The load factor $W_t^{\cdot}$ (from tables 5.2 to 5.5) = 0.7.

The load which may be carried by the journal at ε_B = 0.355 and

Ns 1000 rpm is = $\frac{0.70}{0.62} \times 22270 = 24942$ N *

The load angle γ = 35 degrees (tables 5.3 and 5.4)

In chapter 3, the validity of the computer programmes which have been used for the self generating regime have been examined by using the author's programmes to solve problems where the results are published. With respect to the programmes which have been used in this chapter, there is nothing which has been published about the three lobe bearings as externally pressurized bearings; also there is nothing in the literature about the analysis of externally pressurized bearings which are compensated by the constant volume flow valves. However, the validity of the computer programmes which

* The calculated load of 24942 N with the displacement of 0.0254 mm implies a stiffness of 9.82×10^8 $N m^{-1}$.

have been used in this chapter has already been discussed in paragraph 5.7 with the discussion of the computer programme results. In paragraph 5.7 it has been shown that the solutions produce a symmetric pressure distribution for all the three lobes, and also it has been shown that by increasing the speed parameter the pressure distribution becomes similar to the pressure distribution of the self generating regime. The load angle of a stationary journal is found to be zero; however, in paragraph 5.7 it has been shown that as the speed parameter increases the load angle approaches the load angle of the self generating circumstance. Also the load factor shows a similar behaviour with the speed parameter . All these comparisons between the output of present computer programme and the output of the computer programme used in chapter 3, with the results of the numerical example may show the logic and the correctness of the results obtained from the present programme.

As a further check upon the computer programme, the calculated oil flow is compared with the measured oil flow. In table 5.9 the calculated oil flow for an offset ratio of 0.45 and different conditions of operation are compared with the measured oil flow at the same operating conditions. Quite clearly the results show that a very close agreement exists which again substantiates the validity of the programme.

A comparison between the results of this analysis, the approximate analysis (chapter 2) and the tests results (chapters 4 and 6) will be presented in chapter 8.

Table 5.10. Comparison between the calculated and measured Oil Flow for the Externally Pressurized regime.

Conditions of Calculation and Measurement						Measured	Calculated	
ε_o	$C \times 10^{4}$, m	$Ps \times 10^{-7}$, Nm^{-2}	$P \times 10^{-7}$, Nm^{-2}	P/Ps	μ, poise	Q_t, ℓs^{-1}	q_a	Q_t, ℓs^{-1}
0.45	2.6	1.33	0.665	0.5	0.273	0.186	0.047	0.2
"	"	1.0	0.57	0.57	0.167	0.261	0.052	0.272
"	"	1.33	0.64	0.48	0.22	0.261	0.045	0.240
"	"	0.662	0.43	0.65	0.163	0.186	0.058	0.207
"	"	1.66	0.424	0.26	0.167	0.186	0.024	0.206

C H A P T E R 6

MAIN TEST RIG, EXPERIMENTATION AND RESULTS

6. MAIN TEST RIG, EXPERMENTATION AND RESULTS

6.1. Introduction

The success or otherwise of the bearing which has been described in meeting both the low and high speed aspects of the specification can only be established by an experimental investigation in which the behaviour of the bearing assembly is tested over a wide range of operation. A full scale test rig for the hydrostatic and hydrodynamic investigation of the three lobe journal bearing has been built. Speeds up to 7000 rpm have been reached. Two oils of different viscosities have been used and two different bearing shells have been machined and used in test.

6.2. Test Rig and Instrumentation*

A layout of the test rig is shown in Figure 6.1. The shaft[1] is supported by the wide speed range bearing[2] (i.e. three-lobe bearing), and by the rolling element thrust[4] with the tail bearing[3] in the housing[5] on the right hand side. A hydraulic ram, which is not shown, is used to apply a vertical load via the slave bearing[7] fitted to the overhang of the shaft. The conception of the rig is that it should correspond as closely as is practical with an actual machine tool spindle, for instance the tail and thrust races have been chosen with machine tool duty in mind, and are mist lubricated through the nozzle[8]. The displacement of the journal with respect to the bearing is measured with inductive displacement transducers[9] at each end of the bearing. There are two pairs of transducers arranged to measure vertical and horizontal displacements. Measurements have been made at each end by transferring the transducers. Thermocouples[10] are provided to measure oil and bearing metal temperature. Flow and pressure at both high pressure and low pressure inlets were measured, but the flow was not measured simultaneously because to reduce the provision of

*The writer designed, drew, assembled and commissioned the rig himself. He also carried out some machining and fitting.

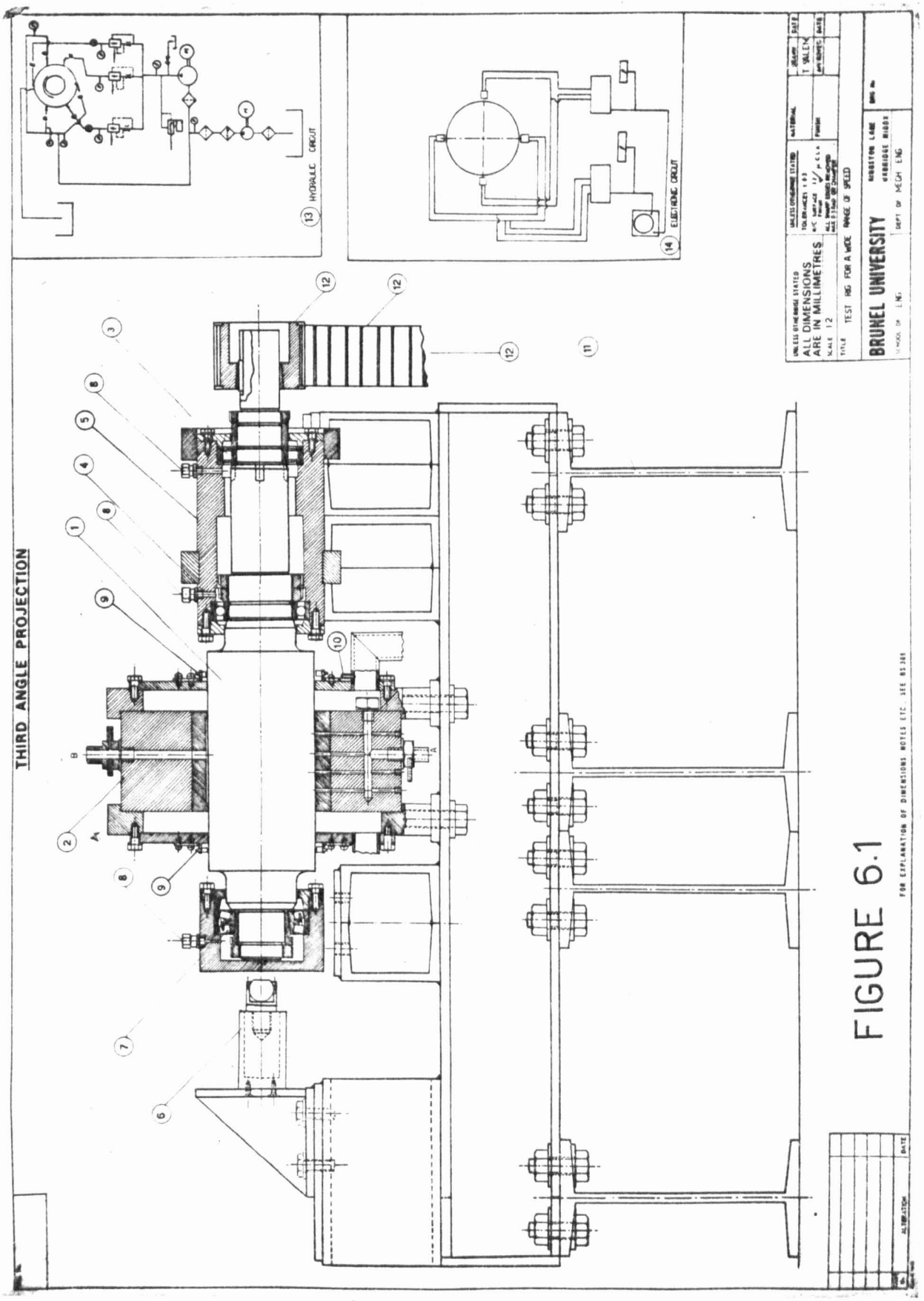
THIRD ANGLE PROJECTION
13 HYDRAULIC CIRCUIT
14 ELECTRONIC CIRCUIT
BRUNEL UNIVERSITY
TEST RIG FOR A WIDE RANGE OF SPEED
ALL DIMENSIONS ARE IN MILLIMETRES
SCALE 1:2

FIGURE 6.1

instruments, the moving of an instrument from one position to another was accepted. Photographs of the test rig with instrumentation are shown in Figures 6.2 and 6.3.

6.2.1. The Three Lobe Bearing

Two test bearings have been machined to provide different diametral clearance* and different dimensions for the axial grooves where the low pressure oil for hydrodynamic operation is delivered. A high pressure oil inlet for the hydrostatic regime is provided at the centre of each lobe. The main dimensions of the test bearings are shown by Figure 6.4. A bearing is also shown by the photograph of Figure 6.5. The machining of a bearing is described in detail in Appendix A.4., and in Appendix A.5 an alternative method is described which has been tested as a process, but no actual bearing machined by the process has been made or tested.

6.2.2. The Design of the Shaft

In the design of the test shaft it was considered that the shaft should be of a form as close as possible to an actual machine spindle. The shaft is illustrated in Figure 6.6. The shaft was designed to provide an extension to carry a slave bearing for overhung loading of the test bearing[7]. (Figure 6.1).

Evaluations by conventional means were made of the bending stress, shear stress and deflection in the shaft. The stresses are low, but at the position of maximum stress, where the dimensions are reduced for the thrust bearing, a very generous filet is provided to avoid any possibility of a fatigue failure.

In a machine tool application the precise axial position of the cutting tool could be important, and with the notion of minimizing

*In principle the same effect could have been achieved by reducing the diameter of the shaft, but it would have been difficult to modify the first bearing in other respects.

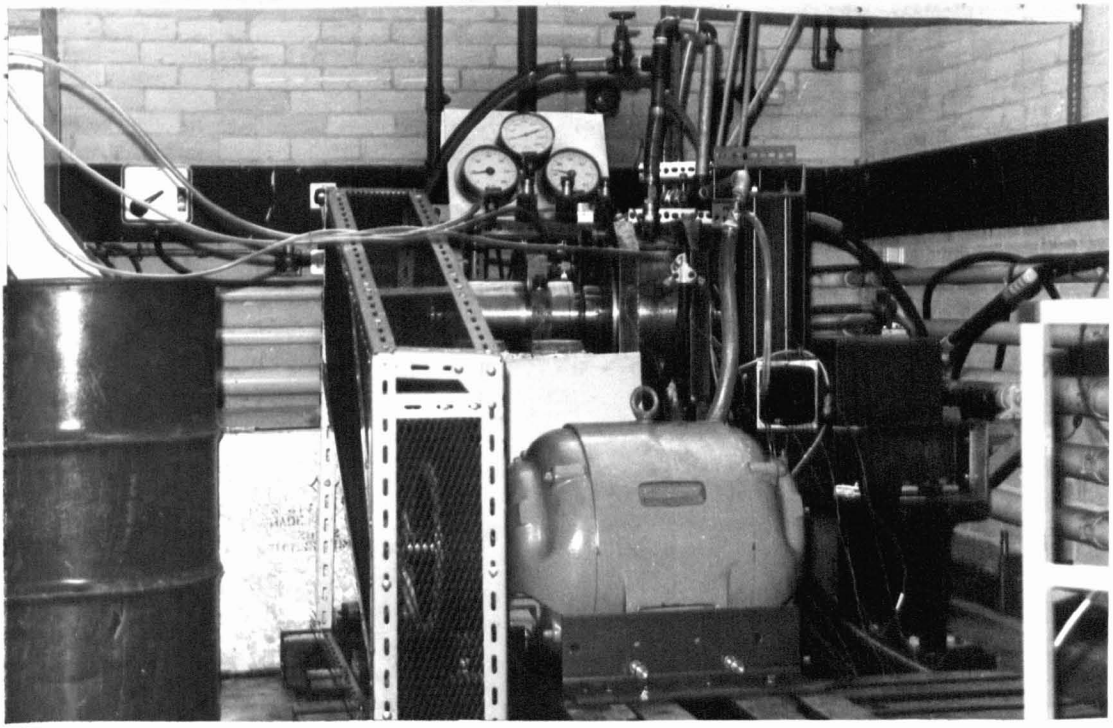

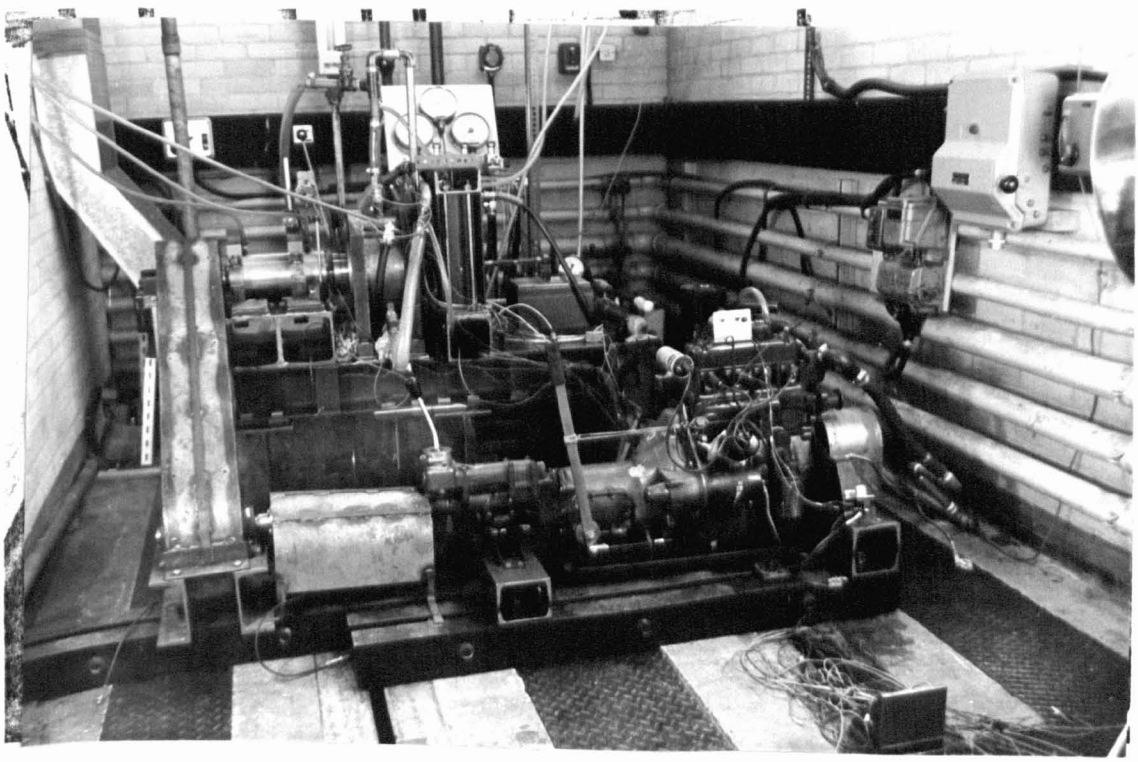

FIG.6.2 TEST RIG.

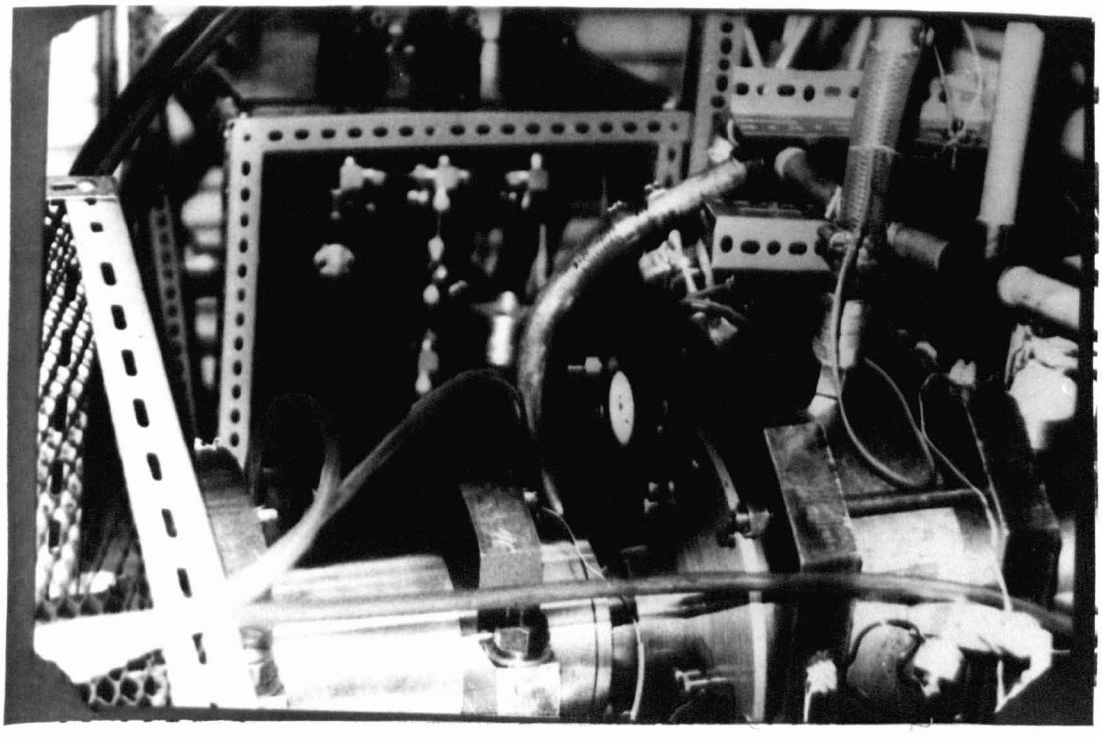

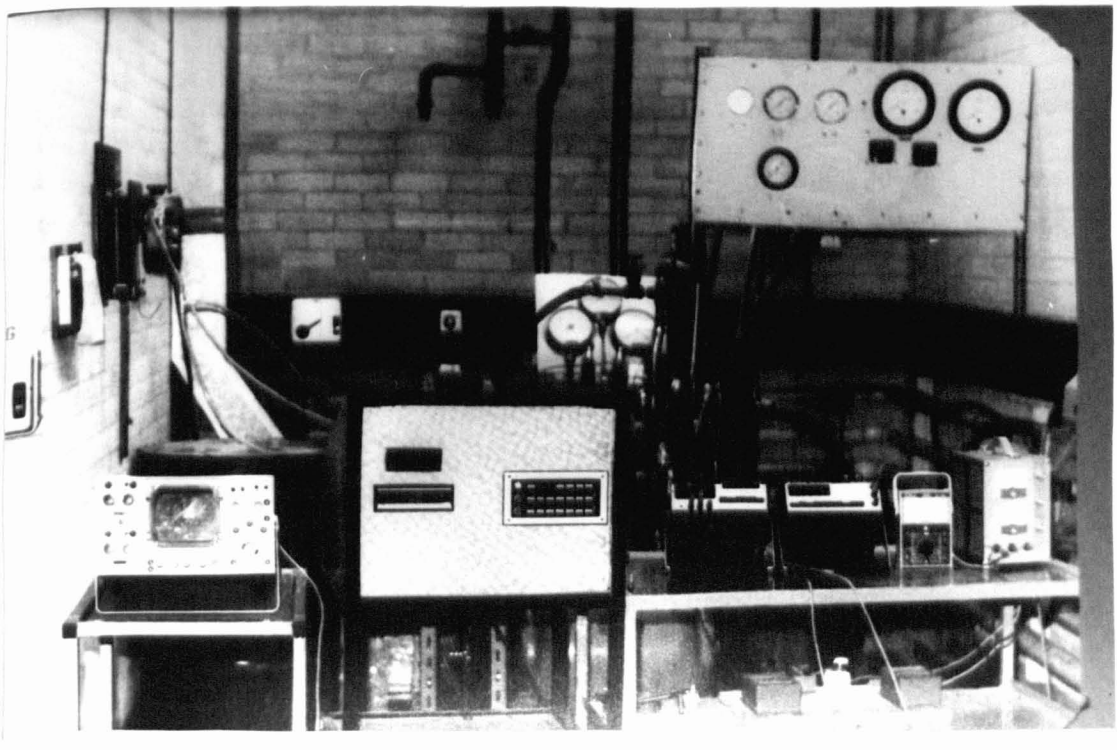

FIG.6.3 TEST RIG AND INSTRUMENTATIONS

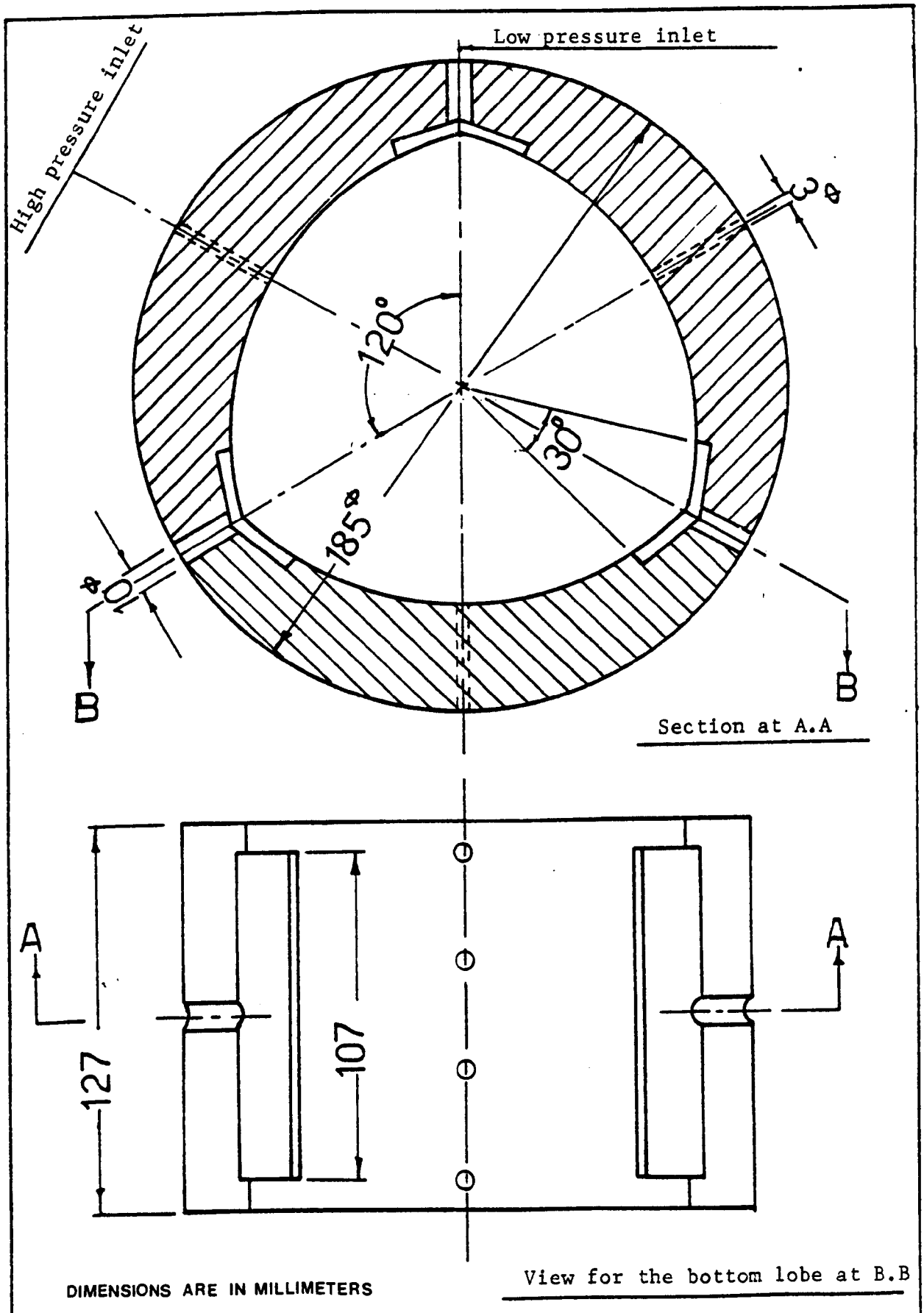

FIG. 6.4 Three lobe-bearing.

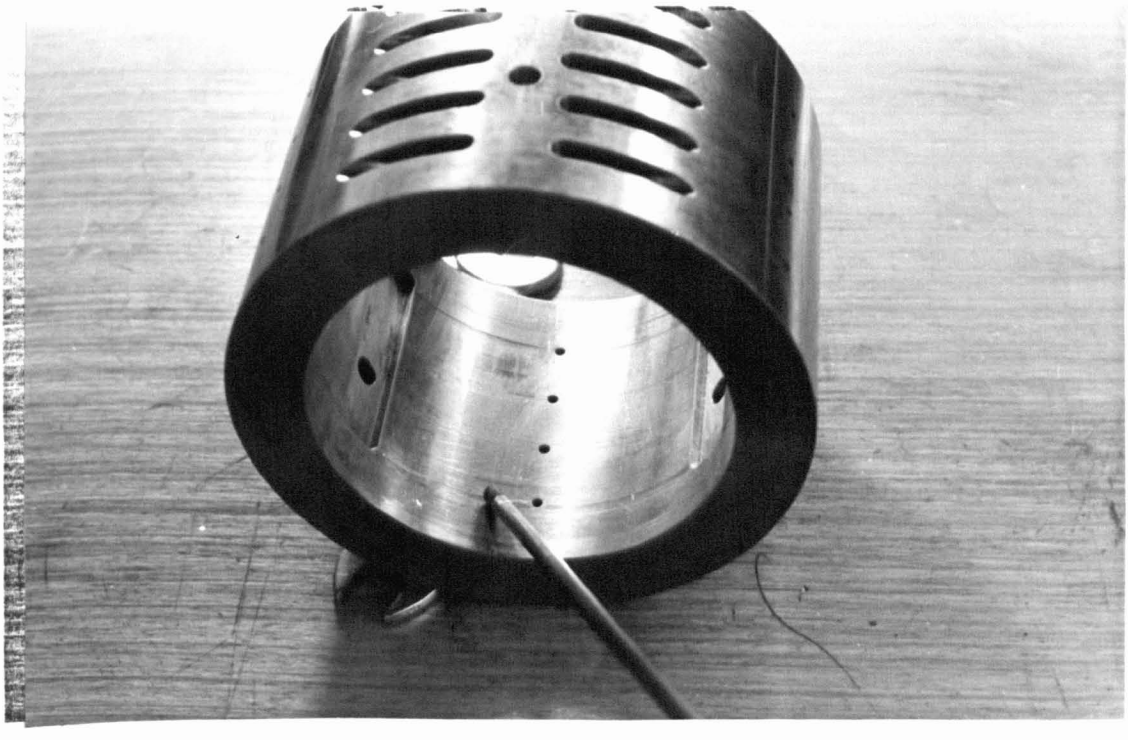

FIG. 6.5 TEST BEARING.

First bearing - the lines in the bore and score marks caused by detritus in the oil ways. The second bearing is completely undamaged.

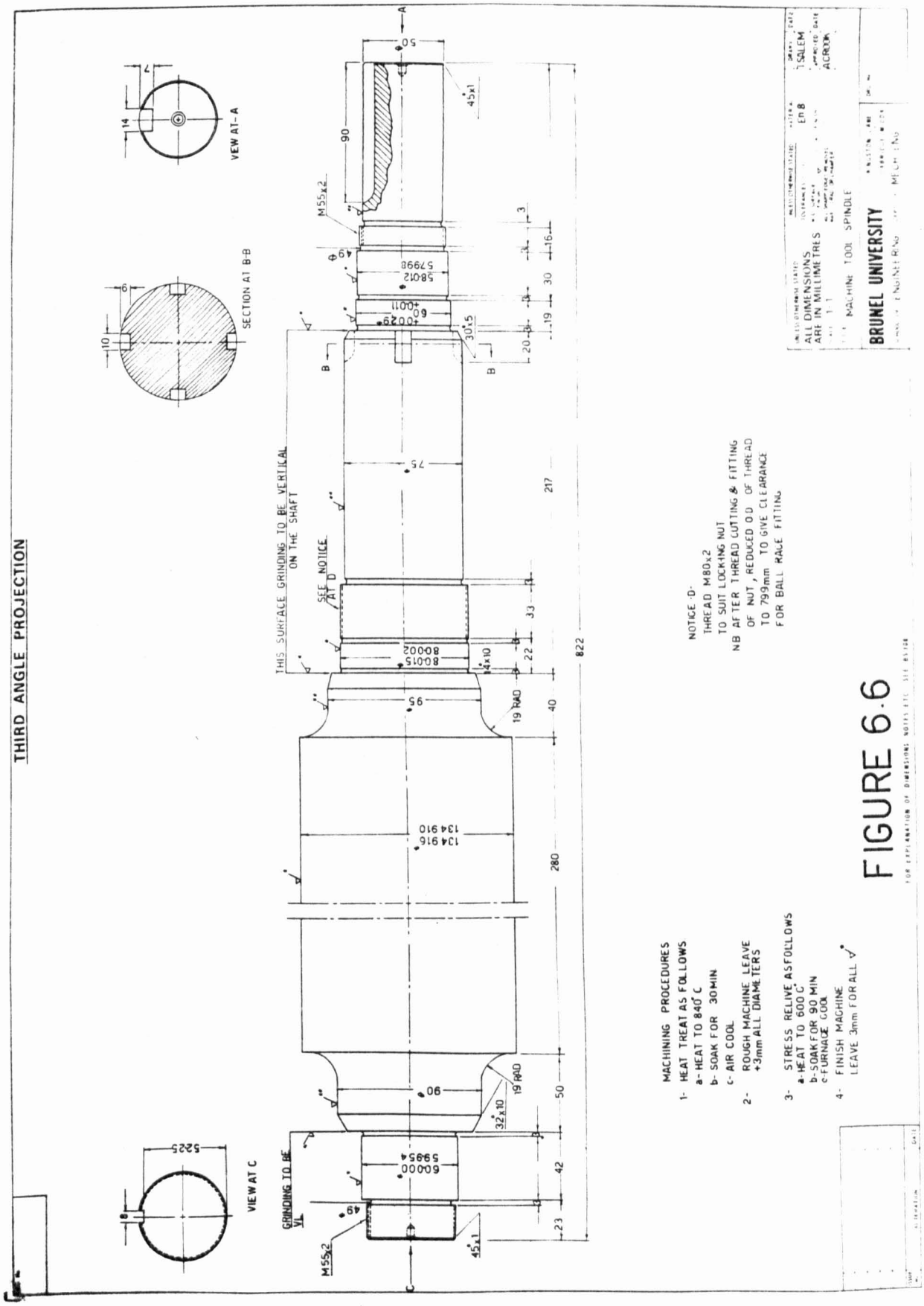
THIRD ANGLE PROJECTION
VIEW AT A-A
SECTION AT B-B
VIEW AT C
THIS SURFACE GRINDING TO BE VERTICAL ON THE SHAFT
SEE NOTICE 'D'
GRINDING TO BE V
MACHINING PROCEDURES
1- HEAT TREAT AS FOLLOWS
a- HEAT TO 840°C
b- SOAK FOR 30MIN
c- AIR COOL
2- ROUGH MACHINE LEAVE +3mm ALL DIAMETERS
3- STRESS RELIVE AS FOLLOWS
a- HEAT TO 600°C
b- SOAK FOR 90 MIN
c- FURNACE COOL
4- FINISH MACHINE LEAVE 3mm FOR ALL
NOTICE 'D'
THREAD M80x2
TO SUIT LOCKING NUT
NB AFTER THREAD CUTTING & FITTING OF NUT, REDUCED O/D OF THREAD TO 799mm TO GIVE CLEARANCE FOR BALL RACE FITTING
ALL DIMENSIONS ARE IN MILLIMETRES
MACHINE TOOL SPINDLE
BRUNEL UNIVERSITY
SALEM
ACROYD

FIGURE 6.6

the effect upon this precison of the thermal expansion of the shaft, it was decided to fit the thrust bearing as close as is possible to the three lobe bearing. This gave rise to a reduced diameter of the tail to permit the fitting of the thrust. However, as will be described later, this was probably a mistake, as it makes the shaft more flexible than would otherwise be so. (The thrust and tail bearings are shown at 4 and 3 respectively - Figure 6.1).

The shaft was roughly machined from normalized En8 steel, the shaft was heat treated for stress relieving (1.5 hours at 690°C, furnace cooled. Shaft rotated in heat treatment) and then it was finally machined to the required dimensions. The positions of the main journal bearing, the thrust bearing and the tail bearing were ground. Details of the manufacturing process are given in Figure 6.6. The machined shaft is shown by the photographs in Figures 6.7 and 6.8.

6.2.3 The Design of the Thrust Bearing

In the design of the thrust bearing, no consideration was given to a specific thrust load and the main criteria, for the design of the thrust bearing was the speed limit and the shaft diameter. It was found that an ordinary roller or ball thrust is not suitable for the required speeds, and that a single row deep groove ball bearing is better suited to accommodate axial loads at high speeds. A deep groove ball bearing of 80 mm. bore was used; this bore diameter is the greatest diameter which is compatible with the maximum speed.

6.2.4 Design of the Tail Bearing

The required load to be supported at the position of the tail bearing was calculated and it was found that the load carrying capacity of the bearing does not introduce a problem. However, for the required running accuracy of a machine tool it is advisable to use cylindrical

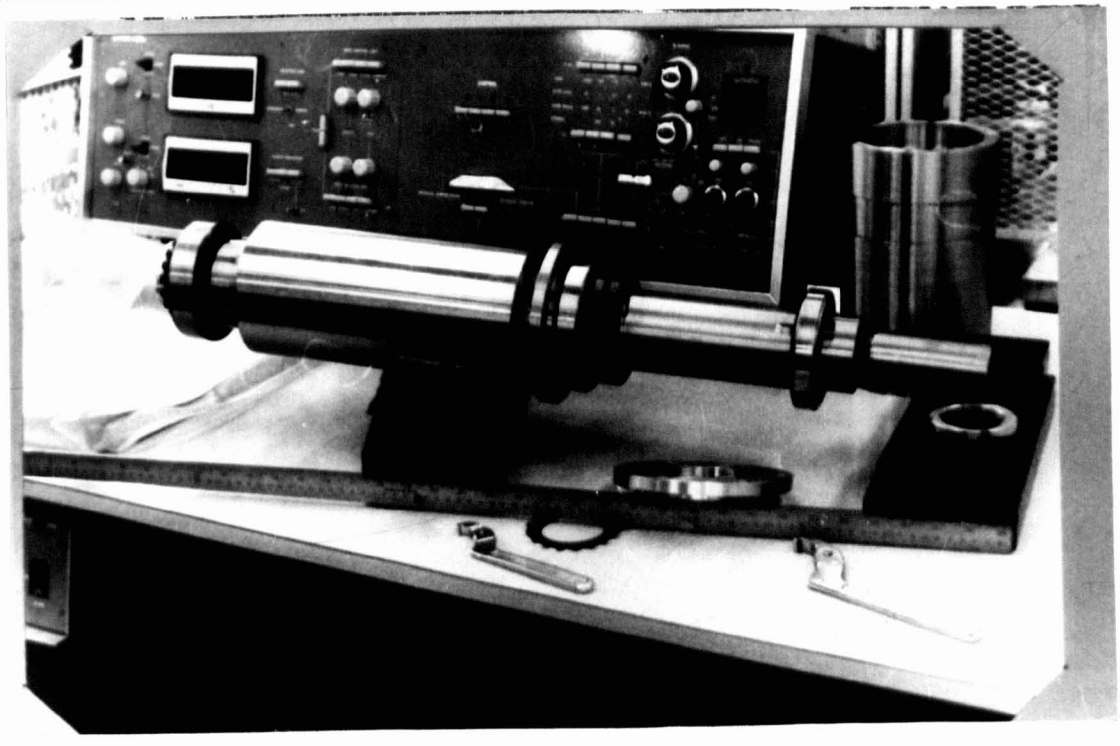

FIG. 6.7 TEST SHAFT WITH MOUNTED ROLLING ELEMENTS.

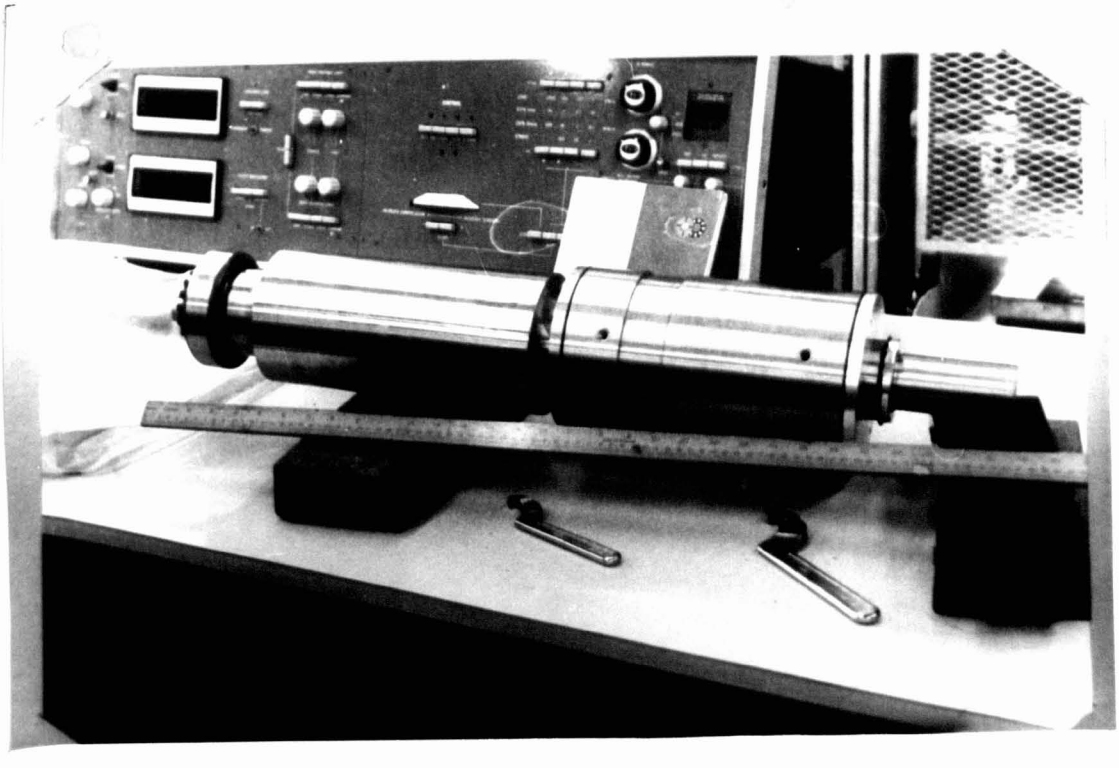

FIG. 6.8 TEST SHAFT WITH THE THRUST AND TAIL BEARINGS HOUSING.

roller bearings. To achieve the speeds of the specification given in Table 1.1, a cylindrical roller bearing of 60 mm bore has been used. Figure 6.7 shows the tail bearing, thrust bearing and the slave bearing mounted on the test shaft.

6.2.5 The Design of the Rolling Bearings Housing

A steel housing to house the thrust bearing and the tail bearing was designed with the following functions in mind:

i) The outer ring of the thrust ball bearing is a clearance fit with the housing. The magnitude of that radial clearance must be greater than the shaft deflection at that point under the maximum load so that the bearing is subjected only to thrust loads.

ii) The outer ring of the tail bearing is an interference fit with the housing. However, dismounting the housing from the shaft could be easily made as the inner and outer rings of the tail bearing are separable. The roller tail bearing provides no constraint of axial movements due to thermal expansion.

iii) The cover plates (i.e. seals), have been machined with a sufficient clearance to give an adequate venting area for the air of the mist lubrication. The flow of air is a provision against the ingress of dirt. Figure 6.8 shows the housing assembled to the shaft, while Figure 6.9 shows the manufacturing drawing for the housing.

6.2.6 The Design of the Rolling Bearings Lubricating System

For high speed bearings, or where high bearing temperatures prevail, the main task of lubricant is to remove heat, and several methods of lubrication are available. One of these is mist lubrication in which

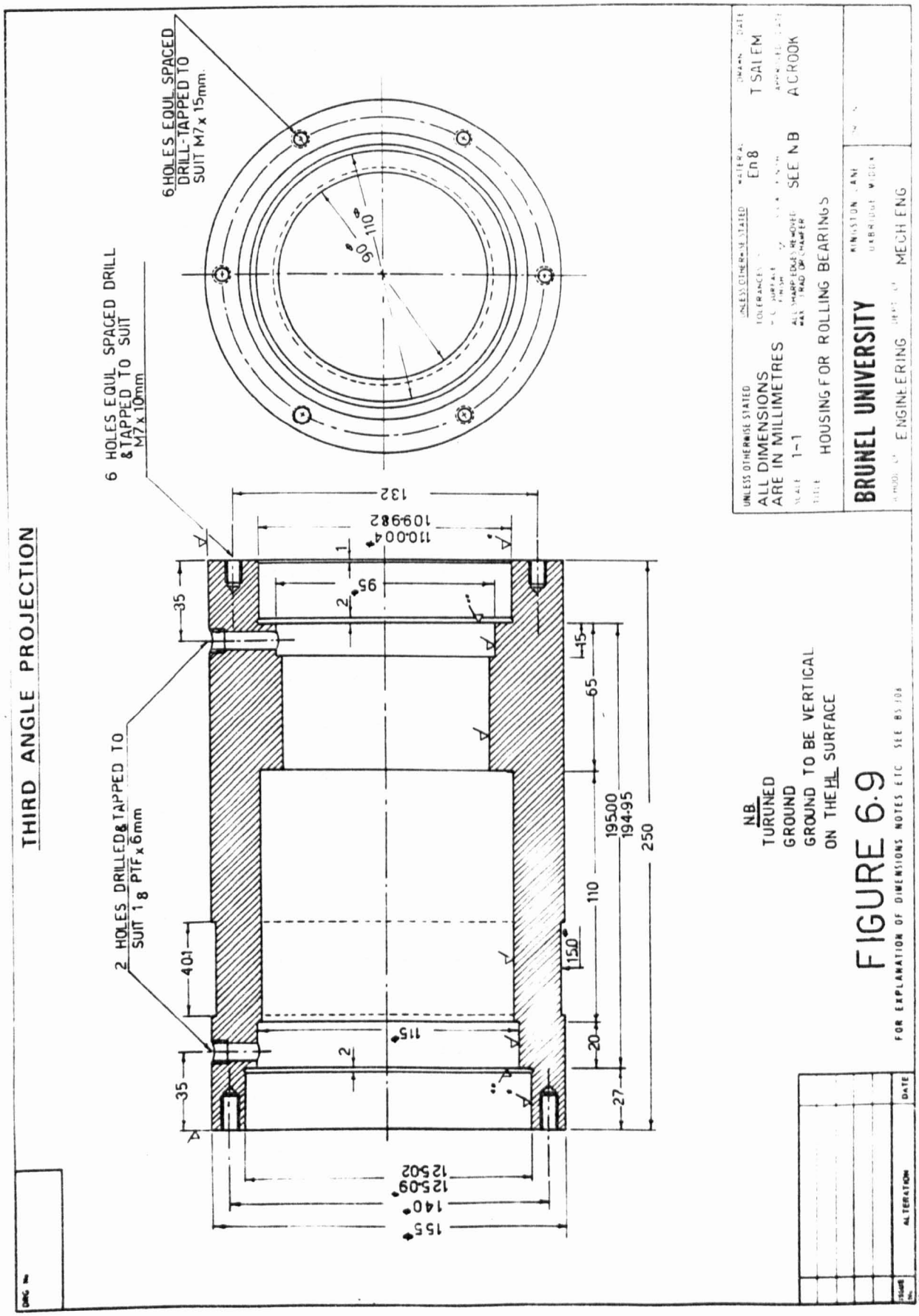
THIRD ANGLE PROJECTION
6 HOLES EQUL SPACED DRILL &TAPPED TO SUIT M7 x 10mm
6 HOLES EQUL SPACED DRILL-TAPPED TO SUIT M7 x 15mm.
2 HOLES DRILLED & TAPPED TO SUIT 1/8 PTF x 6mm
132
110.004
109.982
95
35
40
115
2
150
110
65
45
20
27
195.00
194.95
250
125.02
125.09
140
155
NB
TURUNED
GROUND
GROUND TO BE VERTICAL ON THE HL SURFACE
UNLESS OTHERWISE STATED
ALL DIMENSIONS ARE IN MILLIMETRES
SCALE 1-1
TITLE HOUSING FOR ROLLING BEARINGS
MATERIAL En8
SEE NB
DRAWN T SALEM
APPROVED A CROOK
BRUNEL UNIVERSITY
KINGSTON LANE UXBRIDGE MIDDX
DEPT OF ENGINEERING MECH ENG
FIGURE 6.9
FOR EXPLANATION OF DIMENSIONS NOTES ETC SEE BS 308
ISSUE No.
ALTERATION
DATE
DRG No

a suspension of oil in air is forced through the bearings.

The oil mist consists of atomised oil in air and it is conveyed to the lubricating point where it is completely or partially precipitated. The size of the spray nozzles, quantity of air, quantity of oil, and the air pressure, are supplied by the manufacturer.

Two oils of different viscosities have been used in the mist lubricator. The full specifications are presented in Appendix 6.

6.2.7 Design of the Loading System

To apply a radial load on the three lobe bearing, a hydraulic ram is employed to apply radial loads via a slave bearing, to the overhang of the shaft (Figures 6.10-6.12).

In Figure 6.10 a self-aligning spherical roller bearing[1], is mounted in a bearing housing[2] and the housing is held coaxial with the shaft[3] by the rod[4]. The load is applied through a hydraulic ram[5] of known area and pressure. The loading bearing itself is lubricated through the mist fitting[6] which is connected to the mist lubricator by the plastic tube[7]. The loading bearing was considered to be a sacrificial bearing, but in fact there has been no failure of it.

6.2.8 The Design of Oil Circuit for the Externally Pressurized and Self-Generating Operation.

The oil circuit is illustrated by Figure 6.13. The high and low pressure circuits are arranged so that they can be operated individually or simultaneously. However, an oil cooler is provided only in the low pressure circuit, but the circuit is arranged so that oil from the cooler is passed directly back to the sump if the low pressure supply to the bearing is not required, but it is required to remove

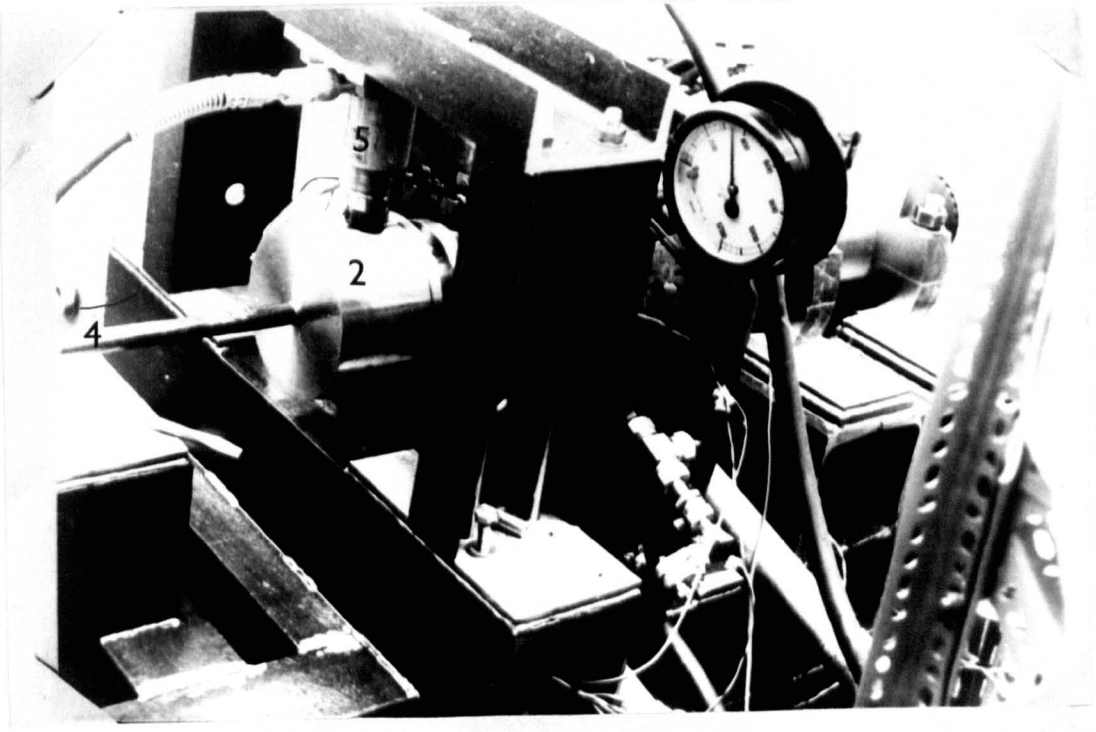

FIG. 6.10 LOADING SYSTEM.

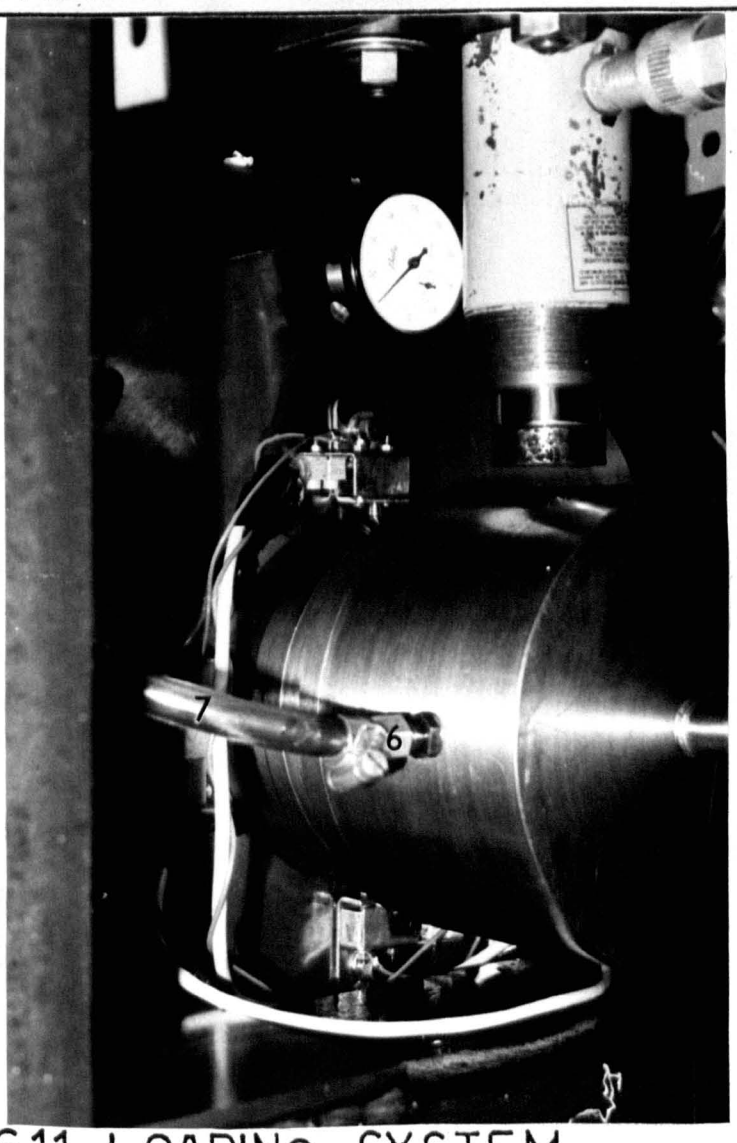

FIG. 6.11 LOADING SYSTEM.

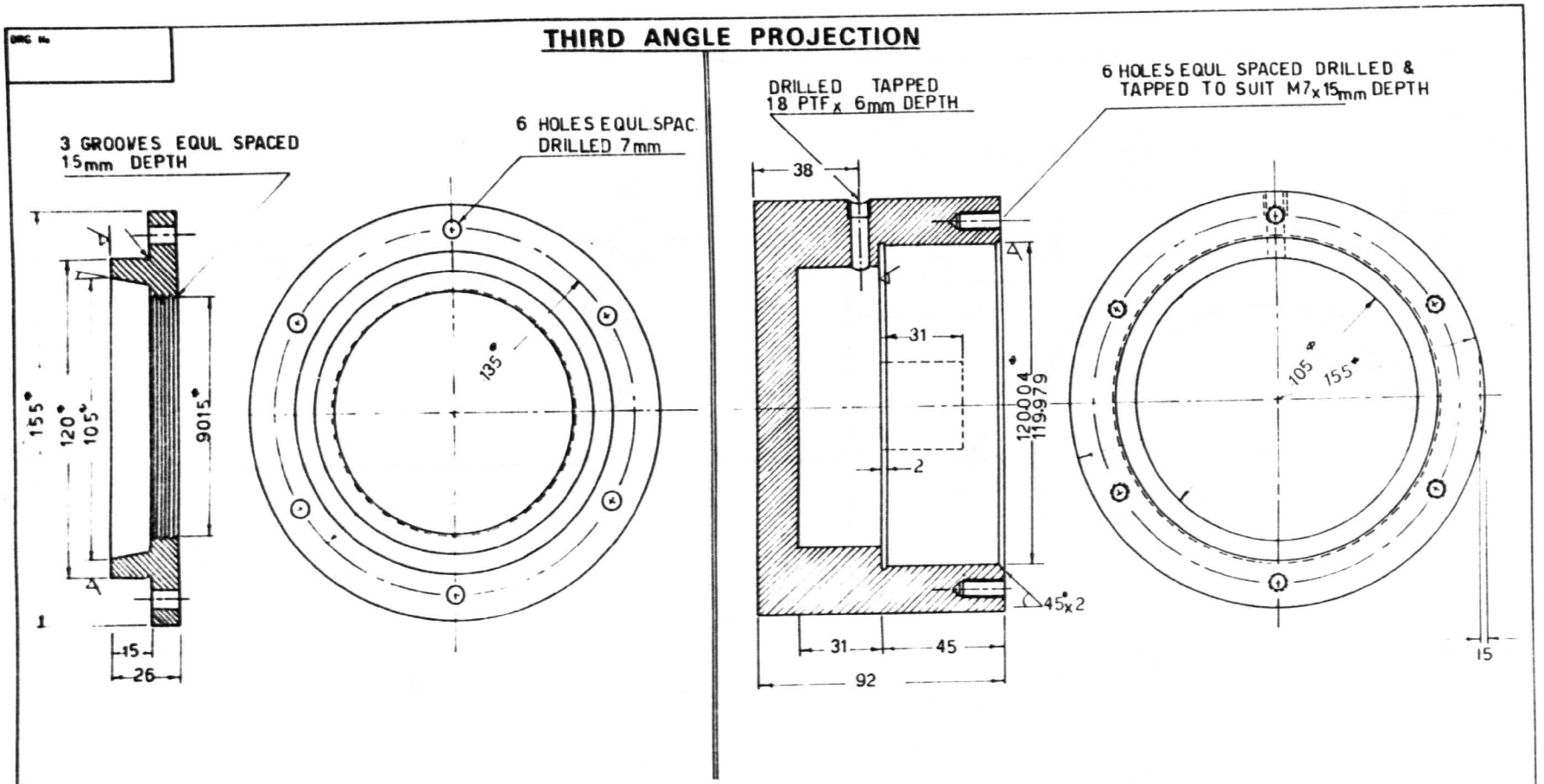

FIGURE 6·12

UNLESS OTHERWISE STATED ALL DIMENSIONS ARE IN MILLIMETRES	UNLESS OTHERWISE STATED TOLERANCES	MATERIAL M.S.	DRAWN T.SALEM DATE
SCALE 1 1	ALL SHARP EDGES REMOVED MAX 1.5 RAD OR CHAMFER		APPROVED A.CROOK DATE
TITLE HOUSING FOR A SLAVE BEARING & A COVER PLATE			
BRUNEL UNIVERSITY KINGSTON LANE UXBRIDGE MIDDX			DRG No
SCHOOL OF ENGINEERING DEPT OF MECH. ENG.			

ISSUE No.	ALTERATION	DATE

FOR EXPLANATION OF DIMENSIONS NOTES ETC SEE BS 308

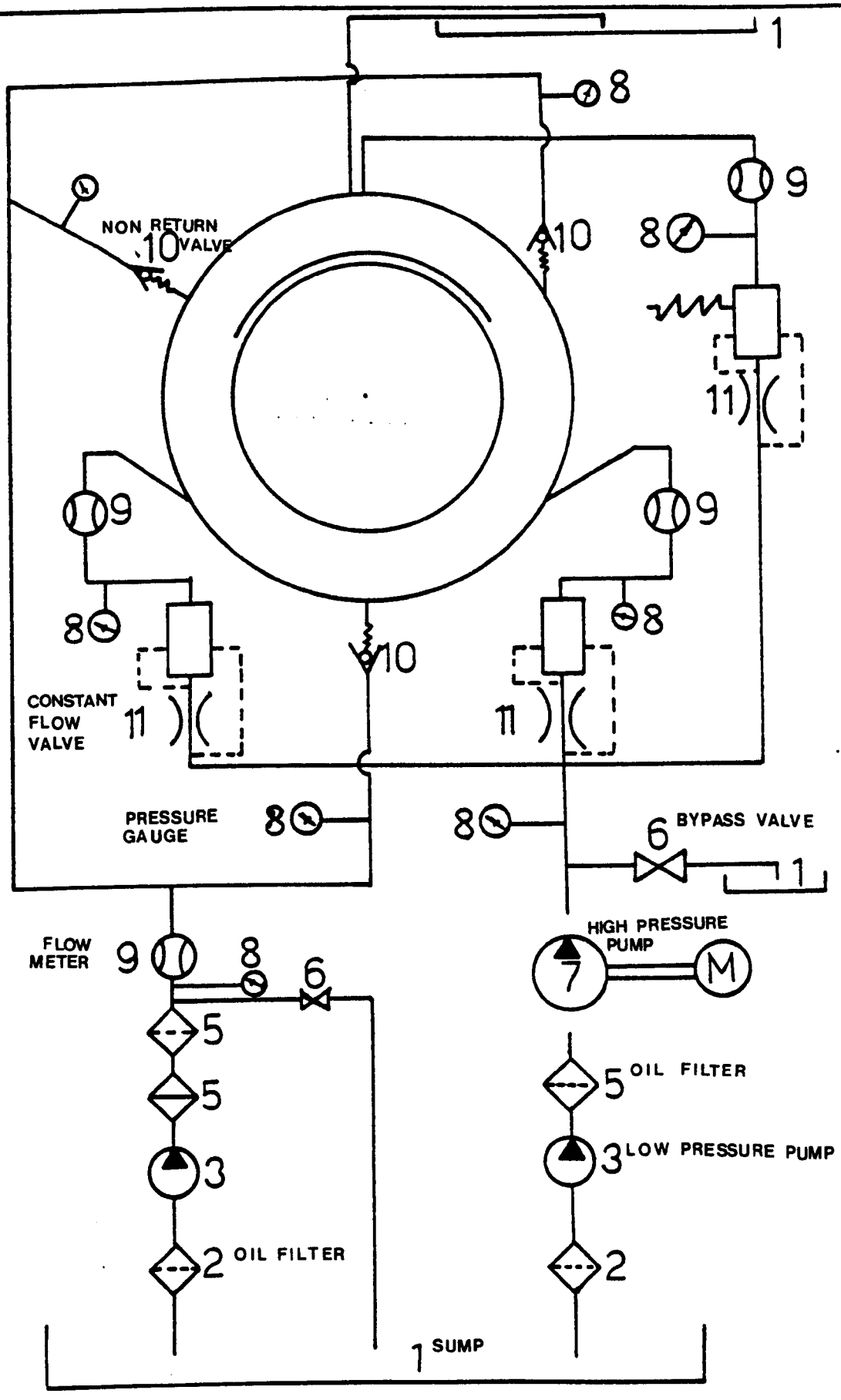

FIG.6.13 Self-generating and externally pressurized oil circuit.

heat generated in the high pressure circuit. The diagram shows four positions for flow measurement. However, only two flow meters were available, and they were moved from position to position as was appropriate for the test to be carried out.

6.2.9 Calibration of the Compensation Devices

The flow characteristics of each valve were tested by measuring volume flows at different valve settings, at different supply pressures, at different back pressures and at different oil temperatures between 22 & 80°C.

The valves were calibrated by subjecting each valve to varying back pressures whilst the pump line pressure was held constant. The flow rates were measured by using the "STOP WATCH AND BUCKET TECHNIQUE". The results show that the valves are working correctly. The variation of the oil viscosity between 250C.S and 17C.S. has resulted in a flow variation of 6%. However, by considering that some difference may occur due to the timing, the flow variation may be considered negligible.

The valve controlled the flow rate by varying the area of an orifice within the valve. To nulify the effects of fluctuating back pressure the valve contains a spring controlled by-pass loop.

The full calibration results are given in Appendix A.7, while in Figure 6.14 a calibration chart for the oil flow against the valve setting is shown.

6.2.10 Calibration of the Flowmeters

The flow meters which were used are of the turbine type, with generation of frequency signal which is directly proportional to the speed of rotation (i.e. the flow through the pipe line) so for high viscosity oil such meters indicate flow rates less than the true flow rates, and it is necessary to calibrate them. The basis of calibration was the

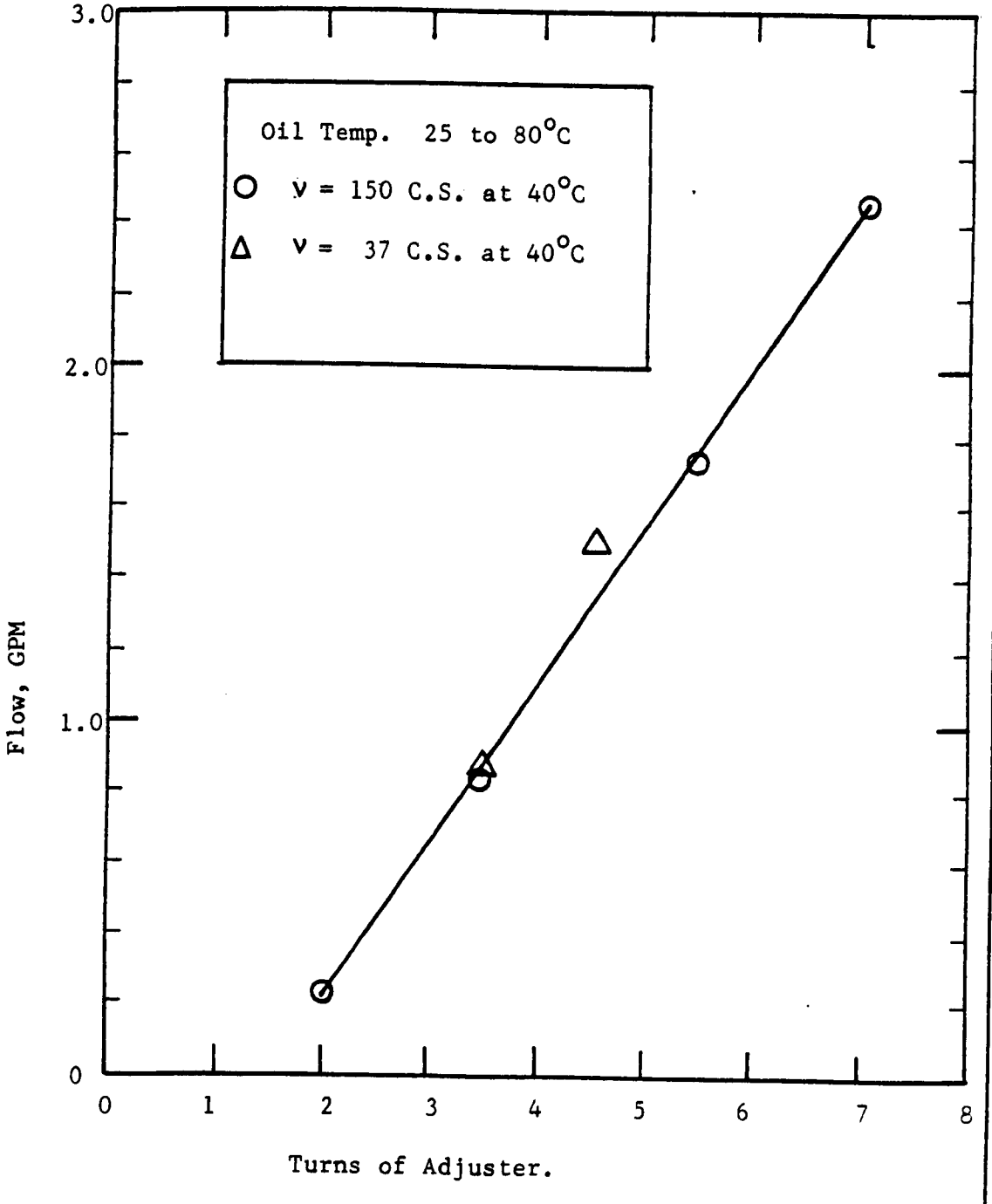

FIG.6.14 VFS 1/100 adjuster calibration curve.

flow associated with particular settings of the constant valves which had already been calibrated over the full range of viscosities by the "bucket and stop watch" technique (Appendix 7). But because the calibration was carried out in the high pressure line with constant flow valves already present, the opportunity was taken to check the calibration of the valves simultaneously. A calibration chart is given in Figure 6.15 where the dotted lines show the flow as measured by "bucket and stop watch" with the settings of the constant volume valve. Quite clearly it would be unrealistic to rely on the nominal reading of the flow meter at temperatures below 60°C, and that was not done. In that range, the high pressure oil flow was based upon the calibration chart of Figure 6.14, while the total oil flow from the bearing was measured by taking the drain to a bucket, and by using the "bucket and stop watch" technique. No internal inconsistency has ever arisen to bring the calibration of the flow meters into doubt.

6.2.11. Measurements of the Shaft Displacements and the Journal Centre Attitude.

The displacements of the journal with respect to the bearing were measured with inductive displacement transducers at each end of the bearing. The transducers were matched in pairs to increase the linearity of the output, and each pair is connected to a carrier frequency amplifier. The output was displayed on a digital millivolt meter. The electrical output from the amplifiers is either a voltage between $\pm$ 10V or a current between $\pm$ 20 ma. The output signal for a given displacement depends upon the initial gap between shaft and transducers and upon the gain of the amplifiers which can be adjusted internally. There are no external knobs for the adjustment of the gain so that gain remains constant until it is deliberately changed by internal adjustment.

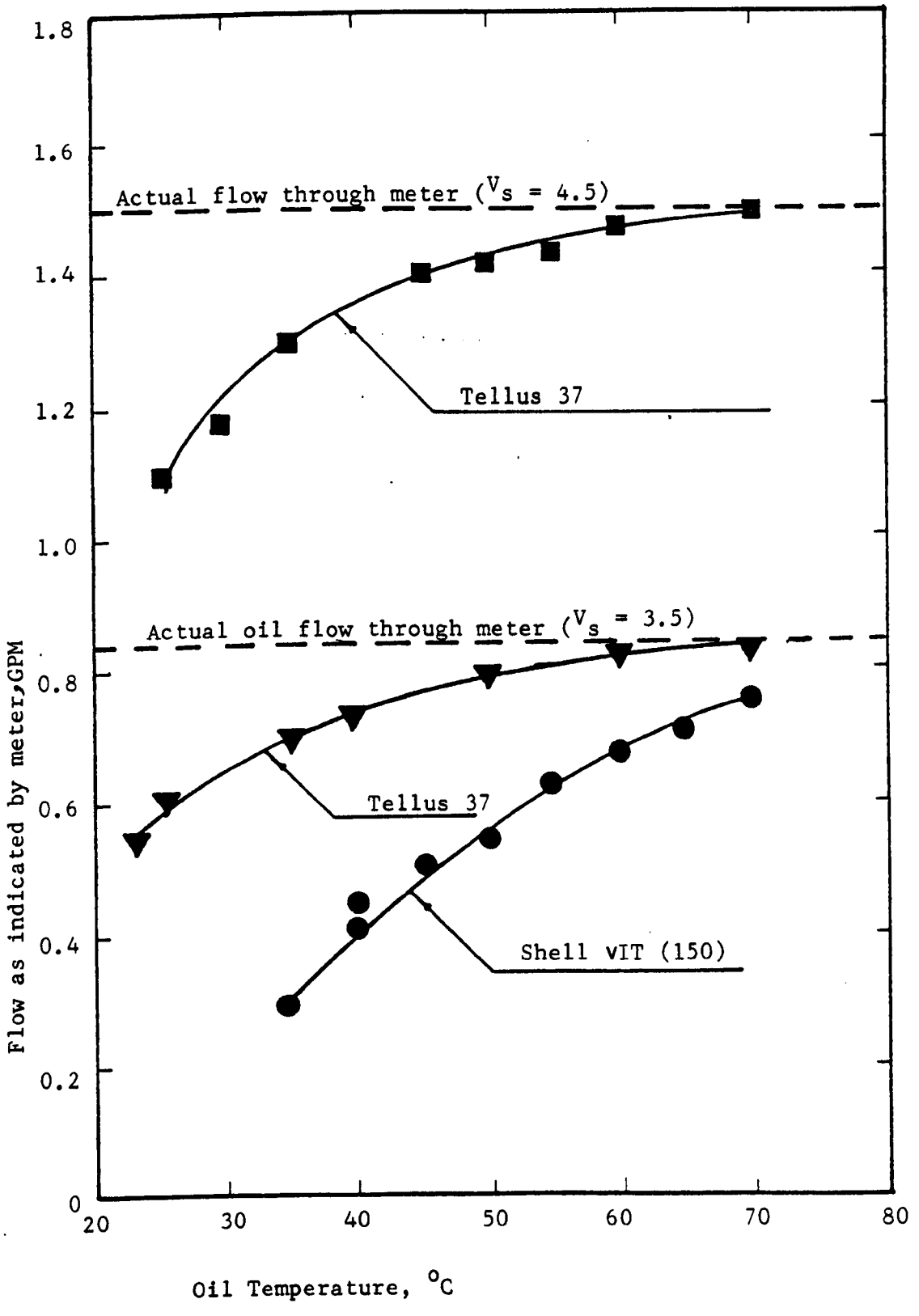

FIG.6.15 Variations of the flow-meter reading with the oil temperature.

The output signal can be brought to zero at will by connecting a potentiometer of a 100Ω to a zero external terminals, and in general the output was brought to zero with the journal in unloaded condition. The measuring circuit is shown by Figures 6.16 and 6.17.

6.2.12. Calibration of the Transducers.

To calibrate the inductive transducers, the high pressure system was engaged to locate the journal centrally within the bearing. The transducers were set by feeler gauges with an initial gap ranging between 0.1524 mm and 0.4 mm. Dial gauges were positioned as near as possible from the transducers. A load was applied to the shaft and the deflection of the shaft was measured by the dial gauges and the change in the output of the transducers was noted. This procedure was repeated at working temperatures ranging from 25°C and up to 85°C, the transducers were recalibrated from time to time (2 times a week) to ensure the accuracy of the results. Typical calibration charts are given in Figure 6.18. The difference between the calibration is attributed to the different gain settings.

6.2.13. Pressure Measurements.

The supply pressure of the high pressure pump, the pressures at the high pressure oil inlets and the pressures at the low pressure inlets were measured by Bourdon gauges which were dead weight calibrated.

6.2.14. Temperature Measurements

To monitor the temperatures of the oil at the bearing inlets, outlets, and bearing metal temperature, thermocouples were provided in 10 positions. The thermocouples were connected to a 'read out' unit with built-in compensations. Thermometer pockets were provided in the high pressure line and these pockets contained thermocouples and mercury in glass thermometers. This dual provision provided a check upon the read out unit.

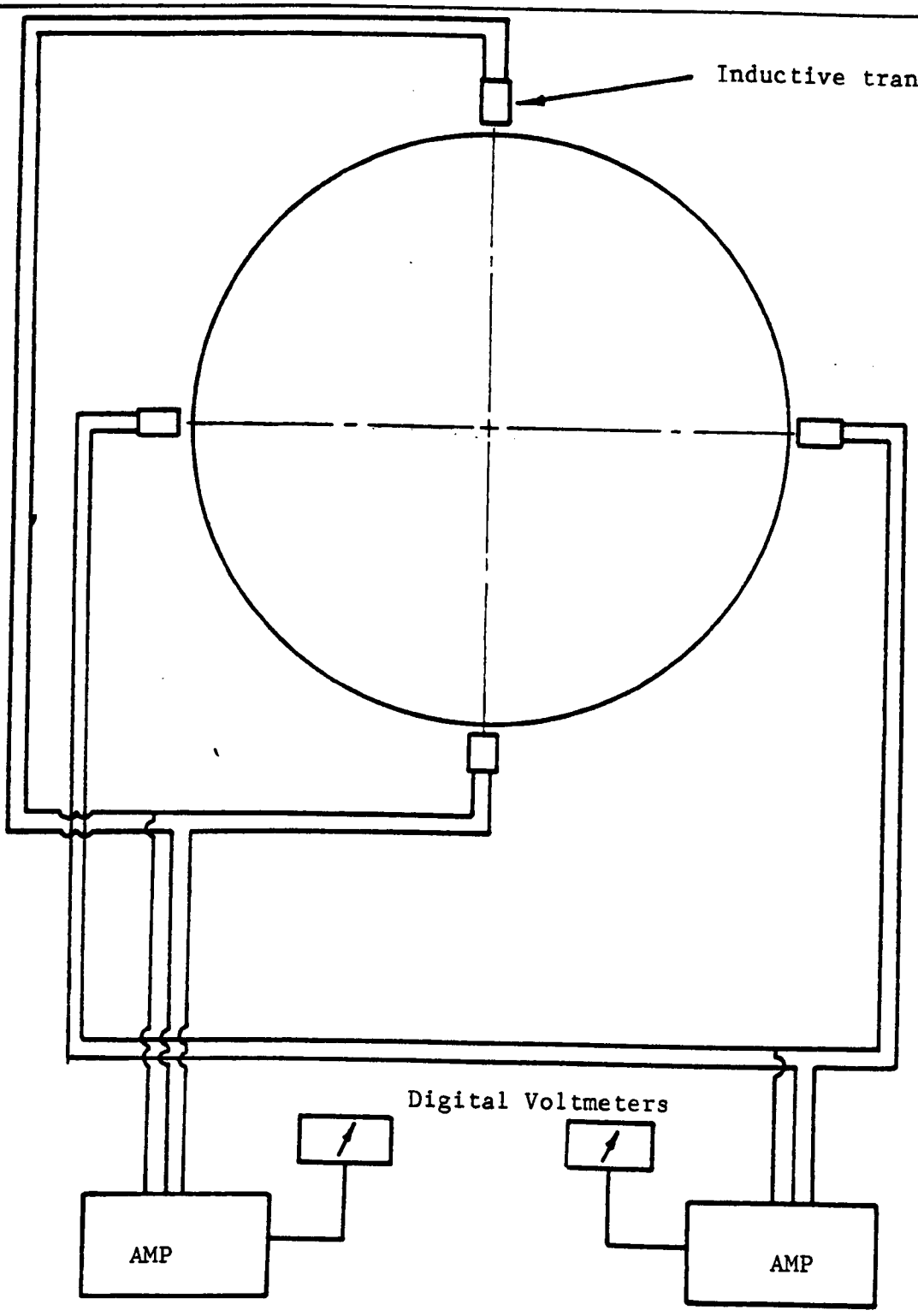

FIG.6.16 The inductive transducers circuit for displacements measurements.

The transducers are set permanently at A.A and B.B.
The transducers are moved to C.C and D.D, as the tests require.

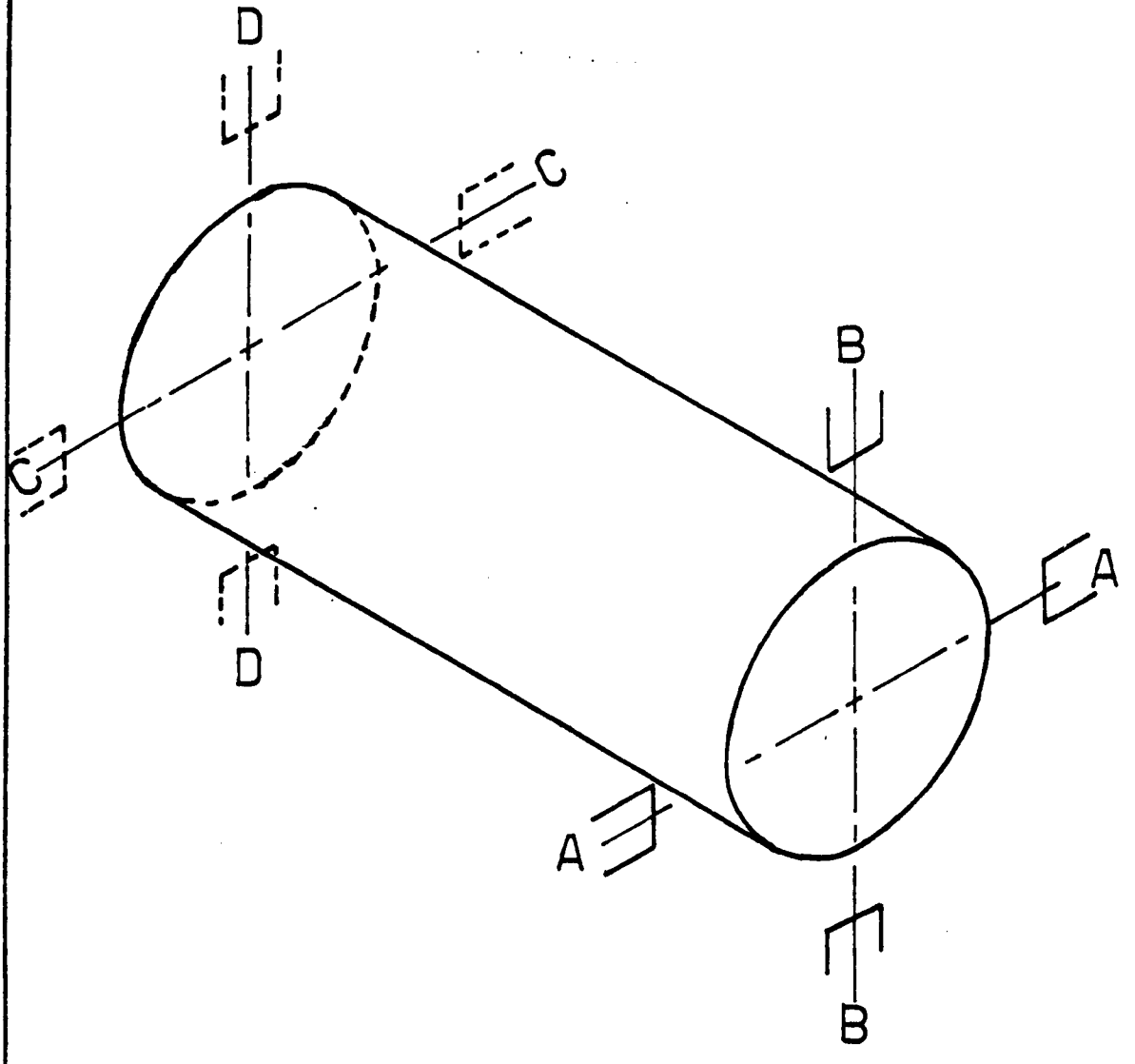

FIG.6.17 Transducers arrangements of the Journal.

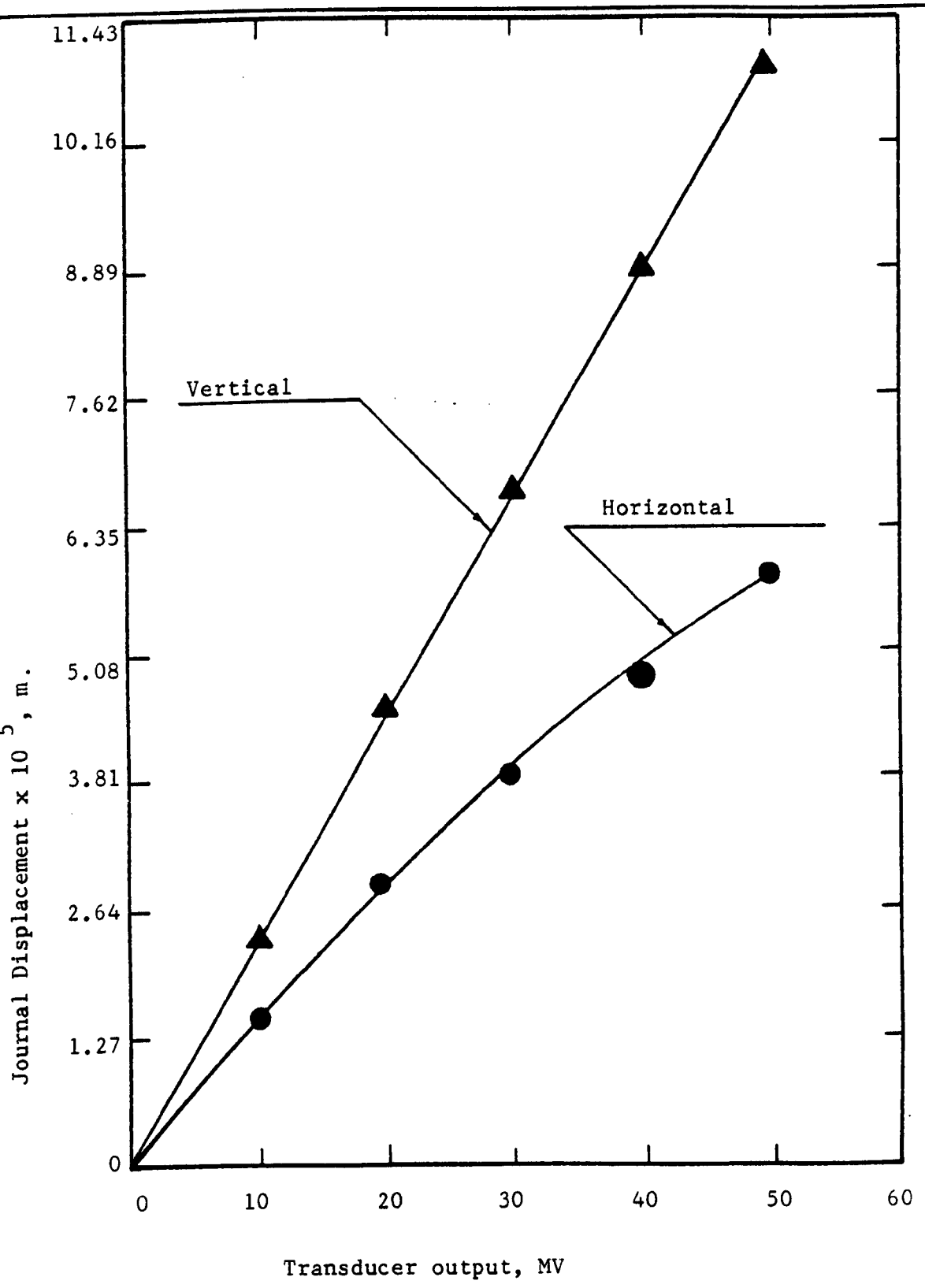

FIG.6.18 Calibration Chart for the displacement transducers.

6.2.15 The Metallic Contact Monitoring

To monitor any occurence there might be of metal to metal contact between journal and bearing,and also to provide a convenient means of judging the maximum allowable load, the electrical resistance between journal and bearing was measured with a meter which imposed less than 3 volts across the oil film. To permit these measurements of resistance the parallel paths such as through the housing of tail and thrust bearing were insulated from the main frame.

6.2.16 Drive Unit

In the early stages of the design, the very approximate estimation of the power loss suggested that a power of approximately 40KW would be required to rotate the test shaft at 9000rpm. (The more refined calculations of Chapter 3, and the experimental test results show that early estimate to be too large by a factor of approximately 2). The provision of a variable speed electrical drive of that power was too expensive to contemplate, and it was decided to use an existing 22KW/1500rpm electrical motor together with a set of timing pulleys and belt to provide various speeds in the range 720 to 4000rpm. The speed of the motor together with limitation of pulleys and belt limited the shaft speed with the motor to 4000rpm. In addition the starting torque imposed a limitation on the speed at which the shaft can be driven. It was seen that these limitations could be over-come by use of a petrol engine which could be run at 4000rpm, and which has a clutch to relieve the starting torque problem. Later a petrol engine drive was provided with belt connection to the shaft and speedsup to 7000rpm were obtained. The limitation on speed then became the maximum safe velocity of the belt itself. Because the test results up to 7000rpm give confidence that may be reasonably extrapolated to 9000rpm,

and because the time and additional cost which would be involved in reaching 9000rpm, the maximum test speed of 7000rpm was deemed to be adequate. The use of a belt drive directly to the end of the shaft inevitably introduces some vibrations, but the vibrations was never excessive. Some form of inline drive is obviously to be preferred.

6.2.17 Selection of the Oil

In the early approximate design investigation, Shell Oil Vitria 150 with kinematic viscosity of 150 centistokes at 40°C had been assumed, and this oil is one of the oils which has been used in the test. In the test programme the disadvantage of an excessive high outlet temperature with this oil emerged, whilst other aspects of the test results indicated that it would be permissible to use an oil of significantly lower viscosity. For instance, in paragraph 6.3.1 to 6.3.6 oil outlet temperatures of 72°C and 95°C are reported at 4000rpm in externally pressurized and in hydrodynamic tests respectively. Because oil temperature rise is approximately proportional to the rotational speed it is quite clear that an excessive oil outlet temperature would arise had the test been continued to higher rotational speeds. Theory indicates that the oil temperature rise is reduced when an oil of lower viscosity is employed. A second oil of lower viscosity "Shell Tellus 37" was employed in a further series of tests. The viscosity-temperature characteristics of these oils are given in Figures 6.19 to 6.20.

6.2.18 Power Loss Measurements

The power absorbed by a bearing has been measured in the usual way from measurements of oil flow and of oil temperature rise as the oil passes through the bearing. However a correction should be added to the

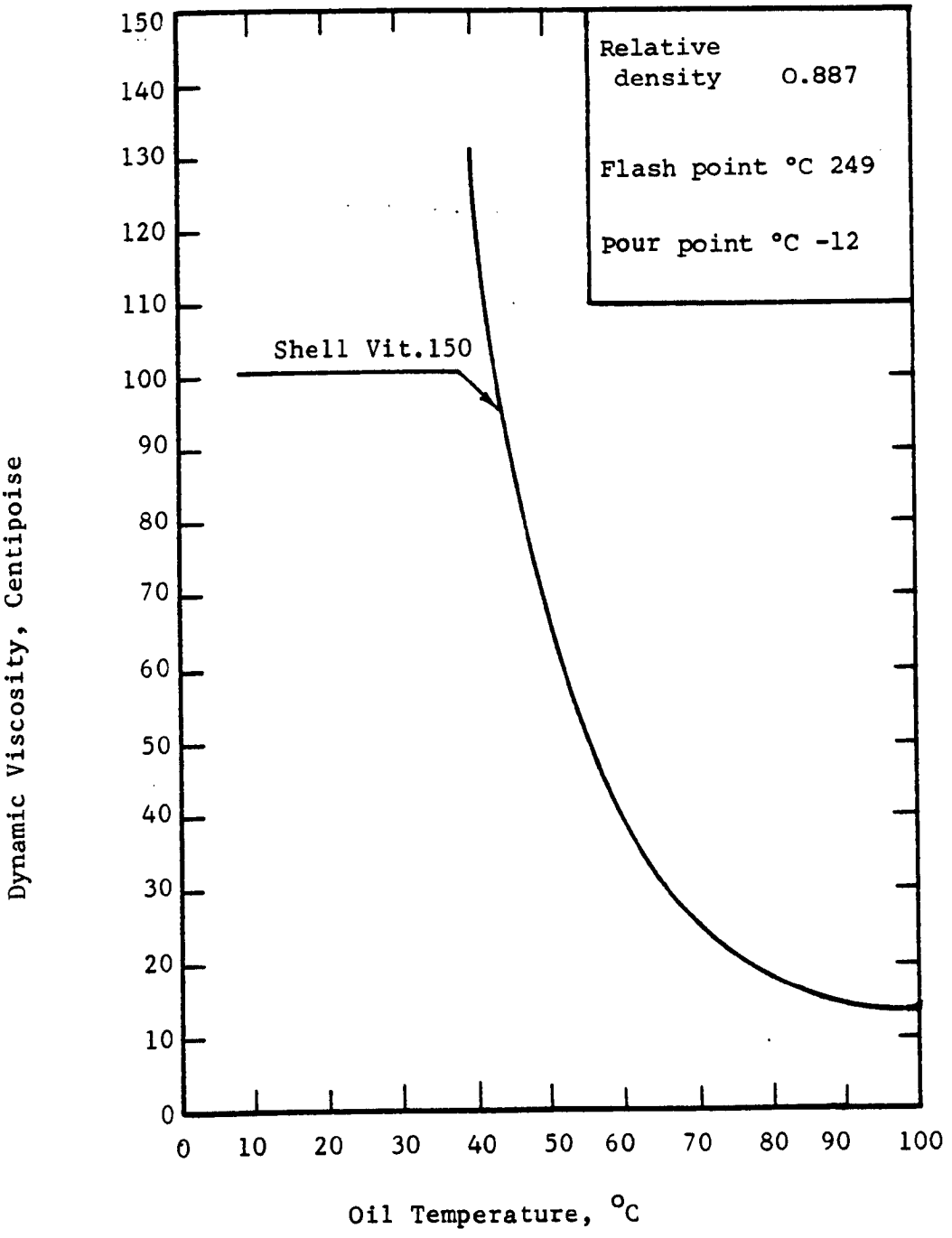

FIG.6.19 Typical viscosity-temperature characteristics of Shell Vitria 150

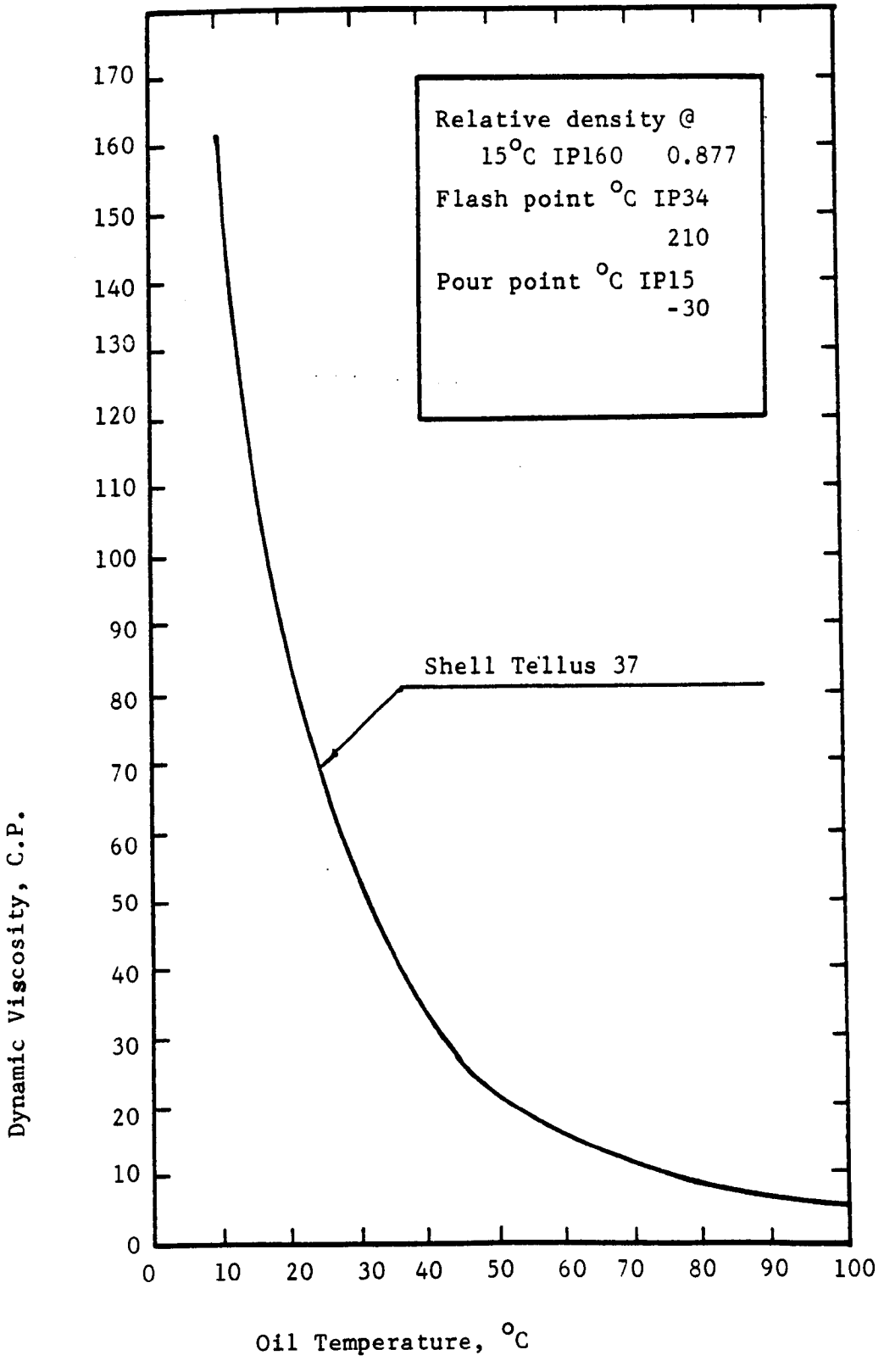

FIG.6.20 Typical viscosity-temperature characteristics of Shell Tellus 37.

power loss given by that calculation which does not include the heat fluxes of conduction along the journal and of heat transfer to the air from the pedestal and journal. The correction is relatively small and approximate means for its assessment will suffice.

If the bearing and journal satisfied the assumptions of Newton's Law of cooling then a quantity k can be defined which is given by

$$K = {}^{C}/_{T} \ln \left\{ \frac{\theta - \theta_e}{\theta_1 - \theta_e} \right\}$$

where k is the heat transfer coefficient, θ is the metal temperature at time T, θ_1 is the metal temperature at time O, θ_e is the ambient temperature which is taken as 22°C and C is the thermal capacity of the metal which may be calculated from

$$C = m C_p (\theta_1 - \theta_e)$$

where, C_p is the specific heat for steel and m is the mass of the bearing and pedestal metal.

The method employed to determine the correction was to take a cooling curve of the bearing pedestal immediately following the arrest of the journal, and the stopping of the oil flow. Typical cooling curves are shown in Figure 6.21. These cooling curves show that the assumptions of Newton's law of cooling do not hold because the curvature of the cooling curve is opposite to that which is required by Newton's Law of cooling. Nevertheless, the end points of the cooling curves have been used for the estimation of k, and of the heat loss to the surroundings. The thermal capacity C was taken to be the thermal capacity of the bearing and its pedestal and that portion of the

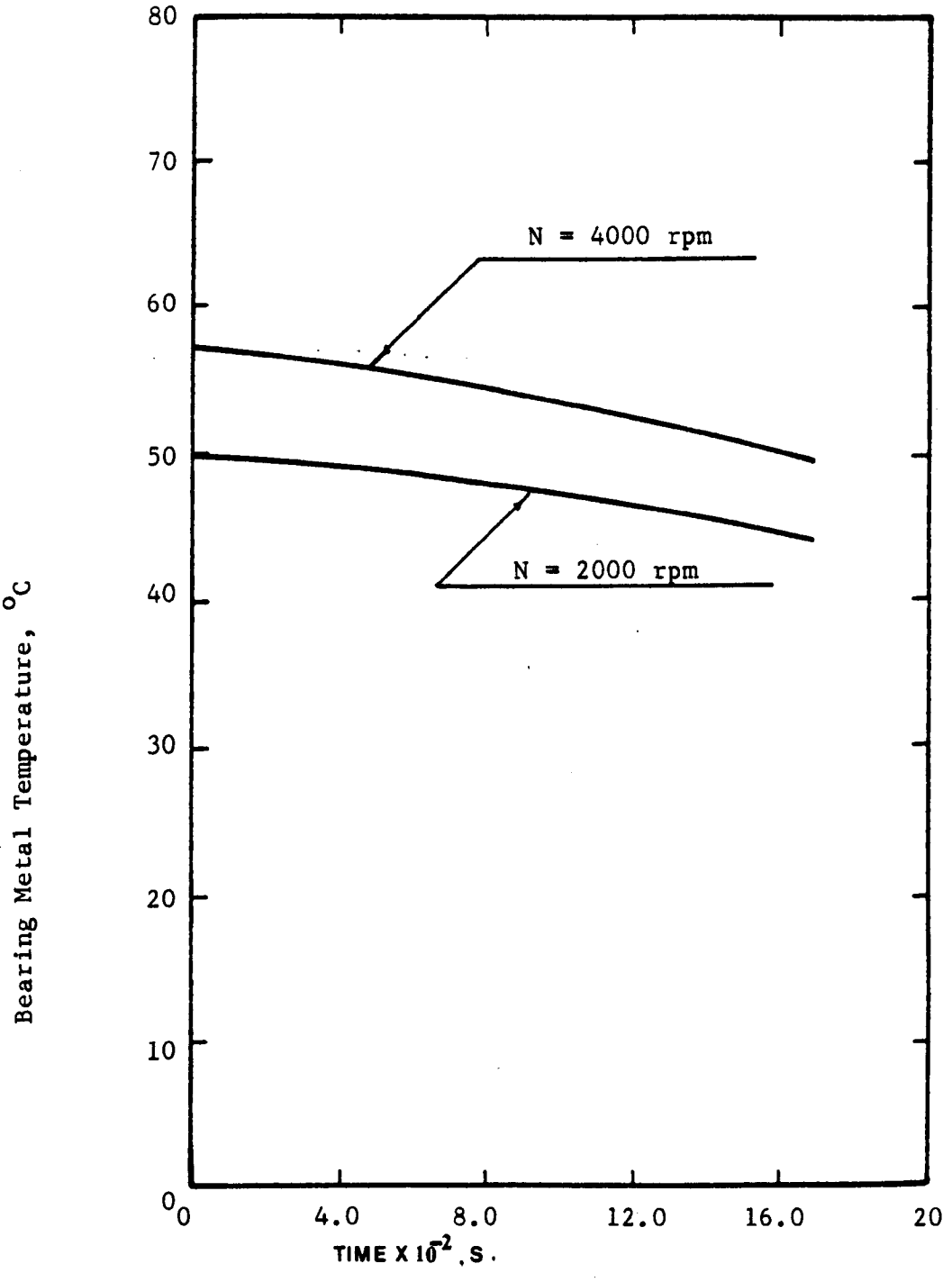

FIG.6.21 Variation of bearing metal temperature with the time.

journal within the bearing. The cooling curves of Figure 6.21 on the above approximate basis gave heat fluxes of 0.397 and 0.584KW respectively which are respectively 9% and 15% of the heat lost by way of the oil itself. These percentages are consistent with a value quoted in the literature, e.g. references 7 and 84 which give 15% as a correction factor for the heat lost by other means, and for the purpose of this investigation a uniform and conservative correction of 20% has been applied to the heat loss by way of the oil in arriving at the total power loss.

6.3 Tests and Test Results of the Externally Pressurized Operation

The following results relate to the bearing being supplied only with high pressure oil via constant volume control valves, and with shaft rotation in the range 0 to 4000rpm when the VIT 150 oil is used and in the range 0 to 6000rpm when Tellus 37 oil is used.

6.3.1 Static Stiffness

6.3.1a Test with VIT 150 Oil

The salient dimensions of the journal and bearing used in the tests are given in Table 6.1. The first test carried out in the main test rig was to measure the hydrostatic stiffness of the bearing, in much the same way as it had been measured in the static rig, and to compare the results with those previously obtained and which are reported in Chapter 4. A vertical load was applied to the shaft over-hang by the hydraulic ram and the displacement of the journal was measured at both ends, both by dial gauges and the inductive transducers which were mounted at positions B-B and D-D. Figure 6.22 shows the measured displacement along the axial length of the journal, the displacements at the AFT, MID, and the FORE planes are deduced

Lobe Diameter D m	Journal Diameter d m	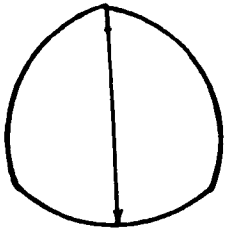 m	Offset Δr m	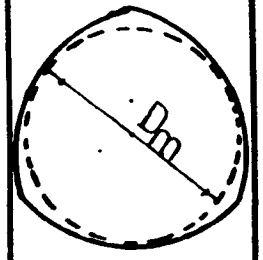	Lobe Diameter Clearance C m	Max. Clearance C_{Max} m	Min. Clearance C_{min} m	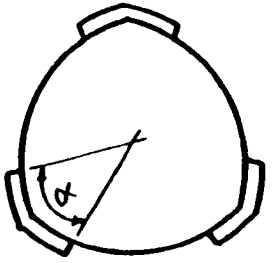	L/D
1.351×10^{-1}	1.349×10^{-1}	-	5.75×10^{-5}	-	2.6×10^{-4}	2.025×10^{-4}	1.45×10^{-4}	16	0.95

TABLE 6.1 Dimensions of the original test bearing.

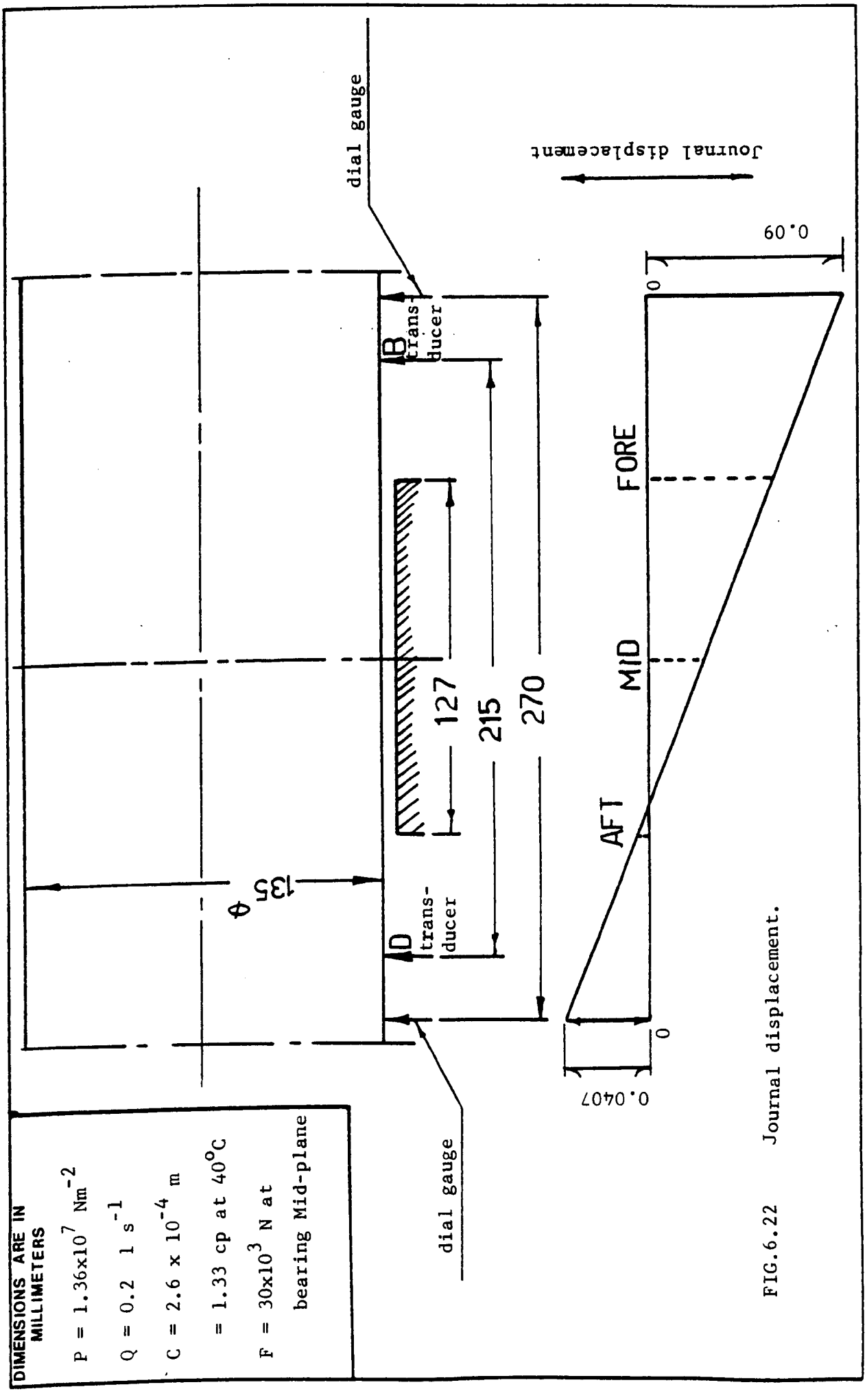

FIG.6.22 Journal displacement.

from the measured displacements at B and D. It may be seen from Figure 6.22 that the displacement varies along the axial length of the bearing. The measured displacement load relationships are shown by Figure 6.23. The magnitude of the displacements are plotted but the displacements of line AFT were in fact of opposite sign to those of lines MID and FORE; the change in sign reflects the bending of the shaft itself. However, line MID, which is the true mean line has been used to derive a mean stiffness which is $1.125 \times 10^{9} Nm^{-1}$, and which is substantially the stiffness as found in the static rig ($1.4 \times 10^{9} Nm^{-1}$). The journal did not tilt in the static rig, and consequently this substantial agreement shows that the tilting of the journal in the bearing, which arose because of the bending of the shaft, has little effect upon the mean stiffness.

The journal displacement was measured in the vertical direction and the horizontal direction. The displacements in the horizontal plane at the AFT, MID, and FORE planes were deduced from the measured displacements, and from the disposition of the planes of measurement as shown by Figure 6.24.

However, for a stationary shaft, the displacement of the journal in the horizontal direction is negligible compared with that in the vertical direction. The results are shown in Figure 6.25 where the displacements are given in the form of a polar diagram.

6.3.1b Test with Tellus 37 Oil

The static stiffness of the bearing was measured in much the same way as it had been measured in paragraph 6.3.1a. The measured displacement load relationships are shown by Figure 6.26. Also Figure 6.26 shows the measured displacements which have been reported in paragraph 6.3.1a.

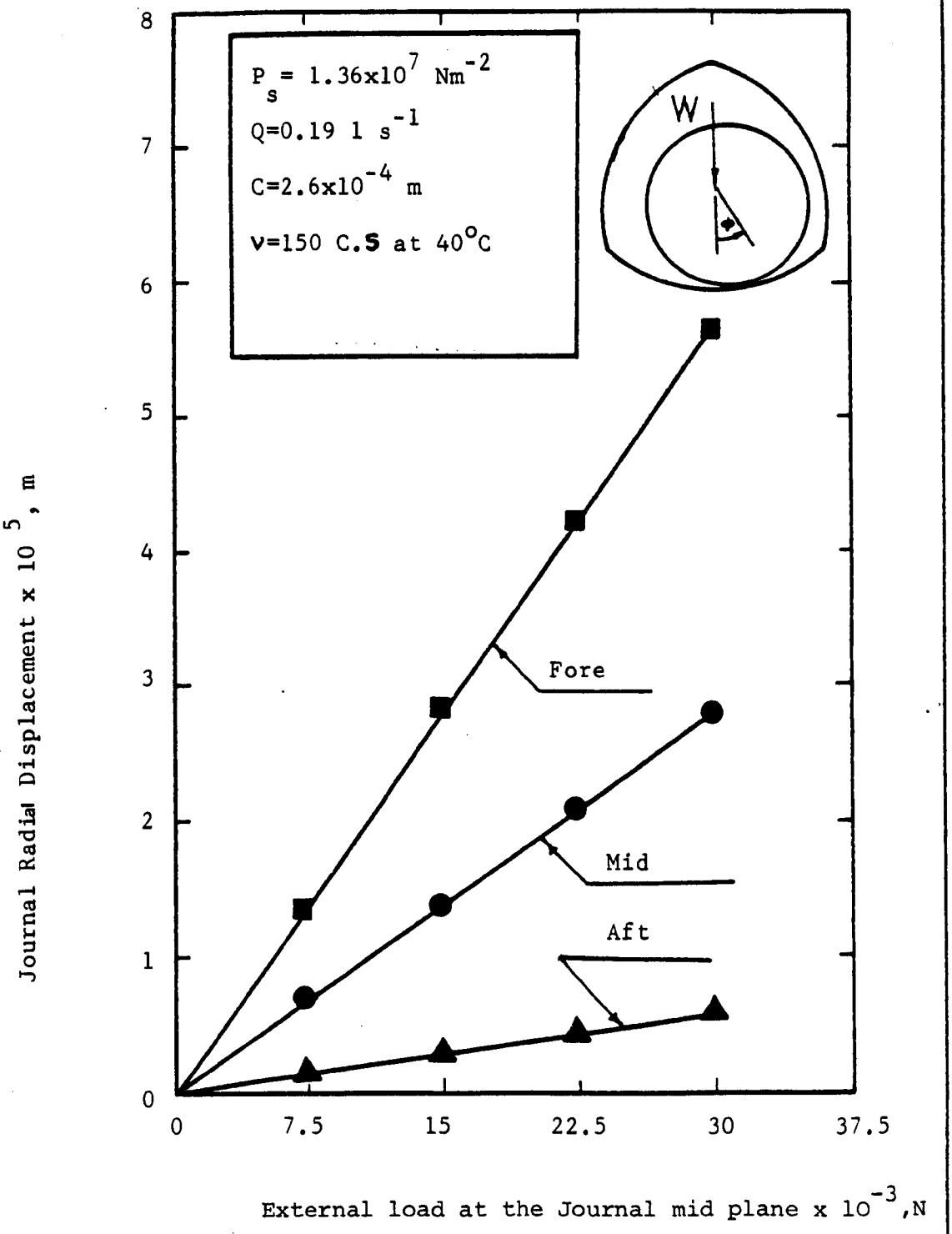

FIG.6.23 Load-displacement relationship (experimental)

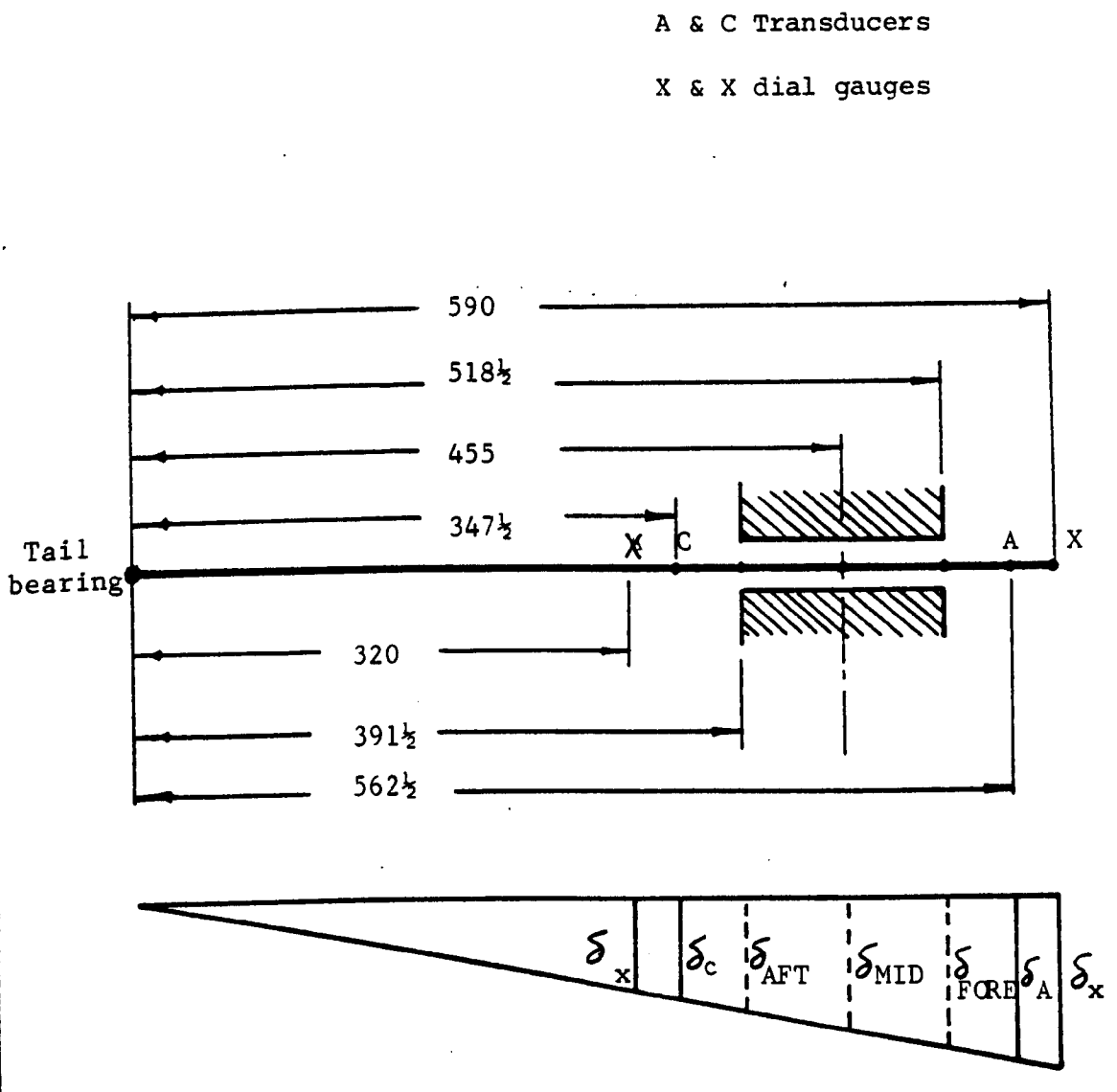

FIG.6.24 Shaft displacement in the horizontal plane.

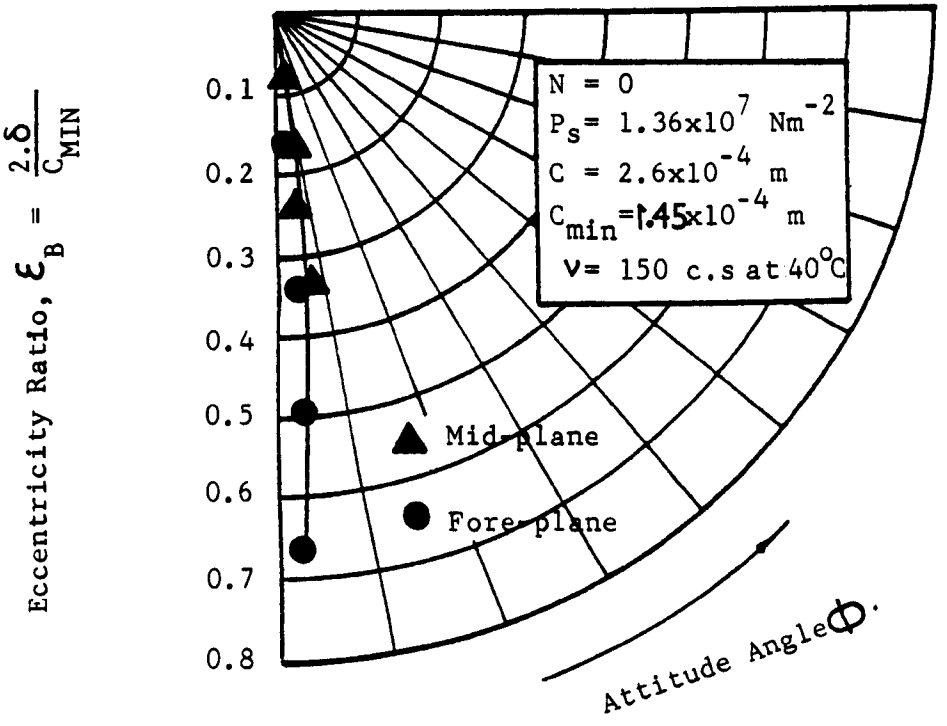

FIG.6.25 Typical locus of Journal centre (experimental).

It may be seen that with the Shell VIT.150 oil and at an operating temperature of 50°C (μ=67CP) the static stiffness at the journal mid-plane was 1.125×10^{9} Nm^{-1}. By using the Tellus 37 oil and at an operating temperature of 65°C ($\mu = 13Cp$) the static stiffness at the journal mid-plane becomes 8.98×10^{8} Nm^{-1}. However, the reduction in the oil viscosity by 80% leads to a reduction in the static stiffness by 20%. Also it may be seen from Figure 6.26 that at operating temperatures between 35 and 42°C the static stiffness given by the low viscosity oil is much the same as that given by a high viscosity oil.

6.3.2. Static Deflection of the Test Shaft

The unexpected change in the sign of the deflection over the length of the bearing suggested that the deflection of the shaft should be measured at as many axial positions as were available. The measured displacements are shown by the circular points in Figure 6.27, and the points suggest a significant bending of the shaft under the moment and shear forces which result from the load. A computer programme* existed for calculating shaft displacements at speed under the influence of any number of out of balance forces and out of balance moments. The programme is based upon the transfer matrix method of Myklestadt and Prohl. This programme was adapted to calculate the bending of the static shaft by entering an insignificant speed of rotation. The result of the calculation is given by the dotted line of Figure 6.27. The tail bearing was assumed to be connected to ground by a spring of stiffness $3 \times 10^{8} Nm^{-1}$, and the journal bearing was represented by 3 springs disposed along its length with stiffnesses adjusted so

* The computer programme has been written by Professor A.W. Crook.

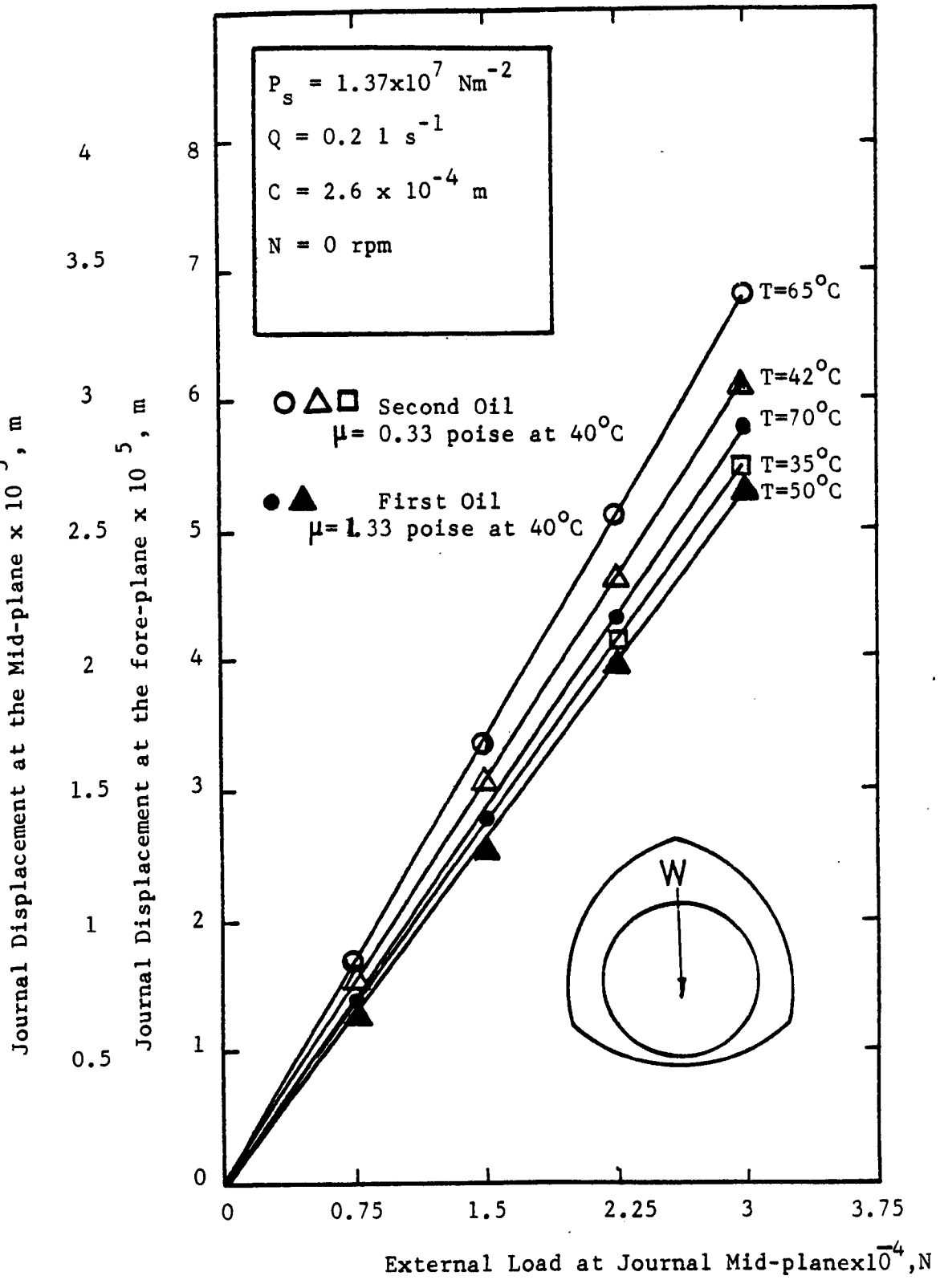

FIG.6.26 Displacement-load relationship for externally pressurized operation (experimental).

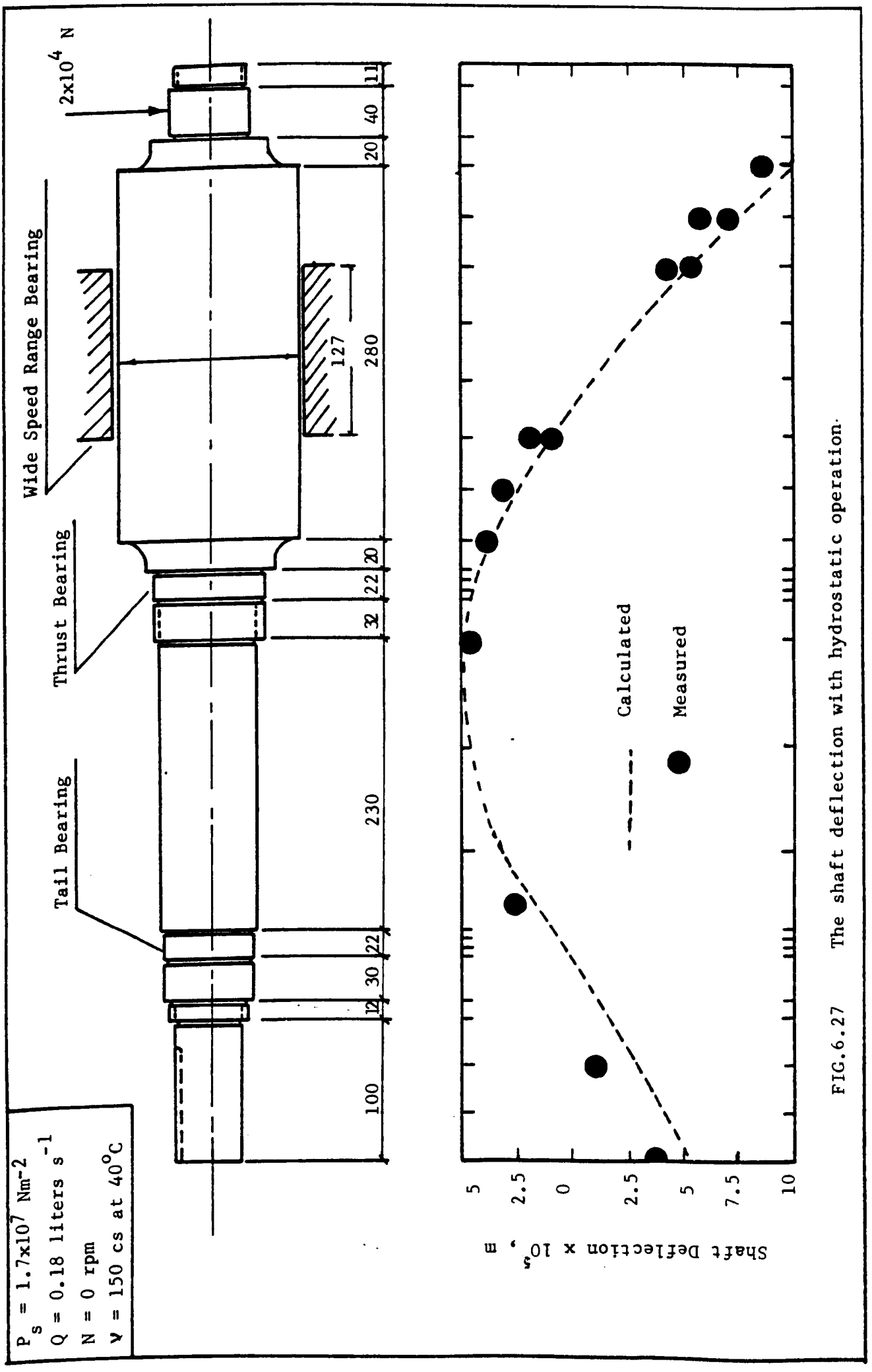

FIG.6.27 The shaft deflection with hydrostatic operation.

that together their effect was equivalent to the measured hydrostatic stiffness of the bearing itself. It may be seen from Figure 6.27 that there is substantial agreement between observed and calculated displacement and it is concluded that the bending of the shaft makes a considerable contribution to the total deflection at the loading position. The programme has been used to investigate different shaft, tail and thrust bearing arrangements and the results are presented and discussed in Chapter 8. The computer programme itself with a sample of the output are presented in Appendix A8.

6.3.3 The Load Speed Relationship of the Externally Pressurized Operation

6.3.3a. Tests with VIT 150 Oil

With shaft rotation the journal displacement at both the bearing ends was measured by the inductive displacement transducers. The transducers were first mounted at positions C-C and D-D and then moved to positions A-A and B-B (Figures 6.17, 6.22 and 6.24). During each test the speed was brought to zero and a check upon the calibration of the inductive transducers against the dial gauges was made. The journal displacements at the AFT, MID and FORE plane positions were deduced from the measured displacements in their planes of measurements. The results are shown in Figures 6.28 and 6.29. The displacements at the AFT plane are not plotted because they were very small ($\sim 5 \times 10^{-6}$ m). The test results are shown in the form of polar diagrams in Figure 6.28. It may be seen from Figures 6.28 and 6.29 that the bearing displacement decreases as the speed increases and that the bearing attitude angle changes marginally as the speed was increased from 1000 to 4000 rpm.

6.3.3b Tests with Tellus 37 Oil

With shaft rotation the journal displacement was measured in much the same way as described in paragraph 6.3.a, except that in

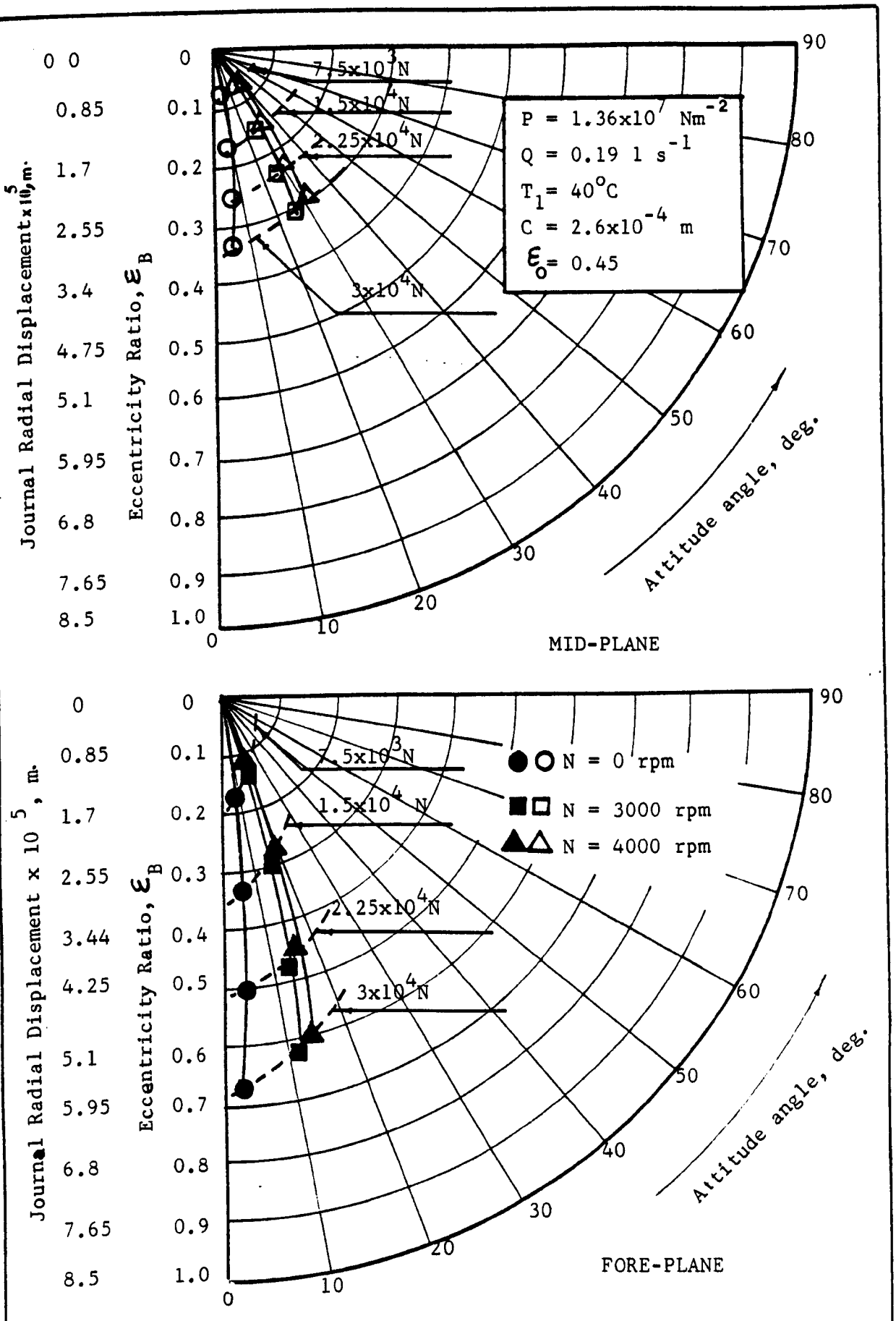

FIG.6.28 Journal centre locus (experimental)

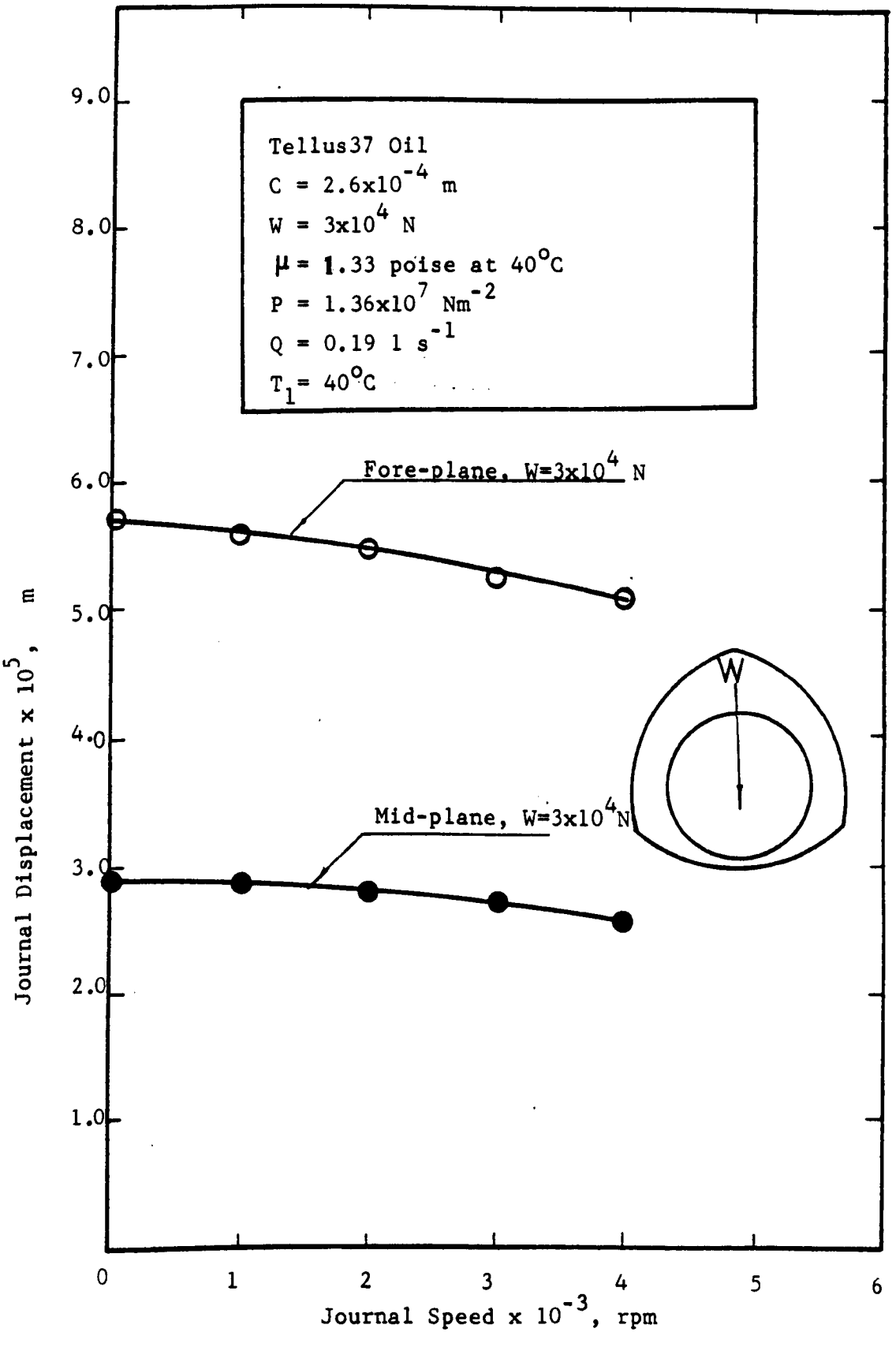

FIG.6.29 Displacement-speed characteristics for the externally pressurized operation.

the present measurements the maximum speed is 6000rpm instead of 4000rpm. The results of measurements are shown in Figure 6.30. It may be seen at 4000 rpm and with a radial force of $3x10^{4}N$, that the radial displacement at the journal mid-plane is $2.65x10^{-5}m$ (i.e. the bearing stiffness is $1.132x10^{9}Nm^{-1}$). The oil outlet temperature was $59^{o}C$. In paragraph 6.3.3b (Figure 6.29) it has been shown that by using a high viscosity oil the radial displacement at the journal mid-plane was $2.55x10^{-5}m$(i.e. the bearing stiffness is $1.176x10^{9}Nm^{-1}$). The oil outlet temperature was $72^{o}C$. However, it may be seen from this example that with shaft rotation there is negligible difference between the stiffness obtained by using an oil of high viscosity and the stiffness obtained by using an oil of low viscosity, but it is quite clear that there is a big difference in the oil outlet temperature which favours the use of the low viscosity oil. Also it may be seen from Figure 6.30 that the journal displacement decreases as the speed increases.

6.3.4 Power Loss, Oil Flow and Oil Temperature Rise for the Externally Pressurized Operation

6.3.4a Tests with the VIT 150 Oil

With a constant oil flow the variation of power loss and of oil temperature rise with journal speed are given respectively in Figures 6.31 and 6.32. Power loss and oil temperature rise are given for various speeds as functions of oil inlet temperature in Figure 6.33. All measurements of power loss have been derived from measurements of oil flow, and oil temperature rise. Corrections were made for the heating of the oil due to the fall in its pressure, and for heat losses to the surroundings. The pressure correction was made by measuring the temperare rise of the oil through the bearing when the journal was stationary and this temperature rise was subsequently

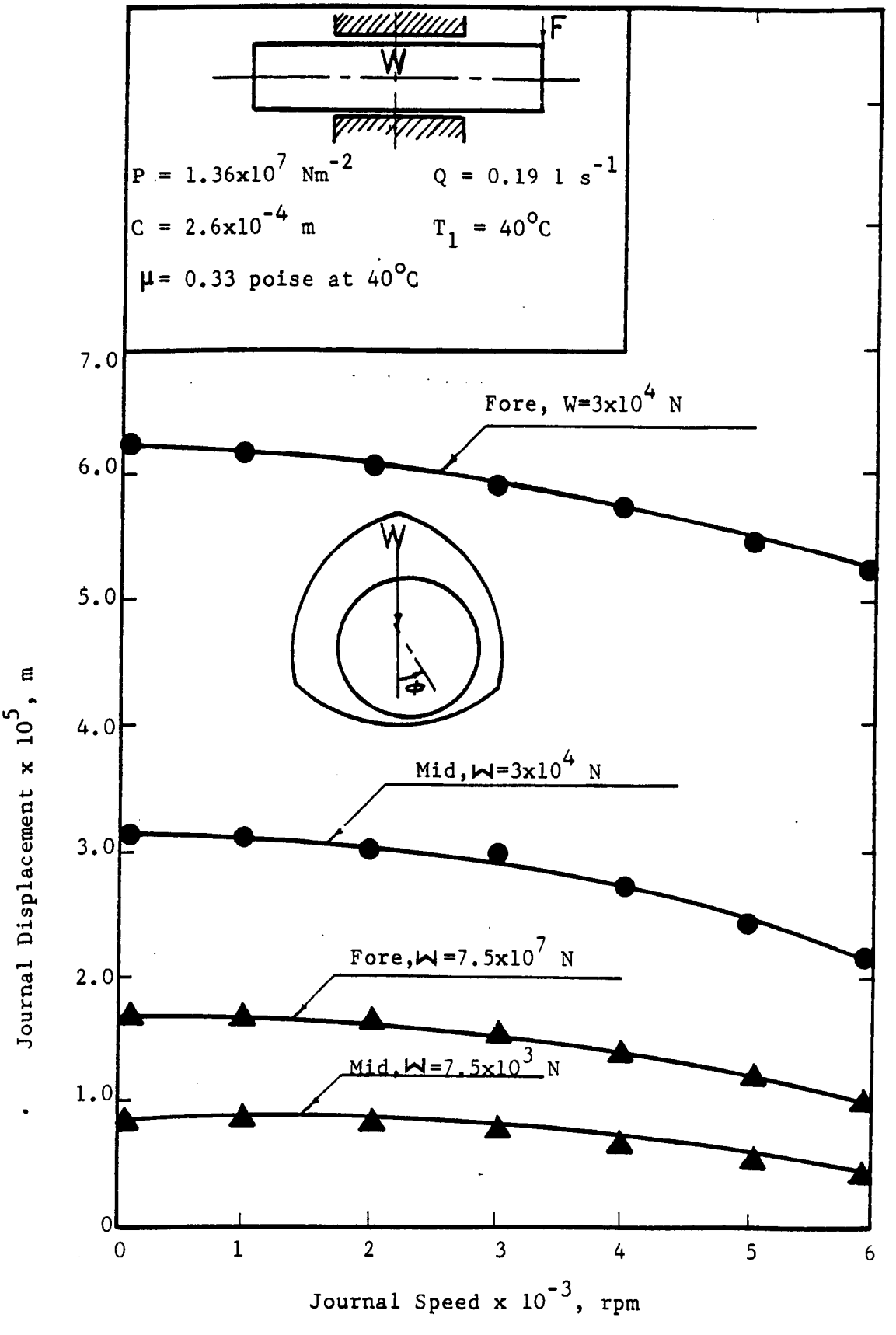

FIG.6.30 Displacement-speed characteristics for the externally pressurized operation.

deducted from the measured temperature rise when the journal was rotating. The measured temperature rise was approximately $4^{o}C$ which is in substantial agreement with a predicted temperature rise of 5°C as calculated from the condition of constant total enthalpy of the oil. The correction for heat loss to the surroundings was found from cooling curves with the journal stationary and with no oil flow (paragraph 6.2.18). This correction was found to be 20% of the total heat loss, and has been applied in the results.

It may be seen from Figure 6.31 that there is no change in the slope of the log-log plot of power loss versus speed up to 4000rpm, which suggests no departure from laminar flow in the oil film. The plotted power loss is for the no load condition; limited tests have been carried out in the loaded condition and the results show that as the load increases there is a slight increase in the oil outlet temperature. In considering this trend it must be recalled that the oil flow was held constant.

The power loss-speed characteristics of Figure 6.31 is expressed by $Hs=3N^{0.89}$. The index is lower than is usual, and the low value of the index is attributed to the volume flow of oil being held constant in contrast with the usual hydrodynamic circumstance in which the oil is freely available. An effect of the constant volume of oil flow can also be seen in the trend of oil outlet temperature with load. The differences between these present results, and the corresponding results with full oil supply, are described and discussed more fully in paragraphs 6.3.6 - 6.4.22 following the presentation of the full flow results.

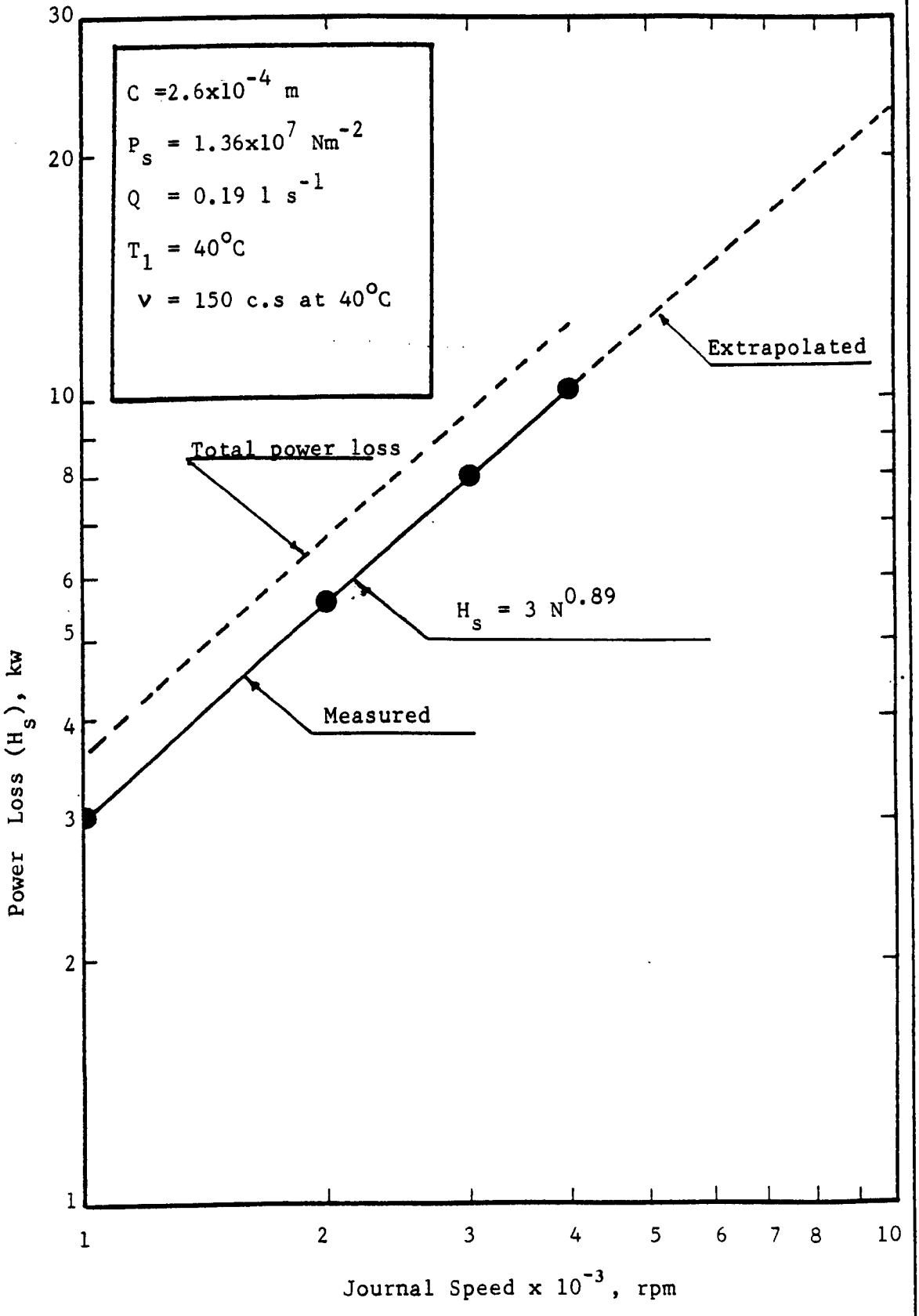

FIG.6.31 Power loss-speed characteristics for the externally pressurized operation (experimental).

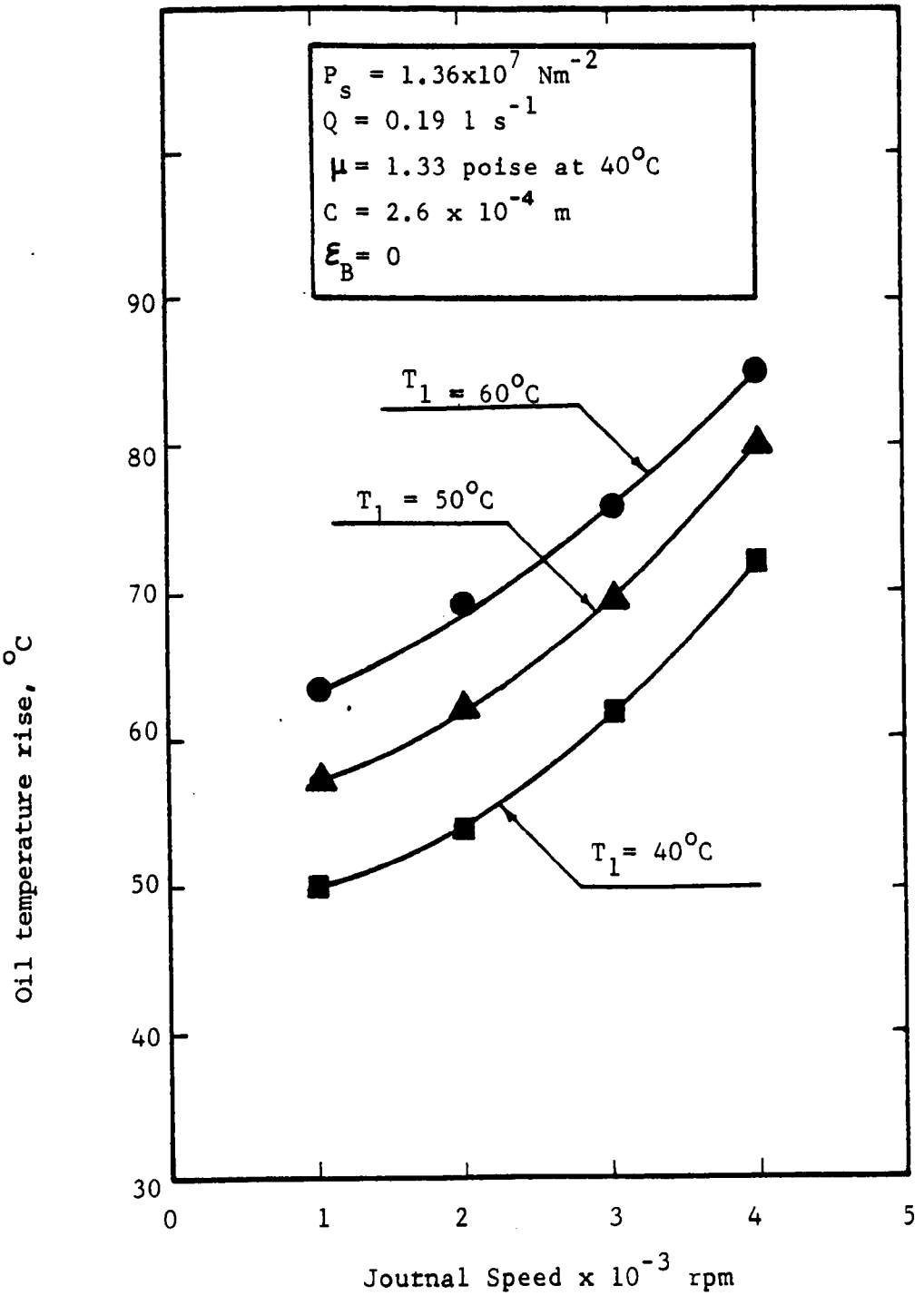

FIG.6.32 Oil outlet temperature-speed characteristics for the externally pressurized operation.

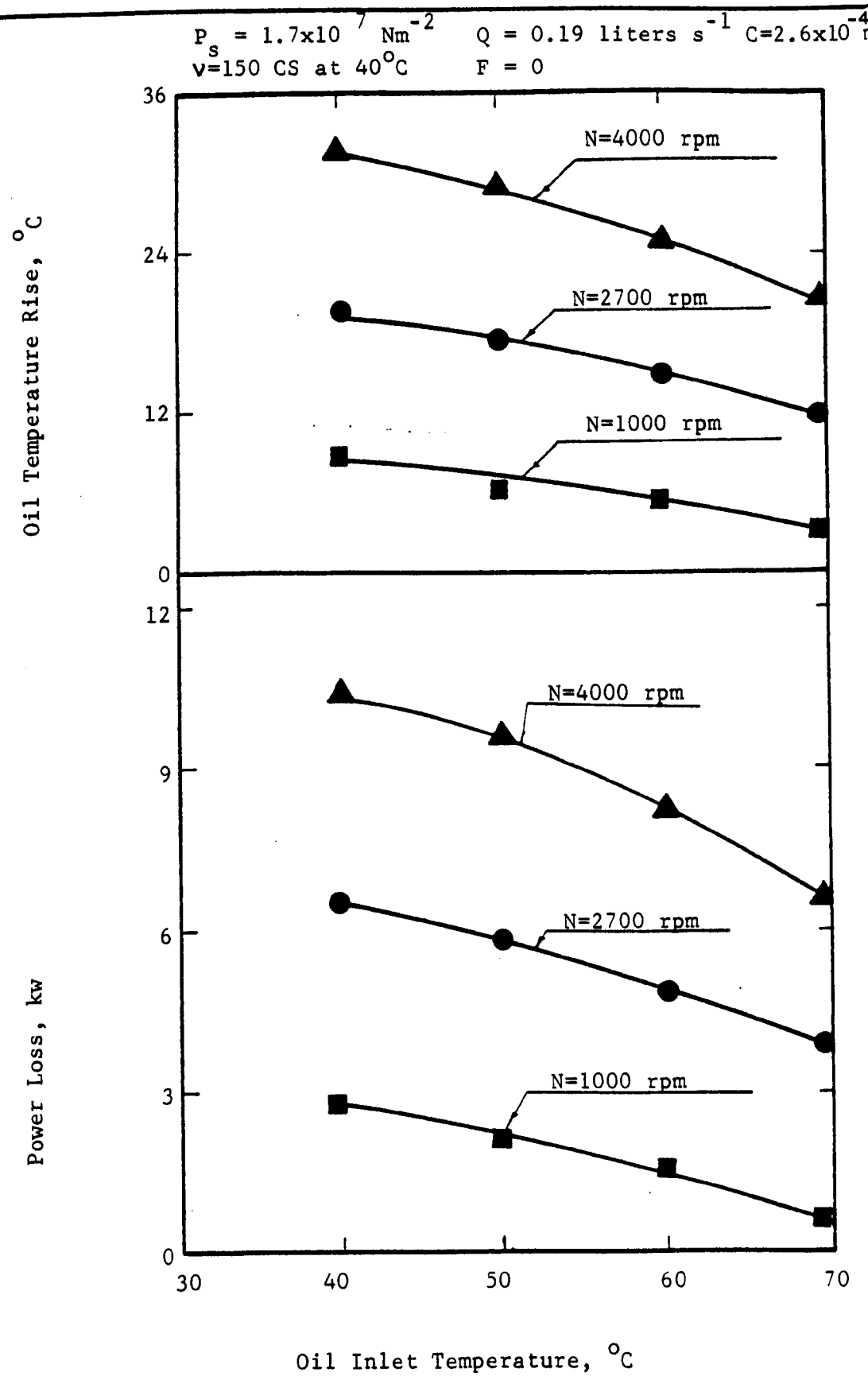

FIG.6.33 Power loss, and oil temperature rise variation with the oil inlet temperature.

6.3.4b Tests with the Tellus 37 Oil

With a constant oil flow the variation of power loss and of oil temperature rise with journal speed are given in Figures 6.34 and 6.35. It may be seen from Figure 6.34 that there is no change in the slope of the log-log plot of power loss versus speeds up to 6000 rpm, which suggests no departure from the laminar flow in the oil film. At 6000 rpm the Reynolds' number for the bearing is approximately 486 while the critical Reynolds' number is 973*. There is some evidence that a departure from laminar conditions occurs at the critical Taylor number (Refs. 82 - 83) and the linearity of the log-log plot against speed up to a speed of 6000 rpm is perhaps to be expected. If the onset of turbulence is delayed until the critical Taylor number is reached then the flow would not become turbulent before a speed of approximately 8400 rpm.

The power loss curves of Figure 6.34 were obtained without journal load. However, because the volume flow of oil is constant, any variation in power loss with journal load would become manifest through a change in oil temperature rise. Several measurements of oil temperature rise were made both with and without journal load and no influence of load upon temperature rise was found. However, it should be mentioned that at the maximum load the bearing eccentricity ratio (ε_B) at the journal mid-plane was 0.3. It is concluded under conditions of externally pressurized operation up to a lobe eccentricity of 0.3 that the power loss is independent of the load.

The power loss speed characteristics of Figure 6.34 is expressed by $Hs = 1.15N^{1.212}$, where Hs is in KW and N is in rpm. Again, as was mentioned in paragraph 6.3.4a, the index is lower than is usual,

* Reynolds' number corresponds to the critical Taylor's number.

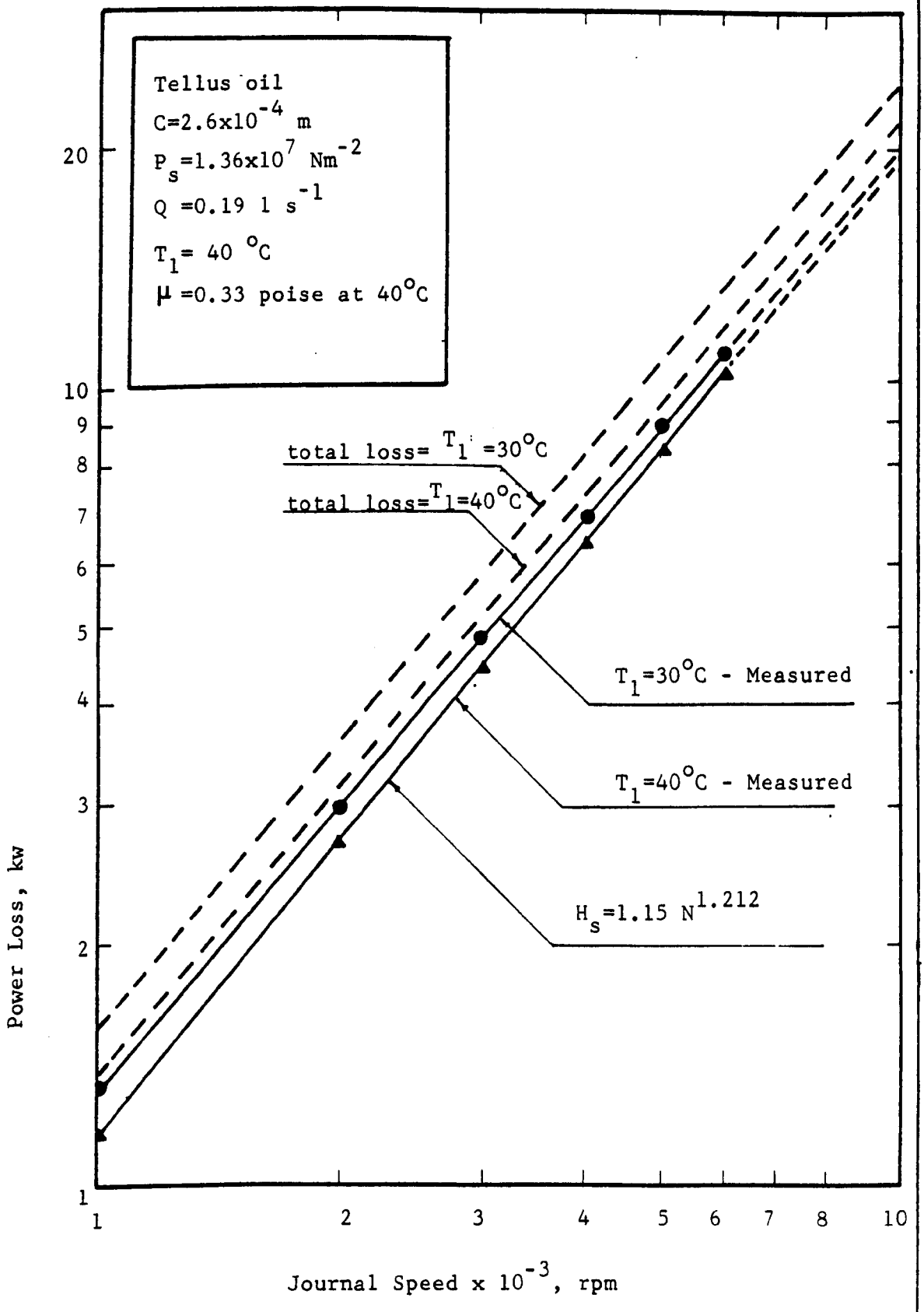

FIG.6.34 Power loss-speed characteristics for externally pressurized operation.

and the low value of the index is attributed to the volume flow of oil being held constant. It may be seen from Figure 6.34 that the measured power loss at 4000rpm is 6.2KW, while the measured power loss with the first oil was 10.3KW (Figure 6.31), (i.e. reduction of power loss by $\sim$ 40%) resulting from the use of low viscosity oil. However, it must be recalled that the drop in the bearing stiffness was approximately 4% at 4000rpm. Quite clearly there is very considerable advantage in the particular instances of this paragraph in the use of the low viscosity oil.

Figure 6.35 shows the variation of the oil temperature rise with the journal speed, while Figures 6.36 and 6.37 show the measured power loss and the measured oil temperature rise with two oils of different viscosities. It may be seen from Figures 6.36 and 6.37 that there is a considerable improvement in the measured power loss and the temperature rise by using low viscosity oil.

6.3.5 Load Speed Relationship in Hydrodynamic Operation

6.3.5a Tests with VIT 150 Oil

The journal displacement with respect to the bearing was measured over a range of speeds from 1000 to 4000rpm. Constant vertical loads of $5.4\text{x}10^3$, $10.8\text{x}10^3$, $16.2\text{x}10^3$ and $21.6\text{x}10^3$N were applied at the shaft overhang. The equivalent loads at the bearing mid-plane are $7.5\text{x}10^3$, $1.5\text{x}10^4$, $2.25\text{x}10^4$ and $3\text{x}10^4$N respectively.

The procedure used in bringing the journal to the desired test conditions was to float the journal hydrostatically, to bring the shaft to speed, to admit low pressure oil, and then to switch off the

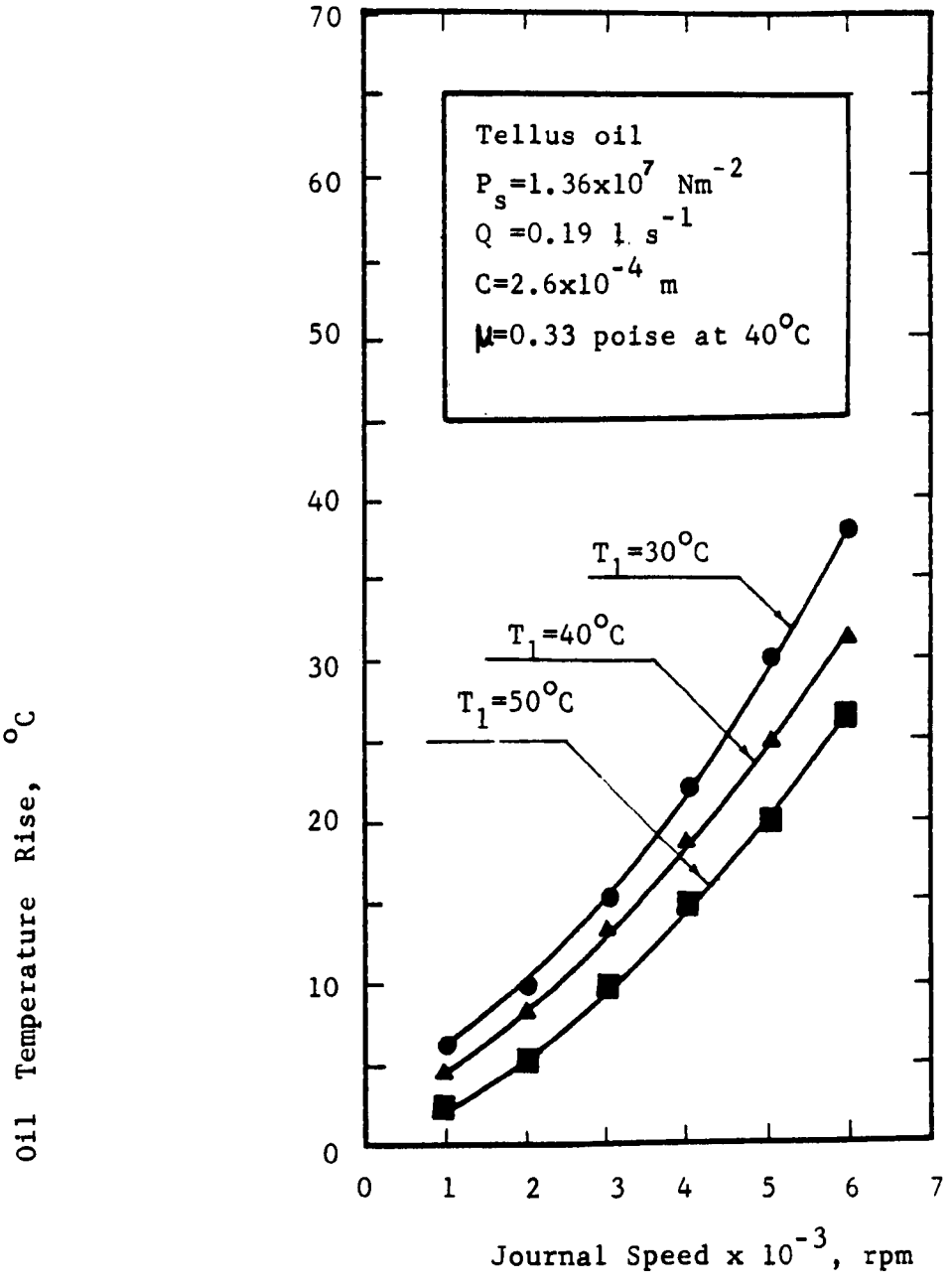

FIG.6.35 Oil temperature rise-speed characteristics for the externally pressurized operation.

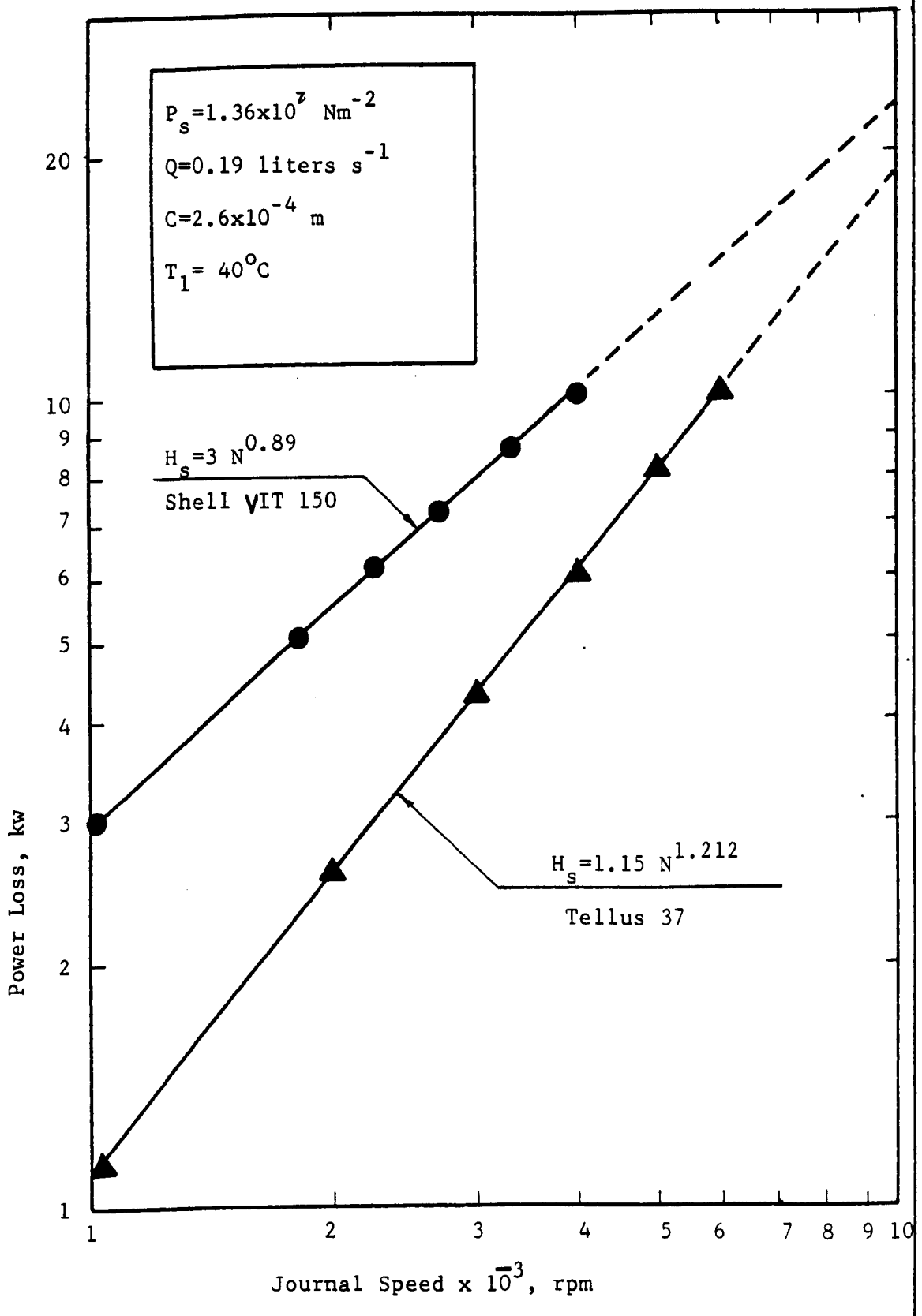

FIG.6.36 Power loss-speed characteristics for the externally pressurized regime.

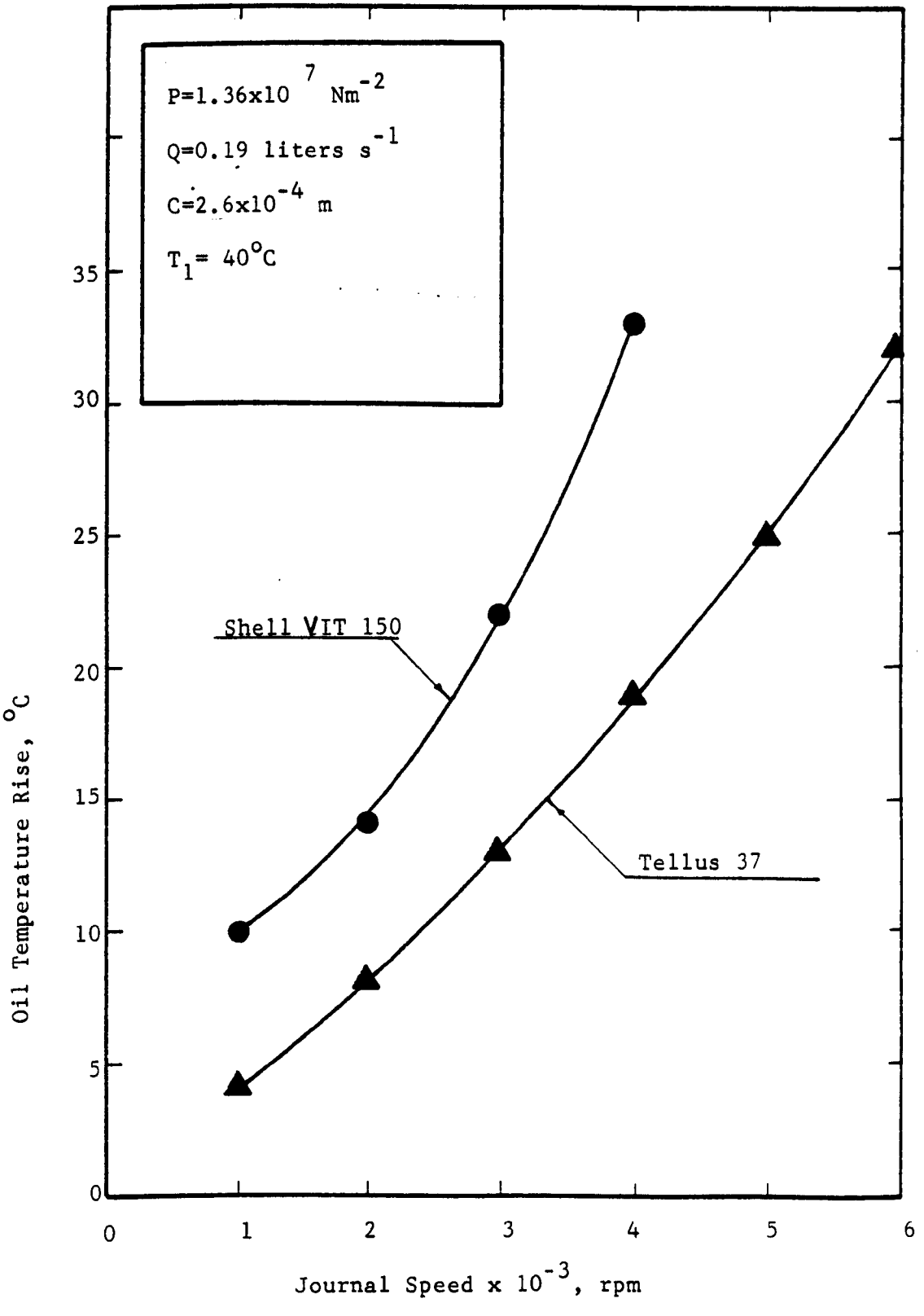

FIG.6.37 Oil temperature rise-speed characteristics for the externally pressurized regime.

high pressure supply of oil. This sequence was followed in reverse order at the end of a test. It was noticed that there was little change in journal attitude when the transfer was made from high pressure oil only to low pressure oil, and such changes as there were diminished as the speed of the journal was increased.

Table 6.2 lists the measurements of journal displacement together with the deduced values of journal displacement at the fore and mid-plane of the bearing. It may be seen that the fore-plane and mid-plane values are in substantially constant proportion, and may therefore be presented graphically simple by adopting appropriate scale. This is done in Figure 6.38 in which the journal radial displacement at the bearing mid-plane and at the bearing fore-plane is shown as a function of the external load at the journal mid-plane. It may be seen that the journal displacement decreased as the speed was increased (i.e. higher load carrying capacity). In Figure 6.39 the results of the measured displacements, load, speed and oil outlet temperature are plotted in a dimensionless form. The bearing duty parameter, which is based upon lobe dimensions, is calculated from $\frac{\mu NLD}{W} (D/C)^2$ and W is load at the journal mid-plane and μ is the oil viscosity at the outlet. The results of the calculated duty parameter are plotted as a function of the bearing eccentricity ratio at both the fore and mid-plane of the bearing. In Figure 6.40 the duty parameter is plotted against the speed.

In Figure 6.41 the position of the centre of the journal with relation to the centre of the bearing is shown. It may be seen at constant load

TABLE 6.2 Measured and deduced displacements along the Journal.

Vertical Plane				Horizontal Plane				Radial	
δ_D $x10^{+5}m$	δ_B	δ_{mid}	δ_{fore}	δ_C	δ_A	δ_{mid}	δ_{fore}	δ_{mid}	δ_{fore}
3.69	0.992	1.349	2.42	1.33	2.16	1.65	1.88	2.13	3.066
4.96	1.314	1.78	3.24	1.72	2.8	2.14	2.44	2.8	4.056
6.36	1.91	2.22	4.12	2.04	3.31	2.53	2.89	3.37	5.04
7.5	2.29	2.62	4.86	2.04	3.31	2.53	2.89	3.5	5.55

For notation see figures 6.21 and 6.23.

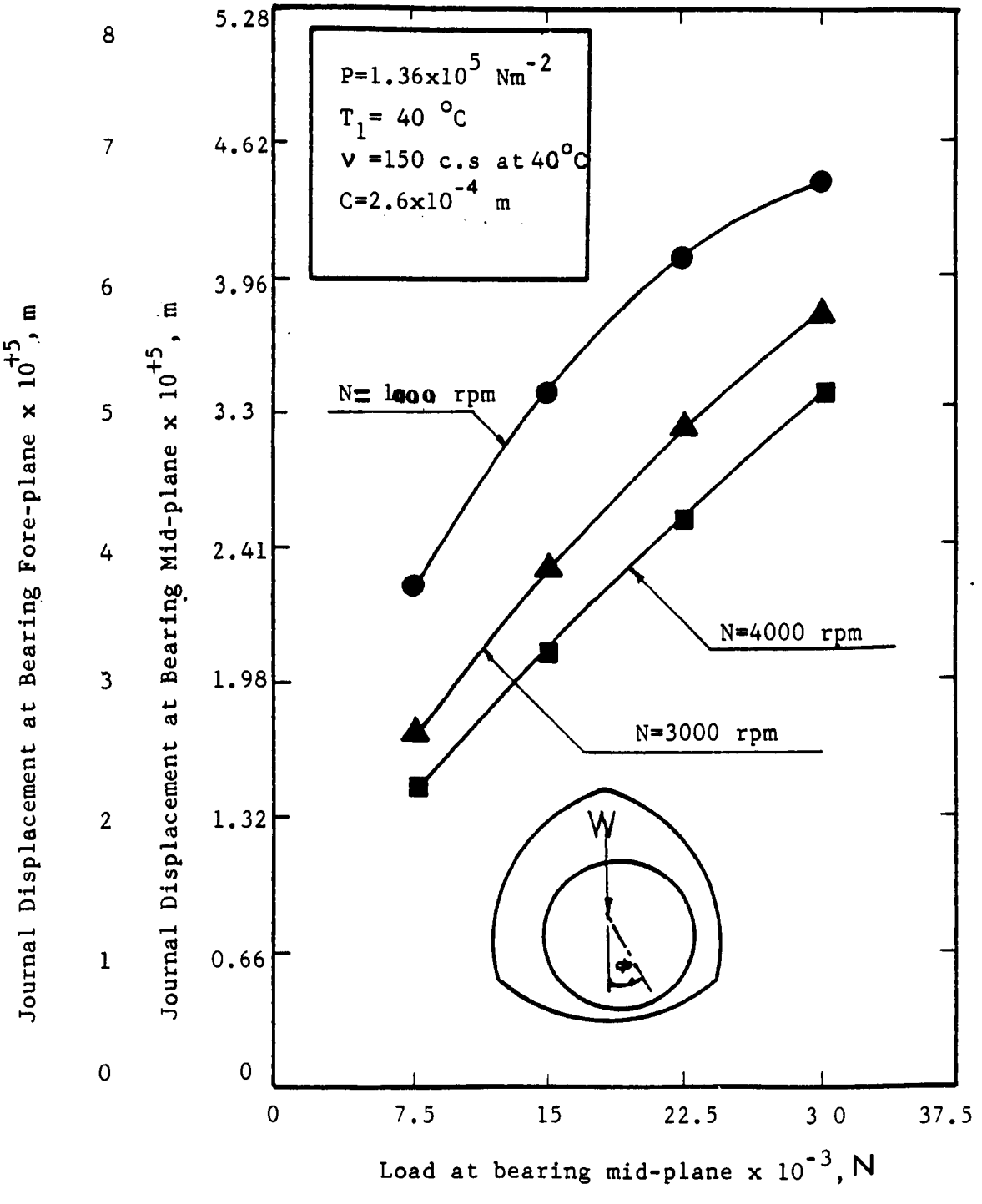

FIG.6.38 Load-displacement characteristics for the hydrodynamic operation (experimental)

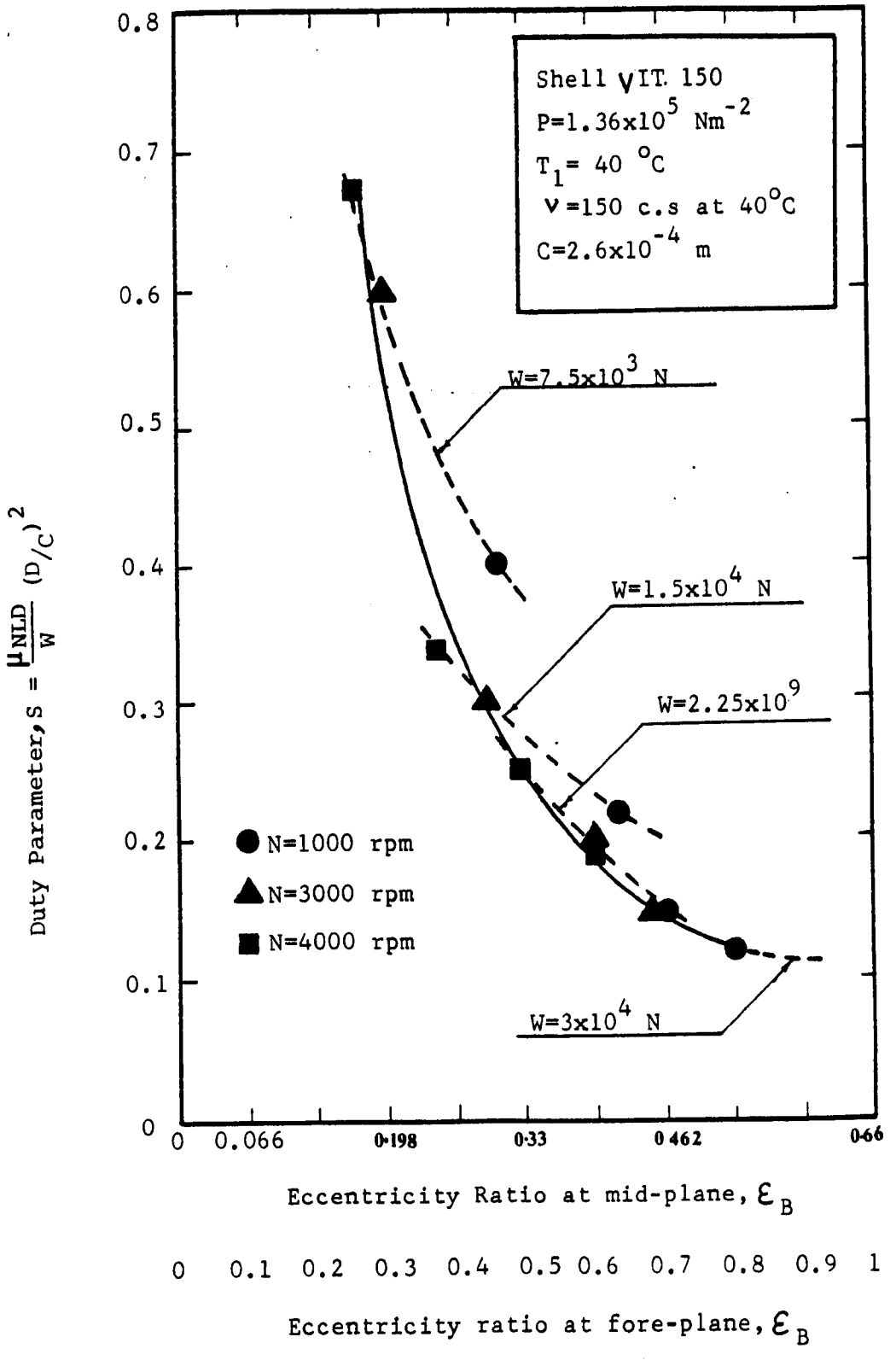

FIG.6.39 Duty parameter variation with eccentricity ratio (experimental)

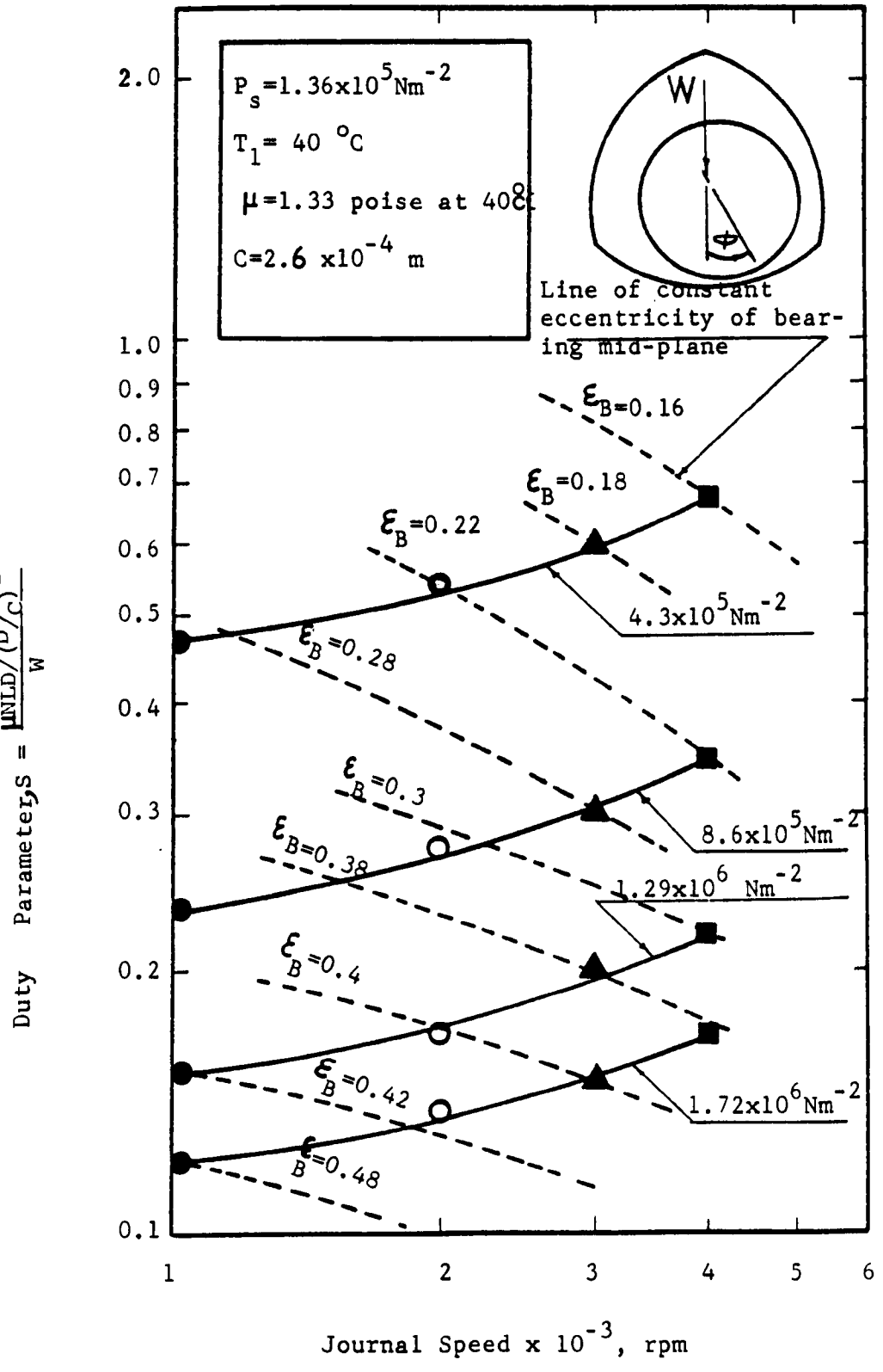

FIG.6.40 Variation of the duty parameter with the Journal speed (experimental)

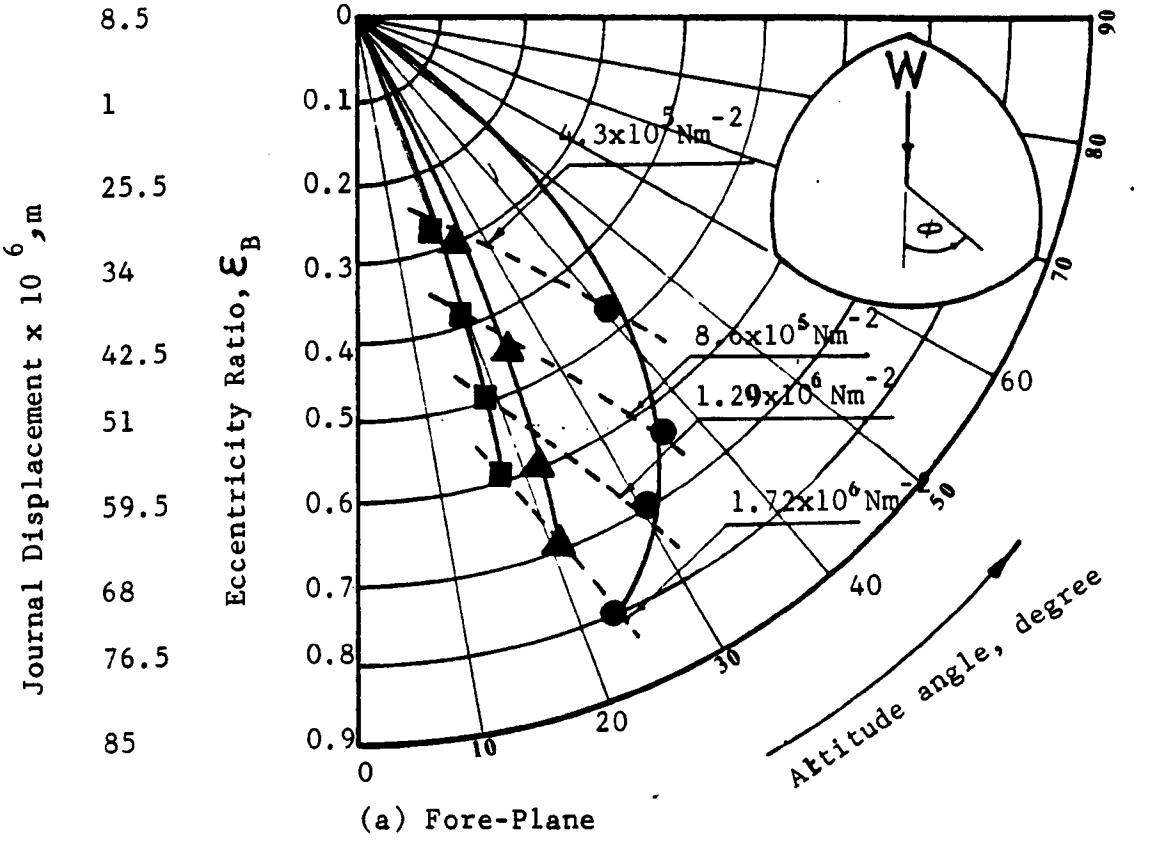

(a) Fore-Plane

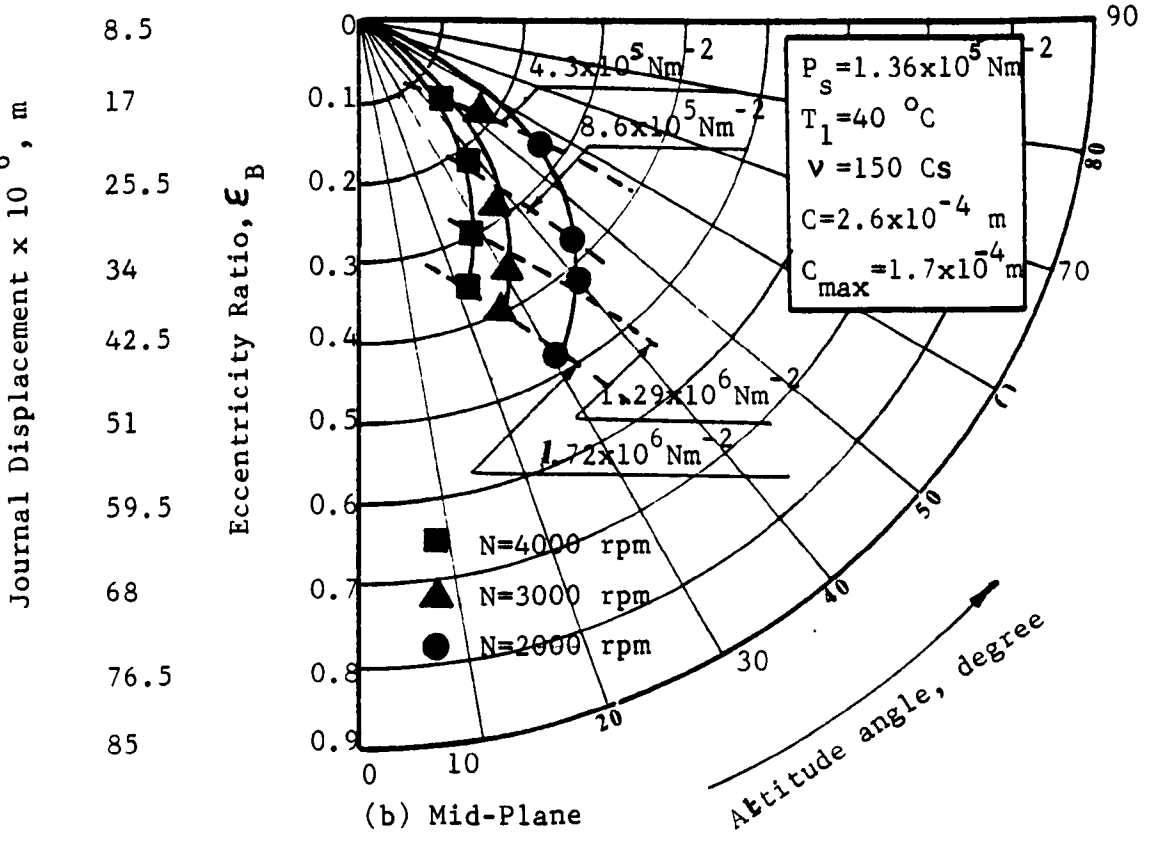

(b) Mid-Plane

FIG.6.41 Variation of attitude with eccentricity ratio (experimental)

that as the speed increases the attitude angle decreases.

6.3.5b Tests with Tellus 37 Oil

The journal displacement with respect to the bearing was measured over a range of speeds from 1000 to 6000rpm. The procedure used in these tests has been described in paragraph 6.3.5a. In Figure 6.42 the journal radial displacement at the bearing mid-plane and at the bearing fore-plane is shown as a function of the journal speed. It may be seen at constant load of 7.5×10^{3}N, that the displacements at the journal mid-plane are 2.85×10^{-5}, 2.4×10^{-5}, 2.0×10^{-5} and 1.75×10^{-5}m at speeds of 10^{3}, 2×10^{3}, 3×10^{3} and 4×10^{4}rpm respectively. The corresponding stiffnesses are 2.63×10^{8}, 3.125×10^{8}, 3.75×10^{8} and 4.286×10^{8} Nm^{-1} respectively. The required stiffness of the functional specification is $3.51 \times 10^{8} Nm^{-1}$ which can be obtained at journal speeds over 2000rpm. From the results which have been reported in paragraph 6.3.5a the displacement at the journal mid-plane was 2.44×10^{-5}, 1.75×10^{-5} and 1.45×10^{-5}m at journal speeds of 1000, 3000 and 4000rpm respectively. However it may be seen from these values that by using a low viscosity oil the journal displacement has been increased by 18% (i.e. the bearing stiffness has been reduced by 18%), but because the stiffness obtained with the low viscosity oil exceeds the stiffness required by the specification the fall in stiffness as the oil viscosity is decreased is of no consequence in the hydrodynamic performance of the bearing.

In Figure 6.43 and 6.44 the results of the measured displacements, load, speed and oil outlet temperature are plotted in a dimensionless

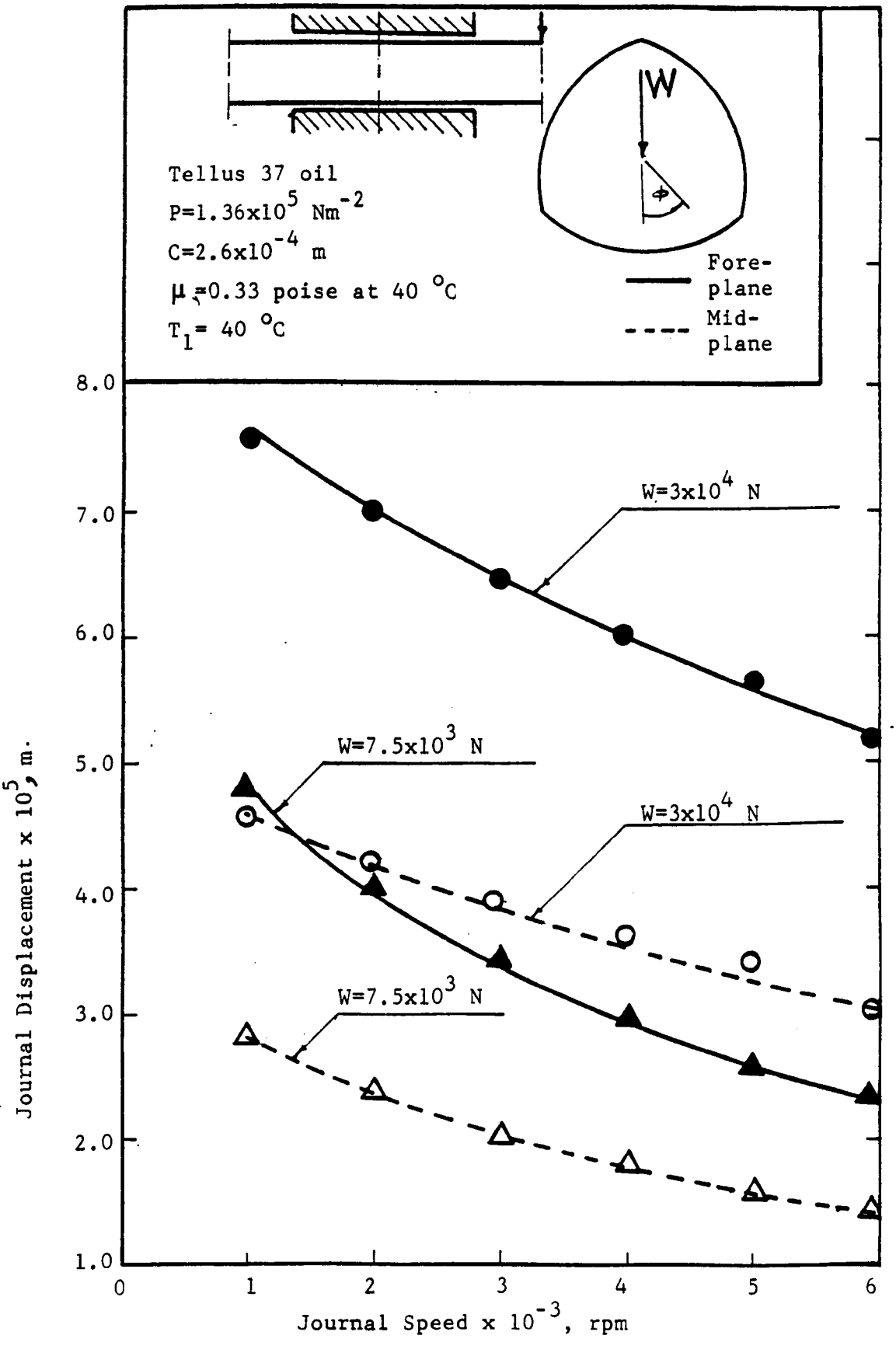

FIG.6.42 Displacement speed characteristics for the self-generating regime.

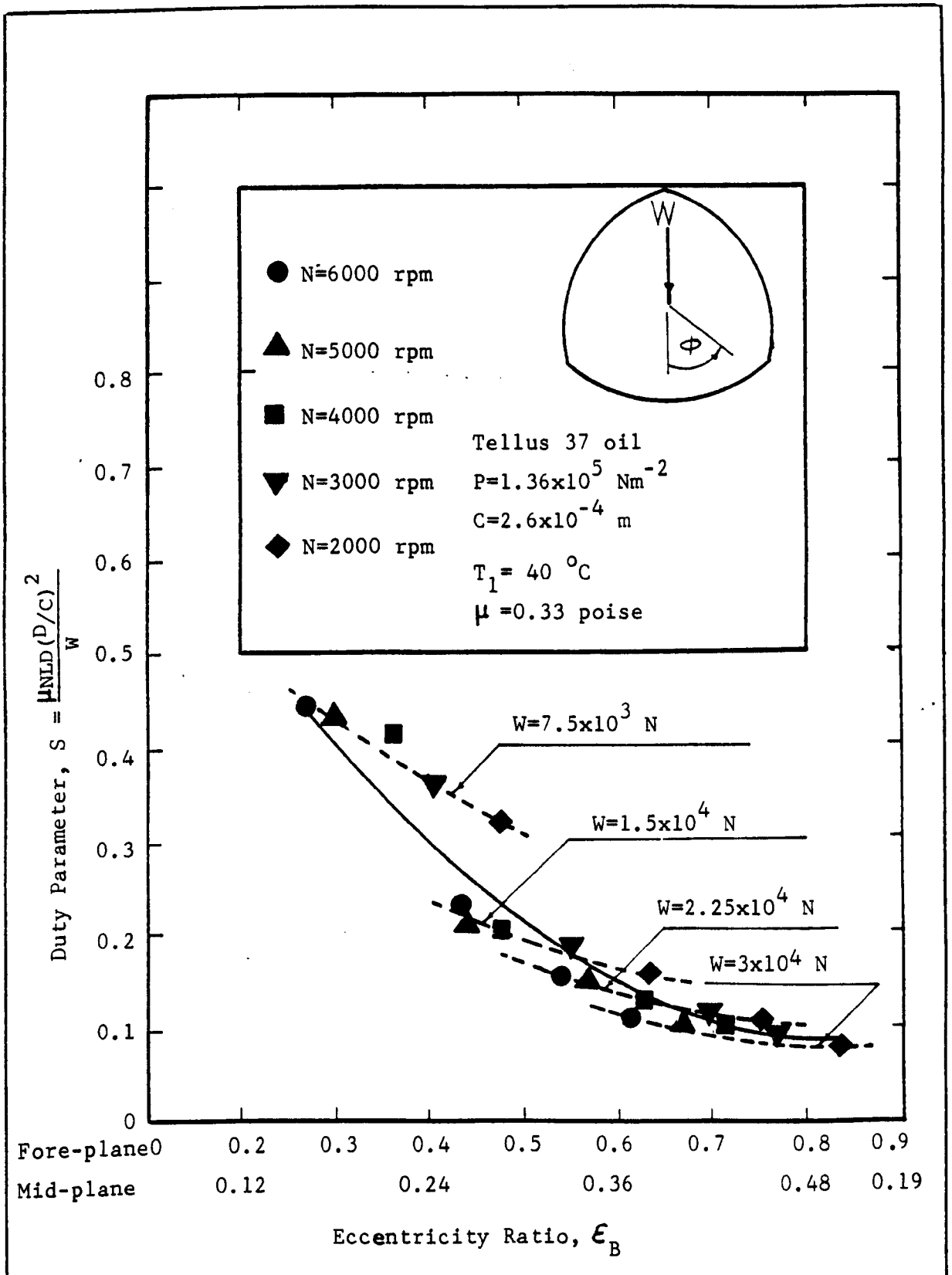

FIG.6.43 Variation of duty parameter with the eccentricity ratio for the self-generating operation.

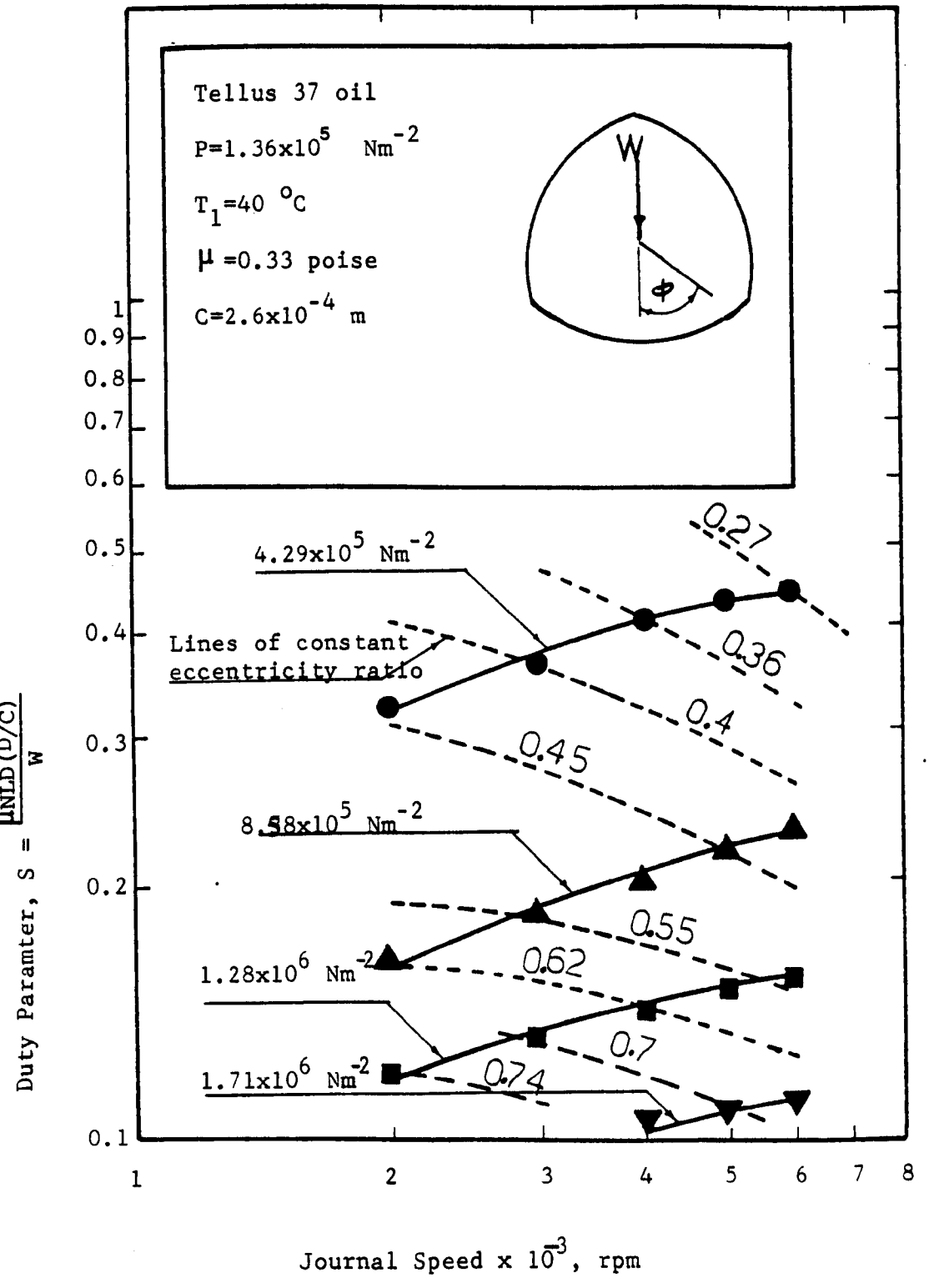

FIG. 6.44 Duty parameter variation with speed for the self-generating regime.

form. The bearing duty parameter which is based upon lobe dimensions is calculated from $\frac{\mu NLD}{W} (D/c)^2$ and W is load at the journal mid-plane and μ is the oil viscosity at the outlet.

6.3.6 Power Loss, Oil Flow and Temperature Rise in Hydrodynamic Operation with Low Pressure Oil only

6.3.6a Tests with VIT 150 Oil

The variation of power loss, oil flow and oil temperature rise with journal speed are presented in Figures 6.45 and 6.46.

In these tests oil flow was measured directly by bucket and stop watch; the flow meter was operating in an inaccurate region because of high oil viscosity and because of low flow.

The results of the measured power loss are shown in Figure 6.45 in which the circular points show the measured power loss as calculated from oil flow and temperature rise. The triangular points have been adjusted by 20% to take into account the heat loss from the rig. The power loss is plotted against speed on a log-log basis and the experimental points lie on a straight line. The dotted extrapolation indicates the power loss to be expected at high speeds for the same type of oil at the same inlet temperature. The exponent in the power loss-speed relationship is now 1.8 in contrast with the exponent of 0.89 which was found with a controlled volume flow of oil (paragraph 6.3.4a Figure 6.31). Limited observations were made of the variation of the power loss with external load and the results showed that as the load increased the oil outlet temperature fell, oil flow increased, and the power loss also. For instance at a load

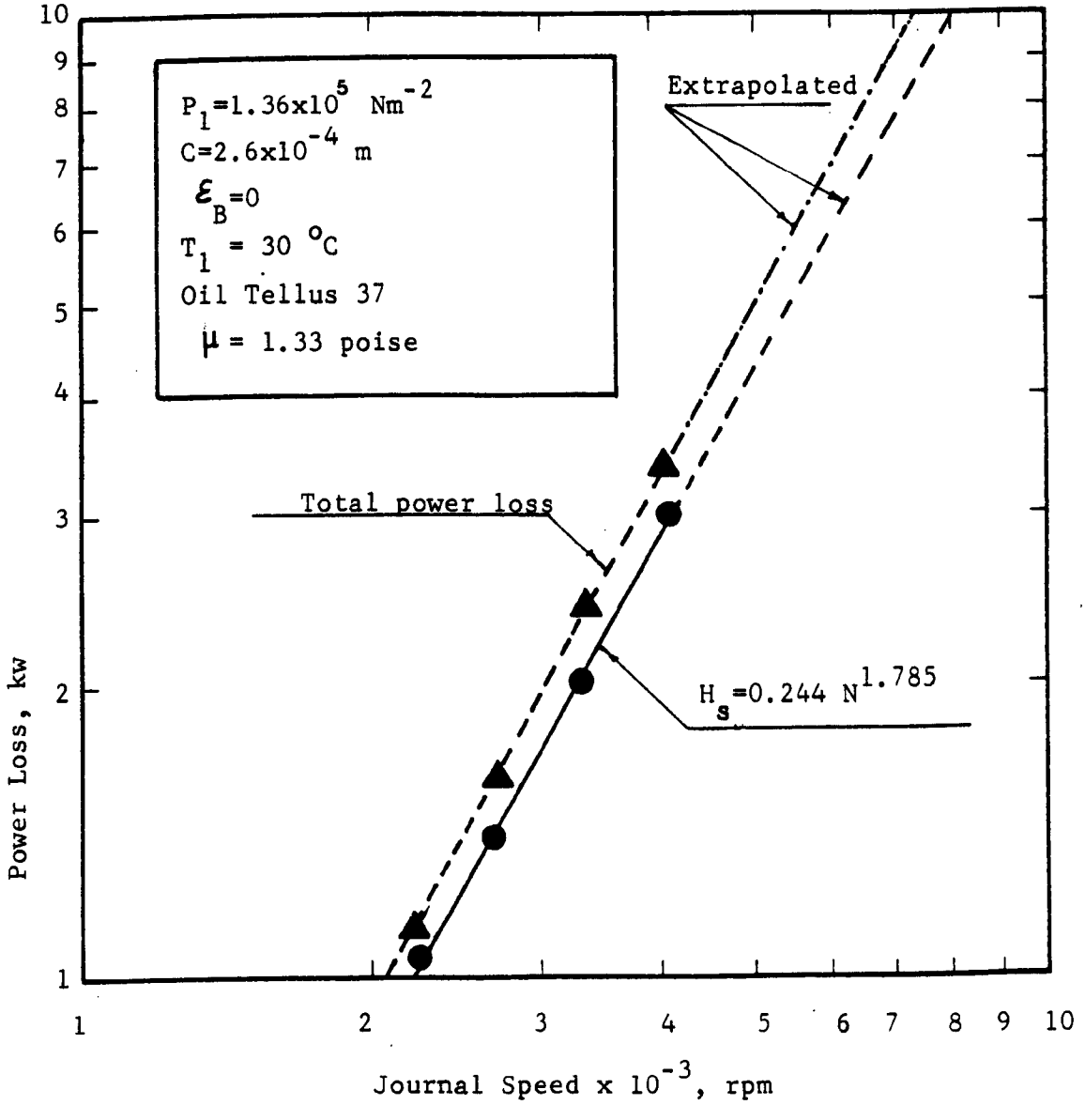

FIG.6.45 Variation of the power loss with the Journal speed for the self-generating regime.

of 1.5×10^4N, a speed of 3000 rpm, the power loss increased by 13%, over the power loss at zero load.

Figure 6.46 shows the variation of the oil outlet temperature and the oil flow with the journal speed. It may be seen that the oil flow is generally very low and that may explain why the oil outlet temperature in the hydrodynamic operation is higher than the oil outlet temperatures which were measured with controlled oil flow. For instance it may be deduced from figure 6.32 for which the oil flow was 0.19 ιs^{-1} that at 2000rpm the temperature rise is $14^{\circ}C$ at an inlet temperature of $30^{\circ}C$, while in the present instance the oil temperature rise is $30^{\circ}C$ with an oil flow of 0.015 ιs^{-1}.

6.3.6b. Tests with Tellus 37 Oil.

The variation of Power Loss, Oil Flow and Oil Temperature rise with journal speed are presented in Figures 6.47 and 6.48. The tests have been carried out in the same way as explained in paragraph 6.3.6a, except that the oil flow has been measured by the flow meter.

The results of the measured power loss are shown in Figure 6.47 in which the circular points show the measured power loss as calculated from oil flow and temperature rise. The triangular points show the measured power loss which has been reported in paragraph 6.3.6a by using an oil of high viscosity. However, it may be seen that there is no difference in the power loss because as the oil viscosity decreased the oil flow is increased and the temperature rise is decreased. With high viscosity oil the oil flow is decreased and the temperature rise is increased but $Q \times \Delta T$ is constant in both cases.

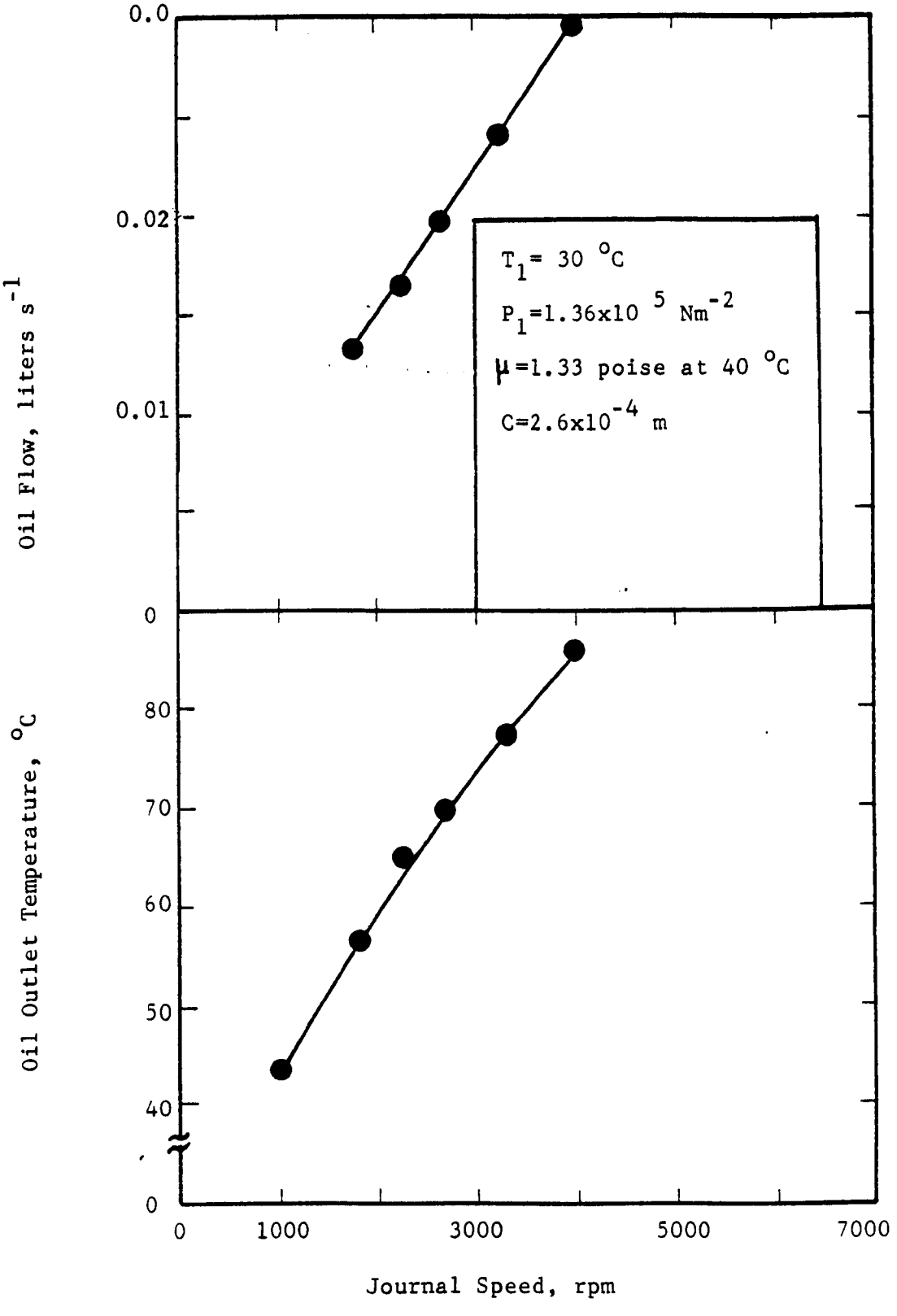

FIG.6.46 Variation of outlet temperature and oil flow with speed for hydrodynamic operation.

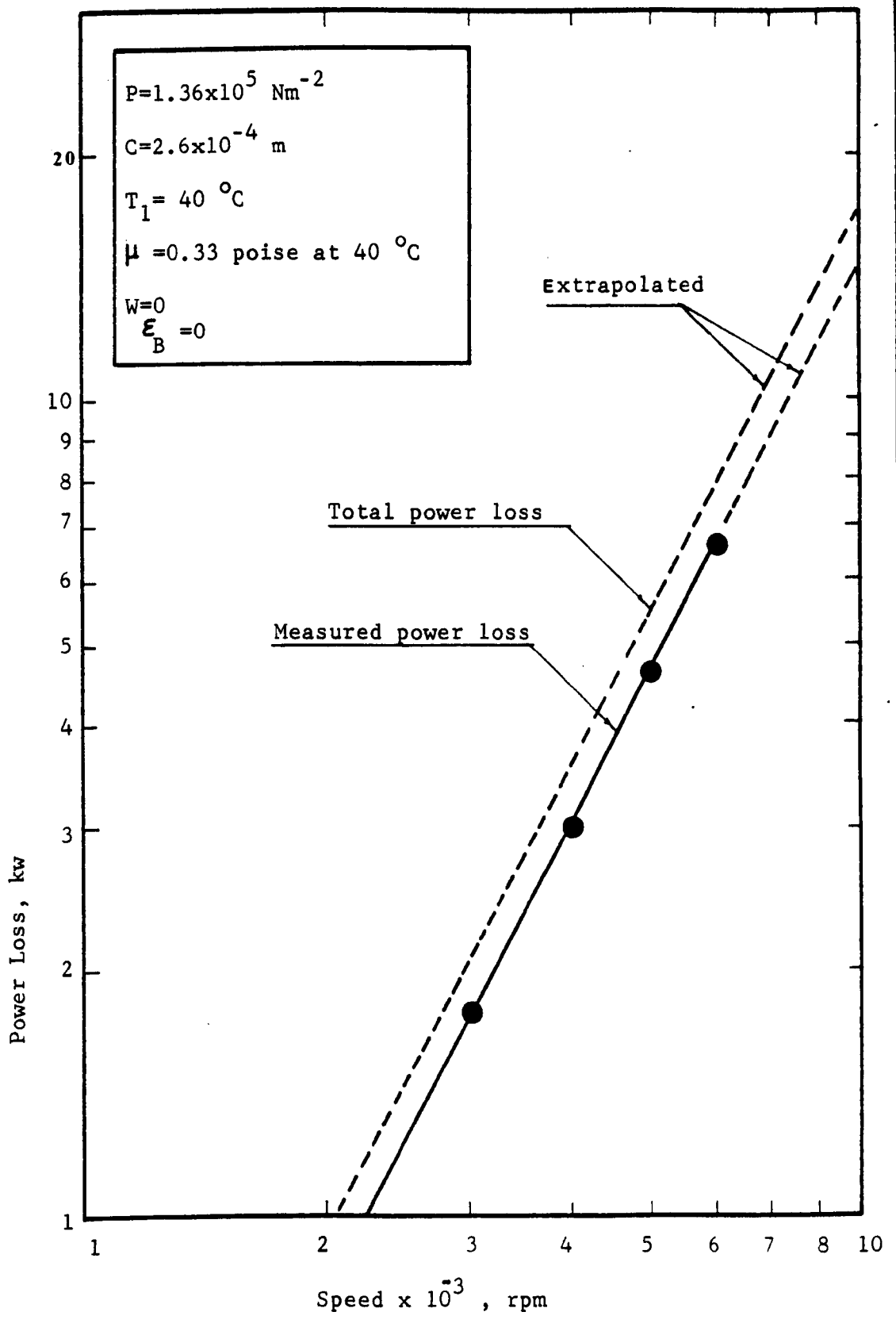

FIG.6.47 Power loss-speed characteristics for the self-generating regime.

This is in contrast with the externally pressurized instance with its constant volume flow in which a change in oil viscosity did lead to a change in power loss. Figure 6.48 shows the variation of the oil temperature rise and the oil flow with journal speed. It may be seen that the oil flow is generally low and the oil flow is increased by increasing the bearing load. The consequence of increasing the oil flow under loading on the temperature rise and power loss will be dealt with in the next section. Figure 6.49 shows the variation of the oil temperature rise and the oil flow with the journal speed. The results are plotted for the two types of oil which have been used in the tests. However, it may be seen that there is considerable difference in the oil flow and the oil temperature rise, and by using an oil of low viscosity, the oil flow increases and the oil temperature rise decreases.

6.4. Tests and Test Results with the Second Bearing.

After the investigation with the first bearing had been completed, a new bearing was machined with a larger lobe diametral clearance and with large axial grooves. This was done for two reasons, firstly to give a more comprehensive picture of the three-lobe bearings in general, together with a more adequate comparison of experimental with theory, and secondly to increase the oil flow in the hydrodynamic regime and to reduce the oil temperature rise so that it becomes more realistic to imagine the bearing being able to run at speeds somewhat higher than have been reached in the present tests.

The machining procedure of the second bearing is given in Appendix A4.

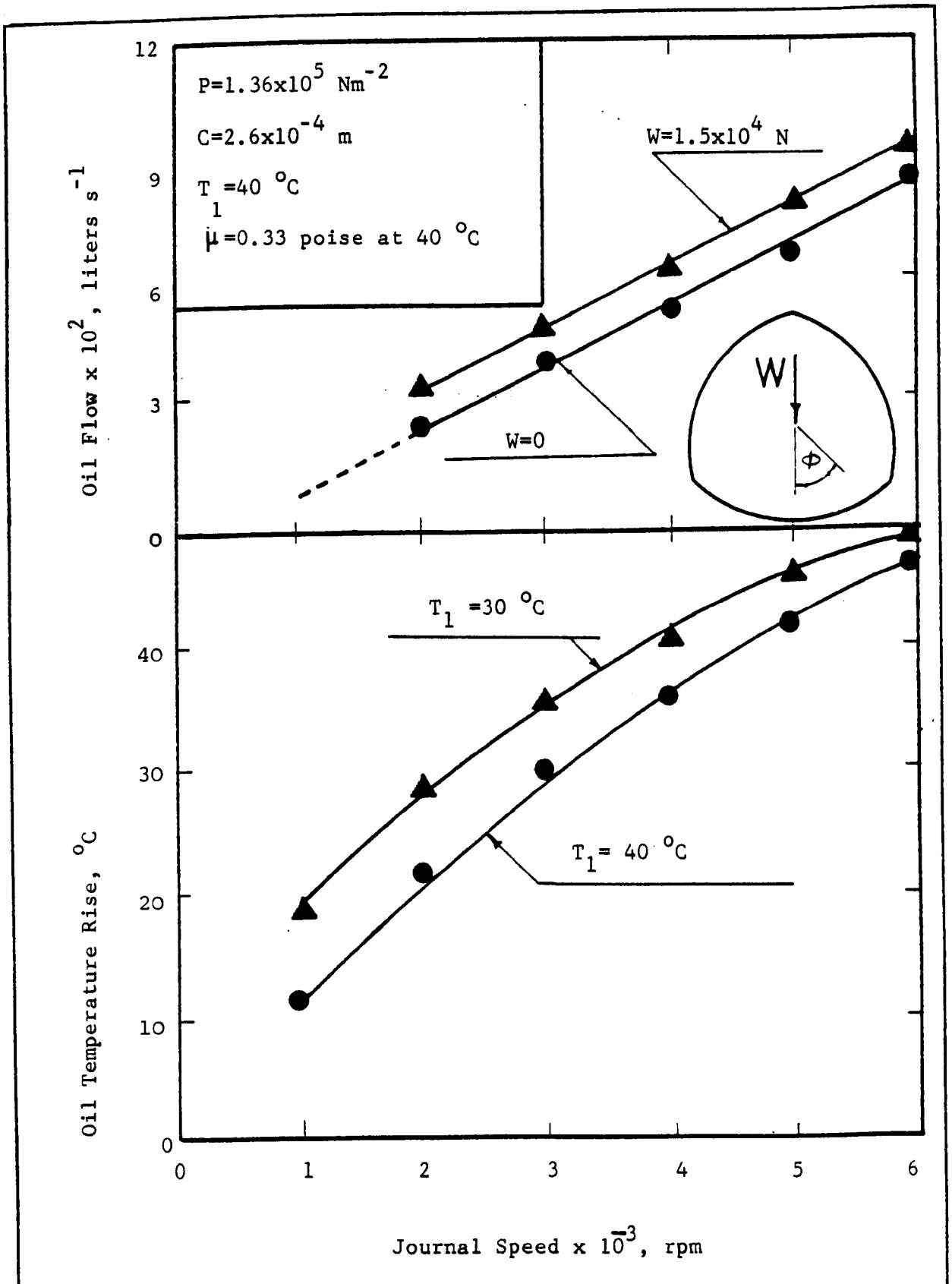

FIG.6.48 Oil temperature rise and oil flow variation with speed for the self-generating regime.

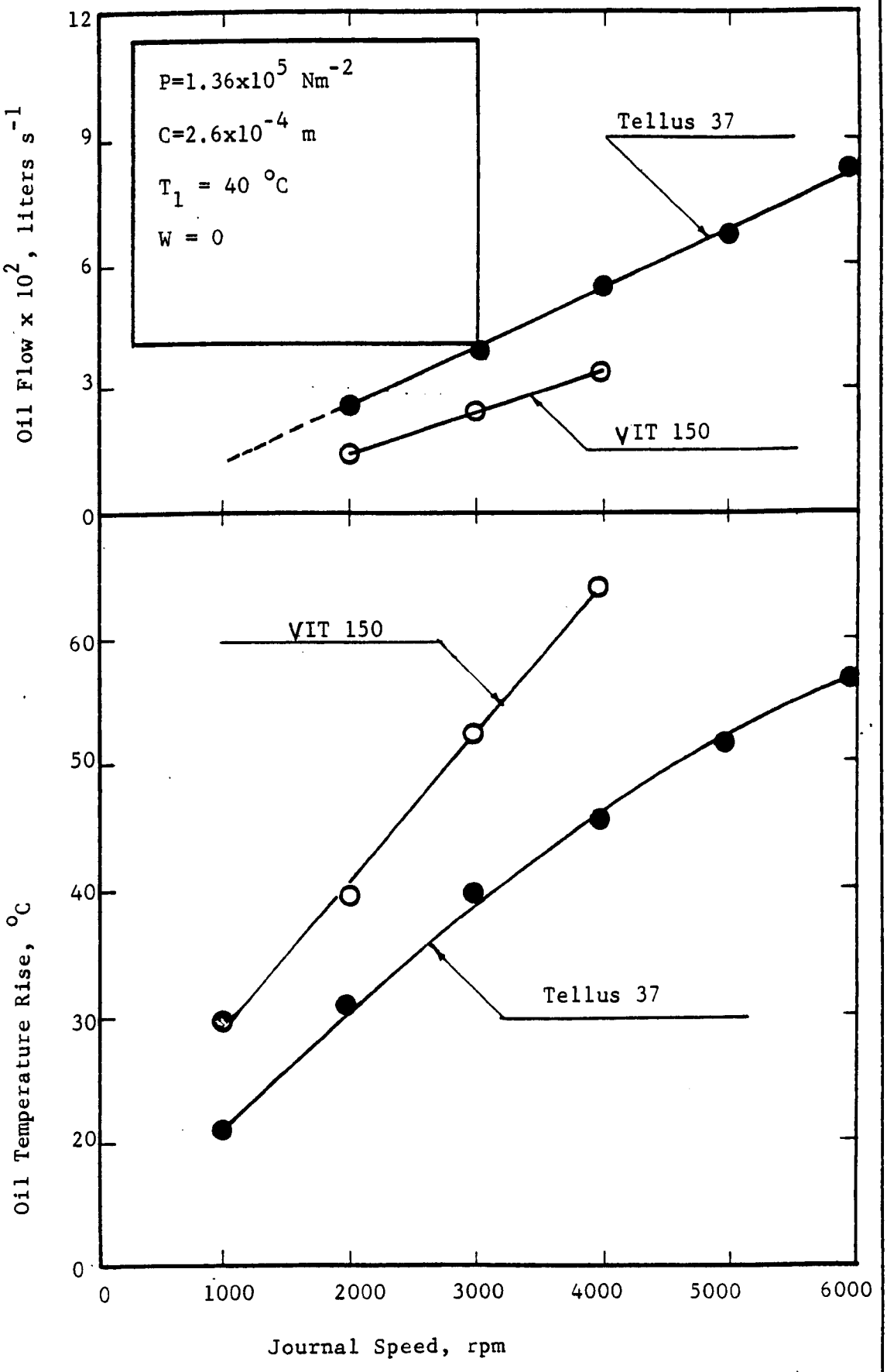

FIG.6.49 Oil flow and oil temperature rise variation with speed for the self-generating regime.

6.4.1 Tests and Test Results of the Externally Pressurized Operation

The salient dimensions of the journal and bearing used in the tests are given in Table 6.3.

The following results relate to the bearing being supplied only with high pressure oil via the constant volume control valves and with shaft rotation in the range 0 to 7000rpm. However, the high pressure oil was supplied in the first instance at mid-lobe position as was the design intention, and secondly the high pressure oil, still via the control valves was supplied to the axial grooves between the pads which by design intention are the low pressure oil inlets.

Oil Shell Tellus 37 was used.

6.4.11 Load-displacement Relationship of the Externally Pressurized Operation

In the first instance the static stiffness of the bearing and the load speed relationship was measured in much the same way as has been described in paragraphs 6.3.1a, b and 6.3.2.a, b. In the second instance the same procedure was adapted, but of course with the change in the position of the oil supply.

Figure 6.50 shows the variation of the journal displacement with the external load at the journal mid-plane. The results obtained in paragraphs 6.3.16 and 6.3.3b are also plotted in the same figure. Quite clearly Figure 6.50 shows the expected result that as the lobe clearance increases the journal displacement increases. At zero speed the stiffness falls from $9.98 \times 10^{8} Nm^{-1}$ to $8.33 \times 10^{8} Nm^{-1}$. (The specifications of Table 1.1 calls for a stiffness of $8.0 \times 10^{8} Nm^{-1}$). Also it may be seen that at the journal mid-plane

Lobe Diameter D mm	Shaf Diameter d mm	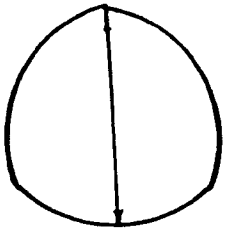 mm	Off-set Δr mm	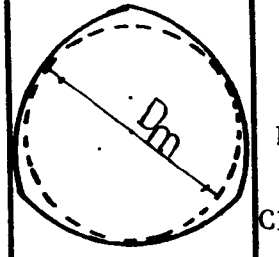 mm	Lobe Diameter Clearance C mm	Max. Clearance C Max mm	Min. Clearance C Min mm	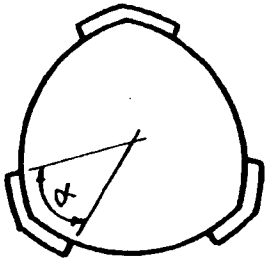 degree	L/D
134.01	133.685	133.905	0.0587	133.877	0.325	0.246	0.192	30	0.95

TABLE.6.3 Dimensions of the second bearing

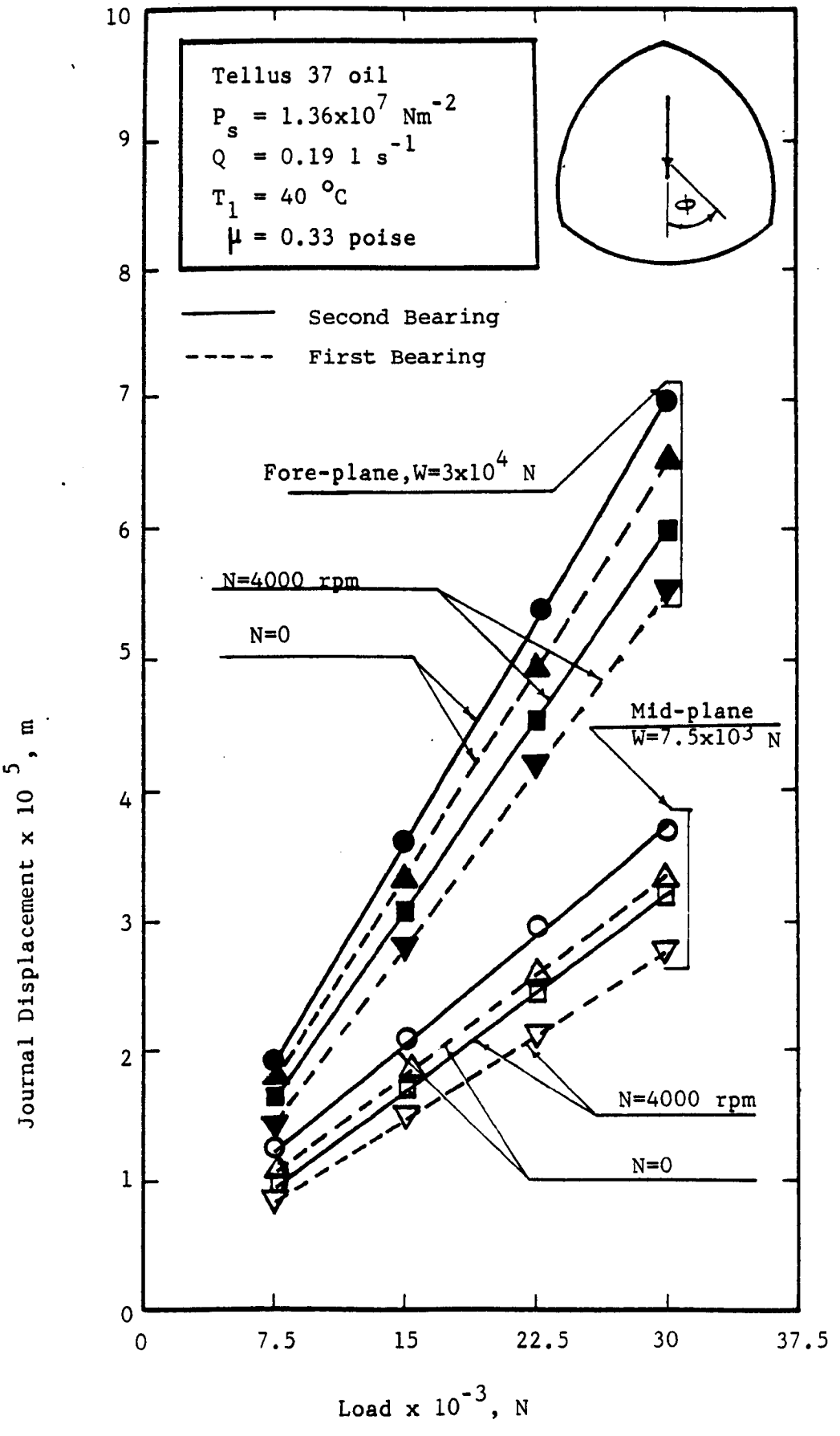

FIG.6.50 Variation of the Journal displacement with the external load for the externally pressurized operation.

and for a load of $3x10^{4}N$, when the lobe clearance is increased from $2.6x10^{-4}m$ to $3.25x10^{-4}m$, the bearing stiffness falls from $1.13x10^{9}Nm^{-1}$ to $9.375x10^{8}Nm^{-1}$. In figure 6.51 the test results are shown in the form of polar diagrams. It may be seen that the bearing attitude angle changed marginally as the speed was increased from 3000 to 5000 rpm.

In the second instance a new feature of the bearing has been tested. In figure 6.52 the load-displacement relationship is shown and it may be seen that for the same oil flow and the same inlet pressure, the bearing stiffness (i.e, force/displacement) has improved by admitting the oil at the axial grooves. It should be mentioned that the axial groove for each lobe is of 30 degree width in the circumferential direction and does not break through at the ends of the bearing. The increase in stiffness is probably due to the inlet grooves acting as a pressure pocket. The disadvantage of this method of pressurization is that as the journal speed is increased the pressure at the bearing inlet decreases and the oil flow must be increased to keep a positive pressure at the bearing inlets.

6.4.12 Power Loss, Oil Flow and Oil Temperature Rise for the Externally Pressurized Operation.

The power loss-speed characteristic is shown in figure 6.53. Lines A and B are both for the second bearing ($C = 3.25x10^{-4}m$) but for different oil flows. It may be seen that the lines are substantially parallel. Line C is for a lobe diametrical clearance of $2.6x10^{-4}m$, (i.e, the original bearing). At low speeds the increase in the lobe clearance leads to a decrease in the shear power loss but as the speed increases line A and line C approach each other and at a speed of 6000rpm the power loss of both lines becomes substantially the same.

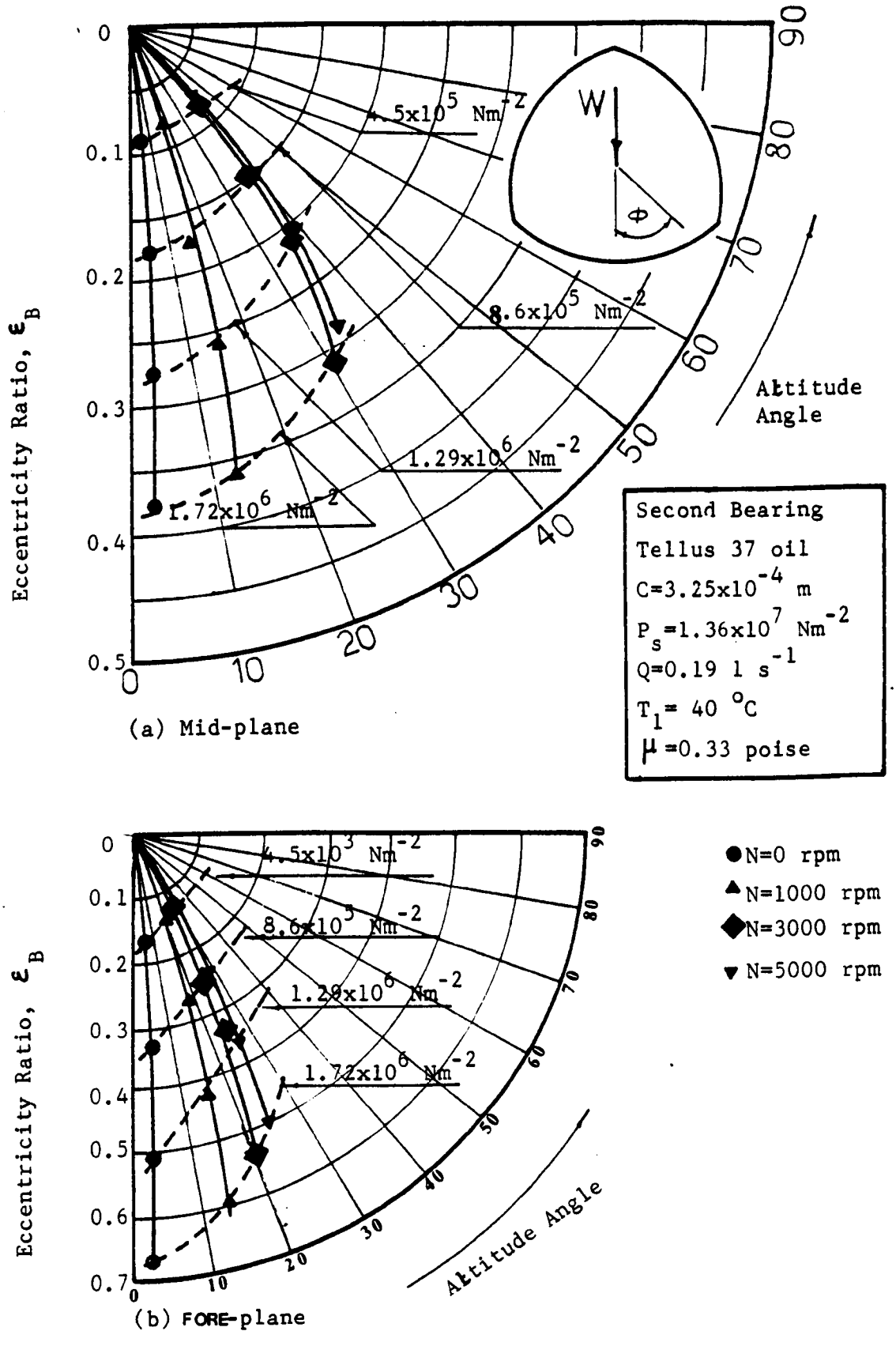

FIG.6.51 Variation of the attitude angle with the eccentricity ratio (externally pressurized)

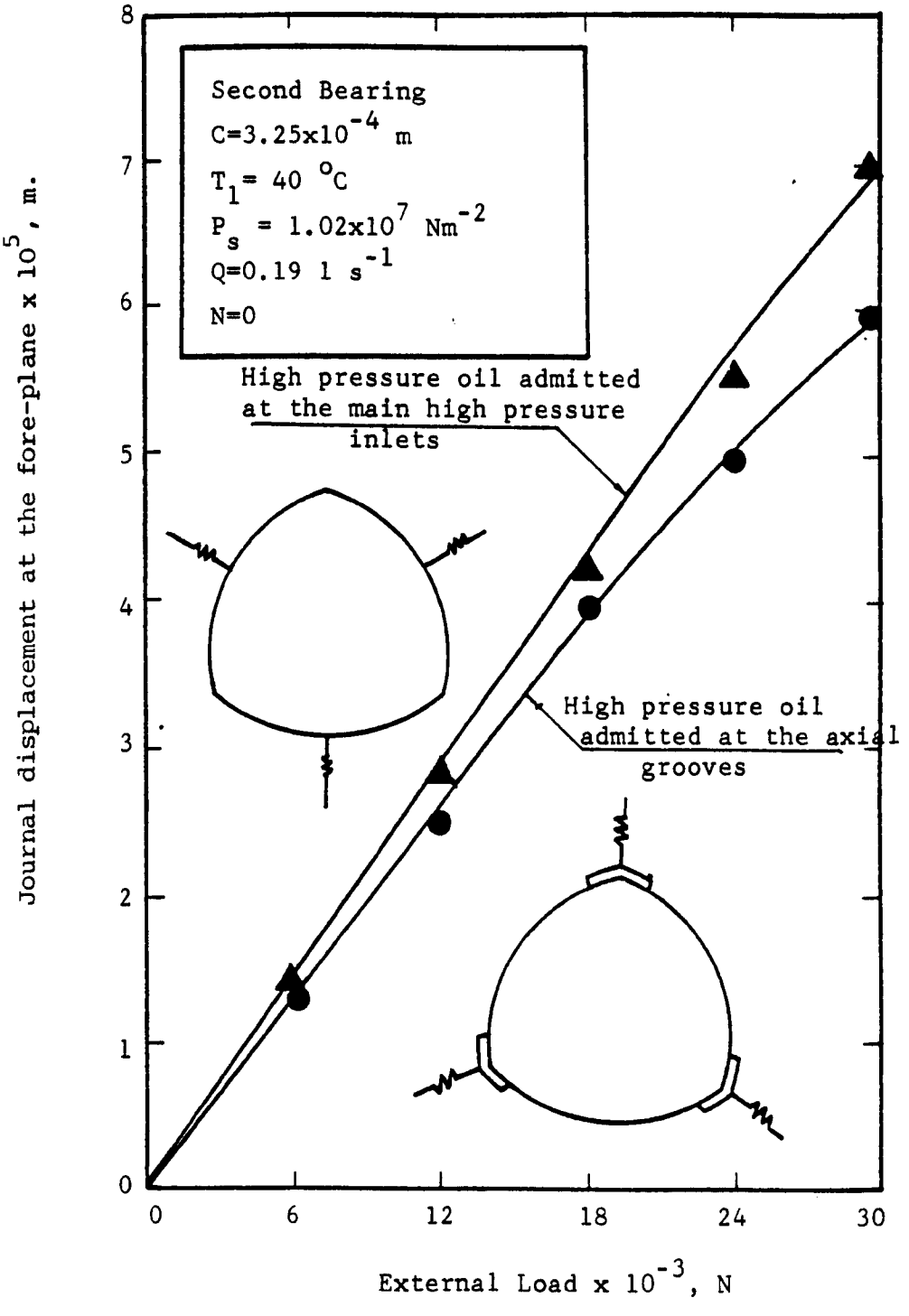

FIG.6.52 Variation of the Journal displacement with the external load.

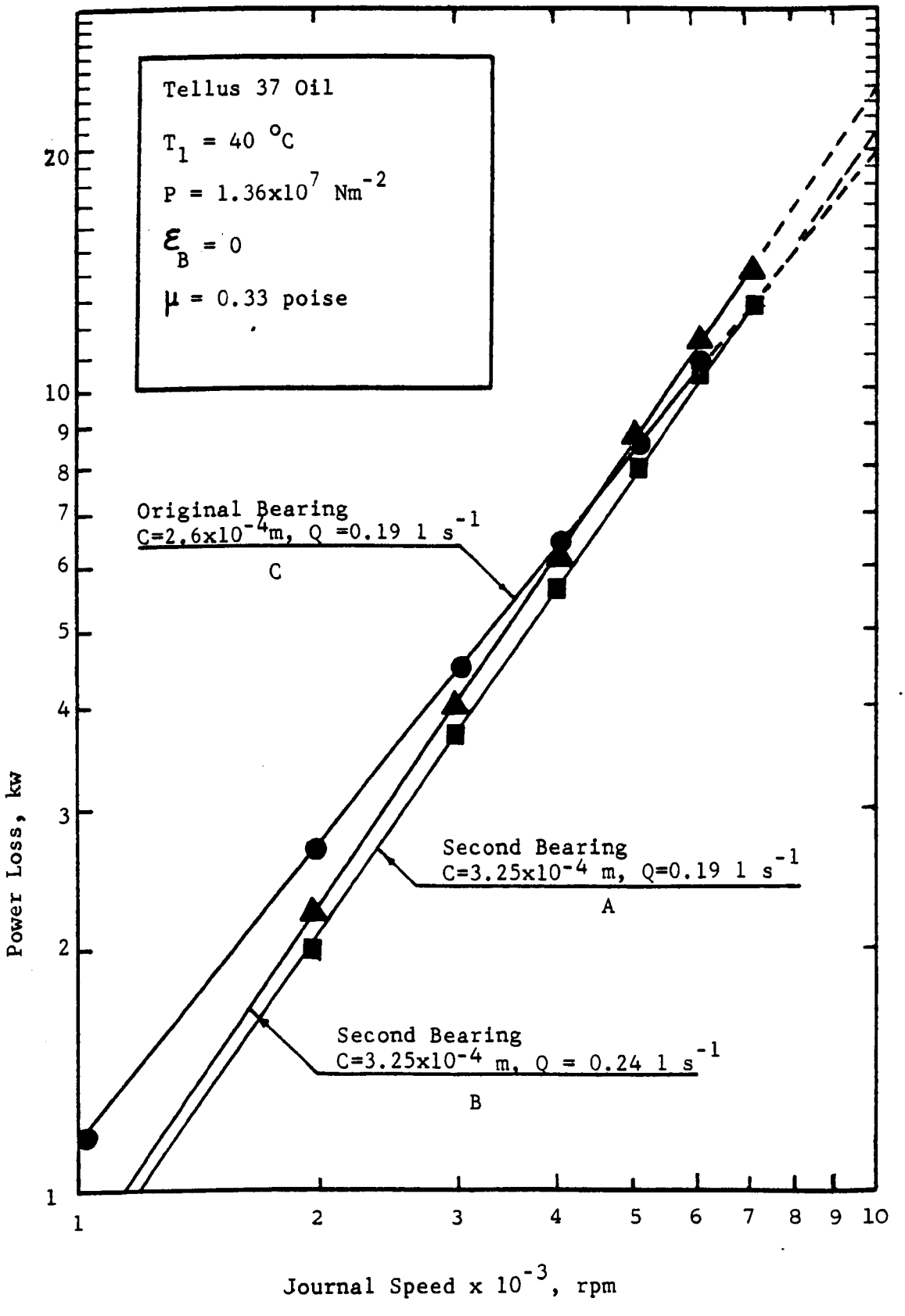

FIG.6.53 Variation of power loss with Journal speed (externally pressurized).

Also it may be seen for the same oil flow that the index of the power loss increases as the lobe clearance increases (lines A & C). Figure 6.54 shows the oil temperature rise-speed characteristic. The characteristics of the original bearing is also shown, and it may be seen that the increase in the lobe clearance has produced a small decrease in the oil temperature rise. That the decrease in the oil temperature rise is only marginal is attributed to that the oil flow was held constant over the full speed range and the oil flow was also held constant for the lobe clearances which have been tested.

Figure 6.55 shows the power loss-speed characteristics for the two different ways in which the high pressure oil was admitted. The triangular points represent the measured power loss when the high pressure oil is admitted at the original high pressure inlets, while the circular points represent the power loss as measured when the high pressure oil is admitted at the axial grooves. It may be seen that the power loss is decreased when the high pressure oil is admitted to the axial grooves, but the difference in the power loss becomes insignificant as the rotational speed is increased. The decrease of the power loss may be understood from the following discussion. When the high pressure oil is admitted at the original high pressure inlets a large proportion of this relatively cold oil is forced to flow in the direction of the journal rotation and tends to decrease the oil film temperature. The decrease in the oil film temperature results in a higher viscosity and somewhat greater power loss. When the high pressure oil is admitted at the axial grooves, a great proportion of the oil escapes out of the bearing from both ends of the axial grooves, so that the oil film temperature becomes somewhat higher than in the previous instance, and the power loss becomes somewhat smaller than the power loss of the original method of pressurization.

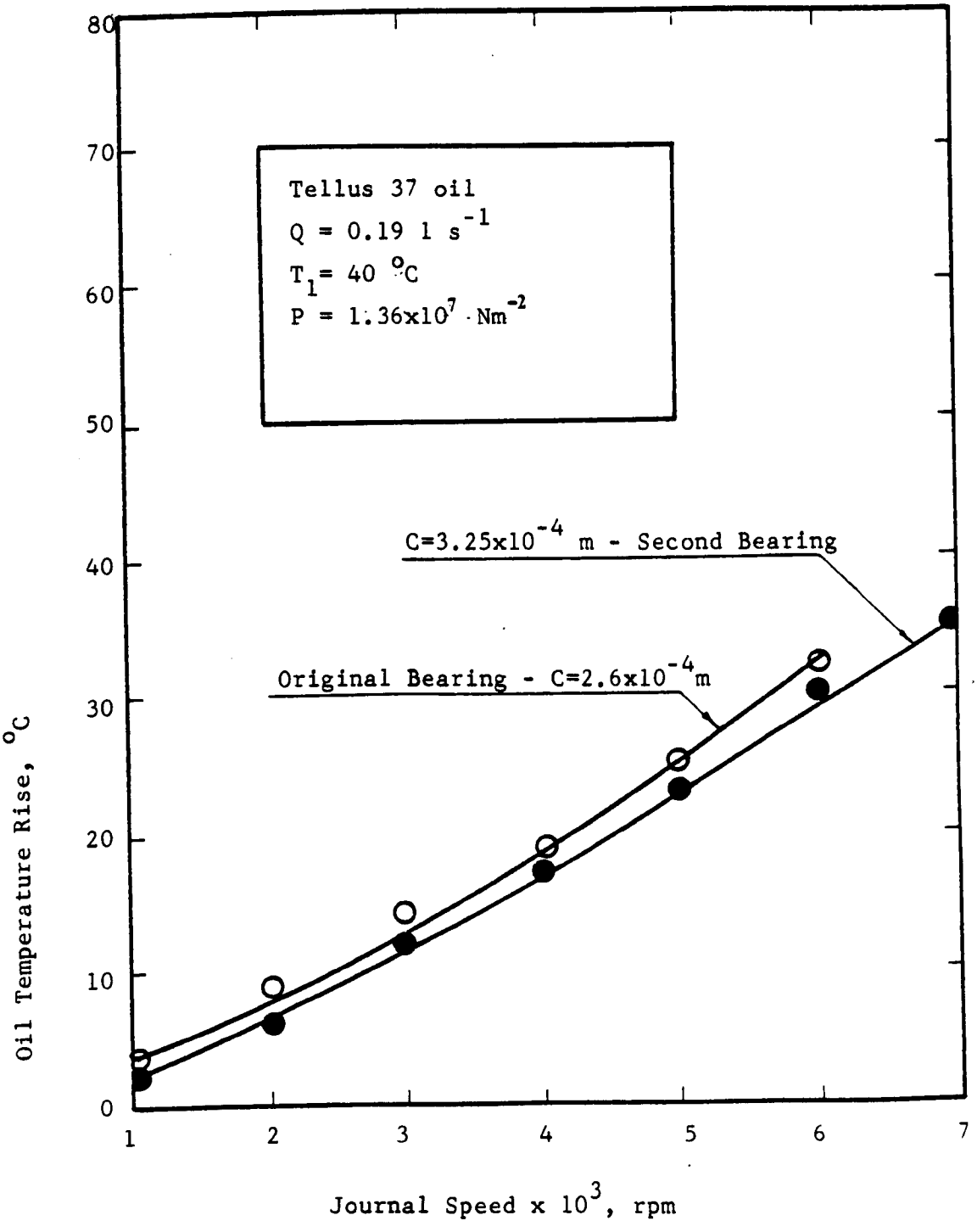

FIG.6.54 Oil temperature rise-speed characteristics for the externally pressurized operation.

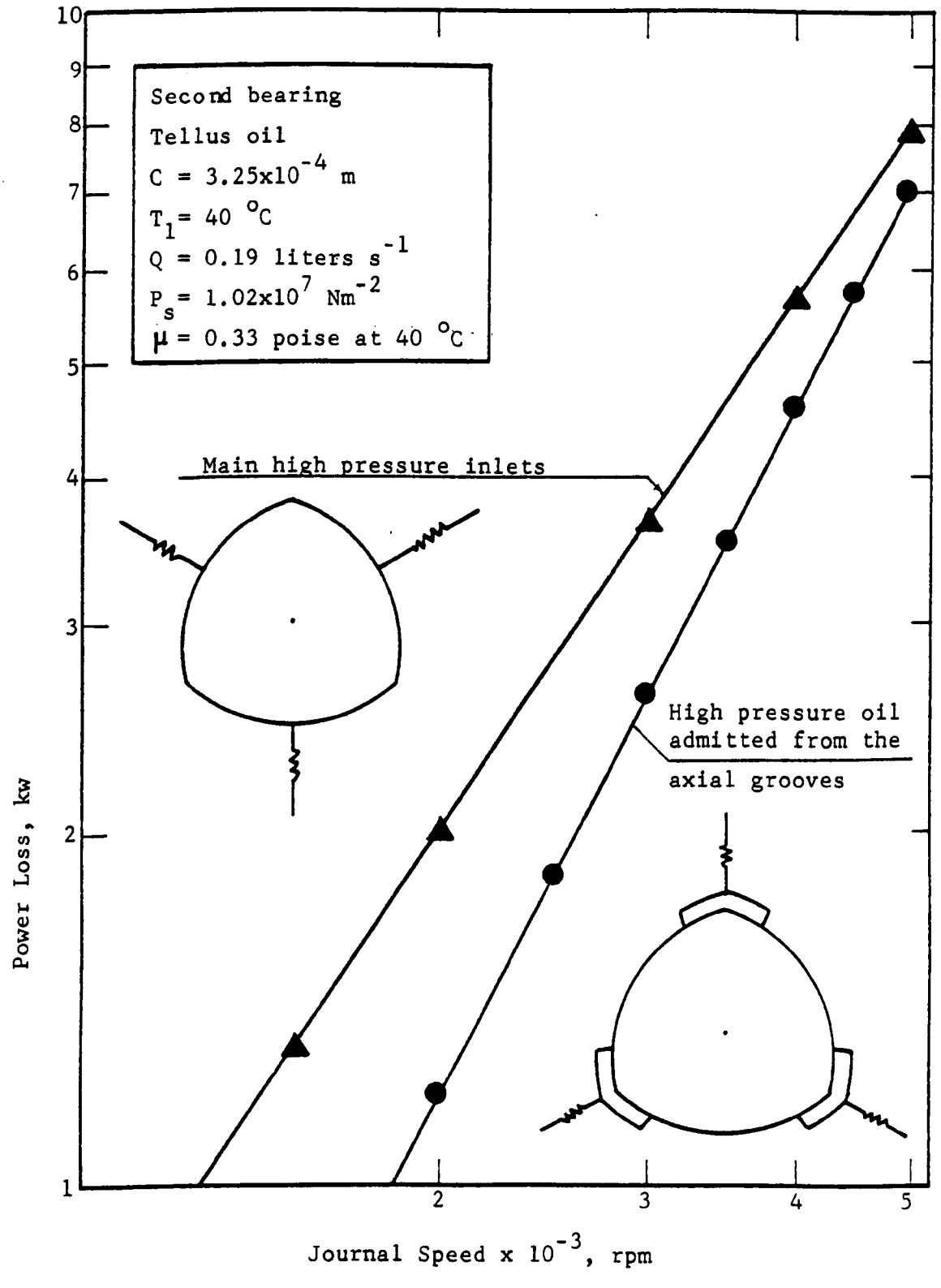

FIG.6.55 Power loss speed characteristics for the externally pressurized operation.

The oil which escapes out of the axial grooves is mixed with the film oil and acts as a cooling media so that the measured oil outlet temperature in the second case is lower than that measured with the original method in which the oil was admitted. When the rotational speed of the journal increases a great proportion of the oil which is supplied at the axial grooves is forced to flow in the direction of rotation due to the pumping action of the journal and consequently as the speed increases the difference in the power loss decreases.

6.4.2 Tests and Test Results of the Self Generating Operation.

The following results relate to the bearing being supplied only with low pressure oil and with shaft rotation in the range 1000 to 7000 rpm. Oil Shell Tellus 37 was used.

6.4.21 Load-Speed Characteristics of the Self Generating Operation.

The test results for the self generating operation are presented in figures 6.56 - 6.58. In figures 6.59 - 6.60 the results have been compared with the test results which have been reported in paragraph 6.3 and as expected the increase in the lobe clearance has resulted in an increase in the journal displacement and consequently the bearing stiffness is decreased.

6.4.22 Power Loss, Oil Temperature Rise and Oil Flow-Speed Characteristics.

The power loss, oil flow and oil temperature rise have been measured in much the same way as has been discussed in paragraph 6.3. Furthermore in the tests with the second bearing the relation between bearing load, power loss, oil temperature rise and oil flow has been investigated as well as the relation between the supply pressure and the oil flow. Also the pressure and the hydrodynamic oilflows have been measured.

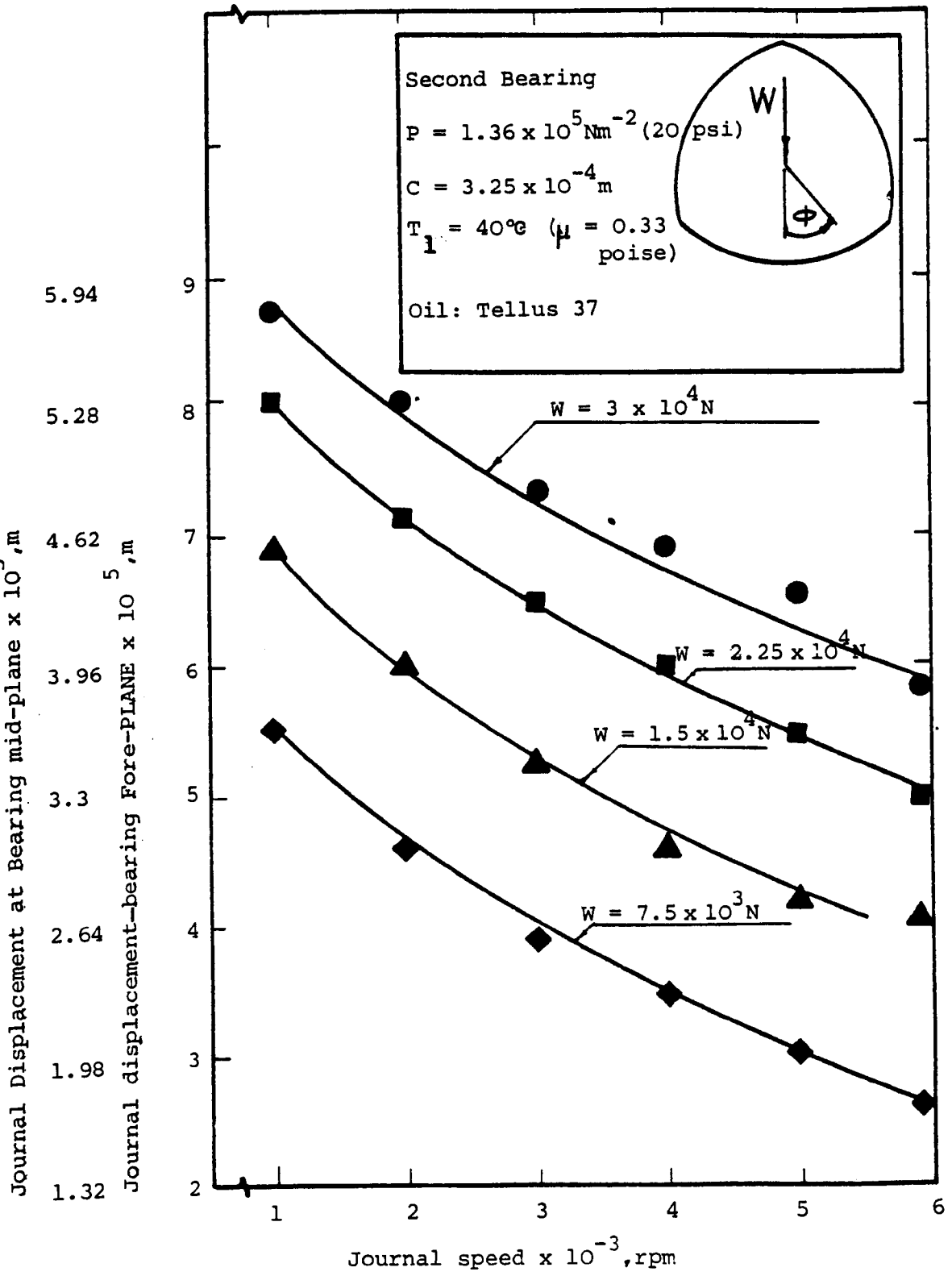

Figure 6.56. Variation of the journal displacement with the speed (self generating).

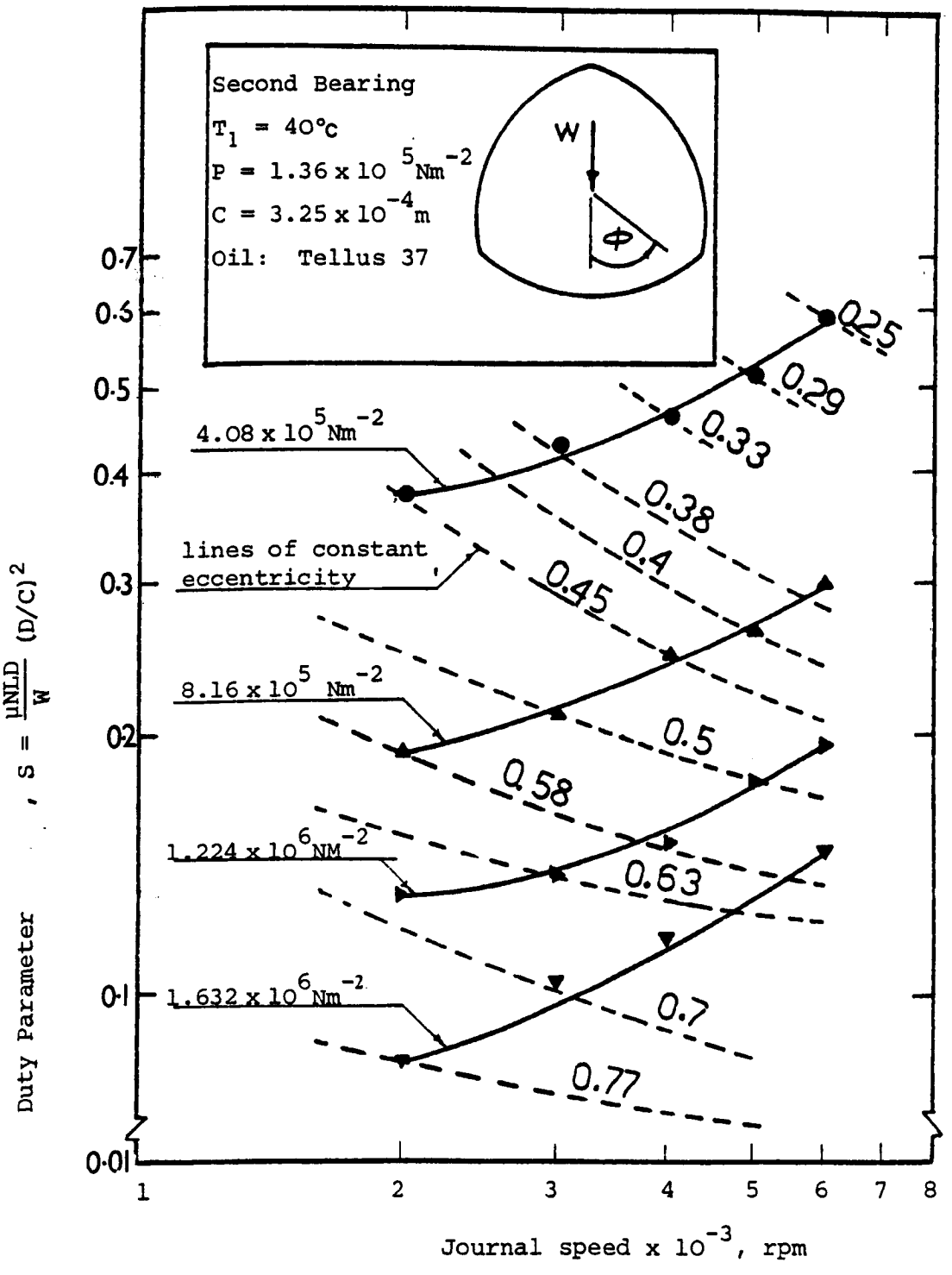

Figure 6.57. Duty Parameter - Speed Characteristics for the self generating operation.

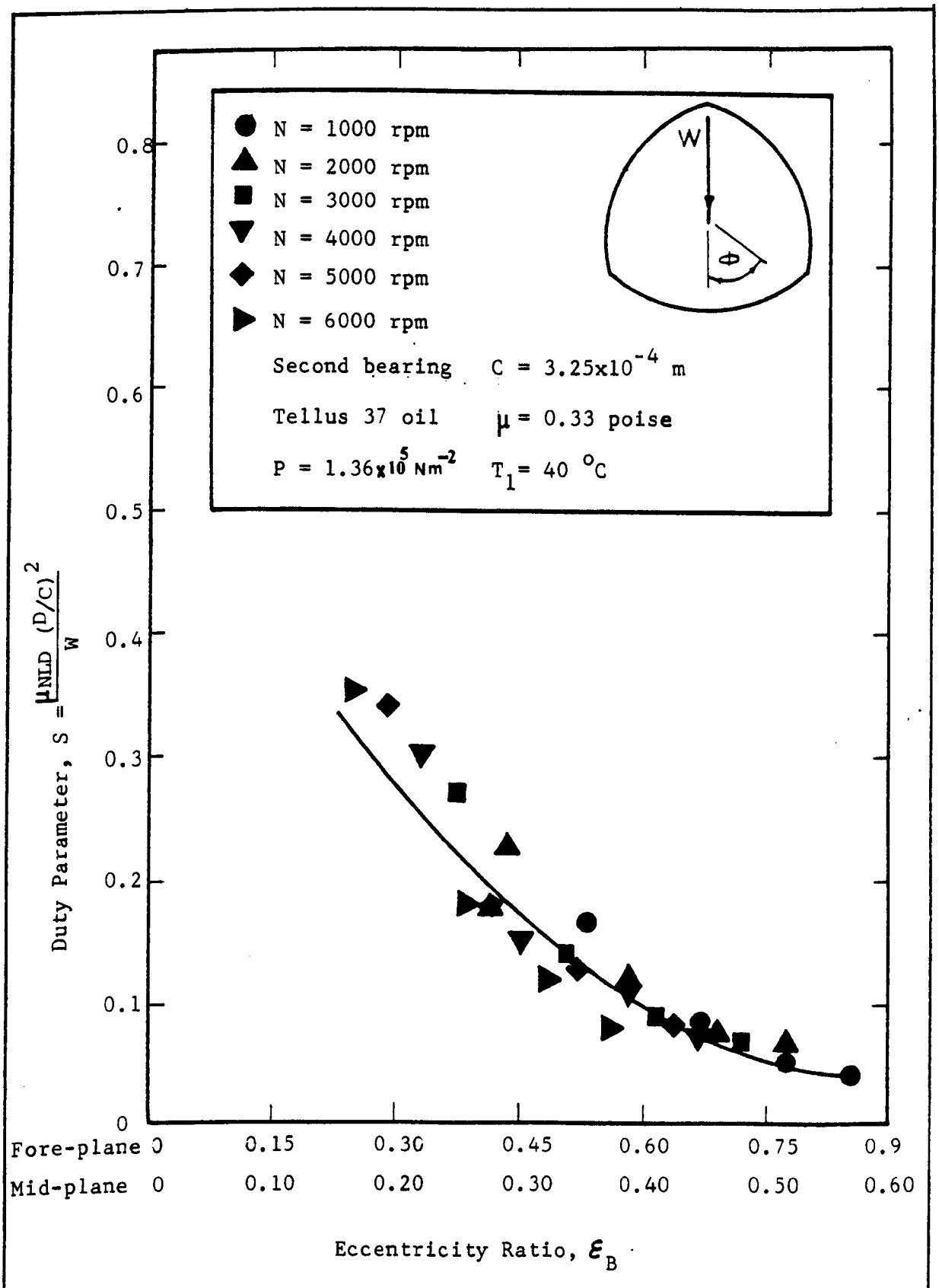

FIG.6.58 Variation of the duty parameter with the eccentricity ratio.

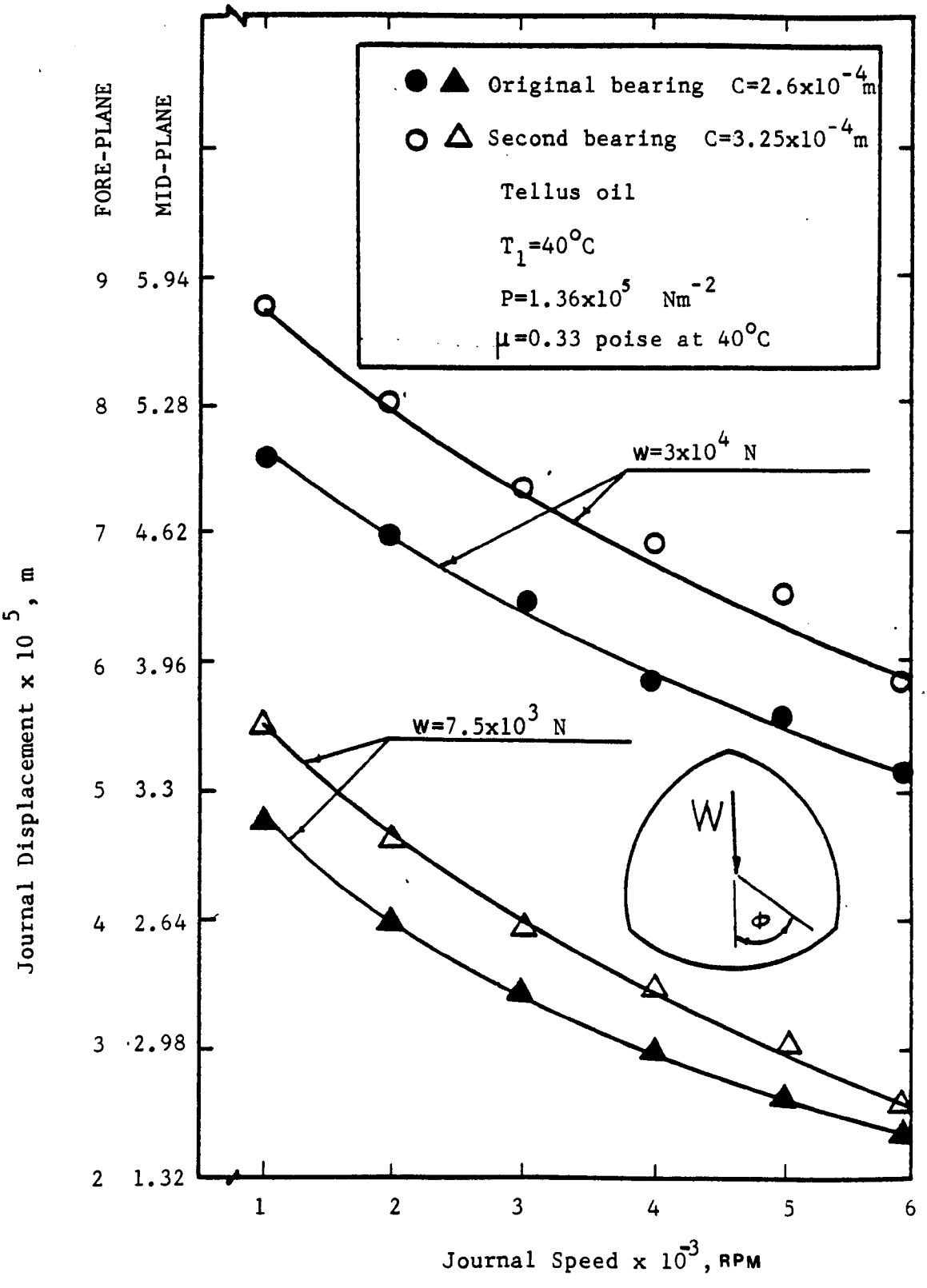

FIG.6.59 Variation of Journal displacement with the Journal speed (self-generating).

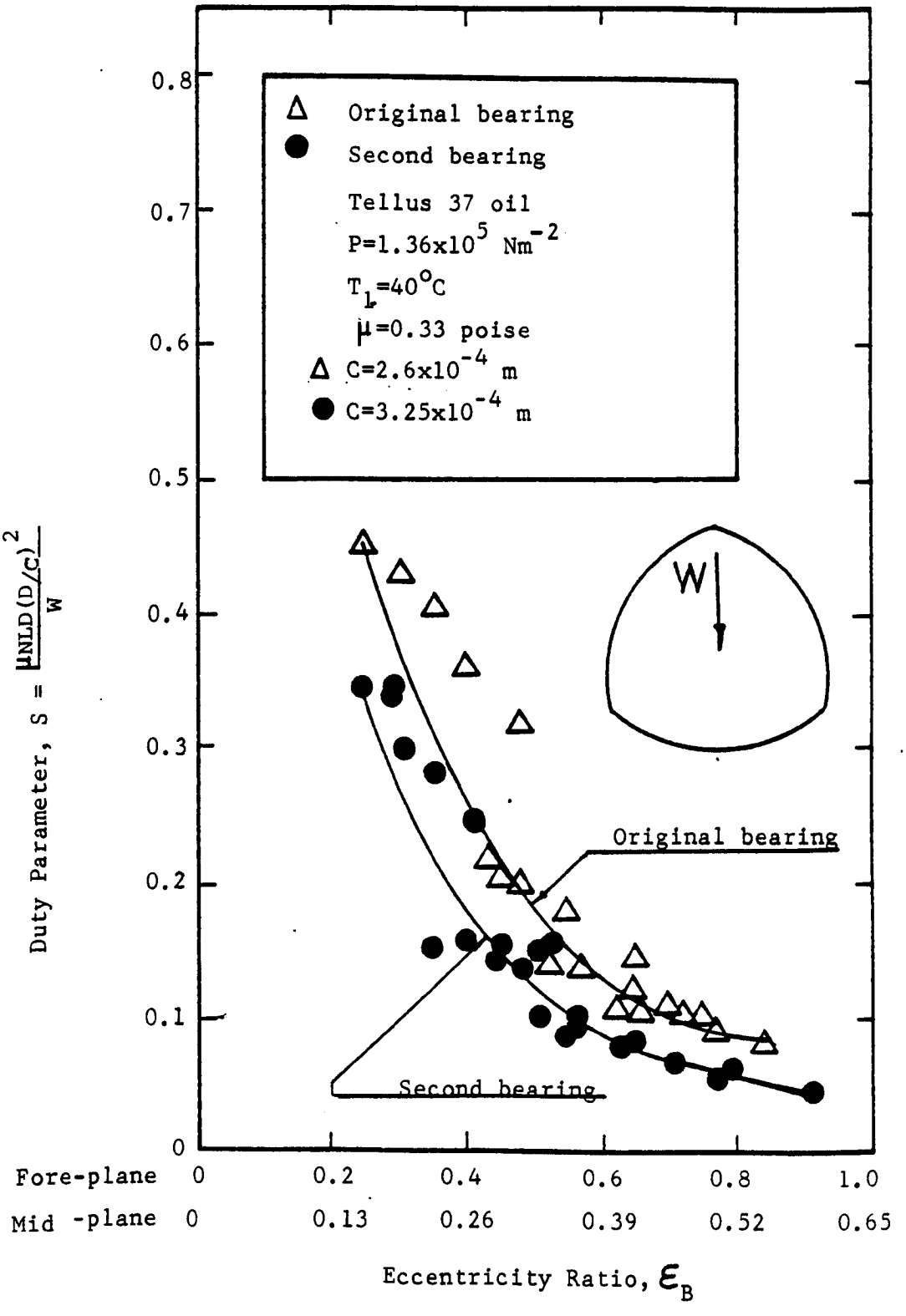

FIG.6.60 Variation of the duty parameter with the eccentricity ratio.

In figures 6.61-6.62, the measured power loss, oil temperature rise and oil flow are plotted versus the journal speed. In figure 6.63 the power loss, oil temperature rise and oil flow at no load of the original bearing are plotted with measured results of the second bearing at no load. It may be seen that the increase in the lobe clearance has increased the power loss marginally and has decreased the oil temperature rise. The decrease may be attributed to the increase in the oil flow.

6.4.23. Power Loss, Oil Temperature rise and Oil flow-load. Characteristics.

The variation of power loss, oil flow and oil temperature rise with journal load for the second bearing are shown in figures 6.64-6.65. Varying the journal load between zero and 22500 N at journal speeds of 3000 rpm and 4000 rpm., resulted in a slight increase in the power loss with increase of the load. The oil flow increased, also the oil temperature rise decreased, but again started to increase as the load was increased over 1.5×10^4 N.

6.4.24. Oil Flow-Inlet Pressure Characteristics.

The effect of varying the oil inlet pressure on the oil flow is shown in figure 6.66, for a journal speed of 4000 rpm and zero journal speed. The measurements were made with no load on the journal and with a journal load of 1.5×10^4 N. At no journal load, increasing the oil inlet pressure resulted in a substantial increase in the oil flow, and it is quite clear that the pressure flow is exceeding the hydrodynamic flow. At a journal load of 1.5×10^4N, increasing the oil inlet pressure resulted in a substantial increase

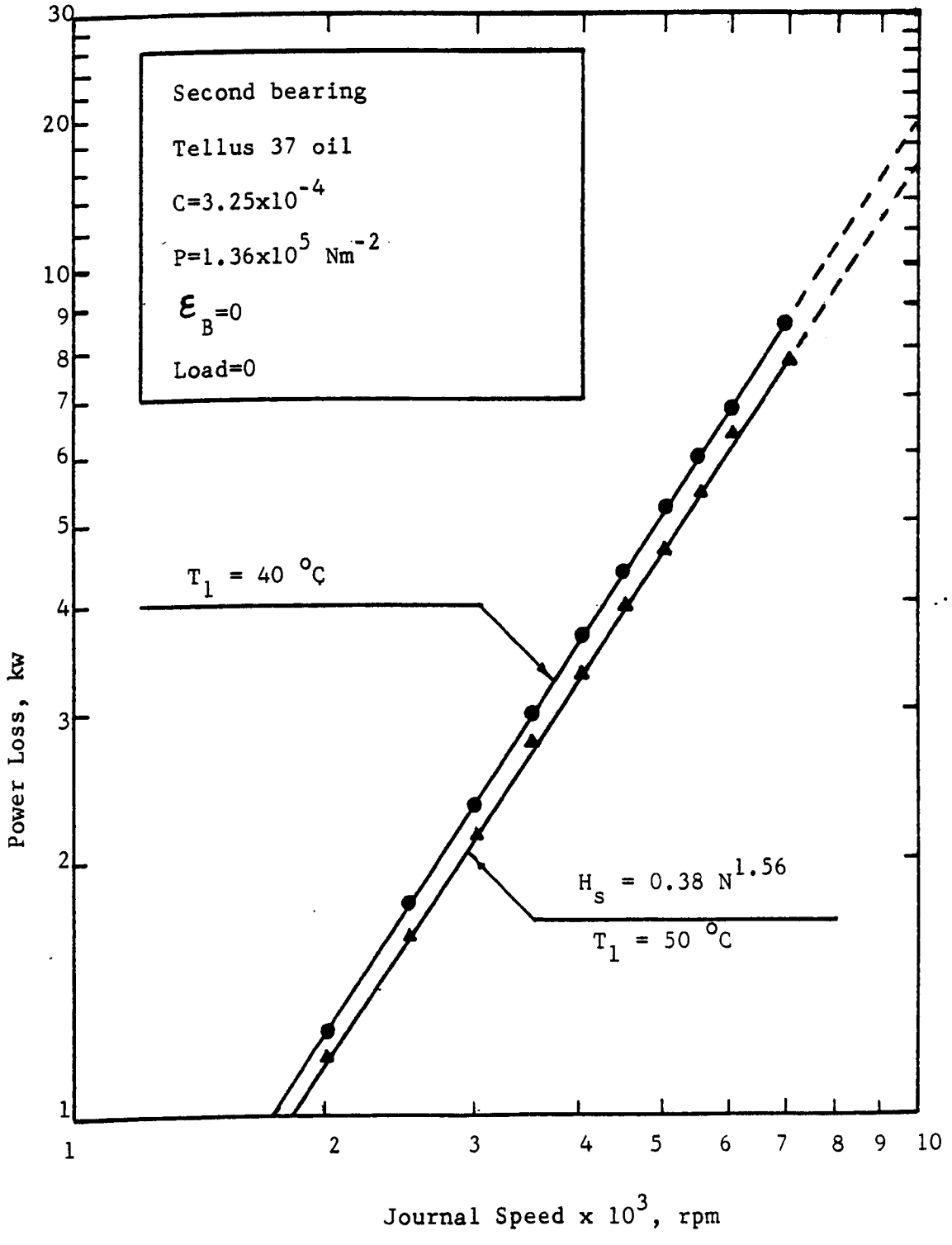

FIG.6.61 Variation of the power loss with Journal speed (self-generating).

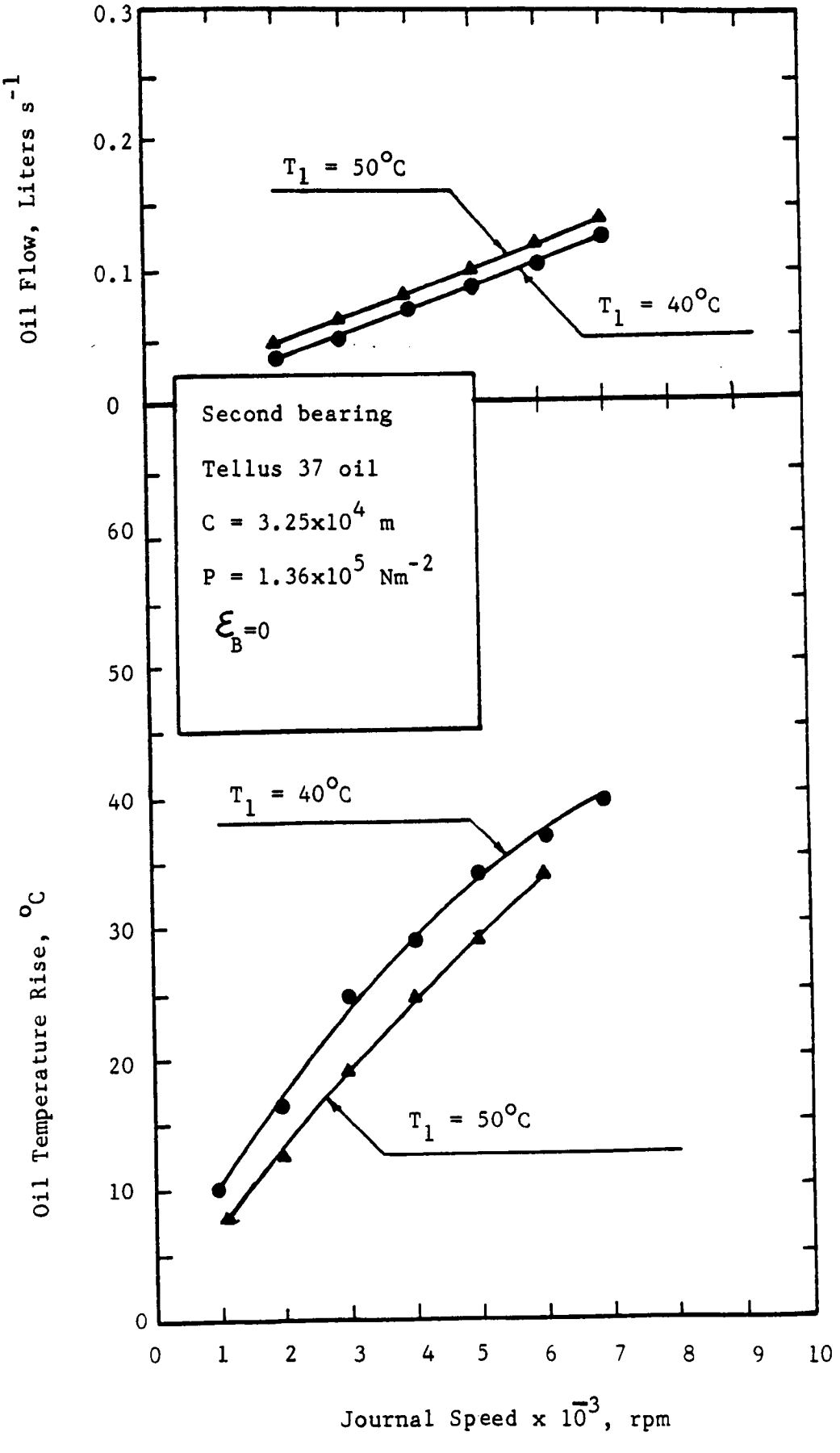

FIG.6.62 Variation of oil temperature rise and oil flow with the Journal speed.

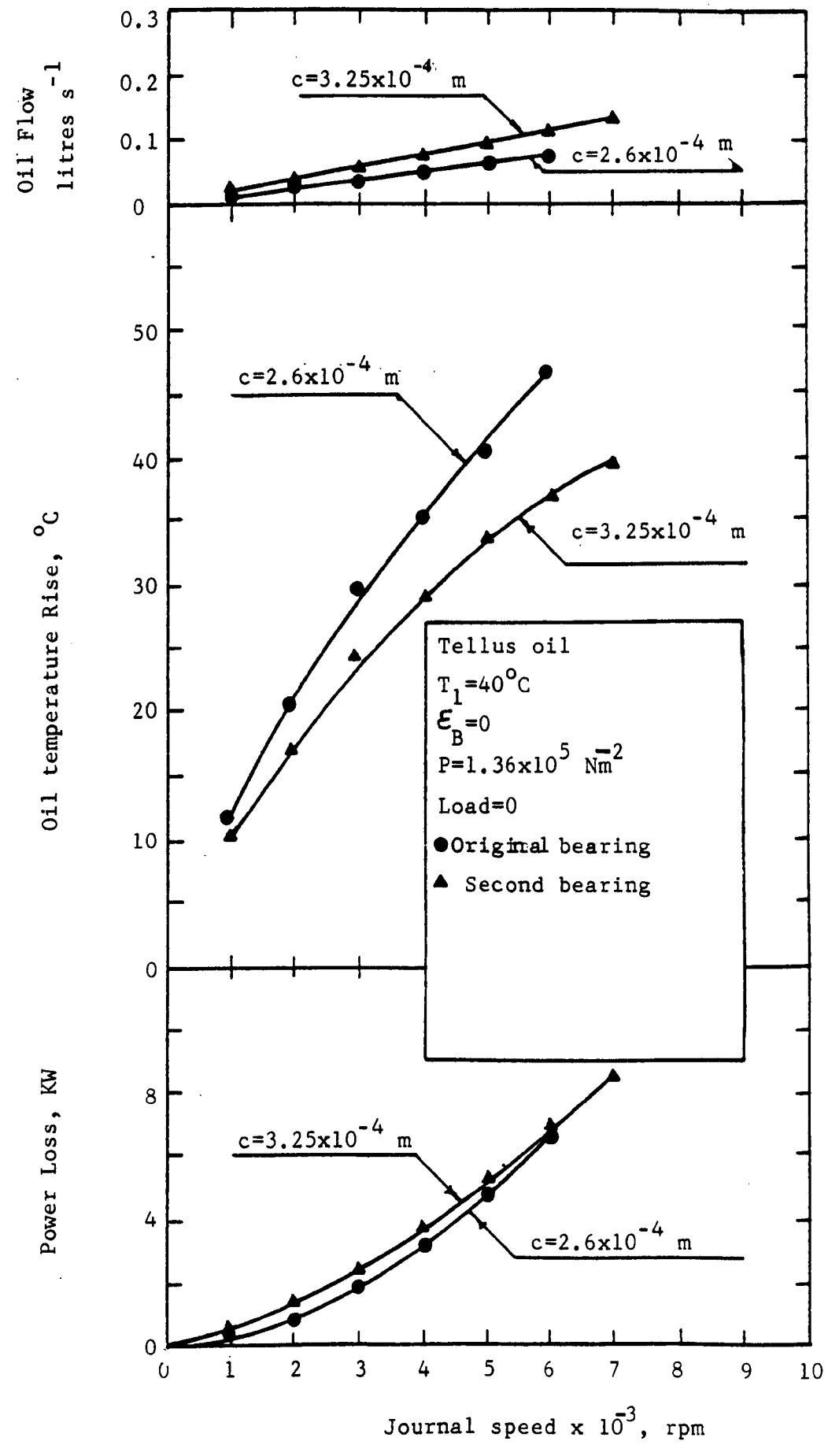

FIG.6.63 Variation of power loss, oil temperature rise, and oil flow with the Journal speed (self-generating).

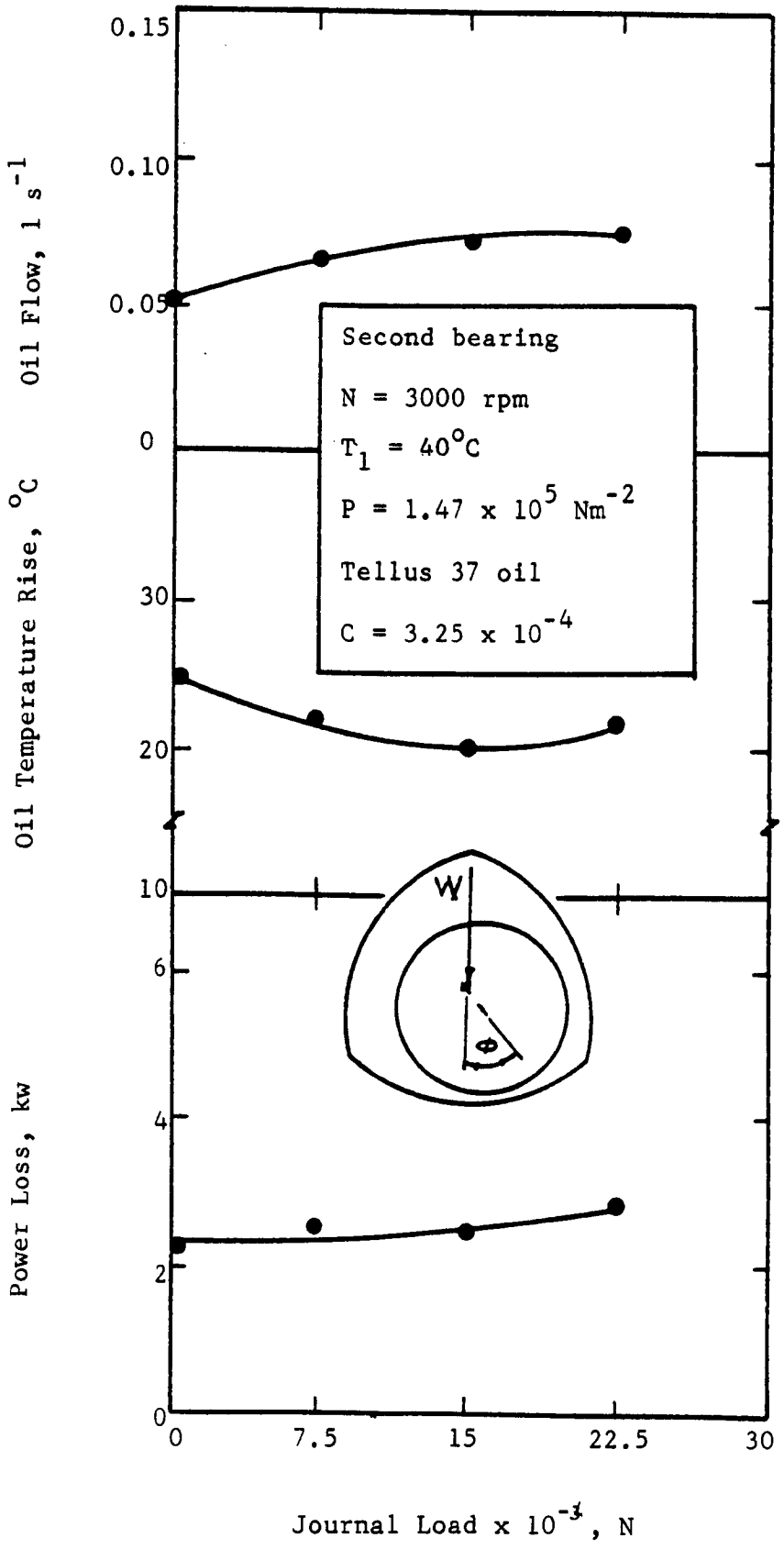

FIG.6.64 Power loss, oil temperature rise and oil flow-load characteristics.

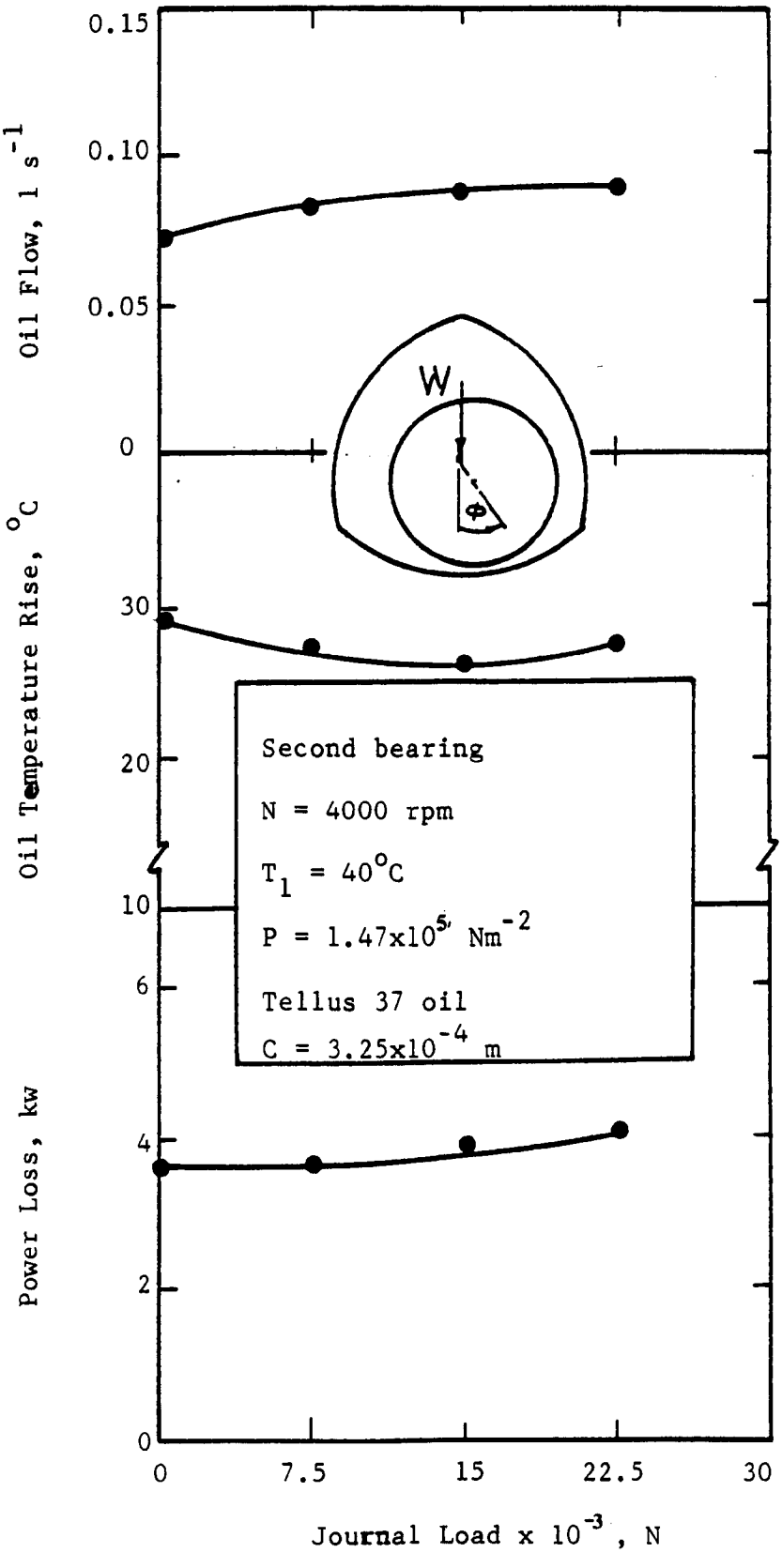

FIG.6.65 Power loss, oil temperature rise, and oil flow-load characteristics.

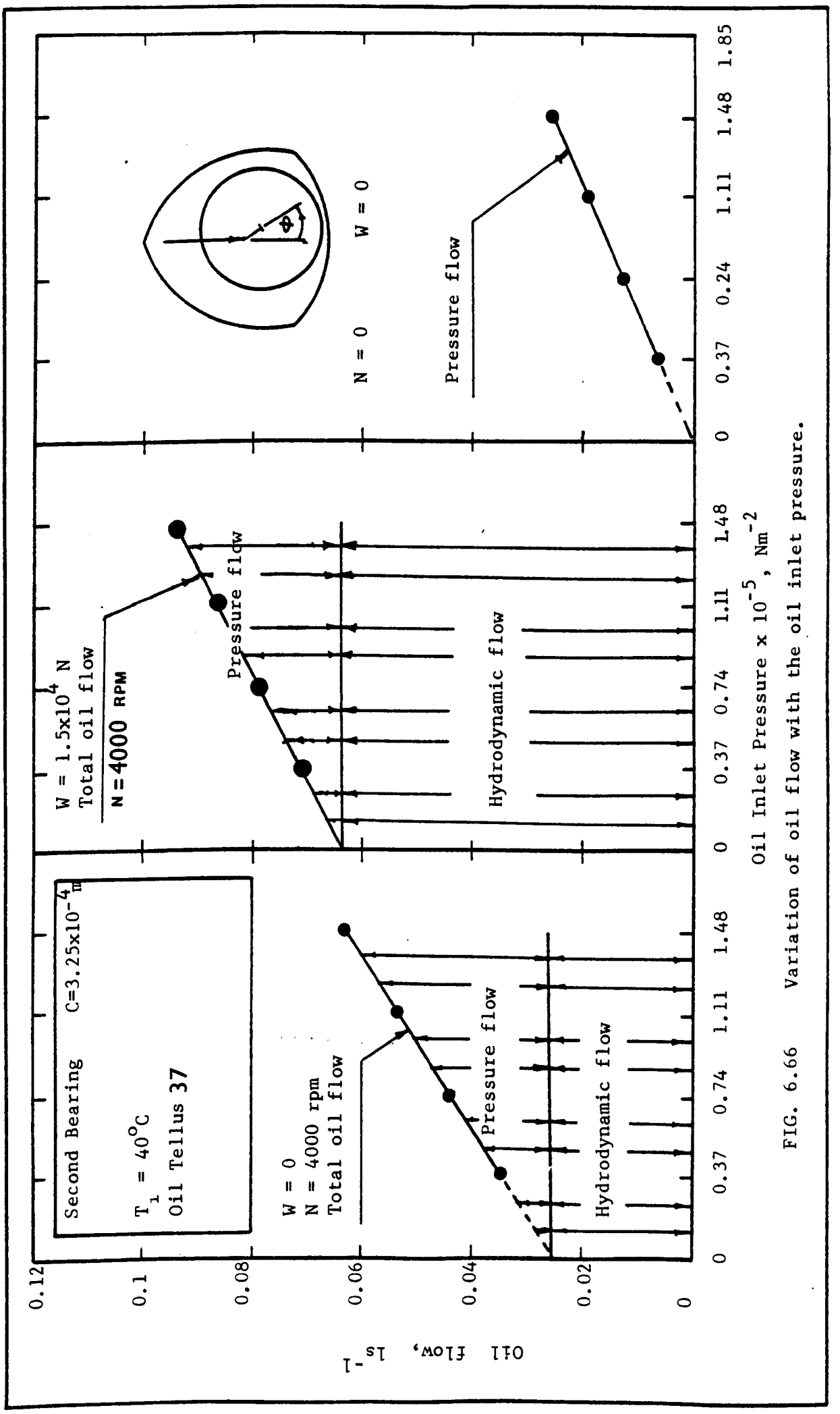

FIG. 6.66 Variation of oil flow with the oil inlet pressure.

in the oil flow, but the hydrodynamic oil flow is also increased and becomes the predominant oil flow. In figure 6.6, the pressure flow at 4000 rpm was 0.038 ℓs^{-1}, while at zero speed the measured pressure flow was 0.025 ℓs^{-1}; however, it may be seen that the pressure flow increases as the speed and the oil temperature increases, as has been considered in chapter 3.

6.5. Discussion of Test Results

The discussion of test results which is given below relates principally to the tests which have been carried out on a 135 mm diameter x 127 mm three lobe journal bearing which has a lobe clearance of 0.26 mm. and an offset ratio of 0.45 (the first bearing). The test results from the second bearing are introduced in the discussion of the effect of the lobe clearance on the bearing performance.

6.5.1. Externally Pressurized Operation with Stationary Shaft.

The tests which have been carried out with three lobe bearings and without shaft rotation have shown clearly that a stiffer spindle should be used if the capability of the bearing is to be realised fully. Despite the bending of the shaft the experimentally determined performance measured at the journal mid-plane, substantially matches or exceeds the functional specification of table 1.1; for instance the stiffness at the bearing mid-plane is 1.125×10^{9} Nm^{-1} (figure 6.23), which is substantially the stiffness as found in the static test rig (chapter 4), which exceeds the functional specification requirements for a stiffness in finishing of 8×10^{8} Nm^{-1} at low speed.

The above results were obtained with Shell VIT. 150 oil (ν = 150 CS. at 40°C), but tests were carried out also with Shell Tellus 37 oil (ν = 37 CS at 40°C). With this lower viscosity oil the bearing stiffness at the bearing mid plane was found to be 9.98×10^8 (figure 6.26), which is approximately 88.6% of the stiffness with the first oil.

Increasing the lobe diameteral clearance from 2.6×10^{-4}m to 3.25^{-4}m (the offset ratio decreased from 0.45 to 0.35) resulted in a decrease in the bearing stiffness from 8.98×10^8 Nm^{-1} to 8.33×10^8 Nm^{-1} (figures 6.26 and 6.50).

6.5.2. Externally Pressurized Operation with Rotating Shaft .

Increasing the journal speed from zero to 4000 rpm resulted in a small increase in the bearing stiffness. For instance the bearing stiffness increased from 1.125×10^9 Nm^{-1} at zero speed to 1.176×10^9 Nm^{-1} at 4000 rpm (figure 6.29). Also increasing the journal speed resulted in an increase in the power loss and in the oil temperature rise. At 4000 rpm the power loss was 10.3 KW., and the oil temperature rise was 32°C (the oil inlet temperature was 40°C - VIT. 150 oil).

Increasing the oil inlet temperature resulted in a decrease in the power loss and in an increase in the oil outlet temperature, whereas, by using a lower viscosity oil (Tellus 37) the power loss and the oil outlet temperature substantially decreased. At 4000 rpm the power loss decreased from 10.3 KW to 6.2 KW, and the oil temperature rise decreased from 32°C to 19°C (figures 6.36 and 6.37).

Increasing the lobe clearance resulted in a marginal decrease in the power loss particularly at low speeds but as the speed increases

the power loss is much the same as found with the original bearing. Also, increasing the lobe clearance has little effect on the oil temperature rise (figures 6.53 - 6.54).

6.5.3. Self Generating Operation

In the self generating regime and with Shell VIT.150 oil, and at a speed of 4000 rpm and a load of 7.5×10^{3}N, the journal displacement at the bearing mid plane was found to be 1.45×10^{-5}m, which corresponds to a stiffness of 5.19×10^{8} Nm^{-1}. Also at 4000 rpm and with no load the power loss was found to be 3.2 KW., the oil flow 0.03 ℓs^{-1} and the oil temperature rise was found to be 57°C.

By using a lower viscosity oil and at 4000 rpm, the journal displacement at the bearing mid-plane increased from 1.45×10^{-5} m to 1.71×10^{-5} m (the stiffness is descreased from 5.19×10^{8} to 4.26×10^{8} Nm^{-1}). Also, at 4000 rpm the oil temperature rise decreased from 57°C to 40°C, but because the oil flow had increased from 0.03 ℓs^{-1} to 0.039 ℓs^{-1}, the power loss is much the same as the power loss measured with the first oil.

Increasing the lobe diameteral clearance from 2.6×10^{-4}m to 3.25×10^{-4}m decreased the bearing stiffness from 4.26×10^{8} Nm^{-1} to 3.58×10^{8} Nm^{-1}, the power loss was little affected, but the oil flow increased and at 4000 rpm the oil temperature rise had decreased from 40°C to 33°C (figures 6.56 to 6.63).

Varying the journal load between zero and 2.25×10^{4}N at journal speeds of 3000 and 4000 rpm, resulted in an increase in the power loss with increase of journal load. The oil flow increased and the oil

temperature rise decreased initially with load, reaching a minimum at a load of 1.5×10^4N, then increased but still remained lower than the oil temperature rise at zero load (figures 6.64 and 6.65).

Increasing the oil inlet pressure resulted in a substantial increase in the oil flow. At no load the pressure flow represents a substantial proportion of the total oil flow, whereas at a load of 1.5×10^4N the hydrodynamic oil flow became dominant.

The test results are summarized in table 6.4, and the following salient factors are drawn from the table:

I. The maximum stiffness at zero speed is 1.125×10^9 Nm^{-1} and the minimum stiffness is 8.98×10^8 Nm^{-1}.

II. In the externally pressurized regime and at 4000 rpm the maximum stiffness is 1.176×10^9 Nm^{-1}, the minimum stiffness is 9.375×10^8 Nm^{-1}, the maximum power loss is 10.3 Kw, the minimum is 5.5 Kw., the maximum oil temperature rise is 32°C and the minimum is 17.5°C.

III. In the self generating regime and at 4000 rpm, the maximum stiffness is 4.286×10^8 Nm^{-1}, the minimum is 3.21×10^8 Nm^{-1}, the power loss is 3 Kw., the maximum oil temperature rise is 51°C and the minimum is 29°C.

IV. At 6000 rpm and with externally pressurized operation the power loss, oil temperature rise and the bearing stiffness are 10.5 Kw., 32°C and 1.39×10^9 Nm^{-1} respectively, whereas with the self-generating operation these became 6.7 Kw., 46°C and 5.34×10^8 Nm^{-1} respectively.

TABLE 6.4. Test Results and Functional Specification.

Regime	Test Results							Functional specification stiffness Nm^{-1}
	Test * Condition	Speed r.p.m.	Power Loss Kw.	Oil flow ℓs^{-1}	Oil Temp. Rise, °C	Load N	Stiffness Nm^{-1}	
External Pressure	A	0	(3)**	0.2	4	3×10^4	1.125×10^9	8×10^8
"	A	4000	10.3(3)	"	32	3×10^4	1.176×10^9	"
"	B	0	- (3)	"	4	3×10^4	8.98×10^8	"
"	B	4000	6.2(3)	"	19	3×10^4	1.132×10^9	"
"	B	6000	10.5(3)	"	32	"	1.39×10^9	"
"	C	0	- (3)	"	4	3×10^4	8.33×10^8	"
"	C	4000	5.5(3)	"	17.5	"	9.375×10^8	"
"	C	6000	10 (3)	"	30	-	-	"
Self-Gen.	A	2000		0.015	23	7.5×10^3	3.52×10^8	3.51×10^8

TABLE 6.3. continued. Test Results and Functional Specification.

Regime	Test Results							Functional specification stiffness Nm^{-1}
	Test * condition	Speed r.p.m.	Power loss Kw.	Oil flow ℓs^{-1}	Oil Temp. Rise. °C	Load N	Stiffness Nm^{-1}	
Self-Gen.	A	4000	3	0.03	51	7.5×10^3	5.19×10^8	3.51×10^8
"	B	2000	-	0.029	20	7.5×10^3	3.125×10^8	"
"	B	4000	3	0.055	35	"	4.286×10^8	"
"	B	6000	6.7	0.088	46	"	5.34×10^8	"
"	C	2000	1.25	0.035	16	"	2.5×10^8	"
"	C	4000	3.7	0.075	29	"	3.21×10^8	"
"	C	6000	6.8	0.11	37	"	4.41×10^8	"
"	C	7000	8.6	0.125	39	-	-	"

Table 6.3. continued

** Test Condition A: D = 135 m m L = 127 m m C = 0.26 m m.

ε_o = 0.45 α = 16°

Oil: Shell VIT. 150.

Test Condition B: As above except that,

Oil: Shell Tellus 37.

Test Condition C: D = 134 m m L = 127 m m C = 0.325 m m

ε_o = 0.35 α = 30°

Oil: Shell Tellus 37.

* Figure in brackets is the pumping power.

CHAPTER 7

ON THE DYNAMIC CHARACTERISTICS OF THREE-LOBE JOURNAL BEARINGS FOR SELF-GENERATING AND EXTERNALLY PRESSURIZATION.

7. ON THE DYNAMIC CHARACTERISTICS OF THREE-LOBE JOURNAL BEARINGS FOR SELF-GENERATING AND EXTERNALLY PRESSURIZATION.

7.1. Introduction

Throughout Chapters 2 to 6, the experimental work and the theoretical analysis have been devoted to the steady state running of the three-lobe journal bearings in both the self-generating and the externally pressurized regimes. Dynamic characteristics have not been calculated comprehensively nor have any tests been carried out. The object of this chapter is to outline how the dynamic characteristics might be calculated, and to comment upon the dynamic implications of such relevant information as has been gathered.

In this chapter a general discussion on the dynamic characteristics of journal bearings is briefly presented with special reference to the method used for the calculation of the dynamic coefficients. The dynamic characteristics of the control device, (i.e. constant volume flow valves) will also be considered. The way in which the computer programmes might be modified to yield the dynamic coefficients is outlined. In chapter 8, the required modifications of the test rig will be discussed.

7.2. Dynamic Characteristics of Journal Bearings.

One of the vibration problems which are associated with journal bearings is oil whirl. Oil whirl is a self excited vibration in which

the vibration is almost exactly half the journal rotation speed. Another type of the self excited vibration is known as oil whip (ref. 2) or as low-frequency whirl (ref. 10) which is a shaft vibration occurring at the natural frequency of the shaft when the rotating speed of the shaft is approximately two or more times the natural frequency. Oil whirl has been the subject of many investigations (references 71 to 80). These kinds of vibration are normally associated with high-speed lightly loaded bearings. The bearing dynamic characteristics play an important role in the stability of high speed machinery. However, stability is determined by both the dynamic characteristics of the rotating parts and by the dynamic characteristics of the journal bearings. Consequently, several bearing designs have been introduced to reduce and to delay the tendency for a shaft to whirl in a bearing. These designs include elliptical bearings, pressure bearings, longitudinal-groove bearings, pivoted-shoe bearings, nut cracker type bearings and the three-lobe bearings (reference 58). In all these designs the bearing bore is far from a complete circle and the surface is always interrupted by axial grooves, which may be used to admit the oil or to act as relief grooves.

In references (10-74-76) the dynamic characteristics of full circular bore journal bearings are presented. In the analysis, it is assumed that the dynamic characteristics with respect to a journal motion of a small amplitude can be represented by linear force displacement, and linear force velocity relations. It is assumed that the force displacement terms can be calculated, as for zero squeeze velocity, by differentia tion of the conventional steady running characteristics, and that the

force velocity terms can be calculated, as for zero displacement*, from the squeeze effects in the film with boundaries fixed as for steady running conditions.

With this assumption and with reference to figure 7.1 the dynamic characteristics can be expressed in the dimensionless form.

$$P_x^* = a_{11}\, x^* + a_{12} y^* + b_{11}(x^*/_w) + b_{12}\,(y^*/_w) \qquad (7.1)$$

$$P_y^* = a_{21}\, x^* + a_{22}\, y^* + b_{21}(x^*/_w) + b_{22}(y^*/_w) \qquad (7.2)$$

where,

$$P_x^* = \frac{P_x}{W} \quad , \quad P_y^* = \frac{P_y}{W}$$

$$x^* = \frac{X}{C} \quad , \quad y^* = \frac{Y}{C}$$

$$x^*/_w = \frac{\dot{X}}{cw} \quad , \quad y^*/_w = \frac{\dot{Y}}{cw}$$

a_{11}, ... and a_{22}: are the displacement coefficients.

b_{11}, ... and b_{22}: are the velocity coefficients

P_x and P_y, are the disturbance forces.

W : is the steady load

c : is the lobe radial . clearance,

and

w : is the angular velocity of the journal.

In references (10-74-76) the displacement coefficients of the full circular bore bearings have been calculated from the steady running characteristics and the velocity coefficients have been calculated from the results which have been obtained by solving Reynolds' equation

* The displacement from steady running position.

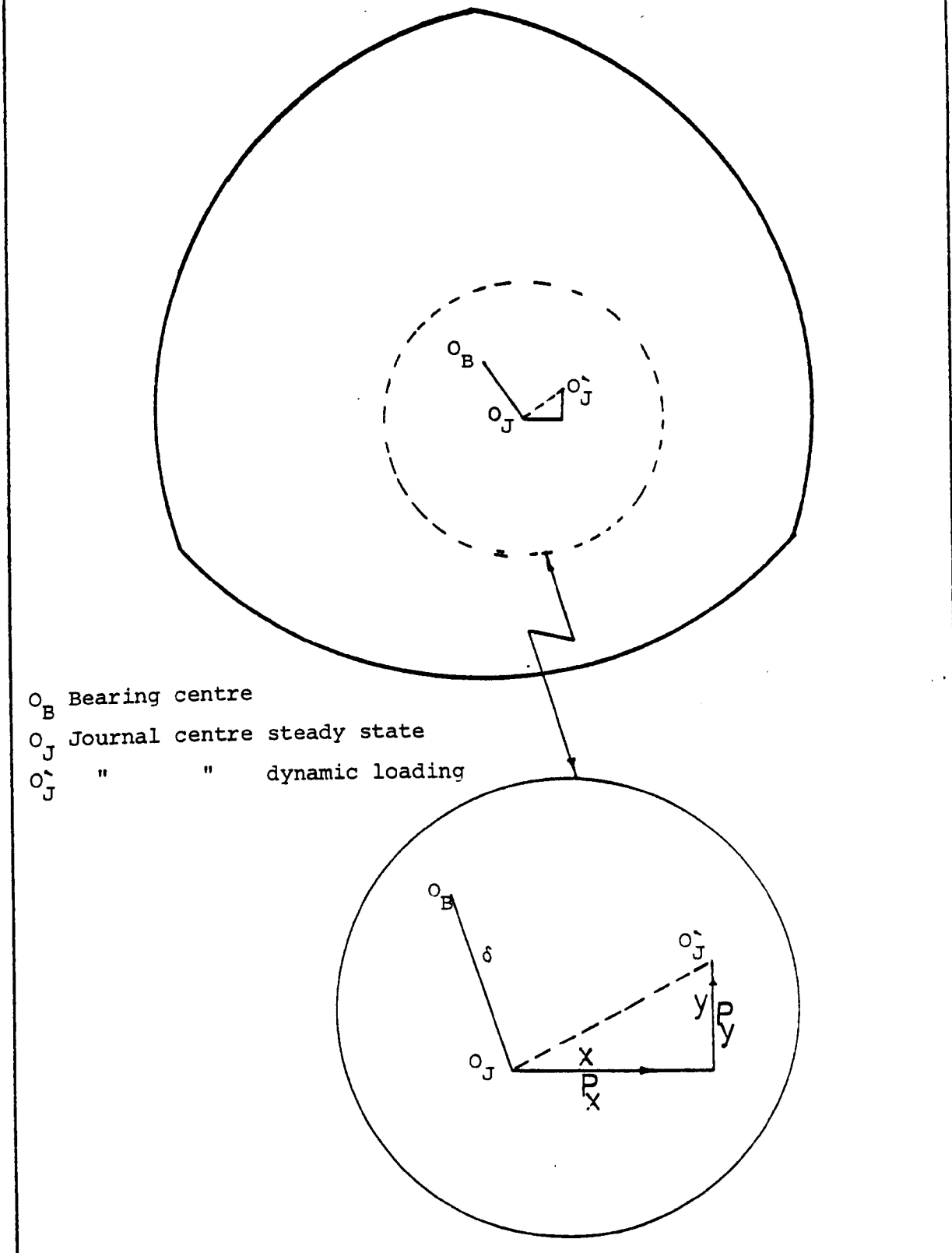

Figure 7.1. Force and displacement characteristics.

which includes the squeeze term as will be explained below.

For the three-lobe bearing, it has been shown in chapter 3 that at higher values of eccentricity ratios the calculated attitude angle and duty parameter are nearly the same as for a circular bore bearing. However, because both the velocity coefficients and the displacement coefficients are functions of the attitude angle and the duty parameter, the dynamic characteristics may be expected to be the same as those calculated for a circular bore bearing. With smaller values of eccentricities, substantial pressure is created in both the bottom and side lobes with consequent effects on the attitude and duty parameter. In Chapter 3 it has also been shown that at small values of eccentricity there is substantial difference between the three-lobe bearings and the full circular bore bearings with respect to the attitude and the duty parameter and this difference increases as the offset ratio increases. In consequence, for a lightly load three-lobe bearing, the dynamic characteristics may be expected to differ from those calculated for a circular bore bearing.

In chapter 3, Reynolds' equation for the steady running condition of the three-lobe bearings has been solved. The attitude angle has been found for a vertical load where the results for different values of L/D, ε_o, ε_B are tabulated in tables 3.4 and 3.5. Those results may be differentiated by a method similar to the method described in references (74-76) to find the displacement coefficients for the three-lobe bearings.

For the calculation of the velocity coefficients Reynolds' equation, which must now include the squeeze term, may be written as

$$\partial/\partial x\left(\frac{h^3}{\mu}\cdot\frac{\partial P}{\partial x}\right)+\frac{\partial}{\partial z}\left(\frac{h^3}{\mu}\cdot\frac{\partial P}{\partial z}\right)=6U\frac{dh}{dx}+12\frac{dh}{dt} \qquad (7.3)$$

Equation (7.3) may be expressed in a dimensionless form and then this equation may be transformed into a finite difference form by the same procedure as has been described in chapter 3.

In reference (10), it has been pointed out that the solution of equation (7.3) for zero velocity and by using the conventional assumptions of boundary conditions which have been described in chapter 3, will give dynamic characteristics which are linear and which are consistent in their force-displacement terms with the terms obtained by differentiation of the steady-running characteristics of the bearing. When the squeeze term is not zero the conventional assumptions no longer define the actual boundary conditions, but the effect of using the conventional assumptions on the dynamic characteristics is, however, very small for perturbing velocities of small amplitude. However, equation (7.3) can be solved by using the same boundary conditions which have been described in chapter 3. The Computer programme itself can be used and the only modification required in the computer routine is to include the squeeze term in the main finite difference equation (equation 3.7).

The velocity coefficients may be calculated from the outputs of the solution of equation (7.3) by a differentiation procedure similar to that described in references (74-76). However, because

in Chapter 3 it has been shown that at small and moderate values of eccentricity the three-lobe bearings has attitude-duty parameter-stiffness characteristics better than that of circular bore bearings or of longitudinal groove bearings or of elliptical bearings, it may be expected that the three-lobe bearings will have improved dynamic and damping characteristics.

The same procedure can also be used with respect of equation (5.5) to calculate the dynamic characteristics of the three-lobe bearings with external pressurization.

7.3. Dynamic Characteristics of the Compensation Devices.

The performance of the three-lobe bearing as an externally pressurized bearing depends on the characteristics of the external compensation device. In the experimental work which has been described in chapters 4 and 6, the bearing has been compensated by constant volume flow valves. Also in the analysis which has been described in chapter 5, the calculations were based upon a constant volume flow delivered to each lobe. Throughout the experimental investigations only a constant undirectional load has been applied on the test shaft. With a constant load it has been found that the control valves perform satisfactorily, and deliver a constant volume flow providing that there is a minimum pressure difference of 6.67×10^5 Nm^{-2} (100 psi) across the valves.

If a machine tool instance is considered in which a milling cutter with 12 cutting edges is rotating at 1000 rpm, then the load on the bearing will change 12,000 times per minute so that the

pressure in the bearing lobes and at each high pressure inlet wil- fluctuate at the same rate. In Appendix A7 it has been shown that the flow through the valve is kept constant by movement of a spool. However, when the pressure is fluctuating at 12,000 times a minute, the spools would also have to move at the same rate to keep the oil flow constant. The constant volume flow valves have not been subject to any dynamic loading so that the dynamic response of these valves is unknown yet. But, if the test results prove that these control devices do not perform satisfactorily under fluctuating load, the constant volume flow valves may be replaced by a constant volume flow pump which would be insensitive to the fluctuations of the load.

CHAPTER 8

Discussion, Conclusions and Recommendations.

8 Discussion, Conclusion and Recommendations.

8.1. Introduction

In Chapters 2, 3 and 5 the theoretical analysis of the three lobe bearing has been presented and discussed. The comparisons between the results of the theoretical analysis and the test results which have been reported in Chapters 4 and 6 were made when it was necessary to make an immediate comparison between theory and experiment. In this chapter a more comprehensive discussion and comparison will be made. Suggestions are made for future work. These include a re-designed system permitting a stiffer shaft to be used, bearings of modified geometry aimed at higher stiffness, lower power loss, and a lower oil temperature rise, and test and theoretical work to explore more thoroughly than has been possible in this thesis, the dynamic characteristics and stability of the bearing.

8.2. Externally Pressurized Operation.

The results of the approximate analysis which has been reported in Chapter 2 and the results of the numerical analysis which have been reported in Chapter 5, will be compared with the test results which have been reported in Chapters 4 and 6.

Figure 8.1 shows the calculated total oil flow and the calculated lobe pressure as functions of lobe diameteral clearance. Line A and line C have been calculated from the results of the numerical solution (paragraph 5.8, Chapter 5), whereas lines B and D have been calculated from the approximate analysis (paragraph 2.11, Chapter 2). It may be seen that lines A and B are in substantial

agreement. However, this agreement is perhaps fortuitous because the approximate calculation in line B includes both the circumferential flow as would be obtained in infinitely wide bearing together with a side leakage flow based upon very approximate assumption. In fact the oil flow should be the side leakage flow alone and on that basis the substantial agreement between the two curves would no longer exist. With reference to lines C and D, both methods predict the lobe pressure correctly in order of magnitude but the more exact numerical solution shows a fall in lobe pressure with increased lobe diameteral clearance, whereas the approximate method has the opposite trend. Line C, the numerical solution, shows the trend also shown by the test results (figure 4.7, Chapter 4), and the trend which one would expect.

In table 8.1 calculated and measured flows are compared. Both the measured and calculated oil flows were carried out for an unloaded journal which is centred in the bearing. It may be seen that there is a good agreement between the measured and numerically calculated oil flow whereas the oil flow calculated by the approximate method is approximately 70% of the measured oil flow.

Figure 8.2 shows the variation of the measured and calculated load factor with the bearing eccentricity ratio. The load factor has been calculated numerically in Chapter 5. At low values of eccentricity, there is a good agreement between test and theory but at higher values of eccentricity the theory predicts a somewhat higher load factor.

The variation of the load angle with the speed parameter is shown in figure 8.3. The solid line relates to the numerically

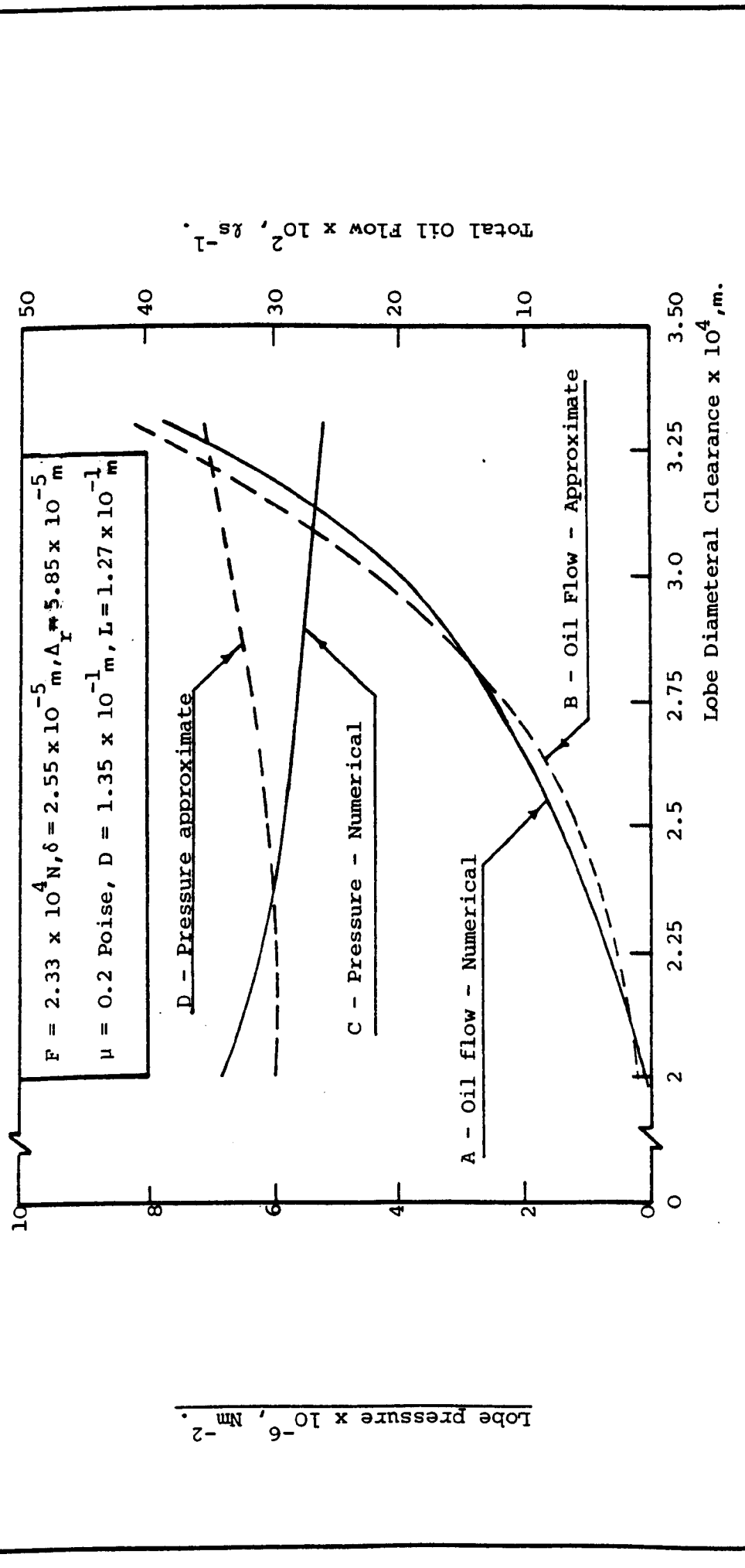

Figure 8.1. Oil Flow and Pressure-Lobe Clearance Characteristics.

Conditions of Measurement and calculation						Measured Q_t ℓs^{-1}	Calculated - Approx.		Calculated - Numerical
ε_o	$C \times 10^4$, M	P_s, NM^{-2}	P, NM^{-2}	P/Ps	μ, Poise		Q_c ℓs^{-1}	Q_t ℓs^{-1}	Q_t ℓs^{-1}
0.45	2.6	1.32×10^7	6.65×10^6	0.5	0.273	0.186	0.109	0.135	0.2
"	"	1.0×10^7	5.7×10^6	0.57	0.167	0.261	0.153	0.186	0.272
"	"	1.33×10^7	6.4×10^6	0.48	0.22	0.261	0.131	0.159	0.240
"	"	6.67×10^6	4.3×10^6	0.65	0.163	0.186	0.118	0.145	0.207
"	"	1.36×10^6	4.24×10^6	0.26	0.167	0.186	0.119	0.146	0.206

Table 8.1. Comparison between the Measured and Calculated Oil Flow for the Externally Pressurized Operation.

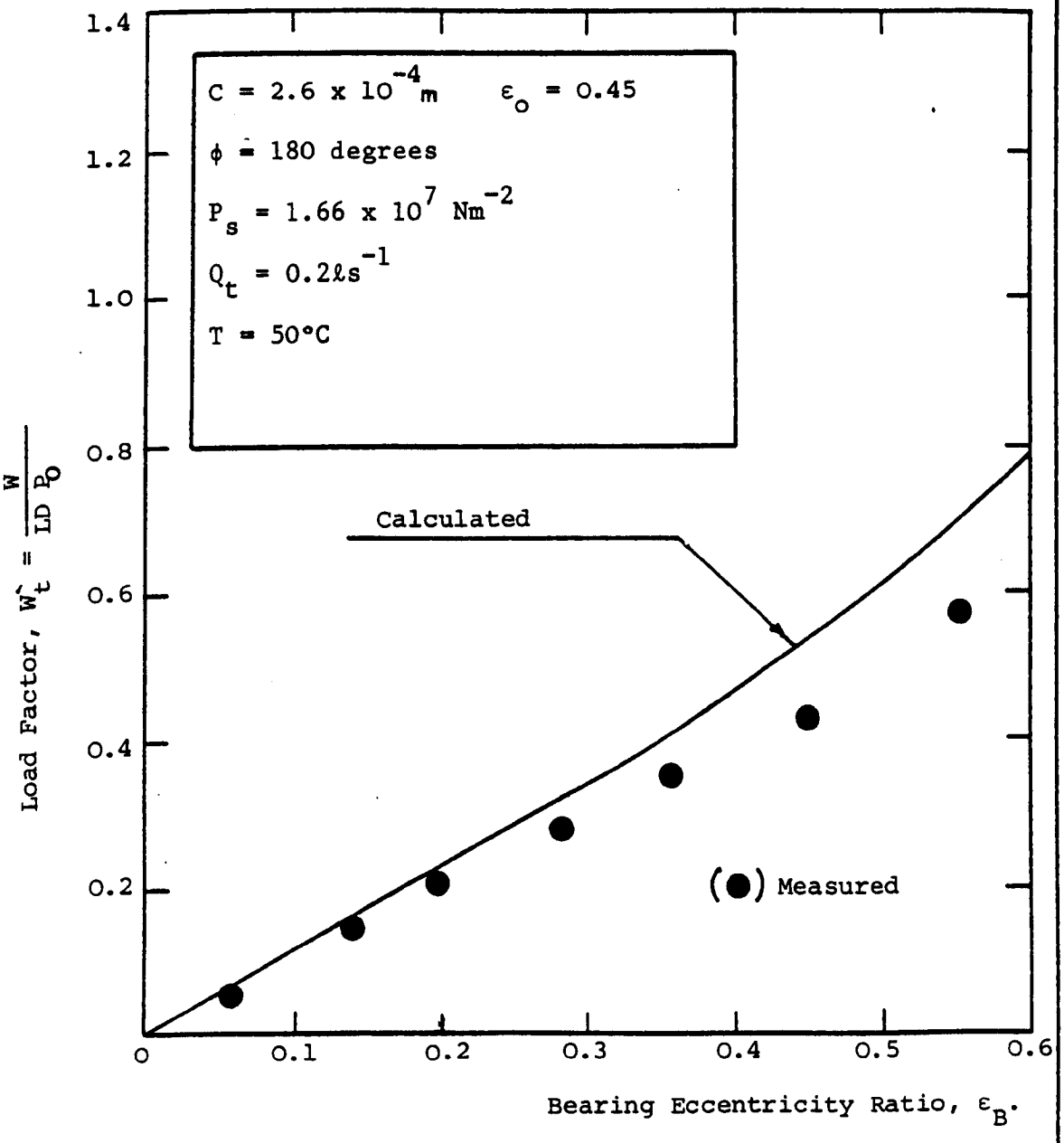

Figure 8.2. Load Factor - Bearing Eccentricity Ratio Characteristics.

calculated load angle (γ) whereas the circular points relate to the measured load angle at the bearing mid plane. In deducing the the speed parameter from the test results, oil viscosity was taken as the viscosity at the oil outlet. Despite the assumptions which have been used in the numerical solution, the variation of journal displacement along the axial width of the bearing in the test, and the assumption that the effective viscosity is the viscosity at oil outlet, it may be seen from figure 8.3, that there is a good agreement between test and theory.

8.3. Power Loss and Oil Temperature Rise in the Externally Pressurized Operation.

The computer programme which has been described in Chapter 3 (the design programme), has been used to calculate the power loss and the oil temperature rise in the externally pressurized regime, simply by inserting the total oil flow rate and by setting the offset ratio to the required value.

The power loss and the oil temperature rise in the externally pressurized regime have been calculated by setting the total oil flow at 0.2 ℓs^{-1}. This value has been chosen because it has been commonly used in the experimental work. In figure 8.4 the calculated power loss for the first bearing, together with the measured power loss as reported in Chapter 6 are shown as functions of journal speed. The circular points relate to the power loss as deduced from measurements of oil flow and of oil temperature rise, whereas the triangular points relate to the total power loss which has been found to be 1.2 x the deduced power loss (Chapter 6, paragraph 6.2.18). It may be seen that measured and calculated power losses are substantially the same.

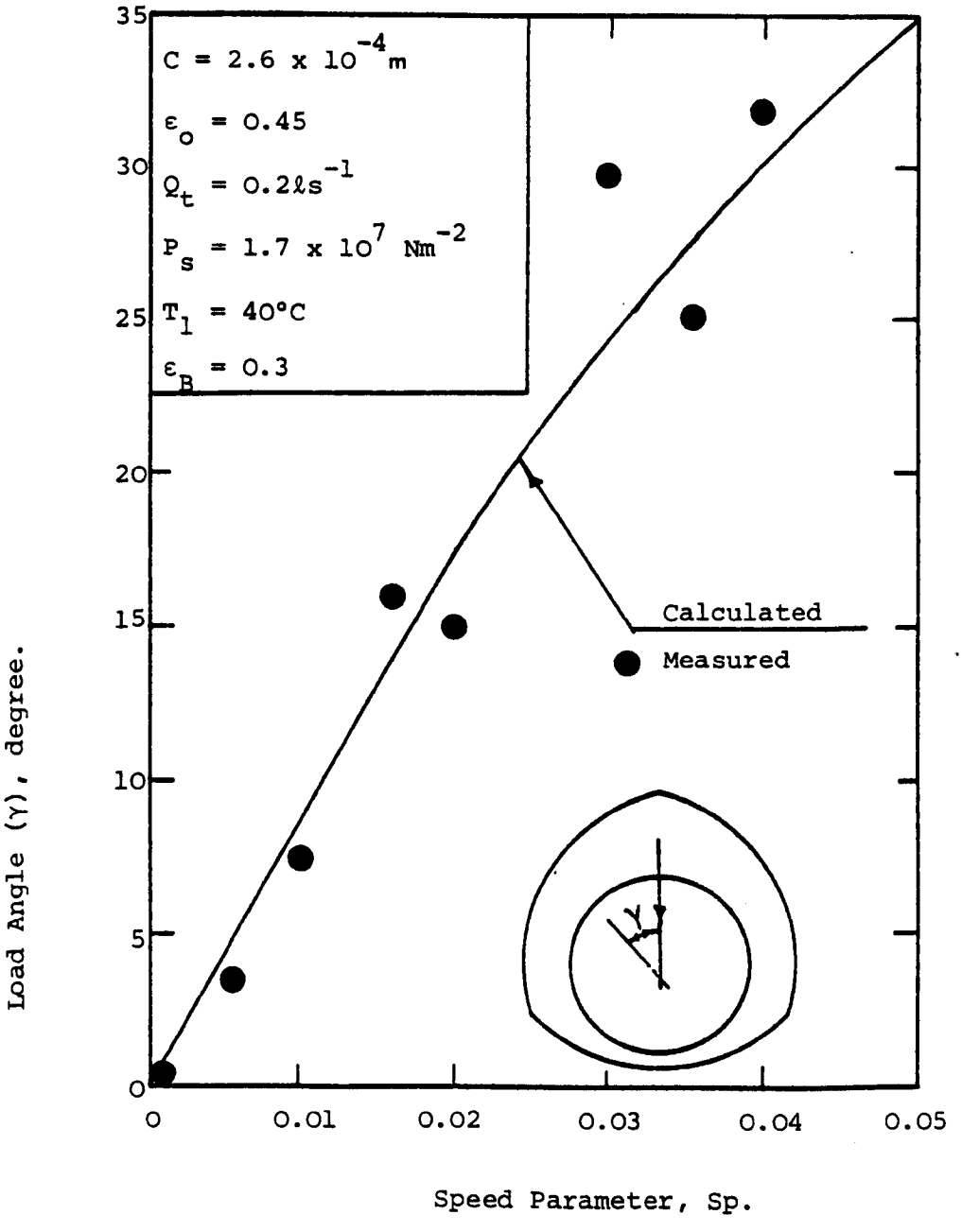

Figure 8.3. Load Angle - Speed Parameter Characteristics.

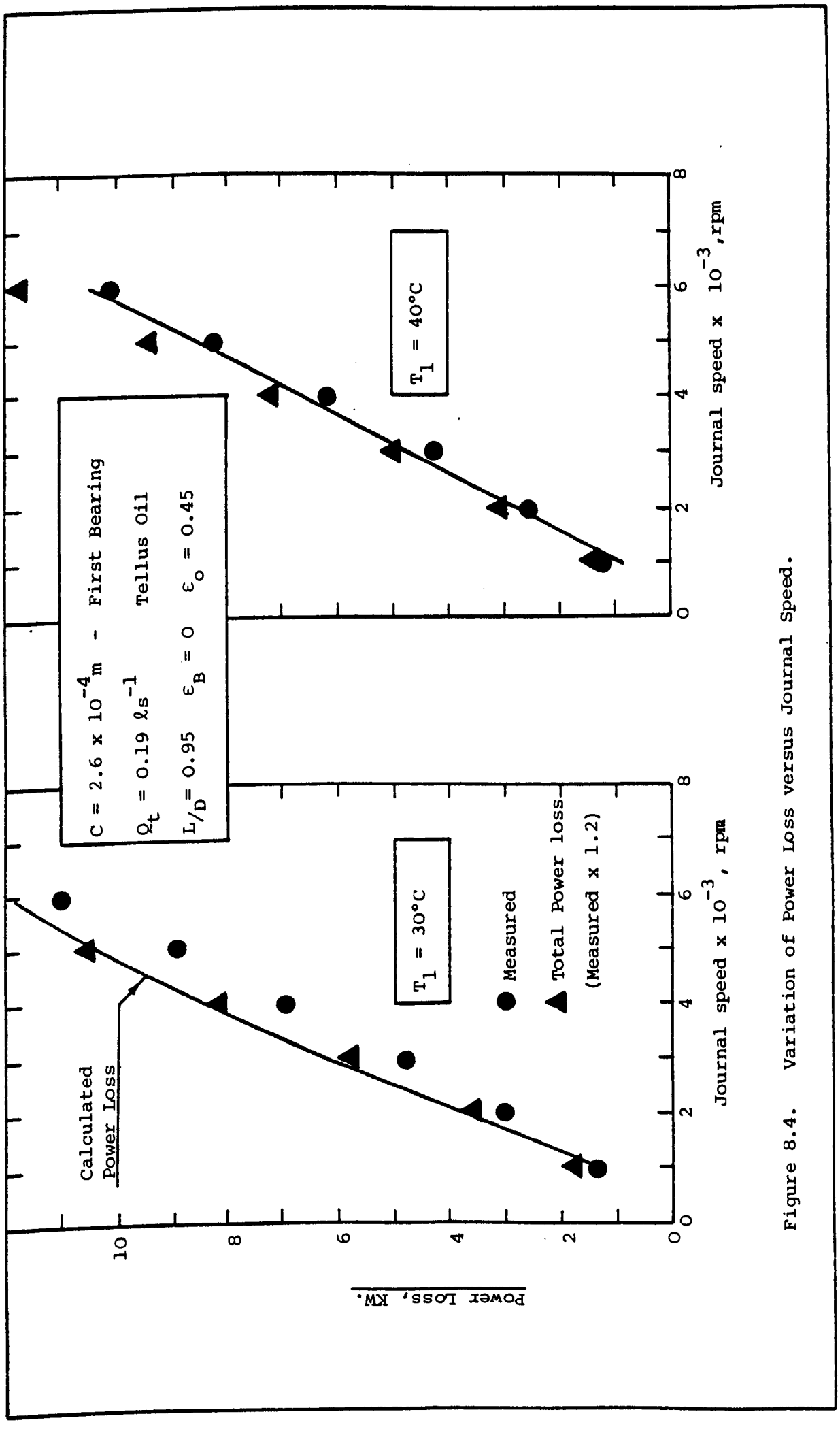

Figure 8.4. Variation of Power Loss versus Journal Speed.

Figure 8.5 shows the variation of both the calculated and measured oil temperature rise with the journal speed. The results are plotted for oil inlet temperatures of 30, 40 and 50°C. It may be seen that the maximum difference between measured and calculated oil temperature rise is approximately $\pm$ 3°C, and a close agreement exists over the full speed range and for all the oil inlet temperatures.

Calculated and measured power loss and oil temperature rise for the second bearing are shown in figure 8.6. as functions of journal speed. The calculated and measured power losses are much the same up to a speed of 5000 rpm, whereas at speeds over 5000 rpm the calculation gives somewhat less power loss, but the maximum difference does not exceed 15%.

In order to consider this difference between calculated and measured power loss further, the Taylor's criterion for the onset of Taylor's vortices has been calculated for the bearing. The critical Reynolds' number is given by $Re = 41.1\ (D/C)^{\frac{1}{2}}$, where $41.1\ (D/C)^{\frac{1}{2}}$ is the onset of Taylor's vortices and pertains to a journal running centrally in a circular bore bearing. In the instance of the three-lobe bearing, the clearance to be taken in the calculation of Reynolds' number and the viscosity of the fluid which is to be taken have to be decided. The decisions made are that the clearance is the lobe clearance, and that the oil viscosity is the viscosity of the oil at outlet. The Reynold's numbers calculated in that way are shown as a function of journal speed in figure 8.7. On the same figure the Reynolds' numbers corresponding with Taylor's criterion are marked as transition Reynolds' numbers, and it may be seen that a transition is not to be

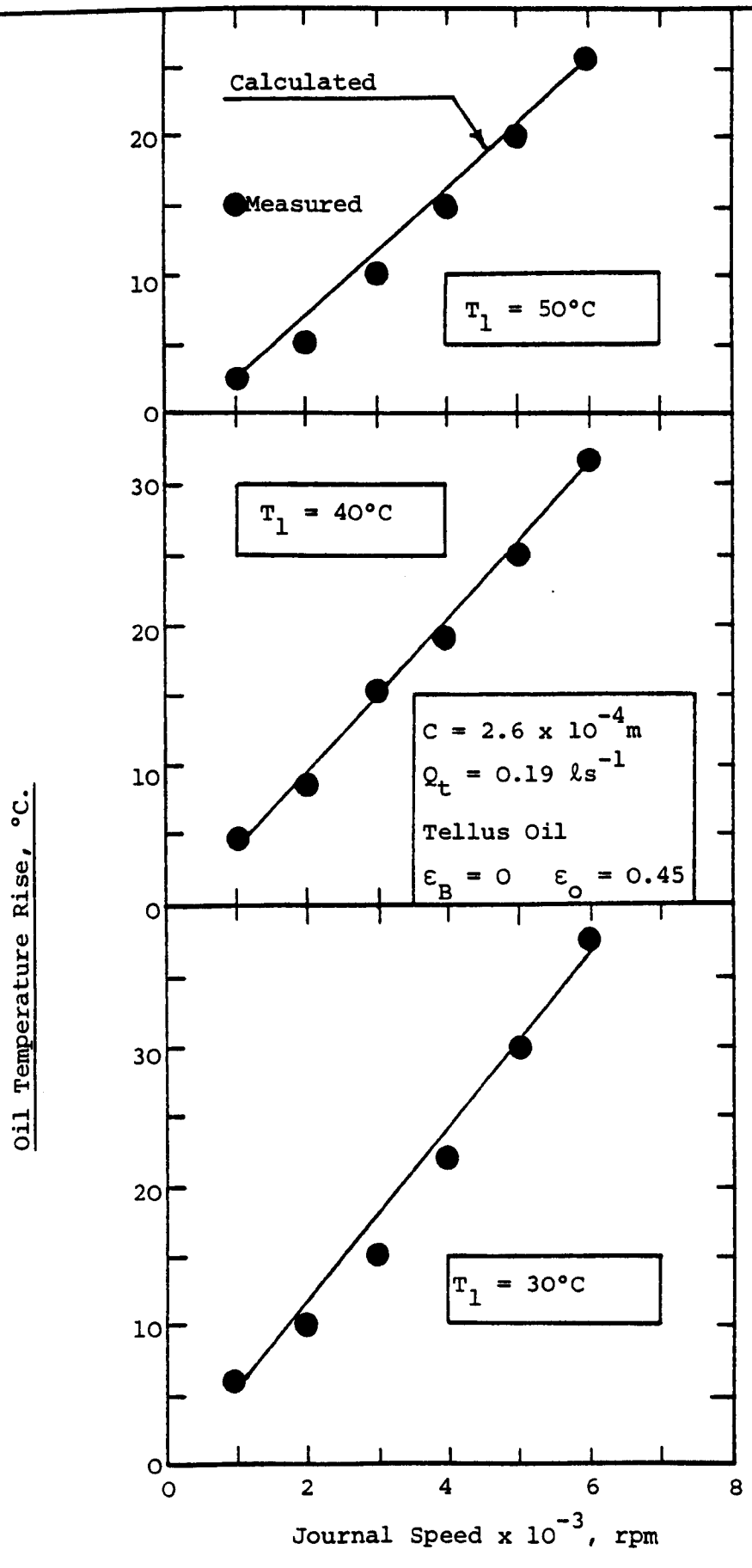

Figure 8.5. Variation of Oil Temperature Rise with Journal Speed.

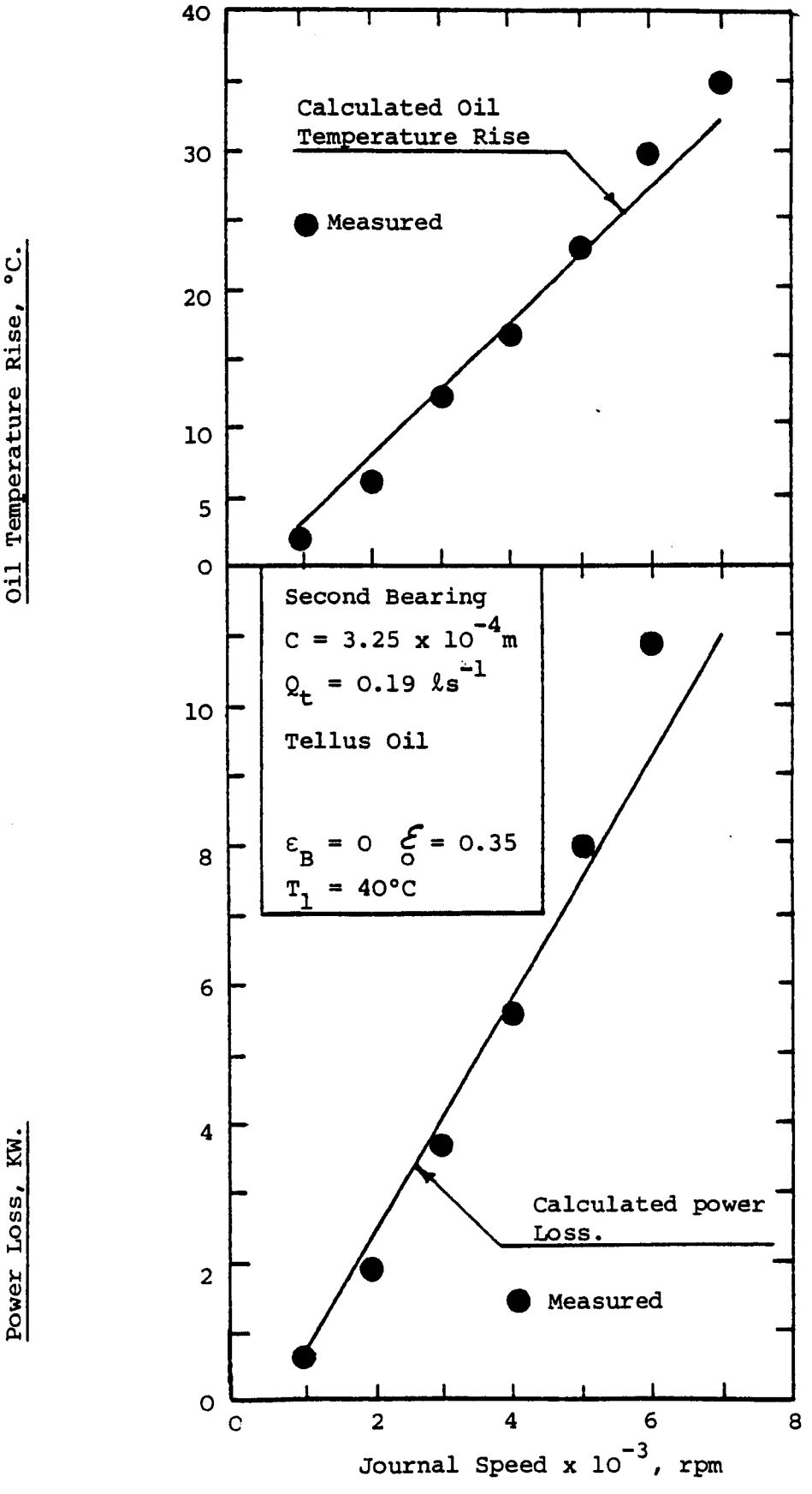

Figure 8.6. Variation of Power Loss and Oil Temperature Rise with journal speed.

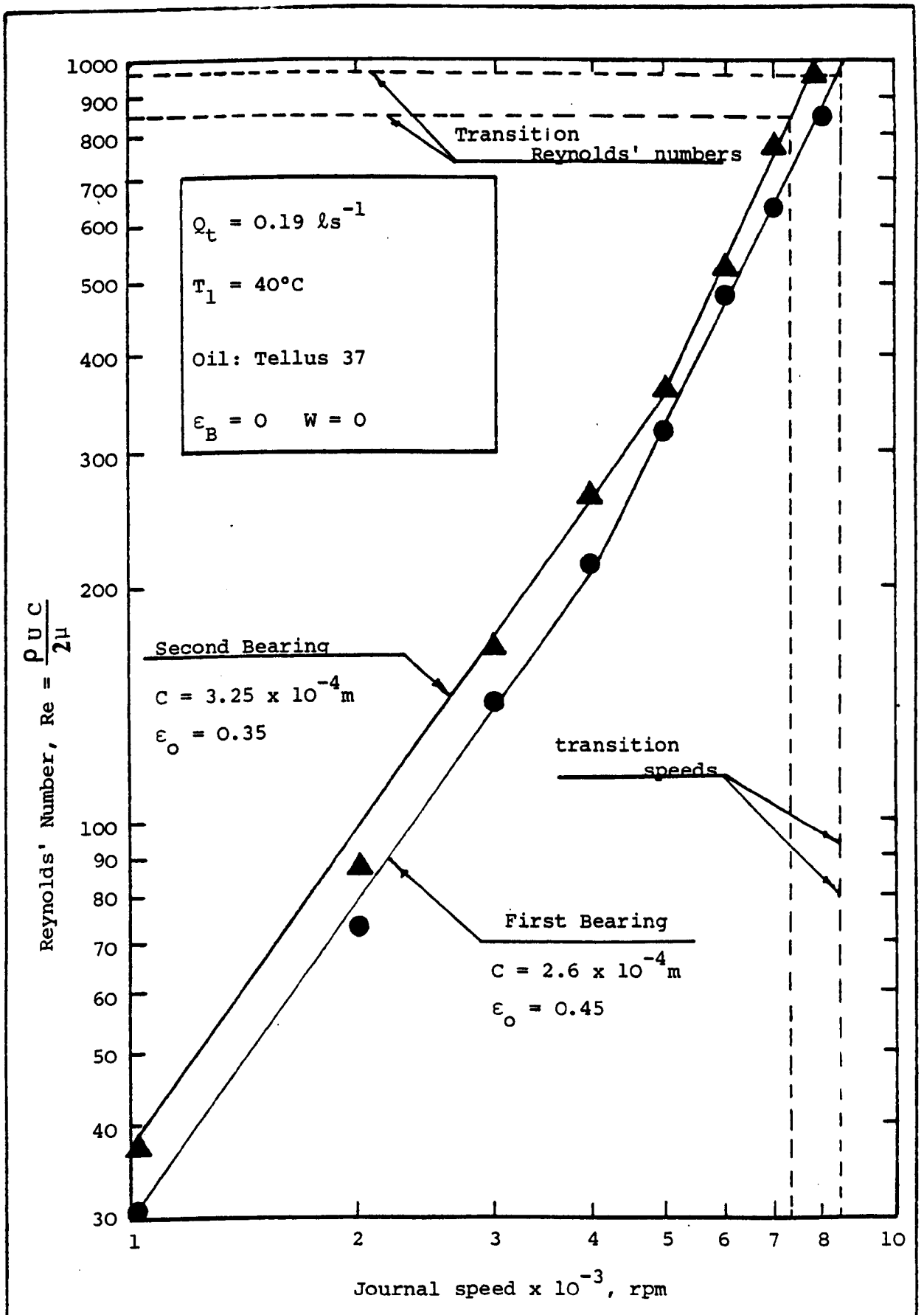

Figure 8.7. Reynolds' Number - Journal Speed Characteristics.

expected at speeds below 7000 rpm. This is a speed higher than the speed at which the calculated power loss falls below the measured power loss, and it is concluded that the difference is not due to a transition from laminar to turbulent flow.

8.4. Self-generating Operation

Figure 8.8 shows a comparison between the measured duty parameter and the calculated duty parameter from the numerical solution. The results of the measured displacements, load, speed and oil outlet temperature are used to calculate the duty parameter (Chapter 6) and the duty parameter was plotted as a function of the bearing eccentricity ratio at both the fore and mid plane of the bearing. This was done because the bending of the shaft brings ambiguities into the eccentricity ratio pertaining to the test results. This has been dealt with by plotting the test results for the eccentricity ratios on both of the fore and mid plane. It may be seen from figure 8.8 that the calculated duty parameter is between the measured duty parameters. At low values of eccentricity the measured duty parameter at the bearing mid plane is close to the calculated duty parameter, whereas at higher values of eccentricities the duty parameter measured at the bearing fore plane becomes closer to the calculated line, but generally there is a reasonable agreement between test and theory.

In figure 8.9, measured and calculated attitude angle are shown as functions of the duty parameter. The calculated curve pertain to an offset ratio of 0.45, the offset ratio of the test

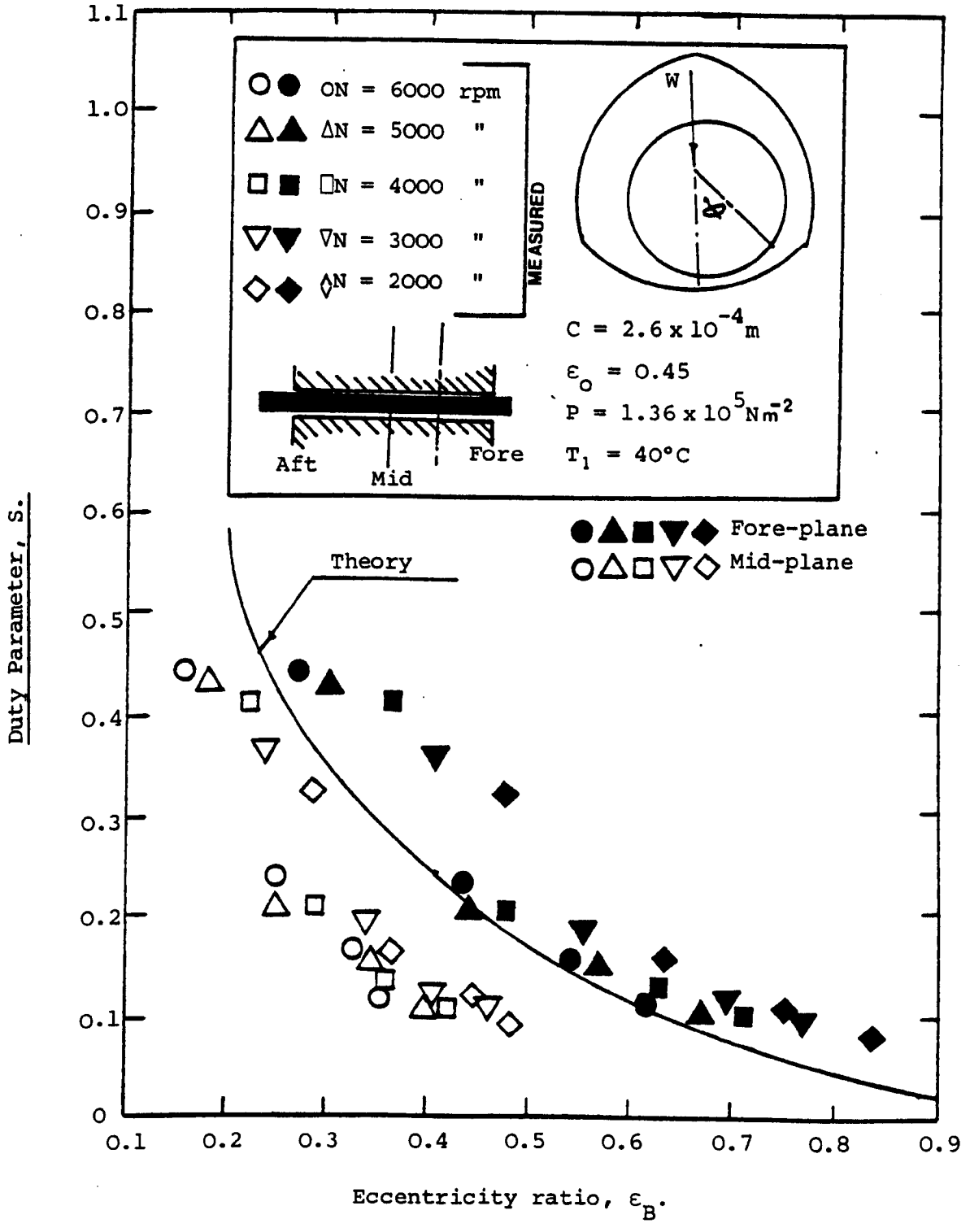

Figure 8.8. Duty Parameter versus Eccentricity Ratio.

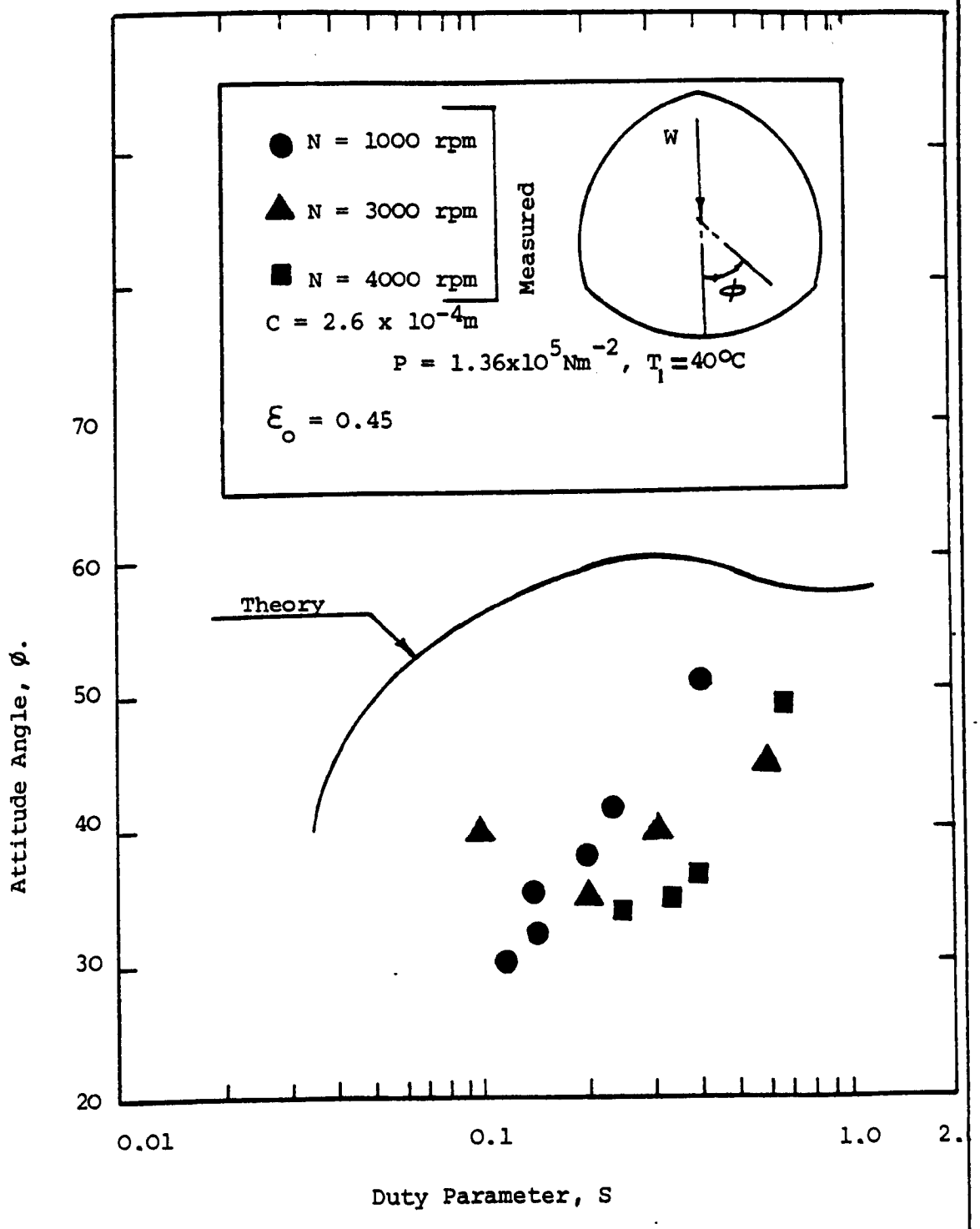

FIG. 8.9 Attitude Angle (Ø) Versus Duty Parameter (S).

bearing, and the calculation was drawn from the results of numerical calculation (Table 3.5). The figures show a substantial difference between calculated and observed attitude angle which is due to the bend of the shaft, which increases the vertical displacement and consequently decreases the attitude angle.

Figure 8.10 shows the variation of the hydrodynamic oil flow coefficient with the duty parameter. The solid line relates to the numerically calculated flow coefficient whereas the points relate to the oil flow coefficient as found from the experiments. It may be seen that a close agreement is obtained between test and theory.

Figure 8.11 shows the variation of both the measured and the calculated stiffness with the journal speed. The measured stiffness at the bearing mid plane is reproduced from figure 6.42, whereas the calculated stiffness is obtained from the design programme simply by running the programme for a journal displacement of 1.27×10^{-5}m and for an offset ratio of 0.45. The measured stiffness is somewhat greater than the stiffness as predicted by the design programme but the maximum difference between measured and calculated stiffness is approximately 20%.

In figures 8.12 and 8.13 the measured and the calculated power loss, oil temperature rise and oil flow are plotted versus the journal speed. The method which has been used in the calculation has previously been described in paragraph 3.8. It may be seen from figures 8.12 and 8.13 that there is close agreement between the measured and calculated power loss, oil flow and oil temperature rise. The agreement implies that laminar conditions persisted throughout, and indeed calculations of the Reynolds' number according to the

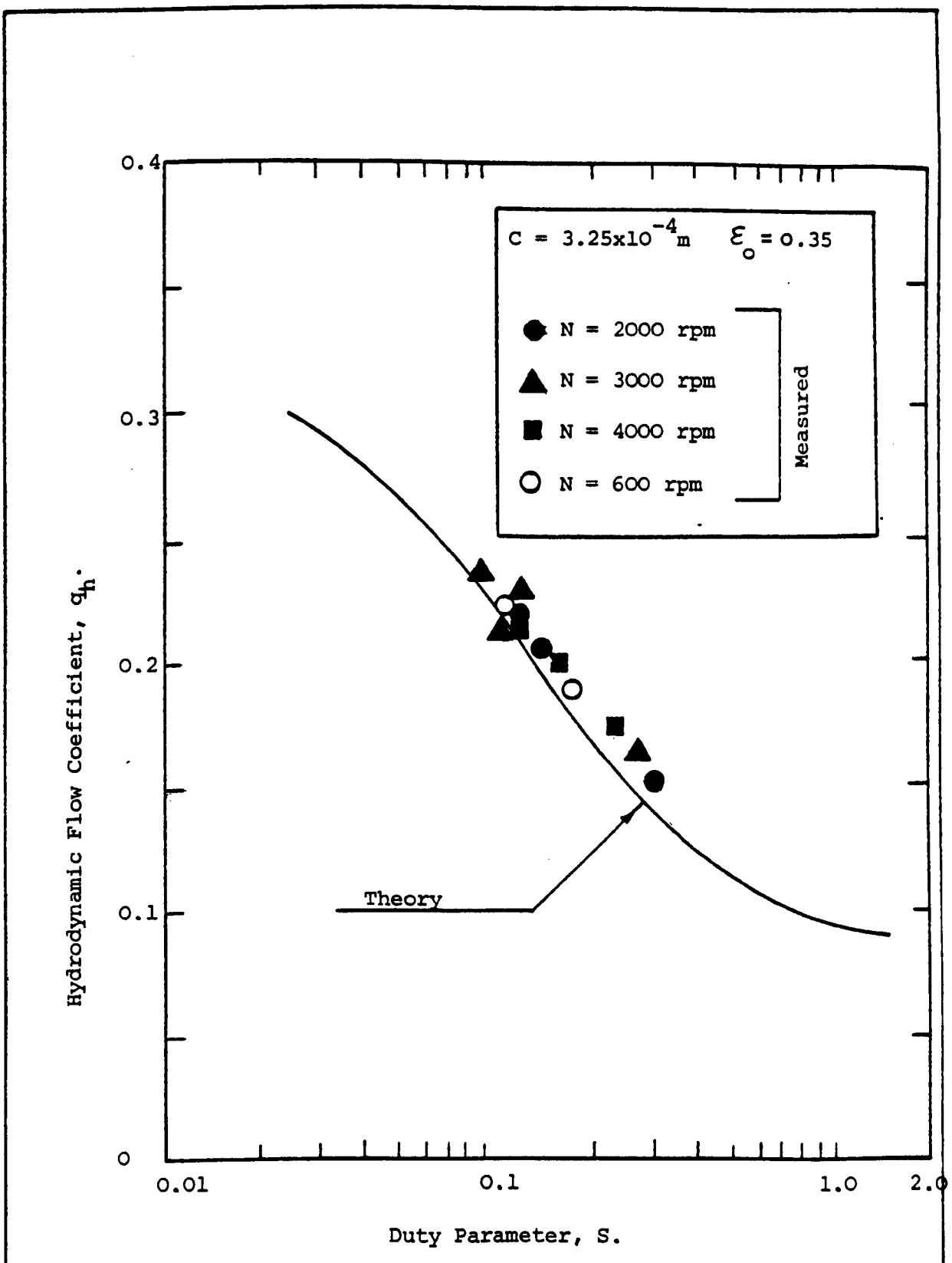

FIG.8.10 Hydrodynamic Flow Coefficient Versus Duty Parameter

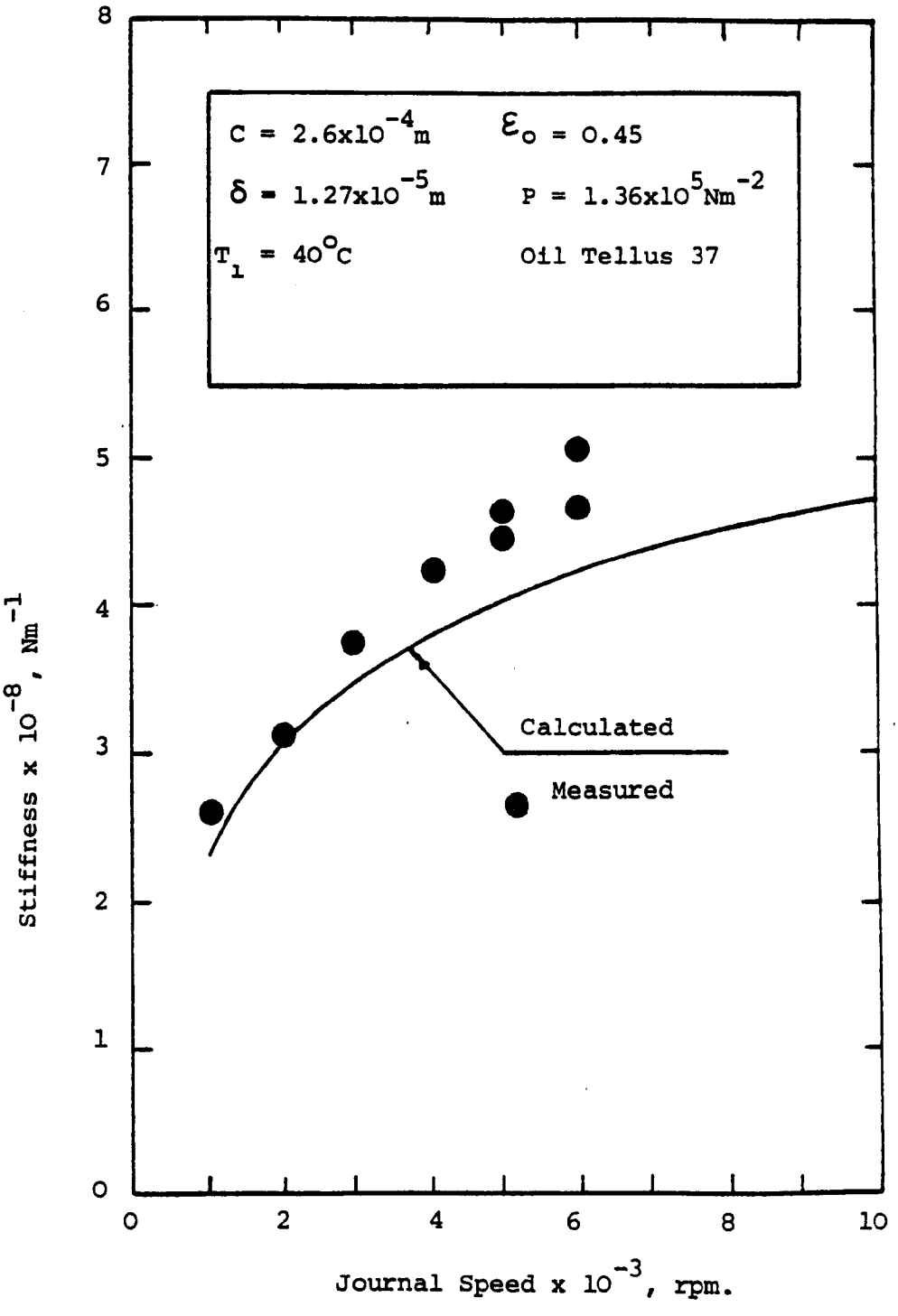

FIG.8.11 Stiffness Versus Journal Speed

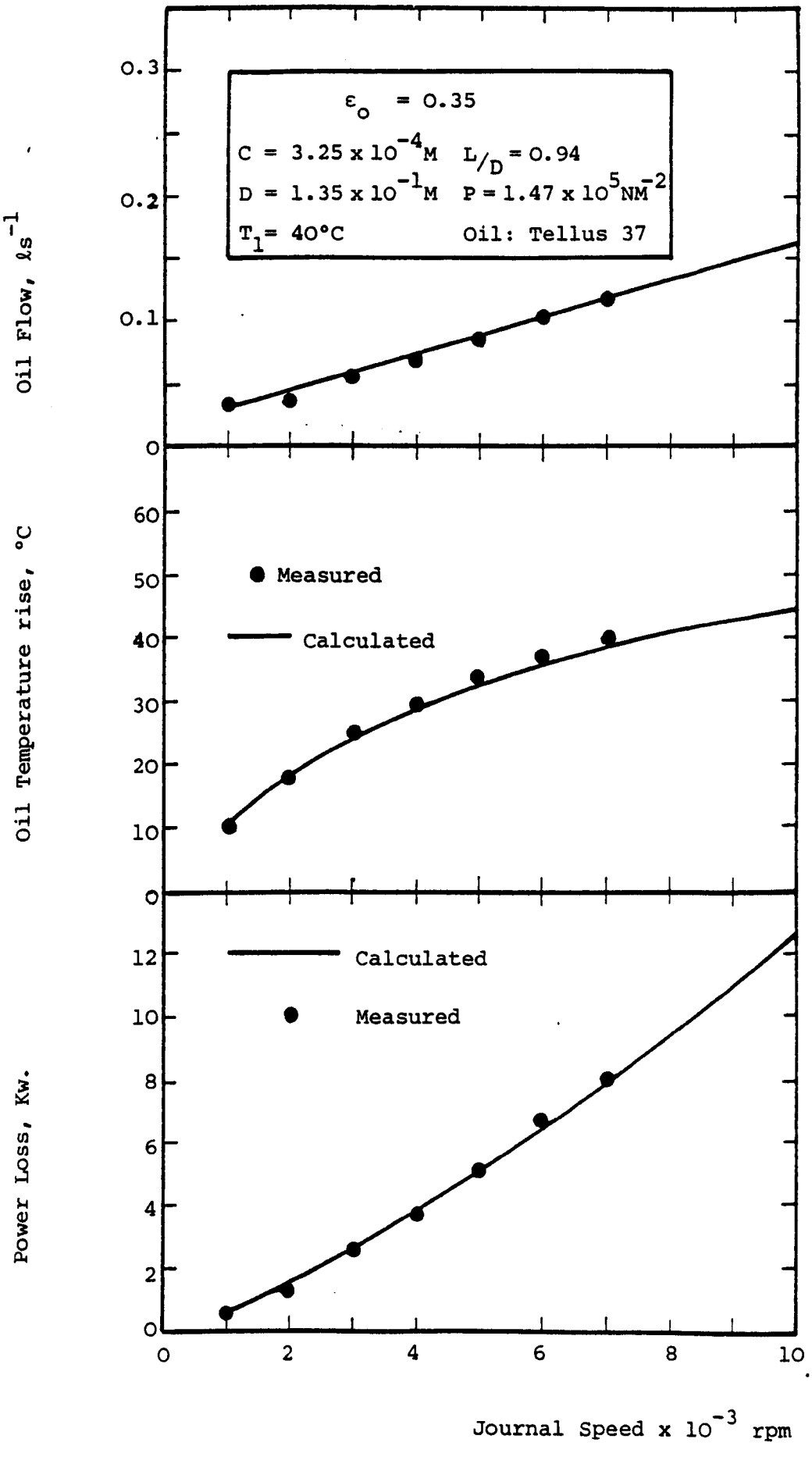

Figure 8.12. Power Loss, Oil Temperature Rise and Oil Flow Versus Journal Speed.

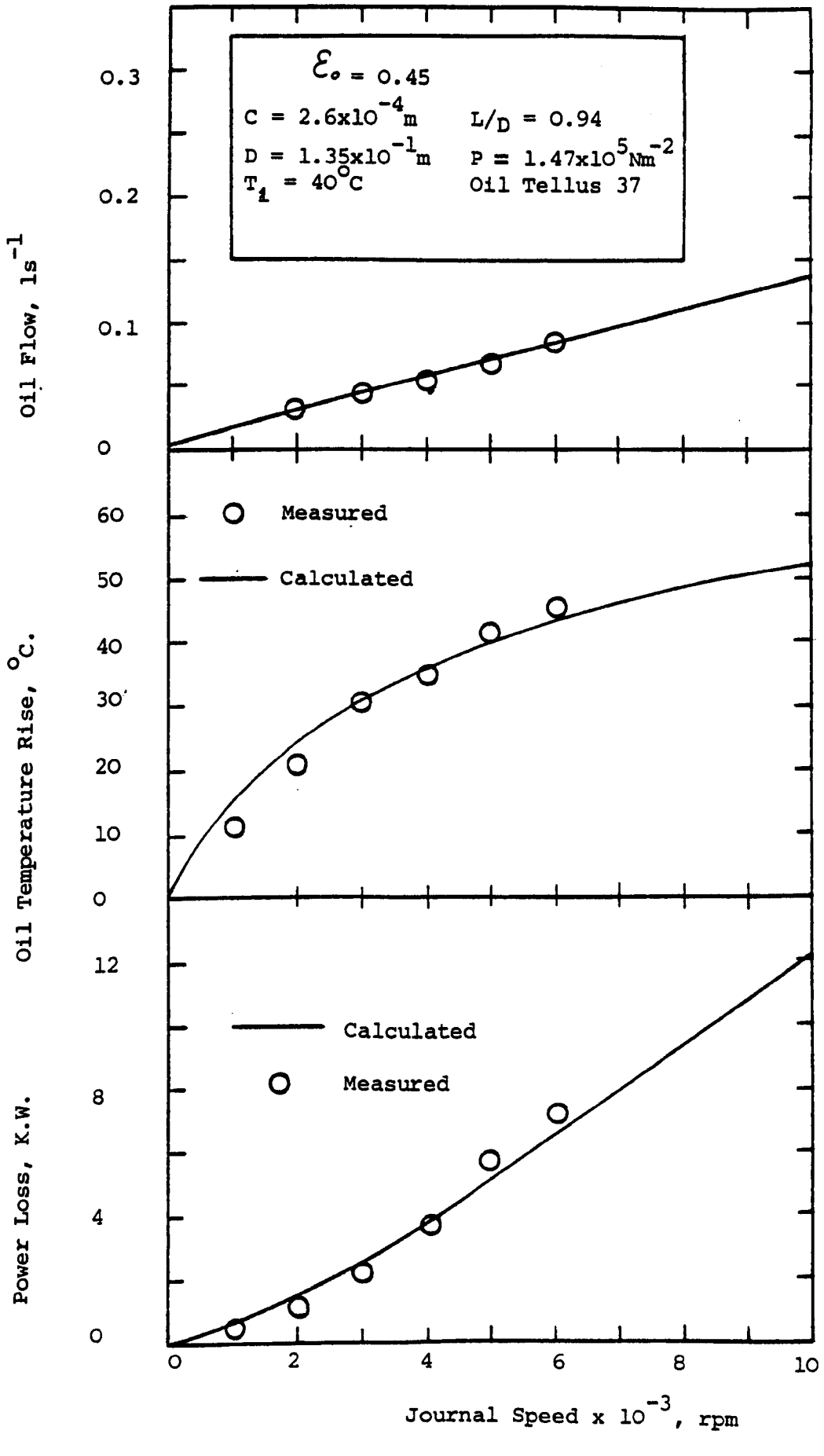

FIG.8.13 Power Loss, Oil Temperature Rise and Oil Flow Versus Journal Speed.

onset of Taylor's vortices (figure 8.14) indicatesthat the transition occurs at speeds exceeding the maximum test speed. However, there is an indication that transition may occur before the maximum speed of the specification (9000 rpm) is reached.

In table 8.2 the measured and calculated performance parameters are listed with the type of agreement which has been achieved between test and theory. It may be seen that a close agreement has been achieved between test and theory for the parameters which have not been affected by the bend of the shaft whereas a reasonable agreement has been obtained when the test results have been affected by the bend of the shaft. A big difference between test and theory was only found with respect to the measured attitude angle.

8.5. Modification of the Test Spindle Assembly.

The design of the spindle used in the test was greatly influenced by the choice of rolling bearing elements for tail and for thrust. This choice has the advantages of cheapness and of minimum power loss, but the rolling elements capable of running up to 9000 rpm, at the required duty,demanded that the diameter of spindle should be substantially reduced outside of the main bearing itself. As has been shown in Chapter 6, the spindle itself bent considerably at the greatest test load and this bending has the effect of reducing spindle stiffness well below the inherent stiffness of the bearing itself, and also it has the effect of greatly complicating the interpretation of bearing behaviour with respect to such quantities as eccentricity ratio and attitude angle.

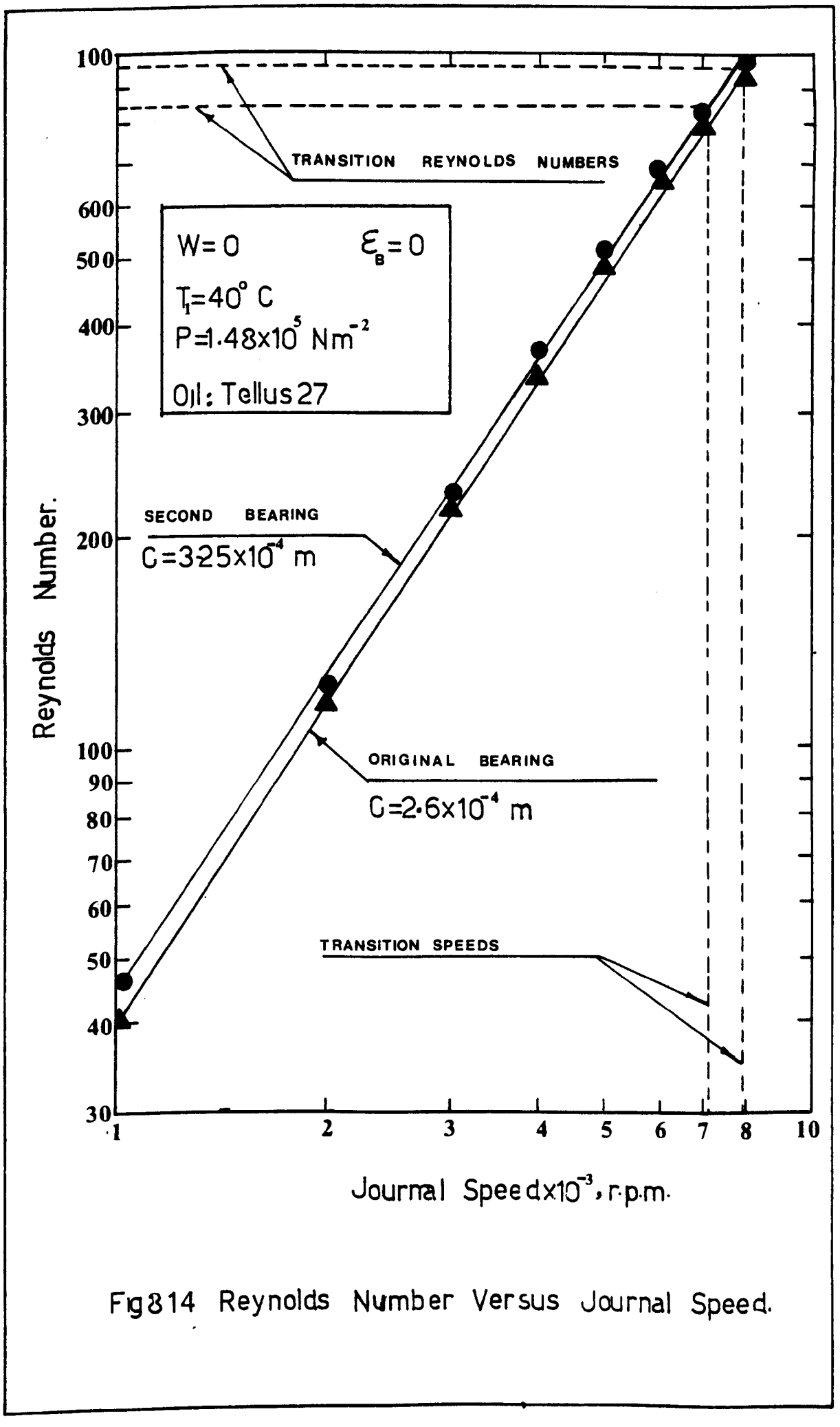

Fig 8·14 Reynolds Number Versus Journal Speed.

TABLE 8.2 Agreement Between Test and Theory

Parameter	Self-generating	Externally pressurized
Power loss	✓✓*	✓✓
Oil Temperature Rise	✓✓	✓✓
Oil Flow	✓✓	✓✓
Hydrodynamic Oil Flow Coefficient	✓✓	–
Total Oil Flow Coefficient (Chapter 6)	✓✓	–
Pressure Oil Flow Coefficient (Chapter 6)	✓✓	–
Stiffness	✓	✓
Load Factor	–	✓
Duty Parameter	✓	–
Attitude Angle	X	–
Load Angle	–	✓
Journal Deflection (Chapter 6)	–	✓✓

* ✓✓ Close agreement

✓ Reasonable agreement

X Big difference

The existence of a computer programme for the calculation of the elastic bending of the shaft, and which has already been referred to in Chapter 6, makes it easy to consider the effects of various redesigns of shaft. The redesigns which have been considered are shown from B to D in figure 8.15 and the deflection of the redesigns, together with the actual test shaft which has been used (A) are given in figure 8.16. It can be seen that the significant matter is to maintain the diameter of the spindle at its full value right down to the tail bearing. In the machine tool context the problem then arises of differential thermal expansion of the shaft relative to the frame of the machine from the thrust face to the cutting tool. In design D a sliding thrust bearing close to the main bearing is suggested.

8.6. Three Lobe Bearings Versus Circular Bore Bearings

The question always arises, is a multi lobe bearing necessary or would a bearing of plain circular bore suffice? To find an answer to this question a comprehensive study of the behaviour of journal bearings which have an offset ratio between zero (circular bore bearings and circular bore bearings with three axial grooves) and 0.8 (three lobe bearings) has been presented in paragraph 3.9 where it has been shown that for bearings of the same minimum clearance the three lobe bearings have the following advantages over the full circular bore bearings. The advantages are:-

I. Higher stiffness. This may be seen from figure 3.26a in which the stiffness increases as the offset ratio is increased (an offset ratio for zero is a bearing of circular bore).

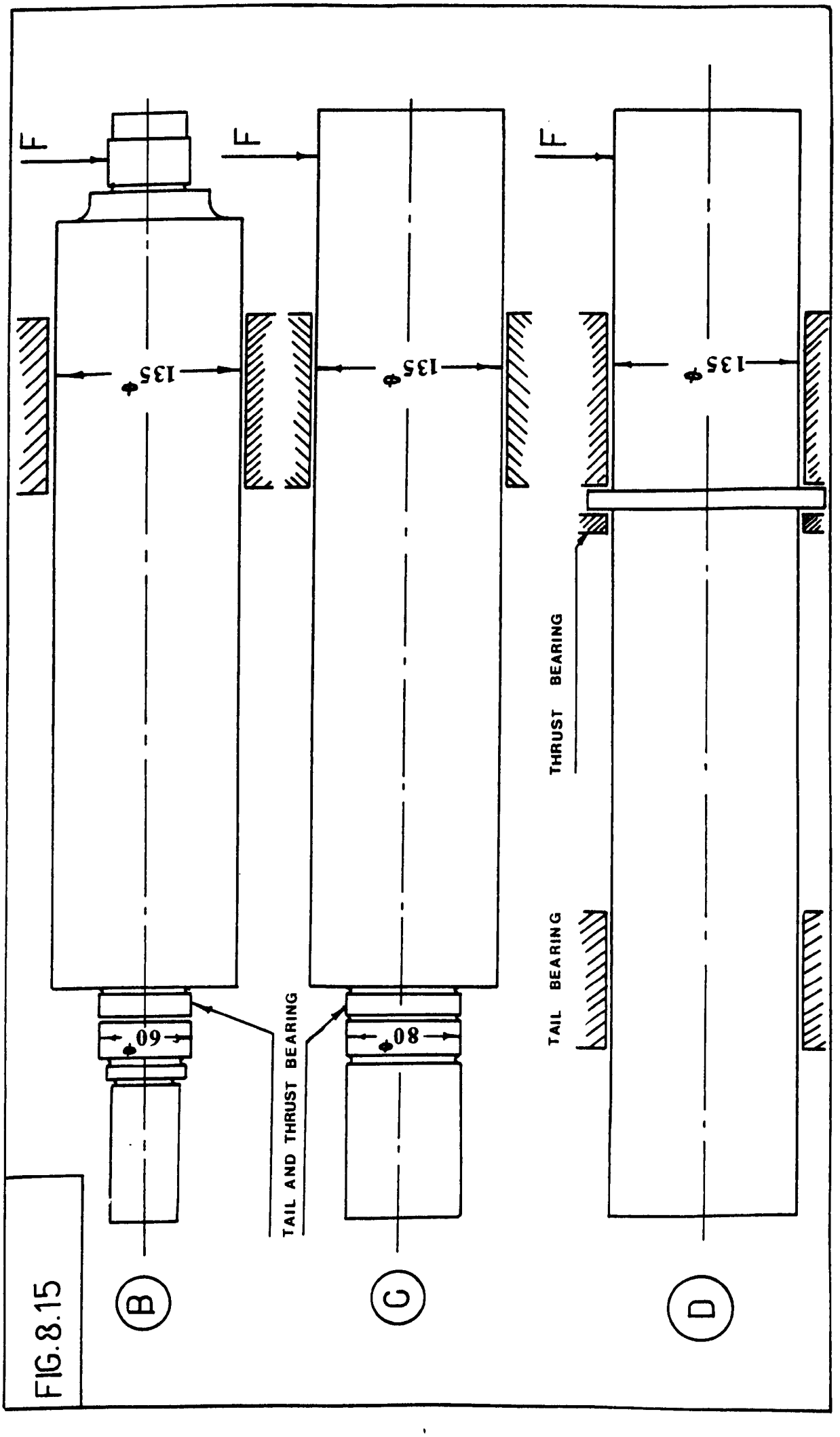
F
F
F
135
135
135
60
80
TAIL AND THRUST BEARING
THRUST BEARING
TAIL BEARING
B
C
D

FIG.8.15

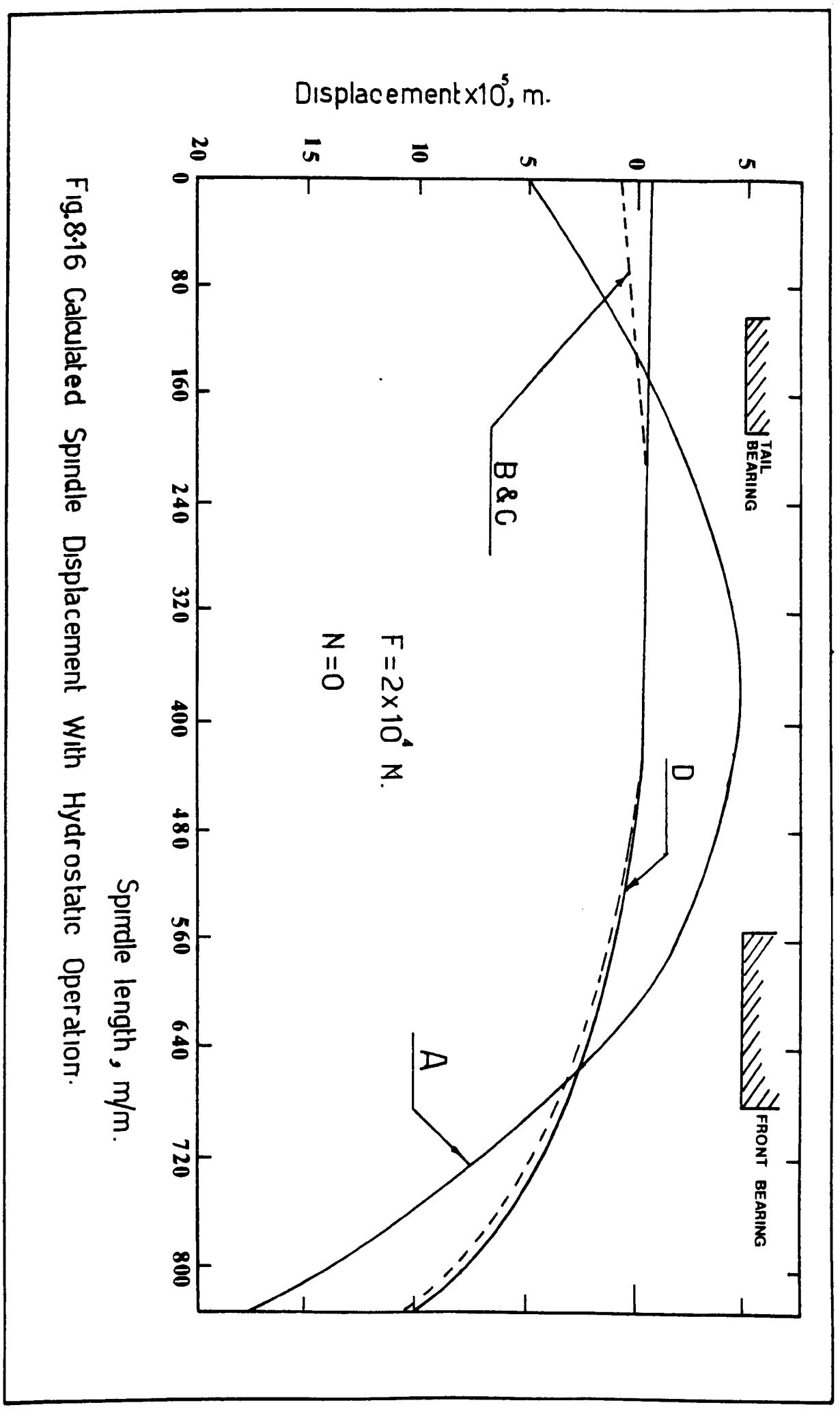

Fig.8.16 Calculated Spindle Displacement With Hydrostatic Operation.

II. Great load capacity. It may be seen from Figure 3.25a that the load given at constant minimum film thickness increases with offset ratio.

III. Lower oil temperature rise. It may be seen from Figure 3.23 that the oil temperature decreases as the offset ratio increases.

The above advantages exist together with a power loss in the three lobe bearing which is substantially the same as the power loss of a bearing of circular bore (3.22). The power loss of the three lobe bearings becomes significantly greater than the power loss of circular bore bearings at offset ratios exceeding 0.6.

8.7. Three lobe bearings for Very High Speed

It became of interest in another context to employ the analysis for a three lobe bearing to predict the behaviour of bearings for a journal of 5.08 cm (2") run up to speeds between 2×10^4 rpm to 3×10^4 rpm. The results of calculation are presented in figure 8.17 which also includes a result for a bearing of circular bore ($\varepsilon_o = 0$). Quite clearly figure 8.17 shows that to achieve a higher bearing load with the minimum possible oil temperature rise, a three lobe bearing with high offset ratio has to be used.

8.8. CONCLUSION

The initial objective of the work described in this thesis was to establish the feasibility of a wide speed range bearing which satisfies the specification given in table 1.1. With the exception

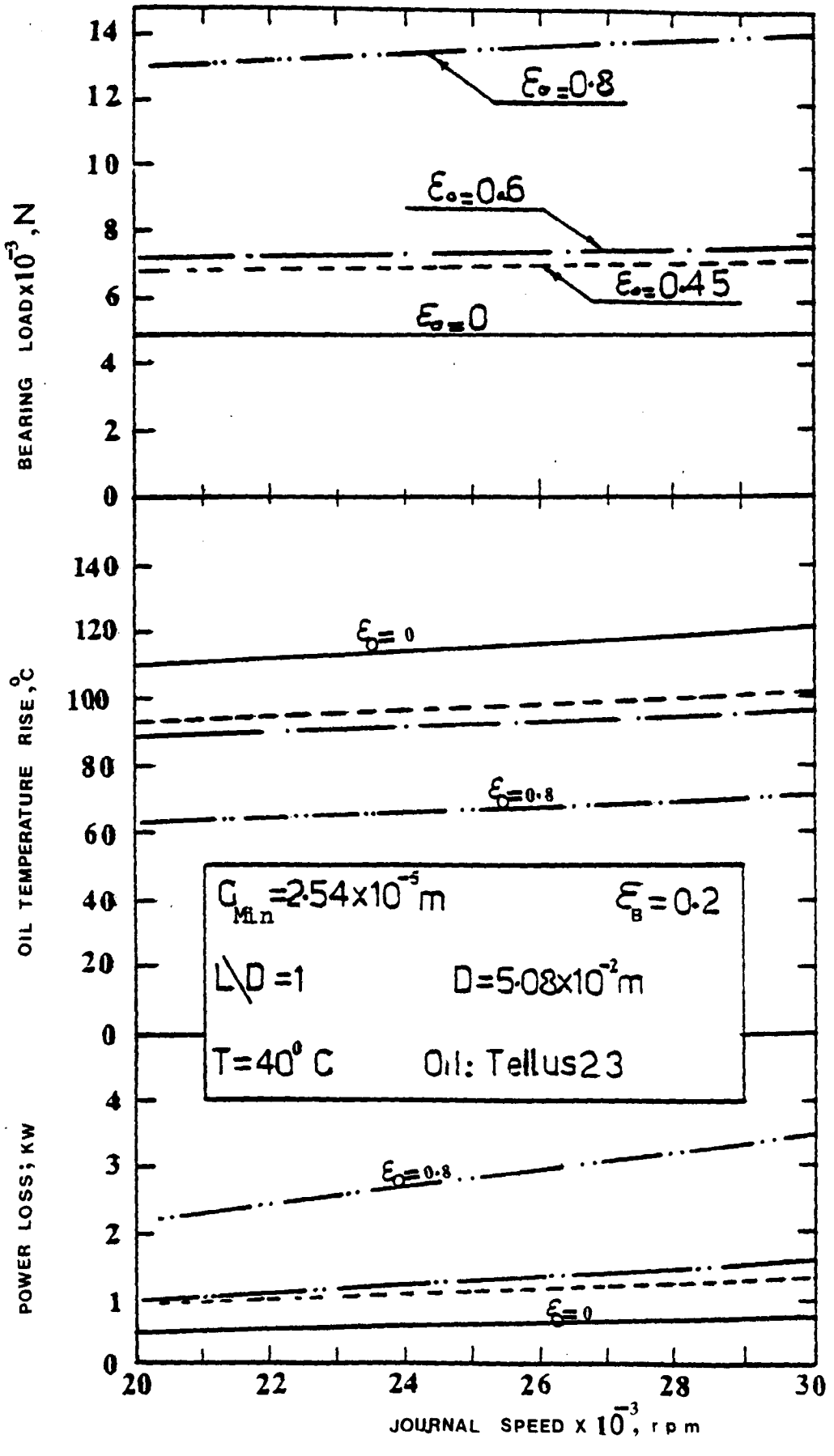

Fig.8-17 Power Loss, Oil Temp. Rise & Bearing Load Versus Journal Speed.

of the speed range of the test rig which has been restricted to 7000 rpm, instead of the 9000 rpm in the specification, feasibility has been established. Tests have been carried out with two bearings of different detailed design and with two oils of different viscosity. In general the preferred arrangement is the first bearing with its high offset ratio combined with the oil of lower viscosity, and with both high and low pressure oil inlets at the conjunction of the lobes as has been tested with the second bearing.

The test work has been paralleled by analytical and computational work which has been checked against the test results and also against published material, particularly upon bearings of circular bore. The computer programmes which have been developed have allowed predictions to be made for a wider range of variables than it has been possible to test. A suggestion from this computer work is that the optimum three lobe bearing with respect of combining stiffness with minimum oil temperature rise and with minimum power loss would be with an offset ratio of 0.6 and with the least possible minimum clearance.

There are, of course, aspects both of the bearing as a bearing and as a bearing in a machine tool spindle context which have not been tested. The loading of the bearing has been limited to a steady load and the field of the dynamic performance of the bearing has not been investigated. The test speed was limited to 7000 rpm due to the use of a belt drive, and it is suggested, particularly if higher speeds are to be attempted, that the final drive of the shaft should be in line. The fitting of a roller element thrust close to the main bearings has produced difficult shaft deflection. A fitting of a thrust in that position is necessary, and clearly much greater

consideration than has been possible should be given to the provision of a sliding element thrust which can be combined with maintenance of full spindle diameter back to the tail bearing. It is possible that the thrust could be combined with the main bearing by making the main bearing of double conical form. The test bearings have been made by elaborate machining and the elastic distortion method, which has only been briefly described, might be pursued. Clearly there is nothing sacrosanct about the precise way in which the profile of the bearings differ from the circle in the sense that the fourier components provided by the machining method might be replaced, equally effectively, by a different set provided by various means of elastic deformation. By adapting the computer programmes which have been developed, the characteristics of bearing profiles produced by more convenient routes could be predicted.

REFERENCES

REFERENCES

1. CAMERON, A. 'Principles of Lubrication', Longman, 1971.

2. PINKUS, O. and STERNLICHT, B. 'Theory of Hydrodynamic Lubrication', McGraw-Hill Book Comp. Inc., (1961).

3. FULLER, D.D. 'Theory & Practice of Lubrication for Engineers', John Wiley & Sons, Inc., 1963.

4. BURWELL, J.T. 'The Effect of diameteral clearance on the load capacity of a journal bearing'. Trans. of the A.S.M.E., July, 1942, (457-461).

5. BOYD, J., and ROBERTSON, B.P. 'Oil flow and temperature relations in lightly loaded journal bearings', Trans. of the A.S.M.E., April 1948, (257-262).

6. WILCOCK, D.F. 'Turbulence in high-speed journal bearings', Trans. of the A.S.M.E., August 1950, (825-834).

7. COLE, J.A. 'An experimental investigation of temperature effects in journal bearings', Proc. of the Inst. Mech.Engrs., Lubrication & Wear, 2nd Convention (1957), p.111.

8. DOWSON, D., and MARCH, C.N. 'A Thermodynamic analysis of journal bearings', Proc. Inst. Mech. Engrs., 1966-1967, Vol. 181, (Pt. 30), (117-126).

9. BRIGHTON, D.K., HOOKE, C.J., and O'DONOGHUE, J.P. 'A theoretical and experimental investigation of the effect of elastic distortions on the performance of journal bearings', Proc. Inst.Mech.Engrs., 1967-68, Vol. 182, pt. 3N, (192-200).

10. SMITH, D.M. 'Journal bearings in turbo-machinery', Champion and Hall Ltd., 1969.

11. CAMERON, A. 'Basic Lubrication Theory', Longman, 1971.

12. FULLER D.D. 'Hydrostatic lubrication, Part II - oil lefts', Machine Design, July 1947, pp 49-52.

13. SHAW, M.C. and MACKS, E.F. 'Analysis and lubrication of bearings', 1949, 287, (McGraw-Hill, New York and London).

14. RAIMONDI, A.A. and BOYD, J. 'An analysis of orifice and capillary compensated hydrostatic journal bearings', A.S.M.E. - A.S.L.E. Ft. Conf. Lubric. Baltimore, 1954 (October).

15. MORI, H and YABE, H. 'A theoretical investigation on hydrostatic bearing', Bull, J.SME. 6 (22), 1963, (354-363).

16. RIPPEL, H.C. 'Design of hydrostatic bearings', Machine Design, 35 (Dec.5, 1963), 158-162.

17. STANSFIELD, F.M. 'The design of hydrostatic journal bearings', Proc. 8th Int. Mach.Tool Des. Res. Conf.(Sept. 1967), Pt. 1, 419,(Pergamon Press, Oxford).

18. OPTIZ, H. 'Pressure pad bearings', Conf. on lubrication and wear, Inst. Mech.Engrs. Session 2, Fluid Film Lub., paper 8, London, sep. 67.

19. ROWE,W.B., and O'DONOGHUE, J.P. 'Hydrostatic bearing design', Tribology 2,No. 1, (Feb. 1969), 25-71.

20. GHIGLIOZZA, R.M. MICHELINI, R.M. and ROSSI, L. 'A design method for externally pressurized journal bearings', Tribology (August 1970), 168-174.

21. DAVIES, P.B. 'A general analysis of multi-recess hydrostatic journal bearings', Proc. Inst.Mech.Engrs., 184, (Part 1), 1969-1970, (827-838).

22. GHOSH, B. 'An exact analysis of a hydrostatic journal bearing with a large circumferential sill', Wear, 21 (1972), 367-375.

23. GHOSH, B. 'Load and flow characteristics of a capillary compensated hydrostatic journal bearing', Wear, 23 (1973), 377-386.

24. CUSANA, C., and CONRY, T.F. 'Design of Multi-Recess journal bearings for minimum total power loss', Trans. of A.S.M.E. Journal of Engineering for Industry, Feb. 1974.

25. CASTEILI, V., and SHAPIRO, W. 'Improved method for numerical solution of the incompressible fluid film lubrication problem', Journal of lubrication technology, Trans. A.S.M.E., Series F, Vol.89, No. 2, April 1967, p.211-218.

26. O'DONOGHUE, J.P. ROWE, W.B., and HOOKE, C.J. 'A comparison of four different computing methods for hydrostatic bearings', Tribology Convention, I.Mech.E., Brighton, May 1970.

27. O'DONOGHUE,J.P., ROWE, W.B., and HOOKE, C.J. 'Computer Analysis of externally pressurized journal bearings', Inst. Mech.Engrs., Proc., Vol. 184, Pt.3L, 1967-1970, Tribology Convention, 1970, Paper 7, p. 48-53.

28. O'DONOGHUE, J.P., ROWE, W.B., and HOOKE, C.J. 'A solution using the super-position technique for externally pressurized multi-recess journal bearings, including hydrodynamic effects', Proc., Inst. Mech. Engrs., 1970/71, 185.

29. ROSENBLATT, M., and WILCOCK, D.F. 'Oil flow, Key Factor in Sleeve Bearing Performance', Trans. A.S.M.E., 74, 849-865, (1952).

30. LOEB, A.M., and RIPPEL, H.C. 'The advantage of flow control valves over orifice and capillaries in compensating hydrostatic bearings', Journal of Franklin Institute, October 1957, pp 339-341.

31. MALONOSKI, A.B., LOEB, A.M. 'The effect of the method of compensation on hydrostatic bearing stiffness', J. Basic Engng., Trans. AM Soc. Mech.Engrs. 1961, 83, 179.

32. MOHSIN, M.E. 'The use of controlled restrictions for compensating hydrostatic bearings', Advances in MTDR, 1963, (Pergamon Press, Oxford).

33. DE GAST, J.G.C. 'A new type of controlled restrictor for double film hydrostatic bearings and its application to high precision machine tools', Proc. of the 7th Int. MTDR. Conference, 1966, p.273.

34. MORSI, S.A. 'Tapered spool controller for pressurized oil film bearings', Proc. Inst. Mech.Engrs., Vol.184 Pt.1, No. 21, (1969-1970).

35. O'DONOGHUE J.P., and HOOKE, C.J. 'Design of inherently stable hydrostatic bearings', Inst. of Mech.Eng., Tribology Convention, paper 23, Proc. Inst. Mech.Engrs. 1967-1968, 182 Pt. 3N.

36. O'DONOGHUE, J.P. and LEWIS, G.K. 'Tapered lands hydrostatic oil bearings', Tribology, January 1968, pp 43-49.

37. MANAM, J., FOWLER, J.H., and CARPENTER, A.L. 'Tapered lands hydrostatic journal bearings', Proc. Inst. Mech.Engrs. 1964-1965, Vol. 179, Pt. 3F, paper No. 22.

38. O'DONOGHUE, J.P. and ROWE, W.B. 'Compensation Methods for externally pressurized bearings', Engrs. Digest, 30, (1969), 49.

39. RIPPEL, H.C. 'Review of hydrostatic lubrication', Franklin Inst. sponsored seminar on computer aided design of hydrostatic bearing system, 1967 (13th December), London.

40. ROYLE, J.K., HOWARTH, R.B., and CASELY-HAYFORD,E.L. 'Application of Automatic Control to pressurized oil film bearings', Proc. Inst.Mech.Engrs. 176, No. 22, (1962).

41. REDDECLIFFE, J.M., and VOHR, J. 'Hydrostatic bearings for cryogenic rocket engine turbo pumps', J.Lubrication Technology, Trans. A.M. Soc. Mech.Engrs. 1969, 91 (Series F), 557.

42. HAHN, R.S. 'Some advantages of hydrostatics in machine tools', ASLE annual meeting, Chicago, 26-28, May 1964.

43. ENNIS, B., and COWLEY, A. 'Applications of sealed hydrostatic bearing to the vertical slide of an horizontal drilling machine', Int. MTDR, (1964), 265-288.

44. RIPPEL, H.C. 'Role of hydrostatic bearings in manufacture'. Horizons in manufacturing seminar, Inst. of Science & Technology, University of Michigan, Ann Arbor, 9 May, 1967.

45. ROWE, W.B. 'Experience with four types of grinding machine spindles', Proc. 8th MTDR Conference, University of Manchester, 12-5, Sept. 1967.

46. RIPPEL, H.C., and FULLER, D.D. 'Advantages offered by hydrostatic bearings in machine tool applications', Franklin Institute Research Laboratories, Report No. 32TR, 68-5, presented at ASME Design Engineering Conference, Chicago 1968.

47. ROWE, W.B., and O'DONOGHUE, J.P. 'The practical use and advantages of externally pressurized liquid bearings', Proc. of Industrial lubrication and Tribology Symposium, London (1969).

48. MOHSIN, M.E., and HODGSON, B. 'A hydrostatically lubricated ram for horizontal milling and boring machines', Proc. of 4th Intn. MTDR Conf., September 1963, pp 111-138, Pergamon Press, 1964.

49. FAVARETO, M., and RAZELLI, G. 'Design of hydrostatic journal bearings under impulsive loads', I.M.T.D.R. (1974), 299-316.

50. GRASSAM, N.S.,and POWELL, J.W. 'GAS Lubricated Bearings', Butterworths, London (1964).

51. DECKER, O. 'Potential of gas lubricated bearings in ultra-precision machine tool applications', Franklin Inst. Research Laboratories, report No. 32TR 68-7, presented at ASME Design Engineering Conf., Chicago, April 1968.

52. WUNCH, M.L., and NIMO, W.H. 'Industrial applications of gas bearings in the U.K.', paper C.18, Conference on externally pressurized bearings, London (November 1971).

53. KHER, A.K., and COWLEY, A. 'The design and performance characteristics of a capillary compensated hydrostatic journal bearings', Proc. 8th M.T.D.R. Conf., University of Manchester, 12-15 September, 1967.

54. DECKER, O., and SHAPIRO, W. 'Computer aided design of hydrostatic bearings for machine tool applications', Part I, Proc. of 9th Intn. M.T.D.R. conference, Sept. 1968, Pergamon Press, 1969.

55 DECKER, O., and SHAPIRO, W. 'Computer aided design of hydrostatic bearings for machine tool applications', Part II, Applications, Proc. of 9th I.M.T.D.R. Conf. Sept. 1968, Pergamon Press, 1969.

56. DAVIES, P.B., and ANDVIG, T.A. 'The Behaviour of a multi-recess hydrostatic journal bearing in the presence of severe shaft bending', presented at 9th Int. M.T.D.R. Conf., University of Birmingham, 1968.

57. PARSIEGLA, K. 'Hydrostatic bearings in heavy duty machine tools with high rotational speed', presented at 6th Conference on the "Optimization problems in design and production of machines", held at INSTYTUT KONSTUKCJI IEKSPLOR TACJI MASZYN i INSTYTUT TECHNOLOGII BUDOWY MASZYN POLITECHNIKI WROCLAWSKIGJ, POLAND, 21-25 September 1978.

58. WILCOCK, D.F. and BOOSER, E.R. 'Bearing design and application', McGraw-Hill Book Company, 1957.

59. SKF 'Bearings in machine tools', Publication No. 2580^{II}E.

60. SKF 'Typical Machine Tool Bearing', Publication No. 2581^{II}E.

61. SHELDON, D.F., O'DONOGHUE, J.P. 'A hydrodynamic pocket journal bearing', Proc. Instn.Mech.Engrs. 1970, 184 (Part 3L), 70-74.

62. ROWE, W.B., KOSHAL, D., and STOUT, K.J. 'Slot-entry bearing for hydrodynamic and hydrostatic operation', Journal of Mech.Engr. Science, Vol. 18, Nov.1976.

63. ROWE, W.B., KOSHAL, D., and STOUT, K.J. 'Investigation of recessed hydrostatic and slot-entry journal bearings for hybrid hydrodynamic and hydrostatic operation'. Wear, 43, (1977), 55-69.

64. SHINKLE, J.N. and HORNUNG, K.G. 'Frictional characteristics of liquid Hydrostatic journal bearings', Journal of Basic Engineering, Transactions of the ABME, March 1965, (163-169).

65. OPTIZ, H., BOTTCHER, R., and EFFENBERGER, W. 'Investigation on the dynamic behaviour of hydrostatic spindle systems', Proc. 10th Int. MTDR Conf., 1969, Pergamon Press, Oxford.

66. DAVIES, P.B., and LEONARD, R. 'Stability of multi-recess hydrostatic journal bearings', Journal of Mech. Engineering Science, Vol. 12, No. 2, 1970.

67. LEONARD, R., and ROWE, W.B. 'Dynamic force coefficient and the mechanism of instability in hydrostatic journal bearings', Wear, 23, (1973) 277-282.

68. PINKUS, O. 'Analysis of Elliptical Bearings', Trans. ASME, Vol. 78, July 1956.

69. PINKUS, O. 'Power loss in elliptical and 3-lobe bearings', Trans. ASME, Vol. 78, July 1956.

70. PINKUS, O. 'Analysis and characteristics of three-lobe Bearings', Trans. ASME, Ser D.Vol. 79, March 1959.

71. POPE, A.W., and HEALY, S.P., 'ANTI-vibration Journal Bearings', Proc. Inst. Mech.Engrs. 1966-1967, Vol. 181, Pt. 3B, 98-115.

72. GLIENICKE, J. 'Experimental investigation of the stiffness and damping coefficients of turbine bearings and their applications to instability prediction', Proc. Inst. Mech.Engrs., 1966-67, Vol. 181, Pt 3B, 116-129.

73. PARSZEWSKI, Z., and CAMERON, A. 'Oil Whirl of Flexible Rotors', Proc. Inst. Mech. Engrs. Vol. 176, No. 22 (1962).

74. MORRISON, D. 'Influence of Plain journal bearings on the Whirling Action of an Elastic Rotor', Proc. Inst. Mech. Engrs., Vol. 176, No.22 (1962).

75. HOLMES, R. 'Oil Whirl Characteristics of a Rigid Rotor in 360° Journal Bearings', Proc. Inst. Mech. Engrs. Vol. 177, No. 11 (1963), 291-307.

76. SMITH, D.M. 'Dynamic Characteristics of Turbine Journal Bearings'. Inst. Mech.Engrs. - Lubrication and Wear Convention (1963), 72-86.

77. HOLMES, R. 'Instability Phenomena due to Circular Bearing Oil Films'. Journal Mechanical Engineering Science, Vol. 8 No. 4 (1966), 419-425.

78. BONES, J.A. and HANNAM, R.G. 'Whirling of Shafts with Asymmetric Stiffness', Journal Mechanical Engineering Science, Vol. 8, No. 4 (1966), 437-447.

79. BADGLEY, R.H. and BOOKER, J.P. 'Turborotor Instability: Effect of initial transients on Plane Motion'. Journal of Lubrication Technology (October 1969), 625-633.

80. AKERS, A., MICHAELSON, S., and CAMERON, A. 'Stability Contours for a Whirling Finite Journal Bearing'. Trans. of ASME, Paper No. 70, Lubs. 3, (1970), 1-7.

81. HEATH, H.H., and COWKING, W. 'MELBA: A suite of computer programmes for analysis of self-acting plain bearings'. GEC journal of Science & Technology, Vol. 45, No.2, (1979), 83-90.

82. PRIVATE COMMUNICATION 'Steady load and Dynamic Characteristics of a 19" dia. x 10" three-hand Bearing'.

83. DUFFIN, S., and JOHNSON, B.T. 'Some Experimental and Theoretical Studies of Journal Bearings for Large Turbine-Generator Sets'. Proc. Inst. Mech. Engrs. 1966-67, Vol. 181, Pt. 3B.

84. DOWSON, D., HUDSON, J.D., HUNTER, B., and MARCH, C.M. 'An Experimental Investigation of the Thermal Equilibrium of Steadily loaded Journal Bearings'. Proc. Inst. Mech. Engrs. 1966-1967, Vol. 181, Pt. 3B.

85. FORSYTHE, S.E. and WASON, W.R. "Finite Difference Methods for Partial Differential Equations". Wiley (1960).

BIBLIOGRAPHY

BIBLIOGRAPHY

1. WILCOCK, D.F. 'Predicting sleeve-bearing performance'. 1957, I.Mech.E.Conf. on Lubrication and Wear, p.82.

2. HAHN, H.W. 'Dynamically Loaded Bearings of Finite Length' 1957, I.Mech.E. Conf. on Lubrication and Wear, p.101.

3. LOEB, A.M. and RIPPEL, H.C. 'Determination of Optimum Proportions for Hydrostatic Bearings'. A.S.L.E. Trans., 1958.

4. LING, M.T.S. 'On the Optimization of the Stiffness of Externally Pressurized Bearings'. Journal of Basic Engineering, March 1962.

5. MAYER, J.E., and SHAW, M.C. 'Characteristics of an Externally Pressurised Bearing Having Variable External Flow Restrictions'. Trans. A.S.M.E. Ser.D, June 1963, p.291.

6. SMITH, D.M. 'Journal Bearing Dynamic Characteristics - Effect of Inertia of Lubricant'. Proc. Inst. Mech.Engrs. 1964-1965, Vol. 179, Pt.3j.

7. WONG, G.S.K. 'Interface Restrictor Hydrostatic Bearing'. International Mach. Tool Des. Research & Design, 1965.

8. HUGGINS, N.J. 'Tests on 24-4n Diameter Journal Bearing: Transition from Laminar to turbulent flow'. Proc. Inst. Mech.Engrs., 1966-1967, Vol.181, Pt. 3B.

9. NEALE, M.J. 'Selection of Bearings'. Proc. Inst. Mech. Engrs. 1967-68, Vol. 182, Pt. 3A.

10. SMALLEY, A.J., and McCALLIN, H. 'The Effect of Journal Misallignment on the Performance of a Journal Bearing under Steady Running Conditions'. Proc. Inst. Mech.Engrs. 1966-67, Vol. 181, Pt. 3B.

11. SMALLEY, A.J., and McCALLIN, H. 'The Influence of Viscosity Variation with the Temperature on Journing Bearing Performance'. Proc. Inst. Mech.Engrs., 1966-67, Vol. 181, Pt.3B.

12. LLOYD T., and McCALLIN, H. 'Recent Developments in Fluid Film Lubrication Theory'. Proc. Inst. Mech.Engrs., 1967-68, Vol. 182, Pt. 3A.

13. HUNT, J.B., and AHMED, K.M. 'Load Capacity, Stiffness and flow characteristics of a hydrostatically lubricated six-pocket Journal Bearing supporting a rotating spindle'. Proc. Inst. Mech.Engrs., 1967-68, Vol. 182,Pt 3N.

14. ETTLES, C. 'Solution for Flow in a Bearing Groove'. Proc. Inst. Mech.Engrs., 1967-68, Vol. 182, Pt. 3N.

15. COWLEY, A., and KHER, A.K. 'The Dynamic Characteristics of a hydrostatically supported spindle bearing system'. Advanced Mach.Tool Des., Res., 1968.

16. GHIGLIAZZA, R., and MICHELINI, R.C. 'Friction in Externally Pressurized Journal Bearings'. Wear, 12, (1968) 241-256.

17. O'DONOGHUE, J.P. ROWE, W.B., and HOOKE, C.J. 'Design of Hydrostatic Bearings using an Operating Parameter'. Wear, 14 (1969), 355-362.

18. HELLER, S., and SHAPIRO, W. 'A numerical solution for the incompressible hybrid journal bearing with covation'. Journal of Lubrication Technology, July 1969.

19. O'DONOGHUE, J.P., ROWE, W.B., and HOOKE, C.J. 'Some Tolerance effects in Hydrostatic Bearings'. Advanced Mach.Tools Des., Res., 1970.

20. ROWE, W.B., O'DONOGHUE, J.P., and CAMERON, A. 'Optimization of Externally Pressurized Bearings for minimum power and low temperature rise.' Tribology, August 1970.

21. KHER, A.K., and COWLEY, A. 'An Experimental Investigation into the temperature effects in hydrostatic journal bearings'. Tribology, August 1970.

22. O'DONOGHUE, J.P., HOOKE, C.J., and COOK, P.J. 'Analysis of the squeeze film in a multi-recess hydrostatic journal bearing'. Inst. Mech. Engrs., (45-171).

23. ROWE, W.B., and O'DONOGHUE, J.P. 'Diaphragm Valves for Controlling Opposed Pad Hydrostatic Bearings'. Proc. Inst. Mech. Engrs., 1970, Vol. 184, Pt. 3L.

24. O'DONOGHUE, J.P. 'Parallel orifice and capillary control for hydrostatic journal bearings' Tribology, April 1972.

25. ROWE, W.B., and STOUT, K.J. 'Viscosity variation in hydrostatic bearings. Triboloty, December 1972.

26. STOUT, K.J. and ROWE, W.B. 'Externally pressurized bearings design for manufacture'. Triboloty Int. June 1974.

27. STOUT, K.J. and ROWE, W.B. 'Externally Pressurized journal bearings for manufacture'. Tribology Int. October 1974.

28. DIXON, R.S., and LENARD, R. 'Formulae defining the performance of hydrostatic journal bearings incorporating 3,4,5 and 6 recesses'. Int.Mach.Tool Des. Res., Vol. 14, pp 85-94, 1974.

29. ETTLES, C. 'The vane bearing: A self-pressurized journal bearing'. Proc. Inst.Mech.Engrs. Vol. 189, 8/75.

30. ROHDE, S.M., and EZZAT, H.A. 'On the dynamic behaviour of hybrid journal bearings'. Journal of Lubrication Technology, June 1976.

31. GHOSH, M.K., and MAJUMDAR, B.C. 'Stiffness and damping characteristics of hydrostatic multi-recessed oil journal bearings'. Advanced Mach.Tool Des. Res., Vol. 18, pp 139-151.

APPENDIX A1

A1.1 A COMPUTER PROGRAMME TO EVALUATE THE PRESSURE, LOAD, FLOW AND THE STIFFNESS PARAMETERS

```
00001:JOB(GREM114,J6,T40,M7600)                    T  M  S A L E M    MECH. ENG. DEPT.
00002:MNF(T)
00003:LDSET(MAP=B/ZZZZMP,PRESET=ZERO)
00004:LGO.
00005:@
00006:      PROGRAM LOBE(INPUT,OUTPUT,TAPE4=INPUT,TAPE3=OUTPUT)
00007:     10 WRITE(3,20)
00008:     20 FORMAT(84H                                        EVALUATION OF PRESSURE,LOAD,F
00009:       2LOW AND STIFFNESS PARAMETERS/,68H                                          FOR TH
00010:       3E THREE-LOBE EXTERNALLY PRESSURIZED/,73H
00011:       4          JOURNAL BEARINGS  -ANALYTICAL SOLUTION)
00012:        WRITE(3,60)
00013:     60 FORMAT(100H****************************************************************
00014:       2****************************************)
00015:        WRITE(3,200)
00016:    200 FORMAT(36H   GAMA1  IS THE SOMMERFELD VARIABLE)
00017:        WRITE(3,300)
00018:    300 FORMAT(50H  SI  IS TH PRESSURE PARAMETER IN EQUATION (2.4.8))
00019:        WRITE(3,400)
00020:    400 FORMAT(49H  EI  IS THE LOAD PARAMETER FROM EQUATION (2.5.2))
00021:        WRITE(3,500)
00022:    500 FORMAT(55H  AK  IS THE AXIAL FLOW PARAMETER IN EQUATION (2.6.2.3))
00023:        WRITE(3,600)
00024:    600 FORMAT(52H  STIF IS THE STIFNESS PARAMETER IN EQUATION (2.7.3))
00025:        THETA1=45.0
00026:        DO 30 J=1,4
00027:        WRITE(3,40)THETA1
00028:     40 FORMAT(73H                                       THE ANGLE MEASURED FROM TH
00029:       2E PAD CENTRE LINE/,63H                                      TO THE START O
00030:       3F THE AXIAL GROOVES/,59H
00031:       4         THETA1 = ,F15.8)
00032:        WRITE(3,50)
00033:     50 FORMAT(99H***************************************************************
00034:       2****************************************)
```

```
      WRITE(3,80)
   80 FORMAT(116H                E                G                SI
     3         EI               AK               STIF               B)
      THETA1=THETA1*3.14/180.0
      E=-0.5
      DO 70 I=1,145
      A=-E+COS(THETA1)
      D=1.0-(E*COS(THETA1))
      GAMA1=ACOS(A/D)
      X1=(1.0-(E**2))**2.5
      X2=GAMA1*(1.0+((E**2)/2.0))
      X3=2.0*E*SIN(GAMA1)
      X4=(E*E/2.0)*SIN(GAMA1)*COS(GAMA1)
      SI=(1.0/X1)*(X2+X3+X4)
      GAMA=0.0
      X5=COS(GAMA)+((E/4.0)*COS(2.0*GAMA))
      X6=COS(GAMA1)+((E/4.0)*COS(2.0*GAMA1))
      X7=(1.0-(E**2))**0.5
      EI=((X5-X6)/(X2+X3+X4))*X7
      THETA2=60.0*3.14/180.0
      X8=THETA2*((1.0+(1.5*(E**2))))
      X9=3.0*E*SIN(THETA2)
      X17=(E**3)*SIN(THETA2)
      X10=0.75*(E**2)*SIN(2.0*THETA2)
      X11=0.333*(E**3)*SIN(3.0*THETA2)
      AK=(X8-X9+X10+X11-X17)
      X12=(1.0-(E**2))**3
      X13=-COS(GAMA)-((E/4.0)*COS(2.0*GAMA))
      X14=-COS(GAMA1)-((E/4.0)*COS(2.0*GAMA1))
      X15=SIN(GAMA)+(0.5*E*SIN(2.0*GAMA))-(0.25*COS(2.0*GAMA))
      X16=SIN(GAMA1)+(0.5*E*SIN(2.0*GAMA1))-(0.25*COS(2.0*GAMA1))
      STIF=1.0/X12*((4.0*E*(X13-X14))+((1.0-(E**2))*(X15-X16)))
      B=EI/SI
      G=GAMA1*180.0/3.14
      WRITE(3,100)E,G,SI,EI,AK,STIF,B
```

A.1.1a. SAMPLE OF THE OUTPUT.

```
00070:  100 FORMAT(7X,F15.8,F15.8,F15.8,F15.8,F15.8,F15.8,F15.8)
00071:      E=E+0.01
00072:   70 CONTINUE
00073:      THETA1=THETA1*180.0/3.14
00074:      THETA1=THETA1+5.0
00075:   30 CONTINUE
00076:      STOP
00077:      END
```

EVALUATION OF PRESSURE,LOAD,FLOW AND STIFFNESS PARAMETERS
FOR THE THREE-LOBE EXTERNALLY PRESSURIZED
JOURNAL BEARINGS -ANALYTICAL SOLUTION

****

THE ANGLE MEASURED FROM TH E PAD CENTRE LINE
TO THE START O F THE AXIAL GROOVES

THETA1 = 60.00000000

****

E	G	SI	EI	AK	STIF
.35000000	79.55009569	5.01062730	.42566014	.37240194	-4.03072825
.36000000	80.17567003	5.12611972	.42566695	.35897912	-4.21245301
.37000001	80.82700960	5.24769307	.42103675	.34575339	-4.40579636
.38000000	81.46694695	5.37040825	.41956836	.33277957	-4.61177500
.39000000	82.15504191	5.51214627	.41745666	.32005246	-4.83142136
.40000000	82.82656210	5.65564785	.41530254	.30756687	-5.06589495
.41000000	83.50716351	5.80749503	.41310413	.29531761	-5.31647525
.42000000	84.19567003	5.96852701	.41086068	.28329940	-5.58457643
.43000000	84.89207595	6.13884421	.40857080	.27150730	-5.87176419
.44000000	85.59604455	6.31861543	.40623244	.25993567	-6.17977500
.45000000	86.30962970	6.51208592	.40384466	.24858001	-6.51055825
.46000000	87.03129626	6.71056862	.40140568	.23743452	-6.86620156
.47000000	87.76192090	6.92454459	.39891585	.22649420	-7.24916036
.48000000	88.50179291	7.15049311	.39636743	.21575586	-7.66209160
.49000000	89.25121400	7.41429543	.39376463	.20520835	-8.10799522
.50000000	90.01053507	7.67914071	.39110355	.19485243	-8.59022988
.51000000	90.77999015	7.96258224	.38838222	.18466093	-9.11258655
.52000000	91.55002452	8.26634675	.38559857	.17466005	-9.67932992

A1.2 A COMPUTER PROGRAMME TO CALCULATE THE OIL FLOW, SUPPLY PRESSURE, STIFFNESS AND PUMPING POWER

```
00006:       PROGRAM ANALAT(INPUT,OUTPUT,TAPE4=INPUT,TAPE3=OUTPUT)
00007:       COMMON E1,E2,E3,S1,S2,S3,AK1,AK2,AK3,STIF1,STIF2,STIF3,ALPHA,OFFSE
00008:      2T,CMIN,EB,E,EL1,EL2,EL3,P1,P2,P3,PS,FT,QCT,QAT,QT,QA1,QA2,QA3,STIF
00009:      3FN,HP,QC1,QC2,QC3,C11,C22,DUMY
00010:C*****************************************************************
00011:       WRITE(3,10)
00012:    10 FORMAT(96H                                          THE CALCULATION OF THE OIL
00013:      2 FLOW RATES,SUPPLY PRESSURE,PAD PRESSURE/,94H
00014:      3          BEARING STIFFNESS,AND THE PUMPING POWER FOR A THREE LOBE
00015:      4JOURNAL/,99H                                          BEARINGS WITH EXTERNAL P
00016:      5RESSURIZATION AND SPECIFIED LOAD,ECCENTRICITY/,45H
00017:      6                 AND TEMPERATURE)
00018:C*****************************************************************
00019:       WRITE(3,20)
00020:    20 FORMAT(69H
00021:      2   S.I.UNITS.)
00022:C*****************************************************************
00023:C*****************************************************************
00024:       C=8.0/39300.0
00025:       DO 1 I=1,6
00026:       DY=1.0/39300.0
00027:C      DY      IS THE JOURNAL DISPLACEMENT UNDER THE EXTERNAL LOAD
00028:C*****************************************************************
00029:       DO 2 J=1,4
00030:       OFFSET=2.3/39300.0
00031:       CMIN=C-(2.0*OFFSET)
00032:       B=0.127
00033:C      B       IS THE BEARING WIDTH
00034:       B1=0.117
00035:C      B1       IS THE AXIAL WIDTH OF THE INLETS
00036:       D=0.135
00037:C      D       IS THE BEARING DIAMETER
00038:       Z=0.2
00039:C      Z       IS THE OIL VISCOSITY
00040:       T=75.0
00041:C      T       IS THE OIL TEMPERATURE AT THE OUTLET
```

```
00042:C      EO       IS THE BEARING OFFSET DIVIDED BY THE RADIAL CLEARANCE
00043:       FT=22320.0
00044:C*****************************************************************
00045:       DO 7 L=1,4
00046:       EO=2.0*OFFSET/C
00047:C      C        IS THE LOBE DIAMETERAL CLEARANCE
00048:       WRITE(3,8)FT
00049:     8 FORMAT(35H                                    FT = ,F20.8)
00050:C*****************************************************************
00051:       WRITE(3,3)DY
00052:     3 FORMAT(35H                                    DY = ,F20.8)
00053:C*****************************************************************
00054:       WRITE(3,4)C
00055:     4 FORMAT(35H                                     C = ,F20.8)
00056:C*****************************************************************
00057:       ALPHA=0.0
00058:C      ALPHA       IS THE BEARING ATTITUDE ANGLE
00059:C      CMIN       IS THE MINIMUM DIAMETERAL CLEARANCE
00060:       EB=2.0*DY/CMIN
00061:C      EB       IS THE BEARING ECCENTRICITY RATIO MEASURED WITH REFFERENCE
00062:C                 TO THE MINIMUM DIAMETERAL CLEARANCE
00063:C      OFFSET       IS THE DISTANCE BETWEEN THE CENTRE OF THE BEARING AND
00064:C                        THE CENTRE OF EACH LOBE
00065:       E=EB*(1.0-EO)
00066:C      E       IS THE BEARING ECCENTRICITY RATIO MEASURED WITH REFFERENCE
00067:C                          TO THE LOBE DIAMETERAL CLEARANCE
00068:C*****************************************************************
00069:       WRITE(3,25)
00070:    25 FORMAT(119H       B          B1          D             C       Z          T
00071:      2             EO       DY       FT                                        )
00072:C*****************************************************************
00073:       WRITE(3,30)B,B1,D,C,Z,T,EO,DY,FT
00074:    30 FORMAT(F10.7,F10.7,F10.7,F10.7,F10.7,F10.7,F10.7,F10.7,F10.2)
00075:C*****************************************************************
00076:       WRITE(3,40)
00077:    40 FORMAT(100H****************************************************
```

```
00078:     2*********************************************)
00079:C*************************************************************************
00080:      WRITE(3,50)
00081:   50 FORMAT(59H                              THE LOAD IS APPLIED VERTICALLY DOWN
00082:     2WOD)
00083:C*************************************************************************
00084:      WRITE(3,60)
00085:   60 FORMAT(60H*************************************************************
00086:     2****)
00087:C*************************************************************************
00088:      EL1=((E**2)+(EO**2)+(2.0*E*EO*COS(ALPHA)))**0.5
00089:C     EL1       IS THE FIRST LOBE ECCENTRICITY RATIO
00090:      EL2=(((E**2)+(EO**2)-(2.0*E*EO*COS((3.14/3.0)-ALPHA))))**0.5
00091:C     EL2       IS THE SECOND LOBE ECCENTRICITY RATIO
00092:      EL3=EL2
00093:C     EL3       IS THE THIRD LOBE ECCENTRICITY RATIO
00094:C*************************************************************************
00095:      IF(EL1.GT.1.0) GO TO 11111
00096:      CALL HESHAM
00097:      WRITE(3,777)S1,S2,S3,E1,E2,E3,STIF1,STIF2,STIF3,AK1,AK2,AK3
00098:  777 FORMAT(F15.7)
00099:      P1=((FT)/((B1*D)*((E1-((((S2/S1)*E2)+((S3/S1)*E2))*COS(60.0*3.14/1
00100:     280.0))))))
00101:      QC1=((P1*B*(C**3)/(24.0*Z*D))*(1.0/S1))*9.81
00102:      QC2=QC1
00103:      QC3=QC2
00104:      QCT=3.0*QC1
00105:      P2=(24.0*Z*D*QC2/(B*(C**3)))*(S2/9.8)
00106:      P3=P2
00107:      QA1=((D*(C**3)*P1)/(48.0*Z*B))*AK1*9.8
00108:      QA2=((D*(C**3)*P2)/(48.0*Z*B))*AK2*9.8
00109:      QA3=QA2
00110:      QAT=QA1+QA2+QA3
00111:      QT=QAT+QCT
00112:      STIFFN=((Z*48.0*D*D*QC1)/(9.81*(C**4)))*(STIF1+(STIF2+STIF3)*0.25)
00113:      PS=P1
```

```
00114:       HP=(QT*PS)/(750.0*1.36)
00115:C*************************************************************************
00116:       CALL SAMIA
00117:C*************************************************************************
00118:11111 ALPHA=180.0*3.14/180.0
00119:       EL1=2.0*(OFFSET-DY)/C
00120:       EL2=(((E**2)+(EO**2)-(2.0*E*EO*COS((3.14/3.0)-ALPHA))))**0.5
00121:       EL3=EL2
00122:C*************************************************************************
00123:       WRITE(3,500)
00124:  500 FORMAT(62H                          OUTPUT FOR A LOAD APPLIED VERTICALLY
00125:     2UPWARD)
00126:C*************************************************************************
00127:       WRITE(3,501)
00128:  501 FORMAT(60H************************************************************
00129:     2****)
00130:C*************************************************************************
00131:       IF(EL2.GT.1.0) GO TO 22222
00132:       CALL HESHAM
00133:       P2=FT/((B1*D*(((E2+E3)*(COS(3.14/3.0))-(E1*S1/S2)))))
00134:       P3=P2
00135:       PS=P2
00136:       QC2=((P2*B*((C**3))/(24.0*Z*D))*(1.0/S2))*9.81
00137:       QC3=QC2
00138:       QC1=QC2
00139:       QCT=3.0*QC2
00140:       P1=((24.0*Z*D*QC1)/(B*(C**3)))*(1.0/9.81)*S1
00141:       QA1=((D*((C**3))*P1)/(48.0*Z*B))*AK1*9.81
00142:       QA2=((D*(C**3)*P2)/(48.0*Z*B))*AK2*9.81
00143:       QA3=QA2
00144:       QAT=QA1+QA2+QA3
00145:       QT=QCT+QAT
00146:       STIFFN=((Z*48.0*D*D*QC2)/(9.81*(C**4.0)))*((STIF2+STIF3)*0.25+STIF
00147:      21)
00148:       HP=(QT*PS)/(750.0*1.36)
00149:C*************************************************************************M
```

```
00150:       CALL SAMIA
00151:22222  DUMY=0.0
00152:       FT=FT+7000.0
00153:     7 CONTINUE
00154:       DY=DY+(1.0/39300.0)
00155:     2 CONTINUE
00156:       C=C+(1.0/39300.0)
00157:     1 CONTINUE
00158:       STOP
00159:       END
00160:       SUBROUTINE HESHAM
00161:       COMMON E1,E2,E3,S1,S2,S3,AK1,AK2,AK3,STIF1,STIF2,STIF3,ALPHA,OFFSE
00162:      2T,CMIN,EB,E,EL1,EL2,EL3,P1,P2,P3,PS,FT,QCT,QAT,QT,QA1,QA2,QA3,STIF
00163:      3FN,HP,QC1,QC2,QC3,C11,C22,DUMY
00164:       THETA1=60.0*3.14/180.0
00165:       A1=-EL1+COS(THETA1)
00166:       BB1=1.0-(EL1*COS(THETA1))
00167:       IF(EL1.GT.1.0) GO TO 12121
00168:       GAMA1=ACOS(A1/BB1)
00169:       X1=(1.0-(EL1**2))**2.5
00170:       X2=GAMA1*(1.0+((EL1**2)/2))
00171:       X3=2.0*EL1*SIN(GAMA1)
00172:       X4=(EL1*EL1/2.0)*SIN(GAMA1)*COS(GAMA1)
00173:       S1=(1.0/X1)*(X2+X3+X4)
00174:       GAMA=0.0
00175:       X5=COS(GAMA)+((EL1/4.0)*COS(2.0*GAMA))
00176:       X6=COS(GAMA1)+((EL1/4.0)*COS(2.0*GAMA1))
00177:       X7=(1.0-(EL1**2))**0.5
00178:       E1=((X5-X6)/(X2+X3+X4))*X7
00179:       THETA2=60.0*3.14/180.0
00180:       X8=THETA2*((1.0+(1.5*(EL1**2))))
00181:       X9=3.0*EL1*SIN(THETA2)
00182:       X99=(EL1**3)*SIN(THETA2)
00183:       X10=0.75*(EL1**2)*SIN(2.0*THETA2)
00184:       X11=0.3333*(EL1**3)*SIN(3.0*THETA2)
00185:       AK1=(X8-X9+X10+X11-X99)
```

```
00186:       X12=(1.0-(EL1**2))**3
00187:       X13=-COS(GAMA)-((E/4.0)*COS(2.0*GAMA))
00188:       X14=-COS(GAMA1)-((E/4.0)*COS(2.0*GAMA1))
00189:       X15=SIN(GAMA)+(0.5*E*SIN(2.0*GAMA))-(0.25*COS(2.0*GAMA))
00190:       X16=SIN(GAMA1)+(0.5*E*SIN(2.0*GAMA1))-(0.25*COS(2.0*GAMA1))
00191:       STIF1=(1.0/X12)*((4.0*E*(X13-X14))+((1.0-(E**2))*(X15-X16)))
00192:       WRITE(3,70)ALPHA
00193:    70 FORMAT(28H                          ALPHA = ,F15.8)
00194:       WRITE(3,80)OFFSET
00195:    80 FORMAT(29H                          OFFSET = ,F15.8)
00196:       WRITE(3,90)CMIN
00197:    90 FORMAT(29H                             CMIN = ,F15.8)
00198:       WRITE(3,100)EB
00199:   100 FORMAT(29H                              EB = ,F15.8)
00200:       WRITE(3,110)E
00201:   110 FORMAT(29H                               E = ,F15.8)
00202:       WRITE(3,120)EL1
00203:   120 FORMAT(29H                             EL1 = ,F20.8)
00204:       WRITE(3,130)EL2
00205:   130 FORMAT(29H                             EL2 = ,F20.8)
00206:       WRITE(3,140)EL3
00207:   140 FORMAT(29H                             EL3 = ,F20.8)
00208:       WRITE(3,150)
00209:   150 FORMAT(30H******************************)
00210:12121 A2=-EL2+COS(THETA1)
00211:       BB2=1.0-(EL2*COS(THETA1))
00212:       IF(EL2.GT.1.0) RETURN
00213:       GAMA21=ACOS(A2/BB2)
00214:       X21=(1.0-(EL2**2))**2.5
00215:       X22=GAMA21*(1.0+((EL2**2)/2.0))
00216:       X23=2.0*EL2*SIN(GAMA21)
00217:       X24=(EL2*EL2/2.0)*SIN(GAMA21)*COS(GAMA21)
00218:       S2=(1.0/X21)*(X22+X23+X24)
00219:       S3=S2
00220:       X25=COS(GAMA)+((EL2/4.0)*COS(2.0*GAMA))
00221:       X26=COS(GAMA21)+((EL2/4.0)*COS(2.0*GAMA21))
```

```
00222:       X27=(1.0-(EL2**2))**0.5
00223:       E2=((X25-X26)/(X22+X23+X24))*X27
00224:       E3=E2
00225:       X28=THETA2*((1.0+(1.5*(EL2**2))))
00226:       X29=3.0*EL2*SIN(THETA2)
00227:       X299=(EL2**3)*SIN(THETA2)
00228:       X210=0.75*(EL2**2)*SIN(2.0*THETA2)
00229:       X211=0.3333*(EL2**3)*SIN(3.0*THETA2)
00230:       AK2=(X28-X29+X210+X211-X299)
00231:       AK3=AK2
00232:       X212=(1.0-(EL2**2))**3
00233:       X213=-COS(GAMA)-((E/4.0)*COS(2.0*GAMA))
00234:       X214=-COS(GAMA21)-((E/4.0)*COS(2.0*GAMA21))
00235:       X215=SIN(GAMA)+(0.5*E*SIN(2.0*GAMA))-(0.25*COS(2.0*GAMA))
00236:       X216=SIN(GAMA21)+(0.5*E*SIN(2.0*GAMA21))-(0.25*COS(2.0*GAMA21))
00237:       STIF2=(1.0/X212)*((4.0*E*(X213-X214))+((1.0-(E**2))*(X215-X216)))
00238:       STIF3=STIF2
00239:       RETURN
00240:       END
00241:       SUBROUTINE SAMIA
00242:       COMMON E1,E2,E3,S1,S2,S3,AK1,AK2,AK3,STIF1,STIF2,STIF3,ALFHA,OFFSE
00243:      2T,CMIN,EB,E,EL1,EL2,EL3,P1,P2,P3,PS,FT,QCT,QAT,QT,QA1,QA2,QA3,STIF
00244:      3FN,HP,QC1,QC2,QC3,C11,C22,DUMY
00245:       WRITE(3,160)QC1
00246:   160 FORMAT(68H                          THE CIRCUMFERENTIAL OIL FLOW RATE PE
00247:      2R PAD QC1 = ,F19.8)
00248:       WRITE(3,170)QA1
00249:   170 FORMAT(66H                          THE AXIAL FLOW RATES FOR THE FIRST L
00250:      2OBE QA1 = ,F20.8)
00251:       WRITE(3,190)QA2
00252:   190 FORMAT(67H                          THE AXIAL FLOW RATES FOR THE SECOND
00253:      2LOBE QA2 = ,F20.8)
00254:       WRITE(3,180)QA3
00255:   180 FORMAT(66H                          THE AXIAL FLOW RATES FOR THE THIRD L
00256:      2OBE QA3 = ,F20.8)
00257:       WRITE(3,200)QT
```

```
00258:  200 FORMAT(65H                    THE TOTAL OIL FLOW RATE FOR THE BEAR
00259:     2ING QT = ,F20.8)
00260:      WRITE(3,210)P1
00261:  210 FORMAT(62H                    THE PRESSURE AT THE FIRST LOBE INLET
00262:     2 P1 = ,F20.8)
00263:      WRITE(3,220)P2
00264:  220 FORMAT(63H                    THE PRESSURE AT THE SECOND LOBE INLE
00265:     2T P2 = ,F20.8)
00266:      WRITE(3,230)P3
00267:  230 FORMAT(63H                     THE PRESSURE AT THE THIRD LOBE INLE
00268:     2T P3 = ,F20.8)
00269:      WRITE(3,240)PS
00270:  240 FORMAT(65H                                  THE SUPPLY PRESS
00271:     2URE PS = ,F20.8)
00272:      WRITE(3,250)STIFFN
00273:  250 FORMAT(65H                                THE BEARING STIFFNES
00274:     2STIFFN= ,F20.8)
00275:      WRITE(3,260)HP
00276:  260 FORMAT(59H                              THE PUMPING POWER    HP
00277:     2 = ,F20.8)
00278:      RETURN
00279:      END
```

A.1.2a. SAMPLE OF THE OUTPUT

THE CALCULATION OF THE OIL FLOW RATES,SUPPLY PRESSURE,PAD PRESSURE
BEARING STIFFNESS,AND THE PUMPING POWER FOR A THREE LOBE JOURNAL
BEARINGS WITH EXTERNAL PRESSURIZATION AND SPECIFIED LOAD,ECCENTRICITY
AND TEMPERATURE

S.I.UNITS.

****

FT = 22520.00000000
DY = .00002545
C = .00050554

B	BT	D	C	Z	I	EO	DY	FT
.1270000	.1170000	.1550000	.0005055	.2000000075.0000000		.5833333	.0000254	22520.00

****

THE LOAD IS APPLIED VERTICALLY DOWN WOD

****

ALPHA = 0
OFFSET = .00005052
GAIN = .00018650
EO = .27027027
E = .1000000
EL1 = .55000000
EL2 = .55252818
EL3 = .55252818

****

THE CIRCUMFERENTIAL OIL FLOW RATE PER PAD QC1 = .00005005
THE AXIAL FLOW RATES FOR THE FIRST LOBE QA1 = .00005014
THE AXIAL FLOW RATES FOR THE SECOND LOBE QA2 = .00005160
THE AXIAL FLOW RATES FOR THE THIRD LOBE QA3 = .00005160
THE TOTAL OIL FLOW RATE FOR THE BEARING QT = .00024563
THE PRESSURE AT THE FIRST LOBE INLET P1 = 6694192.17547953
THE PRESSURE AT THE SECOND LOBE INLET P2 = 2566818.90591873
THE PRESSURE AT THE THIRD LOBE INLET P3 = 2566818.90591873
THE SUPPLY PRESSURE PS = 6694192.17547953
THE BEARING STIFFNESSTIFFN= , -61764996.24361038
THE PUMPING POWER HP = 1.59692702

OUTPUT FOR A LOAD APPLIED VERTICALLY UPWARD

****

ALPHA = 3.14000000

OFFSET = .00005852

CMIN = .00016850

EB = .27027027

E = .1666667

EL1 = .21666667

EL2 = .45855805

EL3 = .45855805

****

THE CIRCUMFERENTIAL OIL FLOW RATE PER PAD QC1 = .00006129

THE AXIAL FLOW RATES FOR THE FIRST LOBE QA1 = .00003852

THE AXIAL FLOW RATES FOR THE SECOND LOBE QA2 = .00003849

THE AXIAL FLOW RATES FOR THE THIRD LOBE QA3 = .00003849

THE TOTAL OIL FLOW RATE FOR THE BEARING QT = .00029916

THE PRESSURE AT THE FIRST LOBE INLET P1 = 2158986.04976982

THE PRESSURE AT THE SECOND LOBE INLET P2 = 6015417.10555815

THE PRESSURE AT THE THIRD LOBE INLET P3 = 6015417.10555815

THE SUPPLY PRESSURE PS = 6015417.10555815

THE BEARING STIFFNESSTIFFN= , -586945781.27990723

THE PUMPING POWER HP = 1.76429169

APPENDIX A2

A2.1 A COMPUTER PROGRAMME FOR THE NUMERICAL SOLUTION OF REYNOLDS EQUATION

```
.NULL.
00001:JOB(GREM114,J12,T600,M7600)              T  M  S A L E M    MECH. ENG. DEPT.
00002:MNF(T)
00003:LDSET(MAP=B/ZZZZMP,PRESET=NGINF)
00004:LGO.
00005:@
00006:       PROGRAM S44(INPUT,OUTPUT,TAPE4=INPUT,TAPE3=OUTPUT)
00007:       DIMENSION P1(30,52),P11(30,52),P2(30,52),P22(30,52),P3(30,52),P33(
00008:      230,52),H1(30,52),H2(30,52),H3(30,52)
00009:       INTEGER U,W
00010:       L=1
00011:       DO 3 U=1,2
00012:       EB=0.1
00013:       DO 1 K=1,9
00014:       EPS=.001
00015:       MAXIT=100
00016:       D=2.0
00017:       M=50
00018:       ELIPIT=0.0
00019:C*************************************************************************
00020:       DX=3.14*100.0/(3.0*FLOAT(M/2)*120.0)
00021:       DY=DX
00022:       N=28
00023:C       N     IS THE NUMBER OF  MESH  POINTS  ACROSS  THE  BEARING
00024:       WRITE(3,630)N
00025:   630 FORMAT(24H                          N = ,I4/,25H**************************
00026:      2*)
00027:C*************************************************************************
00028:C      EPS  IS  THE  REQUIRED  ACCURACY  IN THE SOLUTION
00029:C       MAXIT      IS  THE  MAXIMUM  NUMBER  OF  ITERTATIONS
00030:C*************************************************************************
00031:C       EB       IS  THE  BEARING  ECCENTRICITY RATIO  (BEARING  ECCENTRICITY/MIN
00032:C       NIMUM  CLEARANCE
00033:C*************************************************************************
00034:C       L     IS THE BEARING  LENGTH
```

```
00035:C*************************************************************************
00036:C      D     IS THE BEARING  DAIMETER
00037:C*************************************************************************
00038:C      M     IS  THE NUMBER OF MESH  POINTS AROUND THE  BEARING
00039:C*************************************************************************
00040:C      ELIPIT    IS  THE  CONCETNRIC  ECCENTRICITY RATI   ((THE BEARING OFFSET/
00041:C          LOBE RADIAL CLEARANCE))
00042:C*************************************************************************
00043:       DO 10 J=1,M+1
00044:       DO 10 I=1,N+1
00045:       P1(I,J)=0.0
00046:       P11(I,J)=0.0
00047:       P2(I,J)=0.0
00048:       P22(I,J)=0.0
00049:       P3(I,J)=0.0
00050:       P33(I,J)=0.0
00051:       H1(I,J)=0.0
00052:       H2(I,J)=0.0
00053:       H3(I,J)=0.0
00054:    10 CONTINUE
00055:C*************************************************************************
00056:       WRITE(3,600)
00057:   600 FORMAT(103H                                        THE  SOLUTION  OF  REYNO
00058:      2LDS  EQUATION  FOR  THREE  LOBE  JOURNAL BEARING/,100H************
00059:      3************************************************************
00060:      4**********************)
00061:       WRITE(3,610)
00062:   610 FORMAT(54H      EPS      MAXIT      EB      L      D      M      ELIPIT)
00063:       WRITE(3,620)EPS,MAXIT,EB,L,D,M,ELIPIT
00064:   620 FORMAT(3X,F7.5,4X,I3,3X,F6.4,4X,I5,3X,F5.3,2X,I3,5X,F5.3/,55H***
00065:      2*************************************************)
00066:C*************************************************************************
00067:       EMEU=1.0-(((3.14**2)*(4.0+(3.14*D/FLOAT(L))**2))/(2.0*((FLOAT(
00068:      4M/2))*FLOAT(M/2))+(3.14*D*FLOAT(N)/FLOAT(L))**2)))
00069:C       OMEGA IS THE OVER RELAXATION FACTOR
00070:       OMEGA=2.0*((1.0-(1.0-EMEU**2)**0.5)/(EMEU**2))
```

```
00071:       WRITE(3,680)OMEGA
00072:   680 FORMAT(36H THE OVER RELAXATION FACTOR OMEGA = ,F8.4/,45H**********
00073:      2**********************************)
00074:C*************************************************************************
00075:C       ALPHA     IC  THE  ATTITUDE  ANGLE
00076:       ALPHA=35.0*3.14/180.0
00077:       DO 12345 W=1,8
00078:       ALPHA=ALPHA*180.0/3.14
00079:       WRITE(3,730)ALPHA
00080:   730 FORMAT(91H                                                    THE  B
00081:      2EARING  ATTITUDE  ANGLE  ALPHA  =  ,F10.6/,100H**********************
00082:      3*************************************************************
00083:      4****************)
00084:C*************************************************************************
00085:       ALPHA=ALPHA*3.14/180.0
00086:       E=EB*(1.0-ELIPIT)
00087:C       E       IS THE BEARING ECCENTRICITY RATIO  ((BEARING ECCENTRICITTY/LOBE
00088:C                RADIAL CLEARANCE))
00089:C       EL1,EL2,AND EL3 ARE THE DIFFERENT LOBES ECCENTRICITY RATIO
00090:C       ALPHA1,ALPHA2,AND ALPHA3 ARE THE LOBESATTITUDE ANGLES
00091:C       THETA1,THETA2,AND THETA3 ARE THE ANGLES MEASURED FROM THE OIL INLET
00092:C           POINT TO THE POINT OF MINIMUM OIL FILM THICKNESS IN THE CONVERGINCE
00093:C             ZONE
00094:C*************************************************************************
00095:       EL1=((E**2)+(ELIPIT**2)+(2.0*E*ELIPIT*COS(ALPHA)))**0.5
00096:       ALPHA1=(ASIN((E*SIN(ALPHA)/EL1)))*180.0/3.14
00097:       THETA1=50.0+ALPHA1
00098:       EL2=((E**2+ELIPIT**2-2.0*E*ELIPIT*COS((3.14/3.0)-ALPHA))**0.5)
00099:       ALPHA0=(ASIN((E*SIN((3.14/3.0)-ALPHA)/EL2))-2.0*3.14/3.0)*180.0/3.
00100:      414
00101:       ALPHA2=-ALPHA0
00102:       THETA2=50.0+120.0-ALPHA2
00103:       EL3=((E**2+(ELIPIT**2)+(2.0*E*ELIPIT*COS((3.14*2.0/3.0)-ALPHA)
00104:      2)))**0.5
00105:       ALPHA3=((2.0*3.14/3.0)-(ASIN(E*SIN((3.14*2.0/3.0)-ALPHA)/EL3)))*18
00106:      20.0/3.14
```

```
00143:       DO 100 I=2,N
00144:       DO 100 J=3,M,2
00145:C       THE NEXT STATEMEBT IS THE REYNOLDS EQUATION FOR STEADY STATE CONDITION,
00146:C       REPRSENTED IN A FINITE DIFFEREENCE FORM
00147:C       P(I,J)       IS THE DIMENIONSLESS PRESSURE AT THE MESH POINTS
00148:       A1=((18.84/DX)*(H1(I,J-1)-H1(I,J+1)))
00149:       B1=((R/T)*((H1(I+1,J))**3)*(P1(I+1,J)))
00150:       C1=((1.0/S)*((H1(I,J+1))**3)*(P1(I,J+2)))
00151:       D1=((R/T)*((H1(I-1,J))**3)*(P1(I-1,J)))
00152:       E1=((1.0/S)*((H1(I,J-1))**3)*(P1(I,J-2)))
00153:       F1=((R/T)*((H1(I+1,J))**3))
00154:       Q1=((1.0/S)*((H1(I,J+1))**3))
00155:       Y1=((R/T)*((H1(I-1,J))**3))
00156:       Z1=((1.0/S)*((H1(I,J-1))**3))
00157:       PNEW1=OMEGA*((A1+B1+C1+D1+E1)/(F1+Q1+Y1+Z1))+B*P1(I,J)
00158:C*************************************************************************
00159:       IF(J.GE.(THETA1/2.0)) GO TO 888
00160:       P11(I,J)=P1(I,J)
00161:       RESID=ABS(PNEW1-P11(I,J))
00162:       IF(RESID.GT.DA) DA=RESID
00163:  888 P1(I,J)=PNEW1
00164:       IF(J.GT.(THETA1/2.0).AND.P1(I,J).LT.0.0) P1(I,J)=0.0
00165:  100 CONTINUE
00166:       ITN=ITN+1
00167:       IF(ITN.GT.MAXIT) STOP
00168:       IF(DA.GT.EPS) GO TO 90
00169:C*************************************************************************
00170:       SUMC1=0.0
00171:       SUMC11=0.0
00172:       SUMS1=0.0
00173:       SUMS11=0.0
00174:       G11=(180.0-THETA1)*3.14/180.0
00175:C*************************************************************************
00176:       DO 110 J=1,M+1,2
00177:       DO 120 I=1,N+1
00178:C*************************************************************************
```

```
00179:C       SUMC1,SUMC2,AND SUMC3 ARE THE HYDRODYNAMIC FORCE IN THE DIRECTION OF
00180:C       THE ATTITUDE LINE FROM ONE COLUMN OF THE MESH
00181:C*******************************************************************************
00182:C       SUMC11,SUMC22,AND SUMC33 ARE THE TOTAL HYDRODYNAMIC FORCE IN THE
00183:C       DIRECTION THE ATTITUDE LINE
00184:C*******************************************************************************
00185:C       SUMS1,SUMS2,AND SUMS3 ARE THE HYDRODYNAMIC FORCE IN THE DIRECTION PERPEND
00186:C       ICULAR ON THE ATTITUDE LINE FOR ONE COLUMN OF THE MESH
00187:C*******************************************************************************
00188:C       SUMS11,SUMS22,AND SUMS33 ARE THE TORAL HYDRODYNAMIC FORCE IN THE DIRECTIO
00189:C       N PERPENDICULAR ON THE ATTITUDE LINE
00190:C*******************************************************************************
00191:        SUMC1=SUMC1+P1(I,J)*DX*DY*COS(G11)
00192:        SUMS1=SUMS1+P1(I,J)*DX*DY*SIN(G11)
00193:    120 CONTINUE
00194:C*******************************************************************************
00195:C*******************************************************************************
00196:        G11=G11+(4.0*3.14/180.0)
00197:        SUMC11=SUMC1+SUMC11
00198:        SUMS11=SUMS1+SUMS11
00199:        SUMC1=0.0
00200:        SUMS1=0.0
00201:    110 CONTINUE
00202:C*******************************************************************************
00203:        FCOS1=SUMC11
00204:        FSIN1=SUMS11
00205:C        FROM HERE TO STATEMENT NUMBER 722 THE ROUTINE IS USED FOR THE SECOND LOBE
00206:C*******************************************************************************
00207:        G2=(THETA2)*3.14/180.0
00208:        DO 32 J=1,M+1
00209:        DO 22 I=1,N+1
00210:        H2(I,J)=(1.0-EL2*COS(G2))/2.0
00211:     22 CONTINUE
00212:C*******************************************************************************
00213:     32 G2=G2-(2.0*3.14/180.0)
00214:C*******************************************************************************
```

```
00215:       DO 52 I=2,N
00216:    52 P2(I,1)=0.0
00217:       DO 62 I=2,N
00218:    62 P2(I,M+1)=0.0
00219:       DO 72 J=2,M
00220:    72 P2(1,J)=0.0
00221:       DO 82 J=2,M
00222:    82 P2(N+1,J)=0.0
00223:       ITN=1
00224:       B=1.0-OMEGA
00225:    92 DA=0.0
00226:C*************************************************************************
00227:       DO 102 J=3,M,2
00228:       DO 102 I=2,N
00229:C*************************************************************************
00230:       A2=((18.84/DX)*(H2(I,J-1)-H2(I,J+1)))
00231:       B2=((R/T)*((H2(I+1,J))**3)*(P2(I+1,J)))
00232:       C2=((1.0/S)*((H2(I,J+1))**3)*(P2(I,J+2)))
00233:       D2=((R/T)*((H2(I-1,J))**3)*(P2(I-1,J)))
00234:       E2=((1.0/S)*((H2(I,J-1))**3)*(P2(I,J-2)))
00235:       F2=((R/T)*((H2(I+1,J))**3))
00236:       Q2=((1.0/S)*((H2(I,J+1))**3))
00237:       Y2=((R/T)*((H2(I-1,J))**3))
00238:       Z2=((1.0/S)*((H2(I,J-1))**3))
00239:       PNEW2=OMEGA*((A2+B2+C2+D2+E2)/(F2+Q2+Y2+Z2))+B*P2(I,J)
00240:C*************************************************************************
00241:       IF(J.GE.(THETA2/2.0)) GO TO 882
00242:       P22(I,J)=P2(I,J)
00243:       RESID=ABS(PNEW2-P22(I,J))
00244:       IF(RESID.GT.DA) DA=RESID
00245:   882 P2(I,J)=PNEW2
00246:       IF(J.GT.(THETA2/2.0).AND.P2(I,J).LT.0.0) P2(I,J)=0.0
00247:   102 CONTINUE
00248:C*************************************************************************
00249:       ITN=ITN+1
00250:       IF(ITN.GT.MAXIT) STOP
```

```
00251:       IF(DA.GT.EPS) GO TO 92
00252:       SUMC2=0.0
00253:       SUMC22=0.0
00254:       SUMS2=0.0
00255:       SUMS22=0.0
00256:       G22=(180.0-THETA2)*3.14/180.0
00257:C*************************************************************************
00258:       DO 112 J=1,M+1,2
00259:       DO 122 I=1,N+1
00260:       SUMC2=SUMC2+P2(I,J)*DX*DY*COS(G22)
00261:       SUMS2=SUMS2+P2(I,J)*DX*DY*SIN(G22)
00262:   122 CONTINUE
00263:C*************************************************************************
00264:       G22=G22+(4.0*3.14/180.0)
00265:       SUMC22=SUMC2+SUMC22
00266:       SUMS22=SUMS2+SUMS22
00267:       SUMC2=0.0
00268:       SUMS2=0.0
00269:   112 CONTINUE
00270:       FCOS2=SUMC22
00271:       FSIN2=SUMS22
00272:C*************************************************************************
00273:C       FROM HERE TO STATEMENT NUMBER 723 THE ROUTINE IS USED FOR THE THIRD
00274:C       LOBE
00275:       G3=(THETA3)*3.14/180.0
00276:       DO 33 J=1,M+1
00277:       DO 23 I=1,N+1
00278:       H3(I,J)=(1.0-EL3*COS(G3))/2.0
00279:    23 CONTINUE
00280:    33 G3=G3-(2.0*3.14/180.0)
00281:C*************************************************************************
00282:       DO 53 I=2,N
00283:    53 P3(I,1)=0.0
00284:       DO 63 I=2,N
00285:    63 P3(I,M+1)=0.0
00286:       DO 73 J=2,M
```

```
00287:    73 P3(1,J)=0.0
00288:       DO 83 J=2,M
00289:    83 P3(N+1,J)=0.0
00290:C*************************************************************************
00291:       ITN=1
00292:       B=1.0-OMEGA
00293:    93 DA=0.0
00294:C*************************************************************************
00295:       DO 103 I=2,N
00296:       DO 103 J=3,M,2
00297:C*************************************************************************
00298:       A3=((18.84/DX)*(H3(I,J-1)-H3(I,J+1)))
00299:       B3=((R/T)*((H3(I+1,J))**3)*(P3(I+1,J)))
00300:       C3=((1.0/S)*((H3(I,J+1))**3)*(P3(I,J+2)))
00301:       D3=((R/T)*((H3(I-1,J))**3)*(P3(I-1,J)))
00302:       E3=((1.0/S)*((H3(I,J-1))**3)*(P3(I,J-2)))
00303:       F3=((R/T)*((H3(I+1,J))**3))
00304:       Q3=((1.0/S)*((H3(I,J+1))**3))
00305:       Y3=((R/T)*((H3(I-1,J))**3))
00306:       Z3=((1.0/S)*((H3(I,J-1))**3))
00307:       PNEW3=OMEGA*((A3+B3+C3+D3+E3)/(F3+Q3+Y3+Z3))+B*P3(I,J)
00308:C*************************************************************************
00309:       IF(J.GE.(THETA3/2.0)) GO TO 883
00310:       P33(I,J)=P3(I,J)
00311:       RESID=ABS(PNEW3-P33(I,J))
00312:       IF(RESID.GT.DA) DA=RESID
00313:   883 P3(I,J)=PNEW3
00314:       IF(J.GT.(THETA3/2.0).AND.P3(I,J).LT.0.0) P3(I,J)=0.0
00315:   103 CONTINUE
00316:C*************************************************************************
00317:       ITN=ITN+1
00318:       IF(ITN.GT.MAXIT) STOP
00319:       IF(DA.GT.EPS) GO TO 93
00320:       WRITE(3,693)ITN
00321:   693 FORMAT(21H  CYCLE NUMBER ITN = ,I5//,21H**********)
00322:C*************************************************************************
```

```
00323:       SUMC3=0.0
00324:       SUMC33=0.0
00325:       SUMS3=0.0
00326:       SUMS33=0.0
00327:       G33=(180.0-THETA3)*3.14/180.0
00328:C*************************************************************************
00329:       DO 113 J=1,M+1,2
00330:       DO 123 I=1,N+1
00331:       SUMC3=SUMC3+P3(I,J)*DX*DY*COS(G33)
00332:       SUMS3=SUMS3+P3(I,J)*DX*DY*SIN(G33)
00333:   123 CONTINUE
00334:C*************************************************************************
00335:       G33=G33+(4.0*3.14/180.0)
00336:       SUMC33=SUMC3+SUMC33
00337:       SUMS33=SUMS3+SUMS33
00338:       SUMC3=0.0
00339:       SUMS3=0.0
00340:   113 CONTINUE
00341:C*************************************************************************
00342:       FCOS3=SUMC33
00343:       FSIN3=SUMS33
00344:C*************************************************************************
00345:C       FHT    IS THE SUMMATION OF THE HORIZONTAL COMPONENT OF THE FORCES ((((((
00346:C       FCOS11,FCOS22,FCOS33,FSIN11,FSIN22,FSIN33))))))) FUT MUST BE EQUAL TO
00347:C       ZERO TO SATISFY THE BALANCR CONDITION
00348:C*************************************************************************
00349:C       FVT     IS THE SUMMATION OF ALL THE VERTICAL COMPONENT OF THE FORCES(((((
00350:C       FCOS11,FCOS22,FCOS33,FSIN11,FSIN22,FSIN33)))))).    FVT IS EQUAL TO THE B
00351:C              B E A R I N G    D E U T Y    P A R A M E T E R
00352:C*************************************************************************
00353:       ALPHA1=ALPHA1*3.14/180.0
00354:       ALPHA2=ALPHA2*3.14/180.0
00355:       ALPHA3=ALPHA3*3.14/180.0
00356:       FT1=SQRT((FCOS1**2)+(FSIN1**2))
00357:       IF(FSIN1.EQ.0.0.AND.FCOS1.EQ.0.0) GO TO 7171
00358:       PHI1=ATAN(-FSIN1/FCOS1)
```

```
00359:       GO TO 4141
00360: 7171 PHI1=0.0
00361: 4141 IF(PHI1.GT.ALPHA1) GO TO 9191
00362:       GO TO 9292
00363: 9191 PHI11=(PHI1-ALPHA1)
00364:       FH1=FT1*SIN(PHI11)
00365:       FV1=FT1*COS(PHI11)
00366:       GO TO 9393
00367: 9292 IF(PHI1.LT.ALPHA1) PHI11=(ALPHA1-PHI1)
00368:       FH1=-FT1*SIN(PHI11)
00369:       FV1=FT1*COS(PHI11)
00370: 9393 FT2=SQRT((FCOS2**2)+(FSIN2**2))
00371:       IF(FSIN2.EQ.0.0.AND.FCOS2.EQ.0.0) GO TO 7272
00372:       PHI2=ATAN(-FSIN2/FCOS2)
00373:       GO TO 4242
00374: 7272 PHI2=0.0
00375: 4242 IF(ALPHA2.GT.1.57) GO TO 9494
00376:       GO TO 9595
00377: 9494 PHI22=(ALPHA2-1.57+PHI2)
00378:       FH2=FT2*COS(PHI22)
00379:       FV2=-FT2*SIN(PHI22)
00380:       GO TO 9696
00381: 9595 IF(ALPHA2.LT.1.57) PHI22=(1.57-ALPHA2-PHI2)
00382:       FH2=FT2*COS(PHI22)
00383:       FV2=FT2*SIN(PHI22)
00384: 9696 FT3=SQRT((FCOS3**2)+(FSIN3**2))
00385:       IF(FSIN3.EQ.0.0.AND.FCOS3.EQ.0.0) GO TO 7373
00386:       PHI3=ATAN(-FSIN3/FCOS3)
00387:       GO TO 4343
00388: 7373 PHI3=0.0
00389: 4343 IF(ALPHA3.LT.1.57) GO TO 9797
00390:       GO TO 9898
00391: 9797 PHI33=(1.57-ALPHA3+PHI3)
00392:       FH3=-FT3*COS(PHI33)
00393:       FV3=+FT3*SIN(PHI33)
00394:       GO TO 9899
```

```
00395: 9898 IF(ALPHA3.GT.1.57) PHI33=(ALPHA3-1.57-PHI3)
00396:      FH3=-FT3*COS(PHI33)
00397:      FV3=-FT3*SIN(PHI33)
00398: 9899 FHT=FH1+FH2+FH3
00399:      FVT=FV1+FV2+FV3
00400:      FTO=SQRT(FHT**2+FVT**2)
00401:      IF(FHT.GT.0.0) ALPH11=ACOS(FVT/FTO)
00402:      IF(FHT.LT.0.0) ALPH11=ASIN(FHT/FTO)
00403:      ALPH11=ALPH11*180.0/3.14
00404:C*************************************************************************
00405:  333 WRITE(3,640)
00406:  640 FORMAT(116H        E        EL1        EL2        EL3        ALPHA1
00407:     2   ALPHA2        ALPHA3        THETA1        THETA2        THETA3//,10
00408:     30H**************************************************************
00409:     4**********************************)
00410:      WRITE(3,650)E,EL1,EL2,EL3,ALPHA1,ALPHA2,ALPHA3,THETA1,THETA2,THETA
00411:     13
00412:  650 FORMAT(4X,F7.4,2X,F7.4,2X,F7.4,2X,F7.4,3X,F6.3,7X,F6.3,7X,F6.3,7X,
00413:     4F6.3,7X,F6.3,7X,F6.3/,100H**************************************
00414:     5************************************************************)
00415:C*************************************************************************
00416:      WRITE(3,810)DY,DX
00417:  810 FORMAT(25H                          DY = ,F15.8,45H
00418:     2                    DX = ,F15.8/,100H*****************************
00419:     4************************************************************
00420:     5****)
00421:      ALPHA=ALPHA*180.0/3.14
00422:      WRITE(3,5155)ALPHA
00423: 5155 FORMAT(60H                                    THE  ATTITUDE  ANGLE  ALPH
00424:     2A = ,F10.6/,100H*****************************************************
00425:     4*****************************************)
00426:      WRITE(3,5555)FHT
00427: 5555 FORMAT(67H                                    THE  TOTAL  HORIZONTAL  FO
00428:     2RCE  FHT = ,F15.8/,100H**********************************************
00429:     3*****************************************************)
00430:C*************************************************************************
```

```
00431:       WRITE(3,6666)FVT
00432: 6666 FORMAT(59H                        THE TOTAL VERTICAL   FVT
00433:      2 = ,F15.8/,100H**************************************************
00434:      3**************************************************)
00435:C*****************************************************************************
00436:       WRITE(3,77777)FTO
00437:77777 FORMAT(67H                                              THE  TOTA      FO
00438:      2RCE  FTO = ,F15.8/,100H**************************************************
00439:      3**************************************************)
00440:C*****************************************************************************
00441: 1333 WRITE(3,555)ALPH11
00442:  555 FORMAT(60H                                         THE  LOAD      ANGLE  ALPH
00443:      211= ,F10.6/,100H**************************************************
00444:      4**************************************************)
00445:C       THE FOLLOWING ROUTINE IS USED TO CALCULATE THE FLOW COEFFICIENTFFOR EACH
00446:C       H LOBE
00447:C       FLOCO1 , FLOCO2 , FLOCO3     ARE THE HYDRODYNAMIC OIL FLOW COEFCIENT
00448:C         FOR THE BEARING LOBES
00449:C*****************************************************************************
00450:       FLOCO1=0.0
00451:       FLOCO2=0.0
00452:       FLOCO3=0.0
00453:       DO 1000 J=3,M+1,2
00454:       FLOCO1=FLOCO1+((2.0/(9.42))*((D/FLOAT(L))**2)*(P1(N,J))*((H1(N,J)
00455:      2)**3))
00456:       FLOCO2=FLOCO2+((2.0/(9.42))*((D/FLOAT(L))**2)*(P2(N,J))*((H2(N,J)
00457:      2)**3))
00458:       FLOCO3=FLOCO3+((2.0/(9.42))*((D/FLOAT(L))**2)*(P3(N,J))*((H3(N,J)
00459:      2)**3))
00460: 1000 CONTINUE
00461:       WRITE(3,7777)FLOCO1
00462: 7777 FORMAT(75H                                         THE FIRST  LOBE  FLOW  COE
00463:      2FFICIENT  FLOCO1 = ,F15.8/,100H**************************************
00464:      3**************************************************)
00465:C*****************************************************************************
00466:       WRITE(3,7778)FLOCO2
```

```
00467: 7778 FORMAT(71H                                          THE SECOND LOBE FLOW COEFF
00468:      2ICIENT FLOCO2 = ,F15.8/,100H**************************************
00469:      3**************************************************)
00470:       WRITE(3,7779)FLOCO3
00471: 7779 FORMAT(71H                                          THE THIRD  LOBE FLOW COEFF
00472:      2ICIENT FLOCO3 = ,F15.8/,100H
00473:      3 **************************************************)
00474:C*************************************************************************
00475:C         TFLOCO  IS THE TOTAL OIL FLOW COEFFICITNT
00476:       TFLOCO=FLOCO1+FLOCO2+FLOCO3
00477:       WRITE(3,7770)TFLOCO
00478: 7770 FORMAT(73H                                              THE TOTAL FLOW COEF
00479:      2FICIENT TFLOCO = ,F15.8/,100H**************************************
00480:      3**************************************************)
00481:C      WRITE(3,713)((P1(I,J),J=3,M+1,2),I=2,14)
00482:C 713 FORMAT(2X,12(F9.5))
00483:C*************************************************************************
00484:67676 CONTINUE
00485:       ALPHA=ALPHA*3.14/180.0
00486:       ALPHA=ALPHA+5.0*3.14/180.0
00487:12345 CONTINUE
00488:       EB=EB+0.1
00489:     1 CONTINUE
00490:       L=L+1
00491:     3 CONTINUE
00492:       STOP
00493:       END
BOTTOM
```

The following subroutine can be used with the main computer programme to solve for non-zero boundary conditions at the low pressure inlets. The solution is required to calculate the total oil flow coefficient.

```
00128:       PF=3.0
00129:       DO 50 I=3,27
00130:       DO 50 J=1,5,2
00131:       P1(I,J)=PF
00132:    50 CONTINUE
00133:       DO 60 I=3,27
00134:       DO 60 J=57,61,2
00135:       P1(I,J)=PF
00136:    60 CONTINUE
00150:       DO 100 J=3,M,2
00151:       IF(I.GT.1.AND.I.LT.28) GO TO 1515
00152:       GO TO 2525
00153: 1515 IF(J.GT.0.AND.J.LT.6) GO TO 100
00154:       IF(J.GT.56.AND.J.LT.62) GO TO 100
00224:       DO 52 I=3,27
00225:       DO 52 J=1,5,2
00226:       P2(I,J)=PF
00227:    52 CONTINUE
00228:       DO 62 I=3,27
00229:       DO 62 J=57,61,2
00230:       P2(I,J)=PF
00244: 3535 IF(J.GT.0.AND.J.LT.6) GO TO 102
00245:       IF(J.GT.56.AND.J.LT.62) GO TO 102
00299:       DO 53 I=3,27
00300:       DO 53 J=1,5,2
00301:       P3(I,J)=PF
00302:    53 CONTINUE
00303:       DO 63 I=3,27
00304:       DO 63 J=53,61,2
00305:       P3(I,J)=PF
00320:     5 IF(J.GT.0.AND.J.LT.6) GO TO 103
00321:       IF(J.GT.56.AND.J.LT.62) GO TO 103
```

A.2.1a. SAMPLE OF THE OUTPUT.

THE SOLUTION OF REYNOLDS EQUATION FOR THREE LOBE JOURNAL BEARING

EPS	MAXIT	EB	L	D	ID	ELIPIT
.00100	100	.1000	1	2.000	50	.700

THE OVER RELAXATION FACTOR OMEGA = 1.7910

CYCLE COUNTER ITR = 50

E	EL1	EL2	EL3	ALPHA1	ALPHA2	ALPHA3	THETA1	THETA2
.0500	.7252	.6719	.7056	.027	2.076	2.051	51.528	50.875

DY = -.05466669 DX = -.05488889

THE ATTITUDE ANGLE ALPHA = 40.000000

THE TOTAL HORIZONTAL FORCE FHT = -.02556076

THE TOTAL VERTICAL FVT = 1.11761951

THE TOTAL FORCE FTO = 1.11791177

THE LOAD ANGLE ALPHAT= -1.310855

THE FIRST LOBE FLOW COEFFICIENT FLOCO1 = .11176701

THE SECOND LOBE FLOW COEFFICIENT FLOCO2 = .10291751

THE THIRD LOBE FLOW COEFFICIENT FLOCO3 = .08960848

THE TOTAL FLOW COEFFICIENT TFLOCO = .30429280

THE BEARING ATTITUDE ANGLE ALPHA = 55.000000

E	EL1	EL2	EL3	ALPHA1	ALPHA2	ALPHA3	THETA1	THETA2
.1200	.6013	.5954	.7205	4.9260	115.0972	110.4457	54.928	

CYCLE NUMBER IN = 44

E	EL1	EL2	EL3	ALPHA1	ALPHA2	ALPHA3	THETA1	THETA2
.1200	.7095	.5369	.7405	.1116	2.040	1.936	56.171	55.044

DY = .05486869 DX = .03488889

THE ATTITUDE ANGLE ALPHA = 45.000000

THE TOTAL HORIZONTAL FORCE FHT = .19732651

THE TOTAL VERTICAL FVT = 8.65309570

THE TOTA FO RCE FTO = 8.65534342

THE LOAD ANGLE ALPHT1= 1.307018

THE FIRST LOBE FLOW COEFFICIENT FLOCO1 = .07536860

THE SECOND LOBE FLOW COEFFICIENT FLOCO2 = .05546851

THE THIRD LOBE FLOW COEFFICIENT FLOCO3 = .02994338

THE TOTAL FLOW COEFFICIENT TFLOCO = .15680028

****

THE SOLUTION OF REYNOLDS EQUATION FOR THREE LOBE JOURNAL BEARING

****

EPS	MAXIT	EB	L	D	N	ELIPIT
.00100	100	.1000	1	2.000	50	.800

** **********

THE OVER RELAXATION FACTOR OMEGA = 1.7916

****

THE BEARING ATTITUDE ANGLE ALPHA = 55.000000

****

E	EL1	EL2	EL3	ALPHA1	ALPHA2	ALPHA3	THETA1	THETA2
.0200	.8165	.7819	.8020	.8051	119.3806	118.5759	50.805	50.619

THETA3

48.595

****

DY = .03488889 DX = .03488889

****

THE ATTITUDE ANGLE ALPHA = 55.000000

****

THE TOTAL HORIZONTAL FORCE FHT = -.22175813

****

THE TOTAL VERTICAL FVT = 2.28507890

****

THE TOTAL FORCE FTO = 2.29581407

****

THE LOAD ANGLE ALPHA1= -5.545789

****

THE FIRST LOBE FLOW COEFFICIENT FLOCO1 = .11471675

****

THE SECOND LOBE FLOW COEFFICIENT FLOCO2 = .11155480

****

THE THIRD LOBE FLOW COEFFICIENT FLOCO3 = .10131853

****

A2.2 THE DESIGN PROGRAMME

```
.NULL.
00001:JOB(GREM114A,J9,T30,M7600)          T.  M.  S A L E M     MECH. ENG. DEPT.
00002:MNF(T)
00003:LDSET(MAP=B/ZZZZMP,PRESET=ZERO)
00004:LGO.
00005:@
00006:       PROGRAM BE1(INPUT,OUTPUT,TAPE4=INPUT,TAPE3=OUTPUT)
00007:       COMMON L,D,P,V,EO,C,OFFSET,HF,FO,T1,FLOCO,MEU1,N,TO,MEU2,QO,QH,QT,
00008:      2CMIN,CMAX,CM,A11,A12,A21,A22,PHI,DY,N1,F,HS,T2,PX1T,PY1T,PTOTAL,AL
00009:      3PHA,S,MEU11,MEU22
00010:       REAL L1,L,M,N,MEU1,MEU2,MEU11,MEU22
00011:       INTEGER V
00012:C*************************************************************************
00013:C                        SHELL VIT . 150
00014:C                        ---------------
00015:C                TEMP. DEGREE CEN.                VISCOSITT IN POISE
00016:C                  ------------                    ---------------
00017:C                       30.0                            2.19
00018:C                       35.0                            1.66
00019:C                       40.0                            1.316
00020:C                       45.0                            1.033
00021:C                       50.0                            0.746
00022:C                       55.0                            0.614
00023:C                       60.0                            0.480
00024:C                       65.0                            0.395
00025:C                       70.0                            0.325
00026:C                       75.0                            0.270
00027:C*************************************************************************
00028:C
00029:C
00030:C                              TELLUS  OIL
00031:C                              -----------
00032:C       TEMP.          R41          R33          R27          R23
00033:C       -----          ---          ---          ---          ---
00034:C       30.0           1.4          0.877        0.530        0.310
```

```
00035:C      35.0          1.05          0.658          0.410          0.250
00036:C      40.0          0.81          0.526          0.330          0.200
00037:C      45.0          0.636         0.421          0.260          0.170
00038:C      50.0          0.510         0.342          0.220          0.140
00039:C      55.0          0.377         0.281          0.175          0.127
00040:C      60.0          0.324         0.230          0.150          0.100
00041:C      65.0          0.281         0.193          0.132          0.088
00042:C      70.0          0.232         0.161          0.110          0.075
00043:C      75.0          0.193         0.140          0.096          0.068
00044:C*******==========**********==========**********
00045:       C=0.004*2.54
00046:       DO 34567 V=1,5
00047:       WRITE(3,10)
00048:    10 FORMAT(115H                          THE CALCULATION OF THE POWER LOSS,
00049:      2OUTLET TEMPERATURE,THE OPERATING VISCOSITY AND THE STIFFNESS/,57H
00050:      3                                   FOR THE THREE LOBE BEARING/,111H****
00051:      6**********
00052:      5**********)
00053:       L=12.7
00054:C       L       IS THE BEARING LENGTH
00055:       D=13.5
00056:       MEU11=1.66
00057:       MEU22=0.746
00058:       AA=ALOG(MEU11/MEU22)
00059:       ALPHA=AA/15.0
00060:C       D       IS THE BEARING DIAMETER
00061:       P=1.5
00062:C       P       IS THE SUPPLY PRESSURE
00063:C       EO      IS THE OFFSET RATIO
00064:C       C       IS THE DIAMETERAL CLEARANCE
00065:       EO=0.8
00066:       C=CMIN/(1,0-EO)
00067:       OFFSET=EO*C/2.0
00068:C       OFFSET       IS THE DISTANCE BETWEEN THE LOBE
00069:C                    CENTRE AND THE BEARING CENTRE
00070:C       T1      IS THE OIL INLET TEMPERATURE
```

```
00071:C      CMIN=C-(2.0*OFFSET)
00072:       CMAX=CMIN*(1.0-(EO/2.0))/(1.0-EO)
00073:       CM=CMIN+(0.65*(CMAX-CMIN))
00074:       EB=0.0
00075:       QP=0.0
00076:       QH=0.0
00077:       DO 5 K=1,5
00078:       CALL TAREK3
00079:       T1=30.0
00080:       DO 20 I=1,3
00081:       IF(T1.EQ.30.0) MEU1=0.53
00082:C       MEU1     IS THE OIL VISCOSITY AT THE OIL INLETS
00083:       IF(T1.EQ.40.0) MEU1=0.33
00084:       IF(T1.EQ.50.0) MEU1=0.22
00085:       N=1000.0
00086:C       N       IS THE SHAFT ROTATON SPEED
00087:       DO 30 J=1,10
00088:       TO=70.0
00089:       GO TO 8
00090:     7 TO=TO-1.0
00091:       GO TO 8
00092:    11 TO=TO+1.0
00093:       GO TO 8
00094:    12 TO=TO+0.5
00095:       GO TO 8
00096:    13 TO=TO-0.5
00097:     8 MEU2=MEU11*((2.73)**(-ALPHA*(TO-35.0)))
00098:       PO=(P*60.0*980000.0)*((C/D)**2)/(MEU2*N)
00099:       IF(EO.EQ.0.0.AND.EB.EQ.0.0) FLOCO=0.0+(0.38*PO)
00100:       IF(EO.EQ.0.0.AND.EB.EQ.0.2) FLOCO=0.16+(0.385*PO)
00101:       IF(EO.EQ.0.0.AND.EB.EQ.0.4) FLOCO=0.3+(0.5*PO)
00102:       IF(EO.EQ.0.4.AND.EB.EQ.0.0) FLOCO=098+(0.12*PO)
00103:       IF(EO.EQ.0.4.AND.EB.EQ.0.2) FLOCO=0.115+(0.152*PO)
00104:       IF(EO.EQ.0.4.AND.EB.EQ.0.4) FLOCO=0.17+(0.1906*PO)
00105:       IF(EO.EQ.0.4.AND.EB.EQ.0.6) FLOCO=0.239+(0.2042*PO)
00106:       IF(EO.EQ.0.4.AND.EB.EQ.0.8) FLOCO=0.287+(0.2542*PO)
```

```
00107:       IF(EO.EQ.0.3.AND.EB.EQ.0.0) FLOCO=0.075+(0.205*PO)
00108:       IF(EO.EQ.0.3.AND.EB.EQ.0.2) FLOCO=0.111+(0.209*PO)
00109:       IF(EO.EQ.0.3.AND.EB.EQ.0.4) FLOCO=0.192+(0.2344*PO)
00110:       IF(EO.EQ.0.3.AND.EB.EQ.0.6) FLOCO=0.278+(0.2844*PO)
00111:       IF(EO.EQ.0.3.AND.EB.EQ.0.8) FLOCO=0.362+(0.3556*PO)
00112:       IF(EO.EQ.0.45.AND.EB.EQ.0.0) FLOCO=0.109+(0.11*PO)
00113:       IF(EO.EQ.0.45.AND.EB.EQ.0.2) FLOCO=0.12+(0.117*PO)
00114:       IF(EO.EQ.0.45.AND.EB.EQ.0.4) FLOCO=0.141+(0.14*PO)
00115:       IF(EO.EQ.0.45.AND.EB.EQ.0.6) FLOCO=0.165+(0.153*PO)
00116:       IF(EO.EQ.0.45.AND.EB.EQ.0.8) FLOCO=0.222+(0.185*PO)
00117:       IF(EO.EQ.0.35.AND.EB.EQ.0.0) FLOCO=0.087+(0.16*PO)
00118:       IF(EO.EQ.0.35.AND.EB.EQ.0.2) FLOCO=0.11+(0.16*PO)
00119:       IF(EO.EQ.0.35.AND.EB.EQ.0.4) FLOCO=0.14+(0.18*PO)
00120:       IF(EO.EQ.0.35.AND.EB.EQ.0.6) FLOCO=0.2+(0.22*PO)
00121:       IF(EO.EQ.0.35.AND.EB.EQ.0.8) FLOCO=0.26+(0.27*PO)
00122:       IF(EO.EQ.0.6.AND.EB.EQ.0.0) FLOCO=0.098+(0.054*PO)
00123:       IF(EO.EQ.0.6.AND.EB.EQ.0.2) FLOCO=0.169+(0.056*PO)
00124:       IF(EO.EQ.0.6.AND.EB.EQ.0.4) FLOCO=0.182+(0.062*PO)
00125:       IF(EO.EQ.0.6.AND.EB.EQ.0.6) FLOCO=0.205+(0.074*PO)
00126:       IF(EO.EQ.0.6.AND.EB.EQ.0.8) FLOCO=0.239+(0.0883*PO)
00127:       IF(EO.EQ.0.7.AND.EB.EQ.0.0) FLOCO=0.183+(0.036*PO)
00128:       IF(EO.EQ.0.7.AND.EB.EQ.0.2) FLOCO=0.184+(0.037*PO)
00129:       IF(EO.EQ.0.7.AND.EB.EQ.0.4) FLOCO=0.188+(0.04*PO)
00130:       IF(EO.EQ.0.7.AND.EB.EQ.0.6) FLOCO=0.197+(0.044*PO)
00131:       IF(EO.EQ.0.7.AND.EB.EQ.0.8) FLOCO=0.209+(0.051*PO)
00132:       IF(EO.EQ.0.8.AND.EB.EQ.0.0) FLOCO=0.194+(0.023*PO)
00133:       IF(EO.EQ.0.8.AND.EB.EQ.0.2) FLOCO=0.194+(0.0233*PO)
00134:       IF(EO.EQ.0.8.AND.EB.EQ.0.4) FLOCO=0.195+(0.0277*PO)
00135:       IF(EO.EQ.0.8.AND.EB.EQ.0.6) FLOCO=0.196+(0.0277*PO)
00136:       IF(EO.EQ.0.8.AND.EB.EQ.0.8) FLOCO=0.199+(0.0287*PO)
00137:       IF(EO.EQ.0.0.AND.EB.EQ.0.0) FLOCO1=0.0
00138:       IF(EO.EQ.0.0.AND.EB.EQ.0.2) FLOCO1=0.16
00139:       IF(EO.EQ.0.0.AND.EB.EQ.0.4) FLOCO1=0.3
00140:       IF(EO.EQ.0.4.AND.EB.EQ.0.0) FLOCO1=098
00141:       IF(EO.EQ.0.4.AND.EB.EQ.0.2) FLOCO1=0.115
00142:       IF(EO.EQ.0.4.AND.EB.EQ.0.4) FLOCO1=0.17
```

```
00143:       IF(EO.EQ.0.4.AND.EB.EQ.0.6) FLOCO1=0.239
00144:       IF(EO.EQ.0.4.AND.EB.EQ.0.8) FLOCO1=0.287
00145:       IF(EO.EQ.0.3.AND.EB.EQ.0.0) FLOCO1=0.075
00146:       IF(EO.EQ.0.3.AND.EB.EQ.0.2) FLOCO1=0.111
00147:       IF(EO.EQ.0.3.AND.EB.EQ.0.4) FLOCO1=0.192
00148:       IF(EO.EQ.0.3.AND.EB.EQ.0.6) FLOCO1=0.278
00149:       IF(EO.EQ.0.3.AND.EB.EQ.0.8) FLOCO1=0.362
00150:       IF(EO.EQ.0.45.AND.EB.EQ.0.0) FLOCO1=0.109
00151:       IF(EO.EQ.0.45.AND.EB.EQ.0.2) FLOCO1=0.12
00152:       IF(EO.EQ.0.45.AND.EB.EQ.0.4) FLOCO1=0.141
00153:       IF(EO.EQ.0.45.AND.EB.EQ.0.6) FLOCO1=0.165
00154:       IF(EO.EQ.0.45.AND.EB.EQ.0.8) FLOCO1=0.222
00155:       IF(EO.EQ.0.35.AND.EB.EQ.0.0) FLOCO1=0.087
00156:       IF(EO.EQ.0.35.AND.EB.EQ.0.2) FLOCO1=0.11
00157:       IF(EO.EQ.0.35.AND.EB.EQ.0.4) FLOCO1=0.14
00158:       IF(EO.EQ.0.35.AND.EB.EQ.0.6) FLOCO1=0.2
00159:       IF(EO.EQ.0.35.AND.EB.EQ.0.8) FLOCO1=0.26
00160:       IF(EO.EQ.0.6.AND.EB.EQ.0.0) FLOCO1=0.098
00161:       IF(EO.EQ.0.6.AND.EB.EQ.0.2) FLOCO1=0.169
00162:       IF(EO.EQ.0.6.AND.EB.EQ.0.4) FLOCO1=0.182
00163:       IF(EO.EQ.0.6.AND.EB.EQ.0.6) FLOCO1=0.205
00164:       IF(EO.EQ.0.6.AND.EB.EQ.0.8) FLOCO1=0.239
00165:       IF(EO.EQ.0.7.AND.EB.EQ.0.0) FLOCO1=0.183
00166:       IF(EO.EQ.0.7.AND.EB.EQ.0.2) FLOCO1=0.184
00167:       IF(EO.EQ.0.7.AND.EB.EQ.0.4) FLOCO1=0.188
00168:       IF(EO.EQ.0.7.AND.EB.EQ.0.6) FLOCO1=0.197
00169:       IF(EO.EQ.0.7.AND.EB.EQ.0.8) FLOCO1=0.209
00170:       IF(EO.EQ.0.8.AND.EB.EQ.0.0) FLOCO1=0.194
00171:       IF(EO.EQ.0.8.AND.EB.EQ.0.2) FLOCO1=0.194
00172:       IF(EO.EQ.0.8.AND.EB.EQ.0.4) FLOCO1=0.195
00173:       IF(EO.EQ.0.8.AND.EB.EQ.0.6) FLOCO1=0.196
00174:       IF(EO.EQ.0.8.AND.EB.EQ.0.8) FLOCO1=0.199
00175:C       MEU2       IS THE OIL VISCOSITY AT THE OUTLET
00176:C       TO       IS THE OIL TEMPERATURE AT THE OUTLET
00177:C      M=(1.0/((C/2.0)**3))*((H1**3)+(H2**3)+(H3**3))
00178:       QL=7.3
00179:       B2=(3.14*D)/22.5
```

```
00180:       L1=10.7
00181:C      QP=((((CM**3)*P*D*M)/(96.0*MEU2*L))*((QL+((4.0*B2)/((D*((1.0
00182:C     2-(L1/L)))))))))*980000.0
00183:C      QH=(FLOCO1*3.14*(N/60.0)*D*L*C)/4.0
00184:C      QT=QO+QH
00185:       QT=(FLOCO*3.14*(N/60.0)*D*L*C)/4.0
00186:C       FLOCO       IS THE TOTAL FLOW COEFFICIENT
00187:C       QT       IS THE TOTAL OIL FLOW OUT OF THE BEARING
00188:       N1=N/60.0
00189:       HS=(((1.64E-12)*MEU2*L*(N**2)*(D**3))/C)*((ACOS((-1.0+EO)/
00190:      2(1.0-(EO))))-(ACOS((+EO-0.5)/(1.0-(0.5*EO)))))
00191:      3*(1/((1.0-EO**2)**0.5))
00192:       T2=((HS+(4.19*(1.0E-3)*.877*.47*QT*T1))/(4.19*(1.0E-3)*.877*.47
00193:      2*QT))
00194:C       HS       IS THE SHEAR POWER LOSS
00195:       A=T2-TO
00196:       IF(A.LE.2.0.AND.A.GT.0) GO TO 9
00197:       IF(A.LT.0.0.AND.A.GE.-2.0) GO TO 9
00198:       IF(A.LT.7.0.AND.A.GT.0.0) GO TO 12
00199:       IF(A.LT.0.0.AND.A.GT.-7.0) GO TO 13
00200:       IF(T2.LT.TO) GO TO 7
00201:       IF(T2.GT.TO) GO TO 11
00202:     9 IF(EO.EQ.0.0.AND.CMIN.EQ.0.004*2.54) DUTY=1.0
00203:       IF(EO.EQ.0.0.AND.CMIN.EQ.0.004*2.54+(0.001*2.54)) DUTY=1.33
00204:       IF(EO.EQ.0.0.AND.CMIN.EQ.0.004*2.54+(0.002*2.54)) DUTY=1.6
00205:       IF(EO.EQ.0.0.AND.CMIN.EQ.0.004*2.54+(0.003*2.54)) DUTY=2.0
00206:       IF(EO.EQ.0.0.AND.CMIN.EQ.0.004*2.54+(0.004*2.54)) DUTY=2.5
00207:       IF(EO.EQ.0.35.AND.CMIN.EQ.0.004*2.54) DUTY=0.6
00208:       IF(EO.EQ.0.35.AND.CMIN.EQ.0.004*2.54+(0.001*2.54)) DUTY=0.73
00209:       IF(EO.EQ.0.35.AND.CMIN.EQ.0.004*2.54+(0.002*2.54)) DUTY=0.85
00210:       IF(EO.EQ.0.35.AND.CMIN.EQ.0.004*2.54+(0.003*2.54)) DUTY=1.0
00211:       IF(EO.EQ.0.35.AND.CMIN.EQ.0.004*2.54+(0.004*2.54)) DUTY=1.2
00212:       IF(EO.EQ.0.45.AND.CMIN.EQ.0.004*2.54) DUTY=0.45
00213:       IF(EO.EQ.0.45.AND.CMIN.EQ.0.004*2.54+(0.001*2.54)) DUTY=0.58
00214:       IF(EO.EQ.0.45.AND.CMIN.EQ.0.004*2.54+(0.002*2.54)) DUTY=0.7
00215:       IF(EO.EQ.0.45.AND.CMIN.EQ.0.004*2.54+(0.003*2.54)) DUTY=0.75
00216:       IF(EO.EQ.0.45.AND.CMIN.EQ.0.004*2.54+(0.004*2.54)) DUTY=0.85
```

```
00217:      IF(EO.EQ.0.6.AND.CMIN.EQ.0.004*2.54) DUTY=0.22
00218:      IF(EO.EQ.0.6.AND.CMIN.EQ.0.004*2.54+(0.001*2.54)) DUTY=0.35
00219:      IF(EO.EQ.0.6.AND.CMIN.EQ.0.004*2.54+(0.002*2.54)) DUTY=0.4
00220:      IF(EO.EQ.0.6.AND.CMIN.EQ.0.004*2.54+(0.003*2.54)) DUTY=0.45
00221:      IF(EO.EQ.0.6.AND.CMIN.EQ.0.004*2.54+(0.004*2.54)) DUTY=0.52
00222:      IF(EO.EQ.0.7.AND.CMIN.EQ.0.004*2.54) DUTY=0.17
00223:      IF(EO.EQ.0.7.AND.CMIN.EQ.0.004*2.54+(0.001*2.54)) DUTY=0.265
00224:      IF(EO.EQ.0.7.AND.CMIN.EQ.0.004*2.54+(0.002*2.54)) DUTY=0.31
00225:      IF(EO.EQ.0.7.AND.CMIN.EQ.0.004*2.54+(0.003*2.54)) DUTY=0.375
00226:      IF(EO.EQ.0.7.AND.CMIN.EQ.0.004*2.54+(0.004*2.54)) DUTY=0.43
00227:      IF(EO.EQ.0.8.AND.CMIN.EQ.0.004*2.54) DUTY=0.09
00228:      IF(EO.EQ.0.8.AND.CMIN.EQ.0.004*2.54+(0.001*2.54)) DUTY=0.13
00229:      IF(EO.EQ.0.8.AND.CMIN.EQ.0.004*2.54+(0.002*2.54)) DUTY=0.17
00230:      IF(EO.EQ.0.8.AND.CMIN.EQ.0.004*2.54+(0.003*2.54)) DUTY=0.2
00231:      IF(EO.EQ.0.8.AND.CMIN.EQ.0.004*2.54+(0.004*2.54)) DUTY=0.24
00232:      IF(EO.EQ.0.0.AND.CMIN.EQ.0.004*2.54) STIF=5.0
00233:      IF(EO.EQ.0.0.AND.CMIN.EQ.0.004*2.54+(0.001*2.54)) STIF=5.0
00234:      IF(EO.EQ.0.0.AND.CMIN.EQ.0.004*2.54+(0.002*2.54)) STIF=5.0
00235:      IF(EO.EQ.0.0.AND.CMIN.EQ.0.004*2.54+(0.003*2.54)) STIF=5.0
00236:      IF(EO.EQ.0.0.AND.CMIN.EQ.0.004*2.54+(0.004*2.54)) STIF=5.0
00237:      IF(EO.EQ.0.35.AND.CMIN.EQ.0.004*2.54) STIF=12.5
00238:      IF(EO.EQ.0.35.AND.CMIN.EQ.0.004*2.54+(0.001*2.54)) STIF=11.25
00239:      IF(EO.EQ.0.35.AND.CMIN.EQ.0.004*2.54+(0.002*2.54)) STIF=10.75
00240:      IF(EO.EQ.0.35.AND.CMIN.EQ.0.004*2.54+(0.003*2.54)) STIF=10.25
00241:      IF(EO.EQ.0.35.AND.CMIN.EQ.0.004*2.54+(0.004*2.54)) STIF=10.0
00242:      IF(EO.EQ.0.45.AND.CMIN.EQ.0.004*2.54) STIF=20.0
00243:      IF(EO.EQ.0.45.AND.CMIN.EQ.0.004*2.54+(0.001*2.54)) STIF=17.5
00244:      IF(EO.EQ.0.45.AND.CMIN.EQ.0.004*2.54+(0.002*2.54)) STIF=17.25
00245:      IF(EO.EQ.0.45.AND.CMIN.EQ.0.004*2.54+(0.003*2.54)) STIF=17.0
00246:      IF(EO.EQ.0.45.AND.CMIN.EQ.0.004*2.54+(0.004*2.54)) STIF=16.75
00247:      IF(EO.EQ.0.6.AND.CMIN.EQ.0.004*2.54) STIF=42.5
00248:      IF(EO.EQ.0.6.AND.CMIN.EQ.0.004*2.54+(0.001*2.54)) STIF=40
00249:      IF(EO.EQ.0.6.AND.CMIN.EQ.0.004*2.54+(0.002*2.54)) STIF=37.5
00250:      IF(EO.EQ.0.6.AND.CMIN.EQ.0.004*2.54+(0.003*2.54)) STIF=36.25
00251:      IF(EO.EQ.0.6.AND.CMIN.EQ.0.004*2.54+(0.004*2.54)) STIF=35.0
```

```
00252:       IF(EO.EQ.0.7.AND.CMIN.EQ.0.004*2.54) STIF=73.0
00253:       IF(EO.EQ.0.7.AND.CMIN.EQ.0.004*2.54+(0.001*2.54)) STIF=70.0
00254:       IF(EO.EQ.0.7.AND.CMIN.EQ.0.004*2.54+(0.002*2.54)) STIF=67.5
00255:       IF(EO.EQ.0.7.AND.CMIN.EQ.0.004*2.54+(0.003*2.54)) STIF=66.25
00256:       IF(EO.EQ.0.7.AND.CMIN.EQ.0.004*2.54+(0.004*2.54)) STIF=65.0
00257:       IF(EO.EQ.0.8.AND.CMIN.EQ.0.004*2.54) STIF=210.0
00258:       IF(EO.EQ.0.8.AND.CMIN.EQ.0.004*2.54+(0.001*2.54)) STIF=200.0
00259:       IF(EO.EQ.0.8.AND.CMIN.EQ.0.004*2.54+(0.002*2.54)) STIF=192.0
00260:       IF(EO.EQ.0.8.AND.CMIN.EQ.0.004*2.54+(0.003*2.54)) STIF=187.5
00261:       IF(EO.EQ.0.8.AND.CMIN.EQ.0.004*2.54+(0.004*2.54)) STIF=185.0
00262:       LOAD=(2.86E-5)*(1.0/DUTY)*MEU2*N*((D/C)**2)
00263:       STIFN=(4.233E-4)*MEU2*STIF*N*((D/C)**3)
00264:       CALL TAREK
00265:       N=N+1000.0
00266:    30 CONTINUE
00267:       CALL TAREK
00268:       T1=T1+10.0
00269:    20 CONTINUE
00270:       EB=EB+0.2
00271:     5 CONTINUE
00272:       CMIN=CMIN+(0.001*2.54)
00273:34567 CONTINUE
00274:       STOP
00275:       END
00276:       SUBROUTINE TAREK
00277:       COMMON L,D,P,V,EO,C,OFFSET,HF,FO,T1,FLOCO,MEU1,N,TO,MEU2,QP,QH,QT,
00278:      2CMIN,CMAX,CM,A11,A12,A21,A22,PHI,DY,N1,F,HS,T2,PX1T,PY1T,PTOTAL,AL
00279:      3PHA,S,STIFN,LOAD
00280:       REAL L,M,N,K,MEU1,MEU2,LOAD
00281:       WRITE(3,81818)T1,MEU1,N,MEU2,TO,QH,QP,QT,HS,T2,STIFN,LOAD
00282:81818 FORMAT(2X,F6.3,2X,F6.2,2X,F8.2,2X,F6.2,2X,F6.2,3X,F6.2,3X,F6.2,
00283:      23X,F6.2,3X,F6.2,3X,F6.2,2X,F15.2,F9.1)
00284:       RETURN
00285:       END
00286:       SUBROUTINE TAREK3
```

```
00287:       COMMON L,D,P,V,EO,C,OFFSET,HF,FO,T1,FLOCO,MEU1,N,TO,MEU2,QP,QH,QT,
00288:      2CMIN,CMAX,CM,A11,A12,A21,A22,PHI,DY,N1,F,HS,T2,PX1T,PY1T,PTOTAL,AL
00289:      3PHA,S,STIFN,LOAD
00290:       REAL L,M,N,K,MEU1,MEU2,LOAD
00291:       WRITE(3,40)L
00292:    40 FORMAT(100H                                THE BEARING WIDTH
00293:      2                                                 L = ,F20.8)
00294:       WRITE(3,50)D
00295:    50 FORMAT(100H                                THE BEARING DIAMETER
00296:      2                                                 D = ,F20.8)
00297:       WRITE(3,60)P
00298:    60 FORMAT(100H                                 THE SUPPLY PRESSURE
00299:      2                                                 P = ,F20.8)
00300:       WRITE(3,80)EO
00301:    80 FORMAT(100H                                 THE OFFSET RATIO
00302:      2                                                EO = ,F20.8)
00303:       WRITE(3,90)C
00304:    90 FORMAT(100H                                 THE DIAMETER CLEARANCE
00305:      2                                                 C = ,F20.8)
00306:       WRITE(3,100)OFFSET
00307:   100 FORMAT(98H                                THE BEARING OFFSET DISTANCE
00308:      2                                              OFFET= ,F20.8)
00309:       WRITE(3,140)FLOCO
00310:   140 FORMAT(100H                                THE HYDRODYNAMIC SIDE-LEAKAGE
00311:      2COEFFICIENT                                 FLOCO = ,F20.8)
00312:       WRITE(3,180)ALPHA
00313:   180 FORMAT(100H                                     THE VISCOSITY CONSTANT
00314:      2                                            ALPHA = ,F20.8)
00315:       WRITE(3,230)CMIN
00316:   230 FORMAT(98H                                 THE MINIMUM DIAMETERAL CLEAR
00317:      2ANCE                                        CMIN = ,F20.8)
00318:       WRITE(3,240)CMAX
00319:   240 FORMAT(100H                                 THE MAXIMUM DIAMETERAL CLEARA
00320:      2NCE                                          CMAX = ,F20.8)
00321:       WRITE(3,250)CM
```

```
00322:  250 FORMAT(100H                                THE MEAN DIAMETRAL CLEARANCE
00323:     2                                               CM = ,F20.8)
00324:      WRITE(3,71717)
00325:71717 FORMAT(113H      T1      MEU1       N      MEU2      TO       QH
00326:     2 QP        QT       HS          T2          STIFN          LOAD)
00327:      RETURN
00328:      END
BOTTOM
```

A2.2a. SAMPLE OF THE OUTPUT FOR THE SELF-GENERATING OPERATION.

THE CALCULATION OF THE POWER LOSS, OUTLET TEMPERATURE, THE OPERATING VISCOSITY AND THE STIFFNESS
FOR THE THREE LOBE BEARING

****

THE BEARING WIDTH	L =	12.70000000
THE BEARING DIAMETER	D =	13.50000000
THE SUPPLY PRESSURE	P =	1.50000000
THE OFFSET RATIO	EO =	.35000000
THE DIAMETER CLEARANCE	C =	.01565077
THE BEARING OFFSET DISTANCE	OFFET=	.00273538
THE HYDRODYNAMIC SIDE-LEAKAGE COEFFICIENT	FLOCO =	0
THE VISCOSITY CONSTANT	ALPHA =	.04150197
THE MINIMUM DIAMETERAL CLEAR ANCE	CMIN =	.01016000
THE MAXIMUM DIAMETERAL CLEARANCE	CMAX =	.01289538
THE MEAN DIAMETRAL CLEARANCE	CM =	.01193800

T1	MEU1	N	MEU2	TO	QT	HS	T2	STIFN	LOAD
30.000	.53	1000.00	.11	66.00	8.94	.55	65.43	585930355.51	4004.6
30.000	.53	2000.00	.07	78.00	15.81	1.33	78.59	465653761.24	4857.0
30.000	.53	3000.00	.05	85.50	22.43	2.18	86.39	510966340.53	5329.6
30.000	.53	4000.00	.04	91.00	28.90	3.09	91.87	541716630.87	5650.3
30.000	.53	5000.00	.03	95.50	35.39	4.00	95.43	561358652.84	5855.0
30.000	.53	6000.00	.03	99.00	41.61	4.98	99.27	582170965.07	6072.3
30.000	.53	7000.00	.03	102.00	47.76	5.98	102.48	599366543.64	6251.7
30.000	.53	8000.00	.02	104.50	53.71	7.04	105.85	617206394.41	6437.7
30.000	.53	9000.00	.02	107.00	59.98	8.02	107.46	625046345.21	6525.8
30.000	.53	10000.00	.02	109.00	65.86	9.11	110.12	639562778.54	6670.9
30.000	.53	11000.00	.02	109.00	65.86	9.11	110.12	639562778.54	6670.9
40.000	.53	1000.00	.10	69.50	9.86	.47	67.75	531815609.48	5461.0
40.000	.53	2000.00	.06	80.50	16.88	1.20	81.02	419574502.13	4576.4
40.000	.53	3000.00	.05	87.50	23.58	2.01	89.34	470098721.89	4903.3
40.000	.53	4000.00	.04	93.00	30.35	2.84	94.20	498589572.07	5198.4

40.000	.33	5000.00	.03	97.50	37.14	5.68	97.36	516442185.95	5586.7
40.000	.33	6000.00	.03	101.00	45.65	4.58	100.77	535608324.77	5586.6
40.000	.33	7000.00	.02	104.00	50.06	5.50	103.62	551428584.94	5751.6
40.000	.33	8000.00	.02	106.50	56.26	6.47	106.62	567841585.92	5922.8
40.000	.33	9000.00	.02	108.50	62.08	7.54	110.30	587728154.35	6130.3
40.000	.33	10000.00	.02	111.00	68.93	8.38	110.43	588409885.23	6137.4
40.000	.33	11000.00	.02	111.00	68.93	8.38	110.43	588409885.23	6137.4
50.000	.22	1000.00	.09	72.00	10.61	.43	73.24	298980445.85	3118.5
50.000	.22	2000.00	.06	85.00	18.06	1.08	84.54	378055064.71	3943.3
50.000	.22	3000.00	.04	90.00	25.17	1.81	91.66	423579607.01	4418.1
50.000	.22	4000.00	.03	95.50	32.54	2.56	95.82	449070906.27	4684.0
50.000	.22	5000.00	.03	99.50	39.05	3.39	100.20	475136603.51	4955.9
50.000	.22	6000.00	.02	103.00	45.65	4.21	103.22	492769814.64	5139.8
50.000	.22	7000.00	.02	106.00	52.55	5.06	105.76	507324753.98	5291.6
50.000	.22	8000.00	.02	108.50	59.03	5.96	108.42	522425026.09	5449.1
50.000	.22	9000.00	.02	110.50	65.09	6.93	111.69	540721046.12	5640.0
50.000	.22	10000.00	.02	112.50	71.41	7.88	113.86	552748461.36	5765.4
50.000	.22	11000.00	.02	112.50	71.41	7.88	113.86	552748461.36	5765.4

THE CALCULATION OF THE POWER LOSS, OUTLET TEMPERATURE, THE OPERATING VISCOSITY AND THE STIFFNESS
FOR THE THREE LOBE BEARING

****

THE BEARING WIDTH	L = 12.70000000
THE BEARING DIAMETER	D = 13.50000000
THE SUPPLY PRESSURE	P = 1.50000000
THE OFFSET RATIO	EO = .45000000
THE DIAMETER CLEARANCE	C = .01847273
THE BEARING OFFSET DISTANCE	OFFET= .00415636
THE HYDRODYNAMIC SIDE-LEAKAGE COEFFICIENT	FLOCO = 0
THE VISCOSITY CONSTANT	ALPHA = .04150197
THE MINIMUM DIAMETERAL CLEAR ANCE	CMIN = .01016000
THE MAXIMUM DIAMETERAL CLEARANCE	CMAX = .01451636
THE MEAN DIAMETRAL CLEARANCE	CM = .01286164

T1	MEU1	N	MEU2	TO	QT	HS	T2	STIFN	LOAD
30.000	.33	1000.00	.12	63.50	10.54	.58	62.13	413023211.58	4242.1
30.000	.33	2000.00	.08	74.50	18.56	1.48	76.14	522259964.51	5364.9
30.000	.33	3000.00	.06	82.00	26.57	2.43	83.05	573080870.33	5886.9
30.000	.33	4000.00	.05	87.50	34.44	3.44	87.85	607569253.92	6241.2
30.000	.33	5000.00	.04	91.50	41.93	4.55	92.85	642854767.68	6603.5
30.000	.33	6000.00	.03	95.00	49.48	5.66	96.28	666691572.43	6848.5
30.000	.33	7000.00	.03	98.00	56.98	6.80	99.13	686383637.78	7050.8
30.000	.33	8000.00	.03	100.50	64.29	8.01	102.12	706813509.61	7260.1
30.000	.33	9000.00	.02	103.00	71.89	9.13	103.54	716478787.39	7360.0
30.000	.33	10000.00	.02	105.00	79.13	10.37	105.89	732415633.11	7523.1
30.000	.33	11000.00	.02	105.00	79.13	10.37	105.89	732415633.11	7523.1
40.000	.33	1000.00	.11	67.00	11.48	.51	65.48	356959598.46	3666.8
40.000	.33	2000.00	.07	77.50	19.83	1.51	78.12	460873674.89	4734.3
40.000	.33	3000.00	.05	84.50	28.00	2.19	85.36	516371048.33	5304.4
40.000	.33	4000.00	.04	89.50	35.87	3.17	91.11	558975255.93	5742.0
40.000	.33	5000.00	.04	94.00	44.05	4.10	95.90	579222575.19	5950.0
40.000	.33	6000.00	.03	97.00	51.43	5.21	98.67	613368888.00	6300.8
40.000	.33	7000.00	.03	100.00	59.19	6.26	101.25	631485961.51	6486.9
40.000	.33	8000.00	.02	102.50	66.73	7.37	103.91	650281830.98	6680.0
40.000	.33	9000.00	.02	105.00	74.61	8.40	105.19	659174069.80	6771.3
40.000	.33	10000.00	.02	107.00	82.08	9.54	107.51	673856270.04	6921.9
40.000	.33	11000.00	.02	107.00	82.08	9.54	107.51	673856270.04	6921.9
50.000	.22	1000.00	.10	70.00	12.41	.45	70.81	315002491.09	3235.8
50.000	.22	2000.00	.06	80.50	21.26	1.15	81.56	406702712.67	4177.8
50.000	.22	3000.00	.05	87.00	29.59	1.98	88.08	465273006.56	4779.5
50.000	.22	4000.00	.04	92.00	37.82	2.85	93.67	505661250.06	5193.8
50.000	.22	5000.00	.03	96.00	45.92	3.77	97.57	532895568.01	5474.1
50.000	.22	6000.00	.03	99.50	54.10	4.70	100.25	552672522.72	5677.3
50.000	.22	7000.00	.02	102.50	62.22	5.64	102.49	568996602.11	5845.0
50.000	.22	8000.00	.02	105.00	70.09	6.64	104.85	585932506.49	6018.9
50.000	.22	9000.00	.02	107.00	77.56	7.73	107.69	606452643.04	6229.7
50.000	.22	10000.00	.02	109.00	85.29	8.78	109.00	619942145.28	6368.3
50.000	.22	11000.00	.02	109.00	85.29	8.78	109.00	619942145.28	6368.3

THE CALCULATION OF THE POWER LOSS, OUTLET TEMPERATURE,THE OPERATING VISCOSITY AND THE STIFFNESS
FOR THE THREE LOBE BEARING

****

THE BEARING WIDTH L = 12.70000000
THE BEARING DIAMETER D = 13.50000000
THE SUPPLY PRESSURE P = 1.50000000
THE OFFSET RATIO EO = .70000000
THE DIAMETER CLEARANCE C = .03386667
THE BEARING OFFSET DISTANCE OFFET= .01185333
THE HYDRODYNAMIC SIDE-LEAKAGE COEFFICIENT FLOCO = 0
THE VISCOSITY CONSTANT ALPHA = .04150197
THE MINIMUM DIAMETERAL CLEAR ANCE CMIN = .01016000
THE MAXIMUM DIAMETERAL CLEARANCE CMAX = .02201333
THE MEAN DIAMETRAL CLEARANCE CM = .01786467

T1	MEU1	N	MEU2	TO	QT	HS	T2	STIFN	LOAD
30.000	.53	1000.00	.20	52.50	21.58	.79	51.17	586955246.84	5285.0
30.000	.53	2000.00	.13	62.50	39.45	2.08	60.55	510122672.28	6967.2
30.000	.53	3000.00	.10	68.50	56.67	3.64	67.24	595876446.96	8138.4
30.000	.53	4000.00	.09	72.50	73.28	5.48	73.34	672494152.50	9184.9
30.000	.53	5000.00	.07	76.00	89.96	7.41	77.67	726512159.05	9922.6
30.000	.53	6000.00	.06	79.50	107.07	9.22	79.85	753474388.85	10290.9
30.000	.53	7000.00	.06	82.00	123.57	11.31	82.97	792065791.93	10818.0
30.000	.53	8000.00	.05	84.50	140.56	13.30	84.89	815641241.18	11140.0
30.000	.53	9000.00	.05	86.50	156.79	15.49	87.21	844206085.48	11530.1
30.000	.53	10000.00	.04	88.50	173.45	17.60	88.74	862984004.54	11786.6
30.000	.53	11000.00	.04	88.50	173.45	17.60	88.74	862984004.54	11786.6
40.000	.33	1000.00	.16	57.50	25.36	.64	55.88	514161299.79	4290.8
40.000	.33	2000.00	.11	66.50	41.57	1.76	64.53	431785627.61	5897.3
40.000	.33	3000.00	.09	71.00	58.31	3.28	72.61	536910864.63	7355.1
40.000	.33	4000.00	.08	75.50	75.03	4.84	77.05	593449378.83	8105.3

40.000	.33	5000.00	.07	79.00	92.68	6.54	80.83	641118124.07	8756.3
40.000	.33	6000.00	.06	82.00	109.67	8.31	83.85	678913535.94	9272.5
40.000	.33	7000.00	.05	85.00	127.07	9.98	85.46	698966601.56	9546.4
40.000	.33	8000.00	.05	87.00	143.56	11.99	88.55	734928601.83	10037.6
40.000	.33	9000.00	.04	89.00	160.27	13.96	90.43	760666780.03	10389.1
40.000	.33	10000.00	.04	91.00	177.23	15.85	91.80	777586512.11	10620.2
40.000	.33	11000.00	.04	91.00	177.23	15.85	91.80	777586512.11	10620.2
50.000	.22	1000.00	.13	63.00	25.80	.51	61.43	249800800.03	3411.8
50.000	.22	2000.00	.10	70.00	43.73	1.52	70.15	373175002.22	5096.8
50.000	.22	3000.00	.08	75.00	61.32	2.78	76.25	454460088.23	6207.0
50.000	.22	4000.00	.07	79.00	78.78	4.18	80.75	512894499.25	7005.1
50.000	.22	5000.00	.06	82.50	96.32	5.65	83.96	554092684.13	7567.8
50.000	.22	6000.00	.05	85.50	113.79	7.18	86.53	586757742.92	8013.9
50.000	.22	7000.00	.05	88.00	131.03	8.80	88.90	616810263.49	8424.3
50.000	.22	8000.00	.04	90.00	147.87	10.58	91.45	648545300.53	8857.8
50.000	.22	9000.00	.04	92.00	164.96	12.32	93.24	671258220.50	9168.0
50.000	.22	10000.00	.04	94.00	182.32	13.99	94.43	686189212.02	9371.9
50.000	.22	11000.00	.04	94.00	182.32	13.99	94.43	686189212.02	9371.9

CALCULATION OF THE POWER LOSS, OUTLET TEMPERATURE,THE OPERATING VISCOSITY AND THE STIFFNESS
FOR THE THREE LOBE BEARING

****

THE BEARING WIDTH L = 12.70000000
THE BEARING DIAMETER D = 13.50000000
THE SUPPLY PRESSURE P = 1.50000000
THE OFFSET RATIO EO = .80000000
THE DIAMETER CLEARANCE C = .05080000
THE BEARING OFFSET DISTANCE OFFET= .02032000
THE HYDRODYNAMIC SIDE-LEAKAGE COEFFICIENT FLOCO = 0
THE VISCOSITY CONSTANT ALPHA = .04150197
THE MINIMUM DIAMETERAL CLEAR ANCE CMIN = .01016000
THE MAXIMUM DIAMETERAL CLEARANCE CMAX = .03048000
THE MEAN DIAMETRAL CLEARANCE CM = .02336800

T1	MEU1	N	MEU2	TO	QT	HS	T2	STIFN	LOAD
30.000	.53	1000.00	.25	46.50	55.00	.89	44.79	423538664.45	5697.4
30.000	.53	2000.00	.18	55.00	62.59	2.51	53.21	594373400.46	7995.5
30.000	.53	3000.00	.14	60.50	89.43	4.49	59.06	708911080.52	9536.3
30.000	.53	4000.00	.12	64.50	115.73	6.75	63.79	800062762.52	10762.4
30.000	.53	5000.00	.10	68.00	142.12	9.12	67.16	864327701.10	11626.9
30.000	.53	6000.00	.10	70.00	166.98	12.08	71.90	954237448.59	12836.4
30.000	.53	7000.00	.09	72.50	192.85	14.82	74.50	1003111521.24	13493.8
30.000	.53	8000.00	.08	75.00	219.14	17.44	76.08	1032968642.95	13895.5
30.000	.53	9000.00	.07	77.00	244.93	20.51	78.01	1069144580.24	14382.1
30.000	.53	10000.00	.07	79.00	271.03	23.07	79.28	1092925873.60	14702.0
30.000	.53	11000.00	.07	79.00	271.03	23.07	79.28	1092925873.60	14702.0
40.000	.53	1000.00	.20	52.00	58.32	.71	50.74	336770624.82	4530.2
40.000	.53	2000.00	.15	59.50	66.38	2.08	58.14	492722184.25	6628.1
40.000	.53	3000.00	.12	64.50	95.62	3.80	63.50	600047071.74	8071.8
40.000	.53	4000.00	.10	68.50	120.68	5.72	67.45	677201035.61	9109.7
40.000	.53	5000.00	.09	71.00	146.33	8.05	71.85	762754866.03	10260.5
40.000	.53	6000.00	.08	73.50	172.37	10.44	75.08	824709159.41	11094.0
40.000	.53	7000.00	.07	76.00	198.84	12.81	77.30	866949060.42	11662.2
40.000	.53	8000.00	.07	78.00	224.78	15.39	79.65	911553798.98	12262.2
40.000	.53	9000.00	.06	80.00	251.05	17.92	81.53	943477626.77	12691.6
40.000	.53	10000.00	.06	82.00	277.69	20.36	82.45	964463673.59	12973.9
40.000	.53	11000.00	.06	82.00	277.69	20.36	82.45	964463673.59	12973.9
50.000	.22	1000.00	.15	59.00	43.82	.53	57.02	251549191.69	3385.8
50.000	.22	2000.00	.12	65.00	72.09	1.65	63.28	391780896.96	5270.2
50.000	.22	3000.00	.10	69.50	99.95	3.08	67.87	487166351.54	6553.3
50.000	.22	4000.00	.09	71.50	124.98	5.05	73.37	597603016.21	8038.9
50.000	.22	5000.00	.08	75.00	152.82	6.81	75.81	645605401.85	8684.7
50.000	.22	6000.00	.07	77.50	179.58	8.84	78.50	698062606.00	9390.3
50.000	.22	7000.00	.06	79.50	205.76	11.07	81.15	749269506.01	10079.1
50.000	.22	8000.00	.06	81.50	232.30	13.50	83.16	787819592.78	10597.7
50.000	.22	9000.00	.05	83.50	259.23	15.49	84.60	815409876.90	10968.9
50.000	.22	10000.00	.05	85.00	285.23	17.96	86.47	851100884.46	11449.0
50.000	.22	11000.00	.05	85.00	285.23	17.96	86.47	851100884.46	11449.0

****

THE BEARING LENGTH	L =	12.70000000
THE BEARING DIAMETER	D =	15.50000000
THE SUPPLY PRESSURE	P =	1.50000000
THE OFFSET RATIO	EO =	0
THE DIAMETER CLEARANCE	C =	.01016000
THE BEARING OFFSET DISTANCE	OFFET=	0
THE HYDRODYNAMIC SIDE-LEAKAGE COEFFICIENT	FLOCO =	0
THE VISCOSITY CONSTANT	ALPHA =	.04150197
THE MINIMUM DIAMETERAL CLEARANCE	CMIN =	.01016000
THE MAXIMUM DIAMETERAL CLEARANCE	CMAX =	.01016000
THE MEAN DIAMETERAL CLEARANCE	CM =	.01016000

W	ECCT	S	MESZ	TO	QT	HS	TZ	STIFN	LOAD
50.0000	.55	1000.00	.06	74.50	5.47	.42	74.15	592581641.11	5990.4
50.0000	.55	2000.00	.05	83.00	9.01	.95	87.51	447061146.25	4546.5
50.0000	.55	3000.00	.05	96.00	13.41	1.55	96.19	480446793.09	4866.0
50.0000	.55	4000.00	.05	102.00	17.22	2.12	101.55	498655046.40	5073.2
50.0000	.55	5000.00	.04	106.50	20.78	2.75	106.02	516924520.04	5257.0
50.0000	.55	6000.00	.04	110.50	24.55	3.55	109.05	525051559.24	5339.0
50.0000	.55	7000.00	.04	113.50	27.82	4.05	113.76	540559965.70	5497.3
50.0000	.55	8000.00	.03	116.50	31.52	4.64	115.22	545166817.51	5544.2
50.0000	.55	9000.00	.03	119.00	34.96	5.29	117.57	552023694.70	5620.0
50.0000	.55	10000.00	.03	121.00	38.05	6.01	121.50	564915864.01	5745.0
50.0000	.55	11000.00	.03	121.00	38.05	6.01	121.50	564915864.01	5745.0
40.0000	.55	1000.00	.07	70.50	5.95	.56	77.57	380996549.90	3671.2
40.0000	.55	2000.00	.06	79.50	10.23	.89	90.57	419960306.59	4270.9
40.0000	.55	3000.00	.05	97.50	14.26	1.44	98.41	451526628.59	4569.9
40.0000	.55	4000.00	.05	103.50	18.34	1.99	102.97	488621225.40	4705.7

40.000	.55	3000.00	.02	100.00	22.12	2.56	107.01	4655955571.55	4956.4
40.500	.55	3000.00	.02	111.50	25.59	3.21	112.72	5036106954.56	5121.6
41.000	.55	6000.00	.01	115.00	29.01	3.76	113.94	5077985754.56	5164.2
40.500	.55	6000.00	.01	117.50	32.06	4.45	116.40	5229129484.49	5317.9
40.000	.55	9000.00	.01	120.00	36.47	5.07	120.56	5380634894.57	5390.6
40.000	.55	10000.00	.01	122.50	40.46	5.65	120.75	5386785504.75	5396.8
40.000	.55	11000.00	.01	122.50	40.46	5.65	120.75	5386785504.75	5396.8
50.000	.22	1000.00	.07	69.00	0.00	.55	00.54	5252755574.62	5308.0
50.000	.22	2000.00	.04	91.50	11.12	.82	92.81	5863770204.59	5929.3
50.000	.22	5000.00	.03	99.50	15.52	1.33	99.44	4152308964.10	4222.8
50.000	.22	9000.00	.02	105.00	19.52	1.87	105.57	4402197644.45	4476.9
50.000	.22	5000.00	.02	109.50	23.55	2.43	109.66	4561655574.77	4639.1
50.000	.22	6000.00	.02	113.00	27.24	3.02	114.10	4730945104.56	4811.2
50.000	.22	7000.00	.01	116.50	31.52	3.55	115.25	4770227154.14	4851.2
50.000	.22	8000.00	.01	119.00	34.98	4.10	119.19	4912210619.95	4995.6
50.000	.22	9000.00	.01	121.50	38.83	4.77	121.09	4979562544.09	5063.9
50.000	.22	10000.00	.01	123.50	42.20	5.41	124.29	5090140184.82	5176.5
50.000	.22	11000.00	.01	123.50	42.20	5.41	124.29	5090140184.82	5176.5

A2.2b SAMPLE OF THE OUTPUT FOR THE

EXTERNALLY PRESSURIZED OPERATION.

THE CALCULATION OF THE POWER LOSS, OUTLET TEMPERATURE, THE OPERATING VISCOSITY AND THE STIFFNESS
FOR THE THREE LOBE BEARING

****

THE BEARING WIDTH
THE BEARING DIAMETER
THE SUPPLY PRESSURE
THE OFFSET RATIO
THE DIAMETER CLEARANCE
THE BEARING OFFSET DISTANCE
THE HYDRODYNAMIC SIDE-LEAKAGE COEFFICIENT
THE VISCOSITY CONSTANT
THE MINIMUM DIAMETERAL CLEARANCE
THE MAXIMUM DIAMETERAL CLEARANCE
THE MEAN DIAMETRAL CLEARANCE

L =	12.70000000
D =	13.50000000
P =	1.50000000
EO =	.35000000
C =	.01563077
OFFET=	.00275558
FLOCO =	0
ALPHA =	.04150197
CMIN =	.01016000
CMAX =	.01269538
CM =	.01193800

T1	NEU1	N	NEU2	T0	QT	HS	T2
50.000	.55	1000.00	.36	57.00	189.58	1.85	55.60
50.000	.55	2000.00	.25	46.50	189.58	4.93	45.07
50.000	.55	3000.00	.18	55.00	189.58	7.79	55.79
50.000	.55	4000.00	.13	62.50	189.58	10.13	60.93
50.000	.55	5000.00	.10	68.50	189.58	12.52	67.04
50.000	.55	6000.00	.08	73.00	189.58	14.71	74.93
50.000	.55	7000.00	.07	76.00	189.58	16.26	79.05
50.000	.55	8000.00	.06	82.50	189.58	17.60	85.76
50.000	.55	9000.00	.05	86.50	189.58	18.80	87.59
50.000	.55	10000.00	.04	90.00	189.58	20.12	91.45
50.000	.55	11000.00	.04	90.00	189.58	20.12	91.45
40.000	.55	1000.00	.26	45.50	189.58	1.29	45.93
40.000	.55	2000.00	.19	55.00	189.58	3.76	51.49
40.000	.55	3000.00	.14	61.50	189.58	6.19	58.91
40.000	.55	4000.00	.11	67.00	189.58	8.40	65.04

40.000	.33	5000.00	.09	71.50	189.58	10.86	75.21
40.000	.33	6000.00	.07	77.00	189.58	12.45	78.03
40.000	.33	7000.00	.06	81.50	189.58	14.05	82.91
40.000	.33	8000.00	.05	85.50	189.58	15.53	87.44
40.000	.33	9000.00	.04	89.50	189.58	16.64	90.82
40.000	.33	10000.00	.04	93.00	189.58	17.75	94.23
40.000	.33	11000.00	.04	93.00	189.58	17.75	94.23
50.000	.22	1000.00	.16	54.50	189.58	.86	52.70
50.000	.22	2000.00	.14	60.00	189.58	2.81	56.58
50.000	.22	3000.00	.11	66.50	189.58	4.82	64.73
50.000	.22	4000.00	.09	70.50	189.58	7.26	72.16
50.000	.22	5000.00	.07	76.00	189.58	9.02	77.53
50.000	.22	6000.00	.06	81.00	189.58	10.54	82.19
50.000	.22	7000.00	.05	85.50	189.58	11.89	86.32
50.000	.22	8000.00	.04	89.50	189.58	13.15	90.15
50.000	.22	9000.00	.04	93.00	189.58	14.36	93.92
50.000	.22	10000.00	.03	96.00	189.58	15.67	97.85
50.000	.22	11000.00	.03	96.00	189.58	15.67	97.85

****

THE BEARING WIDTH	L =	12.70000000
THE BEARING DIAMETER	D =	15.50000000
THE SUPPLY PRESSURE	P =	1.50000000
THE OFFSET RATIO	EO =	.45000000
THE DIAMETER CLEARANCE	C =	.01847273
THE BEARING OFFSET DISTANCE	OFFEI=	.00415636
THE HYDRODYNAMIC SIDE-LEAKAGE COEFFICIENT	FLOCO =	0
THE VISCOSITY CONSTANT	ALPHA =	.04150197
THE MINIMUM DIAMETERAL CLEARANCE	CMIN =	.01016000
THE MAXIMUM DIAMETERAL CLEARANCE	CMAX =	.01451636
THE MEAN DIAMETERAL CLEARANCE	CM =	.01286164

T1	mE01	N	mE02	T0	QT	HS	T2
50.000	.55	1000.00	.50	57.00	189.58	1.76	55.39
50.000	.55	2000.00	.25	46.50	189.58	4.75	44.51
50.000	.55	3000.00	.16	54.50	189.58	7.66	55.39
50.000	.55	4000.00	.13	62.00	189.58	9.96	60.42
50.000	.55	5000.00	.10	68.00	189.58	12.12	67.02
50.000	.55	6000.00	.09	72.50	189.58	14.47	74.19
50.000	.55	7000.00	.07	77.50	189.58	15.99	78.85
50.000	.55	8000.00	.06	82.00	189.58	17.51	82.87
50.000	.55	9000.00	.05	86.00	189.58	18.55	86.64
50.000	.55	10000.00	.04	89.50	189.58	19.79	90.43
50.000	.55	11000.00	.04	89.50	189.58	19.79	90.43
40.000	.55	1000.00	.20	45.50	189.58	1.24	43.78
40.000	.55	2000.00	.19	55.00	189.58	5.62	51.07
40.000	.55	3000.00	.14	60.00	189.58	6.09	56.00
40.000	.55	4000.00	.11	66.50	189.58	8.20	65.22
40.000	.55	5000.00	.09	71.00	189.56	10.70	72.07
40.000	.55	6000.00	.07	76.50	189.56	12.25	77.40
40.000	.55	7000.00	.06	81.00	189.58	13.82	82.20
40.000	.55	8000.00	.05	85.00	189.58	15.26	86.00
40.000	.55	9000.00	.04	89.00	189.56	16.57	89.98
40.000	.55	10000.00	.04	92.50	189.58	17.46	93.55
40.000	.55	11000.00	.04	92.50	189.58	17.46	93.55
30.000	.22	1000.00	.16	54.50	189.58	.65	52.60
30.000	.22	2000.00	.14	60.00	189.56	2.71	58.27
30.000	.22	3000.00	.11	66.00	189.56	4.74	64.48
30.000	.22	4000.00	.10	70.00	189.56	6.14	71.80
30.000	.22	5000.00	.08	75.50	189.56	8.87	77.08
30.000	.22	6000.00	.08	80.50	189.58	10.57	81.06
30.000	.22	7000.00	.07	84.50	189.56	11.94	86.47
30.000	.22	8000.00	.06	88.50	189.58	13.20	90.52
30.000	.22	9000.00	.06	92.50	189.58	14.14	93.20
30.000	.22	10000.00	.05	95.50	189.58	15.41	97.06
30.000	.22	11000.00	.05	95.50	189.56	15.41	97.06

APPENDIX A.3.

A.3.1. A COMPUTER PROGRAMME FOR THE NUMERICAL SOLUTION FOR THE THREE-LOBE EXTERNALLY PRESSURIZED JOURNAL BEARING .

"THE HIGH PRESSURE OIL IS ADMITTED AT THE CENTRE OF EACH LOBE".

```
31/05/77 UNIVERSITY OF MINNESOTA 7600 FORTRAN COMPILER SCOPE  2.1.4 VER4.5      15/02/80  18.15.56
      MNF(T)
0000000B        1.        PROGRAM HY5(INPUT,OUTPUT,TAPE4=INPUT,TAPE5=OUTPUT)
0000047B        2.        COMMON QA1,QA2,QA5,QC1,QC11,QC1T,QC2,QC22,QC2T,QC5,QC55,QC5T,Q11
                         2,Q2T,Q3T,FHT,FVT
0000047B        3.        DIMENSION P1(29,182),H1(29,182)
0000047B        4.        INTEGER V
0000047B        5.        EB=0.0
0024544B        6.        DO 71717 K=1,10
0024547B        7.        EPS=0.005
0024547B        8.        MAXIT=80
0024551B        9.        L=2
0024552B       10.        D=2.0
0024553B       11.        M=180
0024554B       12.        ELIPIT=0.4
0024555B       13.        DX=3.14/FLOAT(M/2)
0024560B       14.        DY=DX
0024560B       15.        N=28
0024562B       16.        WRITE(5,600)
0024572B       17.    600 FORMAT(103H                                    THE  SOLUTION  OF  REYNO
                         2LDS  EQUATION  FOR  THE  EXTERNALLY  PRESSURIZED/,96H
                         5           THREE  LOBE JOURNAL BEARINGS   FOR ZERO SPEED CASE
                         4                  /,100H**********************************************
                         5**************************************************)
0024572B       18.        WRITE(5,666)
0024600B       19.    666 FORMAT(88H                                THE HIGH PRESSURE OIL IS SUPPLI
                         2ED FROM THE HIGHPRESSURE GROOVES)
0024600B       20.        WRITE(5,650)N
0024607B       21.    650 FORMAT(24H                          N = ,I4/,25H**************************
                         2*)
0024607B       22.        WRITE(5,610)
0024615B       23.    610 FORMAT(54H      EPS      MAXIT      EB      L      D      M      ELIPIT)
0024615B       24.        WRITE(5,620)EPS,MAXIT,EB,L,D,M,ELIPIT
```

```
0246328       25.    620 FORMAT(3X,F7.5,4X,I3,3X,F6.4,4X,I1,3X,F5.3,2X,I3,5X,F5.3/,55H*****
                     2**************************************************)
0246328       26.         EMEU=1.0-(((3.14**2)*(4.0+(3.14*D/FLOAT(L))**2))/(2.0*((FLOAT(M/2)
                     4*FLOAT(M/2))+(3.14*D*FLOAT(N)/FLOAT(L))**2)))
0246528       27.         OMEGA=2*((1.0-(1.0-EMEU**2)**0.5)/(EMEU**2.0))
                                                                                 (**********
0246628       28.         WRITE(3,680)OMEGA
0246728       29.    680 FORMAT(36H THE OVER RELAXATION FACTOR OMEGA = ,F6.4/,45H**********
                     2**********************************)
0246728       30.         ALPHA=0.0
0246728       31.         WRITE(3,730)ALPHA
0247028       32.    730 FORMAT(91H
                     2    DISPLACEMENT  ANGLE  ALPHA  =  ,F10.6/,100H
                     3****************************************************************
                     4****************)
0247028       33.         ALPHA=ALPHA*3.14/180.0
0247048       34.         E=EB*(1.0-ELIPIT)
0247068       35.         EL1=((E**2)+(ELIPIT**2)+(2.0*E*ELIPIT*COS(ALPHA)))**0.5
0247238       36.         ALPHA1=(ASIN((E*SIN(ALPHA))/EL1))*180.0/3.14
0247368       37.         EL2=((E**2+ELIPIT**2-2.0*E*ELIPIT*COS((3.14/3.0)-ALPHA))**0.5)
0247548       38.         ALPHA2=(ASIN((E*SIN((3.14/3.0)-ALPHA)/EL2))-2.0*3.14/3.0)*(-180.0/
                     43.14)
0247718       39.         EL3=((E**2+(ELIPIT**2)+(2.0*E*ELIPIT*COS((3.14*2.0/3.0)-ALPHA))))*
                     2*0.5
0250078       40.         ALPHA3=((2.0*3.14/3.0)-(ASIN(E*SIN((3.14*2.0/3.0)-ALPHA)/EL3)))*18
                     20.0/3.14
0250258       41.         THETA1=60.0+ALPHA1
0250308       42.         THETA2=180.0-ALPHA2
0250318       43.         THETA3=ALPHA3-60.0
0250338       44.         WRITE(3,640)
0250428       45.    640 FORMAT(116H        E         EL1         EL2         EL3         ALPHA1
```

```
                2   ALPHA2        ALPHA3        THETA1        THETA2        THETA3//,10
               5UH**********************************************************************
               4************************************)
0250428      40.       WRITE(3,650)E,EL1,EL2,EL3,ALPHA1,ALPHA2,ALPHA3,THETA1,THETA2,THETA
               13
0250628      47.   650 FORMAT(4X,F7.4,2X,F7.4,2X,F7.4,2X,F7.4,3X,F7.2,1X,F8.2,6X,F8.2,1X,
               4F6.3,7X,F6.3,7X,F6.3/,100H**********************************************
               5**********************************************************)
              C**********************************************************************
0250628      48.       G1=(180.0-THETA1)*3.14/180.0
0250658      49.       DO 30 J=151,181
0250708      50.       DO 20 I=1,N+1
0251018      51.       H1(I,J)=(1.0+EL1*COS(G1))/2.0
0251018      52.    20 CONTINUE
0251238      53.    30 G1=G1+(2.0*3.14/180.0)
0251308      54.       G4=(180.0-THETA1+60.0)*3.14/180.0
0251348      55.       DO 40 J=1,31
0251408      56.       DO 45 I=1,N+1
0251518      57.       H1(I,J)=(1.0+EL1*COS(G4))/2.0
0251518      58.    45 CONTINUE
0251738      59.    40 G4=G4+(2.0*3.14/180.0)
0252008      60.       G3=(180.0-THETA3)*3.14/180.0
0252038      61.       DO 34 J=31,91
0252078      62.       DO 24 I=1,N+1
0252208      63.       H1(I,J)=(1.0+EL3*COS(G3))/2.0
0252208      64.    24 CONTINUE
0252428      65.    34 G3=G3+(2.0*3.14/180.0)
0252478      66.       G2=(180.0-THETA2)*3.14/180.0
0252528      67.       DO 35 J=91,151
0252568      68.       DO 25 I=1,N+1
0252678      69.       H1(I,J)=(1.0+EL2*COS(G2))/2.0
```

```
025267B        70.     25 CONTINUE
025311B        71.     35 G2=G2+(2.0*3.14/180.0)
025316B        72.        WRITE(3,670)((H1(I,J),J=1,M+1),I=1,2)
025355B        73.    670 FORMAT((10(F7.5,4X)))
              C*****************************************************************
025355B        74.        A4=.4
025355B        75.        A3=0.4
025356B        76.        A2=0.4
025357B        77.        Q0=0.058
025360B        78.    111 B11=0.0
025362B        79.        WRITE(3,929)A2,A3,A4
025374B        80.    929 FORMAT(F10.5)
025374B        81.        DO 50 I=2,N
025404B        82.        P1(I,1)=A2
025404B        83.     50 CONTINUE
025422B        84.        DO 60 I=2,N
025432B        85.        P1(I,61)=A3
025432B        86.     60 CONTINUE
025450B        87.        DO 70 I=2,N
025460B        88.        P1(I,121)=A4
025460B        89.     70 CONTINUE
025476B        90.        DO 94 J=2,M
025506B        91.     94 P1(N+1,J)=0.0
025530B        92.        DO 95 J=2,M
025540B        93.     95 P1(1,J)=0.0
025560B        94.        DO 55 I=2,N
025570B        95.        P1(I,181)=A2
025570B        96.     55 CONTINUE
025606B        97.        ITN=1
025606B        98.        WRITE(3,810)DY,DX
025620B        99.    810 FORMAT(25H                    DY = ,F15.6,45H
                  2                    DX = ,F15.6/,100H********************************
                  4****************************************************************
```

```
                     5****)
025620B      100.      R=(D/FLOAT(L))**2
025622B      101.      S=DX**2
025623B      102.      T=DY**2
025624B      103.      B=1.0-OMEGA
025627B      104.   90 DA=0.0
025631B      105.      DO 100 J=3,M-1,2
025643B      106.      DO 100 I=2,N
025654B      107.      IF(I.GT.2.AND.I.LT.N) GO TO 1
025661B      108.      GO TO 2
025662B      109.    1 IF(J.GE.1.AND.J.LT.2) GO TO 100
025667B      110.      IF(J.GE.181.AND.J.LT.182) GO TO 100
025673B      111.      IF(J.GE.61.AND.J.LT.62) GO TO 100
025677B      112.      IF(J.GT.120.AND.J.LT.122) GO TO 100
025703B      113.    2 SP=0.0
025704B      114.      A1=((18.84/DX)*(H1(I,J-1)-H1(I,J+1)))*SP
025722B      115.      B1=((R/T)*((H1(I+1,J))**3)*(P1(I+1,J)))
025735B      116.      C1=((1.0/S)*((H1(I,J+1))**3)*(P1(I,J+2)))
025752B      117.      D1=((R/T)*((H1(I-1,J))**3)*(P1(I-1,J)))
025764B      118.      E1=((1.0/S)*((H1(I,J-1))**3)*(P1(I,J-2)))
026001B      119.      F1=((R/T)*((H1(I+1,J))**3))
026012B      120.      Q1=((1.0/S)*((H1(I,J+1))**3))
026023B      121.      Y1=((R/T)*((H1(I-1,J))**3))
026034B      122.      Z1=((1.0/S)*((H1(I,J-1))**3))
026045B      123.      PNEW1=OMEGA*((A1+B1+C1+D1+E1)/(F1+Q1+Y1+Z1))+B*P1(I,J)
026060B      124.      IF(J.GE.1.AND.J.LT.62.) GO TO 7
026074B      125.      IF(J.GE.62.AND.J.LT.122) GO TO 9
026100B      126.      IF(J.GE.122.AND.J.LT.182) GO TO 10
026104B      127.    7 THETA=THETA1
026106B      128.      GO TO 617
026107B      129.    9 THETA=THETA2
```

```
026112B      150.          GO TO 617
026113B      151.       10 THETA=THETA3
026116B      152.          RESID=ABS(PNEW1-P1(I,J))
026127B      153.          IF(RESID.GT.DA) DA=RESID
026133B      154.      617 P1(I,J)=PNEW1
026144B      155.        8 IF(J.GT.(THETA/2.0).AND.P1(I,J).LT.0.0) P1(I,J)=0.0
026170B      156.      100 CONTINUE
026176B      157.          ITN=ITN+1
026177B      158.          IF(ITN.GT.MAXIT) GO TO 5
026201B      159.          IF(DA.GT.EPS) GO TO 90
026205B      160.        5 WRITE(3,690)ITN
026214B      161.      690 FORMAT(21H CYCLE  NUMBER ITN=  ,I5//,21H**********************)
                     C      WRITE(3,713)((P1(I,J),J=1,M+1,2),I=1,8)
                     C  713 FORMAT((2X,11(F12.5)))
026214B      162.          QA12=0.0
026214B      163.          DO 1000 J=1,51,2
026217B      164.          QA12=QA12+(D/FLOAT(L))*(DX/(2.0*DY))*(H1(N,J)**5)*P1(N-1,J)
026217B      165.     1000 CONTINUE
026262B      166.          QA11=0.0
026262B      167.          DO 10001 J=151,179,2
026265B      168.          QA11=QA11+(D/FLOAT(L))*(DX/(2.0*DY))*(H1(N,J)**5)*P1(N-1,J)
026265B      169.    10001 CONTINUE
026530B      170.          QA1=QA11+QA12
026532B      171.          QA3=0.0
026532B      172.          DO 1002 J=51,91,2
026536B      173.          QA3=QA3+(D/FLOAT(L))*(DX/(2.0*DY))*(H1(N,J)**5)*P1(N-1,J)
026536B      174.     1002 CONTINUE
026401B      175.          QA2=0.0
026401B      176.          DO 1003 J=91,151,2
026404B      177.          QA2=QA2+(D/FLOAT(L))*(DX/(2.0*DY))*(H1(N,J)**5)*P1(N-1,J)
026404B      178.     1003 CONTINUE
026447B      179.          QC1=0.0
026447B      180.          QC2=0.0
```

```
026450B      161.        QC3=0.0
026450B      162.        QC11=0.0
026451B      163.        QC22=0.0
026451B      164.        QC33=0.0
026452B      165.        DO 1004 I=1,N+1
026462B      166.        QC1=QC1+(FLOAT(L)/D)*(DY/(2.0*DX))*(H1(I,31)**3)*(P1(I,29)-P1(I,33
                        2))
026505B      167.        QC11=QC11+(FLOAT(L)/D)*(DY/(2.0*DX))*(H1(I,151)**3)*(P1(I,153)-P1(
                        2I,149))
026530B      168.        QC3=QC3+(FLOAT(L)/D)*(DY/(2.0*DX))*(H1(I,31)**3)*(P1(I,33)-P1(I,29
                        2))
026552B      169.        QC33=QC33+(FLOAT(L)/D)*(DY/(2.0*DX))*(H1(I,91)**3)*(P1(I,89)-P1(
                        2I,93))
026575B      170.        QC2=QC2+(FLOAT(L)/D)*(DY/(2.0*DX))*(H1(I,91)**3)*(P1(I,93)-P1(I,
                        289))
026620B      171.        QC22=QC22+(FLOAT(L)/D)*(DY/(2.0*DX))*(H1(I,151)**3)*(P1(I,149)-P1(
                        2I,153))
026643B      172.   1004 CONTINUE
026645B      173.        QC1T=QC11+QC1
026647B      174.        QC2T=QC22+QC2
026651B      175.        QC3T=QC33+QC3
026653B      176.        Q1T=QA1+QC1T
026655B      177.        Q2T=QA2+QC2T
026657B      178.        Q3T=QA3+QC3T
026661B      179.        IF(Q1T.LT.0.0) Q1T=Q1T*(-1.0)
                                                  **********************************************
026665B      180.        IF(Q2T.LT.0.0) Q2T=Q2T*(-1.0)
                                                  **********************************************
026670B      181.        IF(Q3T.LT.0.0) Q3T=Q3T*(-1.0)
                                                              ***********************************
026675B      182.        B3=Q1T-Q0
```

```
026674B      183.          CALL HESHAM
026700B      184.          IF(B3.LE..005.AND.B3.GT.0.0) GO TO 180
026705B      185.          IF(B3.LT.0.0.AND.B3.GT.-0.005) GO TO 180
026706B      186.          IF(Q0.GT.Q1T.OR.Q0.LT.Q1T) A2=Q0*A2/Q1T
026715B      187.          IF(Q0.LT.Q2T.OR.Q0.GT.Q2T) A3=Q0*A3/Q2T
026720B      188.          A4=A3
026720B      189.          GO TO 111
                       C 180 WRITE(3,700)
026720B      191.            700 FORMAT(95H                                        J
                              2 SUMCA                                          SUMSA)
026722B      191.            180 SUMSAA=0.0
026724B      192.                SUMSA=0.0
026725B      193.                SUMCAA=0.0
026725B      194.                SUMCA=0.0
026726B      195.                GAA=(180.0-THETA1)*3.14/180.0
026731B      196.                DO 110 J=151,179,2
026735B      197.                DO 120 I=1,N+1
026746B      198.                SUMSA=SUMSA+P1(I,J)*DX*DY*SIN(GAA)
026764B      199.                SUMCA=SUMCA+P1(I,J)*DX*DY*COS(GAA)
026775B      200.            120 CONTINUE
                       C        WRITE(3,910)J,SUMCA,SUMSA
027001B      201.            910 FORMAT(28X,I4,25X,F10.7,23X,F10.7)
027001B      202.                GAA=GAA+(4.0*3.14/180.0)
027005B      203.                SUMCAA=SUMCA+SUMCAA
027005B      204.                SUMSAA=SUMSA+SUMSAA
027007B      205.                SUMCA=0.0
027007B      206.                SUMSA=0.0
027007B      207.            110 CONTINUE
027013B      208.                FCOSA=SUMCAA
027014B      209.                FSINA=SUMSAA
                       C        WRITE(3,720)FCOSA,FSINA
027015B      210.            720 FORMAT(77HTHE TOTAL HYDROSTATIC  FORCE IN THE DIRECTION OF THE ATT
                              2TITUDE LINE FCOSA = ,F10.7,92HTHE TOTAL HYDROSTATIC  FORCE IN TH
```

```
                     3E DIRECTION PERPENDICULAR ON THE AITITUDE LINE  FSINA  =  ,F10.7/,
                     495H**************************************************************
                     6**********************************)
                C      WRITE(3,706)
0270158      211.   706 FORMAT(95H                                          J
                     2 SUMCB                                           SUMSB)
0270158      212.       SUMSBB=0.0
0270168      213.       SUMSB=0.0
0270178      214.       SUMCBB=0.0
0270208      215.       SUMCB=0.0
0270208      216.       GBB=(180.0-THETA1+60.0)*3.14/180.0
0270258      217.        DO 1110 J=1,31,2
0270308      218.       DO 1220 I=1,N+1
0270418      219.       SUMSB=SUMSB+P1(I,J)*DX*DY*SIN(GBB)
0270578      220.       SUMCB=SUMCB+P1(I,J)*DX*DY*COS(GBB)
0270708      221.  1220 CONTINUE
                C      WRITE(3,1910)J,SUMCB,SUMSB
0270748      222.  1910 FORMAT(26X,I4,25X,F10.7,25X,F10.7)
0270748      223.       GBB=GBB+(4.0*3.14/180.0)
0270768      224.       SUMCBB=SUMCB+SUMCBB
0271008      225.       SUMSBB=SUMSB+SUMSBB
0271028      226.       SUMCB=0.0
0271028      227.       SUMSB=0.0
0271028      228.  1110 CONTINUE
0271088      229.       FCOSB=SUMCBB
0271078      230.       FSINB=SUMSBB
0271108      231.       FCOS1=FCOSA+FCOSB
0271128      232.       FSIN1=FSINB+FSINA
                C      WRITE(3,7202)FSIN1,FCOS1
0271148      233.  7202 FORMAT(F12.5)
                C      WRITE(3,703)
```

```
0271148      254.    703 FORMAT(95H                                        J
                        2 SUMC3                                          SUMS3)
0271148      255.        SUMC3=0.0
0271158      256.        SUMC33=0.0
0271158      257.        SUMS3=0.0
0271168      258.        SUMS33=0.0
0271178      259.        G33=(180.0-THETA3)*3.14/180.0
0271228      240.        DO 113 J=31,91,2
0271268      241.        DO 123 I=1,N+1
0271378      242.        SUMC3=SUMC3+P1(I,J)*DX*DY*COS(G33)
0271558      243.        SUMS3=SUMS3+P1(I,J)*DX*DY*SIN(G33)
0271668      244.    123 CONTINUE
                     C      WRITE(3,913)J,SUMC3,SUMS3
0271728      245.    913 FORMAT(28X,I4,25X,F10.7,25X,F10.7)
0271728      246.        G33=G33+(4.0*3.14/180.0)
0271748      247.        SUMC33=SUMC3+SUMC33
0271768      248.        SUMS33=SUMS3+SUMS33
0272008      249.        SUMC3=0.0
0272008      250.        SUMS3=0.0
0272018      251.    113 CONTINUE
0272058      252.        FCOS3=SUMC33
0272068      253.        FSIN3=SUMS33
                     C      WRITE(3,723)FCOS3,FSIN3
0272078      254.    723 FORMAT(38H                                        FCOS3 = ,F10.7,/,38H
                        2                                FSIN3=  ,F10.7,/,90H                ***********
                        4**********************************************************************
                        6)
                     C      WRITE(3,702)
0272078      255.    702 FORMAT(95H                                        J
                        2 SUMC2                                          SUMS2)
0272078      256.        SUMC2=0.0
0272108      257.        SUMC22=0.0
0272118      258.        SUMS2=0.0
```

```
027212B      259.          SUMS22=0.0
027212B      260.          G22=(180.0-THETA2)*3.14/180.0
027216B      261.          DO 112 J=91,151,2
027221B      262.          DO 122 I=1,N+1
027232B      263.          SUMC2=SUMC2+P1(I,J)*DX*DY*COS(G22)
027250B      264.          SUMS2=SUMS2+P1(I,J)*DX*DY*SIN(G22)
027261B      265.       122 CONTINUE
                        C     WRITE(3,912)J,SUMC2,SUMS2
027265B      266.       912 FORMAT(28X,I4,25X,F10.7,23X,F10.7)
027265B      267.          G22=G22+(4.0*3.14/180.0)
027267B      268.          SUMC22=SUMC2+SUMC22
027271B      269.          SUMS22=SUMS2+SUMS22
027273B      270.          SUMC2=0.0
027273B      271.          SUMS2=0.0
027274B      272.       112 CONTINUE
                        C*****************************************************************
027300B      273.          FCOS2=SUMC22
027301B      274.          FSIN2=SUMS22
                        C     WRITE(3,722)FCOS2,FSIN2
027302B      275.       722 FORMAT(38H                                    FCOS2 = ,F10.7,/,56H
                           2                          FSIN2 = ,F10.7,/,90H**************************
                           4*****************************************************************
                           6)
027302B      276.          WRITE(3,715)((P1(I,J),J=1,N+1,2),I=1,16)
027343B      277.       715 FORMAT((2X,11(F12.5)))
027343B      278.          ALPHA1=ALPHA1*3.14/180.0
027345B      279.          ALPHA2=ALPHA2*3.14/180.0
027346B      280.          ALPHA3=ALPHA3*3.14/180.0
027350B      281.          FT1=SQRT((FCOS1**2)+(FSIN1**2))
027360B      282.          IF(FSIN1.EQ.0.0.AND.FCOS1.EQ.0.0) GO TO 7171
027363B      283.          PHI1=ATAN(-FSIN1/FCOS1)
```

```
027371B      284.          GO TO 4141
027372B      285.    7171  PHI1=0.0
027374B      286.    4141  IF(PHI1.GT.ALPHA1) GO TO 9191
027400B      287.          GO TO 9292
027401B      288.    9191  PHI11=(PHI1-ALPHA1)
027405B      289.          FH1=FT1*SIN(PHI11)
027411B      290.          FV1=FT1*COS(PHI11)
027416B      291.          GO TO 9393
027420B      292.    9292  IF(PHI1.LT.ALPHA1) PHI11=(ALPHA1-PHI1)
027426B      293.          FH1=-FT1*SIN(PHI11)
027432B      294.          FV1=FT1*COS(PHI11)
027436B      295.    9393  FT2=SQRT((FCOS2**2)+(FSIN2**2))
027451B      296.          IF(FSIN2.EQ.0.0.AND.FCOS2.EQ.0.0) GO TO 7272
027454B      297.          PHI2=ATAN(-FSIN2/FCOS2)
027462B      298.          GO TO 4242
027463B      299.    7272  PHI2=0.0
027465B      300.    4242  IF(ALPHA2.GT.1.57) GO TO 9494
027471B      301.          GO TO 9595
027472B      302.    9494  PHI22=(ALPHA2-1.57+PHI2)
027477B      303.          FH2=FT2*COS(PHI22)
027503B      304.          FV2=-FT2*SIN(PHI22)
027511B      305.          GO TO 9696
027513B      306.    9595  IF(ALPHA2.LT.1.57) PHI22=(1.57-ALPHA2-PHI2)
027521B      307.          FH2=FT2*COS(PHI22)
027524B      308.          FV2=FT2*SIN(PHI22)
027531B      309.    9696  FT3=SQRT((FCOS3**2)+(FSIN3**2))
027544B      310.          IF(FSIN3.EQ.0.0.AND.FCOS3.EQ.0.0) GO TO 7373
027547B      311.          PHI3=ATAN(-FSIN3/FCOS3)
027555B      312.          GO TO 4343
027556B      313.    7373  PHI3=0.0
027560B      314.    4343  IF(ALPHA3.LT.1.57) GO TO 9797
027564B      315.          GO TO 9898
027565B      316.    9797  PHI33=(1.57-ALPHA3+PHI3)
```

```
0275728      317.        FH3=-FT3*COS(PHI33)
0275778      318.        FV3=+FT3*SIN(PHI33)
0276038      319.        GO TO 9899
0276058      320.   9898 IF(ALPHA3.GT.1.57) PHI33=(ALPHA3-1.57-PHI3)
0276148      321.        FH3=-FT3*COS(PHI33)
0276208      322.        FV3=-FT3*SIN(PHI33)
0276258      323.   9899 FHT=FH1+FH2+FH3
0276328      324.        FVT=FV1+FV2+FV3
0276358      325.        FTO=SQRT(FHT**2+FVT**2)
0276438      326.        IF(FHT.GT.0.0) ALPH11=ACOS(FVT/FTO)
0276538      327.        IF(FHT.LT.0.0) ALPH11=ASIN(FHT/FTO)
0276628      328.        ALPH11=ALPH11*180.0/3.14
0276648      329.        WRITE(3,99994)FTO,ALPH11
0276748      330.  99994 FORMAT(2(F10.5))
0276748      331.         CALL HESHAM
0276778      332.         EB=EB+0.1
0277008      333.  71717 CONTINUE
0277048      334.        STOP
0277058      335.        END


0000008      1.          SUBROUTINE HESHAM
0000008      2.          COMMON QA1,QA2,QA3,QC1,QC11,QC1T,QC2,QC22,QC2T,QC3,QC33,QC3T,Q1T
                        2,Q2T,Q3T,FHT,FVT
0000008      3.          WRITE(3,256)
0000068      4.          WRITE(3,206)QA1
0000158      5.    206 FORMAT(9UH                          THE AXIAL PRESSURE INDUCED FLOW COEF
                        2FICIENT FOR THE FIRST LOBE  QA1 = ,F20.8)
0000158      6.          WRITE(3,256)
0000238      7.          WRITE(3,207)QA2
0000328      8.    207 FORMAT(9UH                          THE AXIAL PRESSURE INDUCED FLOW COEF
```

```
                2FICIENT FOR THE 2 ND  LOBE  QA2 = ,F20.8)
0000328      9.       WRITE(3,256)
0000408     10.       WRITE(3,208)QA3
0000478     11.   208 FORMAT(9UH                        THE AXIAL PRESSURE INDUCED FLOW COEF
                2FICIENT FOR THE THIRD LOBE QA3  = ,F20.8)
0000478     12.       WRITE(3,256)
0000558     13.       WRITE(3,209)QC1
0000648     14.   209 FORMAT(105H                       THE CIRCUMFERENTIAL PRESSURE INDUCED
                2FLOW COEFFICIENT FOR THE  FIRST LOBE AT  61 QC1  = ,F20.8)
0000648     15.       WRITE(3,256)
0000728     16.       WRITE(3,210)QC11
0001018     17.   210 FORMAT(105H                       THE CIRCUMFERENTIAL PRESSURE INDUCED
                2FLOW COEFFICIENT FOR THE  FIRST LOBE AT  1  QC11 = ,F20.8)
0001018     18.       WRITE(3,256)
0001078     19.       WRITE(3,211)QC1T
0001168     20.   211 FORMAT(105H                       THE CIRCUMFERENTIAL PRESSURE INDUCED
                2FLOW COEFFICIENT FOR THE  FIRST LOBE       QC1T = ,F20.8)
0001168     21.       WRITE(3,256)
0001248     22.       WRITE(3,214)QC2
0001338     23.   214 FORMAT(105H                       THE CIRCUMFERENTIAL PRESSURE INDUCED
                2FLOW COEFFICIENT FOR THE SECOND LOBE AT 121 QC2  = ,F20.8)
0001338     24.       WRITE(3,256)
0001418     25.       WRITE(3,215)QC22
0001508     26.   215 FORMAT(105H                       THE CIRCUMFERENTIAL PRESSURE INDUCED
                2FLOW COEFFICIENT FOR THE SECOND LOBE AT 181 QC22 = ,F20.8)
0001508     27.       WRITE(3,256)
0001568     28.       WRITE(3,216)QC2T
0001658     29.   216 FORMAT(105H                       THE CIRCUMFERENTIAL PRESSURE INDUCED
                2FLOW COEFFICIENT FOR THE SECOND LOBE       QC2T = ,F20.8)
0001658     30.       WRITE(3,256)
0001738     31.       WRITE(3,217)QC3
0002028     32.   217 FORMAT(105H                       THE CIRCUMFERENTIAL PRESSURE INDUCED
                2FLOW COEFFICIENT FOR THE  THIRD LOBE AT  61 QC3  = ,F20.8)
```

```
000202B      33.          WRITE(3,256)
000210B      34.          WRITE(3,218)QC33
000217B      35.      218 FORMAT(105H                                THE CIRCUMFERENTIAL PRESSURE INDUCED
                         2FLOW COEFFICIENT FOR THE  THIRD LOBE AT 121 QC33 = ,F20.8)
000217B      36.          WRITE(3,256)
000225B      37.          WRITE(3,219)QC3T
000234B      38.      219 FORMAT(105H                                THE CIRCUMFERENTIAL PRESSURE INDUCED
                         2FLOW COEFFICIENT FOR THE  THIRD LOBE        QC3T = ,F20.8)
000234B      39.          WRITE(3,256)
000242B      40.          WRITE(3,220)Q1T
000251B      41.      220 FORMAT(105H                                THE TOTAL OIL FLOW COEFFICIENT
                         2FOR THE  FIRST LOBE                         Q1T  = ,F20.8)
000251B      42.          WRITE(3,256)
000257B      43.          WRITE(3,222)Q2T
000266B      44.      222 FORMAT(105H                                THE TOTAL OIL FLOW COEFFICIENT
                         2FOR THE SECOND LOBE                         Q2T  = ,F20.8)
000266B      45.          WRITE(3,256)
000274B      46.          WRITE(3,223)Q3T
000303B      47.      223 FORMAT(105H                                THE TOTAL OIL FLOW COEFFICIENT
                         2FOR THE THIRD LOBE                          Q3T  = ,F20.8)
000303B      48.          WRITE(3,256)
000311B      49.      256 FORMAT(121H************************************************************
                         2************************************************************
                         3)
000311B      50.          WRITE(3,77777)FHT
000320B      51.  77777 FORMAT(67H                                   THE  TOTAL  HORIZONTAL  FO
                         2RCE  FHT = ,F15.8/,100H************************************************
                         3************************************************)
000320B      52.          WRITE(3,6666)FVT
000327B      53.  6666 FORMAT(59H                                    THE  LOAD    FACTOR    FVI
                         2 = ,F15.8/,100H************************************************************
                         3******************************************)
000327B      54.          RETURN
000331B      55.          END
```

APPENDIX A.3.1a

SAMPLE OF THE OUTPUT

THE SOLUTION OF REYNOLDS EQUATION FOR THE EXTERNALLY PRESSURIZED
THREE LOBE JOURNAL BEARINGS FOR ZERO SPEED CASE

THE HIGH PRESSURE OIL IS SUPPLIED FROM THE HIGHPRESSURE GROOVES

N = 28

EPS	MAXIT	EB	L	D	H	ELIPII
.00500	80	0	2	2.000	180	.400

THE OVER RELAXATION FACTOR OMEGA = 1.8501

DISPLACEMENT ANGLE ALPHA = 0

E	EL1	EL2	EL3	ALPHA1	ALPHA2	ALPHA3	THETA1	THETA2
0	.4000	.4000	.4000	0	120.00	120.00	60.000	60.000

1.00000
1.00000
1.00000

DY = .05486889 DX = .05488889

CYCLE NUMBER IN= 51

THE AXIAL PRESSURE INDUCED FLOW COEFFICIENT FOR THE FIRST LOBE QA1 = .1162007

THE AXIAL PRESSURE INDUCED FLOW COEFFICIENT FOR THE 2 ND LOBE QA2 = .1154001

THE AXIAL PRESSURE INDUCED FLOW COEFFICIENT FOR THE THIRD LOBE QA3 = .1154007

THE CIRCUMFERENTIAL PRESSURE INDUCED FLOW COEFFICIENT FOR THE FIRST LOBE AT 61 QC1 =

THE CIRCUMFERENTIAL PRESSURE INDUCED FLOW COEFFICIENT FOR THE FIRST LOBE AT 1 QC11 =

```
THE CIRCUMFERENTIAL PRESSURE INDUCED FLOW COEFFICIENT FOR THE  FIRST LOBE        QC11 =          .0003052
*****************************************************************************************
THE CIRCUMFERENTIAL PRESSURE INDUCED FLOW COEFFICIENT FOR THE SECOND LOBE AT 121 QC2  =          -.0000105
*****************************************************************************************
THE CIRCUMFERENTIAL PRESSURE INDUCED FLOW COEFFICIENT FOR THE SECOND LOBE AT 181 QC22 =          -.0001562
*****************************************************************************************
THE CIRCUMFERENTIAL PRESSURE INDUCED FLOW COEFFICIENT FOR THE SECOND LOBE        QC21 =          -.0001487
*****************************************************************************************
THE CIRCUMFERENTIAL PRESSURE INDUCED FLOW COEFFICIENT FOR THE  THIRD LOBE AT  61 QC3  =          -.0001670
*****************************************************************************************
THE CIRCUMFERENTIAL PRESSURE INDUCED FLOW COEFFICIENT FOR THE  THIRD LOBE AT 121 QC33 =          .0000105
*****************************************************************************************
THE CIRCUMFERENTIAL PRESSURE INDUCED FLOW COEFFICIENT FOR THE  THIRD LOBE        QC31 =          -.0001564
*****************************************************************************************
      THE TOTAL OIL FLOW COEFFICIENT FOR THE  FIRST LOBE                        Q11  =          .1185139
*****************************************************************************************
      THE TOTAL OIL FLOW COEFFICIENT FOR THE SECOND LOBE                        Q21  =          .1132515
*****************************************************************************************
      THE TOTAL OIL FLOW COEFFICIENT FOR THE THIRD LOBE                         Q31  =          .1132502


*****************************************************************************************
          THE  TOTAL  HORIZONTAL  FORCE  FHT =                  0
*****************************************************************************************
          THE  LOAD    FACTOR    FVT =                  0
*****************************************************************************************
    *************************************************************************************
                          THE  SOLUTION  OF  REYNOLDS  EQUATION  FOR  THE  EXTERNALLY  PRESSURIZED
                        THREE  LOBE JOURNAL BEARINGS   FOR ZERO SPEED CASE
    ***************************************  ******************************************************
                          THE HIGH PRESSURE OIL IS SUPPLIED FROM THE HIGHPRESSURE GROOVES
                     N =   28
    ***************************
       EPS      MAXIT      EB      L      D      M      ELIPII
     .00500      80     .1000     2    2.000  180        .400
    ***************************************************
    THE OVER RELAXATION FACTOR OMEGA =    1.8501
```

```
**********************************************
                                                    DISPLACEMENT  ANGLE  ALPHA  =            0
                  ***************************************************************************************
      E        EL1        EL2        EL3        ALPHA1        ALPHA2        ALPHA3        THETA1        THETA2

*************************************************************************************************************
     .0600     .4000     .3750     .3757          0          112.00        112.00        60.000        67.996
*************************************************************************************************************


  1.27715
   .90052
   .90052
                  DY =        .05466669                                          DX =        .05466669
*************************************************************************************************************
CYCLE  NUMBER ITN=      16

**********************
 THE AXIAL PRESSURE INDUCED FLOW COEFFICIENT FOR THE FIRST LOBE  QA1 =            .11006561
*************************************************************************************************************
 THE AXIAL PRESSURE INDUCED FLOW COEFFICIENT FOR THE 2 ND  LOBE  QA2 =            .11825202
*************************************************************************************************************
 THE AXIAL PRESSURE INDUCED FLOW COEFFICIENT FOR THE THIRD LOBE QA3  =            .11655163
*************************************************************************************************************
THE CIRCUMFERENTIAL PRESSURE INDUCED FLOW COEFFICIENT FOR THE  FIRST LOBE AT  61 QC1  =            .0033716
*************************************************************************************************************
THE CIRCUMFERENTIAL PRESSURE INDUCED FLOW COEFFICIENT FOR THE  FIRST LOBE AT  1  QC11 =            .0043042
*************************************************************************************************************
THE CIRCUMFERENTIAL PRESSURE INDUCED FLOW COEFFICIENT FOR THE  FIRST LOBE        QC11 =            .0076759
*************************************************************************************************************
THE CIRCUMFERENTIAL PRESSURE INDUCED FLOW COEFFICIENT FOR THE SECOND LOBE AT 121 QC2  =            .0006590
*************************************************************************************************************
THE CIRCUMFERENTIAL PRESSURE INDUCED FLOW COEFFICIENT FOR THE SECOND LOBE AT 181 QC22 =           -.0043042
*************************************************************************************************************
```

```
THE CIRCUMFERENTIAL PRESSURE INDUCED FLOW COEFFICIENT FOR THE SECOND LOBE        QC2T =          -.0036452
**********************************************************************************************
THE CIRCUMFERENTIAL PRESSURE INDUCED FLOW COEFFICIENT FOR THE  THIRD LOBE AT  61 QC3  =          -.0055716
**********************************************************************************************
THE CIRCUMFERENTIAL PRESSURE INDUCED FLOW COEFFICIENT FOR THE  THIRD LOBE AT 121 QC33 =          -.0006590
**********************************************************************************************
THE CIRCUMFERENTIAL PRESSURE INDUCED FLOW COEFFICIENT FOR THE  THIRD LOBE        QC3T =          -.0040507
**********************************************************************************************
      THE TOTAL OIL FLOW COEFFICIENT FOR THE  FIRST LOBE                         Q1T  =           .1177595
**********************************************************************************************
      THE TOTAL OIL FLOW COEFFICIENT FOR THE SECOND LOBE                         Q2T  =           .1140068
**********************************************************************************************
      THE TOTAL OIL FLOW COEFFICIENT FOR THE THIRD LOBE                          Q3T  =           .1143209
**********************************************************************************************
            THE  TOTAL  HORIZONTAL  FORCE  FHT =       -.00193406
**********************************************************************
            THE  LOAD    FACTOR    FVT =        .13400355
**********************************************************************
                                  THE  SOLUTION  OF  REYNOLDS  EQUATION  FOR  THE  EXTERNALLY  PRESSURIZED
                          THREE  LOBE JOURNAL BEARINGS   FOR ZERO SPEED CASE
      ************************************  ************************************************************
                             THE HIGH PRESSURE OIL IS SUPPLIED FROM THE HIGHPRESSURE GROOVES
                        N =   28
      ************************

        EPS      MAXIT      EB       L       D       B       ELIPIT
      .00500      60      .2000     2     2.000   180         .400
      ***************************************************
      THE OVER RELAXATION FACTOR OMEGA =   1.8501
      ******************************************
                                                          DISPLACEMENT  ANGLE  ALPHA  =            0
                     ***************************************************************************
```

```
      E         EL1         EL2         EL3         ALPHA1         ALPHA2         ALPHA3         THETA1         THETA2

*****************************************************************************************************************
      .1200      .5200      .3555      .3557           0           105.00         102.99         60.000         77.002
*****************************************************************************************************************
    1.68537
     .80804
     .80804
*****************************************************************************************************************
  THE AXIAL PRESSURE INDUCED FLOW COEFFICIENT FOR THE FIRST LOBE  QA1 =                .10200661
*****************************************************************************************************************
  THE AXIAL PRESSURE INDUCED FLOW COEFFICIENT FOR THE 2 ND  LOBE  QA2 =                .12250354
*****************************************************************************************************************
  THE AXIAL PRESSURE INDUCED FLOW COEFFICIENT FOR THE THIRD LOBE QA3  =                .12255146
*****************************************************************************************************************
THE CIRCUMFERENTIAL PRESSURE INDUCED FLOW COEFFICIENT FOR THE  FIRST LOBE AT  61 QC1  =              .0087289
*****************************************************************************************************************
THE CIRCUMFERENTIAL PRESSURE INDUCED FLOW COEFFICIENT FOR THE  FIRST LOBE AT   1  QC11 =              .0081885
*****************************************************************************************************************
THE CIRCUMFERENTIAL PRESSURE INDUCED FLOW COEFFICIENT FOR THE  FIRST LOBE         QC11 =              .0169174
*****************************************************************************************************************
THE CIRCUMFERENTIAL PRESSURE INDUCED FLOW COEFFICIENT FOR THE SECOND LOBE AT 121 QC2  =             -.0011491
*****************************************************************************************************************
THE CIRCUMFERENTIAL PRESSURE INDUCED FLOW COEFFICIENT FOR THE SECOND LOBE AT 181 QC22 =             -.0081685
*****************************************************************************************************************
THE CIRCUMFERENTIAL PRESSURE INDUCED FLOW COEFFICIENT FOR THE SECOND LOBE         QC21 =             -.0093576
*****************************************************************************************************************
THE CIRCUMFERENTIAL PRESSURE INDUCED FLOW COEFFICIENT FOR THE  THIRD LOBE AT  61 QC3  =             -.0087289
*****************************************************************************************************************
THE CIRCUMFERENTIAL PRESSURE INDUCED FLOW COEFFICIENT FOR THE  THIRD LOBE AT 121 QC33 =              .0011491
*****************************************************************************************************************
THE CIRCUMFERENTIAL PRESSURE INDUCED FLOW COEFFICIENT FOR THE  THIRD LOBE         QC31 =             -.0075796
*****************************************************************************************************************
      THE TOTAL OIL FLOW COEFFICIENT FOR THE  FIRST LOBE                         Q11  =              .1169241
```

```
**********************************************************************************************
      THE TOTAL OIL FLOW COEFFICIENT FOR THE SECOND LOBE                    Q21  =          .1129658
**********************************************************************************************


      THE TOTAL OIL FLOW COEFFICIENT FOR THE THIRD LOBE                     Q31  =          .1147510
**********************************************************************************************
            THE  TOTAL  HORIZONTAL  FORCE  FHT =       -.00229766
**************************************************************************
            THE  LOAD     FACTOR     FVT =        .29177726
**************************************************************************
                                THE  SOLUTION  OF  REYNOLDS  EQUATION  FOR  THE  EXTERNALLY  PRESSURIZED
                          THREE  LOBE JOURNAL BEARINGS   FOR ZERO SPEED CASE
     ************************************  ************************************************
                            THE HIGH PRESSURE OIL IS SUPPLIED FROM THE HIGHPRESSURE GROOVES
                        N =    28
     ************************
          EPS       MAXIT       EB       L       D       M       ELIPII
        .00500        60      .4000      2     2.000    100        .400
     ************************************************
     THE OVER RELAXATION FACTOR OMEGA =    1.8501
     ******************************************
                                                          DISPLACEMENT  ANGLE  ALPHA  =             0
                        ***************************************************************************
          E         EL1         EL2         EL3         ALPHA1         ALPHA2         ALPHA3         THETA1         THETA2

     ***************************************************************************************************
        .2400      .0400      .5486      .5490            0             65.59          65.40         60.000         90.008
     ***************************************************************************************************
       3.50019
        .05205
        .05205
```

```
**********************************************************************************************
  THE AXIAL PRESSURE INDUCED FLOW COEFFICIENT FOR THE FIRST LOBE  QA1 =              .0665672
**********************************************************************************************
  THE AXIAL PRESSURE INDUCED FLOW COEFFICIENT FOR THE 2 ND  LOBE  QA2 =              .1290106
**********************************************************************************************


  THE AXIAL PRESSURE INDUCED FLOW COEFFICIENT FOR THE THIRD LOBE QA3  =              .1269150
**********************************************************************************************
THE CIRCUMFERENTIAL PRESSURE INDUCED FLOW COEFFICIENT FOR THE  FIRST LOBE AT  61 QC1  =           .0165355
**********************************************************************************************
THE CIRCUMFERENTIAL PRESSURE INDUCED FLOW COEFFICIENT FOR THE  FIRST LOBE AT   1  QC11 =           .0160516
**********************************************************************************************
THE CIRCUMFERENTIAL PRESSURE INDUCED FLOW COEFFICIENT FOR THE  FIRST LOBE        QC1T =           .0325671
**********************************************************************************************
THE CIRCUMFERENTIAL PRESSURE INDUCED FLOW COEFFICIENT FOR THE SECOND LOBE AT 121 QC2  =          -.0011597
**********************************************************************************************
THE CIRCUMFERENTIAL PRESSURE INDUCED FLOW COEFFICIENT FOR THE SECOND LOBE AT 181 QC22 =          -.0160516
**********************************************************************************************
THE CIRCUMFERENTIAL PRESSURE INDUCED FLOW COEFFICIENT FOR THE SECOND LOBE        QC21 =          -.0171713
**********************************************************************************************
THE CIRCUMFERENTIAL PRESSURE INDUCED FLOW COEFFICIENT FOR THE  THIRD LOBE AT  61 QC3  =          -.0165355
**********************************************************************************************
THE CIRCUMFERENTIAL PRESSURE INDUCED FLOW COEFFICIENT FOR THE  THIRD LOBE AT 121 QC33 =           .0011597
**********************************************************************************************
THE CIRCUMFERENTIAL PRESSURE INDUCED FLOW COEFFICIENT FOR THE  THIRD LOBE        QC31 =          -.0155957
**********************************************************************************************
      THE TOTAL OIL FLOW COEFFICIENT FOR THE  FIRST LOBE                        Q1T  =           .1169058
**********************************************************************************************
      THE TOTAL OIL FLOW COEFFICIENT FOR THE SECOND LOBE                        Q2T  =           .1118392
**********************************************************************************************
      THE TOTAL OIL FLOW COEFFICIENT FOR THE THIRD LOBE                         Q3T  =           .1155195
**********************************************************************************************
            THE  TOTAL  HORIZONTAL  FORCE  FHT =       -.0057s096
**********************************************************************
            THE  LOAD    FACTOR    FVT =        .7955o615
**********************************************************************
```

THE SOLUTION OF REYNOLDS EQUATION FOR THE EATERNALLY PRESSURIZED
THREE LOBE JOURNAL BEARINGS FOR ZERO SPEED CASE

THE HIGH PRESSURE OIL IS SUPPLIED FROM THE HIGHPRESSURE GROOVES

N = 20

EPS	MAXIT	EB	L	D	M	ELIPII
.00500	80	.0000	2	2.000	180	.400

THE OVER RELAXATION FACTOR OMEGA = 1.0501

DISPLACEMENT ANGLE ALPHA = 0

E	EL1	EL2	EL3	ALPHA1	ALPHA2	ALPHA3	THETA1	THETA2
9.03449								
.53526								
.53526								

THE AXIAL PRESSURE INDUCED FLOW COEFFICIENT FOR THE FIRST LOBE QA1 = .07002225

THE AXIAL PRESSURE INDUCED FLOW COEFFICIENT FOR THE 2 ND LOBE QA2 = .13565181

THE AXIAL PRESSURE INDUCED FLOW COEFFICIENT FOR THE THIRD LOBE QA3 = .13534095

THE CIRCUMFERENTIAL PRESSURE INDUCED FLOW COEFFICIENT FOR THE FIRST LOBE AT 01 QC1 = .0244688

THE CIRCUMFERENTIAL PRESSURE INDUCED FLOW COEFFICIENT FOR THE FIRST LOBE AT 1 QC11 = .0259001

THE CIRCUMFERENTIAL PRESSURE INDUCED FLOW COEFFICIENT FOR THE FIRST LOBE QC11 = .0463690

THE CIRCUMFERENTIAL PRESSURE INDUCED FLOW COEFFICIENT FOR THE SECOND LOBE AT 121 QC2 = -.0015758

THE CIRCUMFERENTIAL PRESSURE INDUCED FLOW COEFFICIENT FOR THE SECOND LOBE AT 161 QC22 = -.0259001

```
**********************************************************************************************
THE CIRCUMFERENTIAL PRESSURE INDUCED FLOW COEFFICIENT FOR THE SECOND LOBE        QC2I =          -.0254759
**********************************************************************************************
THE CIRCUMFERENTIAL PRESSURE INDUCED FLOW COEFFICIENT FOR THE  THIRD LOBE AT  61 QC3  =          -.0244686
**********************************************************************************************
THE CIRCUMFERENTIAL PRESSURE INDUCED FLOW COEFFICIENT FOR THE  THIRD LOBE AT 121 QC3S =           .0015758
**********************************************************************************************
THE CIRCUMFERENTIAL PRESSURE INDUCED FLOW COEFFICIENT FOR THE  THIRD LOBE        QC3I =          -.0228950
**********************************************************************************************
      THE TOTAL OIL FLOW COEFFICIENT FOR THE  FIRST LOBE                         Q1T  =           .1185912
**********************************************************************************************
      THE TOTAL OIL FLOW COEFFICIENT FOR THE SECOND LOBE                         Q2T  =           .1101758
**********************************************************************************************
      THE TOTAL OIL FLOW COEFFICIENT FOR THE THIRD LOBE                          Q3T  =           .1124476
**********************************************************************************************
            THE  TOTAL  HORIZONTAL  FORCE  FHT =       -.00241427
**********************************************************************
            THE  LOAD    FACTOR    FVT =       2.08259599
**********************************************************************
```

S_P=0.03

```
**********************************************************************************************
                              THE  SOLUTION  OF  REYNOLDS  EQUATION  FOR  THE  EXTERNALLY  PRESSURIZED
                         THREE  LOBE JOURNAL BEARINGS   FOR ZERO SPEED CASE
**********************************  ***************************************************
                           THE HIGH PRESSURE OIL IS SUPPLIED FROM THE HIGHPRESSURE GROOVES
                      N =    28
**************************
    EPS       MAXIT       EB       L       D       M       ELIPIT
   .00500       80      .1000      2    2.0000   180        .400
**********************************************************
THE OVER RELAXATION FACTOR OMEGA =    1.8501
**********************************************
                                                        DISPLACEMENT  ANGLE  ALPHA  =              0
                    ***********************************************************************************
      E         EL1         EL2         EL3         ALPHA1         ALPHA2         ALPHA3         THETA1         THETA2

**********************************************************************************************************
      .0000      .4000      .3736      .3737            0           112.00         112.00         60.000         67.996
**********************************************************************************************************
   1.25005
    .00170
    .00170
                      DY =         -.05425269                                        DX =          .05408589
**********************************************************************************************
```

```
**********************************************************************************************
  THE AXIAL PRESSURE INDUCED FLOW COEFFICIENT FOR THE FIRST LOBE  QA1 =              .10595210
**********************************************************************************************
  THE AXIAL PRESSURE INDUCED FLOW COEFFICIENT FOR THE 2 ND  LOBE  QA2 =              .11870649
**********************************************************************************************
  THE AXIAL PRESSURE INDUCED FLOW COEFFICIENT FOR THE THIRD LOBE QA3  =              .10764401
**********************************************************************************************
THE CIRCUMFERENTIAL PRESSURE INDUCED FLOW COEFFICIENT FOR THE  FIRST LOBE AT  01 QC1  =           -.0255995
**********************************************************************************************
THE CIRCUMFERENTIAL PRESSURE INDUCED FLOW COEFFICIENT FOR THE  FIRST LOBE AT  1  QC11 =            .0508579
**********************************************************************************************
THE CIRCUMFERENTIAL PRESSURE INDUCED FLOW COEFFICIENT FOR THE  FIRST LOBE        QC11 =            .0072584
**********************************************************************************************
THE CIRCUMFERENTIAL PRESSURE INDUCED FLOW COEFFICIENT FOR THE SECOND LOBE AT 121 QC2  =            .0505756
**********************************************************************************************
THE CIRCUMFERENTIAL PRESSURE INDUCED FLOW COEFFICIENT FOR THE SECOND LOBE AT 181 QC22 =           -.0508579
**********************************************************************************************
THE CIRCUMFERENTIAL PRESSURE INDUCED FLOW COEFFICIENT FOR THE SECOND LOBE        QC21 =           -.0002022
**********************************************************************************************
THE CIRCUMFERENTIAL PRESSURE INDUCED FLOW COEFFICIENT FOR THE  THIRD LOBE AT  61 QC3  =            .0255995


**********************************************************************************************
THE CIRCUMFERENTIAL PRESSURE INDUCED FLOW COEFFICIENT FOR THE  THIRD LOBE AT 121 QC33 =           -.0505756
**********************************************************************************************
THE CIRCUMFERENTIAL PRESSURE INDUCED FLOW COEFFICIENT FOR THE  THIRD LOBE        QC31 =           -.0069761
**********************************************************************************************
      THE TOTAL OIL FLOW COEFFICIENT FOR THE  FIRST LOBE                        Q11  =            .1151905
**********************************************************************************************
      THE TOTAL OIL FLOW COEFFICIENT FOR THE SECOND LOBE                        Q21  =            .1105042
**********************************************************************************************
      THE TOTAL OIL FLOW COEFFICIENT FOR THE THIRD LOBE                         Q31  =            .1000670
**********************************************************************************************
           THE  TOTAL  HORIZONTAL  FORCE  FHT =        .0575576
**********************************************************************************************
           THE  LOAD    FACTOR    FVT =        .1554604
**********************************************************************************************
```

S_P=0.03

```
**********************************************************************************************
                              THE  SOLUTION  OF  REYNOLDS  EQUATION  FOR  THE  EXTERNALLY  PRESSURIZED
                        THREE  LOBE JOURNAL BEARINGS   FOR ZERO SPEED CASE
**************************************** ************************************************
                          THE HIGH PRESSURE OIL IS SUPPLIED FROM THE HIGHPRESSURE GROOVES
                     N =    28
**************************
     EPS       MAXIT       EB       L       D       H       ELIPIT
    .00500       80      .4000      2    2.000   180         .400
**********************************************************************
THE OVER RELAXATION FACTOR OMEGA =    1.6501
**************************************
                                                    DISPLACEMENT  ANGLE  ALPHA  =              0
                    ***************************************************************************
      E         EL1         EL2         EL3         ALPHA1         ALPHA2         ALPHA3         THETA1         THETA2

**********************************************************************************************
     .2400      .6400      .3466      .3490            0            63.39          63.40         60.000         96.608
**********************************************************************************************
   5.29754
    .55414
    .55414
```

```
**********************************************************************************************
 THE AXIAL PRESSURE INDUCED FLOW COEFFICIENT FOR THE FIRST LOBE  QA1 =              .0852602U
**********************************************************************************************
 THE AXIAL PRESSURE INDUCED FLOW COEFFICIENT FOR THE 2 ND  LOBE  QA2 =              .12925255
**********************************************************************************************
 THE AXIAL PRESSURE INDUCED FLOW COEFFICIENT FOR THE THIRD LOBE QA3  =              .00432248
**********************************************************************************************
THE CIRCUMFERENTIAL PRESSURE INDUCED FLOW COEFFICIENT FOR THE  FIRST LOBE AT  61 QC1  =          -.0165069
**********************************************************************************************
THE CIRCUMFERENTIAL PRESSURE INDUCED FLOW COEFFICIENT FOR THE  FIRST LOBE AT   1  QC11 =           .0508857
**********************************************************************************************
THE CIRCUMFERENTIAL PRESSURE INDUCED FLOW COEFFICIENT FOR THE  FIRST LOBE         QC11 =           .0343786
**********************************************************************************************
THE CIRCUMFERENTIAL PRESSURE INDUCED FLOW COEFFICIENT FOR THE SECOND LOBE AT 121 QC2  =           .0369657
**********************************************************************************************
THE CIRCUMFERENTIAL PRESSURE INDUCED FLOW COEFFICIENT FOR THE SECOND LOBE AT 181 QC22 =          -.0508857
**********************************************************************************************
THE CIRCUMFERENTIAL PRESSURE INDUCED FLOW COEFFICIENT FOR THE SECOND LOBE         QC2T =          -.0139200
**********************************************************************************************
THE CIRCUMFERENTIAL PRESSURE INDUCED FLOW COEFFICIENT FOR THE  THIRD LOBE AT  61 QC3  =           .0165069
**********************************************************************************************
THE CIRCUMFERENTIAL PRESSURE INDUCED FLOW COEFFICIENT FOR THE  THIRD LOBE AT 121 QC33 =          -.0369657
**********************************************************************************************
THE CIRCUMFERENTIAL PRESSURE INDUCED FLOW COEFFICIENT FOR THE  THIRD LOBE         QC3T =          -.0204588
**********************************************************************************************
      THE TOTAL OIL FLOW COEFFICIENT FOR THE  FIRST LOBE                          QT1  =           .1176050
**********************************************************************************************
      THE TOTAL OIL FLOW COEFFICIENT FOR THE SECOND LOBE                          Q2T  =           .1155525
**********************************************************************************************
      THE TOTAL OIL FLOW COEFFICIENT FOR THE THIRD LOBE                           Q3T  =           .0038056
**********************************************************************************************
            THE  TOTAL  HORIZONTAL  FORCE  FHT =        .29796044
**********************************************************************************************
            THE  LOAD    FACTOR    FVT =        .30782056
**********************************************************************************************
```

A.3.2. A COMPUTER PROGRAMME FOR THE NUMERICAL SOLUTION FOR THE THREE-LOBE JOURNAL BEARING .

"THE HIGH PRESSURE OIL IS ADMITTED AT THE CONJUNCTION OF THE LOBES (i.e. AT THE AXIAL GROOVES)."

```
.NULL.
00001:JOB(GREM114D,J12,T90,M7600)     T.M.SALEM       DEPT.MEC8.ENG.
00002:MNF(T)
00003:LDSET(MAP=B/ZZZZMP,PRESET=ZERO)
00004:LGO.
00005:@
00006:       PROGRAM STAT1(INPUT,OUTPUT,TAPE4=INPUT,TAPE3=OUTPUT)
00007:       COMMON QA201,QA203,QA2,QA1,QA3,QC102,QC103,QC1,QC201,QC203,QC2,QC3
00008:      201,QC302,QC3,QT1,QT2,QT3
00009:       DIMENSION P1(29,182),H1(29,182)
00010:       EPS=0.0005
00011:       L=2
00012:       EB=0.0
00013:       D=2.0
00014:       M=180
00015:       ELIPIT=0.4
00016:       MAXIT=350
00017:       DX=3.14/FLOAT(M/2)
00018:       DY=DX
00019:       N=28
00020:       WRITE(3,600)
00021:   600 FORMAT(103H                                        THE  SOLUTION  OF  REYNO
00022:      2LDS  EQUATION  FOR  THE  EXTERNALLY  PRESSURIZED/,96H
00023:      3           THREE  LOBE JOURNAL BEARINGS   FOR ZERO SPEED CASE
00024:      4                  /,100H****************************************
00025:      5**************************************************)
00026:       WRITE(3,666)
00027:   666 FORMAT(88H                                THE HIGH PRESSURE OIL IS SUPPLI
00028:      2ED FROM THE LOW PRESSURE GROOVES)
00029:       WRITE(3,630)N
```

```
00030:  630 FORMAT(24H                          N = ,I4/,25H**********************
00031:     2*)
00032:      WRITE(3,610)
00033:  610 FORMAT(54H     EPS      MAXIT      EB      L      D      M      ELIPIT)
00034:      WRITE(3,620)EPS,MAXIT,EB,L,D,M,ELIPIT
00035:  620 FORMAT(3X,F7.5,4X,I3,3X,F6.4,4X,I1,3X,F5.3,2X,I3,5X,F5.3/,55H*****
00036:     2**************************************************)
00037:      EMEU=1.0-(((3.14**2)*(4.0+(3.14*D/FLOAT(L))**2))/(2.0*((FLOAT(
00038:     4M/2)*FLOAT(M/2))+(3.14*D*FLOAT(N)/FLOAT(L))**2)))
00039:      OMEGA=2.0*((1.0-(1.0-EMEU**2)**0.5)/(EMEU**2))
00040:      WRITE(3,680)OMEGA
00041:  680 FORMAT(36H THE OVER RELAXATION FACTOR OMEGA = ,F8.4/,45H**********
00042:     2**********************************)
00043:      ALPHA=0.0
00044:  811 WRITE(3,730)ALPHA
00045:  730 FORMAT(91H
00046:     2EARING  ATTITUDE  ANGLE  ALPHA  =  ,F10.6/,100H
00047:     3****************************************************************
00048:     4***************)
00049:      E=EB*(1.0-ELIPIT)
00050:      EL1=((E**2)+(ELIPIT**2)+(2.0*E*ELIPIT*COS(ALPHA)))**0.5
00051:      ALPHA1=(ASIN((E*SIN(ALPHA))/EL1))*180.0/3.14
00052:      EL2=((E**2+ELIPIT**2-2.0*E*ELIPIT*COS((3.14/3.0)-ALPHA))**0.5)
00053:      ALPHA0=(ASIN((E*SIN((3.14/3.0)-ALPHA)/EL2))-2.0*3.14/3.0)*180.0/3.
00054:     414
00055:      ALPHA2=-ALPHA0
00056:      EL3=((E**2+(ELIPIT**2)+(2.0*E*ELIPIT*COS((3.14*2.0/3.0)-ALPHA)
00057:     2)))**0.5
00058:      ALPHA3=((2.0*3.14/3.0)-(ASIN(E*SIN((3.14*2.0/3.0)-ALPHA)/EL3)))*18
00059:     20.0/3.14
00060:      THETA1=60.0+ALPHA1
00061:      THETA2=180.0-ALPHA2
00062:      THETA3=ALPHA3-60.0
00063:      WRITE(3,640)
00064:  640 FORMAT(116H       E        EL1        EL2        EL3        ALPHA1
00065:     2   ALPHA2        ALPHA3        THETA1        THETA2        THETA3//,10
```

```
00066:      30H**********************************************************
00067:      4**********************************)
00068:       WRITE(3,650)E,EL1,EL2,EL3,ALPHA1,ALPHA2,ALPHA3,THETA1,THETA2,THETA
00069:      13
00070:  650 FORMAT(4X,F7.4,2X,F7.4,2X,F7.4,2X,F7.4,3X,F7.2,7X,F8.2,6X,F8.2,7X,
00071:      4F6.3,7X,F6.3,7X,F6.3/,100H**************************************
00072:      5************************************************************)
00073:       G2=(180.0-THETA2)*3.14/180.0
00074:       DO 30 J=1,61
00075:       DO 20 I=1,N+1
00076:       H1(I,J)=(1.0+EL2*COS(G2))/2.0
00077:    20 CONTINUE
00078:    30 G2=G2+(2.0*3.14/180.0)
00079:       G1=(180.0-THETA1)*3.14/180.0
00080:       DO 32 J=61,121
00081:       DO 23 I=1,N+1
00082:       H1(I,J)=(1.0+(EL1*COS(G1)))/2.0
00083:    23 CONTINUE
00084:    32 G1=G1+(2.0*3.14/180.0)
00085:       G3=(180.0-THETA3)*3.14/180.0
00086:       DO 33 J=121,181
00087:       DO 24 I=1,N+1
00088:       H1(I,J)=(1.0+EL3*COS(G3))/2.0
00089:    24 CONTINUE
00090:    33 G3=G3+(2.0*3.14/180.0)
00091:       WRITE(3,660)
00092:  660 FORMAT(50H  THE  OIL  FILM  THICKNESS  AT  THE  MESH  POINTS/,51H*
00093:      2**************************************************)
00094:       WRITE(3,670)((H1(I,J),J=1,M+1),I=1,3)
00095:  670 FORMAT((10(F7.5,4X)))
00096:       A2=0.5
00097:       A3=0.5
00098:       A4=0.5
00099:       Q0=0.0
00100:  111 B11=0.0
00101:       DO 50 I=2,N
```

```
00102:       DO 50 J=1,5,2
00103:       P1(I,J)=A2
00104:    50 CONTINUE
00105:       DO 60 I=2,N
00106:       DO 60 J=57,65,2
00107:       P1(I,J)=A3
00108:    60 CONTINUE
00109:       DO 70 I=2,N
00110:       DO 70 J=117,125,2
00111:       P1(I,J)=A4
00112:    70 CONTINUE
00113:       DO 80 I=2,N
00114:       DO 80 J=177,181,2
00115:       P1(I,J)=A2
00116:    80 CONTINUE
00117:       DO 94 J=2,M
00118:    94 P1(1,J)=0.0
00119:       DO 95 J=2,M
00120:    95 P1(N+1,J)=0.0
00121:       ITN=1
00122:       WRITE(3,810)DY,DX
00123:   810 FORMAT(25H                          DY = ,F15.8,45H
00124:      2                    DX = ,F15.8/,100H**********************************
00125:      4****************************************************************
00126:      5****)
00127:       WRITE(3,25)A2,A3,A4
00128:    25 FORMAT(F15.8)
00129:       R=(D/FLOAT(L))**2
00130:       S=DX**2
00131:       T=DY**2
00132:       B=1.0-OMEGA
00133:    90 DA=0.0
00134:       DO 100 J=3,M,2
00135:       DO 100 I=2,N
00136:       IF(I.GT.1.AND.I.LT.N+1) GO TO 1
```

```
00137:       GO TO 2
00138:     1 IF(J.GT.0.AND.J.LT.6.) GO TO 100
00139:       IF(J.GT.55.AND.J.LT.66) GO TO 100
00140:       IF(J.GT.115.AND.J.LT.126) GO TO 100
00141:       IF(J.GT.175.AND.J.LT.182) GO TO 100
00142:     2 A1=0.0
00143:       B1=((R/T)*((H1(I+1,J))**3)*(P1(I+1,J)))
00144:       C1=((1.0/S)*((H1(I,J+1))**3)*(P1(I,J+2)))
00145:       D1=((R/T)*((H1(I-1,J))**3)*(P1(I-1,J)))
00146:       E1=((1.0/S)*((H1(I,J-1))**3)*(P1(I,J-2)))
00147:       F1=((R/T)*((H1(I+1,J))**3))
00148:       Q1=((1.0/S)*((H1(I,J+1))**3))
00149:       Y1=((R/T)*((H1(I-1,J))**3))
00150:       Z1=((1.0/S)*((H1(I,J-1))**3))
00151:       PNEW1=OMEGA*((A1+B1+C1+D1+E1)/(F1+Q1+Y1+Z1))+B*P1(I,J)
00152:       RESID=ABS(PNEW1-P1(I,J))
00153:       IF(RESID.GT.DA) DA=RESID
00154:   888 P1(I,J)=PNEW1
00155:       IF(J.GE.1.AND.J.LT.62) GO TO 7
00156:       IF(J.GT.62.AND.J.LT.122) GO TO 9
00157:       IF(J.GT.121.AND.J.LT.182) GO TO 10
00158:     7 THETA=THETA1
00159:       GO TO 8
00160:     9 THETA=THETA2
00161:       GO TO 8
00162:    10 THETA=THETA3
00163:     8 IF(J.GT.(THETA/2.0).AND.P1(I,J).LT.0.0) P1(I,J)=0.0
00164:   100 CONTINUE
00165:       ITN=ITN+1
00166:       IF(ITN.GT.MAXIT) GO TO 2323
00167:       IF(DA.GT.EPS) GO TO 90
00168:  2323 WRITE(3,690)ITN
00169:   690 FORMAT(21H  CYCLE NUMBER ITN = ,I5//,21H**********************)
00170:       WRITE(3,713)((P1(I,J),J=1,M+1,2),I=1,8)
00171:   713 FORMAT((2X,9(F12.6)))
00172:       QC201=0.0
```

```
00173:       DO 1005 I=1,N+1
00174:       QC201=QC201+(FLOAT(L)/D)*(DY/(2.0*DX))*(H1(I,31)**3)*(P1(I,29)-P1(
00175:      2I,33))
00176: 1005 CONTINUE
00177:       QC203=0.0
00178:       DO 1006 I=1,N+1
00179:       QC203=QC203+(FLOAT(L)/D)*(DY/(2.0*DX))*(H1(I,151)**3)*(P1(I,153)-P
00180:      21(I,149))
00181: 1006 CONTINUE
00182:       QC2=QC201+QC203
00183:       QC102=0.0
00184:       DO 1007 I=1,N+1
00185:       QC102=QC102+(FLOAT(L)/D)*(DY/(2.0*DX))*(H1(I,31)**3)*(P1(I,33)-P1(
00186:      2I,29))
00187: 1007 CONTINUE
00188:       QC103=0.0
00189:       DO 1008 I=1,N+1
00190:       QC103=QC103+(FLOAT(L)/D)*(DY/(2.0*DX))*(H1(I,91)**3)*(P1(I,89)-P1(
00191:      2I,93))
00192: 1008 CONTINUE
00193:       QC1=QC103+QC102
00194:       QC301=0.0
00195:       DO 1009 I=1,N+1
00196:       QC301=QC301+(FLOAT(L)/D)*(DY/(2.0*DX))*(H1(I,91)**3)*(P1(I,93)-P1(
00197:      2I,89))
00198: 1009 CONTINUE
00199:       QC302=0.0
00200:       DO 1010 I=1,N+1
00201:       QC302=QC302+(FLOAT(L)/D)*(DY/(2.0*DX))*(H1(I,151)**3)*(P1(I,149)-P
00202:      21(I,153))
00203: 1010 CONTINUE
00204:       QC3=QC302+QC301
00205:       QA201=0.0
00206:       DO 1000 J=3,31,2
00207:       QA201=QA201+(D/FLOAT(L))*(DX/(2.0*DY))*(H1(N,J)**3)*P1(N-1,J)
```

```
00208: 1000 CONTINUE
00209:       QA203=0.0
00210:       DO 1001 J=151,181,2
00211:       QA203=QA203+(D/FLOAT(L))*(DX/(2.0*DY))*(H1(N,J)**3)*P1(N-1,J)
00212: 1001 CONTINUE
00213:       QA2=QA201+QA203
00214:       QA1=0.0
00215:       DO 1002 J=31,91,2
00216:       QA1=QA1+(D/FLOAT(L))*(DX/(4.0*DY))*(H1(N,J)**3)*P1(N-1,J)
00217: 1002 CONTINUE
00218:       QA3=0.0
00219:       DO 1003 J=91,151,2
00220:       QA3=QA3+(D/FLOAT(L))*(DX/(2.0*DY))*(H1(N,J)**3)*P1(N-1,J)
00221: 1003 CONTINUE
00222:       QT1=2.0*QA1+QC1
00223:       QT2=2.0*QA2+QC2
00224:       QT3=2.0*QA3+QC3
00225:       CALL HALLAH
00226:       B2=QT2-QT1
00227:       IF(B2.LE..01.AND.B2.GT.0.0) GO TO 18
00228:       IF(B2.GE.-.01.AND.B2.LT.0.0) GO TO 18
00229:       IF(QO.GT.QT1.OR.QO.LT.QT1) A3=QO*A3/QT1
00230:       IF(QO.LT.QT2.OR.QO.GT.QT2) A2=QO*A2/QT2
00231:       IF(QO.LT.QT3.OR.QO.GT.QT3) A4=QO*A4/QT3
00232:       GO TO 111
00233:    18 WRITE(3,700)
00234:   700 FORMAT(95H                                        J
00235:      2 SUMC1                                    SUMS1)
00236:       SUMC1=0.0
00237:       SUMC11=0.0
00238:       SUMS1=0.0
00239:       SUMS11=0.0
00240:       G11=(180.0-THETA1)*3.14/180.0
00241:       DO 110 J=61,121,2
00242:       DO 120 I=1,N+1
00243:       SUMC1=SUMC1+P1(I,J)*DX*DY*COS(G11)
```

```
00244:       SUMS1=SUMS1+P1(I,J)*DX*DY*SIN(G11)
00245:   120 CONTINUE
00246:       WRITE(3,910)J,SUMC1,SUMS1
00247:   910 FORMAT(28X,I2,25X,F10.7,23X,F10.7)
00248:       G11=G11+(4.0*3.14/180.0)
00249:       SUMC11=SUMC1+SUMC11
00250:       SUMS11=SUMS1+SUMS11
00251:       SUMC1=0.0
00252:       SUMS1=0.0
00253:   110 CONTINUE
00254:       FCOS1=SUMC11
00255:       FSIN1=SUMS11
00256:       WRITE(3,720)FCOS1,FSIN1
00257:   720 FORMAT(77HTHE TOTAL HYDROSTATIC  FORCE IN THE DIRECTION OF THE ATT
00258:      2TTITUDE LINE FCOS1 = ,F10.7/,92HTHE TOTAL HYDROSTATIC  FORCE IN TH
00259:      3E DIRECTION PERPENDICULAR ON THE ATTITUDE LINE  FSIN1  =  ,F10.7/,
00260:      495H**************************************************************
00261:      6*****************************)
00262:       WRITE(3,702)
00263:   702 FORMAT(95H                                        J
00264:      2 SUMC2                                      SUMS2)
00265:       SUMC2=0.0
00266:       SUMC22=0.0
00267:       SUMS2=0.0
00268:       SUMS22=0.0
00269:       G22=(180.0-THETA2)*3.14/180.0
00270:       DO 112 J=1,61,2
00271:       DO 122 I=1,N+1
00272:       SUMS2=SUMS2+P1(I,J)*DX*DY*SIN(G22)
00273:       SUMC2=SUMC2+P1(I,J)*DX*DY*COS(G22)
00274:   122 CONTINUE
00275:       WRITE(3,912)J,SUMC2,SUMS2
00276:   912 FORMAT(28X,I2,25X,F10.7,23X,F10.7)
00277:       G22=G22+(4.0*3.14/180.0)
00278:       SUMC22=SUMC2+SUMC22
```

```
00279:       SUMS22=SUMS2+SUMS22
00280:       SUMC2=0.0
00281:       SUMS2=0.0
00282:   112 CONTINUE
00283:       FCOS2=SUMC22
00284:       FSIN2=SUMS22
00285:       WRITE(3,722)FCOS2,FSIN2
00286:   722 FORMAT(38H                                        FCOS2 = ,F10.7/,38H
00287:      2                          FSIN2 = ,F10.7/,90H**************************
00288:      4*************************************************Q*********************
00289:      6)
00290:       WRITE(3,703)
00291:   703 FORMAT(95H                                  J
00292:      2 SUMC3                                  SUMS3)
00293:       SUMC3=0.0
00294:       SUMC33=0.0
00295:       SUMS3=0.0
00296:       SUMS33=0.0
00297:       G33=(180.0-THETA3)*3.14/180.0
00298:       DO 113 J=121,181,2
00299:       DO 123 I=1,N+1
00300:       SUMS3=SUMS3+P1(I,J)*DX*DY*SIN(G33)
00301:       SUMC3=SUMC3+P1(I,J)*DX*DY*COS(G33)
00302:   123 CONTINUE
00303:       WRITE(3,913)J,SUMC3,SUMS3
00304:   913 FORMAT(28X,I2,25X,F10.7,23X,F10.7)
00305:       G33=G33+(4.0*3.14/180.0)
00306:       SUMC33=SUMC3+SUMC33
00307:       SUMS33=SUMS3+SUMS33
00308:       SUMC3=0.0
00309:       SUMS3=0.0
00310:   113 CONTINUE
00311:       FCOS3=SUMC33
00312:       FSIN3=SUMS33
00313:       WRITE(3,723)FCOS3,FSIN3
00314:   723 FORMAT(38H                                        FCOS3 = ,F10.7/,38H
```

```
00315:      2                          FSIN3=   ,F10.7/,90H             **********
00316:      4**************************************************************
00317:      6)
00318:       ALPHA1=ALPHA1*3.14/180.0
00319:       ALPHA2=ALPHA2*3.14/180.0
00320:       ALPHA3=ALPHA3*3.14/180.0
00321:       FT1=SQRT((FCOS1**2)+(FSIN1**2))
00322:       IF(FSIN1.EQ.0.0.AND.FCOS1.EQ.0.0) GO TO 7171
00323:       PHI1=ATAN(-FSIN1/FCOS1)
00324: 7171  PHI1=0.0
00325:       IF(PHI1.GT.ALPHA1) GO TO 9191
00326:       GO TO 9292
00327: 9191  PHI11=(PHI1-ALPHA1)
00328:       FH1=FT1*SIN(PHI11)
00329:       FV1=FT1*COS(PHI11)
00330:       GO TO 9393
00331: 9292  IF(PHI1.LT.ALPHA1) PHI11=(ALPHA1-PHI1)
00332:       FH1=-FT1*SIN(PHI11)
00333:       FV1=FT1*COS(PHI11)
00334: 9393  FT2=SQRT((FCOS2**2)+(FSIN2**2))
00335:       IF(FSIN2.EQ.0.0.AND.FCOS2.EQ.0.0) GO TO 7272
00336:       PHI2=ATAN(-FSIN2/FCOS2)
00337: 7272  PHI2=0.0
00338:       IF(ALPHA2.GT.1.57) GO TO 9494
00339:       GO TO 9595
00340: 9494  PHI22=(ALPHA2-1.57+PHI2)
00341:       FH2=FT2*COS(PHI22)
00342:       FV2=-FT2*SIN(PHI22)
00343:       GO TO 9696
00344: 9595  IF(ALPHA2.LT.1.57) PHI22=(1.57-ALPHA2-PHI2)
00345:       FH2=FT2*COS(PHI22)
00346:       FV2=FT2*SIN(PHI22)
00347: 9696  FT3=SQRT((FCOS3**2)+(FSIN3**2))
00348:       IF(FSIN3.EQ.0.0.AND.FCOS3.EQ.0.0) GO TO 7373
00349:       PHI3=ATAN(-FSIN3/FCOS3)
00350: 7373  PHI3=0.0
```

```
00351:       IF(ALPHA3.LT.1.57) GO TO 9797
00352:       GO TO 9898
00353: 9797 PHI33=(1.57-ALPHA3+PHI3)
00354:       FH3=-FT3*COS(PHI33)
00355:       FV3=+FT3*SIN(PHI33)
00356:       GO TO 9899
00357: 9898 IF(ALPHA3.GT.1.57) PHI33=(ALPHA3-1.57-PHI3)
00358:       FH3=-FT3*COS(PHI33)
00359:       FV3=-FT3*SIN(PHI33)
00360: 9899 FHT=FH1+FH2+FH3
00361:       FVT=FV1+FV2+FV3
00362:       FTO=SQRT(FHT**2+FVT**2)
00363:       IF(FHT.GT.0.0) ALPH11=ACOS(FVT/FTO)
00364:       IF(FHT.LT.0.0) ALPH11=ASIN(FHT/FTO)
00365:       WRITE(3,99992)FCOS1,FSIN1,FCOS2,FSIN2,FCOS3,FSIN3,FH1,FH2,FH3
00366:      2,FV1,FV2,FV3
00367:       WRITE(3,88885)FT1,FT2,FT3
00368:88885 FORMAT(3(F10.5,3X))
00369:       WRITE(3,99993)FHT,FVT
00370:       ALPH11=ALPH11*180.0/3.14
00371:       WRITE(3,99994)FTO,ALPH11
00372:99992 FORMAT(12(F8.5,2X))
00373:99993 FORMAT(2(F10.5))
00374:99994 FORMAT(2(F10.5))
00375:       PHI1=PHI1*180.0/3.14
00376:       PHI11=PHI11*180.0/3.14
00377:       PHI2=PHI2*180.0/3.14
00378:       PHI22=PHI22*180.0/3.14
00379:       PHI3=PHI3*180.0/3.14
00380:       PHI33=PHI33*180.0/3.14
00381:       WRITE(3,99996)PHI1,PHI11,PHI2,PHI22,PHI3,PHI33
00382:99996 FORMAT(6(F10.5,2X))
00383:       CALL HALLAH
00384:       WRITE(3,77777)FHT
00385:77777 FORMAT(67H                                    THE  TOTAL  HORIZONTAL  FO
00386:     2RCE  FHT = ,F15.8/,100H****************************************
```

```
00387:     3**********************************************************)
00388:      WRITE(3,6666)FVT
00389: 6666 FORMAT(59H66)FVT                                    THE   LOAD PARAMETER  FVT
00390:     2 = ,F15.8/,100H**************************************************************
00391:     3**********************************************)
00392:      STOP
00393:      END
00394:      SUBROUTINE HALLAH
00395:      COMMON QA201,QA203,QA2,QA1,QA3,QC102,QC103,QC1,QC201,QC203,QC2,QC3
00396:     201,QC302,QC3,QT1,QT2,QT3
00397:      WRITE(3,255)
00398:      WRITE(3,5)QA201
00399:    5 FORMAT(90 H                                  THE AXIAL PRESSURE INDUCED FLO
00400:     2W COFFICIENT FROM 1 TO 31 QA201 = ,F20.8)
00401:      WRITE(3,255)
00402:      WRITE(3,51)QA203
00403:   51 FORMAT(90H                          THE AXIAL PRESSURE INDUCED FLOW COEF
00404:     2FROM 151 TO 181            QA203 = ,F20.8)
00405:      WRITE(3,255)
00406:      WRITE(3,12)QA2
00407:   12 FORMAT(90H                          THE AXIAL PRESSURE INDUCED FLOW COEF
00408:     2FICIENT FOR THE 2 ND LOBE  QA2 = ,F20.8)
00409:      WRITE(3,255)
00410:      WRITE(3,52)QA1
00411:   52 FORMAT(90H                          THE AXIAL PRESSURE INDUCED FLOW COEF
00412:     2FICIENT FOR THE FIRST LOBE  QA1 = ,F20.8)
00413:      WRITE(3,255)
00414:      WRITE(3,13)QA3
00415:   13 FORMAT(90H                          THE AXIAL PRESSURE INDUCED FLOW COEF
00416:     2FIVIENT FOR THE THIRD LOBE QA3  = ,F20.8)
00417:      WRITE(3,255)
00418:      WRITE(3,14)QC102
00419:   14 FORMAT(105H                         THE CIRCUMFERENTIAL PRESSURE INDUCED
00420:     2FLOW COEFFICIENT FOR THE FIRST LOBE AT 31 QC102= ,F20.8)
00421:      WRITE(3,255)
00422:      WRITE(3,15)QC103
```

```
00423:    15 FORMAT(105H
00424:      2FLOW COEFFICIENT FOR THE FIRST LOBE AT 91 QC103 = ,F20.8)
00425:       WRITE(3,255)
00426:       WRITE(3,16)QC1
00427:    16 FORMAT(105H                        THE CIRCUMFERENTIAL PRESSURE INDUCED
00428:      2FLOW COEFFICIENT FOR THE FIRST LOBE         QC1   = ,F20.8)
00429:       WRITE(3,255)
00430:       WRITE(3,17)QC201
00431:    17 FORMAT(107H                        THE CIRCUMFERENTIAL PRESSURE INDUCED
00432:      2FLOW COEFFICIENT FOR THE SECOND LOBE AT 31 QC201   = ,F20.8)
00433:       WRITE(3,255)
00434:       WRITE(3,18)QC203
00435:    18 FORMAT(104H                        THE CIRCUMFERENTIAL PRESSURE INDUCED
00436:      2FLOW COEFFICIENT FOR THE SECOND LOBE AT151 QC203=,F20.8)
00437:       WRITE(3,255)
00438:       WRITE(3,19)QC2
00439:    19 FORMAT(106H                        THE CIRCUMFERENTIAL PRESSURE INDUCED
00440:      2FLOW COEFFICIENT FOR THE SECOND LOBE         QC2   = ,F20.8)
00441:       WRITE(3,255)
00442:       WRITE(3,224)QC301
00443:   224 FORMAT(105H                        THE CIRCUMFERENTIAL PRESSURE INDUCED
00444:      2FLOW COEFFICIENT FOR THE THIRD LOBE AT  91 QC301= ,F20.8)
00445:       WRITE(3,255)
00446:       WRITE(3,201)QC302
00447:   201 FORMAT(106H                        THE CIRCUMFERENTIAL PRESSURE INDUCED
00448:      2FLOW COEFFICIENT FOR THE  THIRD LOBE AT 151 QC302= ,F20.8)
00449:       WRITE(3,255)
00450:       WRITE(3,202)QC3
00451:   202 FORMAT(105H                        THE CIRCUMFERENTIAL PRESSURE INDUCED
00452:      2FLOW COEFFICIENT FOR THE THIRD LOBE         QC3   = ,F20.8)
00453:       WRITE(3,255)
00454:       WRITE(3,203)QT1
00455:   203 FORMAT(105H                              THE TOTAL QTI FLOW COEFFICIENT
```

```
00456:      2FLOW COEFFICIENT FOR THE FIRST LOBE         QT1   = ,F20.8)
00457:       WRITE(3,255)
00458:       WRITE(3,204)QT2
00459:   204 FORMAT(105H                                THE TOTAL OIL FLOW COEFFICIENT
00460:      2FLOW COEFFICIENT FOR THE 2 NDT LOBE         QT2   = ,F20.8)
00461:       WRITE(3,255)
00462:       WRITE(3,205)QT3
00463:   205 FORMAT(105H                                THE TOTAL OIL FLOW COEFFICIENT
00464:      2FLOW COEFFICIENT FOR THE THIRD LOBE         QT3   = ,F20.8)
00465:       WRITE(3,255)
00466:   255 FORMAT(104H************************************************************
00467:      2************************************************)
00468:       RETURN
00469:       END
BOTTOM
```

The following subroutine can be used with the computer programmes which are given in Appendices A.2 and A.3 when a solution is required for a vertical force which is applied upwards and also this force can be swung $\pm 60^{\circ}$.

```
00076:       ALPHA=0.0*3.14/180.0
00095:       EL1=((E**2)+(ELIPIT**2)-(2.0*E*ELIPIT*COS(ALPHA)))**0.5
00096:       ALPHA1=(ASIN((E*SIN(ALPHA)/EL1)))*180.0/3.14
00097:       THETA1=50.0-ALPHA1
00098:       EL2=((E**2+ELIPIT**2+2.0*E*ELIPIT*COS((3.14/3.0)-ALPHA))**0.5)
00099:       ALPHA2=(3.14/3.0-ASIN((E*SIN((3.14/3.0)-ALPHA)/EL2)))*180.0/3.14
00100:       THETA2=ALPHA2-10.0
00101:       EL3=((E**2+(ELIPIT**2)-(2.0*E*ELIPIT*COS((3.14*2.0/3.0)-ALPHA)
00102:      2)))**0.5
00103:       ALPHA3=((3.14/3.0)-(ASIN(E*SIN((3.14*2.0/3.0)-ALPHA)/EL3)))*18
00104:      20.0/3.14
00105:       THETA3=110.0-ALPHA3
00355:       IF(FSIN1.EQ.0.0.AND.FCOS1.EQ.0.0) GO TO 7171
00356:       PHI1=ATAN(-FSIN1/FCOS1)
00357:       GO TO 4141
00358: 7171  PHI1=0.0
00359: 4141  PHI11=(ALPHA1+PHI1)
00360:       FH1=-FT1*SIN(PHI11)
00361:       FV1=-FT1*COS(PHI11)
00362:       FT2=SQRT((FCOS2**2)+(FSIN2**2))
00363:       IF(FSIN2.EQ.0.0.AND.FCOS2.EQ.0.0) GO TO 7272
00364:       PHI2=ATAN(-FSIN2/FCOS2)
00365:       GO TO 4242
00366: 7272  PHI2=0.0
00367: 4242  IF(ALPHA2.LT.1.57) GO TO 9494
00368:       GO TO 9595
00369: 9494  PHI22=(ALPHA2-PHI2)
00370:       FH2=-FT2*SIN(PHI22)
00371:       FV2=+FT2*COS(PHI22)
00372:       GO TO 9696
```

```
00373: 9595 IF(ALPHA2.GT.1.57) PHI22=(ALPHA2-1.57-PHI2)
00374:      FH2=-FT2*COS(PHI22)
00375:      FV2=-FV2*SIN(PHI22)
00376: 9696 FT3=SQRT((FCOS3**2)+(FSIN3**2))
00377:      IF(FSIN3.EQ.0.0.AND.FCOS3.EQ.0.0) GO TO 7373
00378:      PHI3=ATAN(-FSIN3/FCOS3)
00379:      GO TO 4343
00380: 7373 PHI3=0.0
00381: 4343 IF(ALPHA3.LT.1.57) GO TO 9797
00382:      GO TO 9898
00383: 9797 PHI33=(1.57-ALPHA3-PHI3)
00384:      FH3=FT3*COS(PHI33)
00385:      FV3=FT3*SIN(PHI33)
00386:      GO TO 9899
00387: 9898 IF(ALPHA3.GT.1.57) PHI33=(ALPHA3-1.57+PHI3)
00388:      FH3=FT3*COS(PHI33)
00389:      FV3=-FT3*SIN(PHI33)
```

APPENDIX A.4.

THE DESIGN OF THE BEARING SHELL BY THE MACHINING METHOD.

Appendix A.4. The Design of the Bearing Shell by the Machining Method.

A.4.1. Introduction

The two bearing shells which have been tested were manufactured by cutting a hollow cylinder into three segments. The segments were then assembled together with shims between them and the assembly was bored circular. The required shape of the bearing shell was then obtained by removing the shims.

Theoretically this method should produce the exact shape proposed for the bearing. However, it was found that the segments have to be butted very accurately to obtain an accurate form.

A.4.2. The Bearing Shell Material.

The first bearing shell was machined from a cylinder of 60/40 brass which was cast in the Brunel University foundary. Problems with porosity and inclusions were recognised and attempts were made to alleviate them.

The second bearing shell was machined from a cylinder of gun bronze known commercially as Jml. The metal was stress relieved and tested for porosity by the manufacture.

A.4.3. The Manufacture of the First Bearing Shells.

The bearing shell was machined in six stages, as follows:-

Stage 1.

The brass cylinder was roughly machined. The screw and dowel holes were drilled into the brass cylinder on a vertical milling machine and in conjunction with a universal dividing head. The recesses for the screw and dowel holes were then milled using slot drills and a ball nosed slot drill.

Stage 2.

The brass cylinder was milled into three equal segments using a slitting saw, a horizontal miller and a universal dividing head.

Stage 3.

The three segments were de-burred and assembled together with the 0.102 mm (0.004") thick shims and the screws. Standard silver steel dowels were then fitted. After boring and removing the shims, the resultant shape was found to have large steps at the joints. To remedy the situation stage 3 was recommenced. The faces of the segments were scraped and lapped to obtain good mating surfaces at each joint. The bearing shell was assembled again by means of the screws, and oversize dowel holes were reamed, the shims were tested for constant thickness, inserted between the segments, and the bearing was then assembled with oversize dowels. Chucking of the assembly would have brought distortion so the bearing was mounted on a lathe face plate and bolted in place (figure A.4.1.). Finally the shell was bored to a surface finish of 22 micro inches and by means of "Roundness Measuring Machine" it was found to be circular to within ± 20 micro inches. For the good surface finish required (in the CLA

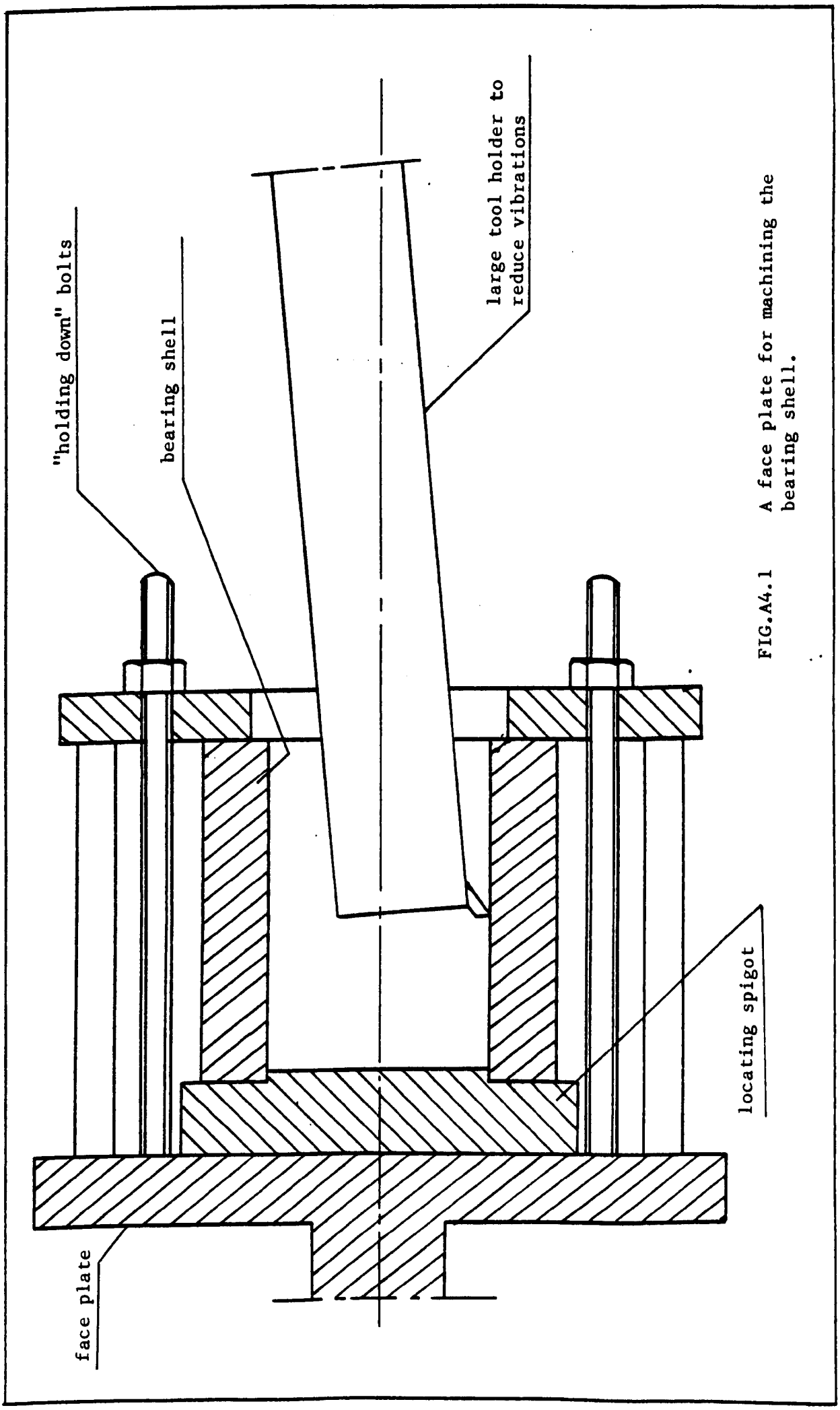

FIG.A4.1 A face plate for machining the bearing shell.

from 6 to 12 micro inches) it was decided to use a diamond tool to bore the shell. However, the best CLA valUe obtained was 15 micro inches.

Stage 4.

The shims were then removed and the bearing shell re-assembled After extensive inspection, the shell was partially disassembled to mill the low pressure oil supply grooves with an end mill.

Stage 5.

The outside diameter of the shell was machined to obtain 0.051 mm interference for the shrink fit. The shell was again mounted on a face plate, with locating spigot, to prevent distortion from a chuck. Finally, pressure relief grooves were machined on the outside of the bearing shell. The aim of these grooves is to prevent oil infiltrating the joints and causing them to separate.

Stage 6.

Due to the high pressure required to operate the bearing at the extreme design conditions, a substantial bearing body was envisaged. A mild steel cylinder of 356 mm. diameter was used. The shell was shrunk into the steel body by heating up the steel body to approximately 200°C. The bearing shell was suspended above the bearing housing and lowered into it. To keep the brass cool until it was in position, the bearing was packed with solid CO_2. The high pressure inlets were drilled into the housing and bearing.

A.4.4. Inspection of the Bearing Shell.

At the end of stages 4 and 5, the bearing shell was tested again on the "Roundness Measuring machine" and a typical result is shown by figure A.4.2. From this figure it is found that the average lobe depth is 0.029 mm. (0.00115").

The full bearing dimensions are listed in table 4.1 (Chapter 4), and the bearing was tested on the simple test rig (Chapter 4).

At this stage the bearing was not provided with the low pressure oil inlet, and it was judged that the axial grooves for the low pressure oil were too small. The bearing shell was then removed from its housing by cooling and by utilizing the differential expansion between brass and steel. The axial grooves were machined to dimensions given in table 6.1. Some difficulties with steps at the joints arose and the bearing was treated from stage (3) onwards. The full final dimensions are given in table 6.1. The bearing was then reassembled in the housing, the journal of the shaft was ground to suit the bearing and the bearing was tested in the main test rig, (Chapter 6).

A.4.5. The Manufacture of the Second Bearing Shell

The first bearing shell suffered from an inadequate appreciation by everyone of the great care required at each stage of manufacture, if the intended result is to be obtained clearly, and without remedial action which can never be fully satisfactory. This lesson had been well learnt when the second bearing came to be manufactured and the careful attention given to the fit at the butts, and to the fit of the dowels, produced a sequence of manufacture ending in the intended

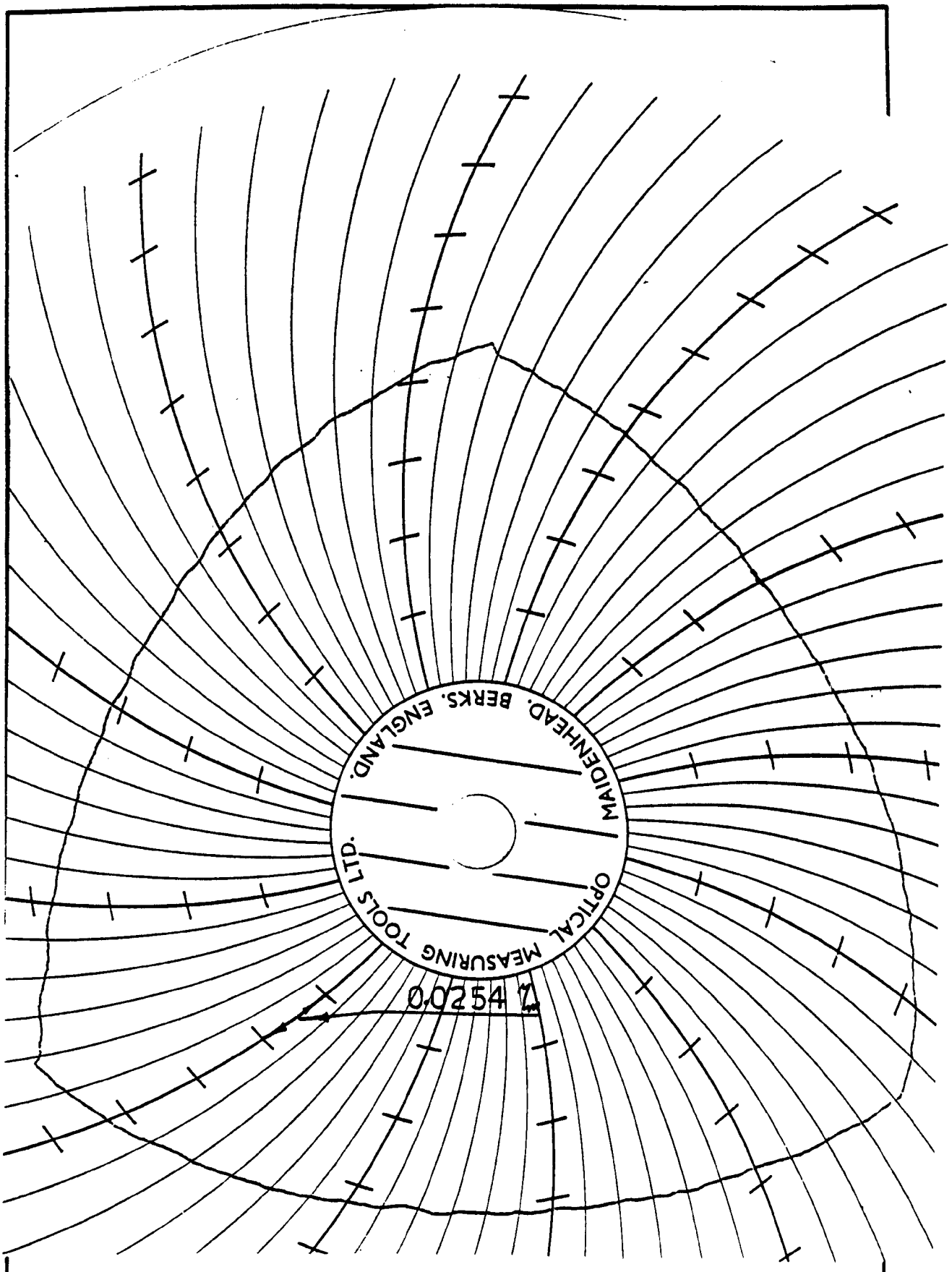

FIG.A4.2 Profile of finished bearing.

result, and without any back-tracking (Figures A.4.3 - A.4.6). This second experience demonstrates that there is nothing impracticable about the method of manufacture, all that is required is an appreciation where extreme care has to be taken. The form achieved is shown in figure A.4.7. The bearing shell was shrunk into the steel housing by freezing the bearing shell to around - 50°C for about 5 hours.

The second bearing shell was tested on the main test rig (Chapter 6).

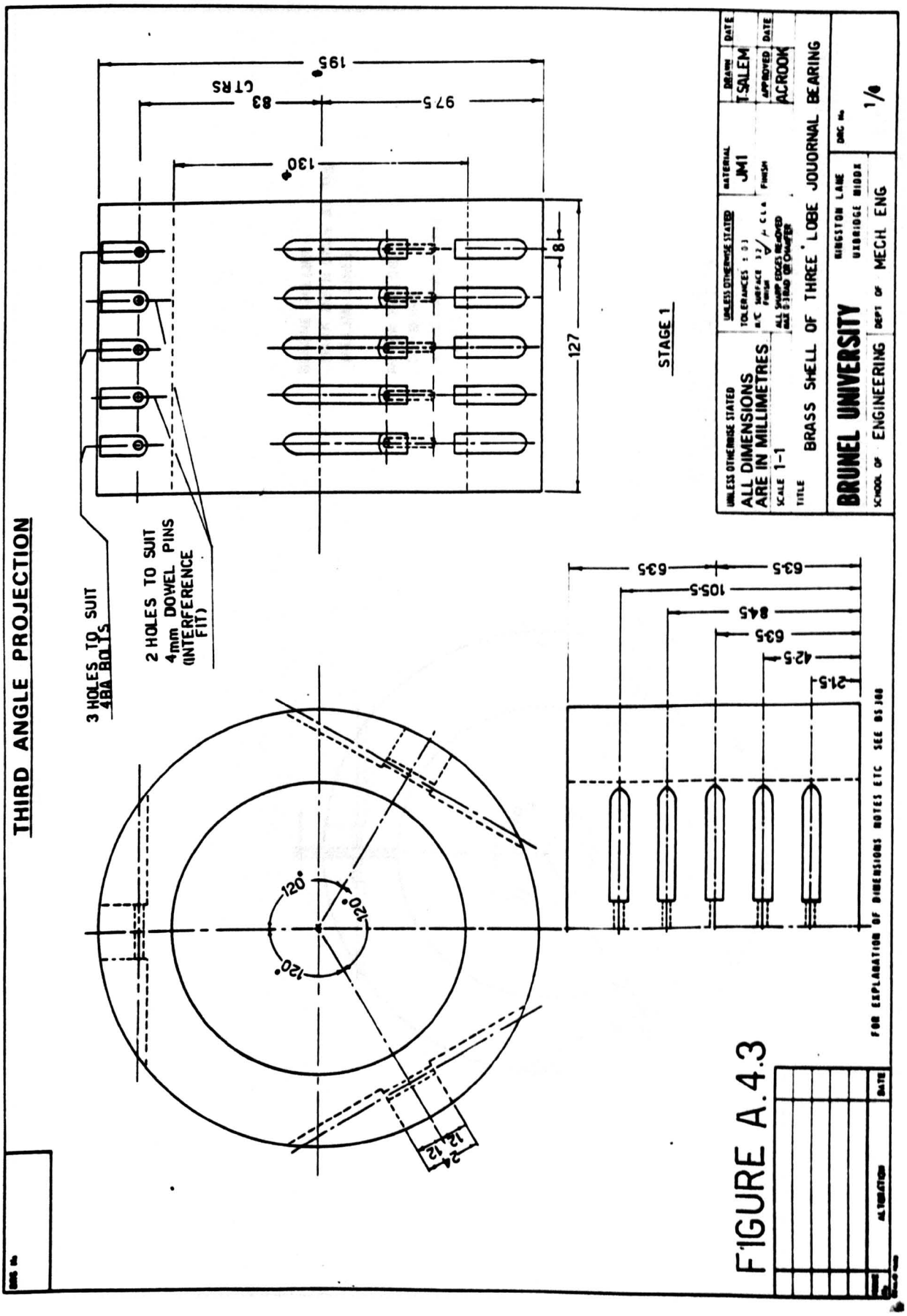
THIRD ANGLE PROJECTION
195
83 CTRS
97.5
130
8
127
3 HOLES TO SUIT 4BA BOLTS
2 HOLES TO SUIT 4mm DOWEL PINS (INTERFERENCE FIT)
STAGE 1
63.5
105.5
84.5
63.5
42.5
21.5
120°
120°
120°
12
12
24
UNLESS OTHERWISE STATED ALL DIMENSIONS ARE IN MILLIMETRES
SCALE 1-1
TITLE BRASS SHELL OF THREE LOBE JOUORNAL BEARING
BRUNEL UNIVERSITY
KINGSTON LANE UXBRIDGE MIDDX
SCHOOL OF ENGINEERING DEPT OF MECH ENG
MATERIAL JM1
DRAWN T.SALEM
APPROVED A.CROOK
1/6
FOR EXPLANATION OF DIMENSIONS NOTES ETC SEE BS308
ALTERATION
DATE

FIGURE A.4.3

THIRD ANGLE PROJECTION

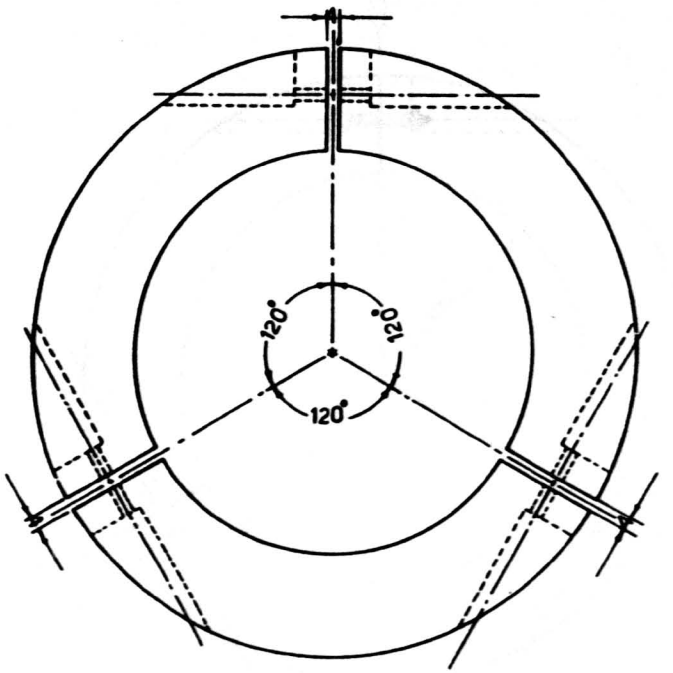

BEFORE MILLING:-
- MARK BOTH ENDS AT THE MILLING LINES.

AFTER MILLING:-
- DE-BURR.
- HAND LAPPING THE FACES.

STAGE 2

FIGURE A·4·4

UNLESS OTHERWISE STATED ALL DIMENSIONS ARE IN MILLIMETRES	UNLESS OTHERWISE STATED TOLERANCES ± 0.1 R/C SURFACE FINISH 32 √ / CLA ALL SHARP EDGES REMOVED MAX 0.3 RAD OR CHAMFER	MATERIAL JM1 FINISH	DRAWN T.SALEM	DATE
SCALE 1:1			APPROVED AG ROOK	DATE
TITLE BRASS SHELL FOR THREE LOBE JOURNAL BEARING				
BRUNEL UNIVERSITY KINGSTON LANE UXBRIDGE MIDDX			DRG No 2\4	
SCHOOL OF ENGINEERING	DEPT OF MECH ENG.			

ISSUED	ALTERATION	DATE

FOR EXPLANATION OF DIMENSIONS, NOTES ETC., SEE BS 308

THIRD ANGLE PROJECTION

FIGURE A·4·5

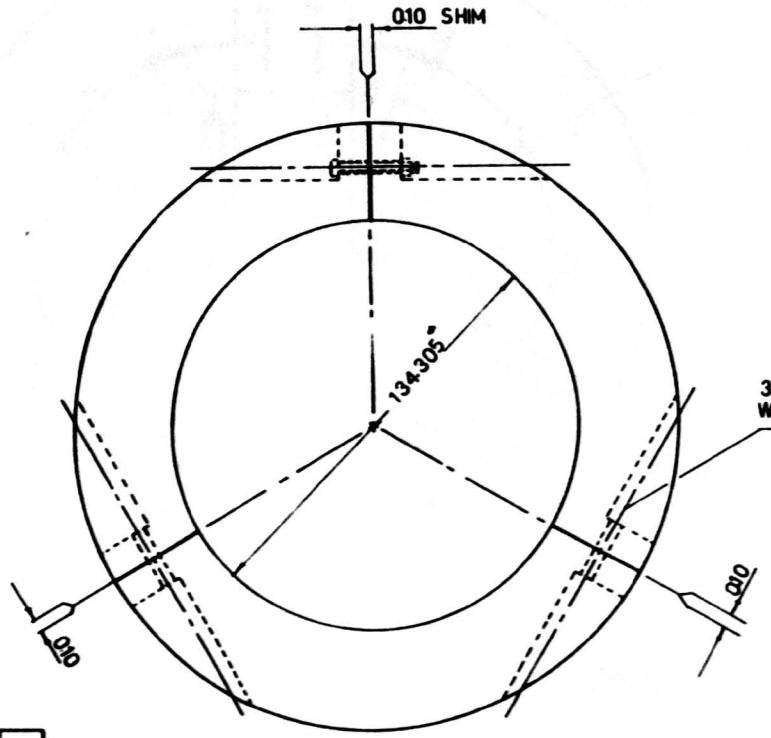

- THE SHIMS THICKNESS IS 0.10mm OR (0.004 INCH)
- HAND FITTING SILVER STEEL DOWLES
- BEFORE REMOVING THE SHIMS TEST THE BORE SIZE AND ROUNDNESS

BORE SURFACE FINISH

TRY TO ACHIVE THE BEST POSSIBLE PLEASE.

3-4 BA SOCKET HEAD CAP SCREWS WITH NUTS PLUS 2.4mm DOWEL PINS

STAGE 3

UNLESS OTHERWISE STATED ALL DIMENSIONS ARE IN MILLIMETRES	UNLESS OTHERWISE STATED TOLERANCES ± .13 N C SURFACE FINISH 12 µ C.L.A. ALL SHARP EDGES REMOVED MAX 0.13 RAD OR CHAMFER	MATERIAL UM1 FINISH	DRAWN T.SALEM	DATE
SCALE 1:1			APPROVED A.CROOK	DATE

TITLE BRASS SHELL FOR THREE LOBE JOURNL BEARING

BRUNEL UNIVERSITY KINGSTON LANE UXBRIDGE MIDDX

SCHOOL OF ENGINEERING DEPT OF MECH. ENG.

DRG No 3/4

	ALTERATION	DATE

FOR EXPLANATION OF DIMENSIONS NOTES ETC SEE BS 308

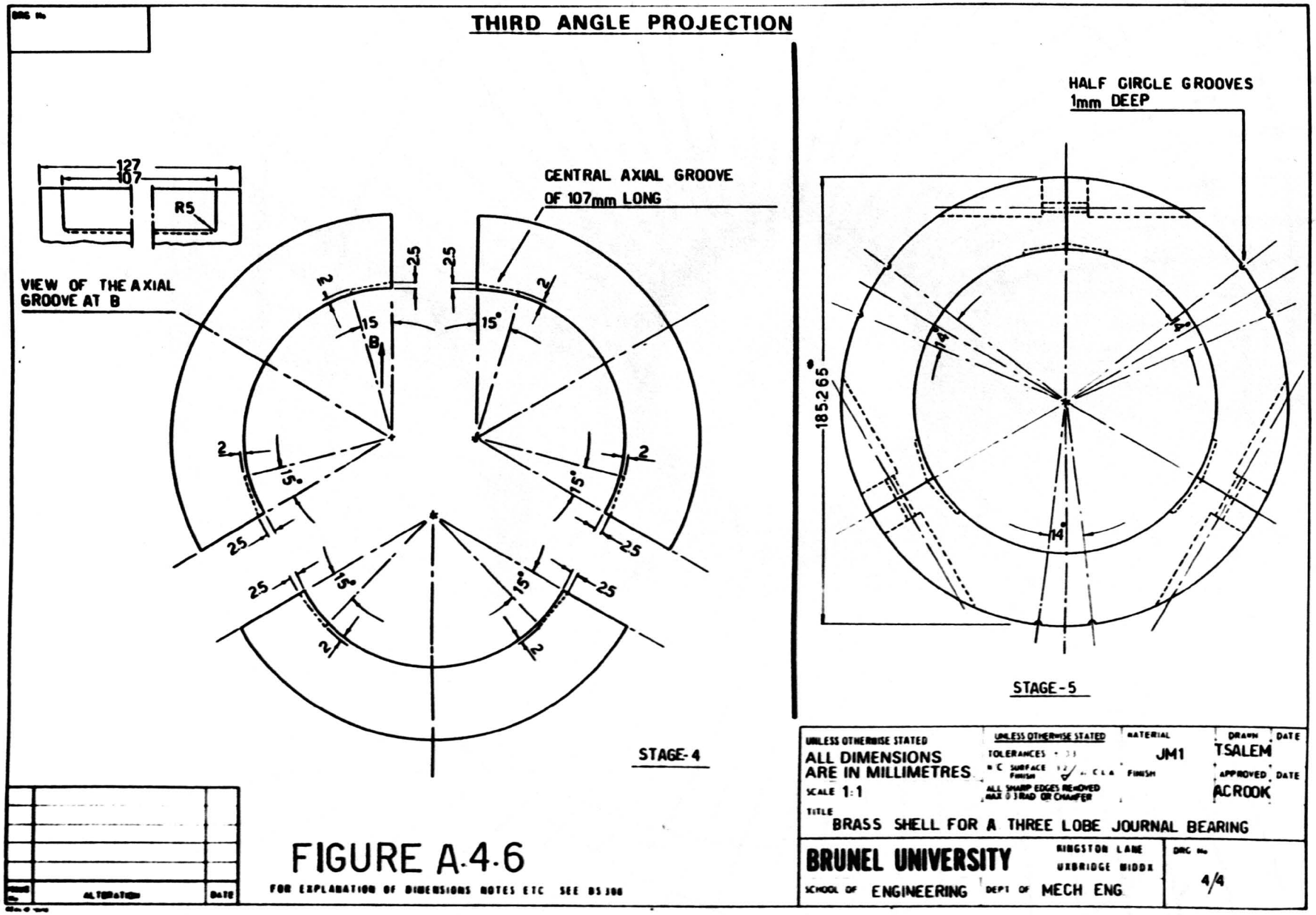

FIGURE A.4.6

FOR EXPLANATION OF DIMENSIONS NOTES ETC SEE BS 308

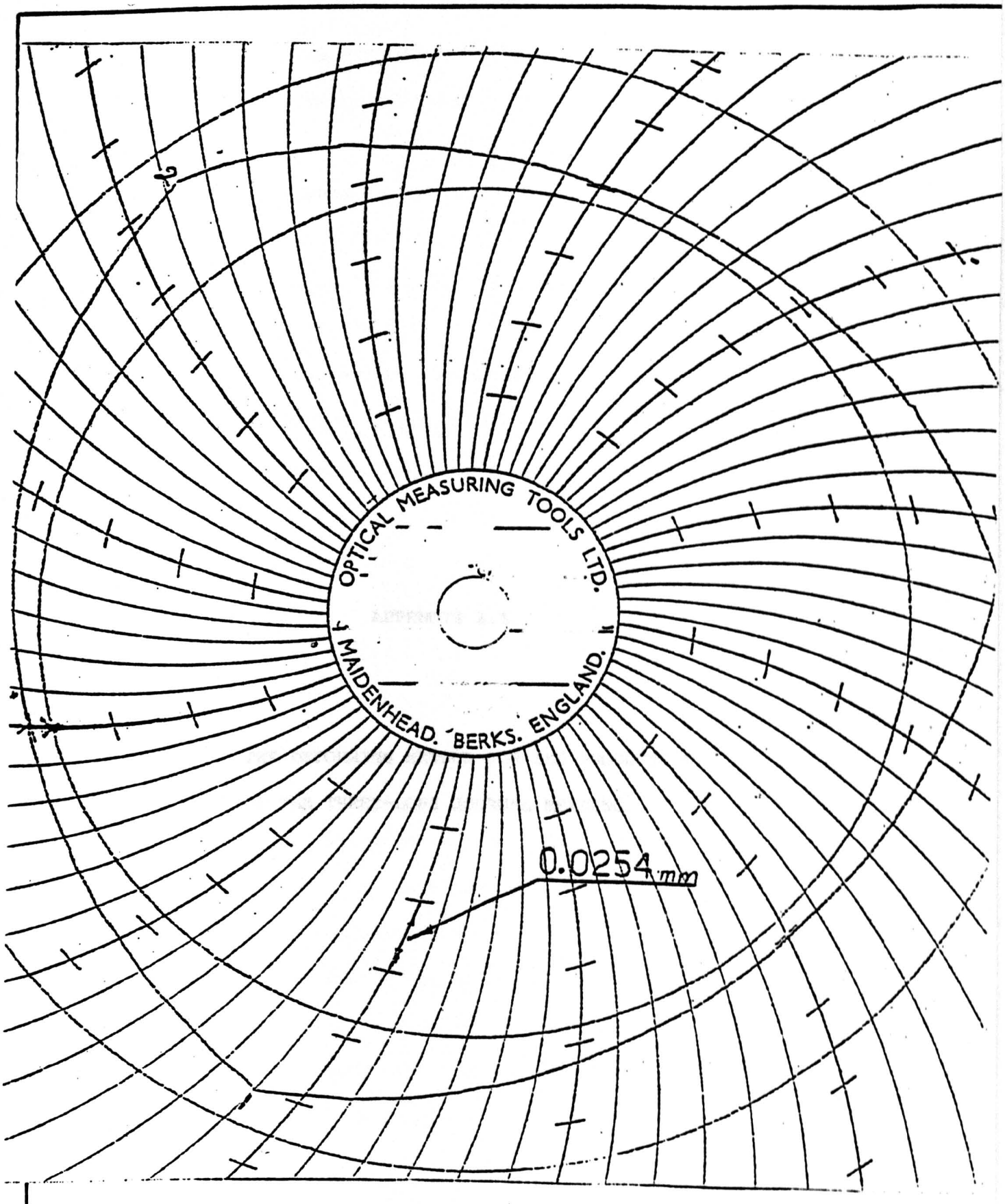

FIG A4.7 Profile of finished bearing.

APPENDIX A.5.

THE DEFORMING METHOD FOR THE PRODUCTION OF THE THREE-LOBE JOURNAL BEARING.

Appendix A.5. The Deforming Method for the Production of a three-lobe Journal Bearing.

A method of manufacture described in Appendix A.4 has produced a very satisfactory form but a simpler method is clearly desirable. A method which has been tried only experimentally is illustrated in Figure A.5.1. It comprises the elastic distortion of the bearing ring within three jaws of a chuck. To give the closest approximation to circular lobes the bearing ring is made less rigid in bending at three places by axial grooves. The distorted ring is machined circular, and then released, and its outer surface is then turned circular. A roundness trace from an experimental ring of 4 mm wall thickness cut from a piece of steel tubing is shown in figure A.4.2. The experiment shows promise.

This method of elastic distortion has also been tried with a circular ring with no axial groove. The theoretical analysis of this situation had suggested that a form of three-lobe could be achieved. However, the experimental test was not a success. The point can be made that the lobes themselves do not necessarily have to be circular and that forms including terms beyond the second degree, such as produced by elastic distortion, might also give satisfactory hydrostatic and hydrodynamic performance. This matter has not been investigated, but the finite difference method does provide a means by which other forms could be examined numerically.

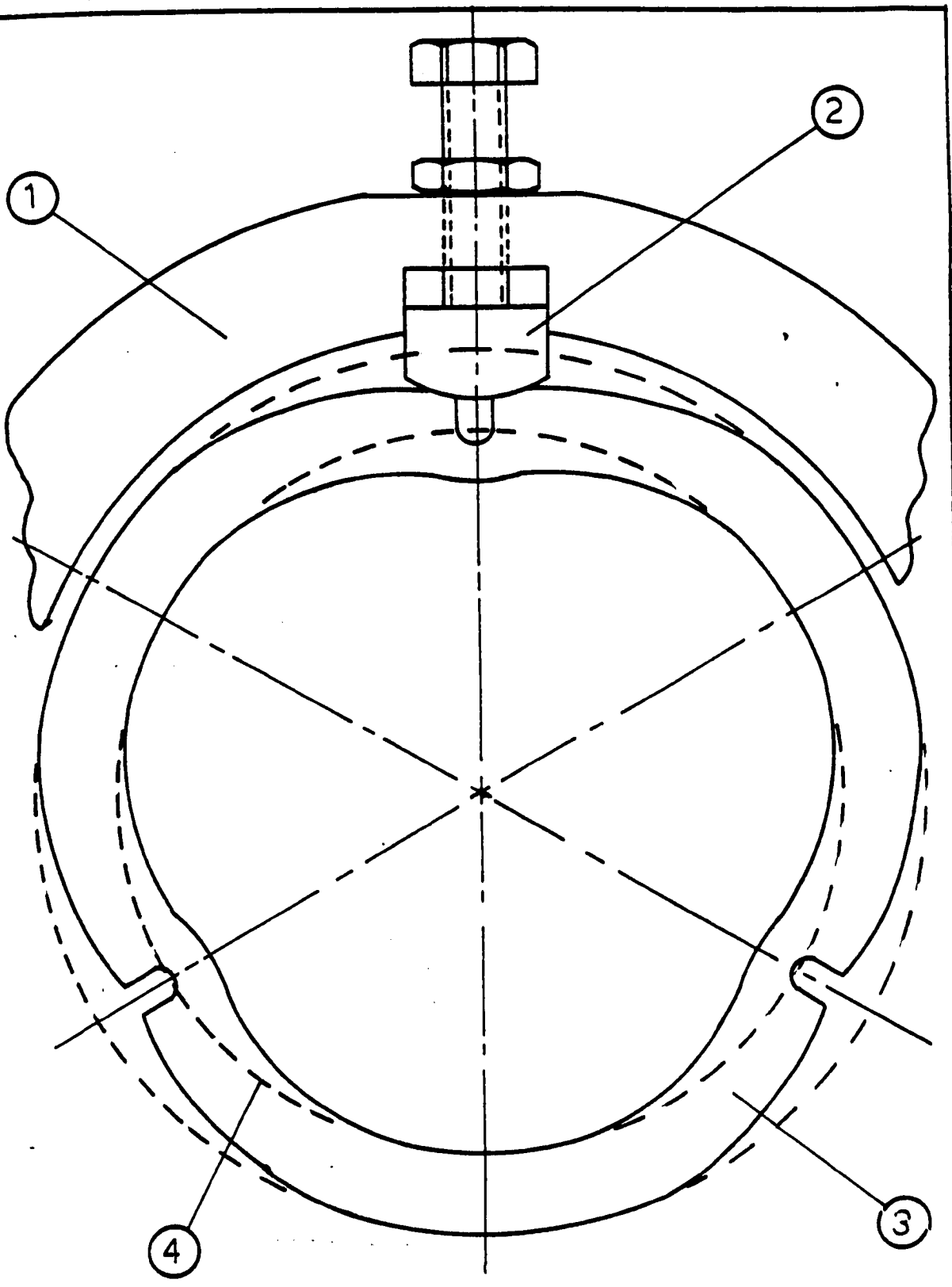

1	Chuck
2	Jaw
3	Elastically distorted ring
4	Circular bore

FIG.A5.1 Jig for manufacturing method.

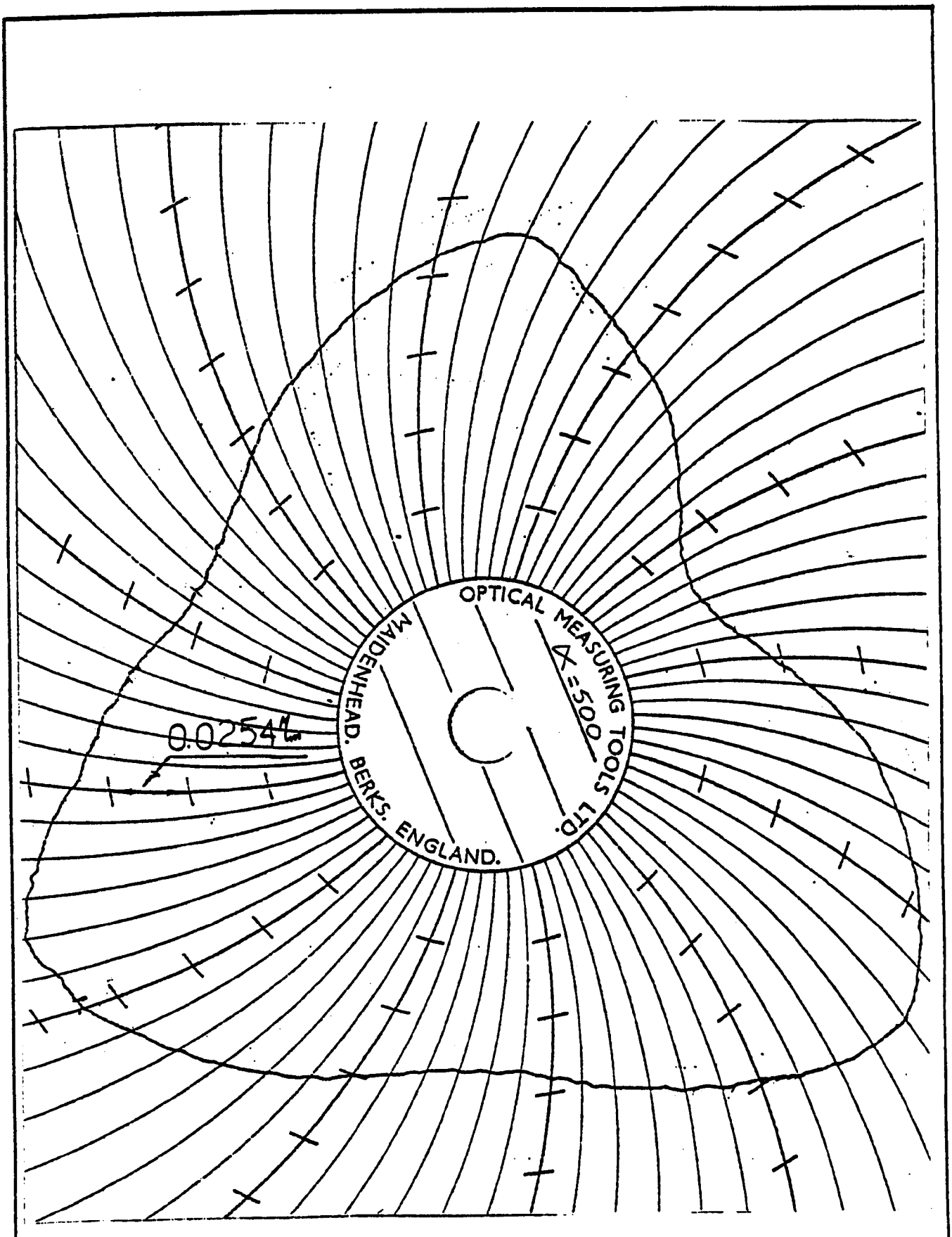

FIG.A5.2 CMT Chart for the deformed bearing shell.

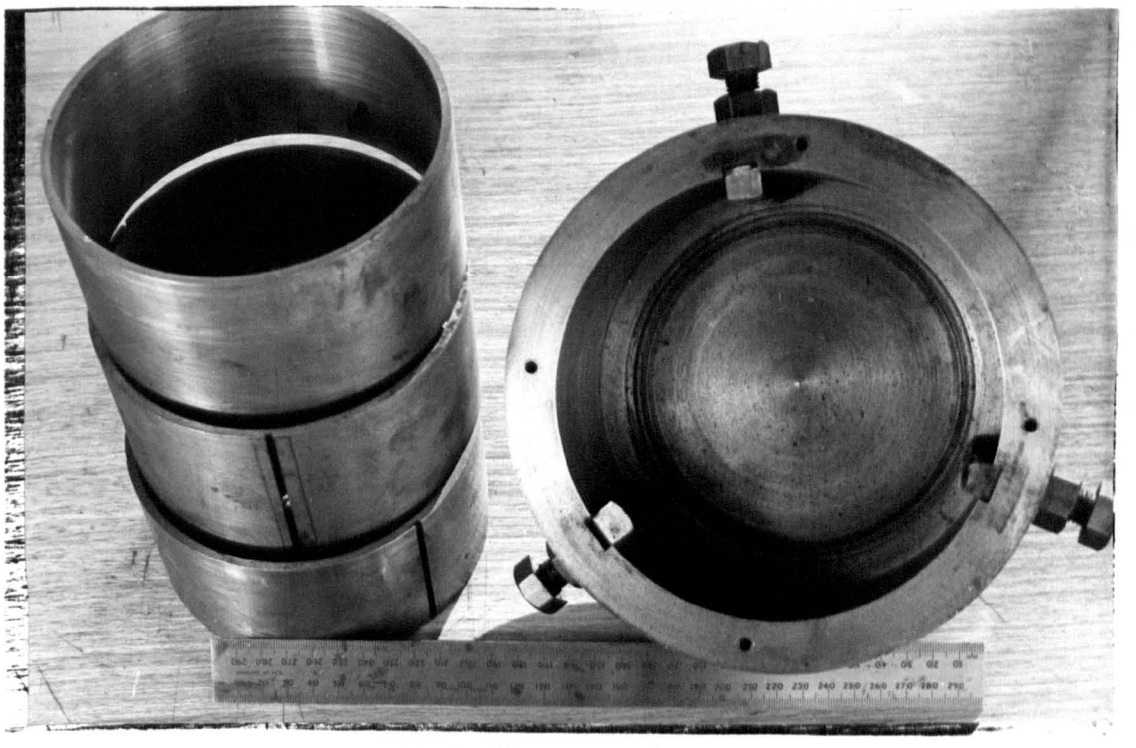

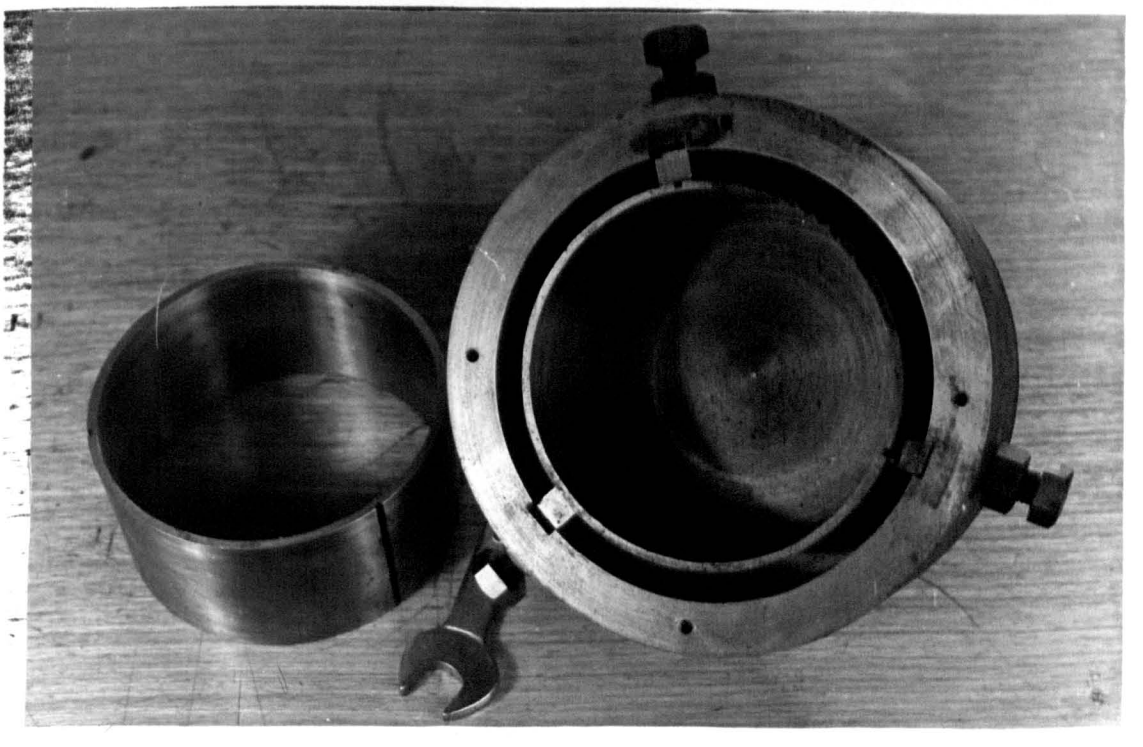

FIG.A.5.3 JIG FOR MAUFACTURING METHOD.

APPENDIX A.6.

THE DESIGN AND THE SPECIFICATION OF THE MIST LUBRICATOR.

Appendix A.6.

A.6.1. SPECIFICATION of the Mist Lubricator

The venting area for each bearing is given by:

$$A_v = \pi/16 (D^2 - d^2)$$

where

D is diameter of the cover plate bore

d " " " " shaft at the cover plate.

And the venting diameter is given by

$$D_v = \sqrt{4Av/\pi}$$

$D_v \geq$ The recommended venting diameter for the selected fittings.

A.6.1. Recommended mist fittings.

1. Tail Bearings and Slave Bearings.

MIST fitting No.381290-4

Venting diameter = 1.575 mm.

AIR FLOW FOR EACH BEARING AT LINE PRESSURE OF 20" HZO

$= .00452\ m^3\ min^{-1}$

TOTAL AIR FLOW $= 0.00805\ m^3\ min^{-1}$

2. Thrust Bearing

MIST fitting No. 381290-6

Venting diameter = 1.981 mm.

AIR FLOW AT PRESSURE LINE OF 20" HO2 $= 0.0068\ m^3\ min^{-1}$

A.6.3. The Design Factors on which the Fittings were selected.

Mist line pressure = 20" H2O

Mean bearing shafts diameter = 80 mm.

Light/medium operating conditions.

A.6.4. Setting the lubricator for operation.

The air pressure gauge (4) should be set at 15 psi (= 1 atm), initially, by using the reducing valve (3), with the oil regulating screw half turned open.

- Unless a manometer is installed in the mist line, for the 20" to be set by the air input valve, the indication of correct system is

  a) No excessive emission of mist from the vents, (bearing in mind that revolving bearing balls will knock the majority of oil from the mist and so reduce the vented material).

  b) Overheating of bearing housing.

A.6.5. Lubricating oils

i - High speed oil VIT. 21 ([illegible] c.s. at 40°C)

ii - Low speed oil SHELL Vit. 25 (ν = 25 c.s. at 40°C).

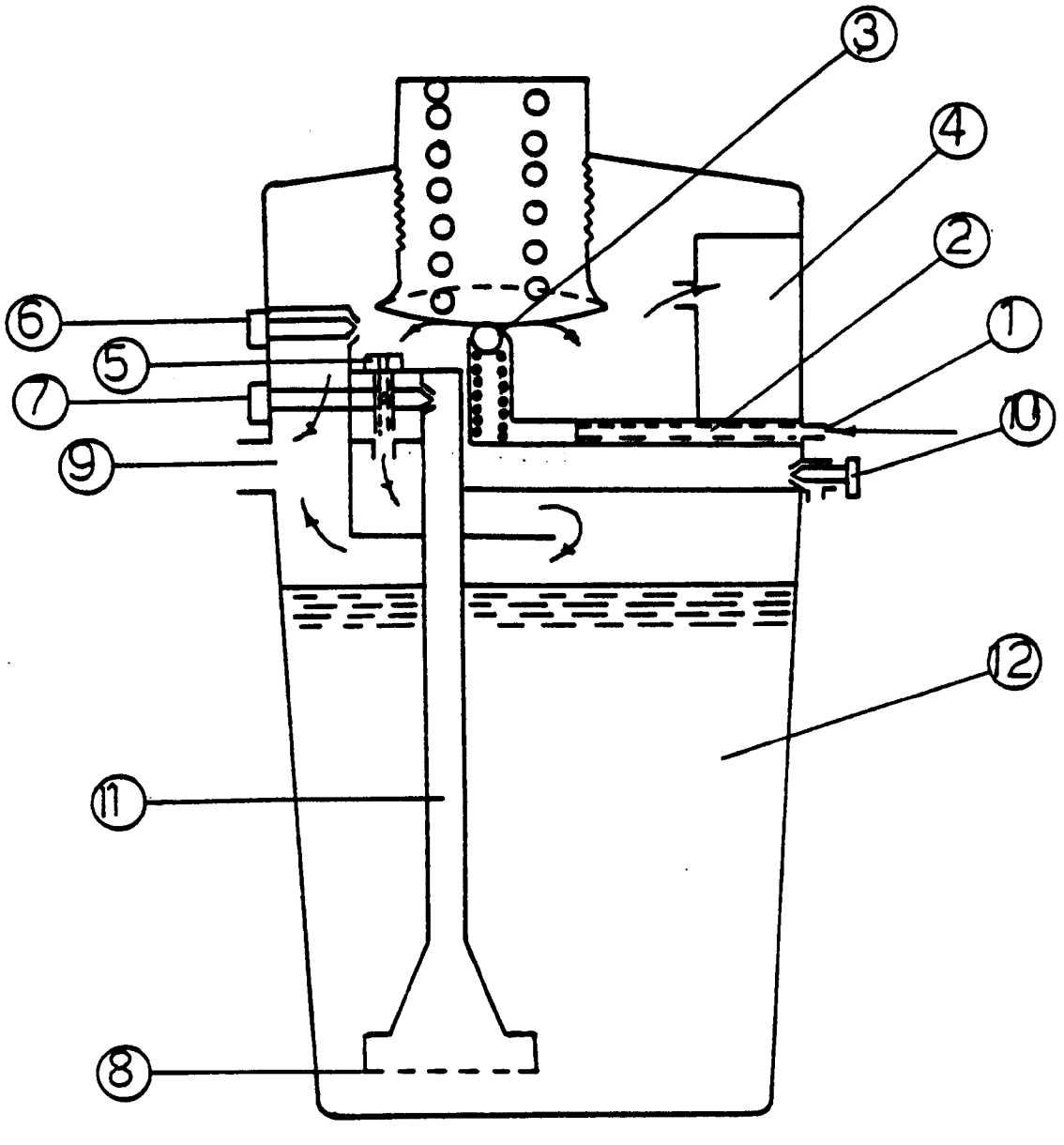

1. Compressed air pipe line
2. Air filter
3. Reduction valve
4. Pressure gauge
5. Atomiser nozzle
6. Air control screw
7. Oil regulating screw
8. Oil filter
9. Oil mist pipe line
10. Water separator drain cock
11. Oil suction pipe
12. Oil container

FIG.A.6.1 Diagram of oil mist lubricator.

APPENDIX A.7.

SPECIFICATION OF THE CONSTANT VOLUME FLOW VALVES.

Appendix A.7. Specifications of the Constant Volume Flow Valves.

Three constant flow valves were needed to couple the high pressure pump to the bearing.

These control the flow rate by varying the area of an orifice within the valve (see table 1.1). To nullify the effects of fluctuating back pressure the valves contain a spring controlled by-pass loop.

Three valves of this type, "Keelavite" hydraulics VFS1/1000 valves were provided. The Manufacturer would not provide performance details for these valves but a data sheet was obtained from them.

The valves were subjected to varying back pressures whilst the pump line pressure was held constant. The flow rates were measured by the "bucket and stop watch" technique, and the results showed that the valves were working correctly. Tables of the results obtained are given, and these show that the valves are controlling the flow despite the variation in the back pressure or the oil temperature.

TABLE 7.1 Specification of Keelavite constant volume valve ($VFS^1/100$)

Maximum pressure	2.04×10^7 Nm^{-2}
Flow Range	0 3.6 gpm(0.273 Ls^{-1})
Pressure drop across valve (assuming normal temperatures)	1.02×10^6 Nm^{-2}
Error in flow setting	$\pm$ 1%
Filtration required for valves	15~20 microns
Frequency response	60×10^{-6} sec.

TABLE A7.2 Results of tests on the flow control valves.

Valve No.3 Valve Setting: 2 Volume: 7.5 litres

Pump Press. $x10^{-7}$ Nm^{-2}	Back Press. $x10^{-7}$ Nm^{-1}	Oil Temp. ^{o}C	Time Second	Flow $L\ S^{-1}$	Flow GPM
0.0667	0.132	26	462	0.0163	0.214
	0.264	28	461	0.0167	0.220
	0.396	30	461	0.0167	0.220
	0.528	31	461	0.0166	0.218
1.334	0.132	27	462	0.0163	0.214
	0.264	30	462	0.0163	0.214
	0.396	31	462	0.0163	0.214
	0.528	34	462	0.0163	0.214
	0.667	36	462	0.0163	0.214
	0.792	39	459.4	0.01633	0.215
	0.924	41	456.3	0.01644	0.217
	1.056	43	456.3	0.01644	0.217
	1.188	47	453	0.01654	0.218
2.000	0.132	50	461	0.0163	0.215
	0.264	55	461	0.0163	0.215
	0.396	55	461	0.0163	0.215
	0.528	63	452	0.0166	0.219
	0.667	78	452	0.0166	0.219
	0.792	80	449	0.0167	0.22
	0.924	88	449	0.0167	0.22
	1.056	88	449	0.0167	0.22
	1.188	90	438	0.0171	0.225
	1.320	92	438	0.0171	0.225
	1.452	93	438	0.0171	0.225

TABLE A.7.3 Results of tests on the flow control valves.

Valve No.3 Valve Setting: 3.5 Volume: 7.5 litres

Pump Press. $x10^{-7}$ Nm^{-2}	Back Press. $x10^{-7}Nm^{-7}$	Oil Temp. ^{o}C	Time Second	Flow $L\ S^{-1}$	Flow GPM
0.667	0.132	24	119	0.063	0.831
	0.264	35	118	0.0636	0.839
	0.396	27	118	0.0636	0.839
	0.528	28	118	0.0636	0.839
1.334	0.132	27	119	0.063	0.831
	0.264	30	118	0.0636	0.839
	0.396	35	118	0.0636	0.839
	0.528	37	118	0.0636	0.839
	0.667	39	118	0.0636	0.839
	0.792	41	118	0.0636	0.839
	0.924	43	118	0.0636	0.839
	1.056	45	118	0.0636	0.839
	1.188	47	118	0.0636	0.839
1.7	0.132	32	118	0.0636	0.839
	0.264	37	118	0.0636	0.839
	0.396	45	118	0.0636	0.839
	0.529	46	118	0.0636	0.839
	0.667	48	118	0.0636	0.839
	0.792	52	118	0.0636	0.839
	0.924	54	118	0.0636	0.839
	1.056	57	118	0.0636	0.839
	1.188	57	118	0.0636	0.839
	1.320	57	118	0.0636	0.839
	1.452	57	118	0.0636	0.839

TABLE A.7.4 Results of tests on the flow control valves.

Valve No.3 Valve Setting: 5.5 Volume: 7.5 litres

Pump Press.	Back Press.	Oil Temp.	Time	Flow $L\ S^{-1}$	Flow GPM
0.667	0.132	34	56.23	0.133	1.76
	0.264	37	55.83	0.134	1.77
	0.396	39	55.83	0.134	1.77
	0.528	41	56.0	0.134	1.77
1.334	0.132	38	57.4	0.131	1.726
	0.264	39	57	0.1316	1.734
	0.396	40	56.42	0.133	1.753
	0.528	41	56.42	0.133	1.753
	0.667	42	56.42	0.133	1.753
	0.792	44	56.42	0.133	1.753
	0.924	50	56.0	0.134	1.765
	1.056	54	56.0	0.134	1.765
	1.188	59	56.0	0.134	1.765
1.88	0.132	30	57.0	0.1316	1.734
	0.264	40	56.91	0.132	1.738
	0.396	45	56.81	0.132	1.738
	0.528	50	56.61	0.132	1.746
	0.667	53	56.61	0.1325	1.746
	0.792	55	56	0.134	1.765
	0.924	55	55.83	0.1342	1.77
	1.056	57	55.83	0.1342	1.77
	1.188	58	55.63	0.135	1.78
	1.320	59	55.63	0.135	1.78
	1.452	61	55.63	0.135	1.78
	1.584	63	55.63	0.135	1.78

TABLE A.7.5 Results of tests on the flow control valves.

Valve No.3 Valve Setting: 7 Volume: 7.5 litres

Pump Press.	Back Press.	Oil Temp.	Time	Flow $L\ S^{-1}$	Flow GPM
0.667	0.132	25	42.7	0.176	2.32
	0.264	27	42.5	0.176	2.33
	0.396	30	42.1	0.178	2.35
	0.528	32	41.7	0.179	2.37
1.334	0.132	34	42.0	0.1786	2.35
	0.264	35	42.0	0.1786	2.35
	0.396	37	42.0	0.1786	2.35
	0.528	38	41.5	0.181	2.37
	0.667	39	41	0.183	2.4
	0.792	41	40.7	0.184	2.43
	1.056	42	40.7	0.184	2.43
	1.188	44	40.4	0.186	2.45
1.88	0.132	39	42.9	0.175	2.31
	0.264	41	42.7	0.176	2.32
	0.396	42	41.5	0.181	2.37
	0.528	44	41.2	0.182	2.4
	0.667	45	40.73	0.184	2.43
	0.792	46	40.73	0.184	2.43
	0.924	46	40.73	0.184	2.43
	1.056	47	40.52	0.185	2.44
	1.188	48	40.52	0.185	2.44
	1.320	50	40.33	0.186	2.45
	1.452	52	40.33	0.186	2.45
	1.584	55	40.33	0.186	2.45

TABLE A.7.6 Results of tests on the flow control valves.

Valve No.1 Valve Setting: 5.5 Measured volume: 7.5 litres

Pump Press.	Back Press.	Oil Temp.	Time	Flow $L\ S^{-1}$	Flow GPM
1.334	0.132	41	56.1	0.134	1.77
	0.264	44	56.1	0.134	1.77
	0.396	47	56.1	0.134	1.77
	0.528	51	56.1	0.134	1.77
	0.667	53	56	0.134	1.77
	0.792	56	55.6	0.135	1.78
	0.924	58	54.6	0.137	1.8
	1.056	61	54.6	0.137	1.8
	1.188	64	54.6	0.137	1.8

Valve No.1 Valve Setting: 5.5 Measured volume: 7.5 litres

P_s	P_i	T °C	Time	Flow $L\ S^{-1}$	Flow GPM
1.334	0.132	22	41.7	0.18	2.37
	0.264	29	41.7	0.18	2.37
	0.396	32	41.7	0.18	2.37
	0.528	32	41.7	0.18	2.37
	0.667	33	41	0.183	2.4
	0.792	35	41	0.183	2.4
	0.924	40	41	0.183	2.4
	1.056	44	40.4	0.186	2.45
	1.188	50	40.4	0.186	2.45

Results in Table A8.1 were obtained by using Shell Vit (150) oil.

TABLE A.7.7 Results of tests on the flow control valves.

Valve No.2 Valve Setting: 3.5 Volume: 7.5 litres

Pump Press.	Back Press.	Oil Temp.	Time	Flow	Flow
1.334	0.132	43	118	0.0636	0.839
	0.264	45	118	0.0636	0.839
	0.396	50	118	0.0636	0.839
	0.528	54	118	0.0636	0.839
	0.667	56	118	0.0636	0.839
	0.792	57	118	0.0636	0.839
	0.924	60	118	0.0636	0.839
	1.056	62	118	0.0636	0.839
	1.188	62	118	0.0636	0.839

Valve No.2 Valve Setting: 7 Volume: 7.5 litres

P_s	P_i	T ^{o}C	Time	Flow $L\ S^{-1}$	Flow GPM
1.334	0.132	38	43.0	0.174	2.3
	0.264	40	42.8	0.175	2.3
	0.396	42	42.7	0.175	2.3
	0.528	45	42.7	0.175	2.3
	0.667	47	42.1	0.178	2.35
	0.792	47	42.1	0.178	2.35
	0.924	49	42	0.178	2.35
	1.056	51	42	0.178	2.35
	1.188	53	41.70	0.18	2.37

TABLE A7.8 Results of tests on the flow meters.

Valve Setting: 3.5 Measured volume: 7 litres

Oil Viscosity: 37 C.S at 40°C

Pump Pressure x 10^{-7} Nm^{-2}	Differential Pressure x 10^{-7} Nm^{-2}	Oil Temp. °C	Time Sec	Measured Flow GPM	Flow Meter Reading
1.334	0.33	22	111	0.83	0.55
		25	111	0.83	0.61
		34	110	0.84	0.7
		40	110	0.84	0.73
		51	110	0.84	0.795
		60	110	0.84	0.82
		70	110	0.84	0.84

Valve Setting: 4.5

Pump Pressure x10^{-7} Nm^{-2}	Differential Pressure x10^{-7} Nm^{-2}	Oil Temp. °C	Time Sec	Measured Flow GPM	Flow Meter Reading
1.334	0.33	20	68	1.44	0.9
		25	68	1.44	1.11
		30	68	1.44	1.17
		35	68	1.44	1.3
		45	68	1.44	1.4
		50	62	1.49	1.41
		55	62	1.49	1.44
		60	62	1.49	1.49
		70	62	1.49	1.50

APPENDIX A.8.

A COMPUTER PROGRAMME FOR THE CALCULATION OF SPINDLE DEFLECTION.

```
.NULL.
00001:   20  PRINT '                    RESPONSE TO UNBALANCE FORCES AND IMPRESSED MOMENTS'
00002:   30  PRINT
00003:   40  PRINT '                                              S.I.UNITS.'
00004:   50  PRINT
00005:   60  PRINT 'TO AVOID RE-ENTRY OF DATA RUN 510. '
00006:   70  PRINT 'INSERT SPEED Z IN R.P.M. IN LINE 510.'
00007:   80  PRINT 'ENTER DATA AS N,E THEN L,R,K,M,M1,P1,P2,DELTA(M*R),FOR EACH STATION.'
00008:   90  PRINT 'DATA STARTS ON LINE 1540'
00009:  100  PRINT 'SUB ROUTINE FOR BEARING SUPPORT ON LINES 1510,1520.'
00010:  110  PRINT
00011:  120  PRINT 'D A T A'
00012:  130  READ N,E
00013:  140  PRINT 'NUMBER OF STATION':N
00014:  141  PRINT 'YOUNGS MODULUS':E
00015:  150  PRINT
00016:  160  Q=1
00017:  180  PRINT 'STATION NO          SEGMENT L                R A D'
00018:  181  PRINT 'BRG STIFFNESS          M A S S'
00019:  190  READ L,R,K,M,M1,P1,P2,F
00020:  200  PRINT Q,L,R,K,M
00021:  210  Q=Q+1
00022:  220  IF Q=N+1 THEN 240
00023:  230  GOTO 190
00024:  240  RESTORE
00025:  250  PRINT
00026:  260  L1=0
00027:  270  Q=1
00028:  290  PRINT 'STATION NO          D I S T                A C C  M A S S'
00029:  291  PRINT 'BASE MASS'
00030:  300  READ N,E
00031:  310  M2=0
00032:  320  READ L,R,K,M,M1,P1,P2,F
00033:  330  M2=M2+M
00034:  340  PRINT Q,L1,M2,M1
```

```
00035: 350  L1=L1+L
00036: 360  Q=Q+1
00037: 370  IF Q=N+1 THEN 390
00038: 380  GOTO 320
00039: 390  RESTORE
00040: 400  PRINT
00041: 410  Q=1
00042: 430  PRINT 'STATION NO        MOMENT P1              MOMENT P2'
00043: 431  PRINT 'DELTA(M*R)'
00044: 440  READ N,E
00045: 450  READ L,R,K,M,M1,P1,P2,F
00046: 460  PRINT Q,P1,P1,F
00047: 470  Q=Q+1
00048: 480  IF Q=N+1 THEN 500
00049: 490  GOTO 450
00050: 500  RESTORE
00051: 510  Z=0
00052: 520  PRINT
00053: 530  PRINT
00054: 540  PRINT 'OUTPUT FOR':Z,'R.P.M.'
00055: 550  W=(3.14*Z*2)/60
00056: 560  DIM A(4,4),C(2,2),E(4,1),F(4,1),G(4,1),H(4,1),J(4,1),X(4,4),Y(4,4)
00057: 570  PRINT
00058: 590  PRINT 'STATION NO          DISPLACEMENT              S L O P E'
00059: 591  PRINT 'M O M                S H E A R'
00060: 610  PRINT 'D I S T            B R G   F                 U N B A L  F'
00061: 611  PRINT 'BASE/ROTOR         EFF STIFFNESS'
00062: 620  PRINT
00063: 630  MAT Y=IDN(4,4)
00064: 640  Q=1
00065: 650  READ N,E
00066: 660  READ L,R,K,M,M1,P1,P2,F
00067: 670  GOSUB 1320
00068: 680  MAT X=A*Y
```

```
00069:  690  MAT Y=X
00070:  700  Q=Q+1
00071:  710  IF Q=N+1 THEN 730
00072:  720  GOTO 660
00073:  730  C(1,1)=Y(3,1)
00074:  740  C(1,2)=Y(3,2)
00075:  750  C(2,1)=Y(4,1)
00076:  760  C(2,2)=Y(4,2)
00077:  770  MAT F=ZER(4,1)
00078:  780  Q=1
00079:  790  RESTORE
00080:  800  READ N,E
00081:  810  READ L,R,K,M,M1,P1,P2,F
00082:  820  G(1,1)=0
00083:  830  G(2,1)=0
00084:  840  G(3,1)=P1
00085:  850  G(4,1)=F
00086:  860  J(1,1)=0
00087:  870  J(2,1)=0
00088:  880  J(3,1)=P2
00089:  890  J(4,1)=0
00090:  900  GOSUB 1320
00091:  910  MAT F=F+G
00092:  920  MAT H=A*F
00093:  930  MAT F=H-J
00094:  940  Q=Q+1
00095:  950  IF Q=N+1 THEN 970
00096:  960  GOTO 810
00097:  970  G1=((C(1,2)*F(4,1))-(C(2,2)*F(3,1)))
00098:  980  G2=-((C(1,1)*F(4,1))-(C(2,1)*F(3,1)))
00099:  990  G3=((C(1,1)*C(2,2))-(C(1,2)*C(2,1)))
00100:  991  MAT PRINT C
00101: 1000  E(1,1)=G1/G3
00102: 1010  E(2,1)=G2/G3
```

```
00103:1020  E(3,1)=0
00104:1030  E(4,1)=0
00105:1040  Q=1
00106:1050  L1=0
00107:1060  PRINT Q,E(1,1),E(2,1),E(3,1),E(4,1)
00108:1070  RESTORE
00109:1080  READ N,E
00110:1090  READ L,R,K,M,M1,P1,P2,F
00111:1100  G(1,1)=0
00112:1110  G(2,1)=0
00113:1120  G(3,1)=P1
00114:1130  G(4,1)=F
00115:1140  J(1,1)=0
00116:1150  J(2,1)=0
00117:1160  J(3,1)=P2
00118:1170  J(4,1)=0
00119:1180  GOSUB 1320
00120:1190  PRINT L1,K3*E(1,1),G(4,1),K4,K3
00121:1200  PRINT
00122:1210  MAT H=A*G
00123:1220  MAT F=A*E
00124:1230  MAT E=F+H
00125:1240  MAT E=E-J
00126:1250  L1=L1+L
00127:1260  Q=Q+1
00128:1270  PRINT Q,E(1,1),E(2,1),E(3,1),E(4,1)
00129:1280  IF Q=N+1 THEN 1300
00130:1290  GOTO 1090
00131:1300  PRINT
00132:1310  END
00133:1320  I=(3.14*R^^4)/4
00134:1330  GOSUB 1510
00135:1340  A(1,1)=1+((M*W^^2)-K)*((L^^3/(6*E*I))-((2.6*L)/(3.14*E*R^^2)))
00136:1350  A(1,2)=L
```

```
00137:1360  A(1,3)=L^^2/(2*E*I)
00138:1370  A(1,4)=(L^^3/(6*E*I))-((2.6*L)/(3.14*(R^^2)*E))
00139:1380  A(2,1)=((M*W^^2)-K)*((L^^2/(2*E*I))-((2.6)/(3.14*E*(R^^2))))
00140:1390  A(2,2)=1
00141:1400  A(2,3)=L/(E*I)
00142:1410  A(2,4)=(L^^2/(2*E*I))-((2.6)/(3.14*(R^^2)*E))
00143:1420  A(3,1)=L*((M*W^^2)-K3)
00144:1430  A(3,2)=0
00145:1440  A(3,3)=1
00146:1450  A(3,4)=L
00147:1460  A(4,1)=(M*W^^2)-K3
00148:1470  A(4,2)=0
00149:1480  A(4,3)=0
00150:1490  A(4,4)=1
00151:1500  RETURN
00152:1510  K3=K
00153:1520  K4=0
00154:1530  RETURN
00155:1540  DATA 27,2.1E+11
00156:1550  DATA .016,.0275,0,.1485,0,0,0,0
00157:1560  DATA .04,.03,0,.259,0,0,0,25000
00158:1570  DATA .02,.045,0,.607,0,0,0,0
00159:1580  DATA .0375,.0675,0,2.556,0,0,0,0
00160:1590  DATA .0375,.0675,0,4.12,0,0,0,0
00161:1600  DATA .0435,.0675,3.E+08,4.49,0,0,0,0
00162:1610  DATA .0435,.0675,6.E+08,4.86,0,0,0,0
00163:1620  DATA .0435,.0675,3.E+08,4.86,0,0,0,
```

```
00164:1630  DATA .0375,.0675,0,4.49,0,0,0,0
00165:1640  DATA .0375,.0675,0,4.12,0,0,0,0
00166:1650  DATA .02,.0475,0,2.61,0,0,0,0
00167:1660  DATA .007,.04,0,.687,0,0,0,0
00168:1670  DATA .007,.04,0,.274,0,0,0,0
00169:1680  DATA .007,.04,0,.274,0,0,0,0
00170:1690  DATA .032,.04,0,1.262,0,0,0,0
00171:1700  DATA .076,.0375,0,2.435,0,0,0,0
00172:1710  DATA .076,.0375,0,2.62,0,0,0,0
00173:1720  DATA .076,.0375,0,2.62,0,0,0,0
00174:1730  DATA .007,.03,6.E+07,1.387,0,0,0,0
00175:1740  DATA .007,.03,1.2E+08,.154,0,0,0,0
00176:1750  DATA .007,.03,6.E+07,.154,0,0,0,0
00177:1760  DATA .03,.03,0,.408,0,0,0,0
00178:1770  DATA .011,.0275,0,.433,0,0,0,0
00179:1780  DATA .033,.025,0,.372,0,0,0,0
00180:1790  DATA .033,.025,0,.54,0,0,0,0
00181:1800  DATA .033,.025,0,.54,0,0,0,0
00182:1810  DATA 0,.025,0,.27,0,0,0,0
BOTTOM
```

A.8.1. SAMPLE OF THE OUTPUT FOR THE TEST SPINDLE .

RESPONSE TO UNBALANCE FORCES AND IMPRESSED MOMENTS

S.I.UNITS.

TO AVOID RE-ENTRY OF DATA RUN 510.
INSERT SPEED Z IN R.P.M. IN LINE 510.
ENTER DATA AS N,E THEN L,R,K,M,M1,P1,P2,DELTA(M*R),FOR EACH STATION
DATA STARTS ON LINE 1540
SUB ROUTINE FOR BEARING SUPPORT ON LINES 1510,1520.

D A T A
NUMBER OF STATION 27
YOUNGS MODULUS 210000000000

STATION NO BRG STIFFNESS	SEGMENT L M A S S	R A D
1	.016	.0275
0	.1485	
2	.04	.03
0	.259	
3	.02	.045
0	.607	
4	.0375	.0675
0	2.556	
5	.0375	.0675
0	4.12	
6	.0435	.0675
300000000	4.49	
7	.0435	.0675
600000000	4.86	
8	.0435	.0675
300000000	4.86	
9	.0375	.0675
0	4.49	
10	.0375	.0675
0	4.12	
11	.02	.0475
0	2.61	
12	.007	.04
0	.687	
13	.007	.04
0	.274	
14	.007	.04
0	.274	
15	.032	.04
0	1.262	
16	.076	.0375
0	2.435	
17	.076	.0375
0	2.62	
18	.076	.0375
0	2.62	
19	.007	.03
60000000	1.387	
20	.007	.03
120000000	.154	
21	.007	.03
60000000	.154	
22	.03	.03

0	.408	
23	.011	.0275
0	.433	
24	.033	.025
0	.372	
25	.033	.025
0	.54	
26	.033	.025
0	.54	
27	0	.025
0	.27	

STATION NO BASE MASS	D I S T	A C C M A S S
1	0	.1485
0		
2	.016	.4075
0		
3	.056	1.0145
0		
4	.076	3.5705
0		
5	.1135	7.6905
0		
6	.151	12.1805
0		
7	.1945	17.0405
0		
8	.238	21.9005
0		
9	.2815	26.3905
0		
10	.319	30.5105
0		
11	.3565	33.1205
0		
12	.3765	33.8075
0		
13	.3835	34.0815
0		
14	.3905	34.3555
0		
15	.3975	35.6175
0		
16	.4295	38.0525
0		
17	.5055	40.6725
0		
18	.5815	43.2925
0		
19	.6575	44.6795
0		
20	.6645	44.8335
0		
21	.6715	44.9875
0		
22	.6785	45.3955
0		
23	.7085	45.8285
0		

```
24                      .7194999999999          46.2005
0
25                      .7524999999999          46.7405
0
26                      .7854999999999          47.2805
0
27                      .8184999999999          47.5505
0

STATION NO          MOMENT P1               MOMENT P2
DELTA(M*R)
1                       0                       0
0
2                       0                       0
25000
3                       0                       0
0
4                       0                       0
OUTPUT FOR 0            R.P.M.

STATION NO              DISPLACEMENT              S L O P E
M O M                    S H E A R
D I S T                 B R G   F                 U N B A L  F
BASE/ROTOR              EFF STIFFNESS

556515500.3511          7345162035.561          86114845.94315
1275789797.457
1                       .0001838713537495       -.0008164717428531
0                       0
0                       0                       0
0                       0

2                       .0001708078058638       -.0008164717428531
0                       0
.016                    0                       25000
0                       0

3                       .0001357649257449       -.0007762181640291
1000                    25000
.056                    0                       0
0                       0

4                       .0001196121612989       -.0007879140072017
1500                    25000
.076                    0                       0
0                       0

5                       8.96264708777E-05       -.0007879756453739
2437.5                  25000
.1135                   0                       0
0                       0

6                       5.983108831315E-05      -.0007777642548482
3375                    25000
.151                    17949.32649394          0
0                       300000000
```

```
7                    2.669426461343E-05   -.0007390164555891
3681.704297513       7050.673506055
.1945                16016.55876806       0
0                    600000000

8                    -4.133501160469E-06  -.0006869374216548
3291.688288616       -8965.885262001
.238                 -1240.050348141      0
0                    300000000

9                    -3.284536628204E-05  -.0006405462495068
2955.614469863       -7725.83491386
.2815                0                    0
0                    0

10                   -5.602770768468E-05  -.0006030603471776
2665.895660593       -7725.83491386
.319                 0                    0
0                    0

11                   -7.786385354282E-05  -.0005687491537998
2376.176851323       -7725.83491386
.3565                0                    0
0                    0

12                   -8.84147827905E-05   -.0005004590382484
2221.660153046       -7725.83491386
.3765                0                    0
0                    0

13                   -9.165679010469E-05  -.0004450175231723
2167.579308649       -7725.83491386
.3835                0                    0
0                    0

14                   -9.451384645897E-05  -.0003904730497032
2113.498464252       -7725.83491386
.3905                0                    0
0                    0

15                   -9.69922311446E-05   -.0003368256178409
2059.417619855       -7725.83491386
.3975                0                    0
0                    0

16                   -.0001047628401985   -.0001710010882736
1812.190902611       -7725.83491386
.4295                0                    0
0                    0

17                   -.0001017923228599   .0002046958512815
1225.027449158       -7725.83491386
.5055                0                    0
0                    0

18                   -7.547050076203E-05  .0004435069317081
637.8639957046       -7725.83491386
.5815                0                    0
0                    0
```

19	-3.62006991986E-05	.0005454321530063
50.70054225117	-7725.83491386	
.6575	-2172.041951916	0
0	60000000	
20	-3.220542766981E-05	.0005714026742878
11.82399151756	-5553.792961944	
.6645	-3864.651320378	0
0	120000000	
21	-2.815236069031E-05	.0005791128772086
2.659635356395E-08	-1689.141641567	
.6715	-1689.141641419	0
0	60000000	
22	-2.409857054985E-05	.0005791128772106
2.556203071435E-08	-1.477310433984E-07	
.6785	0	0
0	0	
23	-6.725184233426E-06	.0005791128772165
2.11300994124E-08	-1.477310433984E-07	
.7085	0	0
0	0	
24	-3.549425840234E-07	.0005791128772197
1.950505793502E-08	-1.477310433984E-07	
.7194999999999	0	0
0	0	
25	1.875578236441E-05	.0005791128772293
1.462993350287E-08	-1.477310433984E-07	
.7524999999999	0	0
0	0	
26	3.786650731311E-05	.0005791128772365
9.254809070727E-09	-1.477310433984E-07	
.7854999999999	0	0
0	0	
27	5.697723226202E-05	.0005791128772411
4.879684638S8E-09	-1.477310433984E-07	
.8184999999999	0	0
0	0	
28	5.697723226202E-05	.0005791128772421
4.879684638S8E-09	-1.477310433984E-07	

A.8.2. SAMPLE OF THE OUTPUT FOR A CONSTANT DIAMETER SPINDLE.

RESPONSE TO UNBALANCE FORCES AND IMPRESSED MOMENTS

S.I.UNITS.

TO AVOID RE-ENTRY OF DATA RUN 510.
INSERT SPEED Z IN R.P.M. IN LINE 510.
ENTER DATA AS N,E THEN L,R,K,M,M1,P1,P2,DELTA(M*R),FOR EACH STATIO
DATA STARTS ON LINE 1540
SUB ROUTINE FOR BEARING SUPPORT ON LINES 1510,1520.

D A T A
NUMBER OF STATION 27
YOUNGS MODULUS 210000000000

STATION NO	SEGMENT L	R A D
BRG STIFFNESS	M A S S	
1	.016	.2
0	7.84	
2	.04	.2
0	27.44	
3	.02	.2
0	29.4	
4	.0375	.2
0	28.175	
5	.0375	.2
0	36.75	
6	.0435	.2
300000000	39.695	
7	.0435	.2
600000000	42.64	
8	.0435	.2
300000000	42.64	
9	.0375	.2
0	39.695	
10	.0375	.2
0	36.75	
11	.02	.2
0	28.175	
12	.007	.2
0	13.23	
13	.007	.2
0	6.86	
14	.007	.2
0	6.86	
15	.032	.2
0	19.11	
16	.076	.2
0	52.92	
17	.076	.2
0	74.48	
18	.046	.2
0	59.74	
19	.0417	.2
300000000	42.93	
20	.0417	.2
600000000	40.86	

21	.0417	.2
300000000	40.86	
22	.0132	.2
0	26.9	
23	.0132	.2
0	12.94	
24	.0132	.2
0	12.94	
25	.0132	.2
0	12.94	
26	.0132	.2
0	12.94	
27	0	.2
0	6.47	

STATION NO BASE MASS	D I S T	A C C M A S S
1	0	7.84
0		
2	.016	35.28
0		
3	.056	64.68
0		
4	.076	92.855
0		
5	.1135	129.605
0		
6	.151	169.3
0		
7	.1945	211.94
0		
8	.238	254.58
0		
9	.2815	294.275
0		
10	.319	331.025
0		
11	.3565	359.2
0		
12	.3765	372.43
0		
13	.3835	379.29
0		
14	.3905	386.15
0		
15	.3975	405.26
0		
16	.4295	458.18
0		
17	.5055	532.66
0		
18	.5815	592.4
0		
19	.6275	635.33
0		
20	.6692	676.19
0		
21	.7109	717.05
0		
22	.7526	743.95
0		

23	.7658	756.8899999999
0		
24	.779	769.8299999999
0		
25	.7922	782.7699999999
0		
26	.8054	795.7099999999
0		
27	.8186	802.1799999999
0		

STATION NO	MOMENT P1	MOMENT P2
DELTA(M*R)		
1	0	0
0		
2	0	0
30000		
3	0	0
0		
4	0	0
0		
5	0	0
0		
6	0	0
0		
7	0	0
0		
8	0	0
0		
9	0	0
0		
10	0	0
0		
11	0	0
0		
12	0	0
0		
13	0	0
0		
14	0	0
0		
15	0	0
0		
16	0	0
0		
17	0	0
0		
18	0	0
0		
19	0	0
0		
20	0	0
0		
21	0	0
0		
22	0	0
0		
23	0	0
0		
24	0	0
0		
25	0	0

OUTPUT FOR 0 R.P.M.

STATION NO M O M D I S T BASE/ROTOR	DISPLACEMENT S H E A R B R G F EFF STIFFNESS	S L O P E U N B A L F
-913807607.0668 -1017597909.298	-2300215632.271	-260745191.6254
1 0 0 0	5.254708103785E-05 0 0 0	-9.569427551826E-05 0
2 0 .016 0	5.101597262956E-05 0 0 0	-9.569427551826E-05 30000
3 1200 .056 0	4.718941483297E-05 30000 0 0	-9.560328370753E-05 0
4 1800 .076 0	4.527841072994E-05 30000 0 0	-9.548954394411E-05 0
5 2925 .1135 0	4.170335089419E-05 30000 0 0	-9.515365620525E-05 0
6 4050 .151 0	3.814388584632E-05 30000 11443.1657539 300000000	-9.465782192409E-05 0
7 4857.222289705 .1945 0	3.404176340419E-05 18556.8342461 20425.05804252 600000000	-9.392332054101E-05 0
8 4775.954554561 .238 0	2.997342497532E-05 -1868.223796414 8992.027492596 300000000	-9.312895598095E-05 0
9 4303.533623489 .2815 0	2.593888219426E-05 -10860.25128901 0 0	-9.238024932386E-05 0
10 3896.274200151 .319 0	2.248573321257E-05 -10860.25128901 0 0	-9.179734669764E-05 0

```
16                      1.242305252268E-05   -9.041641286589E-
2696.216432715          -10860.25128901
.4295                   0                    0
0                       0

17                      5.577914502295E-06   -8.97584357535E-0
1870.83733475           -10860.25128901
.5055                   0                    0
0                       0

18                      -1.22625462044E-06   -8.933828398023E-
1045.458236785          -10860.25128901
.5815                   0                    0
0                       0

19                      -5.33229008231E-06   -8.919951793144E-
545.8866774905          -10860.25128901
.6275                   -1599.687024693      0
0                       300000000

20                      -9.050534859186E-06  -8.914374024281E-
159.7211476685          -9260.564264318
.6692                   -5430.320915512      0
0                       600000000

21                      -1.276747782955E-05  -8.913111442415E-
2.324668457732E-08      -3830.243348806
.7109                   -3830.243348866      0
0                       300000000

22                      -1.648424530104E-05  -8.913111442415E-
2.573506208137E-08      5.972106009722E-08
.7526                   0                    0
0                       0

23                      -1.766077601144E-05  -8.913111442415E-
2.652338007465E-08      5.972106009722E-08
.7658                   0                    0
0                       0

24                      -1.883730672184E-05  -8.913111442415E-
2.731169806793E-08      5.972106009722E-08
.779                    0                    0
0                       0

25                      -2.001383743224E-05  -8.913111442415E-
2.810001606121E-08      5.972106009722E-08
.7922                   0                    0
0                       0

26                      -2.119036814264E-05  -8.913111442415E-
2.88883340545E-08       5.972106009722E-08
.8054                   0                    0
0                       0

27                      -2.236689885304E-05  -8.913111442415E-
2.967665204778E-08      5.972106009722E-08
.8186                   0                    0
0                       0

28                      -2.236689885304E-05  -8.913111442415E-
2.967665204778E-08      5.972106009722E-08
```

APPENDIX A.9

METALLIC CONTACT

MONITORING.

Appendix A.9 Metallic Contact Monitoring

In the hydrostatic tests in the simple test rig (chapter 4), the need arose for a device which would indicate whether the shaft was supported by an oil film or was supported by metal to metal contact. With no load on the journal a metal to metal contact may arise due to a blockage in a high pressure line or in a constant volume flow valve. It was suggested that a measurement of the electric resistance due to the oil film should be monitored. That idea was used on the simple test rig and was also used on the main test rig (chapter 6).

In chapter 6, it has been described how the shaft was insulated from the bearings and from the frame, to make possible measurements of the resistance of the oil film. Duruing the assemply process the bearing housing and the brass shell were cleaned and every care had been taken to ensure that no swarf remained on the warp. After some tests, it was found that the resistance reading was always zero. Several attemps were made to find the reason and finally the shaft was taken out of the bearing. It was found that the journal and bearing surfaces were slightly damaged due to the presence of some metal swarf which had hidden in the high pressure passages. When the high pressure system was operated, that metal swarf came into contact with both the journal bearing surfaces and caused some scoring. The journal was lapped and the bearing was dressed.

The bearing and journal were tested for a long period. High oil film resistance was always observed and no evidence that operation was affected by the scoring. The journal and bearing were removed to fit the second bearing, the surface of the first bearing and the

surface of the journal were as they were after dressing. Figure A.9.1 shows a photograph for the first bearing shell after long operation.

That experience showed the usefulness of the metallic contact monitoring. It can be seen that without this safeguard the bearing and the journal might be rendered useless. It also emphasized that one cannot rely upon shop statements that components have been thoroughly cleaned.

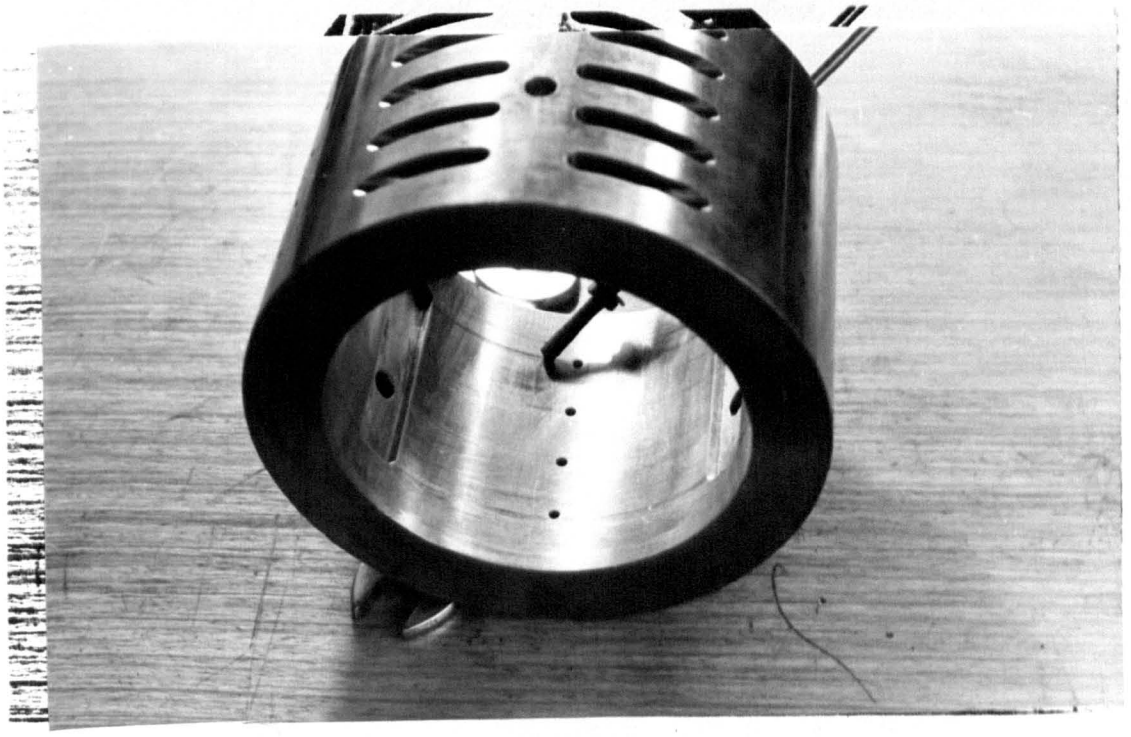

FIG.A.9.1 SCORED BEARING SHELL.

APPENDIX A.10

A COMPUTER PROGRAMME FOR THE NUMERICAL SOLUTION OF REYNOLDS EQUATION FOR THE FULL CIRCULARE BORE JOURNAL BEARING (360° JOURNAL BEARING).

```
.NULL.
00001:JOB(GREM114,J12,M7600,T900)              T  M  S A L E M    MECH. ENG. DEPT.
00002:MNF(T)
00003:LDSET(MAP=B/ZZZZMP,PRESET=ZERO)
00004:LGO.
00005:@
00006:       PROGRAM A35(INPUT,OUTPUT,TAPE4=INPUT,TAPE3=OUTPUT)
00007:       DIMENSION P1(40,122),P11(40,122),H1(40,122)
00008:       INTEGER U,V
00009:       L=1
00010:       DO 3 U=1,3
00011:       E=0.1
00012:       DO 1 K=1,9
00013:       CVN=0.0
00014:       DO 54545 V=1,4
00015:       EPS=0.0001
00016:       MAXIT=200
00017:       D=2.0
00018:       M=120
00019:C*************************************************************************
00020:       DX=(3.14)/90.0
00021:       DY=DX
00022:       N=28
00023:C       N     IS THE NUMBER OF  MESH  POINTS  ACROSS  THE  BEARING
00024:C*************************************************************************
00025:C      EPS  IS  THE  REQUIRED  ACCURACY  IN THE SOLUTION
00026:C       MAXIT      IS  THE  MAXIMUM  NUMBER  OF  ITERTATIONS
00027:C*************************************************************************
00028:C       L     IS THE BEARING  LENGTH
00029:C*************************************************************************
00030:C       D     IS THE BEARING  DAIMETER
00031:C*************************************************************************
00032:C       M     IS  THE NUMBER OF MESH  POINTS AROUND THE  BEARING
00033:C*************************************************************************
00034:       DO 10 J=1,M+1
```

```
00035:       DO 10 I=1,N+1
00036:       P1(I,J)=0.0
00037:       P11(I,J)=0.0
00038:       H1(I,J)=0.0
00039:    10 CONTINUE
00040:C*************************************************************************
00041:       WRITE(3,600)
00042:   600 FORMAT(101H                                        THE  SOLUTION  OF  REYNO
00043:      2LDS  EQUATION  FOR  360 DEGREE JOURNAL BEARING/,102H**********
00044:      3**************************************************
00045:      4**********)
00046:       WRITE(3,610)
00047:   610 FORMAT(54H     EPS      MAXIT              L      D      M            )
00048:       WRITE(3,620)EPS,MAXIT,L,D,M
00049:   620 FORMAT(3X,F7.5,4X,I3,3X,4X,I4,3X,F5.3,2X,I3,5X/,65H*****
00050:      2**************************************************)
00051:C*************************************************************************
00052:8      EMEU=1.0-(((3.14**2)*(4.0+(3.14*D/FLOAT(L))**2))/(2.0*((FLOAT(
00053:      4M/2)*FLOAT(M/2))+(3.14*D*FLOAT(N)/FLOAT(L))**2)))
00054:C       OMEGA IS THE OVER RELAXATION FACTOR
00055:       OMEGA=2.0*((1.0-(1.0-EMEU**2)**0.5)/(EMEU**2))
00056:       WRITE(3,680)OMEGA
00057:   680 FORMAT(36H THE OVER RELAXATION FACTOR OMEGA =  ,F8.4/,45H**********
00058:      2**********)
00059:C*************************************************************************
00060:C       ALPHA    IC  THE  ATTITUDE  ANGLE
00061:C*************************************************************************
00062:C       FROM HERE TO STATEMENT NUMBER 30 THE ROUTINE IS USED TO CALCULE THE
00063:C       OIL FILM THICKNESS AT THE MISH POINTS
00064:       G1=0.0
00065:       DO 30 J=1,M+1
00066:       DO 20 I=1,N+1
00067:       H1(I,J)=(1.0+E*COS(G1))/2.0
00068:    20 CONTINUE
00069:    30 G1=G1+(2.0*3.14/180.0)
00070:C*************************************************************************
```

```
00071:       DO 50 I=2,N
00072:    50 P1(I,1)=0.0
00073:       DO 60 I=2,N
00074:    60 P1(I,M+1)=0.0
00075:       DO 70 J=2,M
00076:    70 P1(1,J)=0.0
00077:       DO 80 J=2,M
00078:    80 P1(N+1,J)=0.0
00079:C*******************************************************************************
00080:       ITN=1
00081:       WRITE(3,810)DY,DX
00082:   810 FORMAT(25H                          DY = ,F15.8,45H
00083:      2                       DX = ,F15.8/,100H*******************************
00084:      4*******************************************************
00085:      5****)
00086:       R=(D/FLOAT(L))**2
00087:       S=DX**2
00088:       T=DY**2
00089:       B=1.0-OMEGA
00090:    90 DA=0.0
00091:C*******************************************************************************
00092:       DO 100 I=2,N
00093:       DO 100 J=3,M,2
00094:C       THE NEXT STATEMEBT IS THE REYNOLDS EQUATION FOR STEADY STATE COITION,
00095:C       REPRSENTED IN A FINITE DIFFEREENCE FORM
00096:C       P(I,J)       IS THE DIMENIONSLESS PRESSURE AT THE MESH POINTS
00097:       A1=((18.8/DX)*(H1(I,J-1)-H1(I,J+1)))
00098:       B1=((R/T)*((H1(I+1,J))**3)*(P1(I+1,J)))
00099:       C1=((1.0/S)*((H1(I,J+1))**3)*(P1(I,J+2)))
00100:       D1=((R/T)*((H1(I-1,J))**3)*(P1(I-1,J)))
00101:       E1=((1.0/S)*((H1(I,J-1))**3)*(P1(I,J-2)))
00102:       F1=((R/T)*((H1(I+1,J))**3))
00103:       Q1=((1.0/S)*((H1(I,J+1))**3))
00104:       Y1=((R/T)*((H1(I-1,J))**3))
00105:       Z1=((1.0/S)*((H1(I,J-1))**3))
00106:       PNEW1=OMEGA*((A1+12.0*CVN+B1+C1+D1+E1)/(F1+Q1+Y1+Z1))+B*P1(I,J)
```

```
00107:C*************************************************************************
00108:       IF(J.GE.(180.0/2.0)) GO TO 888
00109:       P11(I,J)=P1(I,J)
00110:       RESID=ABS(PNEW1-P11(I,J))
00111:       IF(RESID.GT.DA) DA=RESID
00112:   888 P1(I,J)=PNEW1
00113:       IF(J.GT.(180.0/2.0).AND.P1(I,J).LT.0.0) P1(I,J)=0.0
00114:   100 CONTINUE
00115:       ITN=ITN+1
00116:       IF(ITN.GT.MAXIT) GO TO 2
00117:       IF(ITN.LT.10) GO TO 90
00118:       IF(DA.GT.EPS) GO TO 90
00119:     2 WRITE(3,690)ITN
00120:   690 FORMAT(21H  CYCLE NUMBER ITN = ,I5//,21H**********)
00121:       WRITE(3,713)((P1(I,J),J=3,77,2),I=2,15)
00122:   713 FORMAT((2X,12(F9.4)))
00123:C*************************************************************************
00124:       SUMC1=0.0
00125:       SUMC11=0.0
00126:       SUMS1=0.0
00127:       SUMS11=0.0
00128:       G11=0.0
00129:C*************************************************************************
00130:       DO 110 J=1,M+1,2
00131:       DO 120 I=1,N+1
00132:C*************************************************************************
00133:C       SUMC1                    1S THE HYDRODYNAMIC FORCE IN THE DIRECTI. OF
00134:C       THE ATTITUDE LINE FROM ONE COLUMN OF THE MESH
00135:C*************************************************************************
00136:C       SUMC11                      IS THE TOTAL HYDRODYNAMIC FORCE IN THEE
00137:C       DIRECTION THE ATTITUDE LINE
00138:C*************************************************************************
00139:C       SUMS1                    IS THE HYDRODYNAMIC FORCE IN THE DIRECTI PERPEND
00140:C       ICULAR ON THE ATTITUDE LINE FOR ONE COLUMN OF THE MESH
00141:C*************************************************************************
00142:C       SUMS11                     IS THE TOTAL HYDRODYNAMIC FORCE IN THEEDIRECTIO
```

```
00143:C       N PERPENDICULAR ON THE ATTITUDE LINE
00144:C*************************************************************************
00145:        SUMC1=SUMC1+P1(I,J)*DX*DY*COS(G11)
00146:        SUMS1=SUMS1+P1(I,J)*DX*DY*SIN(G11)
00147:   120 CONTINUE
00148:C*************************************************************************
00149:        G11=G11+(4.0*3.14/180.0)
00150:        SUMC11=SUMC1+SUMC11
00151:        SUMS11=SUMS1+SUMS11
00152:        SUMC1=0.0
00153:        SUMS1=0.0
00154:   110 CONTINUE
00155:C*************************************************************************
00156:        FCOS1=SUMC11
00157:        FSIN1=SUMS11
00158:C*************************************************************************
00159:        FT=SQRT(FCOS1**2+FSIN1**2)
00160:        WRITE(3,661)FT
00161:   661 FORMAT(F15.8)
00162:        ALPHA=ATAN(-FSIN1/FCOS1)
00163:        ALPHA=ALPHA*180.0/3.14
00164:        DU=1.0/FT
00165:        WRITE(3,662)ALPHA,FCOS1,FSIN1,DU
00166:   662 FORMAT(4(F15.8))
00167:C*************************************************************************
00168:        FLOCO1=0.0
00169:        DO 1000 J=3,M+1,2
00170:        FLOCO1=FLOCO1+((2.0/(3.0*3.14))*((D/FLOAT(L))**2)*((P1(N,J))
00171:       2)*(H1(N,J)**3))
00172:  1000 CONTINUE
00173:        WRITE(3,7777)FLOCO1
00174:  7777 FORMAT(75H                                        THE                FLOW  COE
00175:       2FFICIENT  FLOCO1 = ,F15.8/,100H*****************************************
00176:       3*************************************************************)
00177:C*************************************************************************
00178:        CVN=CVN+2.0
```

```
00179:54545 CONTINUE
00180:      E=E+0.1
00181:    1 CONTINUE
00182:      L=L+1
00183:    3 CONTINUE
00184:      STOP
00185:      END
BOTTOM
```

This paper has been presented at the 6th Conference 'The Optimization Problems in Design and Production of Machines', held at INSTYTUT KONSTUKCJI IEKSPLOR TACJI MASZYN i INSTYTUT TECHNOLOGII BUDOWY MASZYN POLITECHNIKI WROCLAW SKIGJ POLAND, 21-25 September, 1978.

DEVELOPMENT OF A BEARING FOR A WIDE SPEED RANGE WITH REFERENCE TO MACHINE TOOLS APPLICATION

A.W. CROOK* and T.M. SALEM**

The paper describes work carried out in the development of a bearing for a wide speed range, and of high stiffness. The intended speed range is from zero to 9000 rpm, and the intended load capacity is approximately 6.6×10^4N in the low speed range and 4.0×10^3N in the high speed range.

The bearing is conceived as a hydrostatic bearing at low speeds, and as a self generating bearing at high speeds. The bearing is of three lobe form with the intention of enhancing stiffness in the self generating regime. High pressure inlets with no pockets are provided in the mid lobe positions, and low pressure inlets are provided at the apices of the lobes.

A development bearing of 135 mm bore and 127 mm width has been made and is being tested. Hydrostatic tests without rotation of the journal have shown the stiffness to be satisfactory and substantially as predicted from the analysis of the bearing. Tests with rotation of the journal are currently in progress and tests have been carried out up to a speed of 3000 rpm. The measured power loss and temperature rise are substantially those which had been expected.

* Professor of Mechanical Engineering at Brunel University.

** Research Student, Department of Mechanical Engineering, Brunel University. (Formerly with Helwan University, Egypt).

1. Introduction

The development work described in this paper was originated by an enquiry for a machine tool bearing of 152 mm diameter and with the specification given in Table 1.

It seemed possible, from a feasibility study, that the specification could be met by a bearing which operates hydrostatically at low speed, and which becomes self generating as the speed is increased. In a self-generating bearing of circular bore the stiffness of the bearing arises in the locality of the position of minimum film thickness, and the remainder of the surface contributes little to stiffness but a great deal to the loss within the bearing. However, if the bearing is a multi-lobe bearing then there is a position of film convergence at each lobe, and each lobe contributes to the overall stiffness. By adopting a multi-lobe bearing it was considered that the required stiffness in the self-generating regime could be obtained at a lower power loss than would be possible with a bearing of circular bore. This concept reacted upon the design of the bearing in its hydrostatic aspect.

In a bearing which is entirely hydrostatic the advantages of pockets are well known, but as reported by SHELDON et al[1]*, and ROWE, KOSHAL, and STOUT[2] the consequent removal of surface greatly diminishes the load carrying capacity of the bearing as a self generating bearing. Furthermore, turbulence within the pockets increases the loss. Consequently it was decided that the bearing would be designed without pockets, and that the required characteristics in the hydrostatic regime would be obtained by employing a sufficiently high inlet pressure.

* Numbers in parentheses refer to the References at the end of the paper.

Regime	Speed rpm	Maximum bearing pressure Nm^{-2}	Deflection of spindle m	Mean stiffness Nm^{-1}
Low speed	8 - 40	3.86×10^{6}	Unimportant	-
Roughing	40 - 80	3.86×10^{6}	Unimportant	-
	40 to 1800	1.18×10^{6}	2.5×10^{-5}	8×10^{8}
High speed	1500 to 9000	2.34×10^{5}	1.25×10^{-5}	3.2×10^{8}

For the above bearing pressures maximum loads for a bearing of 135mm diameter and 127 mm long become 6.6×10^{4}N, 6.6×10^{4}N, 2.0×10^{4}N and 4.0×10^{3}N respectively.

Table 1. Specification

2. Notation

C	Diametral clearance	m
C''	Minimum diametral clearance	m
C'	Maximum diametral clearance	m
D	Lobe diameter	m
d	Shaft diameter	m
F_t	External load	N
H_s	Power loss	KW
L	Bearing axial width	m
N	Rotational speed	rpm
P_s	Hydrostatic supply pressure	Nm^{-2}
Q_t	Total rate of flow	litres s^{-1}
Z	Absolute viscosity	cp
Δr	Offset	m

3. The Bearing

The concept of the bearing is illustrated by Figure 1. The bearing comprises three lobes of circular bore with the centre of each lobe displaced from the axis of the bearing. With no external load, the axis of the journal and bearing will be co-linear, but the journal will be forced to run eccentrically with respect to each of the three lobes. Bearings with three lobes have been analysed by PINKUS[3]. They have been proposed as having good anti-whirl properties, and as having high stiffness.

A high pressure oil inlet for the hydrostatic regime is provided at the centre of each lobe, and a low pressure inlet is provided for the self-generating regime at each conjunction of the lobes.

3.1 The development bearing was made by splitting a brass cylinder into three segments, by reassembling the segments but separated by

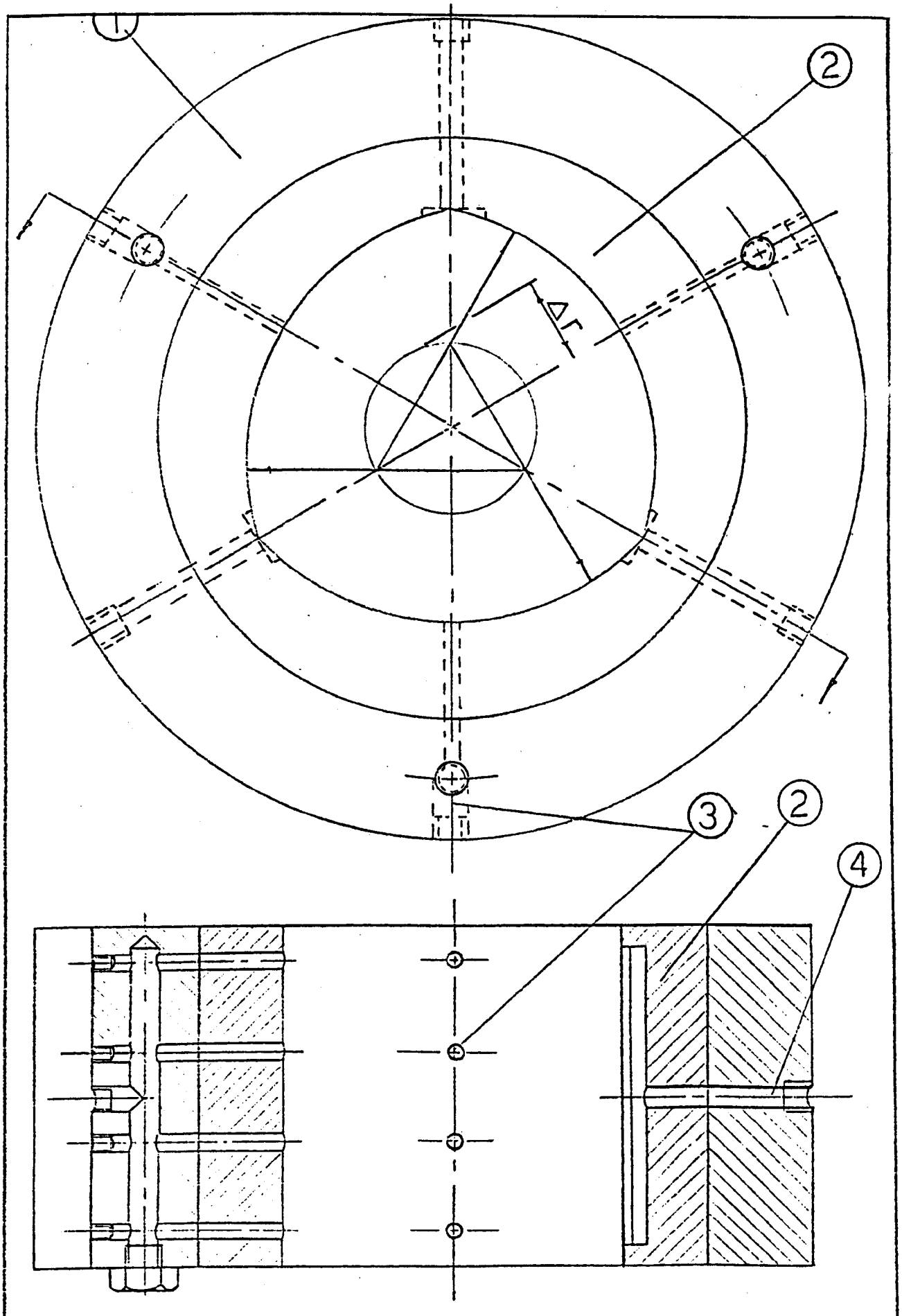

1	Steel housing		
2	Brass shell		
3	High pressure inlet		
4	Low pressure inlet		

FIG.1 Three lobe-bearing for hydrodynamic and hydrostatic operation

shims, by boring the assembly circular, by removing shims and finally by turning the outer surface circular. The thickness of the shims was calculated to provide the required offset of the centres of the lobes (Figure 1). Particular care had to be taken with the abutments of the three segments so that no bending was introduced on tightening. The dimensions of the bearing are given in Table 2, and the form achieved by the process is shown by the roundness chart of Figure 2. The departures from the intended form are negligible.

4. Hydrostatic Tests

4.1 Test Rig

The bearing as arranged for hydrostatic test is shown in Figure 3. The rig does not permit continuous rotation, but the effect of applying the force in different directions with respect to the lobes was tested by rotating the bearing in its frame. The force was applied by a hydraulic ram, the movement of the journal with respect to the bearing was measured with dial gauges, and the absence of metal to metal contact between journal and bearing was monitored by measuring the electrical resistance between journal and bearing. High pressure oil was supplied to the high pressure inlets via individual volume control valves. Volume control valves were chosen in contrast with orifice plates or capillaries to minimise the loss and therefore the pump power, to minimise the pressure of the pump, and also as reported by Malonski and Loeb[4] to provide a greater stiffness. The supply pressure from the pump was measured and oil flow, oil temperature and pressure were measured downstream of each of the three volume control valves.

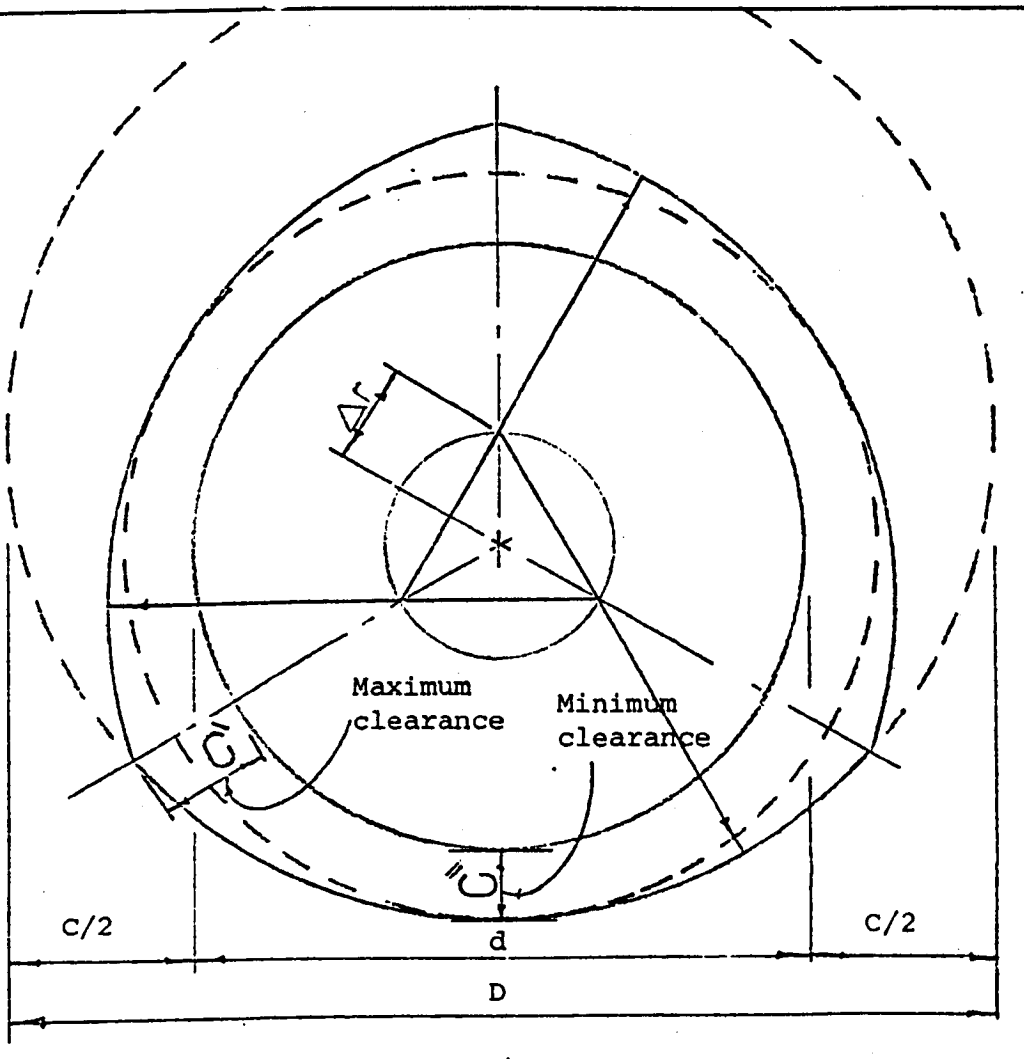

Designation of bearing	D* m	d m	r m	C m	C* m	C` m
1	1.352×10^{-1}	1.349×10^{-1}	5.75×10^{-5}	2.6×10^{-4}	1.45×10^{-4}	2.025×10^{-4}
2	135.2×10^{-1}	1.3487×10^{-1}	5.75×10^{-5}	3.0×10^{-4}	1.85×10^{-4}	2.425×10^{-4}
3	135.2×10^{-1}	1.348×10^{-1}	5.75×10^{-5}	3.7×10^{-4}	2.55×10^{-4}	3.175×10^{-4}

* L/D = 0.94

TABLE 2 DIMENSIONS OF TEST BEARINGS

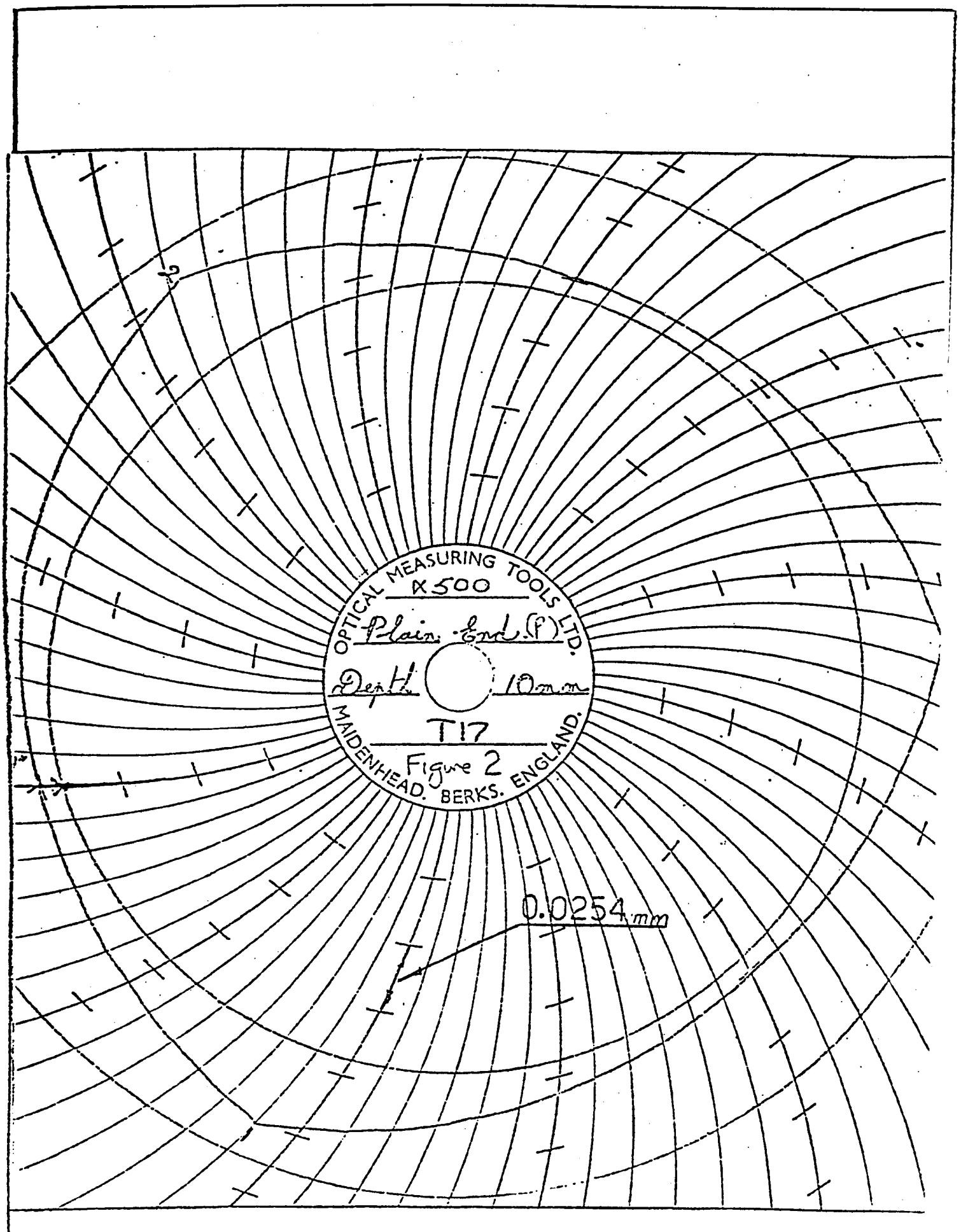

FIG.2 PROFILE OF FINISHED BEARING

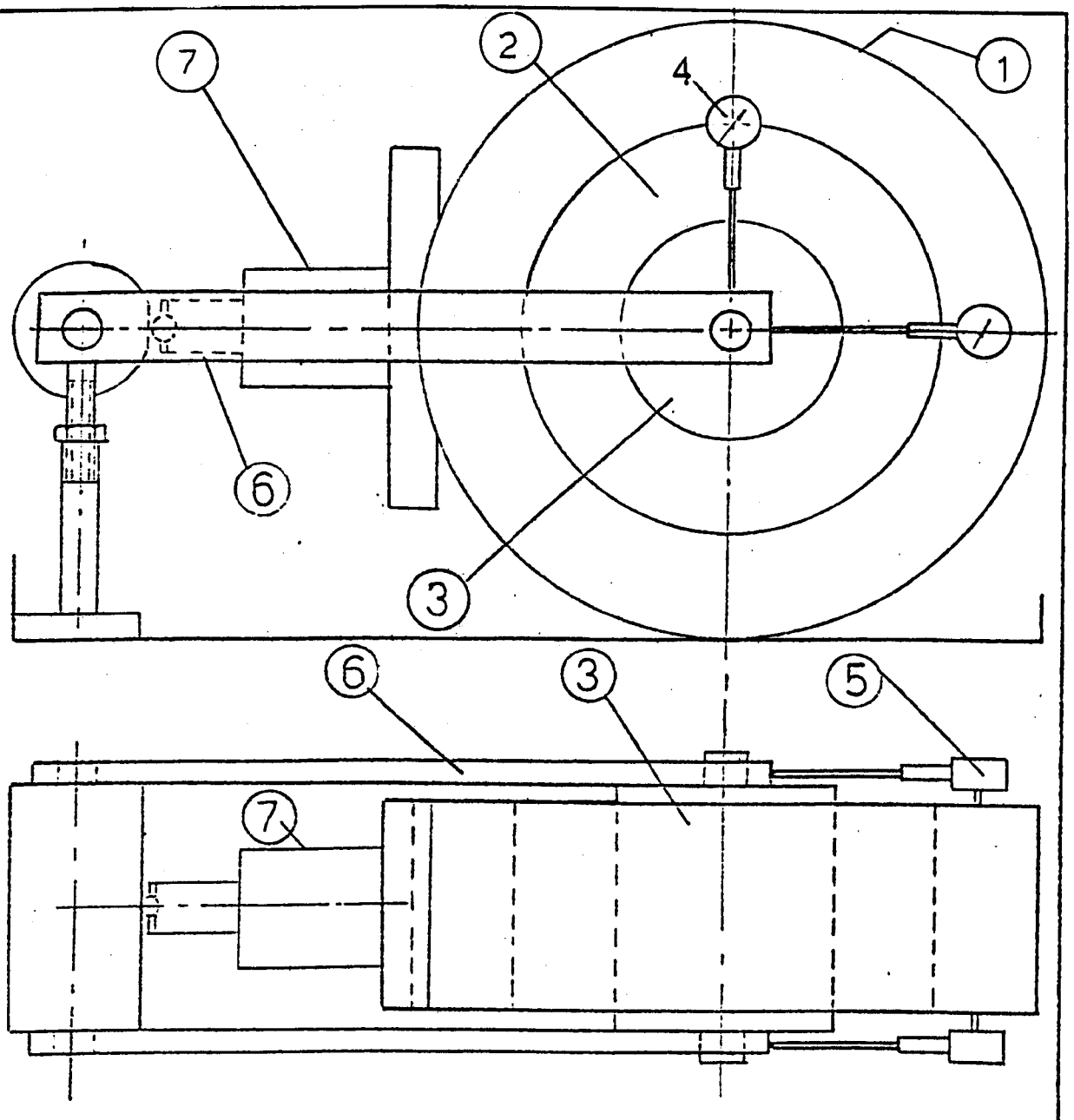

1	Steel housing	7	Hydraulic ram
2	Brass shell		
3	Journal		
4	Dial gauge		
5	Dial gauge		
6	Loading arms		

FIG.3 TEST RIG FOR EXTERNAL PRESSURIZATION

4.2 Results of hydrostatic tests

The tests were carried out with an oil of viscosity of 20cp at 75°C (SHELL VITREA 69 - Industrial Oil). Typical conditions of test were a supply pressure of 1.7×10^{7} Nm^{-2}, a total volume flow of 0.122 litres s^{-1}, a pump power of 3KW and an oil temperature at bearing inlets of 50°C at which the oil has an absolute viscosity of 65cp. A typical result is a stiffness of 1×10^{9} Nm^{-1}, and absence of metal to metal contact up to the maximum load which was applied of 5.6×10^{4}N.

Specific test results are shown in Figures 4 and 5. In Figure 4 displacement is shown as a function of load for three rates of oil flow. In all tests the supply pressure was $1.7 \times 10^{7} Nm^{-2}$ (170 bar). The results show that the displacement load relationship is not exactly linear and that an increase in volume flow produces an increase in stiffness provided that an adequate pressure drop is maintained across the constant volume valves. Figure 5 shows some test results at three different diametral clearances (clearance based upon lobe and journal diameters). The stiffness falls rapidly as the diametral clearance is increased despite the increase in volume flow. The interrupted line shows calculated stiffnesses for the conditions of the tests, and is based upon the infinitely wide bearing theory. However, as may be derived from Figure 4, a stiffness of $1.2 \times 10^{9} Nm^{-1}$ was achieved at a load of 6.4×10^{4} N with a supply pressure of $1.7 \times 10^{7} Nm^{-2}$, a total volume flow of 0.185 litres s^{-1} and with a pumping power of 4.5KW. The diametral clearance was 3×10^{-4}m. There was no metal to metal contact.

The experimentally determined performance exceeds the specification

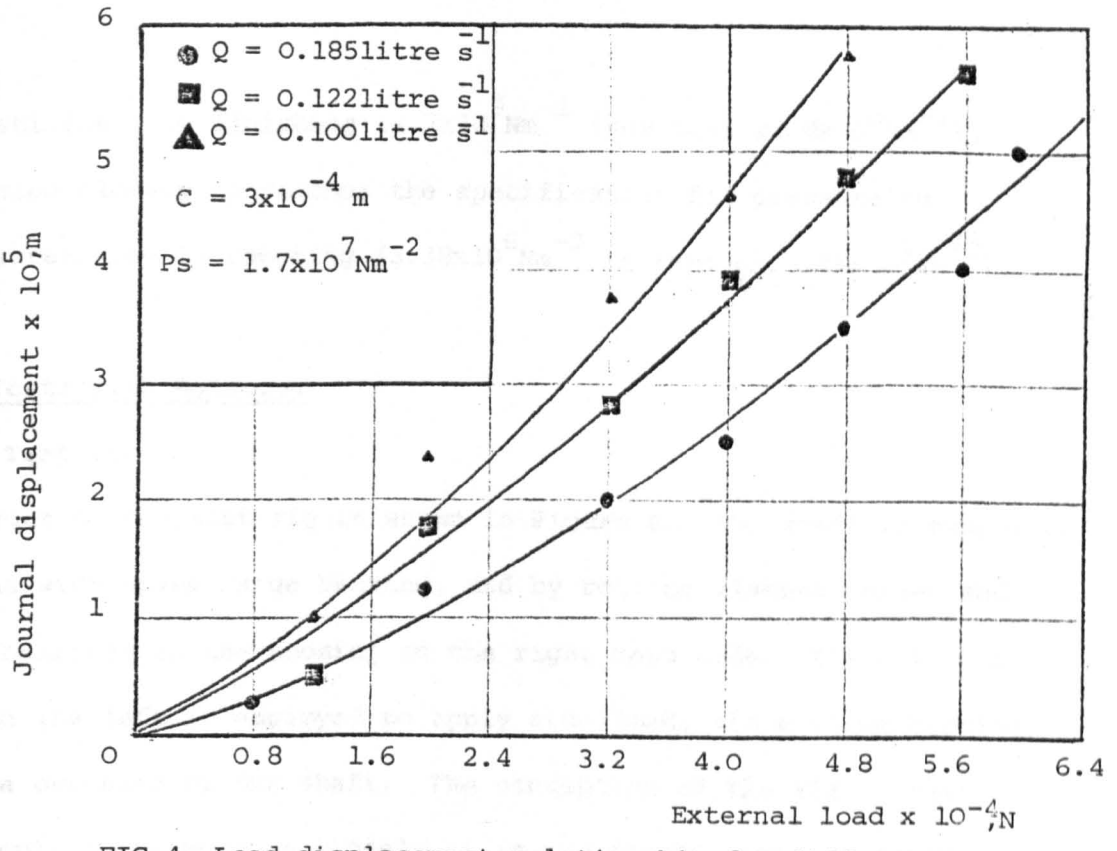

FIG.4 Load displacement relationship for different rates of oil flow

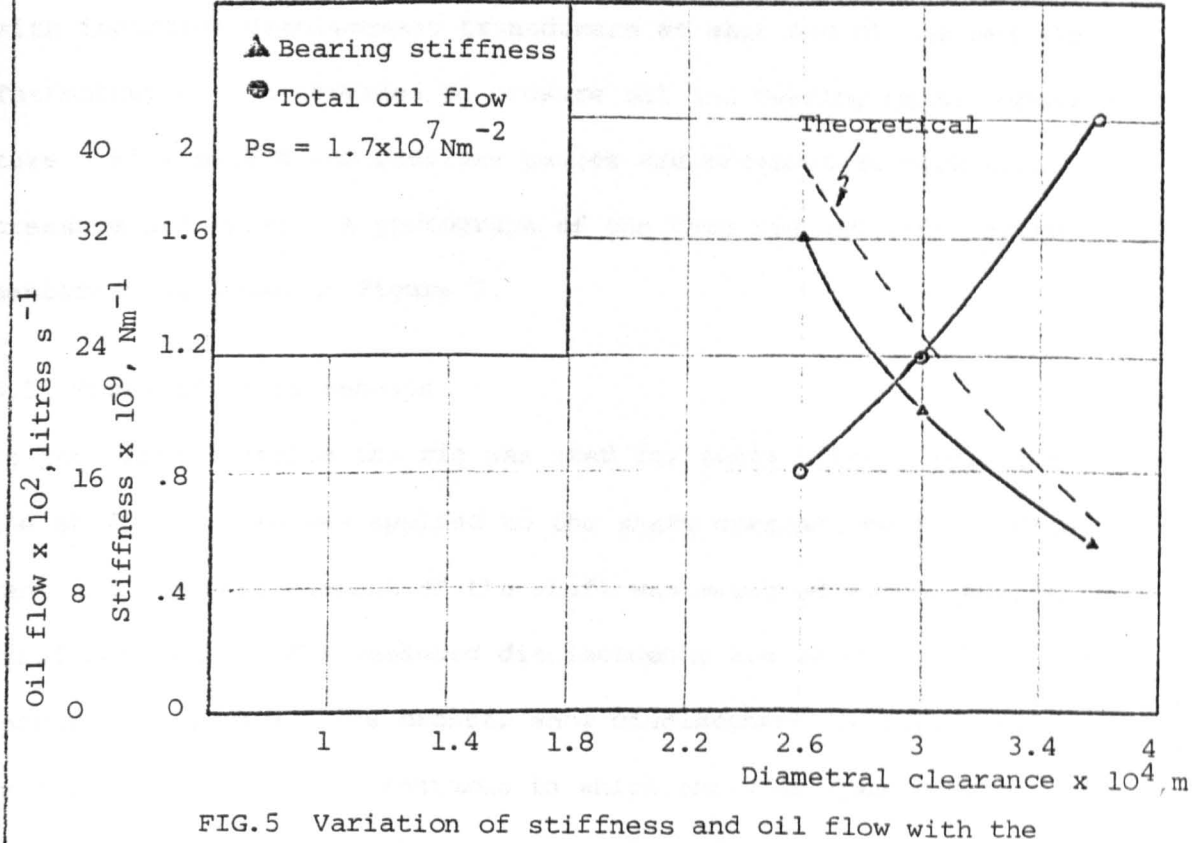

FIG.5 Variation of stiffness and oil flow with the diametral clearance

for stiffness in finishing ($1.2 \times 10^{9} Nm^{-1}$ from test cf $8 \times 10^{8} Nm^{-1}$), and also closely approaches the specification for pressure on projected area in roughing ($3.38 \times 10^{6} Nm^{-2}$ in test cf $3.86 \times 10^{6} Nm^{-2}$).

5. Tests with Rotation

5.1 Test rig

A layout of the test rig is shown in Figure 6. The shaft is supported by the wide speed range bearing, and by rolling element thrust and tail bearings in the housing on the right hand side. The hydraulic ram on the left is employed to apply side load, via a slave bearing, to the overhang of the shaft. The conception of the rig is that it should correspond as closely as is practicable with an actual spindle; for instance the tail and thrust races have been chosen with machine tool duty in mind, and are mist lubricated. The displacement of the journal with respect to the bearing is measured with inductive displacement transducers at each end of the bearing. Thermocouples are provided to measure oil and bearing metal temperature. Flow meters and pressure gauges are provided at each high pressure oil inlet. A photograph of the test rig with its instrumentation is shown in Figure 7.

5.2 Tests and test results

In the first instance the rig was used for tests without rotation of the shaft. A load was applied to the shaft overhang by the hydraulic jack and the displacement of the shaft was measured at the available axial positions. The measured displacements are shown by the circular points in Figure 8. The crosses show displacement as calculated by means of a computer programme in which the wide speed range bearing and the tail bearing were represented by springs of appropriate stiffness. There is substantial agreement between the

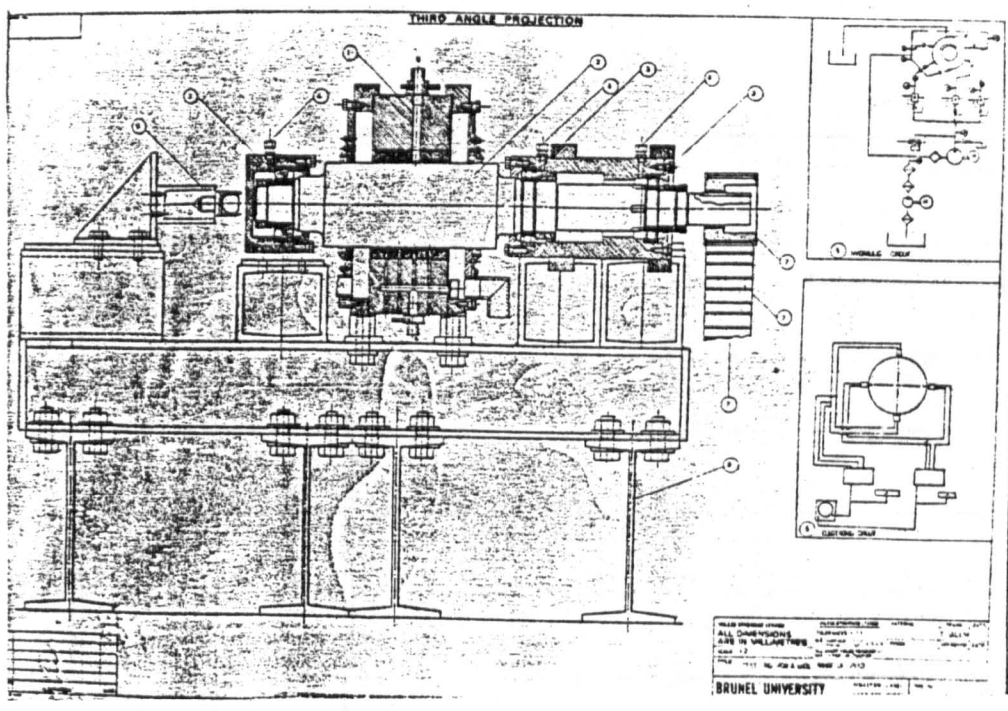

FIG.6 MAIN TEST RIG

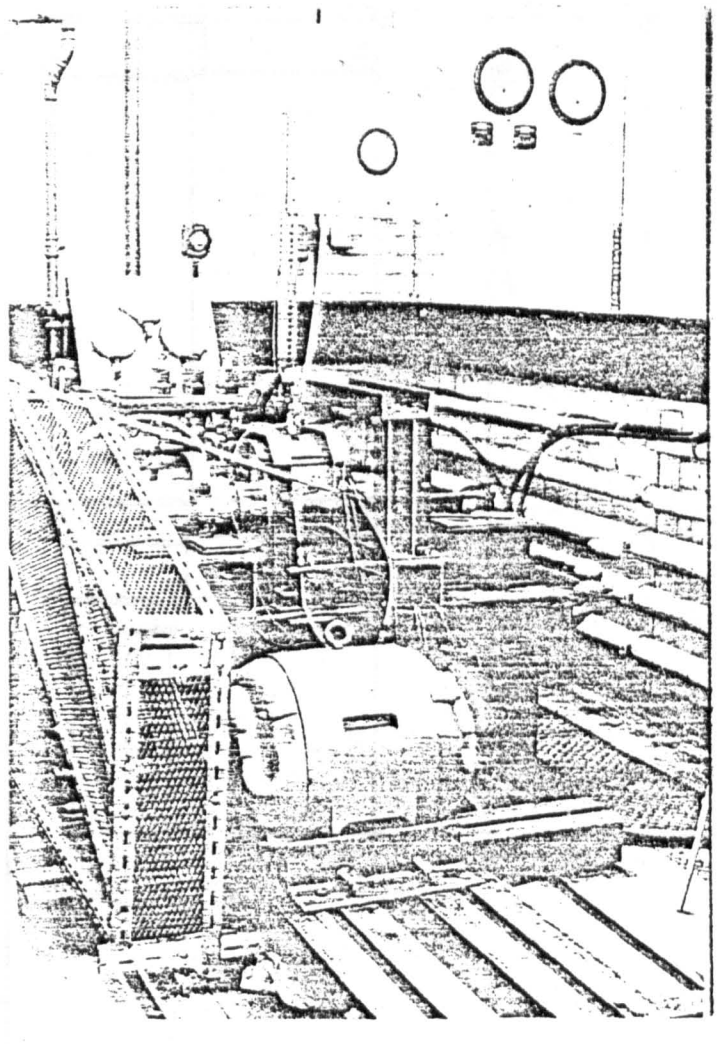

FIG.7 TEST RIG AND INSTRUMENTATIONS

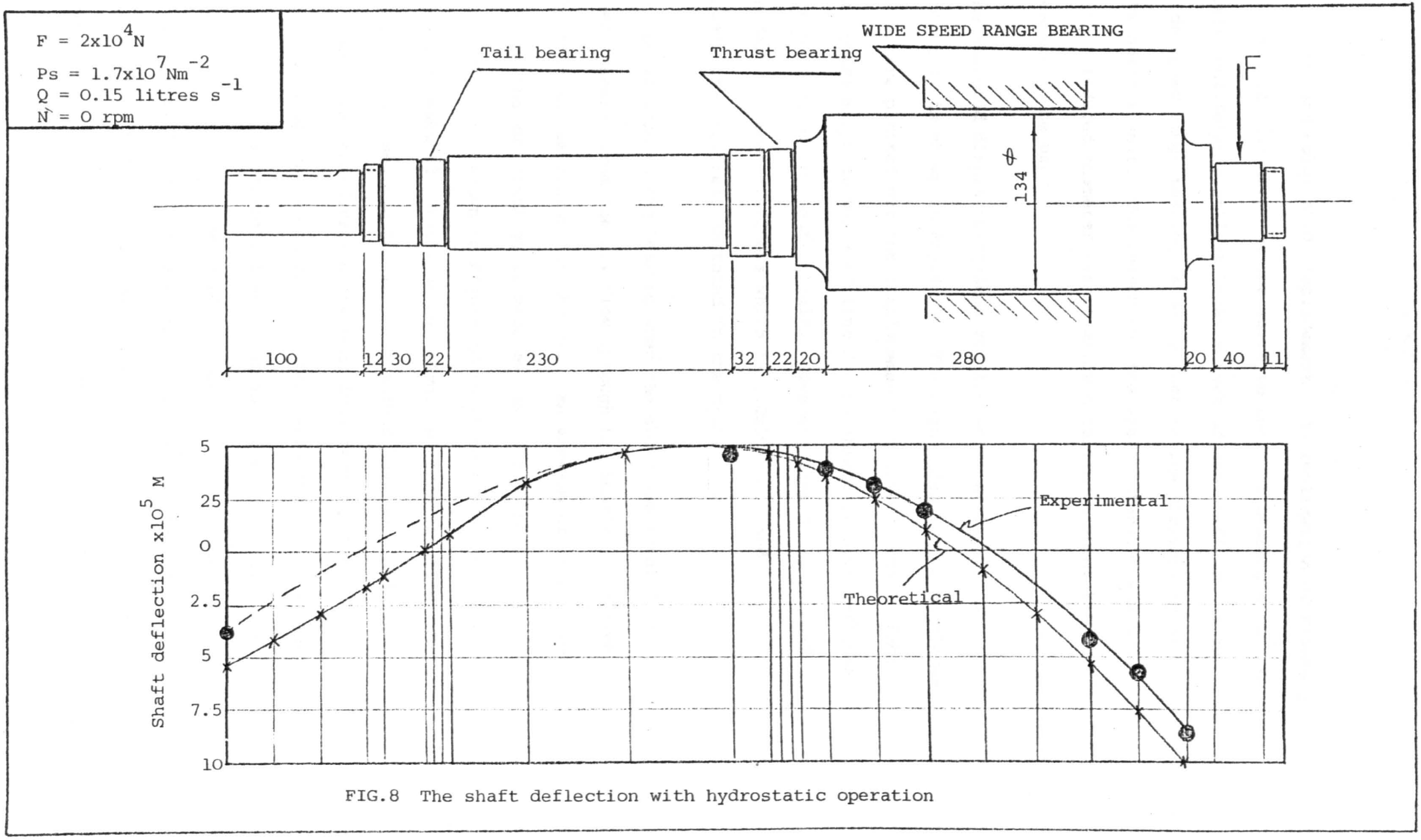

FIG.8 The shaft deflection with hydrostatic operation

observed and calculated displacement. An implication of Figure 8 is that the extension of the shaft to the tail bearing should be made considerably stiffer because much of the stiffness of the wide speed range bearing is being lost in the flexibility of the shaft itself. The reason why the shaft extension was made with a reduced diameter was to allow a rolling element thrust bearing to be used.

The measured displacement-load relationship, again without rotation, is shown in Figure 9. The magnitudes of the displacements are plotted but the displacements of line A were in fact of opposite sign to those of line C; the change in sign reflects the bending of the shaft itself. However, line B may be used to derive a mean stiffness which is $1.2 \times 10^{9} Nm^{-1}$, and which equals the stiffness as found in the static rig.

The power loss in the bearing when the shaft was rotated has been assessed from the oil flow through the bearing, and from the rise in temperature of the oil. An assessment of the heat loss to the surroundings was made by taking cooling curves. The results are shown in Figure 10 in which the triangular points show the measured power loss as calculated from oil flow and temperature rise, and the circular points have been adjusted to take into consideration the heat loss from the rig. The loss is plotted against speed on a log log basis and the experimental points lie on a straight line. The dotted extrapolation indicates the power loss to be expected at high speeds. At the time of writing very limited tests of the stiffness of the bearing when the shaft is rotating have been made. The results indicate a somewhat greater stiffness when rotating than when the journal

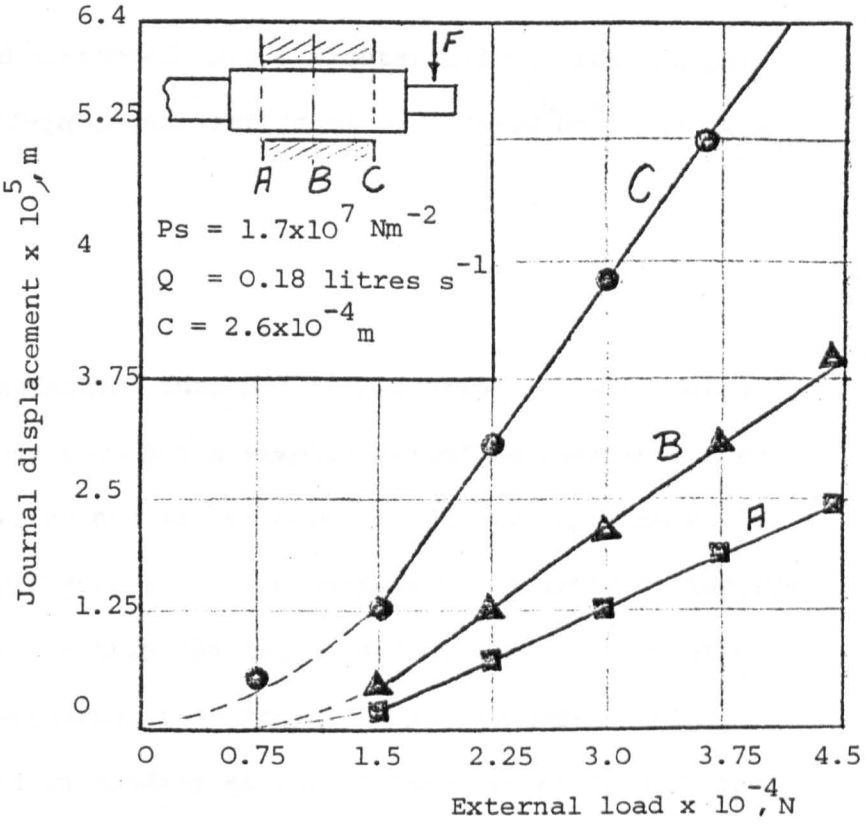

A and C measured. B deduced displacement at centre.

FIG.9 Load displacement relationship

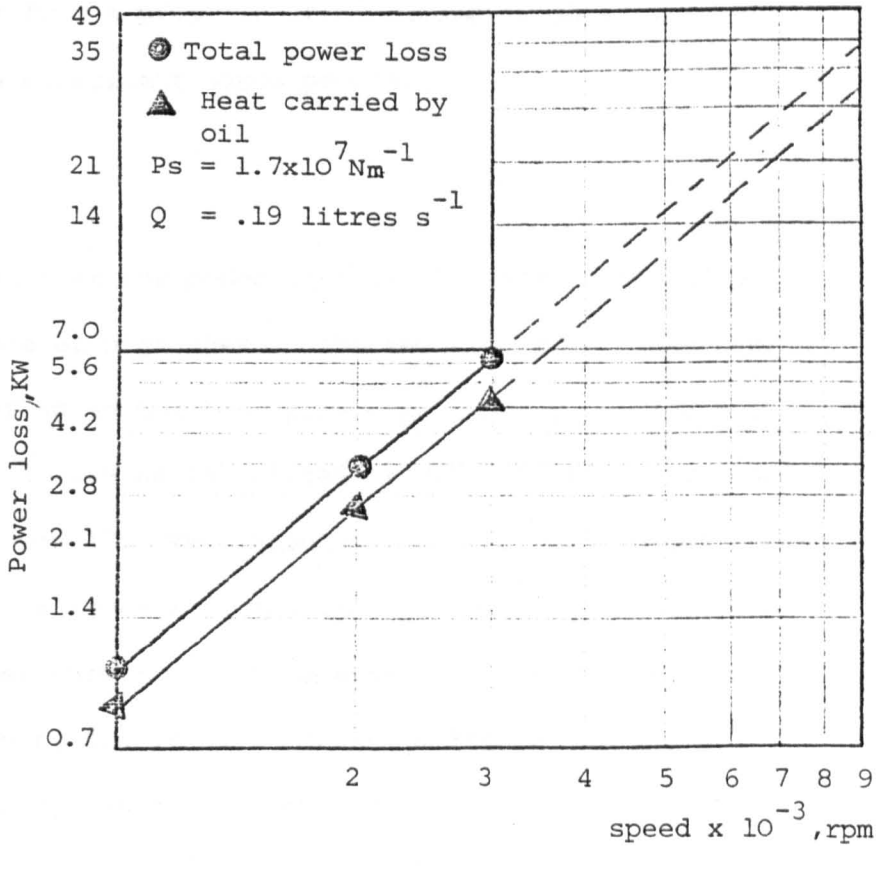

FIG.10 Variation of the power loss with speed

is stationary and supported only hydrostatically. For instance at a speed of 1000rpm a mean stiffness of $1.25 \times 10^{9} Nm^{-1}$ has been found.

6. Manufacture

The method of manufacture outlined in paragraph 3 has produced a very satisfactory form but a simpler method is clearly desireable. A method which has so far been tried only experimentally is illustrated by Figure 11. It comprises the elastic distortion of the bearing ring within the three jaws of a chuck. To give the closest approximation to circular lobes the bearing ring is made less rigid in bending at three places by axial grooves machined in its outer surface. The bore of the distorted ring is machined circular, the ring is then released, and its outer surface is turned circular. A roundness trace from an experimental ring cut from a piece of steel tubing is shown in Figure 12. The experiment shows promise.

7. Power Loss

It is inevitable that the power loss in the bearing should be very considerable at high speed. The measured power loss over a limited range of speed has been presented already in Figure 10. Predicted power losses as calculated by the Petroff relationship are given in Figure 13. The calculations were carried out iteratively so that the power loss and the viscosity of the oil at its outlet temperature are self consistent. The measured power losses are shown by the crossed points in Figure 13, and are substantially in agreement with the predicted losses.

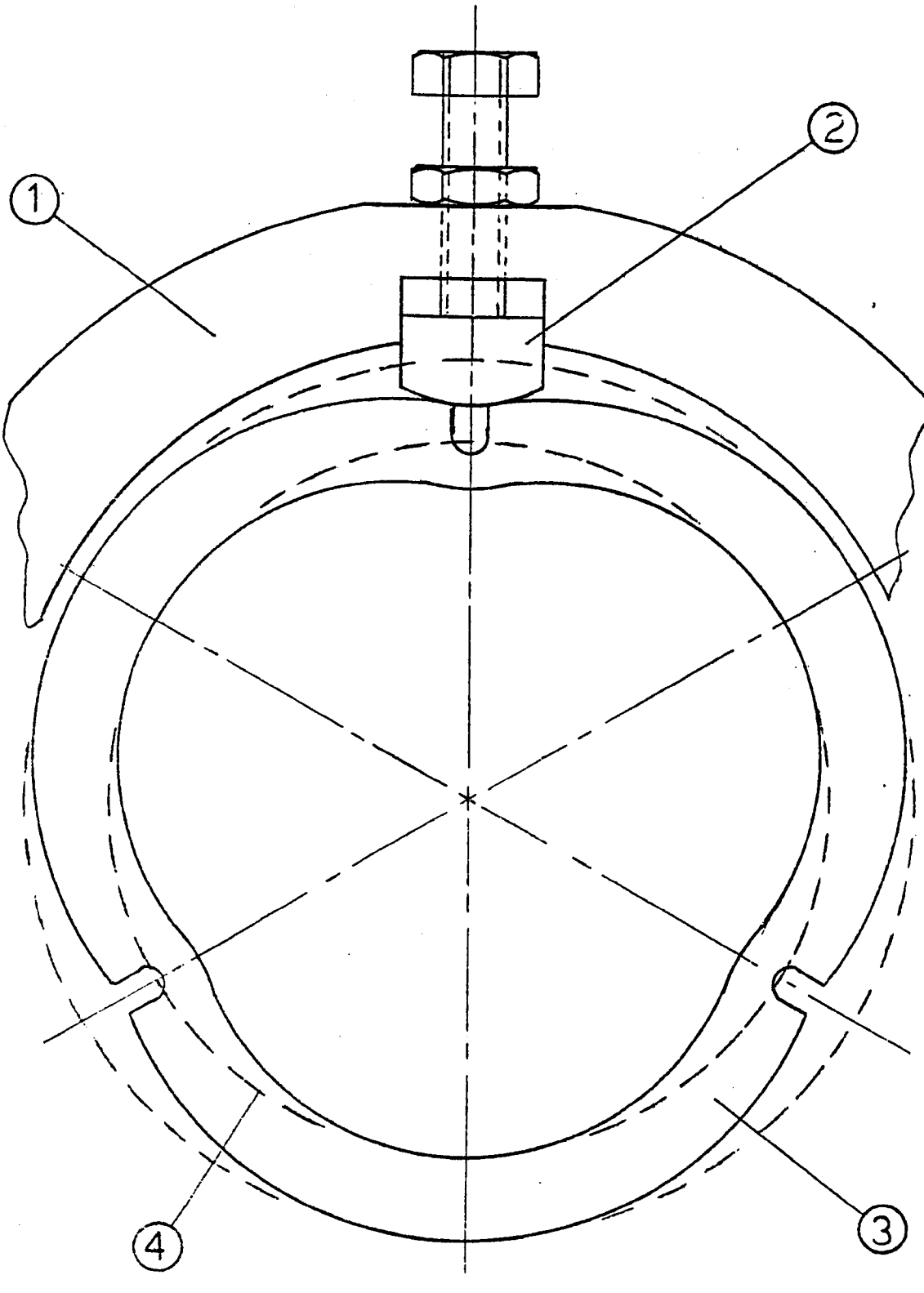

1	CHUCK
2	JAW
3	ELASTICALLY DISTORTED RING
4	CIRCULAR BORE

FIG.11 Jig for manufacturing method

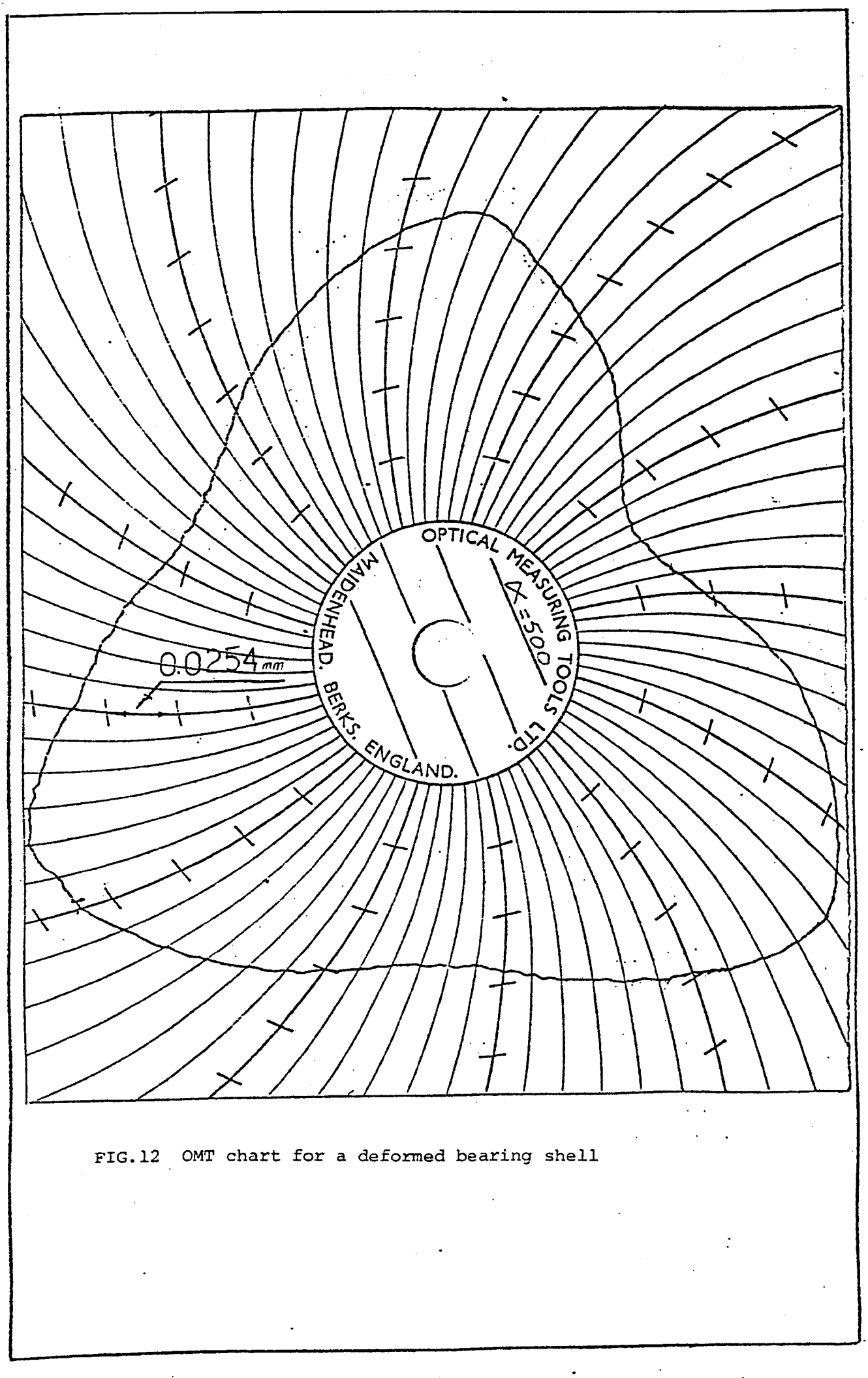

FIG.12 OMT chart for a deformed bearing shell

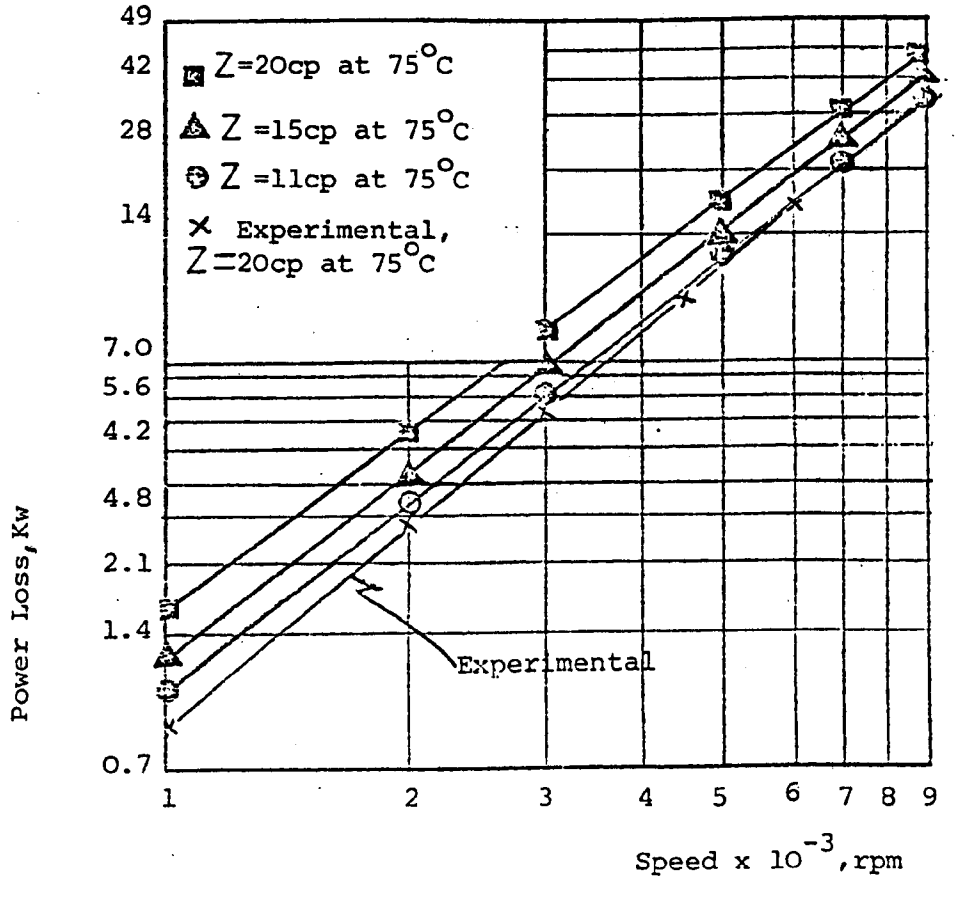

FIG.13 Variation of the Predicted Power Loss with Speed

A principal point of the three lobe bearing in contrast with a bearing of circular bore is to achieve the required stiffnesses with the least possible power loss. A comparison of three lobe and circular bore designs of the same mean stiffness has been carried out on the basis that if a particular oil outlet temperature is permissible with a bearing of circular bore then the same oil outlet temperature is also permitted with a three lobe bearing. The comparison indicates that the power loss in the bearing of circular bore will be approximately 1.5 times greater than the loss in a three lobe bearing of the same mean stiffness, that the oil inlet temperature of the circular bore bearing would have to be impracticably low, and that small clearances difficult to provide would be necessary.

8. Conclusion

From the tests which have been carried out with the three lobe bearing in its hydrostatic regime and without rotation of the journal, and from the limited tests of the bearing with journal rotation which have been carried out upto the time of writing, it seems probable that the three lobe bearing will substantially satisfy the onerous functional specification of Table 1. A point which has become emphasized by the work is that with a bearing of such high stiffness the flexibility of the shaft may become the predominant factor, and shafts of very high stiffness have to be provided if the capability of the bearing is to be realized.

REFERENCES

1. SHELDON, D.F. et al. 'A hydrodynamic pocket journal bearing', Proc.Inst.Mech.Eng. 1970, 184 (Part 32), 70-74.

2. ROWE, W.B., KOSHAL, D., STOUT, K.J., 'Slot entry bearing for hydrodynamic and hydrostatic operation', Journal of Mechanical Engineering Science, Vol.18, No.2. 1976.

3. PINKUS, O., 'Analysis and characteristics of three lobe bearing', Journal of Basic Engineering, March 1959.

4. MALANOSKI, Stanley B., LOEB, Alfred M. 'The effect of compensation on hydrostatic bearing stiffness'. Journal of Basic Engineering, June 1961.

ACKNOWLEDGEMENTS

The Author would like to express his sincere gratitude to his supervisor, Professor A.W. Crook, for the creation of this research subject and feasibility study, and for many constructive comments and criticisms of this material, encouragement and facilities in the work of this investigation. The author would also like to thank his Country for the generous financial support during the time taken to study.

To acknowledge his indebtedness to his wife, Samia, for her great help, patience and forbearance in the period of this investigation.

Not forgetting to thank for the help and assistance of:

Professor G.J. Jackson, Head of Department of Mechanical Engineering.

Dr. A.J. Reynolds, Department of Mechanical Engineering.

Mr. G.R. Halcrow, Department of Mechanical Engineering.

Mr. J.D. Russell, Department of Mechanical Engineering.

Mr. R. Brooks, Department of Mechanical Engineering.

Mr. G. Reading, Department of Mechanical Engineering.

Mr. T. Gates, Department of Mechanical Engineering.

Mr. F. Hawkes, Department of Mechanical Engineering.

Mr. J. Forde, Department of Mechanical Engineering.

Mr. P. Mathers, Department of Mechanical Engineering.

Mr. K. Chambers, Department of Mechanical Engineering.

Mr. S. Aris, Department of Mechanical Engineering.

Mr. S. Hutchinson, Department of Mechanical Engineering.

Mr. D. Gritton, now with British Gas.

Mr. Z. Preece, Department of Mechanical Engineering.

Mrs. D. Woodrow, Department of Mechanical Engineering.

Professor R. New, Department of Production Technology.

Mr. R. Murdock, Central Workshop Supervisor.

Mr. A. Saunders, Central Workshop.

Mr. L. Marke, Central Workshop.

Mr. A. Kettle,Central Workshop.

Mr. C. Ritchie, Computer Centre.

Mrs. J. Gray, Computer Centre.

Mr. A. Smith, now with I.C.L.

Mr. C. Childs, Librarian.

Mr. R. Davies, Foundry.

Mr. H. Lister, Metallurgy.

Mr. E. Cave, Production Technology.

Miss P. Robinson, Metallurgy.